SOVIET PHYSICS

JETP

*A translation of the Journal of Experimental and Theoretical Physics of the USSR.*

SOVIET PHYSICS JETP VOL. 34 (7), NO. 5, pp. 723-937 November, 1958

# *MEASUREMENT OF THE LONGITUDINAL POLARIZATION OF ELECTRONS EMITTED IN THE BETA-DECAY OF* $Tm^{170}$, $Lu^{177}$, $Au^{198}$, $Sm^{153}$, $Re^{186}$, $Sr^{90}$, *AND* $Y^{90}$.* *II*

A. I. ALIKHANOV, G. P. ELISEEV, and V. A. LIUBIMOV

Academy of Sciences, U.S.S.R.

Submitted to JETP editor December 12, 1957

J. Exptl. Theoret. Phys. (U.S.S.R.) **34**, 1045-1057 (May, 1958)

The longitudinal polarization of electrons from Coulomb $\beta$-transitions is measured for various values of the electron energy. The longitudinal polarization was found to be equal to $-v/c$ for all substances investigated. It is shown that the relations $C_T = -C'_T$, $C_S = -C'_S$, $C_V = C'_V$, $C_A = C'_A$ are most probably satisfied by the $\beta$-decay coupling constants.

With the discovery of the violation of the conservation of parity in weak interactions,[1] the $\beta$-decay picture became more complicated. Whereas $\beta$-decay could formerly be characterized by four (more precisely, five) constants of the variants of interaction, the number of constants is now doubled, in so far as half of them reflect nonconservation of parity. And since, in general, the interaction constants can be complex, the number of parameters is increased to 16. However, new effects have come to light, through which connections between constants can be observed by physical measurements. One of these effects is, as is well known, the longitudinal polarization of electrons in the $\beta$-decay of unpolarized nuclei.[2]

Various combinations of the coupling constants can be obtained from the measurement of the longitudinal polarization of the electrons, depending on the type of transition of the $\beta$-active nucleus. It turns out that the maximum possible information about the coupling constants which can, in principle, be given by experiments on the measurement of the longitudinal polarization of electrons from unpolarized nuclei, is obtained by measuring very accurately the longitudinal polarization of the electrons as a function of electron energy, for first forbidden transitions (the so-called Coulomb transitions) in heavy nuclei.

In the present work we attempted to measure longitudinal polarization of electrons of various energies with the greatest possible precision for just the elements with Coulomb transitions, such as $Tm^{170}$ ($\Delta J = 1$; yes), $Re^{186}$ ($\Delta J = 1$, yes), $Sm^{153}$ ($\Delta J = 1, 0$; yes), $Au^{198}$ ($\Delta J = 0$, yes) and $Lu^{177}$ ($\Delta J = 1$, yes) or ($\Delta J = 0$, yes), containing a mixture of Gamow-Teller and Fermi interactions. For comparison, measurements were carried out in the same way for $Sr^{90}$ and $Y^{90}$, which have unique transitions and pure Gamow-Teller interaction, for which there is good reason to expect the electron polarization to be equal to $-v/c$.

## 1. DESCRIPTION OF THE ARRANGEMENT

To measure the longitudinal polarization, we employed the method of Mott scattering, which consisted in measuring the magnitude of the azimuthal asymmetry in a single scattering of transversely polarized electrons through a large angle by a scatterer having a large Z.

To obtain a good stability and reproducibility of results of the measurements, we tried to make the construction of the apparatus as simple as pos-

*This work was reported at the Conference on Mesons and New Particles in Padua-Venice, September 27, 1957, and at the All-Soviet Conference on Nuclear Reactions at Low and Medium Energies in Moscow, November 23, 1957.

sible. We have avoided using external fields, electric or electric + magnetic, for turning the longitudinal polarization into a transverse one, because these means contain sources of errors which are difficult to control. In our case, the longitudinal polarization was turned into a transverse one by deflecting, through an angle of about 90°, the trajectory of the electron in the Coulomb field of the nucleus through multiple scattering by a relatively thick scatterer. In the method where the polarization is transformed by using external fields, for example in a curved condenser, the upper limit on the energy of the electrons, whose polarization can be measured, is very low because it is impossible to obtain a sufficiently large voltage, owing to the possibility of sparking over in the vacuum. It is easy to see that our method does not have this limitation.

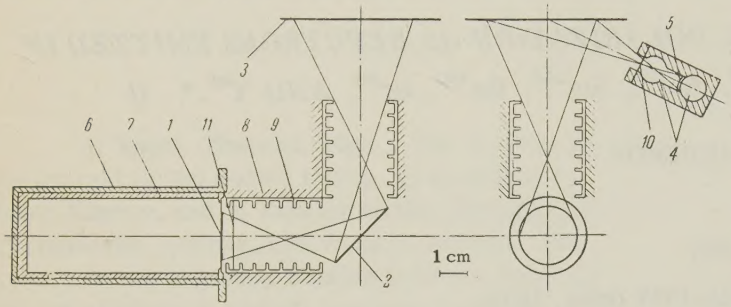


FIG. 1. Scheme of the apparatus. 1 – source, 2 – scatterer I (transformer), 3 – scatterer II (analyzer), 4 – Geiger counters, 5 – aluminum filter between the counters, 6 – brass container, 7 – plexiglass container, 8 – case of the apparatus, 9 – duraluminum diaphragm, 10 – polyethylene film, 11 – thin collodion film.

The scheme of the apparatus is given in Fig. 1. In order to increase the intensity of the apparatus, the channels for the electron traversal were made rather large. However, in spite of the significant spread in angles of the electron trajectories, in so far as the mean angle of scattering of the electrons by the "transforming" scatterer I was near to 90°, the geometrical correction, decreasing the magnitude of the azimuthal asymmetry on account of the angular spread, was equal, in all, to ~6%. The thin gold analyzing scatterer II was placed perpendicular to the axis of the apparatus. Such a position of the scatterer II gave the maximum symmetry for the entire apparatus. Electrons undergoing scattering in the scatterers I and II were counted by a telescope of two Geiger counters connected in coincidence. Between the counters there was placed an aluminum filter, which stopped the low energy electrons. The counters were placed at an angle of 112.5° to the axis of the apparatus, and at a very small angle with respect to the scatterer II so that a rather small solid angle of the counter telescope covered the whole area of the scatterer. Such dispositions of the counters and scatterers II gave the maximum intensity. The counters, together with the scatterer II, could be turned around the axis of the apparatus without destroying the vacuum. In order to decrease the admixture of electrons scattered from the walls of the apparatus, traps made of thin (0.5 mm) duraluminum diaphragms were placed in the canal traversed by the electrons.

The Tm, Lu, Sm, and Sr + Y sources, which were in the form of a finely dispersed active powder, were coated in uniform layers on a 10 $\mu$ thick aluminum foil. The Re was set electrolytically on an aluminum foil covered by a very thin layer of platinum, and the Au was sprayed on an aluminum foil in vacuum. The sources were then activated in the reactor. The foil with the source was fastened to a duraluminum ring, which was placed in a circular brass container, lined with plexiglass. A thin collodion film was placed in front of the source in several cases, to protect the apparatus against contamination by the active material.

Two analogous sets of apparatus were prepared. In the first one (1) the frame was made of brass and lead; in the second (2), of lead and tungsten.

## 2. MEASUREMENTS

The azimuthal asymmetry in the scattering, $\Delta = 200\,(I_1 - I_2)/(I_1 + I_2)$, was measured in a plane perpendicular to the plane in which the electron was turned as a result of the first scattering ($I_1$ is the scattered intensity in the azimuthal direction $\mathbf{v}_2 \times \mathbf{v}_1$, where $\mathbf{v}_1$ and $\mathbf{v}_2$ are the velocities of the electron before and after scattering in scatterer I, and $I_2$ is the intensity in the opposite direction) for several values of the mean electron energy $\overline{E}$. The electrons were separated by energies by placing an aluminum filter of given thickness $\rho$ between the counters, and using a scatterer I of thickness $\tau$. In each experiment with a definite mean energy of the electrons $\overline{E}$, several measurements of the azimuthal asymmetry $\Delta_k$ were carried out for different thicknesses $t_k$ of the scatterer II.

**TABLE I**

| ρ, τ | $\bar{E}$, kev | Element | $\Delta = 200\,(I_1-I_2)/(I_1+I_2)$ for t, mg/cm² Au | | | | | $\bar{\Delta}_0$ | $\bar{\Delta}_{corr}$ | $\bar{\Delta}_{th}$ | $\langle\sigma\rangle/(v/c)$ |
|---|---|---|---|---|---|---|---|---|---|---|---|
| | | | 1.97 | 0.92 | 0.39 | 0.24 | 0.12 | | | | |
| $\rho_1 = 1.0$ mg/cm² Al; $\tau_1 = 3.0$ mg/cm² Au | 145 | Tm 0.8 mg/cm² | | | 22.0±0.9 | 25.3±1.2 | 28.0±2.0 | 33.0±1.3 | 36.6±1.8 | 36.2 | 1.01±0.05 |
| | 140 | Sm 1.1 mg/cm² | | | | 23.1±1.4 | 29.0±1.6 | 32.0±1.5 | 35.7±1.9 | 35.7 | 1.00±0.05 |
| | 130 | Lu 0.3 mg/cm² | | | 15.1±1.9 | 19.0±2.6 | 22.8±2.8 | 26.3±1.9 | 29.6±2.3 | 30.5 | 0.97±0.07 |
| | 130 | Sr + Y 1.5 mg/cm² | | | | 31.6±3.7 | 24.8±2.8 | 33.8±3.6 | 37.3±4.1 | 35.0 | 1.06±0.12 |
| $\rho_2 = 2.6$ mg/cm² Al; $\tau_2 = 6.0$ mg/cm² Au | 260 | Tm | | 22.1±0.9 | 29.8±1.2 | 31.5±1.5 | 33.8±2.8 | 37.5±1.1 | 39.2±1.5 | 42.3 | 0.93±0.04 |
| | 250 | Sm | | | | 31.9±2.5 | | 37.6±3.8 | 39.3±3.8 | 42.1 | 0.93±0.09 |
| | 200 | Lu | 14.0±1.3 | 23.7±2.0 | 30.0±4.0 | | | 42.5±4.4 | 44.4±4.6 | 42.7 | 1.04±0.11 |
| | 260 | Re 0.1 mg/cm² | | 23.3±2.6 | 38.0±4.8 | | | 43.2±4.4 | 45.2±4.6 | 42.7 | 1.06±0.11 |
| | 220 | Sr + Y | | 21.4±1.7 | 35.7±1.8 | 33.6±4.8 | | 41.5±2.5 | 43.4±2.7 | 42.1 | 1.03±0.06 |
| $\rho_3 = 5.2$ Al; $\tau_3 = 13$ Au | 390 | Tm | 18.1±1.3 | 25.7±0.9 | 30.4±1.3 | 33.5±2.8 | | 37.5±1.6 | 41.2±1.9 | 40.6 | 1.01±0.05 |
| | 360 | Sm | | | 30.6±2.3 | | | 36.7±3.0 | 40.4±3.3 | 40.6 | 1.00±0.08 |
| | 390 | Au 0.2 mg/cm² | | | 23.8±2.6 | 36.8±4.0 | | 33.6±2.5 | 36.8±2.9 | 36.6 | 1.00±0.08 |
| | 450 | Sr + Y | 15.5±1.2 | 23.1±1.5 | 28.0±2.0 | | | 33.0±3.1 | 36.2±3.4 | 38.3 | 0.94±0.09 |
| $\rho_4 = 10.4$ Al; $\tau_4 = 20.0$ Au | 520 | Tm | 16.2±2.8 | 27.4±2.1 | 32.0±2.9 | | | 35.2±2.1 | 36.6±2.2 | 37.0 | 0.99±0.06 |
| | 520 | Au | 18.2±2.1 | 24.2±2.6 | 30.0±5.8 | | | 33.3±2.8 | 34.5±2.9 | 35.9 | 0.96±0.08 |
| | 650 | Sr + Y | 18.9±2.2 | 23.6±2.7 | | | | 30.7±3.1 | 31.8±3.2 | 32.5 | 0.98±0.10 |

*Notation: $\rho$ – thickness of the filter between the Geiger counters, $\tau$ – thickness of the transforming scatterer I, $\bar{E}$ – mean electron energy, t – thickness of the analyzing scatterer II, $\bar{\Delta}$ – mean of the measured values of the azimuthal asymmetry, $\bar{\Delta}_0$ – value of the azimuthal asymmetry extrapolated to zero thickness of scatterer II, $\Delta_{corr}$ – azimuthal asymmetry with account of corrections for: 1 – instrumental asymmetry $\Delta_n$, 2 – back scattering of electrons, $\delta_\mu$, 3 – electrons scattered from the walls of the apparatus, $\delta_\eta$; $\Delta_{th}$ is the expected value of the azimuthal asymmetry for electrons, with polarization equal to –v/c, $\langle\sigma\rangle/(-v/c)$ – longitudinal polarization of the electrons in units –v/c.

In all, three series of measurements were carried out: series I, on apparatus 1; series II, on apparatus 2; and series III, on apparatus 2, but using two counter telescopes. The azimuthal asymmetry of the scattering was defined as the mean value of the azimuthal asymmetry in each of the telescopes. These conditions excluded errors due to possible intensity changes in the electron beam during the period of measurement, and also due to possible inhomogeneity in the thickness of the scatterer II.

## Reproducibility of the Measurement Results

In order to rely on the statistical accuracy of the results of a measurement, it is necessary to ascertain that no deviations of nonstatistical character are present. This can be established by the

degree of reproducibility and by the spread of results about the mean value in repeated experiments.

In all, 80 measurements of azimuthal asymmetry in the scattering were carried out, of which 53 were repeated measurements. In spite of the fact that the measurements were carried out on different sets of apparatus, the overwhelming part of the measurements were in agreement with each other. Out of 53 repeated experiments, 40 coincided, within the limits of experimental error, with the mean values, 10 were more than one standard error away, 2 were more than 2 standard errors, and 1, more than three standard errors. The 3 final measurements were not taken into account in the calculation of the mean values in the repeated measurements. The mean values of the measured magnitude of azimuthal asymmetry are given in Table I.

**Control Experiments**

(a) The instrumental asymmetry was measured by scattering electrons from an aluminum foil in place of scatterer II. The instrumental asymmetry could be calculated from this, since the azimuthal asymmetry in scattering in aluminum is about 12 times smaller than that in the same thickness of gold.[3] As the measurements showed, the magnitude of instrumental asymmetry $\Delta_n$ did not depend on the source material, but only on the energy of the electrons and was found to be between 0 and $-2$.

(b) The intensity of the electron flux reflected from the aluminum backing of the source and from the plexiglass container was measured experimentally for a point source covered on top by a small screen, which the electrons could not penetrate, so that direct radiation couldn't penetrate into the counter. The relative fraction of reflected electrons, depending on the electron energy, lay in the interval 0.5 to 1.5%. Since the reflected electrons have essentially a polarization opposite to that of the direct electrons, the corrections $\delta_\mu$ in the measured values of the azimuthal asymmetry should be somewhat larger, 0.8 to 2.0%.

(c) In analogous fashion, the proportion of electrons scattered from the diaphragm and walls of the apparatus lying close to the source was measured. The corrections $\delta_\eta$ to the azimuthal asymmetry in this case were 3.5 to 1.9%.

(d) Measurement of the azimuthal asymmetry for various azimuthal angles showed that at all energies, the effect was maximum in the plane perpendicular to the plane of turning of the trajectory of the electron after scattering in scatterer I.

(e) K. A. Ter-Martirosian has shown that in the multiple scattering of electrons in a light material through angle $\psi$, the spin of the electrons is turned through an angle*

$$\varphi = \psi\,[1 - \sqrt{1-(v/c)^2}]\,.$$

Measurements with Al and Au of equivalent thicknesses as transforming scatterers showed that the effect of azimuthal asymmetry did not depend on the material of scatterer I.

(f) In the case of measurements with $Au^{198}$ as a source, the Geiger counters were subjected to strong $\gamma$-radiation. Measurements of the polarization of electrons were carried out in the 300 to 700 kev energy interval where, between the counters connected in coincidence, there was placed an aluminum filter sufficiently thick so that the electrons from the $\gamma$-rays ($E_\gamma \sim 400$ kev) were practically excluded from giving coincidences in the counters.† The resolution of the counter system was sufficiently high and the background of chance coincidences did not exceed 0.5 to 1.0%. The proportion of photo- and Compton electrons produced by the $\gamma$-rays was measured in an experiment where the source was shielded by a plexiglass screen which could not be penetrated by electrons, but was transparent to $\gamma$-rays. The correction to the magnitude of azimuthal asymmetry caused by this effect constituted $\sim 2\%$.

*For an elementary act of scattering, it is easy to obtain in the Born approximation the angle of turning of the spin in the plane of the scattering. It is given by

$$\sin\varphi_i = \frac{1-(1-\sqrt{1-v^2/c^2})\sin^2(\psi_i/2)}{1-(v^2/c^2)\sin^2(\psi_i/2)}\,(1-\sqrt{1-v^2/c^2})\sin\frac{\psi_i}{2}\,,$$

which for $\psi_i \ll 1$ goes into the formula $\varphi_i = (1-\sqrt{1-(v/c)^2}\,\psi_i$ which is that for the turning of the spin in an electric capacitor.

Terms of order $(Z/137)\,\psi_i/2$, which correct for the use of Born approximation, are small if $\psi_i \ll 1$, even for heavy nuclei. The above formula is therefore expected to be valid for small angles (multiple scattering) even in the case of scattering from heavy nuclei. If multiple scattering takes place in one plane, then it is evident that for the resulting angles $\varphi = \sum_i \varphi_i$, $\psi = \sum_i \psi_i$ the relation given in the text is valid.

†Note added in proof (April 17, 1958). For lower-energy electrons (145 and 260 kev) from $Au^{198}$, the dependence of the longitudinal polarization on the thickness of scatterer II (see below) turned out to be inconsistent with the results of measurements for the remaining elements. In view of the ambiguity in determining the magnitudes of longitudinal polarizations, the data on $Au^{198}$ for electrons of these energies was excluded.

### Determination of the Extrapolated Values of the Azimuthal Asymmetry Corresponding to Single Scattering

In order to determine the polarization of the electrons it is necessary to know the value of the azimuthal asymmetry which corresponds to single scattering of the electrons. In the actual measurements involving electrons scattered in scatterers of finite thicknesses, a fraction of electrons is always muliply scattered, and this leads to a shift in the value of the azimuthal asymmetry. However, this correction can be obtained, experimentally.

As Artsimovich[4] has shown, the scattering intensity of electrons of a given energy in a scattterer of thickness $t$ is

$$I(t) = I_0[t + \gamma(E)t^2] = I'(t) + I''(t),$$

where $I'(t) = I_0 t$ is the intensity of single scattering and $I''(t) = I_0\gamma(t) = I_0\gamma(E)t^2$ is the intensity of multiple scattering. In the scattering of polarized electrons, one would observe an azimuthal asymmetry:

$$\Delta(t) = 200\,\frac{I_1'(t) - I_2'(t) + I_1''(t) - I_2''(t)}{I_1'(t) + I_2'(t) + I_1''(t) + I_2''(t)}$$

$$= 200\,\frac{I_1'(t) - I_2'(t) + I_1''(t) - I_2''(t)}{I'(t) + I''(t)} = 200\,\frac{I_1'(t) - I_2'(t)}{I'(t)[1 + (I''(t)/I'(t))]}$$

$$+ 200\,\frac{I_1''(t) - I_2''(t)}{I''(t)[1 + (I'(t)/I''(t))]} = \frac{\Delta_0}{1 + \gamma(E)t} + \frac{\xi(E)\Delta_0\gamma(E)t}{1 + \gamma(E)t}$$

$$\approx \Delta_0\,\frac{1}{1 + \gamma(E)[1 - \xi(E)]t} = \Delta_0\,\frac{1}{1 + \alpha(E)t},$$

where $\Delta_0 = 200(I_1' - I_2')/I'$ is the azimuthal asymmetry in a single scattering and $\xi(E)\Delta_0$ is the azimuthal asymmetry in multiple scattering, with $\xi(E) >> 1$.

Thus, we find that the inverse of $\Delta_k$, the azimuthal asymmetry for scattering of electrons of a given energy $E$ in scatterers II of various thicknesses $t_k$, is linearly connected with $t_k$:

$$\frac{1}{\Delta_k} = \frac{1}{\Delta_0} + \frac{\alpha(E)t_k}{\Delta_0}.$$

The value of $\overline{\alpha(E)}$ as a function of energy (Fig. 2) has been determined using all the data available for different materials and for different energies. The extrapolated values of $\overline{\Delta}_0$ for each material and each energy were found from the formula

$$\overline{\Delta}_0 = \sum_k \Delta_k[1 + \overline{\alpha(E)}\,t_k]/k$$

subject to the condition $\overline{\alpha(E)}\,t_k > 1$. The extrapolated values $\overline{\Delta}_{corr}$ with account of the corrections indicated above ($\Delta_n$, $\delta_\mu$, $\delta_\eta$) are given in

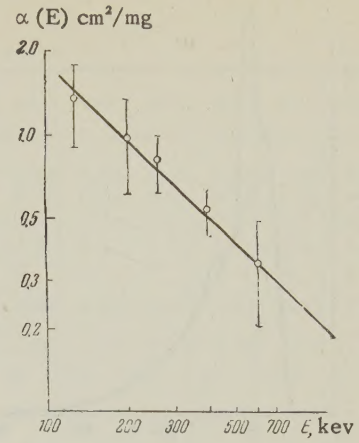


FIG. 2

Table I ($\overline{\Delta}_{corr} = \delta_\mu\delta_\eta \sum_k (\Delta_k - \Delta_n)[1 + \overline{\alpha(E)}\,t_k]/k$).

From these data it can be seen that the measured values of the azimuthal asymmetry change only very slowly in a wide energy interval. This means that, in the given apparatus, a precise knowledge of the form of the electron energy spectrum is not necessary for determination of the degree of polarization of the electrons.

### Energy Spectra of the Electrons

The energy spectrum of electrons undergoing double scattering and registered in the counter can be represented in the form $n = f_0\sigma(\tau)\sigma_0\varphi(\rho)$, where $f_0$ is the electron spectrum at the source, $\sigma(\tau)$ is the cross section for multiple scattering through an angle of 90°, in scatterer I of thickness $\tau$, $\sigma_0$ is the cross section for single scattering through an angle of 112.5°, and $\varphi(\rho)$ is the proportion of electrons going through the aluminum filter of thickness $\rho$. The quantities $\sigma_0$ and $\varphi(\rho)$ are known.[3,5] The energy spectra of electrons from $Au^{198}$ (maximum energy 950 kev) and $Lu^{177}$ (maximum energy 500 kev) undergoing double scattering through an angle of ~90° was carefully measured with a spectrometer. The measurements were carried out for $Lu^{177}$ with scatterers I of thickness 3 mg/cm² and 6 mg/cm² Au, and for $Au^{198}$ with 3 mg/cm² Au, 6 mg/cm² Au, 13 mg/cm² Au, and 20 mg/cm² Au. The electron spectra of Lu and Au contain conversion lines with electron energies 98 and 137 kev for Lu and 325 and ~400 kev for Au. In view of the fact that conversion electrons are unpolarized, their fraction in the spectrum must be taken into account in determining the expected scattered asymmetry. It turned out that this fraction could be determined, knowing the form of the $\beta$-spectrum of electrons

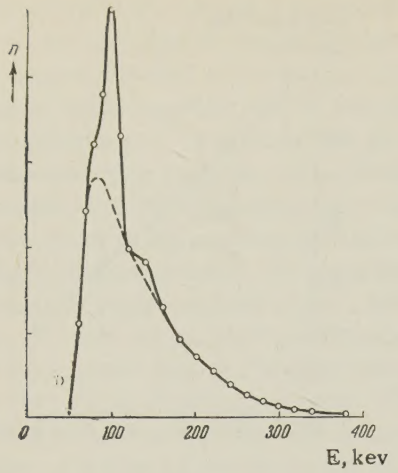


a

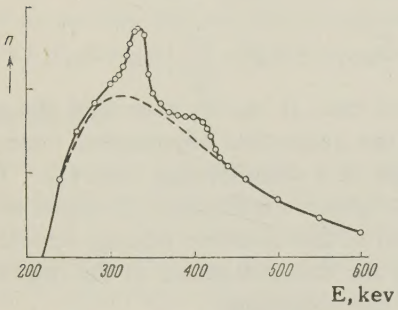


b

FIG. 3. Spectra of electrons undergoing double scattering and producing coincidences in the Geiger counters: a – $Lu^{177}$, $E_1$ = 130 kev, $\rho_1$ = 1.0 mg/cm² Al, $\tau_1$ = 3.0 mg/cm² Au; b – $\overline{E}_3$ = 390 kev, $\rho_3$ = 5.2 mg/cm² Al, $\tau_3$ = 13 mg/cm² Au. Solid lines and o – conversion electron spectra; dashed lines – spectra without conversion electrons.

undergoing multiple scattering, directly from experiment. By way of illustration, spectra of electrons from $Lu^{177}$ ($\overline{E}_1$ = 130 kev) and $Au^{198}$ ($\overline{E}_2$ = 390 kev), after multiple scattering through an angle of 90° and single scattering through 112.5°, are shown in Figs. 3a, b. The spectra of electrons from $Re^{186}$, $Tm^{170}$, and $Sm^{153}$ practically coincide with the spectrum of $Au^{198}$ without conversion electrons. The electron spectra of $Sr^{90} + Y^{90}$ were calculated.

## Calculation of the Expected Value of Azimuthal Asymmetry

In order to determine the degree of longitudinal polarization of electrons in fractions of $-v/c$, it is necessary to compare the measured values with the expected values $\Delta_{th}$ of the azimuthal asymmetry in the scattering of electrons having longitudinal polarization equal to $-v/c$. Their energy spectrum n is known.

$$\overline{\Delta}_{\text{th}_i} = \frac{\sum_j \Delta_{\text{th}_j} n'_{ji}}{\sum_j n_{ji}} = 200\,\frac{v}{c}\,\frac{\sum_j S_j \langle\sigma_\perp\rangle_{ji} \delta_{\Gamma j} \delta_{Zj} \delta_{sj} (1 - \theta_j^2/2)\, n'_{ji}}{\sum_j n_{ji}},$$

where $n'_{ji}$ is the distribution of electrons with respect to energy, excepting conversion electrons, in the i-th experiment, characterized by a filter of thickness $\rho_i$ between counters and a thickness $\tau_i$ of the transforming scatterer I; $n_{ji}$ is the same, but including conversion electrons; $S_j$ is the value of the azimuthal asymmetry in the scattering of electrons of energy $E_j$, completely polarized in the transverse direction by mercury (Z = 80), taken from the table of Sherman;[3] $\delta_{\Gamma j}$ is the correction for the finite solid angle of the apparatus; $\delta_{Zj}$ is the correction to the tabulated value $S_j$, connected with the fact that the scattering took place on gold (Z = 79); $\delta_{sj}$ is the correction connected with the screening effect. (This correction was obtained by extrapolating the results of Mohr and Tassie[6] to the energies of interest; the calculation of these corrections was carried out by K. A. Ter-Martirosian.) $(1 - \theta_j^2/2)$ is the depolarization in the source; $\theta^2$ is the mean square angle for multiple scattering.[5] The latter quantities are given in Table II as functions of the energy. $\langle\sigma_\perp\rangle_{ji}$ is the component of spin perpendicular to the trajectory of the electron of energy $E_j$, undergoing a 90° deflection as a result of multiple scattering in scatterer I of thickness $\tau_i$. The value of this projection was calculated, using the Monte-Carlo method, by G. Adel' son-Vel' skii, A. Birzgal, and A. Kronrod on an electronic computer.* It contains a correction for depolarization of the electrons in scatterer I.

The depolarization of the electrons is due to the turning of the spin in the electric field of the nucleus. In the case where the multiple scattering of the electrons takes place in the plane formed by the initial and final trajectories of the electron in the scatterer, there is no depolarization (if only the trajectory is not a closed loop). If, in the process of scattering, the electron goes out of this plane, then there is depolarization.

Calculations showed that the turning of the spin of the electron in multiple scattering by the Coulomb field was about 5% less than the amount of turning obtained from the "condenser" formula

$$\varphi = \psi(1 - \sqrt{1 - v^2/c^2}).$$

*The authors are grateful to I. S. Bruk, director of the Laboratory of Control Machines of the Academy of Sciences, U.S.S.R., for the possibility of carrying out these calculations.

**TABLE II**

| $E$, kev | 70 | 100 | 150 | 200 | 250 | 300 | 400 | 500 | 600 | 700 | 800 | 900 | 1000 | 1200 | 1400 |
|---|---|---|---|---|---|---|---|---|---|---|---|---|---|---|---|
| $v/c$ | 0.48 | 0.55 | 0.63 | 0.69 | 0.74 | 0.77 | 0.83 | 0.86 | 0.89 | 0.91 | 0.92 | 0.93 | 0.94 | 0.95 | 0.96 |
| S | 0.38 | 0.39 | 0.40 | 0.41 | 0.40 | 0.39 | 0.37 | 0.35 | 0.33 | 0.31 | 0,29 | 0.28 | 0.25 | 0,22 | 0.17 |
| $100\ (\delta_r - 1)$ | —5.2 | —5.5 | —6.2 | —6.8 | —7.3 | —7.7 | —8.1 | —7.8 | —7.1 | —6.2 | —5.1 | —4.1 | —3.0 | —2.0 | —1.5 |
| $100\ (\delta_Z - 1)$ | —2.3 | —2.3 | —2.2 | —2.1 | —2.0 | —1.9 | —1.8 | —1.7 | —1.7 | —1.6 | —1.5 | —1.5 | —1.4 | —1.4 | —1.4 |
| $100\ (\delta_9 - 1)$ | —11.0 | —6.5 | —1.3 | 0 | 0 | 0 | 0 | 0 | 0 | 0 | 0 | 0 | 0 | 0 | 0 |
| $\left(1-\frac{\theta^2}{2}\right)_{Sr+Y}$ | 0.89 | 0.94 | 0.97 | 0.98 | 0.99 | 0.99 | 1.00 | 1.00 | 1.00 | 1.00 | 1.00 | 1.00 | 1.00 | 1.00 | 1.00 |
| $\left(1-\frac{\theta^2}{2}\right)_{Tm}$ | 0.93 | 0.97 | 0.98 | 0.99 | 0.99 | 1.00 | 1.00 | 1.00 | 1.00 | 1.00 | 1.00 | 1.00 | 1.00 | 1.00 | 1.00 |
| $(\Delta_{th})_{Sr+Y}$ | 25 | 33 | 41 | 44 | 44 | 44 | 40 | 37 | 34 | 30 | 28 | 25 | 23 | 17 | 12 |
| $(\Delta_{th})_{Tm,\ Sm}$ | 26 | 34 | 41 | 45 | 44 | 44 | 40 | 37 | 34 | 30 | 28 | 25 | 23 | 17 | 12 |
| $(\Delta_{th})_{Lu,\ Re}$ | 28 | 35 | 42 | 45 | 44 | 44 | 40 | 37 | 34 | 30 | 28 | 25 | 23 | 17 | 12 |

A family of $<\sigma_\perp>_{ji}$ vs. energy curves for electrons scattered by scatterers I of various thicknesses $\tau_i$ is given in Fig. 4.

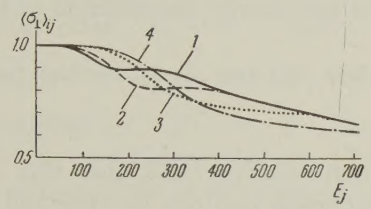


FIG. 4. Dependence of the perpendicular component of spin on the energy of the electron which is deflected by 90° from the original direction as a result of multiple scattering in scatterer I of thickness: 1 – $\tau_1$ = 3.0 mg/cm² Au; 2 – $\tau_2$ = 6.0 mg/cm² Au; 3 – $\tau_3$ = 13.0 mg/cm² Au; 4 – $\tau_4$ = 20.0 mg/cm² Au.

The details of the calculations will be published separately by their authors.

The expected values of the azimuthal asymmetry $\bar{\Delta}_{th}$ for Tm, Lu, Re, Sm, Au, and Sr+Y for various energies are given in Table I.

## 3. DISCUSSION OF RESULTS

The values of the longitudinal polarizations in units of $-v/c$

$$\langle\sigma\rangle_i/(-v/c) = \bar{\Delta}_{corr_i}/\bar{\Delta}_{th_i}$$

are given, as functions of energy, in Fig. 5. From these data it can be seen that the polarization of the electrons $<\sigma>_i/(-v/c)$ for all elements studied does not depend upon energy within the limits of error. In Table III are listed the values $<\bar{\sigma}>_i/(-v/c)$, averaged over energy, for the elements studied. In Fig. 6 are given the mean values $<\bar{\sigma}>_i/(-v/c)$, as functions of the energy, for the Coulomb transitions in comparison with the polarization of electrons of Sr+Y.

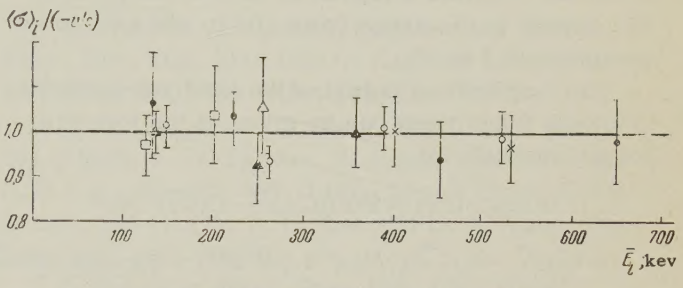


FIG. 5. Longitudinal polarization of the electrons $<\sigma>_i/(-v/c)$ for various energies: ● – $Sr^{90} + Y^{90}$, ○ – $Tm^{170}$, ▲ – $Sm^{158}$, □ – $Lu^{177}$, × – $Au^{198}$, △ – $Re^{186}$.

**TABLE III.** Values of the longitudinal electron polarization $<\bar{\sigma}>/(-v/c)$ averaged over energy. (Statistical errors are shown. The errors, taking into account systematic ones, are shown in parentheses.)

| Element | $<\sigma>/(-v/c)$ |
|---|---|
| $Sr^{90}+Y^{90}$ | 0.99±0.037 (±0.05) |
| $Tm^{170}$ | 0.98±0.015 (±0.03) |
| $Sm^{153}$ | 0.98±0.037 (±0.05) |
| $Lu^{177}$ | 1.00±0.058 (±0.06) |
| $Re^{186}$ | 1.06±0.106 (±0.11) |
| $Au^{198}$ | 0.97±0.055 (±0.06) |
| Average | 0.98±0.01 (±0.03) |

From all of these data it is possible to draw the following conclusions.

1. The longitudinal polarization of the electrons of all measured elements is the same within an accuracy of 2 to 11%. (The errors given do not include systematic errors, which are the same for all elements.)

2. The longitudinal polarization of the electrons

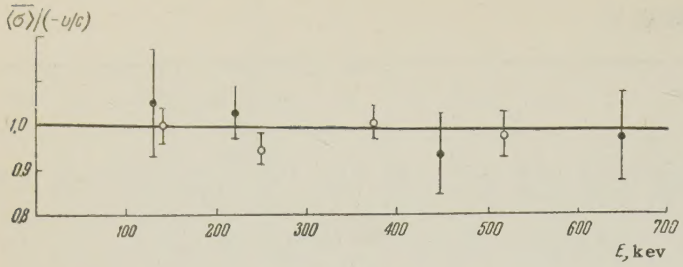


FIG. 6. Energy dependence of the longitudinal polarization of the electrons $\langle\sigma\rangle/(-v/c)$ for Coulomb transitions: ● – $Sr^{90} + Y^{90}$, ○ – Coulomb transitions.

is equal to $-v/c$ to within an accuracy of $\sim 3\%$ for the mean value over all elements.

3. The longitudinal polarization of the electrons from the Coulomb transitions does not depend on the energy in the range from 100 to 600 kev, to an accuracy of 4 to 7%.

The longitudinal polarization for first-forbidden Coulomb transitions can be given in the following form (see Ref. 7):

$$W\langle\sigma_E\rangle/(v/c) = 2\mathrm{Re}\{(C_S C_S'^* - C_V C_V'^*)|M_F|^2 + (C_T C_T'^* - C_A C_A'^*)(|M_{GT}|^2 + |M'_{GT}|^2) + \frac{Z}{137E(v/c)}[(C_T C_V'^* + C_T' C_V^*) M_F^* M_{GT} - (C_S C_A'^* + C_S' C_A^*) M_F M_{GT}^*]\}$$
$$+ 2\mathrm{Im}\{-(C_T C_S'^* - C_A C_V'^*) M_F^* M_{GT} + (C_T'^* C_S - C_A'^* C_V) \times M_F M_{GT}^* + \frac{Z}{137E(v/c)}[(C_S C_V'^* + C_S' C_V^*)|M_F|^2 + (C_T C_A'^* + C_T' C_A^*)(|M_{GT}|^2 + |M'_{GT}|^2)]\};$$
$$W = (|C_T|^2 + |C_T'|^2 + |C_A|^2 + |C_A'|^2)(|M_{GT}|^2 + |M'_{GT}|^2) + (|C_S|^2 + |C_S'|^2 + |C_V|^2 + |C_V'|^2)|M_F|^2 + 2\mathrm{Im}[(C_T^* C_S + C_T'^* C_S' + C_A^* C_V + C_A'^* C_V') M_F M_{GT}^*] + (2\gamma_1/E)\,\mathrm{Re}[(C_S C_V^* + C_S' C_V'^*)|M_F|^2 + (C_T C_A^* + C_T' C_A'^*) \times (|M_{GT}|^2 + |M'_{GT}|^2)] + (2\gamma_1/E)\,\mathrm{Im}[(C_S C_A^* + C_S' C_A'^*) \times M_F M_{GT}^* - (C_T C_V^* + C_T' C_V'^*) M_F^* M_{GT}],$$

where E is the total electron energy in units of $mc^2$; $\gamma_1 = \sqrt{1-(Z/137)^2}$; S, V, T, A, in the subscripts refer to the scalar, vector, tensor and axial-vector variants, respectively.

From the data of our experiment we can set the expression $\langle\sigma_E\rangle$ equal to $-v/c$, independently of energy and independently of the magnitudes of the matrix elements (in so far as the polarization of electrons for the measured elements is the same, and different elements should have different matrix elements). We then obtain 9 equations for the coupling constants

$$|C_S + C_S'|^2 + |C_V - C_V'|^2 = 0, \quad (1)$$
$$|C_T + C_T'|^2 + |C_A - C_A'|^2 = 0, \quad (2)$$
$$\mathrm{Re}(C_S C_V'^* + C_S' C_V'^*) = 0, \quad (3)$$
$$\mathrm{Re}(C_T C_A'^* + C_T' C_A'^*) = 0, \quad (4)$$
$$\mathrm{Im}(C_S C_V'^* + C_S' C_V^*) = 0, \quad (5)$$
$$\mathrm{Im}(C_T C_A'^* + C_T' C_A^*) = 0, \quad (6)$$
$$\mathrm{Im}(C_T C_S'^* - C_S C_T'^* + C_V C_A'^* - C_A C_V'^* + C_T C_S^* - C_T'^* C_S + C_A C_V^* - C_A'^* C_V') = 0, \quad (7)$$
$$\mathrm{Im}(-C_S C_A^* - C_S' C_A'^* + C_T C_V^* + C_T' C_V'^*) = 0, \quad (8)$$
$$\mathrm{Re}(-C_S C_A'^* - C_S' C_A^* + C_T C_V'^* + C_T' C_V^*) = 0. \quad (9)$$

It is easy to see that the maximum number of relations, which can be determined from experiments with measurement of longitudinal polarization of electrons from unpolarized nuclei, have been obtained. Equations (3) and (4) were obtained earlier (absence of Fierz terms). Equations (1) and (2) were obtained in experiments measuring longitudinal polarization (accuracy of measurement 10 – 20%) in allowed and other transitions without measurement of the energy dependence of the polarization.[8]

From Eqs. (1) and (2) follow the relations

$$C_S = -C_S', \quad C_T = -C_T', \quad C_V = C_V', \quad C_A = C_A'.$$

If these relations are valid, then this is the maximum information that can be obtained from the magnitude of longitudinal polarization of electrons from unpolarized nuclei. In fact, all equations are identically zero with this choice. However, the accuracy with which these relations can be obtained from Eqs. (1) and (2) is not high. In fact, let us take, for simplicity, only the tensor variant. Then we have $|C_T + C_T'|^2 = \delta(|C_T|^2 + |C_T'|^2)$, where $\delta$ is the difference of the polarization of the electrons from $-v/c$. In our case this represents an accuracy of measurement equal to 0.03.

In first approximation $C_T = -C_T'(1+\alpha)$, $\alpha^2 = 2\delta = 0.06$; $\alpha \approx 0.25$. Thus, the relation between the constants can be determined from Eqs. (1) and (2) to an accuracy no better than 20 to 30%.

We consider another possibility. Let us assume that the absolute values of C and C′ are equal:

$$|C| = |C'|$$

and $C = -C'$; this indeed occurs in the model of the two component neutrino, but $|C_V|$ and $|C_A|$ are small, for otherwise there would be a contradiction to known experiments.[8] We assume, for simplicity, that there are only the tensor and vector variants of interaction. Then, for the allowed transitions, which lead only to Eqs. (1) and (2), we obtain

$$\frac{-|C_T|^2|M_{GT}|^2 + |C_V|^2|M_F|^2}{|C_T|^2|M_{GT}|^2 + |C_V|^2|M_F|^2} = -\frac{1-|\rho|^2}{1+|\rho|^2}$$

$$\approx (1-2|\rho|^2) = -1+\delta,$$

$$|\rho| = \frac{|C_V||M_F|}{|C_T||M_{GT}|} \approx \sqrt{\frac{\delta}{2}} \approx 0.2,$$

where $\delta = 0.1$ is the best accuracy with which, at the present time, the polarization of electrons for the allowed transitions has been measured.

The energy dependence of the polarization of electrons in Coulomb transitions, as already stated, is also given by Eqs. (3) to (9). It turns out that the Eqs. (3) to (6), (8), and (9) are very sensitive to the relations between the constants. From these equations it follows that the following relations should hold between the coupling constants

$$C_T/C_T' = C_S'/C_S = -C_V/C_V' = -C_A'/C_A,$$

and from the fact that the polarization of electrons, for example, from $Sr^{90}$ (pure Gamow-Teller transition) is negative, and of the positrons from $Cl^{34}$ (pure Fermi transition) is positive,[9] it follows, under the assumption $|C| = |C'|$, that

$$C_T = -C_T', \quad C_S = -C_S', \qquad C_V = C_V', \quad C_A = C_A',$$

with high accuracy.

In fact, in this same example, we have for the polarization of electrons in the case of a Coulomb transition

$$\frac{-|C_T|^2|M_{GT}|^2+|C_V|^2|M_F|^2 \pm [2Z/137E\,(v/c)]\,C_T C_V^* |M_{GT}||M_F|}{|C_T|^2|M_{GT}|^2+|C_V|^2|M_F|^2}$$

$$= -\frac{1-|\rho|^2 \pm [2Z/137E\,(v/c)]\,\rho}{1+|\rho|^2} \approx -1 \pm 1.5\rho = -1+\delta.$$

from which

$$\rho = C_V^*|M_F|/C_T^*|M_{GT}| \approx 0.03, \text{where} Z/137 \approx 0.5,$$
$$E \approx 1.2, \quad v/c \approx 0.6; \quad \delta \approx 0.05.$$

Since the polarization of electrons of all of the Coulomb transitions measured by us is the same, and it is unlikely that the ratio $|M_F|/|M_{GT}|$ is small for all of these, then it follows that the fraction of the vector variant, for which $C_V = -C_V'$ is very small. This is also valid with respect to the axial-vector variant of the interaction.

On the basis of the above, we come to the conclusion that the results of measurement of the longitudinal polarization of electrons in Coulomb transitions as a function of the energy, which we obtained in this work, indicate that most probably the following relations between the coupling constants in $\beta$-decay are satisfied

$$C_T = -C_T', \quad C_S = -C_S', \quad C_V = C_V', \quad C_A = C_A',$$

which correspond to the model of the two-component electron. If the vector and axial-vector constants or scalar and tensor constants are pair-wise equal to zero, the present experiment agrees also with the model of the two-component neutrino.

The authors would like to express their gratitude to K. A. Ter-Martirosian, who calculated several corrections in the present experiments and took an active part in discussion of the results obtained; to G. Adel' son-Bel' skii, A. P. Birzgal, A. S. Kronrod, and V. B. Berestetskii, who calculated the correction for depolarization of the electrons in multiple scattering; to E. F. Tret' iakov and G. I. Grishuk, who measured the spectrum of $Au^{198}$ and $Lu^{177}$ electrons scattered through an angle of $\sim 90°$ by multiple scattering; to M. P. Anikina, who prepared the $\beta$-active sources, and to B. L. Ioffe and A. P. Rudik for discussions.

[1] Wu, Ambler, Hayward, Hoppes, and Hudson, Phys. Rev. **105**, 1413 (1957); Garwin, Lederman, and Weinrich, Phys. Rev. **105**, 1415 (1957).

[2] T. D. Lee and C. N. Yang, Phys. Rev. **104**, 254 (1956); L. D. Landau, J. Exptl. Theoret. Phys. (U.S.S.R.) **32**, 405, 407 (1957), Soviet Phys. JETP **5**, 336, 337 (1957); T. D. Lee and C. N. Yang, Phys. Rev. **105**, 1671 (1957).

[3] N. Sherman, Phys. Rev. **103**, 1601 (1956).

[4] L. A. Artsimovich, J. Exptl. Theoret. Phys. (U.S.S.R.) **9**, 927 (1939).

[5] Ed. E. Segrè, Experimental Nuclear Physics (Russ. Transl.), IIL, M., 1955, Vol. 1, p. 239-241, 247-257. [Wiley, N. Y., 1953].

[6] C. B. O. Mohr and L. F. Tassie, Proc. Phys. Soc. **A67**, 711 (1954).

[7] V. B. Berestetskii, B. L. Ioffe, A. P. Rudik, K. A. Ter-Martirosian, Phys. Rev. **111**, 522 (1958).

[8] Frauenfelder, Bobone, Von Goeler, Levine, Lewis, Peacock, Rossi, and De Pasquali, Phys. Rev. **106**, 386 (1957); Alikhanov, Eliseev, Liubimov, and Ershler, J. Exptl. Theoret. Phys. (U.S.S.R.) **32**, 1344 (1957), Soviet Phys. JETP **5**, 1097 (1957); Vishnevskii, Grigor' ev, Ergakov, Nikitin, Pushkin, and Trebukhovskii, Nucl. Phys. **4**, 271 (1957); Cavanagh et al., Nucl. Phys. **5**, 11 (1958); Koller, Schwarzschild, Vise, and Wu, Phys. Rev., (in press;) Boehm, Novey, Barnes, and Stech, Phys. Rev. **108**, 1497 (1957).

[9] Deutsch, Gittelman, Bauer, Grodzins, and Sunyar, Phys. Rev. **107**, 1733 (1957).

Translated by G. E. Brown
223

# *RARE-EARTH FISSION PRODUCTS IN URANIUM FISSION INDUCED BY 660-Mev PROTONS*

F. I. PAVLOTSKAIA and A. K. LAVRUKHINA

Institute for Geochemistry and Analytic Chemistry, Academy of Sciences, U.S.S.R.

Submitted to JETP editor October 31, 1957

J. Exptl. Theoret. Phys. (U.S.S.R.) **34**, 1058-1069 (May, 1958)

Data on fission products in the rare-earth region for uranium bombarded by 660-Mev protons have been obtained by a radiochemical method. The total rare-earth yield was $0.7 \times 10^{-24}$ cm$^2$, corresponding to approximately 20% of the total fragment yield. In the case of highly asymmetric fission the yields of stable nuclides and nuclides with neutron excess or deficiency are found to be approximately the same. The maximum yield in the light rare earths is for stable nuclides whereas the heavy rare-earth fission products are predominantly neutron-deficient. It is shown that the distribution of rare-earth elements found in nature cannot be explained by fission of heavy nuclei by high-energy particles.

IN an earlier work[1] we have indicated that the rare-earth region is a very convenient one for investigations designed to delineate the role of nuclear reactions in the creation of the elements. The importance of establishing basic trends in the production of rare-earth elements has been pointed out several times by A. P. Vinogradov in connection with some fundamental geochemical problems. For these reasons the study of uranium fission, which is a basic nuclear reaction in the heavy-element region, can not be complete without a knowledge of the yield of the rare-earth elements, which comprise a considerable fraction of the fission products. The yields of these nuclides can then be used to investigate the nature of highly asymmetric fission, a phenomenon which has not been studied to any great extent at the present time.

The rare-earth elements, furthermore lie in an interesting nuclear region in which shell-structure effects become important. It is well-known that there is a marked change in nuclear properties in the rare-earth region: for example, the excitation energy of the first collective level, the quadrupole moment, the isotopic shift of spectral lines, nuclear deformation, and so on. Some of the first members of this group have a shell containing 82 neutrons and gadolinium has a clearly defined sub-shell of 64 protons. All these factors provide motivation for examining the effects of nuclear structure on the fission process.

The determination of the yields of radioactive isotopes of the rare-earths formed in uranium fission induced by high-energy protons involves the solution of two basic problems in method: the effective separation of the elements of this group and a determination of the yields of nuclides which decay by K-capture. The problem of separating the elements has been discussed in Ref. 1; in the present paper main emphasis has been given to the development of a method for determining the yields of the nuclides indicated above.

## METHOD OF INVESTIGATION

A target of spectrally pure metallic uranium, 0.5 to 1 gram in weight, was first irradiated in

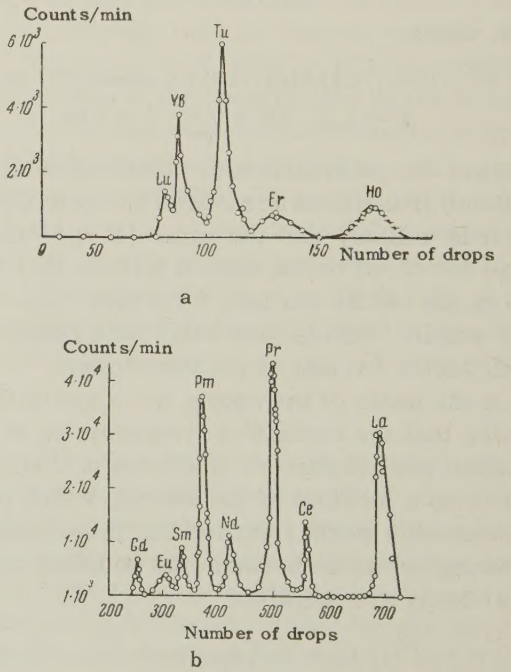


FIG. 1. Separation of rare-earth elements by a 3.6 percent solution of ammonium lactate (pH = 3.4 to 3.5): a – heavy rare earths, b – light rare earths.

TABLE I

| Isotope | Decay mode | Observed half-life | Observed energy | | Production cross section $10^{-27}$ cm² |
|---|---|---|---|---|---|
| | | | β-radiation, Mev | γ-radiation, kev | |
| $_{57}$La 140 | β⁻,γ | 38.5 hours | 1.418 | 110; 165; 350; 480; 875; 1590 | 13.3 |
| $_{58}$Ce 134 | K | 3.5 days | | 510 | 0.6 |
| 139 | K,γ | 145 „ | | | |
| 141 | β⁻,γ | 29 „ | 0.437 | 145 | |
| 143 | β⁻,γ | 35 hours | 1.2 | 38; 62; 114; 305; 635; 755 | 17.3 |
| 145 | β⁻,γ | 2.5 „ | | | |
| $_{59}$Pr 137 | β+ | 1.4 „ | | | |
| 139 | K,β+,γ | 4.2 „ | | | |
| 142 | β⁻,γ | 20 „ | | | 6.3 |
| 143 | β⁻ | 13.5 days | 1.0 | | 24.3 |
| 145 | β⁻ | 4.5 hours | | | |
| $_{60}$Nd 139 | K,β+,γ | 5.75 „ | 2.3 | | 1.3 |
| 140 | K | 3.4 days | | | 3 |
| 147 | β⁻,γ | 10.5 „ | 0.9 | 39; 90; 190; 263; 310; 410; 520; 730 | 4.9 |
| $_{61}$Pm 148 | β⁻,γ | 42.5 „ | | | 5.6 |
| 149 | β⁻,γ | 54 hours | 0.92 | | 14 |
| 150 | β⁻,γ | 4 „ | | | |
| 151 | β⁻,γ | 26.5 „ | 0.92 | 41; 65; 100; 135; 160; 175; 230; 290; 350—385 | 8.3 |
| $_{62}$Sm 145 | K,γ | 113.3 days | | | |
| 153 | β⁻,γ | 48 hours | 0.6 | 40; 70; 100; 155 | 6 |
| 156 | β⁻ | 10 „ | | | 2.6 |
| $_{63}$Eu 146 | K | 36 „ | | 35; 155; 237 | 0.36 |
| 148 | K,γ | 50.5 days | | | |
| 152 | K,β⁻,γ | 9.5 hours | 1.65 | | 3 |
| 156 | β⁻,γ | 14.6 days | 0.59 | | 2 |
| 157 | β⁻,γ | 15.4 „ | | | |
| $_{64}$Gd 149 | α,K(?) | 10.3 „ | | | 0.9 |
| 159 | β⁻,γ | 17 hours | | | 0.075 |
| $_{67}$Ho 161 | K,γ | 3.5 „ | | | |
| 162 | K,β⁻,γ | 65 days | | | |
| 163 | K,γ | 7.5 „ | | | |
| 166 | β⁻,γ | 28 hours | 1.62; 0.3 | | 0.6 |
| $_{68}$Er 160 | K | 28 „ | | 47; 88; 136; 180—190; 1500 | 0.1 |
| 169 | β⁻ | 9.5 days | 0.35 | | 0.4 |
| 171 | β⁻,γ | 7 hours | | | 0.012 |
| $_{69}$Tu 165 | K,γ | 33 „ | | | 0.3 |
| 166 | K,γ | 8 „ | | | 1.1 |
| 167 | K,γ | 9.3 days | | | 1.6 |
| 170 | β⁻,γ | 140 „ | 0.66 | | 0.09 |
| $_{70}$Yb 166 | K | 36 hours | | 52—55; 84; 115; 185 | 0.5 |
| 169 | K,γ | 28.5 days | | | 0.1 |
| 175 | β⁻,γ | 106 hours | | | 0.02 |
| $_{71}$Lu 170 | K,γ | 1.75 days | | | 0.4 |
| 172 | K,γ | 6.75 „ | 1.2 | | 0.13 |
| 174 | K,β⁻,γ | 175 „ | | | |
| 176 m | β⁻,γ | 3 hours | | | 0.01 |
| 177 | β⁻,γ | 6.75 days | 0.5 | | 0.02 |

the internal 660-Mev proton beam at the synchrocyclotron of the Laboratory for Nuclear Problems of the Joint Institute for Nuclear Research for 1 to 1.5 hours and then dissolved in several milliliters of concentrated hydrochloric acid containing 10 to 20 mg of cerium and hydrogen peroxide. The solution was passed through a column (0.8 × 10 cm) of Dowex — 1 — X8 in equilibrium with concentrated hydrochloric acid and the resin was washed by double the volume of this acid. The solution from the column was diluted to 0.5 to 3 N in HCl and again passed through the column with the anionoid in equilibrium with hydrochloric acid of corresponding concentration. The cerium hydroxide was then precipitated by ammonia and the precipitate dissolved in concentrated nitric acid; 1 to 2 mg of zirconium in the form of the oxychloride was added and the zirconium iodate was precipitated for sep-

aration of the thorium radioisotopes. The cerium hydroxide and zirconium iodate were precipitated several times. Double precipitation of the hydroxide and oxalate of cerium from the filtrate was carried out. The last precipitate of the hydroxide was dissolved in hydrochloric acid and from a 0.3 N hydrochloric acid solution the absorption of the rare-earth elements was carried out in Dowex $-50$ in $NH_4$ form. The cationoid was carried to the upper part of the column ($25 \times 0.2$) cm, filled with the cationoid in equilibrium with the eluent. The elution was carried out with a 3.6 percent solution of ammonium lactate (pH = 3.4 to 3.5) at the rate of one drop per minute (approximately 0.03 ml/min) at 75 to 80°C. Each drop was deposited on a thin sheet of tracing cloth, dried under a lamp, and then measured for activity. In Fig. 1 are shown the elution curves for radioisotopes of the rare-earths formed in uranium fission induced by 660-Mev protons. The yttrium peak is not shown on the figure.

Each peak of this chromatogram was identified individually by half-life of each form of radiation ($\beta^-$, $\beta^+$, $\gamma$ and x-ray) and by energy of the $\beta$- and $\gamma$-radiations. The measurements were carried out with both a magnetic analyzer with two end counters and with an ordinary apparatus with an end tube. The energy of the $\beta$-radiation was determined by absorption in aluminum while the energy of the $\gamma$-radiation was determined with a luminescent $\gamma$-spectrometer. The identification of the isotopes by $\gamma$-radiation consisted of taking the $\gamma$-spectra for each peak of the chromatogram and determining the half-life for the individual lines of the spectrum.[2]

## DETERMINATION OF YIELDS OF RARE-EARTH NUCLIDES

The determination of the yields of $\beta^-$- and $\beta^+$-active nuclides was carried out by the method described earlier.[3] The determination of the yields of nuclides which decay by means of K-capture, however, was difficult because of the absence of any reliable method. Several methods are described in the literature. Murin and his colleagues[4,5] have used a method described by Wilkinson[6] for determining the absolute yields of K-capture radioisotopes of the heavy elements; this method is based on measurements of the different radiations using an argon counter and successive absorption in aluminum, beryllium, and lead foils. The counting was carried out using the x-ray K-radiation at low efficiency (0.5 to 1 percent).

In measuring the yields of the K-capture radioisotopes of elements of intermediate atomic weight, Mekhedov and Kurchatov[7] have used a magnetic analyzer with two end counters. The x-ray radiation and the $\gamma$-radiation were recorded by a krypton-filled end counter which had a high counting efficiency for the x-ray K-radiation for nuclei of intermediate atomic weight (50 to 70%). A shortcoming of both methods is the fact that it is necessary to take account of the decay scheme, the ratio of L/K captures, and soft $\gamma$-radiation; furthermore, the geometry is poor in the second method.

Recently, Malysheva[8] has proposed a method for measuring the K-capture decay isotopes of mercury, bismuth, and gold formed in the disintegration of bismuth by 660-Mev protons. This method makes use of the secondary x-ray L-radiation, using a standard argon counter. In this case the detection efficiency for the L-radiation of the heavy elements is 20% while the efficiency for the K-radiation is 0.5 to 1%. The latter can be neglected and account need be taken of K-capture only in the secondary L-radiation (with an error of less than 10%). The advantage of this method is the high counting efficiency for the L-radiation as compared with K-radiation and the fact that

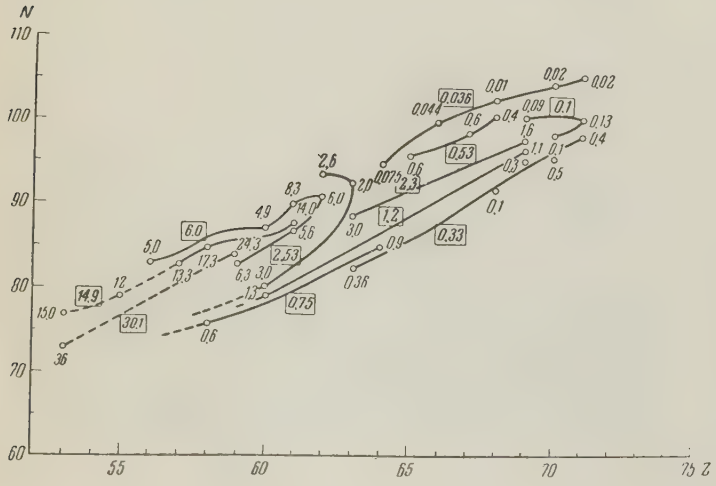


FIG. 2. Yields of radioisotopes of the rare earths.

there is no need to take account of soft $\gamma$-radiation nor of the exact ratio of L/K captures. The last factor is especially important since this quantity is either completely unknown or not known reliably in the majority of neutron-deficient nuclides.

The first method was found to be poorly suited to the present work so that the second was used. For this purpose we have determined the counting efficiency for x-ray K- and L-radiation for the rare-earth elements. The appropriate calculations show that the counting efficiency for K-radiation is 1% for cerium, less than 1% for lutetium and 95 and 55% respectively for L-radiation in these elements. In the remaining rare-earth elements the efficiency lies between these values. The magnitudes which have been obtained indicate a very high counting efficiency for L-radiation in the rare-earth elements and consequently indicate the convenience of the method described above for determining the yields of K-capture isotopes of these elements.

In the activity measurements made with the ordinary end counter corrections were introduced for the following factors.

1. Absorption of L-radiation in the counter window, in the air gap, and in the sample covering (16% for cerium and 22% for lutetium).

2. Absorption of the L-radiation in the ineffective counter volume which was (20% for cerium and 6% for lutetium).

3. L-fluorescent yield (using the data reported by Burhop[9]).

In addition, using the known decay schemes a correction was introduced for the fraction of x-ray K-radiation due to electronic conversion. The error in the determination of the yields was 40 to 50% for the known decay schemes and less than 100% for the unknown decay schemes.

## DISCUSSION OF THE RESULTS

The yields obtained for the radioisotopes of the rare-earths are shown in Table I. Using a method of interpolation and extrapolation which has been described in detail in Refs. 10 to 12, the yields of a large number of stable and unidentified radioactive isotopes were plotted on an isotope chart in N — Z coordinates (Fig. 2). Using the experimental and interpolated data, distribution curves were plotted for the yield of the various elements as a function of mass number; these are shown in Fig. 3. These curves, which are more or less dome-shaped, make it possible to extrapolate the yields of the other isotopes of the rare-earth elements. The yields of the isotopes of dysprosium and terbium, which could not be separated in a pure radioactive state, were determined in this way. This situation arises because of the fact that these two elements are eluted after yttrium, which has a very large yield, and the yttrium peak on the chromatogram tends to mask the dysoprosium and holmium peaks. The superposition of peaks, in separating various amounts of rare-earth elements, has been noted earlier.[13,14]

From the complete pattern of experimental and interpolated data it is possible to obtain a complete picture of the rare-earth fission products for uranium fissioned by 660-Mev protons and to estimate the fraction of stable nuclides and nuclides with neutron deficiency and neutron excess.

It follows from Table II that the yields for all three types of nuclides are approximately the same. Thus stable nuclides comprise 38.6%, the neutron-excess nuclides 36.6%, and the neutron-deficient nuclides 24.8% of the total rare-earth yield. However there is a marked dependence of the yield of these various types of nuclides on atomic number. For example, yields of stable nuclides and neutron-excess nuclides are reduced as Z increases whereas the yield of neutron-deficient isotopes increases as Z is increased. The dependence on atomic number is also observed in the position of maximum-yield nuclides with respect to the line of nuclear stability drawn through nuclides of greatest abundance in nature (solid line in Fig. 4). It is apparent from this figure that a line drawn through nuclides of maximum yield (dashed line) tends to move in the direction of neutron-deficient nuclei as the atomic number of the rare-earth element increases.

The data in Table II indicate a significant reduction in the total yield of rare-earth nuclides with increasing Z. The nature of this dependence is shown in the curve in Fig. 5, from which it is apparent that the yield of lutetium isotopes (Z = 71) is 150 times smaller than the yield of cerium isotopes (Z = 58). The smooth behavior of this curve is disturbed beyond gadolinium (Z = 64); this effect may be interpreted as an indication of the clearly defined sub-shell of 64 protons.

The total yield of rare-earth nuclides is $0.7 \times 10^{-24}$ cm$^2$, about 20% of the yields of all fission products of uranium if it is assumed that the total fission cross section for uranium is $1.65 \times 10^{-24}$ cm$^2$ (Ref. 11) and that this cross section does not change greatly as the energy is increased from 480 Mev to 660 Mev. The ratio of these quantities can be used to estimate the fraction of asymmetric fission which leads to the formation of elements with Z = 30 — 37 and Z = 57 — 71 (40% of the

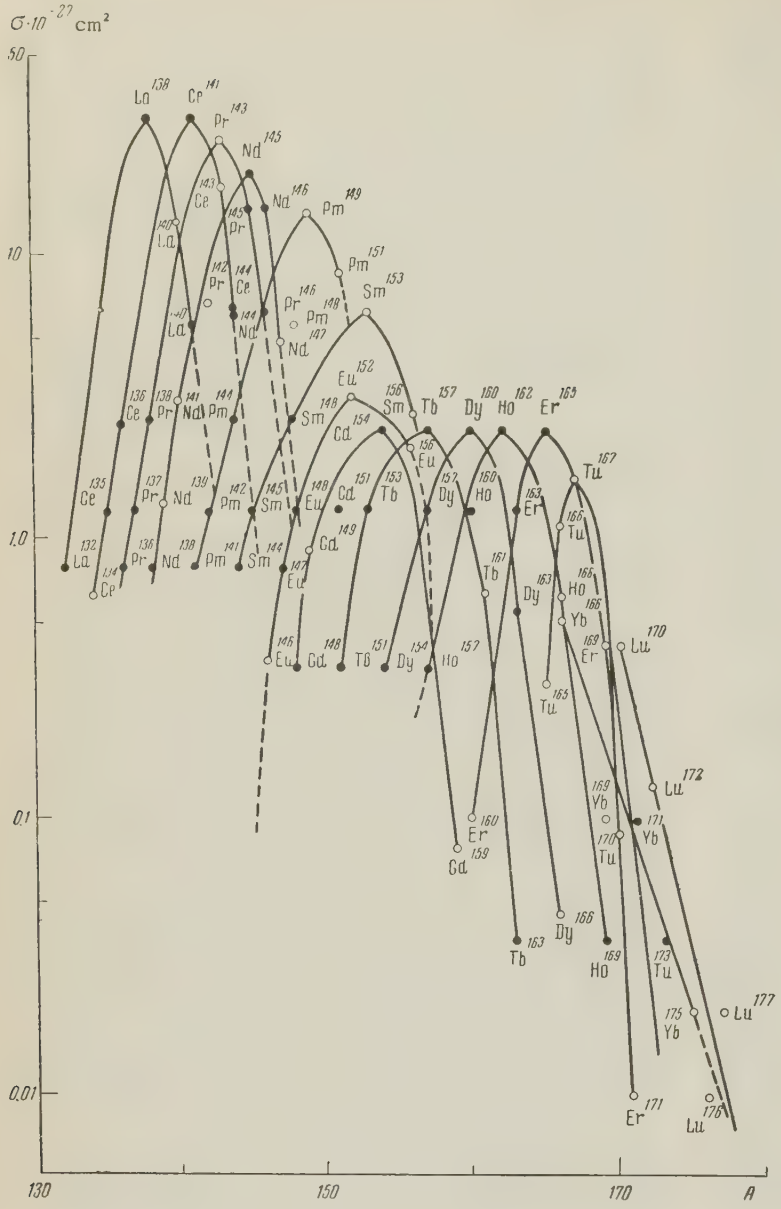


FIG. 3. Yields of rare-earth isotopes as a function of mass number. ● – interpolated data. ○ – experimental data.

TABLE II

| Z | Element | Total isotopic yield, $10^{-27}$ cm² | Stable isotope yield | | Yield of neutron-excess isotopes | | Yield of neutron-deficient isotopes | |
|---|---|---|---|---|---|---|---|---|
| | | | $10^{-27}$ cm² | % | $10^{-27}$ cm² | % | $10^{-27}$ cm² | % |
| 57 | La | 131.1 | 53.1 | 40.5 | 21.2 | 16.2 | 56.8 | 43.3 |
| 58 | Ce | 137.5 | 59.5 | 43.3 | 55.9 | 40.6 | 22.1 | 16.0 |
| 59 | Pr | 107.0 | 15.5 | 14.5 | 71.5 | 66.7 | 20.0 | 18.8 |
| 60 | Nd | 88.0 | 72.2 | 82.0 | 5.5 | 6.3 | 10.2 | 11.7 |
| 61 | Pm | 65.3 | — | — | 54.9 | 84.0 | 10.4 | 16.0 |
| 62 | Sm | 44.0 | 23.7 | 53.8 | 17.6 | 40.0 | 2.7 | 6.2 |
| 63 | Eu | 23.2 | 5.7 | 24.5 | 13.3 | 57.5 | 4.2 | 18.0 |
| 64 | Gd | 14.3 | 8.4 | 58.9 | 0.08 | 0.5 | 5.8 | 40.6 |
| 65 | Tb | 15.3 | 1.5 | 9.8 | 1.8 | 11.8 | 12.0 | 78.4 |
| 66 | Dy | 13.0 | 8.7 | 67.0 | 0.2 | 1.4 | 4.1 | 31.6 |
| 67 | Ho | 13.0 | 1.1 | 8.5 | 2.6 | 20.0 | 9.3 | 71.5 |
| 68 | Er | 11.6 | 7.3 | 62.8 | 0.4 | 3.4 | 3.9 | 33.8 |
| 69 | Tu | 4.9 | 0.6 | 12.0 | 0.2 | 4.1 | 4.1 | 83.9 |
| 70 | Yb | 1.6 | 0.6 | 37.3 | 0.03 | 1.9 | 1.0 | 60.8 |
| 71 | Lu | 0.9 | 0.03 | 3.3 | 0.03 | 3.3 | 0.8 | 93.4 |
| Total | | 670.7 | 257.9 | 38.5 | 245.3 | 36.5 | 167.6 | 25.0 |

total fission cross section for uranium).

The data on yields for all isotopes of the rare-earth elements can also be used to establish the distribution of isotopes over mass number (Fig. 3) and the distributions of isobars over atomic number (Fig. 6). These distributions are of the nature of identical dome-shaped curves for all elements, excluding the heavy elements, in which all nuclides are in the right-hand branch. In the distribution of isobars over Z there are noticeable deviations in the region Z = 64. This gives an indication of the role of shell structure in the fission process.

The information on yields for all rare-earth nuclides supplements the picture of uranium fission given earlier[11] and gives a detailed picture of the heavy fragments of highly asymmetric fission. Among these, neutron-deficient nuclides comprise a large fraction. This is in contrast with the light fission fragments, for which there is a clear predominance of neutron-excess nuclei. The quantity $Z_p$ (the most probable charge for a given mass number) found from the isotope chart (Fig. 2), just as in Ref. 11, departs significantly from the line of nuclear stability and tends to be on the neutron-deficient side. This departure increases with increasing mass number (Fig. 7). On this figure the line of nuclear stability is characterized by a dependence of the quantity $Z_A$ (the most probable charge of the stable nuclei) on mass number.[15] In light fission fragments[11] $Z_p$ lies in the immediate vicinity of the line of nuclear stability. It should be noted that in uranium fission by slow neutrons the quantity $Z_p(n)$ lies in the region of high neutron excess.[15] The ratio n/p for heavy fragments is 1.3 to 1.51 whereas it is much lower for light fragments (1.14 to 1.4). The maximum is found for a nuclide with ratio n/p = 1.42 to 1.47. The considerable difference in the magnitude of n/p in the heavy fragments and light fragments indicates that uranium fission does not involve an emission mechanism since this mechanism is characterized by the same value of n/p for all fission fragments.

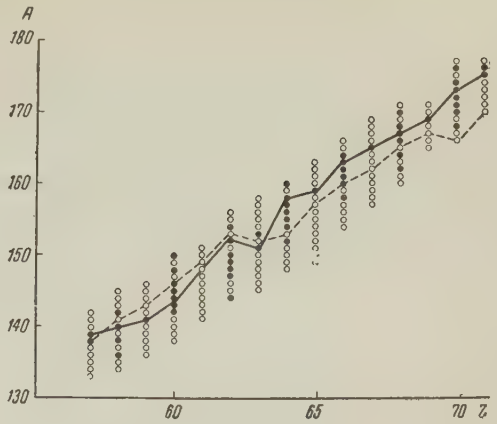


FIG. 4. Products of uranium fission in the rare-earth region. ● – stable isotopes, o – radioactive isotopes.

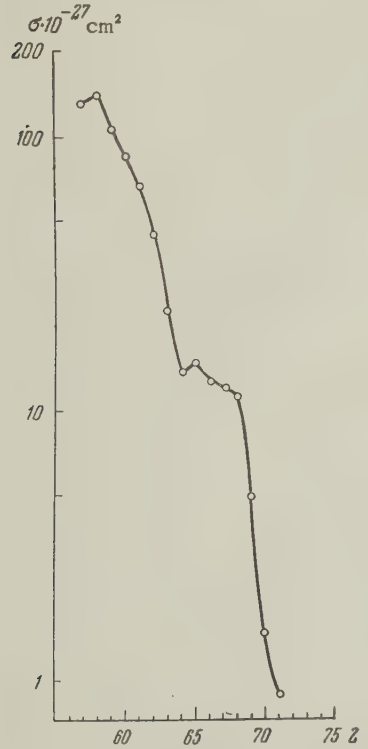


FIG. 5

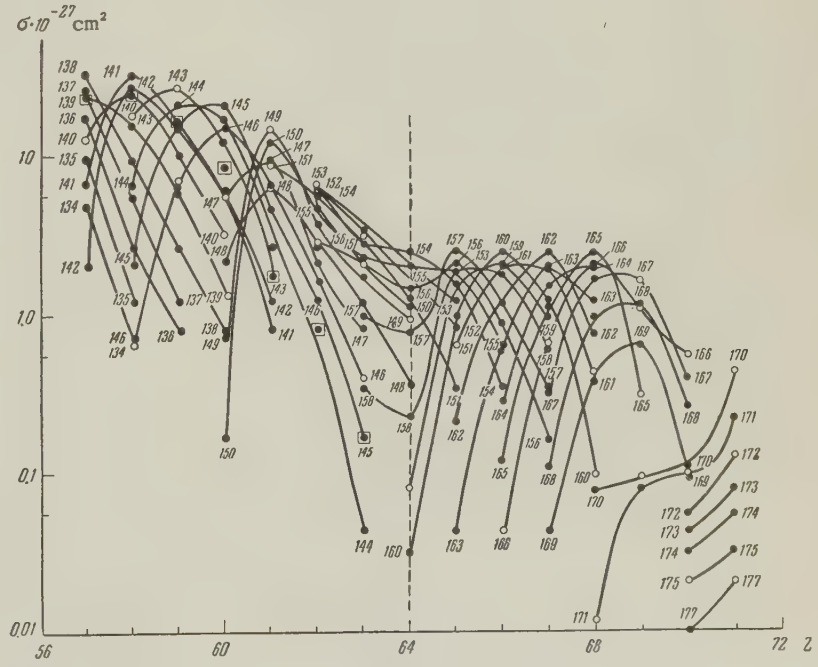


FIG. 6

FIG. 5. Total yields for isotopes of the rare earths as a function of atomic number.
FIG. 6. Distribution of isobars as a function of atomic number. ● – interpolated data, o – experimental data.

## EFFECT OF NUCLEAR STRUCTURE

At the present time the effect of shell structure on the slow-neutron process in heavy nuclei is more or less established. The asymmetric nature of slow-neutron fission in these nuclei is considered by many authors[16,17] to be the result of the shell structure of the fissioning nucleus.

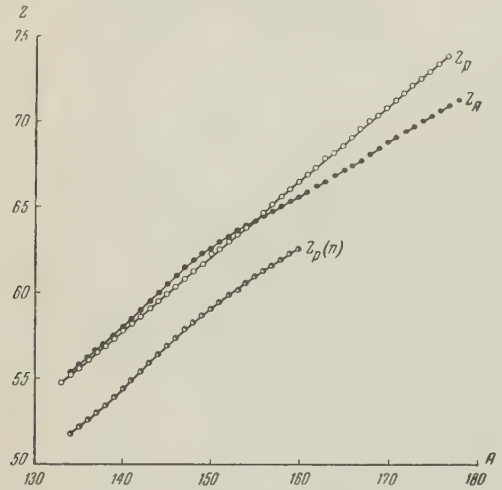


FIG. 7. The quantities $Z_A$ and $Z_p$ as functions of mass number in the rare-earth region for uranium fission induced by 660-Mev protons.

The fine structure in the yield curve for fission products of $U^{233}$, $U^{235}$, $U^{238}$, and $Pu^{239}$ close to mass 133, 100, 84 and others,[18-25] which is observed by mass-spectroscope and radiochemical techniques, may be also be basically attributed to shell structure effects in nuclei with 50 and 82 neutrons. This fine structure is not observed at high bombarding-particle energies, however. This is an indication that the excitation energy of the fissioning nucleus is high. Thus the shell structure of the nucleus becomes apparent only in the last stage of the evaporation process, when the excitation of the nucleus has become small.

A consideration of the yield distribution curves for isobars as a function of atomic number, shown in Fig. 6, shows a marked departure in the behavior of these curves in the region of gadolinium ($Z = 64$). There is a marked reduction in yield for isobars containing 64 protons, corresponding to the filling of a sub-shell.[26] In isobars having a closed neutron shell at $N = 82$ there is also a very marked reduction in yield as the sub-shell of 64 protons is approached (in Fig. 6 isobars with $N = 82$ are enclosed in squares). In general these isotopes are not observed in gadolinium. In Fig. 5, as has already been indicated, there is a sharp break in the behavior of the distribution curve for the total yields of the rare-earth elements in the vicinity of gadolinium ($Z = 64$).

The reduction in yield which is observed for nuclei having a closed sub-shell can be explained from the point of view of the statistical model. It is well-known that nuclei with closed sub-shells have an abnormally low level density. In Ref. 27 it has been shown that in the evaporation process the yield of nuclei with low-level densities is considerably smaller than those with high-level densities.

The fact that uranium fission induced by 660-Mev protons exhibits nuclear shell structure effects, as in the neutron evaporation process, is evidence of the evaporation of neutrons from excited fragments. This finding tends to support the viewpoint that uranium fission is due to a barrier mechanism.

## ORIGIN OF THE RARE-EARTH ELEMENTS

Any explanation of the origin of the elements must provide an understanding of the nuclear abundances found in nature. To delineate the role of the fission process in the formation of the rare-earth elements we have compared the natural abundances of stable isotopes of these elements

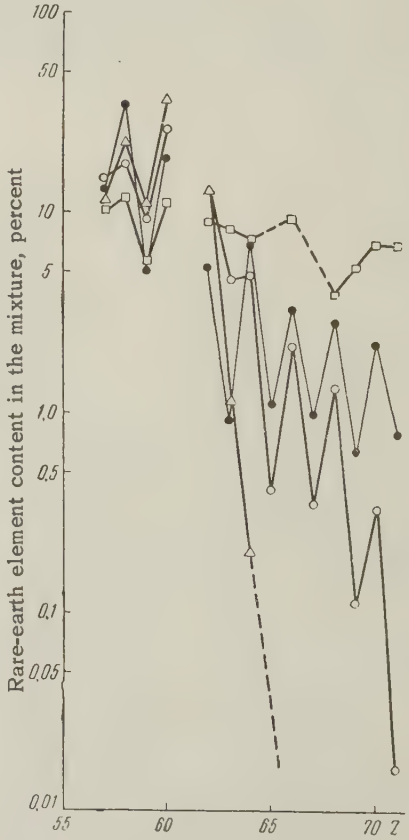


FIG. 8. Rare-earth content as a function of atomic number: ● – in the earth's crust, □ – in the sun and in certain stars, △ – in products of thermal-neutron fission of $U^{235}$, ○ – in products of fission of natural uranium by 660-Mev protons.

TABLE III

| Element | Mass number | Content, percent: In the earth's crust[28] | Content, percent: In fission products |
|---|---|---|---|
| $_{57}$La | 138 | 0.089 | 34.1 |
| | 139 | 99.911 | 65.9 |
| $_{58}$Ce | 136 | 0.193 | 2.5 |
| | 138 | 0.25 | 12.1 |
| | 140 | 88.48 | 55.9 |
| | 142 | 11.07 | 29.5 |
| $_{59}$Pr | 141 | 100.0 | 100.0 |
| $_{60}$Nd | 142 | 27.13 | 8.6 |
| | 143 | 12.2 | 30.7 |
| | 144 | 23.87 | 24.65 |
| | 145 | 8.3 | 22.9 |
| | 146 | 17.18 | 11.9 |
| | 148 | 5.72 | 1.16 |
| | 150 | 5.6 | 0.09 |
| $_{62}$Sm | 144 | 3.16 | 1.05 |
| | 147 | 15.07 | 22.2 |
| | 148 | 11.27 | 12.4 |
| | 149 | 13.84 | 27.35 |
| | 150 | 7.47 | 21.5 |
| | 152 | 26.63 | 8.4 |
| | 154 | 22.53 | 7.1 |
| $_{63}$Eu | 151 | 47.77 | 58.6 |
| | 153 | 52.23 | 41.4 |
| $_{64}$Gd | 152 | 0.2 | 12.9 |
| | 154 | 2.15 | 17.1 |
| $_{64}$Gd | 155 | 14.73 | 26.3 |
| | 156 | 20.47 | 21.2 |
| | 157 | 15.68 | 13.5 |
| | 158 | 24.87 | 6.4 |
| | 160 | 21.90 | 2.6 |
| $_{65}$Tb | 159 | 100.0 | 100.0 |
| $_{66}$Dy | 156 | 0.0524 | 1.05 |
| | 158 | 0.0902 | 22.2 |
| | 160 | 2.294 | 12.4 |
| | 161 | 18.88 | 27.35 |
| | 162 | 25.53 | 21.5 |
| | 163 | 24.97 | 8.4 |
| | 164 | 28.18 | 7.1 |
| $_{67}$Ho | 165 | 100.0 | 100.0 |
| $_{68}$Er | 162 | 0.136 | 4.9 |
| | 164 | 1.56 | 24.2 |
| | 166 | 33.41 | 30.2 |
| | 167 | 22.94 | 24.6 |
| | 168 | 27.07 | 15.6 |
| | 170 | 14.88 | 0.5 |
| $_{69}$Tu | 169 | 100.0 | 100.0 |
| $_{70}$Yb | 168 | 0.140 | 15.0 |
| | 170 | 3.03 | 35.9 |
| | 171 | 14.31 | 25.8 |
| | 172 | 21.82 | 10.7 |
| | 173 | 16.13 | 7.0 |
| | 174 | 31.84 | 4.8 |
| | 176 | 12.73 | 0.8 |
| $_{71}$Lu | 175 | 97.40 | 83.3 |
| | 176 | 2.60 | 16.7 |

with the fission yields. In Fig. 8 are shown the rare-earth abundances in the earth's crust,[28] in the sun, and in various types of stars,[29] together with yield curves for the stable isotopes of these elements in thermal-neutron $U^{235}$ fission[30,31] and fission of natural uranium by 660-Mev protons. The yields and abundances are plotted as functions of atomic number (the percentage of each element in the rare-earth totals). In estimating the stable-isotope yields the contribution of radioactive chains has been taken into account.

An examination of these curves shows the same increase in the even elements both in nature and in the uranium fission products. The relative positions of these curves in Fig. 8 indicates that the rare-earth abundances observed in nature can not be explained by thermal-neutron fission of $U^{235}$, since elements heavier than terbium are not formed in this process. The fission-product curve for 660-Mev proton-induced fission in uranium differs from the natural abundance curve only in the region of heavy rare-earth elements. If it is assumed, however, that the heavy rare-earth yield increases with increasing proton energy at cosmic-ray energy, one would expect completely similar behavior for the two curves. For this reason there would seem to be little basis for the proposal that the abundances of the rare-earth elements observed in nature can be explained by fission of heavy heavy nuclei by high-energy protons.

A detailed examination of the data in Table III indicates a noticeable difference between the isotopic composition of the even rare-earth elements found in nature and those produced in the fission process. In fission due to fast protons there is a clear preponderance of light isotopes as compared with the natural distribution, especially for heavy elements. This preponderance of light isotopes becomes more pronounced as the proton energy is increased. Thus, fission of heavy elements by high-energy particles would not seem to be a likely mechanism for explaining the abundances of the rare-earth elements which are presently observed in nature.

The authors wish to express their gratitude to A. A. Sorokin and L. S. Novikov for the $\gamma$-radiation identifications and for computing the yields of some of the isotopes which decay by electron capture.

[1] F. I. Pavlotskaia and A. K. Lavrukhina, Атомная энергия (Atomic Energy) No. 5, 115 (1956).

[2] Sorokin, Novikov and Pavlotskaia, Заводск. лабор. (Industrial Laboratory) (In Press).

[3] Vinogradov et al., Conference of the Academy

of Sciences, U.S.S.R. on the Peaceful Use of Atomic Energy (Sessions of the Division of Chemical Sci.), 97, Academy of Sciences Press, Moscow, 1955.

[4] Nikitin et al., Тр. Радиевого ин-та (Trans. Radium Institute) **7**, 101 (1956).

[5] Murin, Preobrazhenskii and Titov, Izv. Akad. Nauk SSSR, Div. of Chem. Sci. No. 4, 577 (1955).

[6] G. Wilkinson, Phys. Rev. **75**, 1019 (1949).

[7] Kurchatov et al., Conference of the Academy of Sciences, U.S.S.R. on the Peaceful Use of Atomic Energy (Sessions of the Division of Chemical Sci.), 178, Academy of Sciences Press, Moscow, 1955.

[8] T. V. Malyshev, Атомная энергия (Atomic Energy) 1957 (In Press).

[9] E. Burhop, The Auger Effect, Cambridge, 1952.

[10] A. K. Lavrukhina, Doctoral Dissertation, Institute for Geochemistry, Academy of Sciences U.S.S.R., Moscow, 1955.

[11] A. K. Lavrukhina and L. D. Krasavina, Атомная энергия (Atomic Energy) No. 2, 27 (1957).

[12] Lavrukhina et al., Атомная энергия (Atomic Energy) No. 2, 345 (1957).

[13] Lavrukhina et al., Журн. неорг. хим. (Journal of Inorganic Chemistry) **3**, 82 (1958).

[14] W. E. Nervik, J. Phys. Chem. **59**, 690 (1955).

[15] Glendenin, Coryell, and Edwards, Radiochemical Studies:- The Fission Products, McGraw-Hill, New York, 1951, Vol. I, p. 489.

[16] R. D. Hill, Phys. Rev. **98**, 1272 (1955).

[17] M. D. Curie, Compt rend. **235**, 1286 (1952); **237**, 1401 (1953).

[18] H. G. Thode, Trans. Roy. Soc. Can. **45**, 3 (1951).

[19] R. K. Wanless and H. G. Thode, Canad. J. Phys. **31**, 517 (1953); **33**, 541 (1955).

[20] W. H. Fleming and H. G. Thode, Phys. Rev. **92**, 378 (1953).

[21] Glendenin, et al., Phys. Rev. **84**, 860 (1951).

[22] Krizhanskii et al., Атомная энергия (Atomic Energy) No. 2, 276 (1957).

[23] Petruska, Thode, and Tomlinson, Canad. J. Phys. **33**, 693 (1955).

[24] Petruska, Melaika, and Tomlinson, Canad. J. Phys. **33**, 640 (1955).

[25] Melaika, Parker, et al., Canad. J. Chem. **33**, 830 (1955).

[26] L. K. Peker and L. A. Sliv, Abstracts of Reports for the Seventh Annual Conference on Nuclear Spectroscopy, Leningrad, January 25 — 31, 1957, p. 16, Academy of Sciences Press, 1957.

[27] J. W. Meadows, Phys. Rev. **91**, 885 (1953).

[28] A. A. Saukov, Геохимия (Geochemistry) GIGL, 1951, p. 52.

[29] H. Russell, Astrophys. J. **70**, 11 (1929).

[30] Inghram, Hayden and Hess, Phys. Rev. **79**, 271 (1950).

[31] Gorshkov et al., J. Atomic Energy, No. 3, 11 (1957).

Translated by H. Lashinsky
224

# *ELECTRICAL RESISTANCE OF IRON, COPPER AND NICKEL – COPPER ALLOYS AT LOW TEMPERATURES*

E. I. KONDORSKII, O. S. GALKINA and L. A. CHERNIKOVA

Moscow State University

Submitted to JETP editor November 6, 1957

J. Exptl. Theoret. Phys. (U.S.S.R.) **35**, 1070-1076 (May, 1958)

The electrical resistance of nickel, iron, and copper alloys of nickel, containing up to 25% copper, have been measured in the temperature interval from 2 to 78°K. It has been found that in the region $4° < T < 78°K$, within experimental error, the temperature dependence of the electrical resistance is given by formulas (3) or (4) where $m \approx 3/2$, $l \approx n \approx 5$, where the phonon terms $T^l$ and $T^n$ become important only at temperatures above 20 to 30°K. Assuming a three-halves law for the temperature dependence of the spontaneous magnetization $I_S$, it is easy to relate the electrical resistance $\rho$ to the ferromagnon concentration $n = 1 - I_S/I_0$, (where $I_0$ is the magnetization at $T \to 0$) and to obtain a numerical value for the coefficient $(\rho - \rho_0)/n$, where $\rho_0$ is the residual resistance. A comparison of this coefficient in nickel with the quantity $\Delta\rho/\Delta n$, where $\Delta\rho$ and $\Delta n$ are the changes in $\rho$ and n due to changes in the true magnetization in strong magnetic fields, shows that these quantities are approximately the same. This may be taken as indirect evidence of the validity of the assumption that the electrical resistance of ferromagnetic metals at low temperatures is related to scattering of electrons by inhomogeneities in the magnetization of the lattice (scattering by ferromagnons).

THE electrical resistance of iron, nickel and nickel-copper alloys has been studied in a number of papers,[1-5] but only in a relatively narrow temperature range. Thus, in our previous paper[4] the electrical resistance of nickel and nickel-copper alloys was studied between 2 and 4.2°K and between 14 and 20.4°K. In the present work the temperature dependence of the electrical resistance of these metals and alloys was studied over the entire temperature region from 2 to 78°K. The data obtained help evaluate the validity of various theoretical expressions[6,7] and establish the relation between changes in electrical resistance and spontaneous magnetization in ferromagnets in the low temperature region.

## 1. METHOD OF MEASUREMENT. SAMPLES.

The resistance was measured by a potentiometer method (using a PPTN-1 potentiometer). The samples were wires 0.1 to 0.2 mm in diameter and 150 to 160 mm long wound on a copper coil which was placed in a copper container 8 mm high for the measurement. The compositions of the alloy samples are given in the table. The iron samples were made from Armco iron wire. The nickel was chemically pure and its residual resistance was approximately $0.2 \times 10^{-6}$ ohm-cm rather than $1.54 \times 10^{-6}$ ohm-cm for the nickel sample used earlier.[4]

All samples were annealed in vacuum at 900°C for an hour and then slowly cooled at the rate of

| Specimens | $\rho_0 \cdot 10^6$, Ω·cm | $\rho_{01} \cdot 10^6$, Ω·cm | $\alpha \cdot 10^{10}$, Ω·cm/deg | $\beta \cdot 10^{10}$, Ω·cm/deg$^2$ | $\gamma \cdot 10^{14}$, Ω·cm/deg$^5$ | $a \cdot 10^{10}$, Ω·cm/deg$^{3/2}$ | $b \cdot 10^{16}$ Ω·cm/deg$^5$ | $m$ | $n$ | $l$ |
|---|---|---|---|---|---|---|---|---|---|---|
| Nickel | 0.20 | — | 1 | 0.4 | 0.2 | 2 | 5 | 1.51 | 4.9 | 5.6 |
| Iron | 1.458 | 1.44 | 3 | 0.4 | 1.5 | 1.8 | 7.7 | 1.50 | 4.8 | 5.2 |
| Alloy of Ni-Cu (annealed) | | | | | | | | | | |
| 4.6% Cu | 4.95 | — | 17 | 0.4 | 0.8 | 4.5 | 8.2 | 1.49 | 4.8 | 5.3 |
| 9.9% Cu | 9.27 | — | 30 | 0.4 | — | 8.0 | — | 1.48 | — | — |
| 15.1% Cu | 12.65 | — | 40 | 0.4 | 0.2 | 8.4 | 5 | 1.47 | 4.8 | 5.6 |
| 20.0% Cu | 16.22 | — | 49 | 0.6 | — | 15.0 | — | 1.51 | — | — |
| 25.1% Cu | 20.25 | 19.85 | 51 | 1.1 | — | — | — | — | — | — |
| Alloy of Ni-Cu (hardened) | | | | | | | | | | |
| 9.9% Cu | 10.0 | 9.78 | 36 | 0.5 | — | — | — | — | — | — |
| 15.1% Cu | 14.26 | 13.74 | 58 | 0.6 | — | — | — | — | — | — |
| 20.0% Cu | 17.80 | 17.70 | 70 | 0.6 | — | — | — | — | — | — |

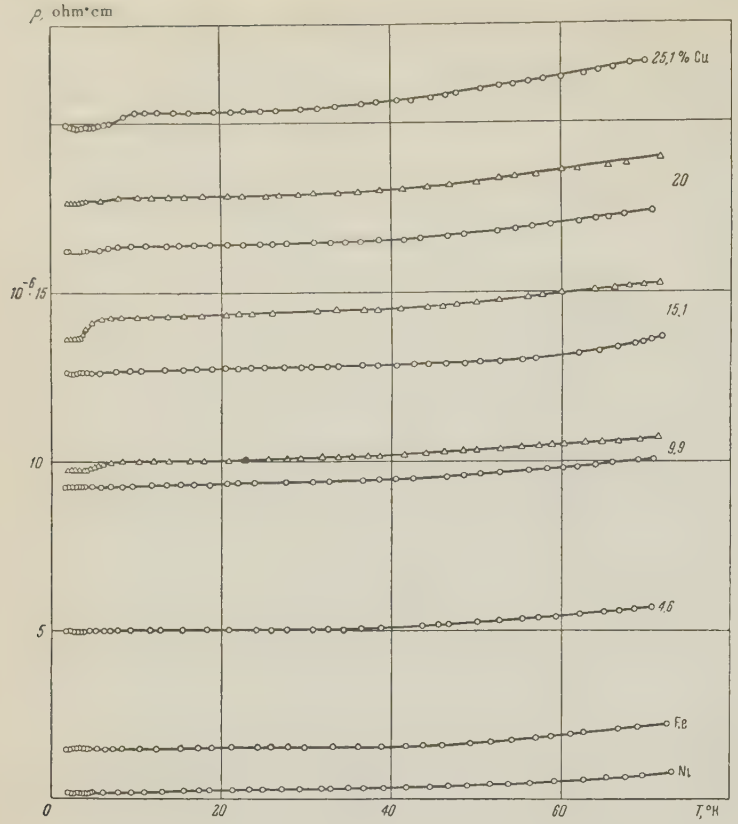


FIG. 1. Electrical resistance of nickel, iron and nickel-copper alloy as a function of temperature: ○ – after annealing, △ – after hardening.

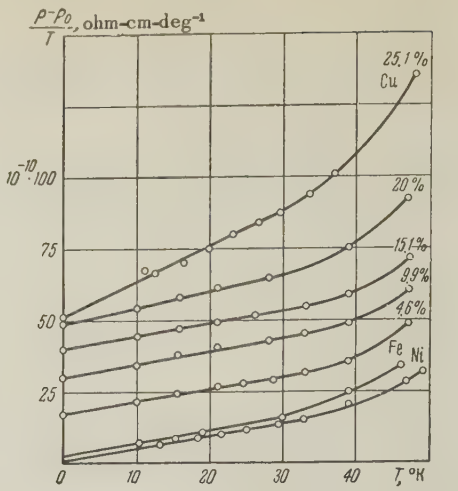


FIG. 2

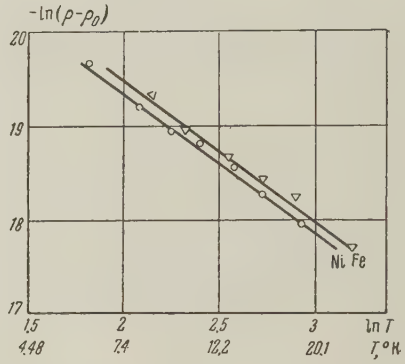


FIG. 3

100 degrees per hour. In addition, three samples were fabricated for which the annealing at 900°C for an hour was followed by rapid cooling (hardening) in air.

The temperature in the intervals 2 to 4.2°K, 14 to 20.4°K and 63.1 to 77.3°K was determined by measuring the pressure. In the measurements in the temperature region 4.2 to 14°K and above 20.4°K the container with the sample was suspended in a Dewar flask above the level of liquid and the temperature measured with a carbon resistance thermometer which had been calibrated against a gas thermometer. The error in the measurements in the 4.2 to 20°K region was 0.1 degree; in the region above 20.4°K the error was 0.5 degrees.

## 2. RESULTS

In Fig. 1 are shown curves which indicate the temperature dependence of the electrical resistance $\rho$ in iron, nickel and nickel-copper alloys. In the curves for certain alloys there are "steps" in the temperature region 3 to 10°K. In the annealed samples these "steps" are generally smaller than in those which were hardened. In our earlier work[4] data have been given concerning the effect of magnetic field on the size and position of these "steps." It is possible that these "steps" are due to the presence of inclusions of superconducting materials which are not detected in chemical or spectral analysis; however, it is also possible that what is being observed is an anomaly, similar to that which was found in Refs. 8 and 9 in certain non-ferromagnetic alloys. In the present paper we shall not discuss these "steps" and consider the temperature dependence of the electrical resistance only outside the region in which they appear.

At the outset, we remove from $\rho$ the residual resistance term $\rho_0$ which is independent of temperature. In many cases $\rho_0$ can be determined by linear extrapolation of the left-hand part of the curve of $\rho(T)$ to zero; however, this extrapolation procedure is not very accurate. We have determined $\rho_0$ by expanding $\rho(T)$ in a power series

$$\rho(T) = \rho_0 + \alpha T + \beta T^2 + \ldots \qquad (1)$$

In this case, if the first three terms are considered, the error in the determination of $\rho_0$ does not exceed the error in the measurements. In those cases

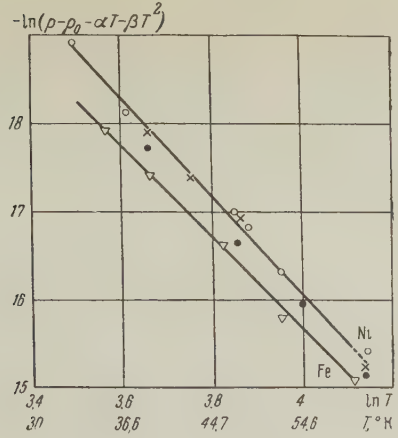


FIG. 4. o – nickel, ▽ – iron, ● – alloy with 4.6 % copper, × – alloy with 15.1% copper.

in which "steps" are observed on the $\rho(T)$ curve, two values of the residual resistance are taken, namely: $\rho_0$ for the part of the curve lying to the right of the step, in which case the expression in (1) is used, and $\rho_{01}$ which is obtained by linear extrapolation to zero of the part of the $\rho(T)$ curve lying to the left of the step ($T < 3°K$). The values of $\rho_0$ and $\rho_{01}$ and $\alpha$ and $\beta$, obtained in this way for the different samples, are shown in the table.

The quantity $(\rho - \rho_0)/T$ as a function of T and the quantity $\ln(\rho - \rho_0)$ as a function of ln T are shown in Figs. 2 and 3 respectively. Departures from a straight line are observed in Fig. 2 starting at $T > 30°K$. In the temperature region $4 < T < 18°K$ the dependence of the electrical resistance on temperature may be described by three terms in the formula in (1) or by the formula*

$$\rho = \rho_0 + aT^m, \qquad (2)$$

where a and m are constants. The values of these constants are given in the table. In all samples the exponent m is approximately $3/2$.

The sharp increase in electrical resistance at temperatures greater than 20 to 30°K indicates that we may be dealing here with a $T^5$ relation. To verify this assumption the curves shown in Figs. 4 and 5 were plotted; in these curves the quantities $\ln(\rho - \rho_0 - \alpha T - \beta T^2)$ and $\ln(\rho - \rho_0 - aT^m)$ are plotted against ln T. In both figures

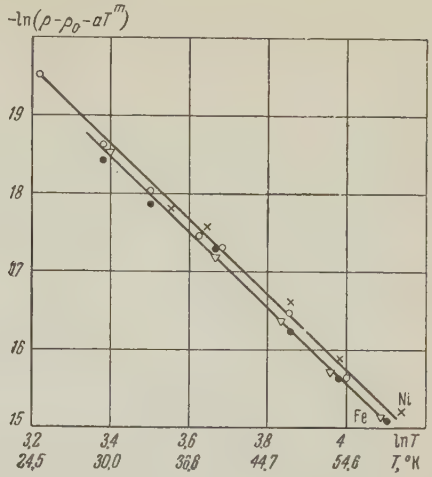


FIG. 5. o – nickel, ▽ – iron, ● – alloy with 4.6 % copper, × – alloy with 15.1% copper.

the points lie on straight lines. Thus the temperature dependence in the region $4°K < T < 77°K$ is given either by

$$\rho = \rho_0 + \alpha T + \beta T^2 + \gamma T^l \qquad (3)$$

or

$$\rho = \rho_0 + aT^m + bT^n, \qquad (4)$$

where $l$ and n are approximately 5. The values of $l$, n and the coefficients $\gamma$ and b are shown in the table.

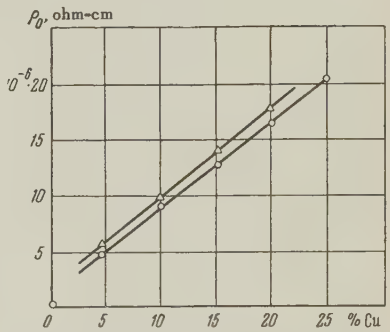


FIG. 6. Residual electrical resistance of a nickel-copper alloy as a function of composition. o – after annealing, △ – after hardening.

Figure 6 shows the residual resistance $\rho_0$ as a function of the copper concentration in nickel-copper alloys for hardened samples and annealed samples. This relation is linear up to copper concentrations of 25%. Points corresponding to $\rho_{01}$ in samples in which "steps" were observed, as is apparent from the table, lie below the lines which pass through the $\rho_0$ points in the "normal" samples. Thus the anomaly is observed as a reduction in the resistance as compared with "normal" behavior; this is the basis for the assumption that the effect is due to superconducting inclusions.

*The fact that there are two formulas for the temperature dependence in a limited low-temperature range is not inconsistent. It is apparent that the formula for $\rho$ can be written in the form of a power series, using any parameter which is small close to absolute zero. Such a parameter could be T or $T^m$ with $m > 0$. The present experimental data indicates that in the region 4 – 20°K the dependence of $\rho$ on T is given by the first three terms in the power series or two terms in the series in powers of $T^{3/2}$.

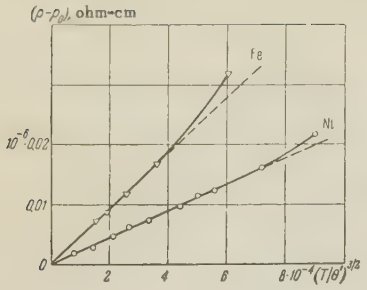


FIG. 7. Increase in electrical resistance with reduction in spontaneous magnetization.

## 3. DISCUSSION OF RESULTS

The electrical resistance of metals is related to scattering of electrons by thermal vibrations of the lattice (phonon scattering), scattering by inhomogeneities in the magnetization (in ferromagnetic materials — scattering by ferromagnons) and scattering by impurity ions which appear in the lattice. From the results which have been given above it follows that in iron, nickel, and nickel-copper alloys the phonon term, which is proportional to $T^5$ in the Bloch theory, is important at temperatures above 18 to 30°K. We may note that if the Bloch relation

$$\rho_1 = 497.6\,(\rho_2 / \Theta_d^4\, T_2)\, T^5$$

(where $\Theta_d$ is the Debye temperature $T_1 \ll \Theta_d \ll T_2$) is used to compute the $T^5$ coefficient in nickel, a value of $9.5 \times 10^{16}$ is obtained and this is close to the value of b given in the table.

Scattering by inhomogeneities in the magnetization of the lattice (ferromagnons) has been considered theoretically by Vonsovskii and Turov.[6,7] The quantity $\Delta\rho$, that part of the electrical resistance of a ferromagnetic metal which depends on the inhomogeneity in the magnetization, is given by Turov in the form $\Delta\rho = c_1 T + c_2 T^2$, which yields the same relation between $\rho$ and T as the empirical relation in (1). The theory does not give the values of the coefficients $c_1$ and $c_2$ and thus cannot be compared quantitatively with the experimental results. However, using the experimental data it is possible to show indirectly that the temperature dependence of the resistance $\rho$ in the ferromagnetic metals investigated in the region from 4 to 18°K is actually related to inhomogeneities in the magnetization and to make a rough estimate of the interaction energy which characterizes the scattering of electrons on the indicated inhomogeneities. For this purpose we have compared the change in $\rho$ in the indicated temperature region with the isotropic changes in this quantity in strong magnetic fields. The latter are proportional to the true magnetization and are thus directly related to the concentration of ferromagnons. We have also compared both quantities with the change in residual resistance in nickel-copper alloys as the copper concentration is changed.

In the low temperature region, it follows from the Bloch theory and has been shown experimentally,[10,11] that

$$(I_0 - I_s)/I_0 = (T/\Theta')^{3/2},$$

where $I_0$ is the magnetization at $T = 0$ and $\Theta'$ is a parameter related to the exchange energy. In Fig. 7 the values of $\rho - \rho_0$ are plotted against $(T/\Theta')^{3/2}$. In plotting these curves the values of $\Theta'$ for nickel and iron were taken from Refs. 10 and 11. In Fig. 7, as can also be seen directly from Fig. 3 and Eq. (2), in the temperature region 4 to 18°K $\rho$ is a linear function of $(T/\Theta')^{3/2}$, and thus of $I_0 - I_S / I_0 = n$, i.e., the concentration of ferromagnons (in the region 4 to 18°K, $n < 0.001$). According to the present data the quantity $(\rho - \rho_0)/n$ is $2.2 \times 10^{-5}$ in nickel and $4.4 \times 10^{-5}$ in iron.

We now compare $(\rho - \rho_0)/n$ with $I_0 \Delta\rho/\Delta I_S = \Delta\rho/\Delta n$ where $\Delta\rho$ is the change in electrical resistance which accompanies a change $\Delta I_S$ in the true magnetization in strong magnetic fields. In nickel, in the region from 4,000 to 18,000 oersteds, we have at room temperature $\Delta\rho/\rho\Delta H = 0.25 \times 10^{-6}$ (Ref. 12), $\Delta I_S/\Delta H = 1.3 \times 10^{-4}$, (Ref. 13), $0.7 \times 10^{-4} < \Delta I_S/\Delta H < 1.2 \times 10^{-4}$ (Ref. 14), and $\rho = 11 \times 10^{-6}$ ohm-cm. Assuming $I_0 = 509$ we have $\Delta\rho/\Delta n \approx 10^{-5}$, or $2.0 \times 10^{-5} > \Delta\rho/\Delta n > 1.1 \times 10^{-5}$. These quantities are of the same order of magnitude as $(\rho - \rho_0)/n$, and this may be considered an indirect verification of the fact that the electrical resistance of ferromagnetic metals and alloys in the low-temperature region is related to scattering of electrons by inhomogeneities in magnetization of the lattice.

In those cases in which electron scattering is due to an irregular static potential due to impurities or inhomogeneities in the lattice, this potential, which is usually taken as a small perturbation, can be estimated roughly from the difference in the ionization potentials of the host atoms and the impurity atoms. If, using this very rough estimate, we take the perturbing potential in the lattice of a nickel-copper alloy as the difference in the ionization potentials for copper and nickel, a value of approximately 0.07 ev is obtained. The magnitude of the perturbing potential due to an inhomogeneity in the magnetic moment corresponds, in order-of-magnitude terms, to the exchange integral, i.e., 0.01 to 0.1 ev. Thus, in the first approximation electron scattering on inhomogeneities in the magnetization of the nickel lattice and electron scattering by copper ions in copper-nickel alloys should

lead to a change in the electrical resistance which is of the same order of magnitude. On the other hand, as the change in electrical resistance is the same for identical increases in the concentration of ferromagnons in the nickel lattice and copper ions in the alloy lattice it may be concluded that the exchange integral for the s and d electrons is a quantity of the order of 0.01 to 0.1 ev.

The curve shown in Fig. 6 indicates that the residual resistance of nickel-copper alloys increases in proportion to the copper concentration $\nu$ for $\nu < 0.25$ and $\Delta\rho_0/\nu = 7.7 \times 10^{-5}$ where $\Delta\rho_0$ is the difference in the values of $\rho_0$ for an alloy sample with a copper concentration equal to $\nu$ and a nickel sample. Comparing these quantities with $(\rho - \rho_0)/n$ for nickel we see that both are approximately the same order of magnitude. From a comparison of $\Delta\rho_0/\nu$ and $(\rho - \rho_0)/n$ it is apparent that electron scattering on impurities in the copper is somewhat stronger than on inhomogeneities in the magnetization.

The authors wish to take this opportunity to thank A. I. Shal'nikova for many discussions concerning the procedure used in the experimental parts of the present work.

[1] W. Meissner and B. Voigt, Ann. Physik **7**, 892 (1930).

[2] H. Masumoto and J. Shirakawa, Sci. Rep. Tokyo Univ. **25**, 104 (1936).

[3] J. Smit, Physica **17**, 612 (1951).

[4] Kondorskii, Galkina and Chernikova, Proceedings of the Conference on Physics of Magnetic Effects, Moscow 1946; Izv. Akad. Nauk SSSR, Ser. Fiz. **21**, 1123 (1957).

[5] A. I. Sudovtsev and E. E. Semenenko, J. Exptl. Theoret. Phys. (U.S.S.R.) **31**, 525 (1956); Soviet Phys. JETP **4**, 592 (1957).

[6] S. V. Vonsovskii and E. A. Tirov, J. Exptl. Theoret. Phys. (U.S.S.R.) **24**, 420 (1953).

[7] E. A. Turov, Izv. Akad. Nauk SSSR, Ser. Fiz. **19**, 474 (1955).

[8] E. Mendoza and J. G. Thomas, Phil. Mag. **42**, 291 (1951); **43**, 900 (1952); A. N. Gerritsen and J. O. Linde, Physica **17**, 573 (1951); **18**, 877 (1952); A. N. Gerritsen, Physica **19**, 61 (1953).

[9] W. B. Teutsch and W. E. Love, Phys. Rev. **105**, 487 (1957); D. A. Spor and R. T. Webber, Phys. Rev. **105**, 1427 (1957).

[10] M. Fallot, Ann. phys. **6**, 305 (1936).

[11] E. I. Kondorskii and L. N. Fedotov, Izv. Akad. Nauk SSSR, Ser. Fiz. **16**, 432 (1952).

[12] E. Englert, Ann. Physik **14**, 589 (1932).

[13] R. Becker and W. Döring, Ferromagnetismus, Berlin, 1939, p. 174. H. Polley, Ann. Physik **36**, 625 (1939).

[14] P. Weiss and R. Forrer, Ann. phys. **12**, 279 (1929); A. R. Kaufmann, Phys. Rev. **55**, 1142 (1939).

Translated by H. Lashinsky
225

# THE STRUCTURE OF EXTENSIVE AIR SHOWERS AT SEA LEVEL

A. T. ABROSIMOV, N. N. GORIUNOV, V. A. DMITRIEV, V. I. SOLOV' EVA, V. A. KHRENOV, and G. G. KHRISTIANSEN

P. N. Lebedev Physics Institute, Academy of Sciences, U.S.S.R. and Moscow State University

Submitted to JETP editor December 3, 1957

J. Exptl. Theoret. Phys. (U.S.S.R.) **34**, 1077-1089 (May, 1958)

The lateral distribution of electrons and of nuclear-active and nuclear-passive particles in extensive air showers containing from $4 \times 10^4$ to $4 \times 10^5$ particles at sea level was studied by means of correlated hodoscopes. The experimental data indicate that cascades of high-energy nuclear-active particles, which determine the development of extensive air showers, are present in the showers in the lower layers of the atmosphere. The energy carried by a cascade is concentrated in a small region with a radius of the order of a few meters around the shower axis.

## INTRODUCTION

THE study of the nucleo-cascade process which manifests itself as an extensive air shower requires detailed information concerning the structure of the shower at different heights in the atmosphere. None of the several recent investigations[1-5] of the lateral distributions of the various shower components has been sufficiently thorough. In the present work we endeavored to obtain as complete and accurate quantitative information as possible regarding the lateral distribution of electrons, penetrating nuclear-interacting or "nuclear-active" (n.a.) particles, and "nuclear-passive" (n.p.) particles at sea level. This was a continuation and expansion of the work reported in Ref. 6. The measurements were performed at Moscow from April to June of 1954.

## DESCRIPTION OF APPARATUS

We used the well-known method of correlated hodoscopes, described in Ref. 7. The charged-particle distribution was determined by more than 2000 Geiger-Müller counters combined in hodoscope groups that were placed in the plane of observation. Most of these groups (1536 counters) were used to measure the density of all charged particles. The remaining 540 counters detected penetrating n.p. and n.a. particles. Figure 1 shows the general arrangement of the apparatus.

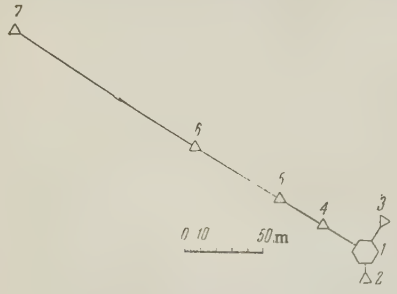


FIG. 1. General arrangement of the apparatus.

The geometry of the apparatus differs from that of Ref. 6 by the presence of the additional hodoscopic stations 5, 6, and 7 located 60, 120 and 250 m, respectively, from the center of station 1.

TABLE I

| Number of point | Number of counters: In charged-particle density indicators | Number of counters: In penetrating particle detectors |
|---|---|---|
| 1 | 1128 | 216 |
| 2 | 72 | 0 |
| 3 | 72 | 72 |
| 4 | 72 | 72 |
| 5 | 36 | 36 |
| 6 | 54 | 54 |
| 7 | 90 | 90 |
| Total | 1536 | 540 |

Table I gives the numbers of counters at stations 1 to 7. The detectors of penetrating particles at stations 1, 3, and 4 were similar to those in Ref. 6, except for the fact that the lead absorber placed above them was increased in thickness from 8 to 13 cm, while the lead shielding at the sides and ends was increased from 10 to 15 cm. Figure 2 is a cross section of the detectors at stations 5, 6, and 7.

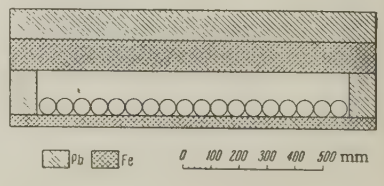


FIG. 2 Detector of penetrating particles at stations 5, 6, and 7.

The hodoscopic arrangement employed in the present work was triggered as described in Ref. 6 by coincidences of six counter groups each of 0.132 $m^2$ area. The geometry and coincidence arrangement made it possible to study the lateral distributions of all charged particles and n.p. particles 2 to 250 m from the shower axis and of n.a. particles 2 to 30 m from the axis. The total number of particles varied from $10^4$ to $10^6$ in the showers studied.

In the present work we used GK-6 Korablev hodoscopes at all stations except 7. Because of the time lag of the gaseous discharge in the nonfilamentary thyratrons of the GK hodoscopes, special attention was paid to bringing about agreement between the lag of the master pulse (resulting from the inclination of the shower axis and passage along a high-frequency cable) and the resolving time of each individual hodoscope unit. The latter was measured by the method described in Ref. 8. For units with $6 \times 55$ $cm^2$ counters the average resolving time was 12 microseconds; for $3.3 \times 30$ $cm^2$ counters the resolving time was 8 microseconds and for $2 \times 12$ $cm^2$ counters it was 5 microseconds. With this resolving time, each master pulse was accompanied by not more than a single chance discharge of a counter in the entire hodoscopic system 1 — 6. The number of counters triggered legitimately at each of stations 1 — 6 considerably exceeded the number due to chance.

With the given system of shower selection the particle density at station 7 is so small that the resolving time must be made as small as possible. Therefore the hodoscope units at station 7 included electron tubes with delay lines and had a resolving time of 2.5 microseconds. This permitted us to study showers at distances of 1 to 250 m from the axis with a minimum of $\sim 10^4$ particles.

## METHODS AND RESULTS

The apparatus which has been described furnished a quite detailed picture of the charged particle density distribution near the axis of each recorded shower. This enabled us to determine the required individual characteristics of the shower, which are the position of its axis and the number of shower particles.

In a considerable number of instances the axes of recorded showers passed close to the center of station 1 and the hodoscope groups of counters obtained a good determination of the particle density distribution. In these instances the location of the shower axis was determined without any special assumption regarding the lateral distribution of the shower particles except that of circular symmetry around the axis.

The position of the axis was determined as follows. As the zeroth approximation, the axis was located at the middle of the region of maximum particle density. This region is easily found if the hodoscopes provide a good determination of particle density. For the next approximation we considered the hodoscope groups forming a symmetrical configuration with respect to the middle of the region that had been obtained. Because of the uniform arrangement of hodoscope groups within station 1, a considerable number of these groups entered into this configuration. The "center of gravity" of the region determined in this way was obtained from the formula

$$X_0 = \sum x_i \rho_i / \sum \rho_i, \quad Y_0 = \sum y_i \rho_i / \sum \rho_i,$$

where $x_i$, and $y_i$ are the coordinates of the i-th hodoscope group and $\rho_i$ is the shower particle density above this group. The point $X_0, Y_0$ is near the shower axis as the "center of gravity" of the entire shower.

For the second approximation we considered the hodoscope groups forming a symmetrical configuration around $X_0, Y_0$ and determined their center of gravity. In practice the second approximation is unnecessary since the inaccuracy in the determination of $X_0, Y_0$ is usually much greater than the difference between the first and second approximations.

When the axis passed through the edge or outside of the station its position was determined by making use of the lateral distribution function of shower particles. (This distribution had already been obtained for showers whose axes were located by the method described above.) In such cases we used the fact that the shower axis had to lie on a straight line drawn through the "center of gravity" of the entire hodoscopic station 1 and through its center of symmetry.* We note that when the shower axis passed outside of station 1 but not more distant than stations 2, 3 and 4 its location was also determined, but less accurately. This permitted a considerable increase in the number of showers selected for determination of the particle density at large distances from the axis (stations 5, 6 and 7), where the above-mentioned reduced accuracy evidently played no part.

The average error in locating the axis was 1.5 m when the axis passed within station 1, and 3 m when it passed outside of station 1. When the axis passed within station 1, its rms deviation from this error did not exceed 1 m.

*The hodoscope groups were arranged symmetrically with respect to the center of station 1.

The second shower characteristic, the total number N of the particles, was determined after locating the axis. As a measure of the total number of particles we used the number of particles in the central region of the shower, which was determined directly from the data as $\alpha N = \sum_i \bar{\rho}_i 2\pi r_i \Delta r_i$. Here $\bar{\rho}_i$ is the experimentally observed particle density at distance $r_i$ from the shower axis. In practice this determination of $\alpha N$ is laborious. Therefore, after determining the lateral particle distribution in the central shower region, we followed a different procedure. If the lateral distribution $\rho(r)$ is of the form $\rho(r) = kNf(r)$ the sum of experimentally observed densities is given by $\Sigma\rho_i = kN\Sigma f(r_i)$. Thus $kN = \Sigma\rho_i / \Sigma f(r_i)$. We note that the denominator is independent of the selected form of the lateral distribution function close to its experimental value. The measure kN of the number of particles was determined with an average accuracy of 15%. The number of particles was determined from kN and k, obtained from the form of the lateral distribution function at both small and large distances from the shower axis.

### (a) Lateral Distribution of Electrons, Nuclear-Active, and Nuclear-Passive Particles

From a knowledge of the individual shower characteristics and the particle densities at various distances from the axis, we can plot the lateral particle distribution in a single shower. For this purpose it is useful to divide the entire plane of observation into a number of rings around the intersection, with the axis as a center. Since the shower axis is determined with a certain error there is a definite probability that a given ring will include hodoscope counters from within adjacent rings and that some of the counters of the given ring will be found in other rings. The particle density at distance r from the shower axis is determined from the ratio of the average number of triggered and untriggered counters in a given ring of radius r.

However, the lateral distribution of all particles in a single shower is determined with small accuracy. Also, the lateral distribution of penetrating particles cannot be determined for a single shower because the basic construction of the detectors of such particles does not permit obtaining of the particle density in each instance. It is therefore useful to obtain the lateral distribution averaged over a large number of showers with approximately equal total numbers of particles. This lateral distribution is plotted by calculating the particle densities for groups of showers with numbers of particles from N to $N + \Delta N$ striking at distance r from the indicator. Several different cases are possible.

1. The number m of triggered counters is not small compared with the total number n of counters. The average density $\rho$ can then be obtained as the mathematical expectation from the individual densities normalized to the total particle number $\bar{N}$, which is the average for the group of showers under consideration:

$$\bar{\rho} = \sum_i \rho_i (\rho_i/\Delta\rho_i)^2 (\bar{N}/N_i) \Big/ \sum_i (\rho_i/\Delta\rho_i)^2,$$

where $\rho_i\sigma = \ln[n/(n-m)]$ and $\sigma$ is the area of a single counter. This case occurs in determining the density of all charged particles at stations 1, 2, 3 and 4.

2. The number of triggered counters is subject to the condition $m \ll n$. Then

$$\rho\sigma = \sum_{m=1}^{n} x_m m/n \Big/ \sum_{m=0}^{n} x_m,$$

where $x_m$ is the number of showers corresponding to the triggering of m counters. This definition of the density applies to the calculation for stations 5, 6 and 7 as well as for 2, 3 and 4 in the case of non-dense showers.

3. In determining the density of n.p. and n.a. particles the hodoscopic groups do not give a detailed representation of the density or number of particles striking the counters in a given shower. A hodoscope gives evidence of either the presence or absence of particles. If C is the total number of showers striking at distance r from the detector, $C_c$ is the number of showers registered in the detector of n.p. particles, $\varphi(\rho)d\rho$ is the differential density spectrum of all charged particles which is produced by all of the recorded showers, $\delta$ is the fraction of n.p. particles by comparison with all charged particles and S is the detector area, then

$$C_c/C = \int (1 - e^{-\delta\rho S})\,\varphi(\rho)\,d\rho \Big/ \int \varphi(\rho)\,d\rho.$$

The density spectrum $\varphi(\rho)d\rho$ can be found if we know the spectrum of the number of recorded showers $W(N)dN$ and the lateral distribution of charged particles. When $\delta\rho S \ll 1$ the equation becomes $C_c/C = \delta\bar{\rho}S$. For n.a. particles the same equation can be used but with S replaced by $S(1 - e^{-\mu d})$, where $1/\mu$ is the mean interaction path of n.a. particles* in g/cm$^2$ and d is the quantity of matter in the detector above the lowest tray

*For Pb $1/\mu$ was taken as 160 g/cm$^2$, and 105 g/cm$^2$ for Fe.

of hodoscope counters* in g/cm$^2$.

The type of penetrating particles in the detector was determined from the pattern of discharged counters. The recorded patterns were divided into the following groups:

1. No counter was discharged.
2. One counter or several counters in a single tray were discharged.
3. A single counter was discharged in each of at least two trays. The discharged counters were in a straight line when one counter in each of three trays was discharged.
4. A single counter was discharged in each of at least two trays, but a second counter was discharged in one of these trays.
5. The pattern is a combination of patterns 3 and 4.
6. Several ($\geq 3$) counters were discharged in one tray; otherwise a single counter in a tray.
7. At least two counters were discharged in one tray and at least four counters in another tray.
8. The counters were discharged at random, but in one tray at least two and in another tray at least three counters were discharged.

TABLE II

| Group | 1 | 2 | 3 | 4 | 5 | 6 | 7 | 8 |
|---|---|---|---|---|---|---|---|---|
| No. of photographs | 509 | 33 | 14 | 7 | 4 | 8 | 16 | 4 |

Table II gives the distribution of photographs of one of the multi-tray detectors for $\overline{N} = 5 \times 10^4$ according to the groups listed above. The 33 events of group 2 were distributed as follows: One counter was discharged in 25 events, two counters in seven events and three counters in one event.

In the case of penetrating n.p. particles $C_C$ was given by the showers which discharged a single counter in at least two trays (group 3) and C was given by the sum of $C_C$ and $C_0$, the number of showers which passed through the detector without discharging a single counter (group 1). The density of n.p. particles at distances $\geq 60$ m from the shower axis was determined by single-tray detectors. The density of the nuclear-active component at such distances is negligibly small compared with the density of n.p. particles. The firing of each counter was assumed to represent the passage of a single n.p. particle; it was considered that the passage of 7% of the n.p. particles was accompanied by $\delta$ electrons and that in such cases two adjacent counters were discharged in a single-tray detector.

In determining the density of n.a. particles $C_C$ was given by the number of showers whose passage through the detector was observed to be accompanied by the formation of a local shower. The observed pattern of the local shower could belong either to group 7 (criterion I for the selection of n.a. particles) or to one of groups 6, 7, or 8 (criterion II).

To plot the lateral distribution we selected showers in which the total number of particles was of the same order of magnitude. To plot the lateral distribution of n.a. and n.p. particles we selected showers with a total number of particles between $2.5 \times 10^4$ and $10 \times 10^4$ for one group and between $2.5 \times 10^5$ and $10 \times 10^5$ for another group of showers. $\rho(r)$ was thus determined for a shower in which the total number of particles $\overline{N}$ was the arithmetical mean of N for all the showers striking at a distance r from the center of the detector. At different distances $\overline{N}$ did not vary by more than 10 to 15%. To plot the lateral distribution function we normalized $\rho(r)$ at all distances r to a single value of $\overline{N}$.

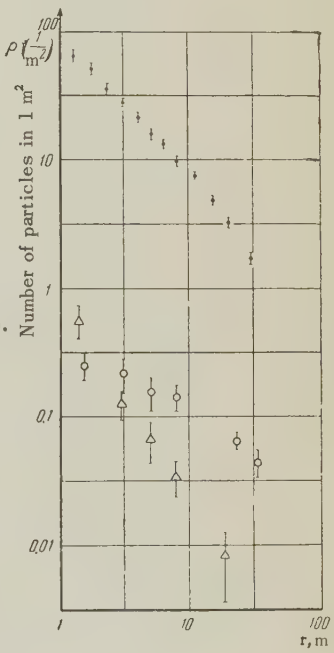


FIG. 3. Lateral distribution: ● – electrons, $N = 4.3 \times 10^4$; △ – n.a. particles, $N = 5 \times 10^4$ (criterion I); ○ – n.p. particles, $N = 5 \times 10^4$; r – distance from shower axis.

The lateral distribution functions are shown in Figs. 3 and 4. Fig. 3 gives the lateral distributions of electrons, n.a. and n.p. particles near the shower axis. Figure 4 gives the lateral distribution of all charged particles and n.p. particles at distances from 2 to 250 m from the shower axis.

Our experimental data on the lateral distribution of all charged particles can be approximated by the function $kNr^{-1}e^{-r/R}$ with $R = (60 \pm 6)$ m

*If we neglect absorption of electron-nucleonic showers in matter we can write

$$C_c/C = \sum_{n=1}^{\infty} \frac{e^{-\delta\rho S}}{n!} (\delta\rho S)^n (1 - e^{-n\mu d}) = 1 - e^{-\delta\rho S (1 - e^{-\mu d})}.$$

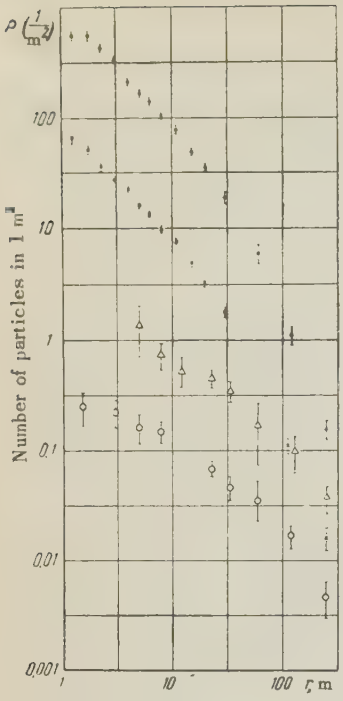


FIG. 4. Lateral distribution of electrons (● – for $N = 4.3 \times 10^4$, × – for $N = 4.3 \times 10^5$) and of n.p. particles (△ – for $N = 5 \times 10^4$, ○ – for $N = 5 \times 10^5$).

for $2 \ll R(n-1)$ and the power law $k_1 N r^{-n}$ for $r \geq R(n-1)$ with $n = 2.6 \pm 0.4$. The coefficients k and $k_1$ are found by normalizing the lateral distribution function:

$$\int \rho(r)\, 2\pi r dr = N$$

and equating the functions $kNr^{-1}e^{-r/R}$ and $k_1 N r^{-n}$ at the point $r = R(n-1)$. In this way the value $(2.0 \pm 0.3) \times 10^{-3}$ was found for k.

We also note that by using data on the lateral distributions of n.a. and n.p. particles we can determine the minimum numbers of these particles in showers with different $\bar{N}$. These results are given in Table III.

TABLE III

| | $\bar{N} = 5 \cdot 10^4$ | $\bar{N} = 5 \cdot 10^5$ |
|---|---|---|
| Number of n.a. particles in a circle of radius R = 22 m | 31 ± 6 | 330 ± 50 |
| Number of n.p. particles in a circle of radius R = 106 m | 1860 ± 350 | 10800 ± 4000 |

### (b) Absolute Number of Showers

Our hodoscopic setup served at the same time to determine the number of recorded extensive air showers with a given number N of particles. From this number, the absolute number of showers with N particles and with axes, striking at an angle $\theta = 0$ with the vertical, per unit area and unit solid angle, can be obtained from the following equation:

$$C(N)\Delta N = \int_0^{\pi/2} \int_0^{2\pi} \int_S F(N, \theta)\, W(N, \theta, \varphi, x, y) \times \cos\theta \sin\theta\, d\theta\, d\varphi\, dx\, dy\, \Delta N.$$

Here $C(N)\Delta N$ is the number of recorded showers with N to $N + \Delta N$ particles and axes striking the region S of the xy plane; $F(N, \theta)$ is the number of showers with N particles and axes inclined at angle $\theta$ to the vertical on the xy plane, per unit area in the xy plane, per unit interval of N, and per unit solid angle:

$$F(N, \theta) = F(N, 0) \cos^{\nu}\theta;$$

$$W(N, \theta, \varphi, x, y) = \prod_{i=1}^{n} (1 - e^{-\rho_i \sigma_i})$$

is the probability that the control system will record a shower with N particles, with its axis striking the point x, y at angle $\theta$ to the vertical and with the azimuthal angle $\varphi$; $\rho_i = Nf[r_i(\theta, \varphi)]$ $r_i$ is the distance from the shower axis to counter group i connected for coincidences in the plane perpendicular to the shower axis.

Station 1 was taken for the region S, since the location of a shower axis passing through this station and the number of shower particles are obtained most accurately. Then $r_i$ is the distance from the shower axis to the center of station 1, which is the location of the counter groups included in the control system.

For a sufficiently steep angular distribution of the axes and sufficiently slow decline of particle density away from the axis $C(N)\Delta N$ can be written as follows:*

$$C(N)\Delta N = \int_0^{\pi/2} \int_0^{2\pi} F(N, 0) \cos^{\nu+1}\theta \sin\theta\, d\theta\, d\varphi \times \int_S W(N, x, y)\, dx\, dy\, \Delta N.$$

For showers with a large number of particles $N \gg 1/\sigma f(r)$

$$\int_S W(N, x, y)\, dx\, dy \approx 1,$$

$$C(N)\Delta N = F(N, 0)(2\pi/\nu + 2) S \Delta N.$$

For showers with smaller N, this integral was calculated numerically.

Table IV gives data on $F(N, 0)$ at sea level assuming that the angular distribution of shower axes is represented by $\cos^2\theta$ with $\nu = 7.5$ (Ref. 9) for showers with different numbers N of particles.

*For the recorded showers, when account is taken of the fact that the recording probability W is dependent on $\theta$ and $\varphi$, there is not more than a 5% change in $C(N)\Delta N$.

## DISCUSSION

The data of the present work, together with an investigation of shower structure at mountain altitudes, permit us to draw certain conclusions regarding the character of the nucleonic cascade.

TABLE IV*

| $N \pm \Delta N$ | $F(N,0)$ N 1/cm²-sec-sterad |
|---|---|
| $2.6 \cdot 10^5 \pm 3.4 \cdot 10^4$ | $1.43 \cdot 10^{-10} \pm 2.86 \cdot 10^{-11}$ |
| $2.7 \cdot 10^4 \pm 4.0 \cdot 10^3$ | $4.1 \cdot 10^{-9} \pm 8.2 \cdot 10^{-10}$ |

*We here consider only a small fraction of all recorded showers with large N.

These conclusions are derived indirectly, not on the basis of an experimental study of the nucleonic cascade itself, but from analysis of experimental material concerning the different components of an extensive air shower which accompany that process. We also note that these experimental results represent averaged characteristics rather than any single shower.

We shall first consider the general behavior of a shower in the lower layers of the atmosphere. Figure 5 shows the lateral distribution of electrons in extensive air showers at sea level (from data of the present work) and at a mountain altitude (Ref. 10) in showers with similar total numbers of particles. The unit of length is the Molière parameter $r_1 = E_S x_0/\beta$, where $E_S = 19$ Mev, $\beta$ is the critical energy for air, and $x_0$ is the length of one radiation unit in meters at the level of observation. The figure shows that when a quantity proportional to $x_0$ is taken as the unit of length the lateral distribution of electrons is identical at sea level and at a mountain altitude.

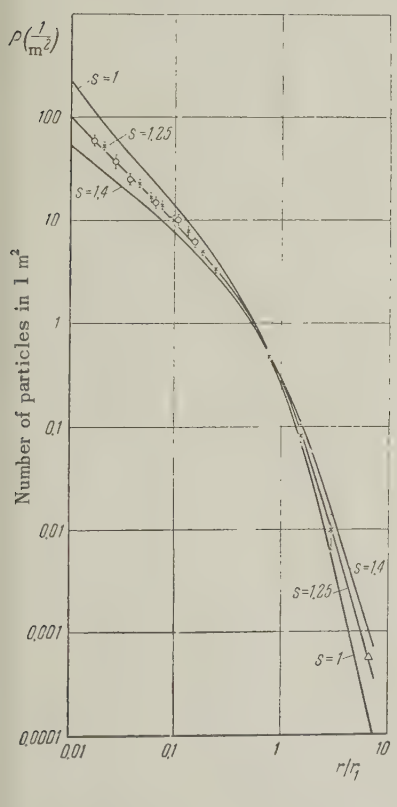


FIG. 5. Lateral distribution of electrons: × – at Moscow with $\bar{N} = 4.3 \times 10^4$, o – at the Pamir mountain site with $\bar{N} = 7 \times 10^4$ and the curves of Nishimura and Kamata for $s = 1$, 1.25 and 1.4. The observations were normalized with the curve for $s = 1.25$ to the number of particles in a circle of 250 m radius. $r/r_1$ is the distance from the shower axis in units of $r_1$.

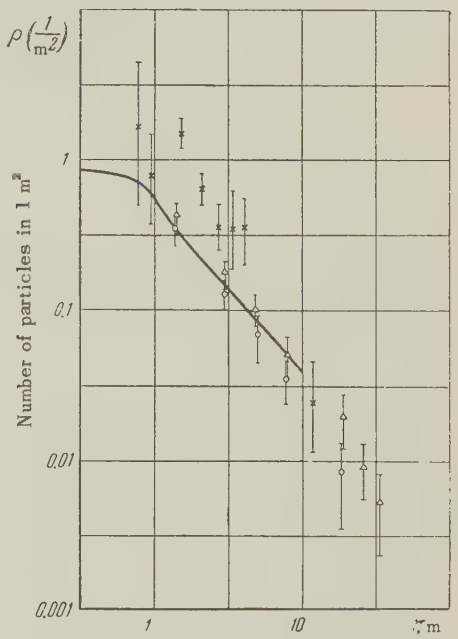


FIG. 6. Lateral distribution of n. a. particles at Moscow for $\bar{N} = 5 \times 10^4$: o – criterion I, Δ – criterion II; × – the same at the Pamir altitude for $\bar{N} = 6.5 \times 10^4$. The solid curve was calculated from Eq. (1) for $\rho(r)$, where r is the shower axis for Moscow.

Figure 6 shows the lateral distribution of n.a. particles in extensive air showers at sea level and a mountain altitude.[11] The distance from the shower axis is measured in units of length which are inversely proportional to the atmospheric pressure at the level of observation. The two distribution functions are seen to have approximately the same shape. We also note that the same data give approximately the same absolute number of n.a. particles at both altitudes in showers with similar N. Finally, Fig. 7 gives the lateral distribution of $\mu$ mesons at sea level and a mountain altitude[12] in showers with the same N.

On the basis of the data presented we can state that in the investigated range of distances from the shower axis the $\mu$-meson component is identical in showers at different altitudes. There are two possible explanations of this observed similarity at two altitudes.

1. The observed similarity is associated with the characteristics of the development of a nucleonic cascade in the lower atmospheric layers.

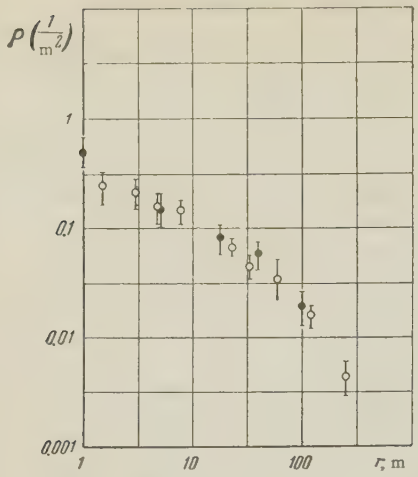


FIG. 7. Lateral distribution of nuclear passive (n.p.) particles: o – at Moscow, $N = 5 \times 10^4$, • – for the Pamir altitude, $\bar{N} = 5 \times 10^4$, r – distance from the shower axis.

2. The similarity results from the fact that showers observed at different altitudes are on the average at the same stage of development.

According to the second explanation the generation of the observed showers must occur not only in high atmospheric layers but also deep in the atmosphere, which is actually possible with a sufficiently small interaction cross section for the primary particles that initiate the showers.

In this connection, let us consider the data on the lateral distribution of $\mu$ mesons, which is determined by the angular divergence of the $\pi$ and K mesons from which the $\mu$ mesons originate and also, as was shown in Ref. 13, to a considerable extent by Coulomb scattering. Thus the lateral distribution of $\mu$ mesons is very sensitive to the height at which they are generated. In the second explanation of the similarity it is assumed that this height of generation, measured in $g/cm^2$, is approximately the same for the two altitudes of observation. It would thus follow that the lateral divergence of $\mu$ mesons at sea level would be smaller than at mountain altitudes. According to observations (Refs. 14 and 15) the lateral distribution of $\mu$ mesons at sea level is characterized by a more slowly diminishing function than at mountain altitudes. We shall therefore dwell in greater detail on the first explanation and shall consider the characteristics of the development of the nucleonic cascade which follow from the results of shower observations.

We now turn to an analysis of data on the electronic component, whose lateral distribution must be determined by Coulomb scattering of electrons and possibly by the lateral distribution of the cores of elementary cascades which results from the angles of emission of $\pi^0$ mesons in elementary acts of the nucleonic cascade process. The problem of the lateral distribution of electrons in electron-photon cascades characterized by the shower development parameter s has been solved by Nishimura and Kamata and by Greisen.[16] Figure 5 gives the lateral distribution of electrons and the theoretical curves for different s.

The lateral distribution due to Coulomb scattering is known to be determined by the energy spectrum of the electrons $N(>E) \sim E^{-s}$. From data on the barometric effect and angular distribution of shower axes[16] it follows that $s = 1.2$, since the absorption coefficient of the number of particles in a shower is $\lambda(s) = 1/200$ g/cm$^2$. Direct measurements of electron energy spectrum in extensive air showers[17] are not in disagreement with this value of s. Figure 5 shows that the theoretical curve of Nishimura, Kamata and Greisen with this value of s furnishes the best agreement with observation.

Agreement of the theoretical and experimental curves over the broad distance interval $0.02 < r/r_1 < 3$ cannot, of course, be fortuitous. It is thus reasonable to conclude that the lateral divergence of individual electron-photon cascade cores does not essentially influence the lateral distribution of electrons. Thus the energy borne by a nucleonic cascade must be well concentrated around the shower axis. The degree of this concentration can be estimated directly. If the divergence of electrons from the shower axis is due only to Coulomb scattering the distribution of the energy of the electron-photon component near the shower axis must be $1/r^2$ * according to cascade theory. If the lateral distribution of electrons with the given energy spectrum is to be essentially that due to Coulomb scattering alone, then the lateral distribution of the energy borne by a nucleonic cascade must be steeper than that borne by the electron-photon component, that is, it must be steeper than $1/r^2$. From the form of the lateral distribution of electrons it is also possible to estimate the energy of n.a. particles which produce electron-photon showers through $\pi^0$ mesons. Such an estimate,[18] based on the fact that s is independent of distance from the shower axis, gives $E_{n.a.} \geq 10^{11}$ ev.

Let us now consider our data on the nuclear-active component in the central region of a shower. From the preceding analysis it appears that most of the shower of a nucleonic cascade is concentrated close to the shower axis. An analysis of the lateral distribution of n.a. particles can indicate the effective size of this circumaxial region.

*Observation[17] of the energy distribution of the electron-photon component near the shower axis also agrees with $\sim 1/r^2$.

We have calculated the lateral distribution of n.a. particles using the following assumptions. The flux of high-energy n.a. particles is concentrated in a circle of radius a around the axis of an extensive air shower. Our recorded n.a. particles of relatively low energies are generated by the high-energy n.a. particles isotropically within a certain angle $\theta$ in the laboratory system. Neglecting the absorption coefficient of both high-energy and low-energy n.a. particles, the density of n.a. particles with low energies is given by

$$\rho(r) = \int_0^{2\pi} \int_0^a \int_{x_{\min}}^{\infty} \frac{x\,dx\,r'\,dr'\,d\varphi}{[r^2 + r'^2 - 2rr'\cos\varphi + x^2]^{3/2}};$$

$$x_{\min} = \frac{\sqrt{r^2 + r'^2 - 2rr'\cos\varphi}}{\tan\theta}, \qquad (1)$$

where x is the height above the altitude of observation, r is the distance from the shower axis to the point of observation, $x_{min}$ is the minimum height beginning with which particles start to strike at the distance r from the axis after being emitted at the angle $\theta$, and the vector $\mathbf{r}'\{r', \varphi\}$ defines the position of high-energy n.a. particles with respect to the shower axis. Integration gives*

$$\rho(r) = \begin{cases} 4Cr\left[E\left(\frac{a}{r}\right) + \left(\frac{a^2}{r^2} - 1\right)K\left(\frac{a}{r}\right)\right]; & \frac{a}{r} < 1 \\ 4CaE\left(\frac{r}{a}\right); & \frac{a}{r} > 1, \end{cases}$$

where C is a constant depending on the angle $\theta$. The function $\rho(r)$ calculated in this way is shown in Fig. 6; comparison with observation shows that a must be $\gtrsim 1$ m.

We shall use this result to estimate the energy of n.a. particles in a nucleonic cascade. It is known that the average angle of nuclear scattering cannot be smaller than $\mu_\pi c^2/E$ (as a result of the meson character of nuclear forces). This angular deviation is acquired on the average in one mean free nucleon path. Thus we must have $(\mu c^2/E)X \leq a$, whence†

$$E > 5 \cdot 10^{10}\ \text{ev}.$$

The combined experimental data on the electron-photon and nuclear-active components of extensive air showers at different altitudes lead to the conclusion that in the lower layers of the atmosphere down to sea level the high-energy ($\gtrsim 10^{11}$ ev) n.a. particles which determine the development of the entire shower are concentrated around the shower axis. Thus the nucleonic cascade plays an essential role in shower development within low-lying atmospheric layers. The development of the electron-photon component will then be closely related to the development of the nucleonic cascade. When n.a. cascade particles interact with the nuclei of air atoms a portion of their energy is imparted to $\pi^0$ mesons. Photons from the decay of the $\pi^0$ mesons give rise to elementary electron-photon cascades. Thus at a depth t of observation the number of electrons is

$$N(t) = \int_{E_0} \int_0^t f(E_0, t')\, N(E_0, t - t')\, dE_0\, dt',$$

where $f(E_0, t')$ is the number of photons with energy $E_0$ which result from the decay of $\pi^0$ mesons generated at depth t' in the atmosphere and $N(E_0, t - t')$ is the total number of electrons at the level of observation from a photon of energy $E_0$.

The absorption of the electron component of a shower in the lower atmosphere will be determined to a considerable extent by the form of $f(E_0, t')$. In the limiting case equilibrium is possible between the electron component and the nucleonic cascade.* For this case, assuming that the total energy F(t) imparted to $\pi_0$ mesons varies with the depth as $\sim e^{-\mu t}$ and using the theorem of the mean, we have

$$N(t)\beta = \int_{E_0} f(E_0, t - t^*) \int_0^t N(E_0, t - t')\,\beta\, dt'\, dE_0$$

$$= \int_{E_0} f(E_0, t - t^*)\, E_0 dE_0 = F(t - t^*) = F(t)\, e^{\mu t^*},$$

since the essential values of $(t - t')$, much less than t and t*, have a slight logarithmic dependence on $E_0$. Thus in equilibrium the number of shower particles diminishes according to the same law as the energy of the nucleonic cascade.

Table IV gives the absolute intensity of showers with different N at sea level. At the Pamir altitude Nikol'skii et al. similarly obtained the absolute number of showers with $N \approx 2.6 \times 10^5$ assuming the angular distribution of shower axes to be $\cos^2\theta$ with $\nu = 5.5$ (Ref. 9). Their result was $(1.37 \pm 0.27) \times 10^{-9}$ cm$^{-2}$-sec$^{-1}$-sterad$^{-1}$. From the absolute shower intensities at the two altitudes we can determine the absorption coefficient of showers with a given number of particles and the absorption coefficient of the number of particles in a shower. The latter coefficient was calculated to be $1/\mu = 1/200$ cm$^2$/g and, as indicated above,

*E(a/r) and K(a/r) are complete elliptic integrals (see Ref. 19).

†G. T. Zatsepin was the first to estimate the energy of n.a. particles from the same considerations; see also Ref. 20.

*Equilibrium between the electron-photon component and the nucleonic cascade was also considered by G. T. Zatsepin and I. L. Rozental' (report at a seminar of the Physics Institute, Academy of Sciences, U.S.S.R.)

can be regarded as the absorption coefficient of the energy borne by the nucleonic cascade in the equilibrium case.

All these observations (identity of the lateral distributions at the two altitudes, approximately identical variations with height of both electrons and nuclear-active particles) can be explained by postulating equilibrium between the electron component and the low-energy nuclear-active component on the one hand, and the energy of the nucleonic cascade of the shower core on the other hand.

In conclusion, we shall estimate the minimum total energy of a nucleonic cascade close to the level of observation assuming that the $\pi^{\pm}$ mesons produced in interactions have only a small probability of decaying to $\mu$ mesons. For equilibrium we have

$$N(t)\beta = F(t)e^{\mu t^*}.$$

We assume the energy of the nucleonic cascade to be $W(t) = F(t)/\mu$. Hence the energy of a nucleonic cascade which has reached the depth t is

$$W(t) = W_0 e^{-\mu t} = N(t)\beta/\mu e^{\mu t^*}.$$

The magnitude of $t^*$ is evidently close to the mean path of an elementary electron-photon cascade. Thus, taking $t^* = \ln E_0/\beta$, we have

$$W(t) = N(t)\beta/\mu (E_0/\beta)^{\mu}.$$

Assuming $E_0 = 10^{10}$, $\beta = 7 \times 10^7$ ev and $\mu = 0.17$, we obtain for $N \approx 10^4$

$$W(t) \approx 10^{12} \text{ ev}.$$

In conclusion, the authors wish to thank N. A. Dobrotin for considerable assistance and interest, and S. N. Vernov and G. T. Zatsepin for discussions of the results. G. V. Bogoslovskii, V. I. Zatsepin, V. Ia. Markov, A. M. Mozhaev, B. V. Subbotin, M. S. Tuliankina, and E. I. Tukish, who assisted with the adjustment of the apparatus and with the measurements, are also entitled to the thanks of the authors.

[1] H. L. Kasnitz and K. Sitte, Phys. Rev. **94**, 977 (1954).

[2] S. R. Haddara and D. Jakeman, Proc. Phys. Soc. (London) **A66**, 549 (1953).

[3] R. E. Heinman, Phys. Rev. **96**, 161 (1954).

[4] G. Fujioka, J. Phys. Soc. Japan **10**, 246 (1955).

[5] Hazen, Williams and Randall, Phys. Rev. **93**, 578 (1954).

[6] Abrosimov, Bedniakov, Zatsepin, Nechin, Solov'eva, Khristiansen, and Chikin, J. Exptl. Theoret. Phys. (U.S.S.R.) **29**, 693 (1955), Soviet Phys. JETP **2**, 357 (1956).

[7] G. T. Zatsepin, Dissertation Phys. Inst., Acad. Sci. U.S.S.R., 1954.

[8] G. B. Khristiansen, Приборы и техника эксперимента (Instruments and Instr. Engg.) **1**, 48 (1958).

[9] H. L. Kraybill, Phys. Rev. **93**, 1362 (1954).

[10] Vavilov, Nikol'skii, and Tukish, Dokl. Akad. Nauk SSSR **93**, 233 (1953).

[11] Batov, Nikol'skii, and Vavilov, Dokl. Akad. Nauk SSSR **111**, 71 (1956), Soviet Phys. "Doklady" **1**, 625 (1957).

[12] Dovzhenko, Nelepo, and Nikol'skii, J. Exptl. Theoret. Phys. (U.S.S.R.) **32**, 463 (1957), Soviet Phys. JETP **5**, 391 (1957).

[13] G. B. Khristiansen, J. Exptl. Theoret. Phys. (U.S.S.R.) **34**, 956 (1958), Soviet Phys. JETP 661 (1958).

[14] Antonov, Vavilov, Zatsepin, Kuruzov, Skvortsov, and Khristiansen, J. Exptl. Theoret. Phys. (U.S.S.R.) **32**, 227 (1957), Soviet Phys. JETP **5**, 172 (1957).

[15] Eidus, Adamovich, Ivanovskaia, Nikolaev, and Tuliankina, J. Exptl. Theoret. Phys. (U.S.S.R.) **22**, 440 (1952).

[16] K. Greisen, Progress in Cosmic Ray Physics, Ed. Wilson, **3** (Amsterdam, 1956).

[17] Ivanovskaia, Kulikov, Rakobol'skaia, and Sarychev, J. Exptl. Theoret. Phys. (U.S.S.R.) **33**, 358 (1957), Soviet Phys. JETP **6**, 276 (1958).

[18] G. B. Khristiansen, Oxford Conference on Extensive Air Showers, 1956.

[19] I. N. Bronshtein and K. A. Semendiaev, Справочник по математике (Mathematics Handbook), 1953.

[20] Iu. N. Vavilov, J. Exptl. Theoret. Phys. (U.S.S.R.) **33**, 179 (1957), Soviet Phys. JETP **6**, 141 (1958).

Translated by I. Emin
226

# DETERMINATION OF SPIN-LATTICE RELAXATION TIME FROM PARALLEL-FIELD ABSORPTION CURVE

K. P. SITNIKOV

Kazan' State University

Submitted to JETP editor November 30, 1957

J. Exptl. Theoret. Phys. (U.S.S.R.) **34**, 1090-1092 (May, 1958)

It is shown that the spin-lattice relaxation time can be determined from the paramagnetic absorption curve in parallel fields. The method has been verified using the normal paramagnetic material $MnSO_4 \cdot 4H_2O$. Results of measurement of $\rho$ at low temperature for various values of the constant magnetic field are presented for the salts $CrK(SO_4)_2 \cdot 12H_2O$, $FeNH_4(SO_4)_2 \cdot 12H_2O$ and $CuSO_4 \cdot 5H_2O$ for which the values of $\rho$ have hitherto been unknown.

1. As is well known (cf. Ref. 1), at sufficiently low frequencies paramagnetic absorption in parallel fields is due exclusively to spin-lattice relaxation and is described by the expression

$$\chi'' / \chi_0 m = \rho\nu F / (1 + \rho^2\nu^2), \tag{1}$$

where $\chi''$ is the imaginary part of the complex magnetic susceptibility, $\chi_0$ is the equilibrium susceptibility per unit mass, m is the mass of the sample, $\rho$ is the spin-lattice relaxation time, $\nu$ is the frequency of the oscillation field, and F is a function of the fixed field. We have used Eq. (1) to measure $\rho$. The absorption curves were observed using the Zavoiskii method;[2] the apparatus is described in detail in Ref. 3.

2. For convenience we write Eq. (1) in the form

$$\chi''(H_c) = FD, \tag{2}$$

where (cf. Ref. 1)

$$F = H_c^2 (b/c + H_c^2)^{-1}, \tag{3}$$

$$D \equiv \rho\nu/(1 + \rho^2\nu^2), \tag{4}$$

$$\chi''(H_c) \equiv \chi''(\chi_0 m)^{-1}. \tag{5}$$

Here $H_C$ is the fixed magnetic field, b is the heat capacity of the spin system, and c is the Curie constant.

The Debye function D is a function of frequency $\nu$ and the fixed field $H_C$ since[4]

$$\rho = \rho_0 (b/c + H_c^2) / (b/c + pH_c^2), \tag{6}$$

where $p < 1$. It is apparent that D will be an increasing function of the field $H_C$ if the frequency $\nu$ and region of variation of $H_C$ are chosen in such a way that $\rho\nu < 1$; conversely this quantity is a decreasing function if $\rho\nu > 1$. For a certain value of $\nu$ and region of variation of $H_C$ the function $D(H_C)$ will have a maximum. Consequently (cf. Ref. 5) the absorption curve $\chi''(H_C)$, given by Eq. (2), depending on the choice of frequency $\nu$ and region of variation of $H_C$, can be increasing (if $\rho\nu < 1$) and have a maximum (if $\rho\nu > 1$). This means that even if we do not analyze the absorption curve, but know its shape and the oscillator frequency, it is possible to find the spin-lattice relaxation time $\rho$. For an increasing absorption function $\chi''(H_C)$ we have $\rho < \nu^{-1}$; for an absorption function having a maximum, $\rho > \nu^{-1}$.

3. Suppose now that the absorption function $\chi''(H_C)$ is measured in the sample material

$$\chi''(H_c) = FD \tag{2}$$

and in a reference material (in which $\rho_{ref}$ is known):

$$\chi''(H_c)_{ref} = F_{ref} D_{ref}. \tag{7}$$

From Eqs. (2) and (7) we have

$$D = \chi''(H_c) F_{ref} D_{ref} / \chi''(H_c)_{ref} F. \tag{8}$$

The right-hand side of Eq. (8) is known since the ratio of the quantities $\chi''(H_C)$ and $\chi''(H_C)_{ref}$ is equal to the ratio of the corresponding readings in the grid circuit (cf. Ref. 2). Thus, using Eq. (8) the quantity D can be found from measurements; whence, using Eq. (4), for $\rho$ we have:

$$\rho = (1/\nu)(1/2D \pm \sqrt{(2D)^{-2} - 1}). \tag{9}$$

We rewrite Eq. (9) in the form

$$\rho\nu = K \pm \sqrt{K^2 - 1}, \tag{10}$$

where $K \equiv (2D)^{-1}$; it is easy to see that $K > 1$ both when $\rho\nu < 1$ and $\rho\nu > 1$. For an increasing absorption curve, or what is the same thing, for an increasing Debye function D, we have $\rho\nu < 1$,

TABLE I

| Frequency Mcs | 1.0 | | 1.95 | | 7.4 | | 13 | |
|---|---|---|---|---|---|---|---|---|
| $H_c$, Oe | $D$ | $\rho \cdot 10^7$ sec | $D$ | $\rho \cdot 10^7$ sec | $D$ | $\rho \cdot 10^7$ sec | $D$ | $\rho \cdot 10^7$ sec |
| 800 | 0.30 | 3.4 | 0.45 | 3.2 | 0.38 | 3.4 | 0.20 | 3.4 |
| 1600 | 0.35 | 4.1 | 0.47 | 3.6 | 0.30 | 3.6 | 0.18 | 4.1 |
| 2400 | 0.41 | 5.2 | 0.50 | 5.1 | 0.23 | 5.2 | 0.14 | 5.2 |
| 3200 | 0.45 | 6.4 | 0.49 | 6.2 | 0.18 | 7.0 | 0.12 | 6.4 |
| 4000 | 0.47 | 7.5 | 0.45 | 8.0 | 0.16 | 7.6 | 0.10 | 7.5 |
| 4800 | 0.49 | 8.2 | 0.44 | 8.5 | 0.15 | 8.3 | 0.09 | 8.6 |
| 5600 | 0.50 | 10.0 | 0.42 | 10.4 | 0.14 | 9.5 | 0.08 | 9.6 |

TABLE II

| Frequency Mcs | 18 | | 7.4 | | 18 | |
|---|---|---|---|---|---|---|
| Material | $CrK(SO_4)_2 \cdot 12H_2O$ | | $Fe(NH_4)(SO_4)_2 \cdot 12H_2O$ | | $CuSO_4 \cdot 5H_2O$ | |
| $H_c$, Oe | $D$ | $\rho \cdot 10^8$ sec | $D$ | $\rho \cdot 10^8$ sec | $D$ | $\rho \cdot 10^8$ sec |
| 800 | 0.05 | 0.3 | 0.12 | 1.7 | 0.10 | 0.5 |
| 1600 | 0.10 | 0.5 | 0.14 | 2.0 | 0.18 | 1.1 |
| 2400 | 0.15 | 0.8 | 0.14 | 2.0 | 0.25 | 1.5 |
| 3200 | 0.19 | 1.0 | 0.15 | 2.1 | 0.31 | 1.9 |
| 4000 | 0.21 | 1.2 | 0.15 | 2.1 | 0.34 | 2.1 |
| 4800 | 0.22 | 1.3 | 0.16 | 2.2 | 0.35 | 2.3 |
| 5600 | 0.24 | 1.4 | 0.16 | 2.2 | 0.37 | 2.5 |
| 6400 | 0.24 | 1.4 | 0.16 | 2.2 | 0.38 | 2.6 |
| | $\rho_0 = 0.13$<br>$\rho_\infty = 1.7$<br>$p = 0.08$ | | $\rho_0 = 0.9$<br>$\rho_\infty = 2.3$<br>$p = 0.4$ | | $\rho_0 = 0.13$<br>$\rho_\infty = 2.9$<br>$p = 0.08$ | |

so that the minus sign must be taken in (9); for a decreasing Debye function $\rho\nu > 1$ in which case the plus sign must be taken in (9).

**4.** The method proposed here for measuring $\rho$ was verified experimentally in $MnSO_4 \cdot 4H_2O$. The results of the measurement of D and the calculation of $\rho$ at various frequencies are shown in Table I. It is apparent from the table that the Debye function is an increasing function at 1 Mcs and a decreasing function at 7.4 and 13 Mcs; at 1.95 Mcs the function exhibits a maximum. The quantity $\rho$ was computed from Eq. (9) using the proper sign (cf. above, end of Sec. 3). As is apparent from the table the values of $\rho$ found at different frequencies are in good internal agreement. They are also are in good agreement with the values obtained by other methods (cf. Ref. 1).

**5.** Using the above method, measurements have been made at room temperature of the values of $\rho$ in $CrK(SO_4)_2 \cdot 12H_2O$, $FeNH_4(SO_4)_2 \cdot 12H_2O$ and $CuSO_4 \cdot 5H_2O$. The results of these measurements are shown in Table II. No room-temperature measurements of $\rho$ were ever made for these materials, nor was its value known at all for copper sulfate. The quantity $\rho_0$, the spin-lattice relaxation time at $H_C = 0$, and the parameter p were computed from the measurements using Eq. (6) while $\rho_\infty$ is $\rho_0/\rho$ and characterizes the spin-lattice relaxation time for $H_C \to \infty$.

**6.** In all cases the reference material was $Mn(NH_4)_2(SO_4)_2 \cdot 6H_2O$.

[1] J. G. Gorter, Paramagnetic Relaxation, Amsterdam, 1947.

[2] E. K. Zavoiskii, Dissertation, Physics Inst. Acad. Sci. U.S.S.R., 1944.

[3] S. G. Salikhov, J. Exptl. Theoret. Phys. (U.S.S.R.) **17**, 1070 (1947).

[4] J. H. Van Vleck, Phys. Rev. **57**, 426 (1940).

[5] K. P. Sitnikov, Dissertation, Kazan' State University, 1954.

Translated by H. Lashinsky
227

# EXPERIMENTAL VERIFICATION OF THE THERMODYNAMIC THEORY OF SPIN-SPIN PARAMAGNETIC RELAXATION IN PARALLEL FIELDS

K. P. SITNIKOV

Kazan' State University

Submitted to JETP editor December 4, 1957

J. Exptl. Theoret. Phys. (U.S.S.R.) **34**, 1093-1095 (May, 1958)

Paramagnetic spin-spin absorption has been investigated in a number of materials at $\nu =$ 600 Mcs at room temperature. It has been established that the absorption relation which follows from the Shaposhnikov analysis[1] is in good agreement with experiment if it is assumed that the corresponding relaxation time is independent of the constant field. The quantity b/c has been measured for certain materials for which it has been hitherto unknown.

1. The thermodynamic theory of paramagnetic relaxation in parallel fields[1] leads to the following expression for the imaginary part of the complex magnetic susceptibility

$$\chi''/\chi_0 m = F/\rho\nu + (1-F)^2\rho_s\nu, \qquad (1)$$

where $\chi_0$ is the equilibrium specific susceptibility, m is the mass of the material being investigated, $\rho$ is the spin-lattice relaxation time, $\rho_S$ is the spin-spin relaxation time, $\nu$ is the frequency of the oscillating field, and F is a function of the constant field $H_C$, which will be discussed in detail below. The expression in (1) applies to the case in which $\rho_S \ll \rho$, $\rho_S\nu \ll 1$ and $\rho\nu \gg 1$. If the difference between $\rho_S$ and $\rho$ is large, by making the frequency $\nu$ high enough the first term in (1) becomes much smaller than the second. In this case the paramagnetic absorption is described by the relation

$$\chi''/\chi_0 m = (1-F)^2\rho_s\nu \qquad (2)$$

and can be discussed in terms of only one internal relaxation mechanism in the spin system.

Equation (2) has been checked by Garif'ianov[2] who has shown that it gives good agreement with experiment if it is assumed that $\rho_S$ is independent of the constant field $H_C$. However, the sample in which this test was made was small. In Ref. 3 an investigation was made of spin-spin absorption in paramagnets in a much larger sample and it was established that in all cases considered the absorption takes place in accordance with Eq. (2) with $\rho_S$ independent of $H_C$.

2. Assuming that $\rho_S$ is independent of $H_C$, we write Eq. (2) in the form

$$\chi''(H_c) = (1-F)^2, \qquad (3)$$

where $\chi''(H_C) \equiv \chi_0 m\rho_S\nu$. The readings in the grid circuit are proportional to the quantity $\chi'(H_C)$. The function F varies over the range $0 < F < 1$ when its argument $H_C$ varies from zero to infinity since[4]

$$F = H_c^2\,(b/c + H_c^2)^{-1}, \qquad (4)$$

where b is the heat capacity of the spin system and c is the Curie constant (normal ferromagnets are being considered). From Eqs. (3) and (4) it follows that the spin-spin absorption $\chi''(H_C)$ is a decreasing function of $H_C$. Furthermore, when $H_C = 0$, we have $\chi''(0) = 1$ which we will use in converting between the meter readings and $\chi''(H_C)$ in absolute units. Writing, for convenience,

$$F \equiv 1/n, \qquad (5)$$

we rewrite Eq. (3) in the form

$$\chi''(H_c) = (1-n^{-1})^2; \qquad (6)$$

furthermore, from Eqs. (4) and (5) we have

$$b/c = (n-1)\,H_c^2. \qquad (7)$$

If it is assumed that (2) is valid, Eq. (7) is convenient for experimental determination of the constant b/c. Actually, giving n an arbitrary value $n_1$ (greater than unity) and using Eq. (6) we can find $\chi''(H_{C_1})$ and then, going over to the corresponding point of the experimental curve by using the relation $\chi''(0) = 1$, we can find $H_{C_1}$; substituting $n_1$ and $H_{C_1}$ in Eq. (7) we then find b/c. If, however, b/c is known from other sources, Eq. (7) can be used conveniently for experimental verification of the expression given in (2). Both procedures have been used in this work: Eq. (2) was verified in several materials in which the con-

stant b/c was known and then the constant b/c was found by the method indicated above in a number of materials for which it had been hitherto unknown.

The absorption curve, the ordinates of which are proportional to the quantity $\chi''(H_C)$, was obtained using the method given by Zavoiskii.[5] In essence this method consists of using the experimentally determined linear relation between the grid current in an electronic oscillator and the magnitude of a small dissipative load. In measuring the absorption, a glass ampoule containing the material being investigated is introduced into a coil which is inductively coupled to the resonant circuit of the oscillator. The sample coil is oriented in a fixed magnetic field so that the oscillating field of the coil is parallel to the fixed field. When the fixed field is changed the dissipative load on the oscillator changes and there is a change in the grid current, which is detected by an appropriate instrument. A detailed description of the oscillator and its operation is given in Ref. 6. The sample is prepared from crystals which have been stored in the host solution to retain the water of crystallization. The neck of the ampoule containing the sample material (in powdered form) is sealed with paraffin. All measurements are carried out at 600 Mcs at room temperature.

**3.** The experimental spin-spin absorption curves obtained in the present work are all similar and differ only in intensity and half width. Hence it is sufficient to discuss one of them. In Table I are shown the results of an analysis of the curve for $MnSO_4 \cdot 4H_2O$; the quantity $\overline{\chi''}(H_C)$ denotes the readings corresponding to $\chi''(H_C)$. It is apparent from the table that Eq. (2) is in good agreement with the absorption curve; the value $b/c = 6.3 \times 10^6$ oersted$^2$ agrees with $b/c = 6.2 \times 10^6$ obtained by Tennyson and Gorter using a beat method (cf. Ref. 4). In all other cases investigated, which have been described in detail in Ref. 3, there is also substantial agreement between the experimental data and the theoretical expression (2) under the assumption that $\rho$ is independent of $H_C$. It should be added that spin-spin relaxation has been investigated at ultrahigh frequencies by Kurushin[7] who has also obtained results which verify the Shaposhnikov theory[1] with $\rho$ independent of $H_C$. On the other hand, there are recent experimental data on spin-spin absorption[8-11] which have as yet not received theoretical explanation.

TABLE I

| $n$ | $\chi''(H_C)$ $(\chi''(0)=1)$ | $\overline{\chi''}(H_C)$ $(\overline{\chi''}(0)=84)$ | $H_C$ | $b/c \cdot 10^{-6}$ Oe$^2$ |
|---|---|---|---|---|
| 1.5 | 1/9 | 9.3 | 3400 | 5.9 |
| 2 | 1/4 | 21.0 | 2500 | 6.2 |
| 3 | 4/9 | 37.3 | 1780 | 6.4 |
| 4 | 9/16 | 47.2 | 1450 | 6.3 |
| 5 | 16/25 | 53.7 | 1240 | 6.0 |
| 6 | 25/36 | 58.3 | 1150 | 6.6 |
| 7 | 36/49 | 61.7 | 1040 | 6.5 |
| 8 | 49/64 | 64.3 | 960 | 6.4 |

Average: 6.3

TABLE II

| Material | $b/c \cdot 10^{-6}$ Oe$^2$ Author's data | $b/c \cdot 10^{-6}$ Oe$^2$ Ref. 4 and others |
|---|---|---|
| $CrK(SO_4)_2 \cdot 12H_2O$ | 0.66 | 0.64 |
| $[Cr\,4H_2O\,2Cl]\,2H_2OCl$ | 4.6 | 4.5 |
| $Cr(NO_3)_3 \cdot 9H_2O$ | 1.2 | 1.1 |
| $MnCl_2 \cdot 4H_2O$ | 19.3 | 19.5 |
| $MnSO_4 \cdot 4H_2O$ | 6.3 | 6.2 |
| $Mn(NH_4)_2(SO_4)_2 \cdot 6H_2O$ | 0.65 | 0.65 |
| $Fe(NH_4)(SO_4)_2 \cdot 12H_2O$ | 0.28 | 0.27 |
| $[CuCl_4](NH_4)_2 \cdot 2H_2O$ | 2.5 | — |
| $Cu(CH_3COO)_2 \cdot H_2O$ | 0.93 | — |
| $CuSO_4 \cdot 5H_2O$ | 0.47 | — |
| $[Cu(NH_3)_4]SO_4 \cdot H_2O$ | 0.30 | — |
| $CuCl_2 \cdot 2H_2O$ | 0.35 | — |
| $Cr(OH)_3$ | 2.8 | — |

**4.** A summary of the results of the determination of b/c (both for materials in which it has been known and in which it is reported for the first time) is given in Table II. The values given in the last column of this table are taken from Gorter.[4]

We wish to take this opportunity to express our gratitude to B. M. Kozyrev, S. G. Salikhov, S. A. Al'tshuler, and I. G. Shaposhnikov for a discussion of the results.

[1] I. G. Shaposhnikov, J. Exptl. Theoret. Phys. (U.S.S.R.) **18**, 533, (1948).

[2] N. S. Garif'ianov, J. Exptl. Theoret. Phys. (U.S.S.R.) **25**, 359 (1953).

[3] K. P. Sitnikov, Dissertation, Kazan' State University, 1954.

[4] C. J. Gorter, Paramagnetic Relaxation, Amsterdam, 1947.

[5] E. K. Zavoiskii, Dissertation, Phys. Inst. Acad. Sci. U.S.S.R., 1944.

[6] S. G. Salikhov, J. Exptl. Theoret. Phys. (U.S.S.R.) **17**, 1070 (1947).

[7] A. I. Kurushin, Izv. Akad. Nauk SSSR, Ser. Fiz. **20**, 1232 (1956).

[8] L. J. Smits et al., Physica **22**, 773 (1956).

[9] A. I. Kurushin, J. Exptl. Theoret. Phys. (U.S.S.R.) **32**, 938 (1957); Soviet Phys. JETP **5**, 766 (1957).

[10] C. J. Gorter, Izv. Akad. Nauk SSSR, Ser. Fiz. **21**, 1083 (1957).

[11] P. G. Tishkov, J. Exptl. Theoret. Phys. (U.S.S.R.) **32**, 620 (1957); Soviet Phys. JETP **5**, 514 (1957).

Translated by H. Lashinsky
228

# *INVESTIGATION OF (p, pxn) REACTIONS ON IODINE*

M. Ia. KUZNETSOVA, V. N. MEKHEDOV, and V. A. KHALKIN

Joint Institute for Nuclear Research

Submitted to JETP editor December 7, 1957

J. Exptl. Theoret. Phys. (U.S.S.R.) **34**, 1096-1100 (May, 1958)

Formation of the radioactive isotopes $A^{126}$, $I^{125}$, $I^{124}$, $I^{123}$, $I^{121}$, and $I^{120}$ from $I^{127}$ was investigated by radiochemical methods. The isotopes were produced with 100, 170, 300, 480, and 660 Mev protons. The experimental data are analyzed and compared with the results of investigations of similar reactions on other elements. The fraction of K capture in $I^{126}$, $I^{124}$, $I^{121}$, and $I^{120}$ was determined.

In most radiochemical investigations where various elements are split by fast particles, not enough attention has been paid to the nuclei formed by the (p, xn), (p, pxn), and (p, 2pxn) reactions. Yet it is quite probable that a study of these reactions would yield additional data on the development of the intranuclear cascade, inasmuch as the radiochemical procedure makes possible observation of neutron emission.

The most suitable for the study of (p, pxn) reactions is $I^{127}$. It is possible to trace reactions with this nuclide over sufficiently wide range of x (from $x = 1$ to $x = 7$).

This article contains the results of a study of (p, pxn) reactions on iodine bombarded by protons of energies ranging from 100 to 660 Mev.

## EXPERIMENTAL PROCEDURE

KI specimens weighing 0.1 g were prepared for the experiments. In the latest experiments of this series, specimens of elementary iodine (0.1 to 0.3 g) were sealed in thin-wall glass ampoules.* The proton beam was monitored by the yield of $Na^{24}$ from the aluminum foil in which the irradiated specimens were rolled up.

The energy of the bombarding particles was varied by varying the radius of the synchrocyclotron circular beam with which the target was irradiated.

The iodine was separated from the bulk of the other radioactive products by double distillation from a nitrate solution, containing sodium nitrite. The final purification of the iodine (essentially removal of the bromine and the chlorine) was by two sequential extraction cycles: the iodine was extracted with chloroform from a 1 m solution in $HNO_3$, the chloroform layer was twice washed with water, the iodine was converted into an aqueous solution with the aid of $Na_2SO_3$, the iodide was again oxidized with the sodium nitrite and the iodine extracted with chloroform, the washing with water was repeated, and the iodine was reextracted in a solution of sodium sulphite.

The targets for the measurements were made in the form of AgI. All targets were scanned with a magnetic analyzer,[1] which made it possible to detect the decay in each component of the emitted radiation: x-rays, positrons, electrons, and gamma-quanta. The x-ray intensity decay curves plotted from the measured data consist of five periods: 60, 13, 4.5 days, 13 hours, and 1.8 hours. The positron component of radiation contains three half lives — 4.5 days, 18 hours, and 30 minutes, while the electron component contains only one — 13 days.

The calculated half lives of the various iodine isotopes are:

$J^{126}$ ($\beta^-$, $K$) $T_{1/2} = 13$ days; $J^{125}$ ($K$) $T_{1/2} = 60$ days;
$J^{124}$ ($\beta^+$, $K$) $T_{1/2} = 4.5$ days; $J^{123}$ ($K$) $T_{1/2} = 13$ hr;
$J^{121}$ ($\beta^+$, $K$) $T_{1/2} = 1.8$ hr; $J^{120}$ ($\beta^+$) $T_{1/2} = 30$ min.

The x-ray decay curve was resolved into components so as to produce a best fit to the known values of the periods, and also to the probabilities of the K-capture fraction. The K-fraction capture for the $I^{126}$, $I^{124}$, and $I^{121}$ isotopes was established as 50, 58, and 58% respectively. These values are obtained by averaging 10 to 12 readings. The obtained K-capture probabilities for $I^{126}$ and $I^{124}$ agree with the literature data ($\sim 58$ and $\sim 70\%$, Ref. 2). The K-capture fraction for $I^{124}$ also agrees with the theoretical value (46%), and is

*In both cases the cross sections obtained were equal, within experimental errors. This suggests that the radioactive iodine does not volatilize from a KI target heated above 100°C in the high vacuum of the synchrocyclotron chamber.

somewhat too low for $I^{121}$ (theoretical value 82%), but lies within the experimental error. No x-radiation was observed for $I^{120}$, in agreement with the theoretical values of the K-capture for this isotope (5 to 10%). The theoretical values were calculated using the formulas of Ref. 3.

To detect the presence of soft x-rays, the x-ray energy was determined by its absorption in aluminum. No soft gamma-ray component was observed, and the wavelength of the x-rays emitted by the $I^{121}$ and $I^{123}$ was found to be 0.46 A. This quantity is in good agreement with the expected value $\lambda$ = 0.455 A (Ref. 4). A separate experiment has confirmed that no buildup of $Te^{125m}$ ($T_{1/2}$ = 60 days) takes place at a gamma-ray energy of 0.35 Mev.[5]

To reduce the errors, the isotope yields were calculated from the data obtained by measuring the corpuscular radiation, using the K-capture fraction previously obtained. Only for $I^{123}$ and $I^{125}$ was the yield calculated by analysis of the decay curves of the electromagnetic-radiation activity.

## EXPERIMENTAL RESULTS

Table I lists the cross sections for the production of light radioactive isotopes of iodine from $I^{127}$ at various proton energies. The indicated deviations at 660 Mev are mean arithmetic values calculated from the results of five experiments, while the remaining cases represent averaged limits of yields obtained from 2 or 3 experiments. The next to the last column gives the total cross sections for the production of all the iodine isotopes; the last column indicates the average values of the emitted particles in reactions of the (p, pxn) type, obtained by averaging the cross sections.

The data obtained show that the energy dependences of the production cross sections of almost all of the isotopes are approximately the same. The reaction cross sections change little in the energy range from 300 to 600 Mev and increase with diminishing energy. For example, the total cross section for 100-Mev protons is almost three times that of 300 to 660 Mev ones. Figure 1 shows the dependence of the cross section on the energy of the incident protons for the various iodine isotopes.

The maximum yield at all proton energies is that of $I^{126}$. The yields of the remaining nuclides diminish gradually with increasing x. An exception is $I^{121}$, with a production cross section larger than that of the neighboring nuclides and fluctuating sharply with varying particle energies. There are

TABLE I

| Proton energy, Mev | Production cross section × $10^{-27}$, cm² | | | | | | | Average number of emitted particles |
|---|---|---|---|---|---|---|---|---|
| | $J^{126}$ (p, pn) | $J^{125}$ (p, p2n) | $J^{124}$ (p, p3n) | $J^{123}$ (p, p4n) | $J^{121}$ (p, p6n) | $J^{120}$ (p, p7n) | Sum over all isotopes | |
| 660 | 51 ± 10 | 31 ± 4.6 | 17.3 ± 3 | 12 ± 1.5 | 16.3 ± 2.5 | 5.1 ± 1.5 | 133 | 3.7 |
| 480 | 70 ± 9 | 32 ± 5 | 19.5 ± 4.6 | 10.5 ± 3 | 27.5 ± 6.6 | 5.6 ± 1.8 | 165 | 3.6 |
| 300 | 53 ± 8 | 37 ± 7 | 28 ± 10 | 12 ± 2.1 | 50 ± 10 | 7.9 ± 2.1 | 188 | 4.3 |
| 170 | 64 ± 9 | 44 ± 9 | 54 ± 12 | 13.5 ± 2.4 | 20.5 ± 3.2 | 6.8 ± 1.1 | 203 | 3.6 |
| 100 | 126 ± 26 | 100 ± 26 | 50 ± 7 | 44 ± 11 | 105 ± 16 | 8.9 ± 3.6 | 434 | 4.0 |

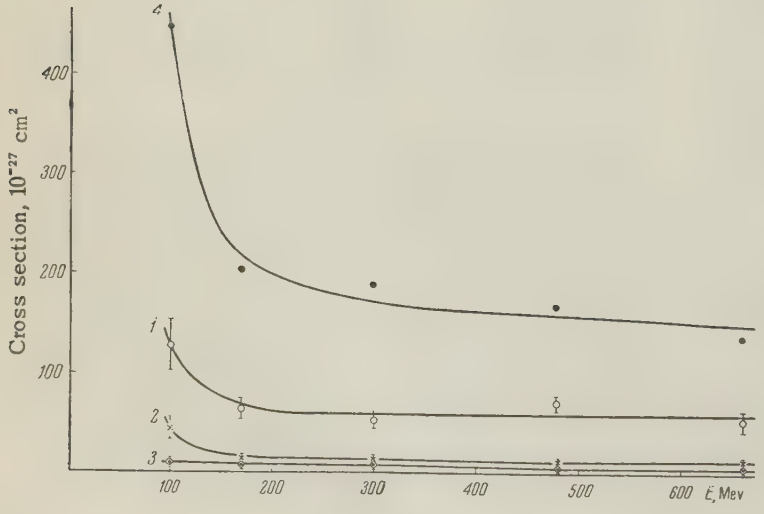


FIG. 1. Dependence of the cross sections of individual products on the proton energy. 1 – $I^{126}$ (p, pn); 2 – $I^{123}$ (p, p4n); 3 – $I^{120}$ (p, p7n); 4 – total cross section.

TABLE II

| Type of reaction | $Co^{59}$ | | | | $Cu^{63}$ | $Cu^{65}$ | $Y^{89}$ | $Cs^{133}$ | | $Th^{232}$ | $U^{238}$ | | |
|---|---|---|---|---|---|---|---|---|---|---|---|---|---|
| | 100 Mev [8] | 100 Mev [7] | 240 Mev [7] | 370 Mev [9] | 100 Mev [13] | 100 Mev [13] | 240 Mev [10] | 100 Mev [14] | 240 Mev [11] | 340 Mev [12] | 100 Mev | 200 Mev | 340 Mev |
| (p, pn) | 135 | 370 ± 180 | 120 ± 60 | 121 ± 60 | 120 | 1155 | 93 ± 15 | 890 | 59 | 40 | 93 | 67.5 | 85 |
| (p, p2n) | 31.5 | — | — | (37) | 70 | — | > 23 ± 4 | 500 | 460 | (35) | — | — | — |
| (p, p3n) | 3 | 89 ± 45 | 22 ± 11 | 15.2 ± 3.8 | — | 80 | < 28.2 ± 5 | — | — | (35) | — | — | — |
| (p, p4n) | 7.8 | 21 ± 4 | 6.6 ± 1.3 | 5.2 ± 1.3 | — | 37 | 15.8 ± 3 | 116 | 15 | 30 ± 3 | — | — | — |
| (p, p5n) | — | — | — | (1.7) | — | — | } 2.3 ± 0.5 | — | — | 22 ± 5 | — | — | — |
| (p, p6n) | — | — | — | — | — | — | | 15.4 | 4.5 | 17 ± 0.3 | — | — | < 4 |
| (p, p7n) | — | — | — | — | — | — | 0.08 ± 0.04 | — | — | — | — | — | — |
| (p, p8n) | — | — | — | — | — | — | — | — | — | — | 0.41 ± 0.03 | 0.41 | 0.35 |
| (p, p9n) | — | — | — | — | — | — | — | — | — | — | 0.046 | 0.1 | 0.06 |
| (p, p10n) | — | — | — | — | — | — | — | — | — | — | 0.012 | 0.03 | 0.038 |
| Sum of all products | 177 | 480 ± 230 | 149 ± 62 | 180 ± 65 | — | 272 | 162 ± 27 | — | — | 179 | — | — | — |

not enough experimental data on hand* to explain the causes of such fluctuations. The greatest deviation is at 300 Mev. The yield of the (p, p7n) reaction is the smallest and varies little with proton energy.

The average number of emitted particles, for all energies, is somewhat greater than 3.2, which is the calculated average number of cascade particles, emitted by interaction between a 400-Mev proton and a nucleus with A = 100 (Ref. 6). This indicates that the observed products are due not only to knockout but also to evaporation of nuclides, particularly for the lighter iodine isotopes.

Our results are in sufficiently good agreement with the literature data in the compared energy interval (see Table II).

The figures in the parentheses in Table II are the interpolated cross sections of the products, not observed experimentally. With the exception of cesium, the atomic weight of each isotope is one less than that of the target nucleus.

We did not observe the relative increase in the cross section of the (p, p2n) reaction, compared with the (p, pn) reaction, with increasing proton energy, as noted in Ref. 11, although iodine and cesium have nearly equal atomic and mass numbers.

Comparison of our results with the literature data lead to certain conclusions concerning the dependence of (p, pxn) reactions on the atomic number of the target element. Naturally, it is possible to compare only results obtained at nearly equal proton energies. Therefore, all that will be said below pertains to (p, pxn) reactions on cobalt,[9] iodine, and thorium[12] at proton energies of 300 to 370 Mev (see Tables I and II). At other proton energies, these relations are less clearly pronounced, owing to the lack of coordination in the experimental data.

The first striking factor is that the total cross sections for the above elements are nearly the same: 180 ± 65, 188 ± 40, and 179 ± 10 millibarns for Co, I, and Th respectively. Nearly-equal cross section are found also for the most probable (p, pn) reaction, this cross section being almost the same (~ 40 mbn) for carbon[14,15] as for the (p, pn) reaction on iodine and thorium. Next, the greater the atomic number of the target, the higher the relative cross sections for the production of the light isotopes (see Fig. 2). For example, if the yield of the (p, pn) reactions is taken to be unity, then the relative cross sections for the production of $Co^{55}$, $I^{123}$, and $Th^{228}$ by the (p, p4n) reaction are respectively $0.045^{+0.065}_{-0.02}$, $0.23^{+0.1}_{-0.05}$ and 0.75 ± 0.1 (Fig. 2).

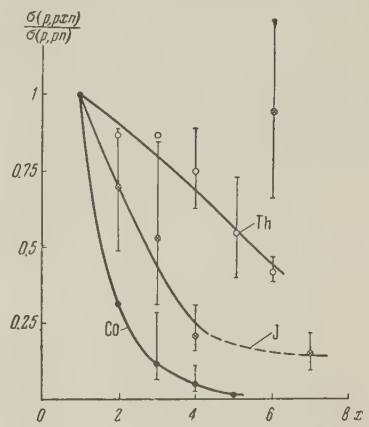


FIG. 2. Dependence of the ratio σ (p, pxn)/σ (p, pn) on the number of emitted neutrons, x, for cobalt, iodine, and thorium.

Such an increase in the yield is quite justified, since the increase in the excess neutrons over protons in the nuclei should favor the emission of neutrons and lead to an increase in the cross section

*Note added in proof (April 19, 1958). It is indicated in Ref. 18 that the 1.8-hour half life belongs to several iodine isotopes.

for the formation of products that are farther away from the initial nucleus.

The observed energy dependencies of the (p, pn) and (p, p2n) reactions can be explained in terms of the energy relations of the cross sections of the elementary nucleon-nucleon elastic cross sections. It is known, for example, that the cross sections of the (p, p) and (n, p) interactions are of approximately the same magnitude and are almost constant over the particle energy range from 200 to 260 Mev.[16,17]

In those cases, when the production of the isotopes cannot be explained as a result of nucleon knockout, we should not observe a similar dependence of the yield of the reaction products, due to the energy dependence of the elementary nucleon interactions. The relative constancy of the yield of $I^{120}$ at all proton energies is apparently due to the fact that its production is caused by another mechanism, the evaporation of the nuclides.

We take this opportunity to thank V. P. Dzhelepov for valuable remarks and I. Iu. Levenberg for help rendered in the performance of this work.

[1] M. Ia. Kuznetsova and V. N. Mekhedov Тр. VII ежегодн. конф. по ядернои спектроскопии, 1957 г. (Trans. of VII Annual Conf. on Nuclear Spectroscopy, 1957); Izv. Akad. Nauk SSSR, Ser. Fiz. **21**, 1020 (1957) [Transl. By Columbia Tech Transl., p. 1021]

[2] Seaborg, Pearlman, and Hollander, Table of Isotopes, Revs. Mod. Phys. **25**, 469 (1953).

[3] B. S. Dzhelepov and A. V. Kudriavtseva, J. Exptl. Theoret. Phys. (U.S.S.R.) **19**, 761 (1949).

[4] A. H. Compton and S. K. Allison, X-Rays in Theory and Experiment, N. Y. Van Nostrand, 1939.

[5] G. Friedlander and W. C. Orr, Phys. Rev. **84**, 484 (1951).

[6] Bernardini, Booth, and Lindenbaum, Phys. Rev. **85**, 826 (1952); **88**, 1017 (1952).

[7] G. Wagner and E. O. Wiig, Phys. Rev. **96**, 1100 (1954).

[8] Sharp, Diamond, and Wilkinson, Phys. Rev. **101**, 1493 (1956).

[9] E. Belmont and I. Miller, Phys. Rev. **95**, 1554 (1954).

[10] A. A. Caretto and E. O. Wiig, Phys. Rev. **103**, 236 (1954).

[11] R. W. Fink and E. O. Wiig, Phys. Rev. **96**, 185 (1954).

[12] M. Lindner and R. N. Osborn, Phys. Rev. **103**, 378 (1956).

[13] J. W. Meadows, Phys. Rev. **91**, 885 (1953).

[14] Aamodt, Peterson, and Phillips, Phys. Rev. **88**, 739 (1957).

[15] Iu. D. Prokoshkin and A. A. Tiapkin, J. Exptl. Theoret. Phys. (U.S.S.R.) **32**, 177 (1957), Soviet Phys. JETP **5**, 148 (1957).

[16] Dzhelepov, Satarov, and Golovin, Dokl. Akad. Nauk SSSR **104**, 717 (1955).

[17] N. P. Bogachev, Dokl. Akad. Nauk SSSR **108**, 806 (1956), Soviet Phys. "Doklady" **1**, 361 (1956).

[18] J. Inorg. Nucl. Chem. **5**, 105 (1957).

Translated by J. G. Adashko
229

# ANGULAR ANISOTROPY IN $\pi^+ - \mu^+ - e^+$ DECAY OBSERVED IN A PROPANE BUBBLE CHAMBER

A. I. ALIKHANIAN, V. G. KIRILLOV-URGIUMOV, L. P. KOTENKO, E. P. KUZNETSOV, and Iu. S. POPOV

P. N. Lebedev Physics Institute, Academy of Sciences, U.S.S.R.

Submitted to JETP editor December 12, 1957

J. Exptl. Theoret. Phys. (U.S.S.R.) 1101-1109 (May, 1958)

The angular anisotropy in $\mu^+ - e^+$ and $\pi^+ - \mu^+$ decays was measured. The dependence of the $\mu^+ - e^+$ decay anisotropy on the electron energy is not inconsistent with the two-component-neutrino theory. No angular anisotropy is displayed by $\pi^+ - \mu^+$ decays.

## 1. INTRODUCTION

THE experimental data accumulated on angular correlation in $\mu - e$ and $\pi - \mu$ decays is currently of interest. In the former case, it can be used to verify the two-component neutrino theory and to understand the nature of the depolarization of the $\mu$ mesons remaining in media. In the latter case it can essentially establish the presence or absence of the correlation itself.

As was shown by Lee and Yang,[1] Landau,[2] and others[3,4] who have developed the theory of the two-component neutrino, the degree and character of the angular anisotropy in $\mu - e$ decay depend substantially on the energy of the decay electrons. Let $\epsilon$ be the decay-electron energy in units of maximum energy in the $\mu - e$ decay. The angular distribution is then, according to the two-component neutrino theory,

$$dN \sim 2\varepsilon^2 [(3 - 2\varepsilon) + \xi \cos\vartheta (2\varepsilon - 1)]\, d\varepsilon\, d\Omega, \qquad (1)$$

where $\vartheta$ is the angle between the momentum of an electron emitted inside a solid angle $d\Omega$ and the spin of the $\mu$ meson (in the $\pi^+ - \mu^+ - e^+$ decay with stoppage of the $\pi^+$ meson the spin is parallel to the momentum of the $\mu^+$ meson), and $\xi$ is a parameter that takes the character of the interaction into account. Integration of (1) over all electron energies yields

$$dN \sim (1 + {}^1/_3 \xi \cos\vartheta)\, d\Omega = (1 + a\cos\vartheta)\, d\Omega. \qquad (2)$$

The theoretical value of $\xi$ ranges from $-1$ to $+1$ and a lies accordingly between $-{}^1/_3$ and $+{}^1/_3$. The coefficient a of formula (2) is a parameter of the theory, while the experimentally-determined coefficient depends on the degree of depolarization of the $\mu$ mesons. We shall therefore denote the experimental value of this coefficient by A, and the correction for depolarization by a.

We have studied the angular anisotropy in the $\pi^+ - \mu^+ - e^+$ decay with discrimination by decay-electron energy.

## 2. EXPERIMENTAL CONDITIONS

The $\pi^+ - \mu^+ - e^+$ decays were registered in a 750-cc propane bubble chamber.[5] The chamber was exposed in a $\pi^+$-meson beam using the phasotron of the Joint Institute for Nuclear Research. The $\pi^+$ mesons were formed on an external polyethylene target by protons with energies of $\sim 660$ Mev. The target was 70 cm long, making it possible to increase the $\pi^+$-meson yield through the use of the two reactions of $\pi^+$-meson creation, $p + p \rightarrow \pi^+ + p + n$ and $p + p \rightarrow \pi^+ + d$.

The $\pi^+$ mesons, with an appr$\frac{de}{}$imate energy

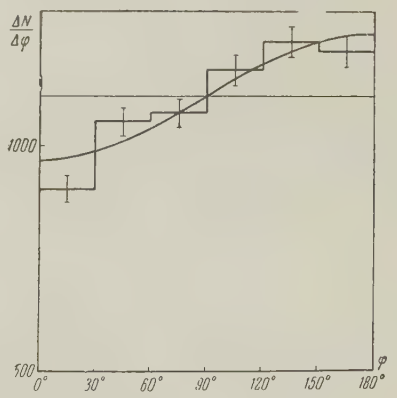


FIG. 1. Angular distribution of electron momenta relative to the $\mu$-meson momentum in $\pi^+ - \mu^+ - e^+$ decay. The abscissas indicate the projection of the spatial angle $\varphi$ between the $\mu$-meson and the electron momenta, and the ordinate indicates the number of electrons over the interval of the angle $\varphi$. The smooth curve corresponds to $dN \sim [(1 + A(\pi^2/16)\cos\varphi)\, d\varphi]$ at $A = -0.22 \pm 0.03$. Horizontal line – isotropic distribution. N = 6670.

of 180 Mev, were aimed with a deflecting magnet into a collimator, and were then slowed down by a copper absorber so that they were stopped inside the chamber. The total distance from target to chamber was 7 m.

To prevent distortion of the angular distribution by precession of the stopped $\pi^+$ mesons in the stray field of the accelerator, the chamber was shielded and the field inside the chamber did not exceed one gauss. The accelerator beam was switched off during the dead time of the chamber. This made possible, in particular, to regular visual monitoring of the quality of the tracks in the chamber. Approximately 8,000 photographs were made during the time of chamber operation, and 6,670 $\pi^+ - \mu^+ - e^+$ decay events were registered.

## 3. ANGULAR ANISOTROPY IN $\mu^+ - e^+$ DECAY. DEPENDENCE OF ANGULAR ANISOTROPY ON THE DECAY-ELECTRON ENERGY

We have measured the projections of the spatial angles between the momenta of the $\pi^+$ meson and the electron on the plane of the camera film. Compared with the measurements of spatial angles, the measurement of angle projections, in addition to being relatively simple, has also the advantage that it becomes unnecessary to introduce corrections for the angle distortion in the propane (the orthogonal projections of spatial angles do not change in a refracting medium). The error in the measurement of the angle was 1 to 3°, depending on the length of the track. To eliminate possible edge effects, which can distort the angular distribution, the only events analyzed were those in which the $\mu^+$ meson was not closer than 3 mm from the wall of the chamber. Events identified as decay of stopped $\mu^+$ mesons may include $\mu^+$ mesons scattered prior to stopping or a $\pi^+$ meson decaying in flight. An estimate shows that these extraneous events comprise not more than 1% of the total number of $\pi^+ - \mu^+ - e^+$ decays.

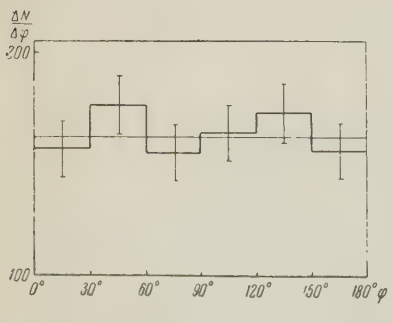


FIG. 2. The same as in Fig. 1 for the group of $\pi^+ - \mu^+ - e^+$ decays with soft electrons; N = 980.

In the case when the projections of the spatial angles on a plane is measured, the distribution (2), as can be readily shown (see Appendix), is transformed into

$$dN \sim [1 + a(\pi^2/16)\cos\varphi]\, d\varphi, \qquad (3)$$

provided the directions of the $\mu$-meson momenta are distributed in space isotropically (as will be shown below, this condition is satisfied for $\pi^+ - \mu^+ - e^+$ decays). Here $\varphi$ is the projection of the spatial angle $\vartheta$. Figure 1 shows the distribution of the projections of the angles between the initial momenta of the $\mu^+$ meson and the electron for 6,670 events of $\pi^+ - \mu^+ - e^+$ decay. It is seen that the experimental distribution is well approximated by formula (3).

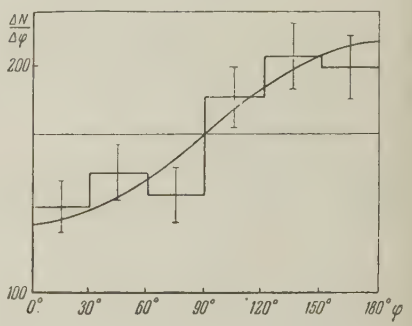


FIG. 3. The same as in Fig. 1 for the group of $\pi^+ - \mu^+ - e^+$ decays with hard electrons. The smooth curve corresponds to $dN \sim (1 + 0.715 A \cos\varphi)\, d\varphi$ at $A = -0.33 \pm 0.07$; N = 1023.

The coefficient A, obtained from the "forward-backward" ratio (the ratio of the number of electrons emitted in the 90 — 180° interval to the number of electrons emitted between 0 and 90°) is $A = -0.22 \pm 0.03$ (Ref. 6).

The error in A is the statistical rms error. It must be noted that had we measured the spatial angles, we would have decreased the error in A by merely 22%.

To estimate the correctness of the two-component neutrino theory, it would be interesting to separate the various groups with decay electrons of different energies from the total number of $\pi^+ - \mu^+ - e^+$ decay events, and to compare the anisotropy for these groups with that predicted by the two-component neutrino theory. In the group of events with low-energy electrons, we have selected such decay events, in which, over a propane path 2 cm long, the electrons experienced multiple Coulomb scattering at an angle not less than 2 to 3°, corresponding roughly to a limiting energy of 30 to 40 Mev for these events. A total of 980 such events was found. The histogram for the projections of the angles between the momenta of the $\mu^+$ meson and the electron, plotted for these events, is shown in Fig. 2. It is seen that we have here complete isotropy. If we calculate formally the coefficient A, using the above method, we find

$$A_s = -0.014 \pm 0.08.$$

Figure 3 shows the histogram for $\pi^+ - \mu^+ - e^+$

decays with hard electrons. This group includes events in which the electrons were scattered not more than 2 mm over 3 to 4 cm of their path projections. A total of 1023 such events was found. Such a selection does not include events with decay electrons that have a small projection, the numerical coefficient in formula (3) is not $\pi^2/16 = 0.616$, but greater. Calculations show that it amounts to 0.715. The coefficient A for events with hard electrons, found from the "forward-backward" ratio, is

$$A_h = -0.33 \pm 0.07.$$

The isotropy for cases with soft electrons, and the increased anisotropy compared with the integral histogram for the cases with hard electrons, are in qualitative agreement with the concepts of the theory of the two-component neutrino, according to which the anisotropy should lead to an increase in the decay electron energy.

For a quantitative comparison it is essential, first of all, to take into account the depolarization of the stopped $\mu^+$ mesons in the propane. We shall not carry out a quantitative comparison for cases with hard electrons, owing to the difficulties in estimating their energy, and also owing to the small difference (taking the errors into account) between the coefficient $A_s$ and the integral coefficient A, which equals $-0.22 \pm 0.03$. We took account of the depolarization in propane in the manner used by Chadwick, Wilkinson et al.,[7,8] who introduced a depolarization correction for emulsion. It is known from experiments in which the angular correlation in $\mu^+ - e^+$ decay is measured with the aid of counters, that maximum anisotropy, which incidentally is of constant value, is observed when a $\mu^+$ meson decays in graphite and in certain pure metals, for example aluminum and magnesium.[9,10] Furthermore, this anisotropy is the same for all these materials. It can be assumed that there is no depolarization in these substances. However, the coefficient A obtained in these experiments cannot be identified with the parameter a of Eq. (1), for the degree of polarization of the $\mu^+$-meson beam is not known exactly, nor do we know the cutoff limit of the decay-electron spectrum on the low-energy side. Depolarization in propane can be accounted for by measuring the coefficients A for carbon and propane, in the same setup, by the counter method. Such measurements are available in Ref. 10, which gives for carbon $A = -0.27 \pm 0.02$ and for propane $A = -0.18 \pm 0.015$.

The ratio of these two quantities will characterize the change in the coefficient A due to depolarization in propane. To introduce a correction for the depolarization in our measurements, it is necessary to multiply our measured values of the coefficient A by this ratio. We then obtain for the entire electron spectrum

$$a = A(0.27/0.18) = -0.33 \pm 0.06.$$

According to the theory of the two-component neutrino, a can range from $-0.33$ to $+0.33$, i.e., there is agreement with experiment. Introducing the depolarization correction for the group of decays with soft electrons (980 events), we get

$$a_s = A_s(0.27/0.18) = -0.02 \pm 0.11.$$

To calculate the theoretical values of the parameter $a_s$, it is necessary to integrate the distribution (1) to the limiting energy of the soft electrons. For a more accurate determination of the limiting energy, we selected approximately 200 events of $\pi^+ - \mu^+ - e^+$ decays with an electron track length not less than 2 cm. We then calculated the ratio of the number of events with soft electrons to the number of remaining events, and obtained a value of 0.375. Then, integrating (1) over the angles, we obtained the distribution over the electron energies only: $dN(\epsilon) \sim \epsilon^2(3 - 2\epsilon)\,d\epsilon$ (which coincides with the well-known Michel formula with the parameter $\rho = 0.75$). The limiting energy was found from the relation

$$\int_0^{\epsilon_{lim}} dN(\varepsilon) \Big/ \int_1^{\epsilon_{lim}} dN(\varepsilon) = 0.375.$$

We obtained $\epsilon_{lim} = 0.56$ or $E_{lim} = 30$ Mev (at $E_{max} = 53.6$ Mev).

Next, integrating (1) to $\epsilon_{lim}$, we get

$$dN \sim (1 + a_s \cos\vartheta)\,d\Omega$$

for $a = -0.33$, and $a_s = +0.07$. Our value, $a_s = -0.02 \pm 0.11$, agrees with the theoretical within experimental error. Thus, the quantitative reduction in angular anisotropy, observed with diminishing electron energies in the $\mu^+ - e^+$ decay, is in agreement with the predictions of the two-component neutrino theory.

The table lists data of five measurements of the angular $\mu - e$ anisotropy in $\pi^+ - \mu^+ - e^+$ decay in propane bubble chambers. We took into account the correction for depolarization (fourth and fifth column), and averaged the parameter a from the five sets of data. In the next to the last line we give the average value of a obtained by Wilkinson[8] from eight investigations in emulsion. There is good agreement between the values of the parameter a obtained in emulsion and in a propane chamber. This indicates, in particular,

| Method | Reference | $A$ | $a$ | $\xi$ | Number of events |
|---|---|---|---|---|---|
| Propane chamber | [11] | $-0.18\pm0.05$ | $-0.27\pm0.08$ | $-0.81\pm0.24$ | 1188 |
| " | [12] | $-0.19\pm0.04$ | $-0.285\pm0.07$ | $-0.85\pm0.20$ | 3500 |
| " | [13] | $-0.16\pm0.03$ | $-0.24\pm0.05$ | $-0.72\pm0.17$ | 3734 |
| " | [14] | $-0.19\pm0.03$ | $-0.285\pm0.05$ | $-0.85\pm0.16$ | 6760 |
| " | Our data | $-0.22\pm0.03$ | $-0.33\pm0.06$ | $-0.99\pm0.17$ | 6670 |
| | Average | $-0.19\pm0.02$ | $-0.28\pm0.03$ | $-0.84\pm0.09$ | 21802 |
| Ilford G-5 emulsion | Average[8] | | $-0.287\pm0.039$ | $-0.87\pm0.12$ | 16000 |
| Average values obtained with emulsions and propane chambers | | | $-0.283\pm0.023$ | $-0.85\pm0.07$ | |

that correct allowance has been made for the depolarization in media. The last line gives the average values of the parameters a and $\xi$ obtained with propane chambers and with emulsions. The parameter a does not exceed the maximum value (with a minus sign) called for by the theory of the two-component neutrino, i.e., $-0.33$, and accordingly $\xi$ does not exceed $-1$.

## 4. ANGULAR DISTRIBUTION IN $\pi^+ - \mu^+$ DECAY

Figure 4 shows a distribution histogram of the projections of the angles between the $\pi^+$- and $\mu^+$-meson momenta for the same 6,670 $\pi^+ - \mu^+ - e^+$ decay events. It is seen that the distribution is isotropic between 0 and 150°. The smaller number of particles in the last angle interval is due to oversights. We have noted that the greater the number of extraneous particles in the chamber, the more oversights occur for decays in which the projection of the angle between the $\pi^+$ and $\mu^+$-meson momenta is close to 180°. If a series of measurements is made with small chamber loading, isotropy is observed over the entire interval of angles, i.e., from 0 to 180°. The distribution of the angles between the $\pi^+$ and $\mu^+$-meson momenta can thus be assumed isotropic.

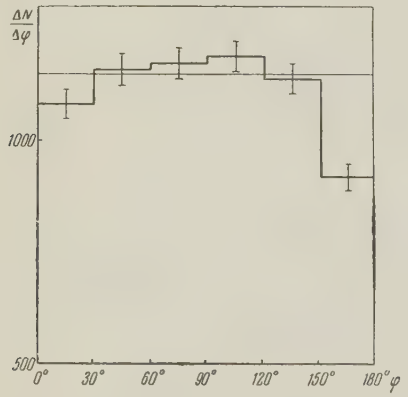


FIG. 4. Angular distribution of $\mu$-meson momenta relative to the $\pi$-meson momentum in $\pi+-\mu+-e+$ decay. The abscissas indicate the projection of the spatial angle between the $\pi$- and $\mu$-meson momenta at the decay point, and the ordinates the number of mesons within the angle interval. The horizontal line represents isotropic distribution. N = 6670.

Since in our case of the momentum of the $\pi^+$ meson did not deviate more than 18° from the beam axis at the end of the range of the $\pi^+$ mesons, it follows from the isotropy in the angular distribution between the $\pi^+$ and $\mu^+$-meson momenta that the distribution of the angles between the momentum of the $\mu^+$ meson and the axis of the beam is also isotropic in $\pi^+ - \mu^+$ decays.

## CONCLUSIONS

1. An increase in angular anisotropy with electron energy is observed in $\mu^+ - e^+$ decay; this increase does not contradict the two-component neutrino theory.

2. The value of the coefficient A in the distribution of the angles between the $\mu^+$-meson and the electron momenta, obtained in the registration of $\pi^+ - \mu^+ - e^+$ decays in a propane chamber, is

$$A = -0.22 \pm 0.03.$$

The value of this parameter, averaged over five investigations in propane chambers, with correction for depolarization, is

$$a = -0.28 \pm 0.03,$$

which agrees with the average values of the parameter, $a = -0.287 \pm 0.039$, obtained in nine emulsion investigations.[8] The average a obtained in both propane and emulsion is

$$a = -0.283 \pm 0.023$$

and correspondingly, the value of $\xi$ is

$$\xi = -0.85 \pm 0.07.$$

3. The angles between the meson momenta are

isotropically distributed in $\pi^+ - \mu^+$ decay.

We take this occasion to thank Professor V. P. Dzhelepov for the opportunity to carry out the experiment with the phasotron of the Joint Institute for Nuclear Research, to B. A. Dolgoshein for useful discussions, to L. A. Kuzin, A. V. Samoilov, and F. M. Sergeev for participating in the processing of the material, and to A. A. Bedniakov for helping in the work with the phasotron.

## APPENDIX

## CONNECTION BETWEEN SPATIAL ANGLE DISTRIBUTION AND THE DISTRIBUTION OF THE PLANE PROJECTIONS OF THE ANGLES IN $\mu - e$ AND $\pi - \mu - e$ DECAYS

### 1. Isotropic Distribution in Projection ($\pi - \mu$ Decays)

Let a beam of particles move in the direction Ox and decay at the point 0, the angular distribution of the decaying particles being isotropic. We then have (Fig. 5)

$$dN = \text{const} \cdot d\Omega = \text{const} \cdot \sin\theta \, d\theta \, d\varphi.$$

In observing the decay along the z axis, i.e., in projecting the spatial distribution on the XY plane, we fix the projection of the spatial angle $\vartheta$ between the initial direction Ox and the momentum of the particle OA. Here the projection of the angle $\vartheta$ coincides with the angle $\varphi$. The observer, so to speak, integrates over the angle

$$dN(\varphi) = \text{const} \cdot d\varphi \int_0^\pi \sin\theta \, d\theta = 2\,\text{const} \cdot d\varphi = \text{const} \cdot d\varphi.$$

Consequently, we also have an isotropic angular distribution in the projection.

### 2. Distribution $dN \sim (1 + a\cos\vartheta)\,d\Omega$ In Projection on a Plane ($\mu - e$ Decays).

The distribution of the momenta of the decaying particles about Ox is now expressed by the formula

$$dN \sim (1 + a\cos\vartheta)\, d\Omega.$$

The problem consists of expressing this distribution in terms of the projection of the angle $\vartheta$ on the plane XY, i.e., in terms of $\varphi$ (see Fig. 5).

It is easy to show that the connection between the angles, $\theta$, $\varphi$, and $\vartheta$ is given by

$$\sin\theta\cos\varphi = \cos\vartheta.$$

Inserting this expression into the formula for the distribution over $\vartheta$ and integrating again over $\theta$, we get

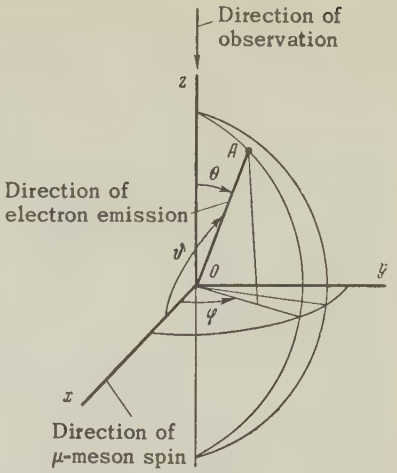


FIG. 5

$$dN(\varphi) \sim \int_0^\pi (1 + a\sin\theta\cos\varphi)\sin\theta \, d\theta \, d\varphi$$

$$= 2[1 + (a\pi/4)\cos\varphi]\, d\varphi,$$

$$dN(\varphi) \sim [1 + (a\pi/4)\cos\varphi]\, d\varphi.$$

### 3. Distribution $dN \sim (1 + a\cos\vartheta)\,d\Omega$ in Plane Projection, Subject to the Condition that the Direction from which $\vartheta$ is Measured is Isotropically Distributed in Space ($\pi - \mu - e$ Decays)

The problem is as follows: The $\pi$ meson moves along Ox, and the decay $\mu$ mesons are emitted isotropically. The momenta of the decay electrons have a spatial distribution $dN \sim (1 + a\cos\theta')\,d\Omega$ relative to the direction of the $\mu$ meson (see Fig. 6). The observer sees the pic-

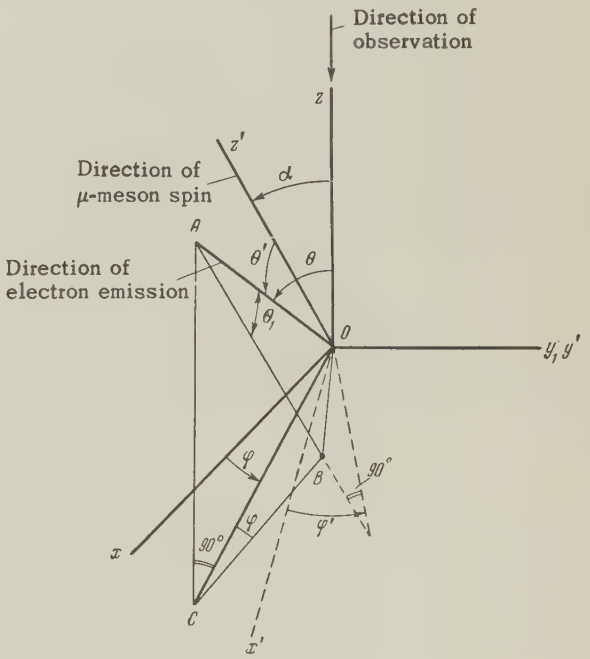


FIG. 6

ture in the XY plane. It is required to find the distribution of the projections of the spatial angles $\theta'$ relative to the projection of the $\mu$-meson momentum on the XY plane.

Since we always measure the projection of the angle between the meson and the electron, we can consider the projection of the momentum of the meson to be directed at all times along Ox (the $\mu$ meson moves in the ZX plane), and we have the picture shown in Fig. 6.

In $x'y'z'$ coordinates the electron distribution is

$$dN = \text{const} \cdot (1 + a\cos\theta')\, d\Omega.$$

But now the momentum of the $\mu$ meson makes an angle $(90 - \alpha)$ with the plane of observation.

It is necessary to find the connection between the angles $\alpha$, $\varphi$, $\theta$, and $\theta'$. Then, integrating over the corresponding angles (taking into account the isotropic distribution of the $\mu$-meson momenta in space), we find the dependence of the electron emission on the angle $\varphi$. This dependence is of the form

$$\cos\theta' = \sin\theta\sin\alpha\cos\varphi + \cos\theta\cos\alpha.$$

Putting AO = a, AB = b, CB = c, OC = d, and AC = f, and noting that $\angle \text{OAD} = \theta'$ and $\angle \text{OCB} = \varphi$, we write for OB

$$a^2 + b^2 - 2ba\cos\theta' = c^2 + d^2 - 2cd\cos\varphi,$$

where

$$b = f/\cos\alpha = a\cos\theta/\cos\alpha;$$

$$c = f\tan\alpha = a\cos\theta\tan\alpha;\quad d = a\sin\theta.$$

Solving this equation with respect to $\cos\theta'$, we obtain the relation given above between the angles $\alpha$, $\varphi$, $\theta$, and $\theta'$. It must be noted that the angle $\alpha$ assumes values from 0 to $\pi$ and, in addition, we assume an isotropic distribution of the $\mu$-meson momenta in space. To take this factor into account we must multiply the entire distribution by $\sin\alpha$:

$$dN = \text{const} \cdot [1 + a(\cos\theta\cos\alpha + \sin\theta\sin\alpha\cos\varphi)]\sin\alpha\, d\alpha\, d\Omega,$$

where $d\Omega = \sin\theta\, d\theta\, d\varphi$. Here the angles $\alpha$ and $\theta$ vary from 0 to $\pi$. Integrating over $\theta$ and $\alpha$ we get

$$\int_0^\pi\int_0^\pi \sin\alpha\sin\theta\, d\theta\, d\varphi = 4;$$

$$a\int_0^\pi\int_0^\pi \cos\theta\cos\alpha\sin\theta\sin\alpha\, d\theta\, d\alpha = 0;$$

$$a\cos\varphi\int_0^\pi\int_0^\pi \sin\theta\sin\alpha\sin\theta\sin\alpha\, d\theta\, d\alpha = (a\pi^2/4)\cos\varphi,$$

i.e.,

$$dN \sim [1 + (\alpha\pi^2/16)\cos\varphi]\, d\varphi.$$

[1] T. D. Lee and C. N. Yang, Phys. Rev. **105**, 1671 (1957).

[2] L. D. Landau, J. Exptl. Theoret. Phys. (U.S.S.R.) **32**, 407 (1957), Soviet Phys. JETP **5**, 336 (1957).

[3] A. Salam, Nuovo cimento **5**, 299 (1957).

[4] B. F. Touchek, Nuovo cimento **5**, 754 (1957).

[5] Kotenko, Popov, and Kuznetsov Приборы и техника эксперимента (Instr. and Meas. Engg) No. 1, 1957, p. 36.

[6] Alikhanian, Kirillov-Ugriumov, Kotenko, Kuznetsov, and Popov, J. Exptl. Theoret. Phys. (U.S.S.R.) **34**, 253 (1958), Soviet Phys. JETP **7**, 176 (1958).

[7] Chadwick, Durrani, Eisberg, Tones, Wignall, and Wilkinson, Phil. Mag. **2**, 684 (1957).

[8] D. H. Wilkinson, Nuovo cimento **6**, 517 (1957).

[9] Barley, Coffin, Garwin, Lederman, and Weinrich, Bull. Am. Phys. Soc. Ser. II **2**, 205 (1957).

[10] Swanson, Campbell, Garwin, Sens, Telegdi, Wright, and Yovanovich, Bull. Am. Phys. Soc. Ser. II **2**, 205 (1957).

[11] Pless, Brenner, Williams, Barrari, Hildebrand, Milburn, Ramsey, Shapiro, Strauch, Street, and Young, Report of the 1957 Rochester Conference.

[12] S. C. Wright, Report of the 1957 Rochester Conference.

[13] Aliston, Evans, Morgen, Newport, Williams, and Kirk, Phil. Mag. **2**, 1143 (1957).

[14] Barmin, Kanavets, Morozov, Pershin, J. Exptl. Theoret. Phys. (U.S.S.R.) **34**, 830 (1958), Soviet Phys. JETP **7**, 573 (1958).

Translated by J. G. Adashko
230

# OBSERVATION OF DECAYS OF CHARGED PARTICLES IN A DOUBLE CLOUD CHAMBER*

Z. Sh. MANDZHAVIDZE, N. N. ROINISHVILI, and G. E. CHIKOVANI

Physics Institute, Academy of Sciences, Georgian S.S.R. Tbilisi State University

Submitted to JETP editor April 19, 1957

J. Exptl. Theoret. Phys. (U.S.S.R.) **34**, 1110-1115 (May, 1958)

The authors analyze ten events, observed in a cloud chamber, of the decay of unstable charged particles produced in penetrating showers by cosmic rays at an altitude of 1800 meters above sea level. The $V^{\pm}$ decays are divided into two groups, depending on the place of generation. The upper limit of the mean lifetime for one of these groups is estimated to be $\tau \leq (1.44 \pm 0.83) \times 10^{-10}$ seconds. An analysis is proposed for one anomalous decay, which cannot be explained on the basis of any of the K-particle or hyperon decay schemes existing at present.

1. The first to estimate the lifetime of charged $V^{\pm}$ particles was Barker,[1] who has shown, that the lifetime of the decaying particles lies in the range $10^{-8} \geq \tau \geq 10^{-9}$ seconds. Further investigations[2-4] have shown that $V^{\pm}$ events contain both a long-lived K component with a lifetime longer than $10^{-9}$ seconds, as well as a short-lived one, on the order of $10^{-10}$ seconds.

Jork et al.,[2] using two cloud chambers with an absorber placed between them, obtained a uniform distribution of the decay points, with an average ratio $x/x_0 = 0.46 \pm 0.05$, for the charged particles produced in a generator placed over the chambers. On the other hand, the decays connected with the interaction in the middle absorber gave a clearly pronounced asymmetry with a ratio $x/x_0 = 0.31 \pm 0.05$. These data have led the authors to conclude the existence of a short-lived component with a lifetime in the interval $1.5 \times 10^{-10} \leq \tau \leq 2.8 \times 10^{-10}$ sec. The presence of protons[2,5] among the products of the short-lived component indicates, in the authors' opinion, the presence of hyperons among the decaying particles. However, in some cases it was possible to identify decays of lighter particles, making it difficult to attribute the short-lived components to decays of hyperons alone. Later investigations made by the same group[6] and carried out under somewhat different conditions, have not confirmed the preceding results, which apparently are explained by the impossibility of observing decays in the direct vicinity of the generator in this series of experiments.

Thompson[4] et al. also found a short-lived component with a decay point near the upper wall of the chamber, and a long-lived component with uniform distribution of events. In this experiment, unlike in those of Jork et al,[2] negative particles predominate in the short-lived components.

2. In this work we analyzed ten events of decay of heavy charged particles, observed with a setup similar to that of Jork.[2] The observations were made at the El'brus High-Altitude Cosmic Laboratory, 1800 meters above sea level. The apparatus consisted of a rectangular double cloud chamber[7] placed in a magnetic field. The principal diagram of the setup is shown in Fig. 1.

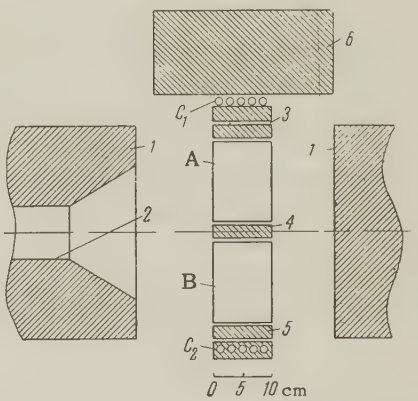


FIG. 1. Principal diagram of apparatus: A, B – working chambers; $C_1$ and $C_2$ – Geiger-Müller counters; 1 – poles of electromagnets, 2 – opening for photography, 3, 4, 5, 6 – absorber.

The cloud chamber combines in one housing two independent working chambers each 280 × 100 × 110 mm, and three absorber compartments, isolated from the working chambers. The chamber was filled with argon to a pressure of 1,000 mm

*Delivered at the Conference on Cosmic Ray Physics, Tbilisi, October, 1956.

TABLE I. Data for Ten Events of Decay of V Particles

| Number of event | Momentum of primary particle, $P_1(10^9$ ev/c) | Momentum of secondary particle, $P_2(10^9$ ev/c) | Ionization of primary particle, $(J/J_0)_1$ | Ionization of secondary particle $(J/J_0)_2$ | Aperture angle $\theta°$ | Sign |
|---|---|---|---|---|---|---|
| 82,179 | Not measured | $1.72^{+0.88}_{-0.44}$ | 1 | 1 | 76 | + |
| 92,98 | " | $3.60^{+2.30}_{-1.02}$ | <1.5 | 1 | 60 | + |
| 101,14 | " | Not measured | 2—4 | 1 | 42 | ? |
| 105,90 | " | $1.09^{+0.04}_{-0.04}$ | 15—20 | 1 | 107 | + |
| 101,76 | " | Not measured | <1.5 | <1.5 | 31 | ? |
| 115,115 | " | $1.07^{+0.23}_{-0.16}$ | >6 | 1 | 124 | — |
| 117,61 | " | $3.52^{+0.94}_{-0.61}$ | >20 | <1.5 | 95 | + |
| 117,85 | " | $0.62^{+0.04}_{-0.04}$ | 1 | 1.5—3 | 25 | — |
| 132,12 | " | $1.43^{+0.32}_{-0.32}$ | 1 | 1 | 86 | — |
| 147,69 | $5.78^{+3.10}_{-1.49}$ | $2.59^{+1.60}_{-0.72}$ | <1.5 | 1 | 28 | — |

Hg. The condensate employed was a mixture of 70% ethyl alcohol and 30% water. The working chambers were illuminated from both directions with IPS-1500 photoflash lamps. The tracks were photographed on "Panchrom 10-800" film with two "Helios-42" objectives at an effective aperture of 10. The base of the photograph is 42.8 mm, and the average magnification is 15. The chamber is controlled by penetrating showers, sorted out by a system consisting of two series of Geiger counters, connected for 1 — 4 coincidence. The showers were generated in absorbers 55 and 25 mm thick located correspondingly over the working volumes of the chamber. To shield against the soft-component, the entire setup was covered with an absorber 160 mm thick.

Copper absorbers were used in one series of experiments, and lead was used in the other.

A magnetic field was produced with a type SP-13 electromagnet with stabilized supply.[8] The field intensity in the working volume of the chamber was approximately 4300 oersted with no more than 5% deviation.

3. After 2836 hours of operation, 11,559 photographs with records of 2269 penetrating showers were obtained. Ten fork-like tracks, which could be interpreted as V decays were observed in these photographs. In addition, we found 22 $V^0$ decays, a $\tau^+$-meson decay, decays of two $\pi$ mesons in flight, and 13 stars in the gas of the chamber. The sorted $V^{\pm}$ decays were thoroughly checked for the presence of a common peak for the two tracks and for the absence of a recoil nucleus at the bend. The momenta and the arrangements of the tracks were determined by the coordinate method,[9,10] used in our laboratory during the past few years. The rms error in the curvature of tracks 10 cm long was 48 $m^{-1}$, corresponding to a maximum measured momentum of 6 Bev/c. The error in the depths of the points of the track was ±1.4 mm. The error in the angle between the tracks was not more than 3 to 4°. The ionizing ability of the particles was estimated by measuring the optical density of the tracks with a microphotometer. Unity blackening was taken to be the optical density of tracks of relativistic particles located in the same frame. The measured momenta and angles, and estimates of the ionization, are given in Table I.

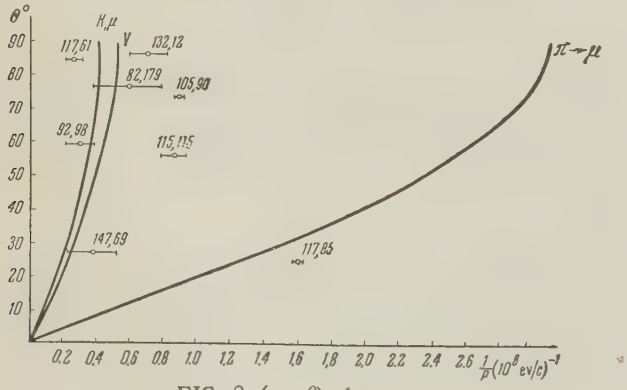


FIG. 2. ($p_2$, $\theta$) plot.

Since the momenta of the decaying particles cannot be measured, in most cases, owing to the short length of the tracks, it is impossible to carry out a complete analysis of each event. Nevertheless, some information can be gained from the dynamics of the decay and from the ionization measurements.

If $p^*_{max}$ is the maximum value of the momentum of the decay product in the rest system, and $p_t$ is the transverse component of the momentum, then it follows from the relation $p_t \leq p^*_{max}$ that

$$1/p_2 \geqslant \sin\theta / p^*_{max}, \qquad (1)$$

where $\theta$ is the emission angle and $p_2$ is the mo-

mentum of the charged product in the laboratory system.

Figure 2 gives the limit curves obtained from (1) for various decay schemes and from the $(p_2, \theta)$ plot of the observed decays, with the exception of two unmeasured events. All decays, with the exception of 117,61, lie within the allowed region for hyperons and K mesons, within the experimental error. Decay of the $\pi$ meson is excluded in event 117,85, since at the observed momentum and emission angle of the secondary particle, the $\pi$ meson should be at least triply ionized. Only one event, namely 147,69, for which the momenta of both tracks could be measured, can reliably be interpreted as a K-meson decay; it is impossible to distinguish between K and Y decays in the remaining cases. It must be noted that not one proton was observed among the decay products.

It is difficult to explain event 117,61, which lies outside the allowed region for Y and K decays, on the basis of experimental error. It will be analyzed separately in Sec. 5.

4. The $V^{\pm}$ decays can be divided into two groups in accordance with the character of their production.

The six relativistic particles, comprising the first group, are accompanied by penetrating showers from the upper and middle absorbers. This group of events features minimum ionization by the primary particles and decay points that are distributed near the generator.

The second group consists of four slow highly-ionized particles which are not connected with visible interaction and which enter into the illuminated portion of the chamber from the side of the electromagnet poles; they are apparently generated far away from the decay point.

The distribution of the decay points of the particles of the first and second group is shown in Figs. 3 and 4. The corresponding real and virtual

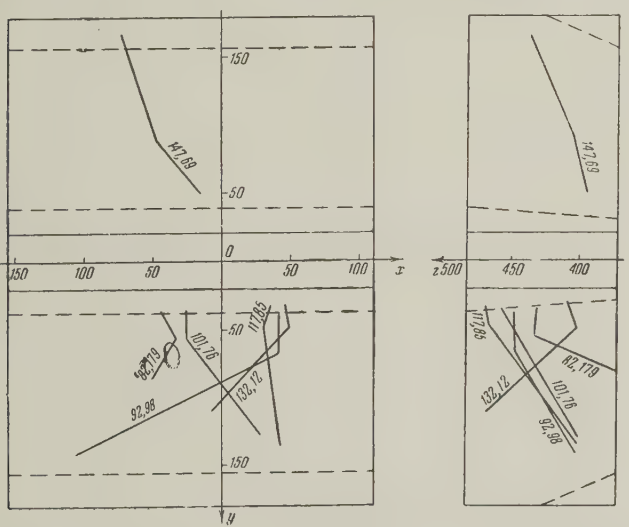


FIG. 3. Distribution of the decays of the first group in the chamber. The origin coincides with the optical center of one of the objectives. The distances are in millimeters.

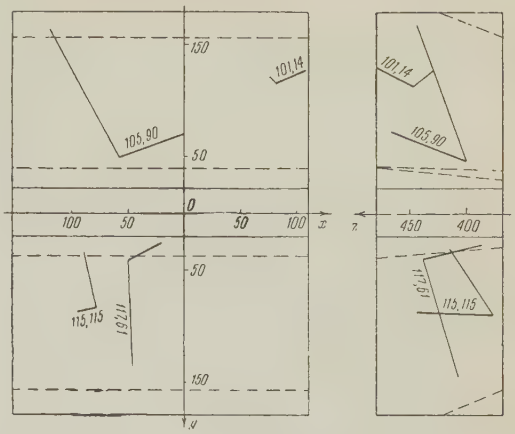


FIG. 4. Distribution of the decays of the second group in the chamber.

ranges are given in Tables II and III. The mean values of the ratios of the real ranges to the virtual ones is 0.30 for the particles of the first group, and 0.64 for the particles of the second group.

TABLE II. Real and Virtual Ranges of Particles Accompanied by Showers from the Upper and Middle Absorber

| Number of event | Real range x, cm | Virtual range $x_0$, cm | $x/x_0$ |
|---|---|---|---|
| 82,179 | 2.7 | 14.1 | 0.19 |
| 92,98 | 4.0 | 13.4 | 0.30 |
| 101,76 | 2.3 | 11.6 | 0.20 |
| 117,85 | 2.0 | 14.6 | 0.16 |
| 132,12 | 2.5 | 6.7 | 0.37 |
| 147,69 | 9.1 | 15.4 | 0.59 |

The difference in the distribution of the decay points and in the ionization indicates a shorter lifetime for the first group of particles. Starting with minimum ionization of the primary particles, it is possible to determine the upper limit of the lifetime, assuming that their velocities are $\beta \geq 0.7$, i.e., ionization of not more than a multiple of 1.5. Calculation by the maximum probability method,[11]

TABLE III. Real and Virtual Ranges of Particles Without Visible Shower Accompaniment

| Number of event | Real range x, cm | Virtual range $x_0$, cm | $x/x_0$ |
|---|---|---|---|
| 101,14 | 4.7 | 13.8 | 0.34 |
| 105,90 | 9.5 | 12.9 | 0.74 |
| 115,115 | 7.3 | 7.7 | 0.94 |
| 117,61 | 6.2 | 11.1 | 0.56 |

based on this assumption, shows that the average lifetime of the particles of the first group is

$$\tau \leqslant (1.44 \pm 0.83) \cdot 10^{-10} \text{ sec.}$$

If an attempt is made to attribute our relatively short mean lifetimes to the structural features of the cloud chamber, features which made it possible to observe particles in the nearest vicinity of the middle absorber, it becomes advisable to consider separately the five particles coming from this absorber. By so doing, we eliminate event 147,69 from the first group, which we identified as a K-meson decay. The average real to virtual range ratio for particles generated in a middle absorber is 0.23. The probability of effecting such a selection from uniform distribution is less than 0.24%. The average lifetime calculated under the assumption $\beta \geq 0.7$ does not exceed

$$\tau \leqslant (1.00 \pm 0.54) \cdot 10^{-10} \text{ sec.}$$

5. Event 117,61 is of particular interest.

As indicated in Section 3, in the $(p_2, \theta)$ plot decay 117,61 lies outside the allowed region for hyperons, K-mesons and $\pi$ mesons (see Fig. 2). We consider it therefore necessary to analyze this case in detail.

A slow particle, with ionization not less than a multiple of 20, without visible accompaniment of nuclear interaction, enters into the chamber from the forward side. Without experiencing noticeable scattering, it decays in the well-illuminated region into a like charged particle having minimum ionization. The charged decay product is emitted at an angle of 95° to the direction or motion of the primaries and has a momentum $352^{+94}_{-61}$ Mev/c. The momentum of the transverse component, in this case 351 Mev/c, is substantially less than the maximum momentum of the decay product in the proper system for all known decay schemes of hyperons and K mesons. In fact, at a given positive-particle momentum and a given emission angle, the negative product can be not more than triply ionized for all three schemes, although the ionization observed is more than by a factor of 20.

The anomaly of this case is difficult to attribute to the experimental errors. The track of the secondary particle is 10 cm long and has a smooth curvature. Since it passes near a cloud cluster, we measured several tracks of hard $\mu$ mesons without a magnetic field, passing through similar photography defects. Measurements have shown that these clusters do not lead to track distortion.

The measured momenta could not be sensitive to systematic errors in the measurement of the curvature, since such errors amount to 0.03 $m^{-1}$ in our chamber. To attribute this event to K-meson decay it becomes necessary to assume errors equal to three standard deviations, an assumption having a probability of 0.3%.

All this gives ground for assuming that in this case the decaying particle is heavier than a K meson. It is possible to assume that this case is a charged analogue of the neutral meson, whose decay was observed by Cowan.[12]

We have included a photograph of this event in an earlier preliminary report.[13]

The authors consider it their duty to thank Professor E. L. Andronikashvili for supervision of this work, and also to thank the Associates of the Tbilisi State University, L. D. Gedevanishvili and E. I. Tsagareli, and to R. I. Dzidziguri, A. I. Tsintsabadze, and V. D. Tsintsadze of the Institute of Physics, who participated in this work.

[1] Barker, Butler, Sowerby, and York, Phil. Mag. **43**, 1201 (1956).

[2] York, Leighton, and Bjornerud, Phys. Rev. **95**, 159 (1954).

[3] Buchanan, Cooper, Millar, and Newth, Phil. Mag. **45**, 1025 (1954).

[4] Kim, Burwell, Huggett, and Thompson, Phys. Rev. **96**, 229 (1954).

[5] York, Leighton, and Bjornerud, Phys. Rev. **90**, 167 (1953).

[6] G. H. Trilling and R. B. Leighton, Phys. Rev. **100**, 1468 (1955).

[7] Z. Sh. Mandzhavidze and G. E. Chikovani, Приборы и техника эксперимента (Instr. and Meas. Engg) No. 6, 1957, p. 30.

[8] Z. Sh. Mandzhavidze and G. E. Chikovani, Приборы и техника эксперимента (Instr. and Meas. Engg.), No. 3, 1957, p. 69.

[9] Mandzhavidze, Roinishvili, et al. Тр. Ин-та физики АН ГрузССР (Trans. Phys. Inst. Acad. Sci. Georgian S.S.R.) **3**, 15 (1957).

[10] Dzidziguri, Kotliarevskii, et al., Вестник АН ГрузССР (Bull. Acad. Sci. Georgian S.S.R.) **19**, 143 (1957).

[11] H. S. Bartlett, Phil. Mag. **44**, 249 (1953).

[12] E. W. Cowan, Phys. Rev. **94**, 161 (1954).

[13] Mandzhavidze, Roinishvili, and Chikovani, J. Exptl. Theoret. Phys. (U.S.S.R.) **33**, 303 (1957), Soviet Phys. JETP **6**, 263 (1958).

Translated by J. G. Adashko
231

# *INVESTIGATION OF THE THERMAL PROPERTIES OF SUPERCONDUCTORS. II*

N. V. ZAVARITSKII

Institute for Physical Problems, Academy of Sciences, U.S.S.R.

Submitted to JETP editor October 21, 1957; resubmitted January 29, 1958

J. Exptl. Theoret. Phys. (U.S.S.R.) **34**, 1116-1124 (May, 1958)

The specific heat, thermal and temperature conductivity of aluminum and zinc have been measured between 1.5 and 0.15°K by the temperature wave method described in Ref. 1. Results of measurement of the normal-state specific heat are identical with those obtained at higher temperatures. The temperature dependence of the electron specific heat in the superconducting state is given by Eq. (2), where $\alpha = 1.2$ for Al and $\alpha = 1.03$ for Zn. The heat conductivity of electrons in a superconductor also depends exponentially on the ratio $T_k/T$. In this case, in contrast to the electrons of normal metals, $K_{es}/c_{es}$ depends on the temperature. The results obtained are compared with the results of measurement of the specific heat of other superconductors and with the results of the microscopic theory of superconductivity.[2,3]

RECENTLY, it has been shown in a series of papers[1,4-7] that the specific heat of electrons in a superconductor depends exponentially on $T_k/T$. However, it is still not clear whether this dependence is general for all superconductors, and whether one can speak of a law of corresponding states for their properties. To clarify these questions, a study was undertaken of the thermal properties of aluminum and zinc — metals which possess relatively low temperatures of transition to the superconducting state.

A study of these metals is also of interest from the viewpoint of the possibility of direct measurement of the specific heat and thermal conductivity of electrons. Thus, while in tin the specific heat of the electrons at the critical temperature amounts to only about 60% of the total specific heat, in aluminum and zinc it amounts to 98%.

The method of measurement was not fundamentally different from that used to investigate the thermal properties of tin.[1] The thermal conductivity and the thermometric conductivity $a^2 = K/c\rho$ were determined by direct measurements, from which the specific heat was calculated. Cylindrical specimens with diameters of about 1.5 mm and length 100 mm were employed. The zinc samples were single crystals, grown in thin glass capillaries. The angle between the (001) direction and the axis of the sample was about 30°. The aluminum crystals consisted of large crystals with the length of the sample equal to several times the diameter. Before the investigation, the aluminum was annealed in a vacuum at ~600°C for 4 hours.

The results of the direct measurement of the thermal and thermometric conductivities are shown in Figs. 1 – 4. Experiments with each of the specimens were carried out over a period of several days. The mean spread of the results amounted to 10 and 4%, respectively, for the thermal and temperature conductivities. On lowering the temperature to 0.2°K and in the region of a strong dependence of the thermal conductivity on the temperature, the accuracy of the determination of the thermal conductivity was decreased. This condition was connected with the fact that at reduced absolute temperature the errors in its determination increased, reaching 3 – 4% near 0.2°K. In the

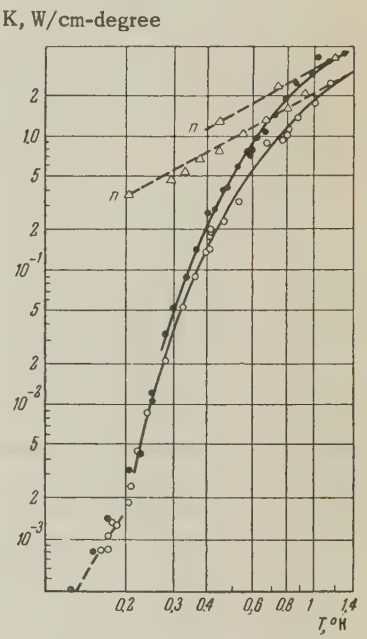


FIG. 1. Thermal conductivity of aluminum. ● – Al-1; o – Al-2; n – thermal conductivity in the normal state, △ – measurements in a magnetic field.

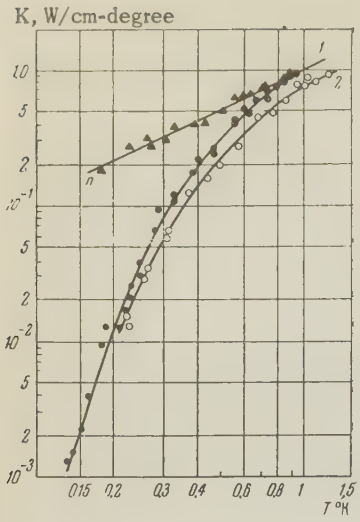


FIG. 2. Thermal conductivity of zinc. 1 – Zn-1; 2 – Zn-2; ▲ – measurements in a magnetic field.

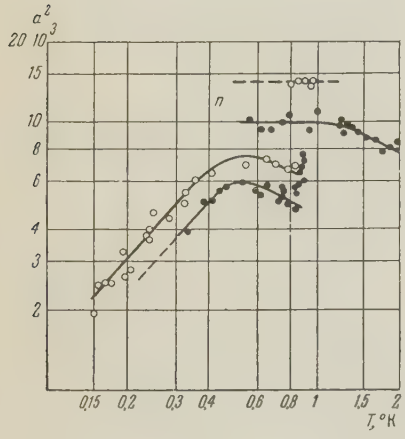


FIG. 4. Temperature conductivity of zinc. ○ – Zn-1, ● – Zn-2; n – normal state.

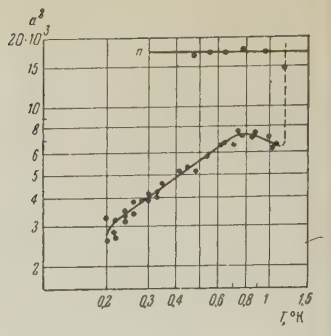


FIG. 3. Temperature conductivity of aluminum. Sample Al-2; n – normal state.

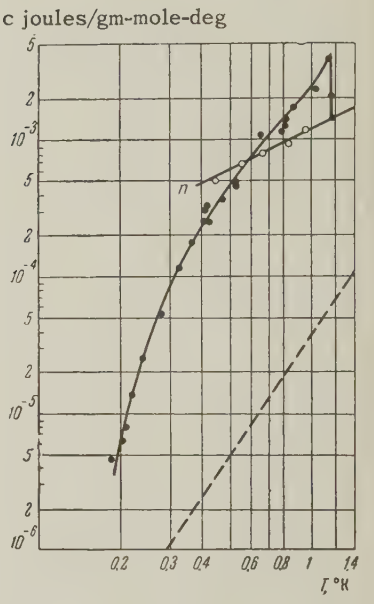


FIG. 5. Specific heat of aluminum; n – normal state, dashed line – lattice specific heat.

case of a strong change in the thermal conductivity with temperature, this is equivalent to the presence of a several times larger error in the magnitude of the thermal conductivity also.[1] Since such errors are determined in fact by the accuracy of establishing the absolute temperature, they always impose a certain limit on the determination of the temperature dependence of physical quantities beyond the dependence on the methods of their determination.

Measurements of the specimens in the superconducting state were carried out in a magnetic field which was compensated to 0.2 oersted. As in the investigation of the properties of tin, control experiments showed that the results were independent of whether the transition from the normal to the superconducting state took place in this same magnetic field or in a field ~ 10 oersted, perpendicular to the axis of the specimen. In the normal state, at temperatures below critical, measurements were carried out in a field parallel to the axis of the specimen and amounting to 115 oersted for Al and 60 oersted for Zn.

The specific heat of aluminum is shown in Fig. 5. The calculation was carried out in terms of the thermal and thermometric conductivities of the sample Al-2. The plotted points were obtained by calculation on the curve of Fig. 3, and from the results of measurement of the thermal conductivity of Fig. 1. The specific heat of zinc is plotted in Fig. 6. Calculations were carried out on the curves of Figs. 2 and 4 for each of the samples studied; the results led to numbers agreeing within the limits of error (~10%).

## DISCUSSION OF THE RESULTS

### Specific Heat

We first consider the results of the measurement of the specific heat in the normal state. As is well known, for sufficiently low temperatures, the specific heat of metals can be represented as

$$c_n = \gamma T + 1944\,(T/\Theta)^3 \quad \text{joule/g-mole-degree}, \qquad (1)$$

where $\Theta$ is the Debye temperature. The first term is due to the specific heat of the electrons, the second is due to the specific heat of the lattice. The value of the linear term for Al and Zn, ob-

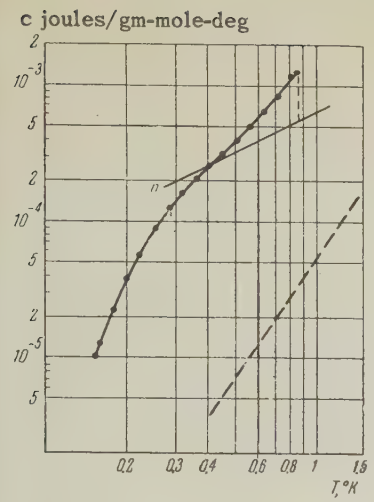


FIG. 6. Specific heat of zinc; n – normal state, dashed line – lattice specific heat.

tained on the basis of our measurements, is shown in Table I. For Zn, this value agrees, within experimental error, with the results of measurement at temperatures above 1.5°K; for aluminum, it is somewhat smaller than the literature value, although the deviation is also at the limit of the accuracy of measurement.

The thermometric conductivity $a^2$ of zinc in the normal state changes with temperature, as is seen from Fig. 4. Evidently this is connected with the specific heat of the lattice. Actually, since the thermal conductivity of metals is directly proportional to the temperature, we have

$$a^2 = D/(1 + qT^2),$$

where D is a constant and $q = 1944/\gamma\Theta^3$. Analysis of the resultant data shows that $q = 0.07 \pm 0.02$ for Zn; this corresponds to $\Theta = 340 \pm 20°$. This value of $\Theta$ agrees within experimental error with the results of measurement for temperatures above 1.5°K (see Table I). All these results are of interest from the point of view of confirming the validity of Eqs. (1) down to temperatures ~0.5°K.

**TABLE I.** Characteristics of metals studied

| Sample | Per cent impurity | Results of measurement | | Literature values | | Reference |
|---|---|---|---|---|---|---|
| | | $\gamma\cdot10^3$, j/g-mole-deg$^2$ | $K_0$, W/cm-deg$^2$ | $\gamma\cdot10^3$, j/g-mole-deg$^2$ | $\Theta$,°K | |
| Al-1 | 0.01 | | 3.02±0.08 | 1.44±0.05 | 408 | [8] |
| Al-2 | 0.01 | 1.27 ±0.1 | 2.17±0.08 | 1.37±0.05 | 375 | [9] |
| | | | | 1.40±0.07 | | [5, 12] |
| Zn-1 | 0.0001 | 0.67 ±0.04 | 1.02±0.05 | 0.654 | 321 | [10] |
| Zn-2 | 0.0001 | 0.645±0.04 | 0.75±0.04 | 0.66 | 296 | [11] |

Earlier investigation[1] of the thermal properties of tin has shown that in the transition to the superconducting state only the specific heat of the electrons undergoes a significant change; the specific heat of the lattice remains practically unchanged. This allows us, by making use of data of the specific heat of the lattice in the normal state, to estimate its contribution to the total specific heat, and to separate the specific heat associated with the electrons. For both aluminum and zinc, the lattice specific heat is a relatively small quantity, not exceeding 10% of the total specific heat in the entire interval.

The transition of the metal into the superconducting state is accompanied by a discontinuity in the specific heat $\Delta c$. The relative magnitude $\Delta c/c_n(T_k)$ of the discontinuity can be determined from a measurement of the thermometric conductivity for the critical temperature. Specifically, inasmuch as the heat conductivity in the normal and superconducting states are the same at $T_k$,

$$\Delta c / c_n(T_k) = (a_n^2 - a_s^2)/a_s^2.$$

Analysis of the results of the measurement (Figs. 3 and 4) show that $\Delta c/c_n(T_k) = 1.60 \pm 0.15$ for Al and $\Delta c/c_n(T_k) = 1.25 \pm 0.15$ for Zn. These values practically coincide with the values of $\Delta c/\gamma T_k$ for Al and Zn, since the specific heat of the lattice in these cases amounts to less than 3% of the total specific heat (at $T_k$).

The dependence of the specific heat of the electrons $c_{es}$ on $T_k/T$ is plotted in semilogarithmic scale in Fig. 7. For $T < 0.7\ T_k$, it can be writ-

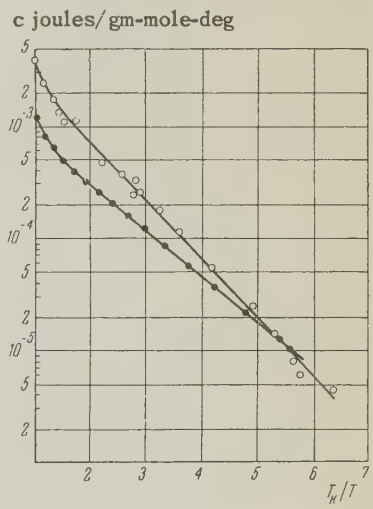


FIG. 7. Specific heat of electrons: o – aluminum, ● – zinc.

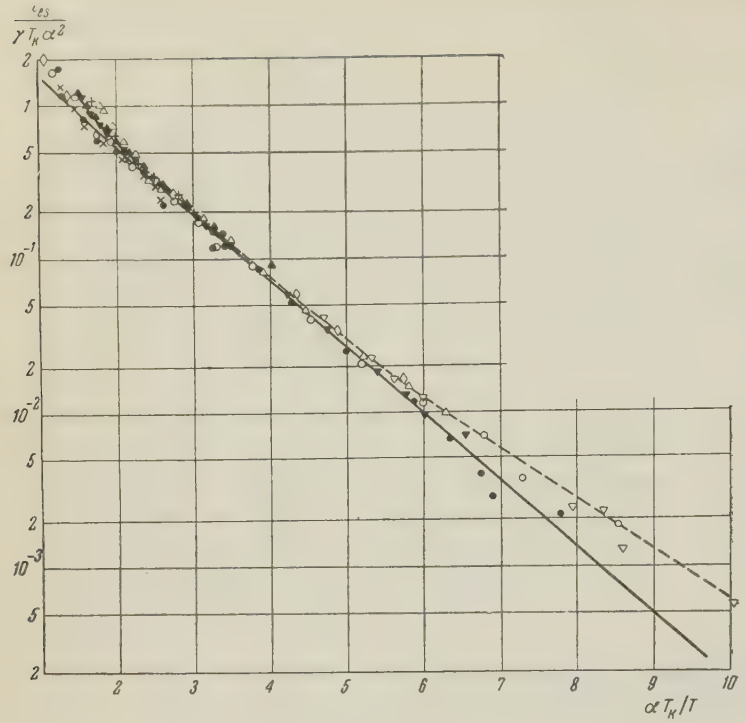


FIG. 8. Specific heat of electrons in superconductors. △ – Nb; ▼ – V; ▲ – Ta; + – In; × – Tl; ◊ – Zn; ---, ▽ – Sn; ●, ○ – Al (---, ● – measurements of author; ▽, ○ – measurements of Goodman[12]). Solid line – Eq. (2). Values of $\gamma$, $T_k$, $\alpha$ are given in Table II.

ten as

$$c_{es} = A \exp(-\alpha T_k / T),$$

where $A = (8.2 \pm 1) \times 10^{-3}$ joule/gram-mole-degree, $\alpha = 1.20 \pm 0.08$ for Al and $A = (2.3 \pm 0.3) \times 10^{-3}$ joule/gram-mole-degree, $\alpha = 1.03 \pm 0.08$ for Zn, under the assumption of $T_k = 1.17°K$ for Al and $T_k = 0.84°K$ for Zn (the errors in A and $\alpha$ are functionally related). The value of $\alpha$ obtained for Al differs somewhat from the value of 1.28 established by Goodman[5] by analyzing the results of direct calorimetric measurements of the specific heat of Al down to 0.25°K; however, new data by Goodman[12] also agree better with $\alpha = 1.20$ (see Fig. 8). There is a systematic deviation of about 10% in the absolute magnitude between the results obtained and the data of Goodman (see Table I).

The exponential dependence of the specific heat of the electrons, which was first discovered in vanadium, is also observed in tin, aluminum, and zinc. Probably, this dependence is a characteristic of all superconductors. However, the quantity $\alpha$, which determines the dependence of $c_{es}$ on the relative temperature, changes from one metal to another. By the same token, if a law of corresponding states is established for the specific heat of superconductors, the quantity $\alpha$ ought to appear in it along with $\gamma$ and $T_k$.

From this point of view, we have analyzed all the results of the investigations which are suitable for the determination of the dependence of $c_{es}$ on $T_k/T$ in a sufficiently wide temperature range, in particular, for Nb, V, Ta, Sn, In, Tl, Al, and Zn. In all these metals, there exists a clearly delineated region of exponential dependence of $c_{es}$ on $T_k/T$. In this region, in first approximation,

$$c_{es} = 4\gamma T_k \alpha^2 \exp(-\alpha T_k / T). \qquad (2)$$

The values of $\gamma$, $T_k$, $\alpha$ are given in Table II. Thus, while the absolute values of $c_{es}$ in the various superconductors at $T_k$ differ by as much as a factor of 500, the expression $c_{es}/\gamma\alpha^2 T_k$ does not change by more than ~10% (Fig. 8). This variation can be ascribed in significant measure to errors in the determination of $\gamma$, $c_{es}$, $\alpha$. Of course, the presence of a general relation among $c_{es}$, $\gamma$, $T_k$, $\alpha$ for all superconductors is due to the thermodynamic connection between the thermal properties in the normal and superconducting states of the metal. We note that deviations from a simple exponential law (2) possibly exist not only close to the critical temperature for $T > 0.7\ T_k$, but also in the region of very low temperatures,[1] for $T < 0.2\ T_k$ (see Fig. 8).

The difference in the dependence of the thermal properties of superconductors on the relative temperature $T/T_k$ is defined by the quantity $\alpha$. This quantity changes from one superconductor to another in a systematic manner. It is likely that some sort of relation exists between $\alpha$ and $T_k/\Theta$ of the superconductor (Fig. 9a), although the small number of metals for which $\alpha$ can be compared makes this conclusion not very trustworthy. Close

TABLE II. Characteristics of thermal properties of superconductors

| Metal | $\gamma \cdot 10^3$, j/g-mole-deg | $\Theta$,°K | $T_k$,° K | $\alpha$ | Reference |
|---|---|---|---|---|---|
| Nb | 8.54 | 252 | 8.7 | 1.80 | [13] |
| V | 9.26 | 338 | 5.03 | 1.50 | [4,14] |
| Ta | 5.44 | 231 | 4.4 | 1.49 | [14] |
| Sn | 1.75 | 200 | 3.72 | 1.50 | [1, 6] |
| In* | 1.81 | 109 | 3.4 | 1.60 | [15] |
| Tl* | 2.55 | 86.6 | 2.36 | 1.30 | [7] |
| Al | 1.27 | 390 | 1.17 | 1.20 | |
| Zn | 0.65 | 340 | 0.84 | 1.03 | |

*One must regard the thermal characteristics of these metals with some caution, since their electron specific heat over the whole range of measurement amounted to only a small fraction of the total specific heat. This especially applies to Tl, for which the $\gamma$ obtained on the basis of calorimetic measurements is substantially different from the value of 1.53 determined on the basis of magnetic measurements.[16]

to the critical temperature, the thermal properties are determined by the size of the discontinuity in the specific heat for the transition from the normal state to the superconducting. A comparison of the relative discontinuity $\Delta c/\gamma T_k$ shows that the change in this quantity is apparently also connected with $T_k/\Theta$ (Fig. 9b). In this case, since calorimetric measurements in a narrow range of temperatures close to $T_k$ can also be used for the determination of the quantity $\Delta c/\gamma T_k$, the number of superconductors whose properties can be compared according to this characteristic is increased. A significant deviation from the general dependence of $\Delta c/\gamma T_k$ on $T_k/\Theta$ is observed only for thallium, if we make use of $\gamma$ obtained from calorimetric measurements (see note on Table II). In the presence of a general law for the change in the specific heat of the electrons in the superconductor with the temperature, $\Delta c/\gamma T_k$ and $\alpha$ are probably interrelated. From this viewpoint, the data of Fig. 9b serve as additional proof of the presence of a connection between the quantity $\alpha$ and $T_k/\Theta$.

It is natural to compare all these results in the first place with the recently developed[2,3] microscopic theory of superconductivity. In first approximation, the theory describes the change in the specific heat of superconductors with temperature with sufficient accuracy. The theoretical values $\Delta c/\gamma T_k = 1.4$, $\alpha = 1.44$ also agree with the experimental values. However, according to the theoretical model, these quantities should be constant for all superconductors; in reality they vary considerably. This change could be corrected, for example, with the appearance of an anisotropy in the electron spectrum in the real metal, from which the specific heat at sufficiently low temperatures will be determined by the change of the sums of exponents. Here, however, one would expect a connection between $\alpha$ and the crystallographic structure of the metal, a relation which has not as yet been discovered. Moreover, only the decrease of $\alpha$ in comparison with $\alpha_{theor}$ could be explained in this way, whereas, for a series of metals, $\alpha > \alpha_{theor}$. All this shows that a further refinement of the model currently considered is necessary to explain quantitatively the properties of superconductors. Since the value of $\alpha$ is connected with the temperature dependence of the value of the energy gap $\Delta$, then the experimental data (Fig. 9) should be regarded as indicative of the presence

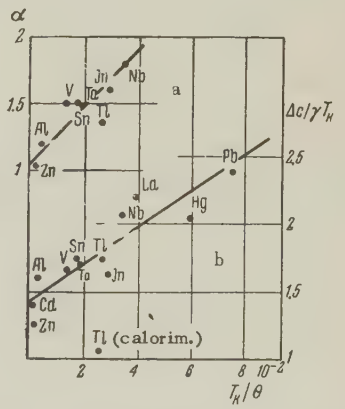


FIG. 9. (a) $\alpha$ and $T_k/\Theta$ of superconductors. The researches involved are enumerated in the text; (b) $\Delta c/\gamma T_k$ and $T_k/\Theta$ of superconductors. For Cd,[17] and especially for La,[18] the data are not very trustworthy; for Hg,[16,19] the data are from magnetic measurements; for Pb, the data of Refs. 20, 21 are used, for the other metals, the results of the researches enumerated in the text were employed.

of a dependence of $\Delta$ on $T/\Theta$ as well as the dependence of $\Delta$ on $T/T_k$ considered in the theory.

### Thermal Conductivity

In the normal state, the thermal conductivity $K_n$ of the metals under consideration is linearly proportional to the temperature in all intervals of measurement:

$$K_n = K_0 T.$$

The quantity $K_0$ is connected with the chemical and physical impurities of the specimen, just as is the residual resistance. The values obtained for $K_0$ (see Table I) confirm the relatively high purity of the samples under investigation.

It is known that for sufficiently low temperatures, transfer of heat to the superconductor is entirely governed by the lattice. In our measurements this temperature region is achieved for aluminum only below 0.2°K, where a sharp change is observed in the thermal conductivity in both samples. At the higher temperatures for Al, and over the whole range of measurements for Zn, the transfer of heat is essentially related to the thermal conductivity of the electrons, $K_{es}$. The dependence of $K_{es}$ on $T_k/T$ is shown in Fig. 10; it can be represented by

$$K_{es} = k_{0s} \exp(-\beta T_k/T),$$

where the values of $\beta$ are $1.5 \pm 0.1$ for Al and $1.30 \pm 0.1$ for Zn; $k_{0s}$ is a constant, related to the quantity $K_0$ of the given sample. This is the same law (but with other values of $\beta$) established previously for tin.

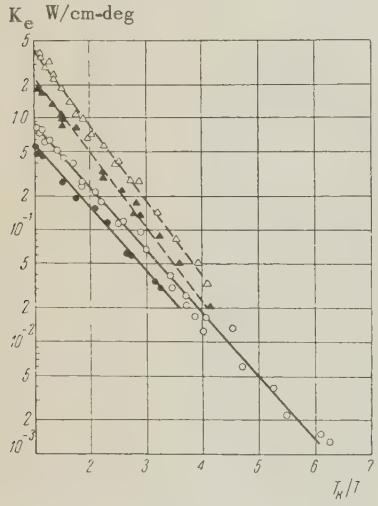


FIG. 10. Thermal conductivity of electrons: o – Zn-1; • – Zn-2; △ – Al-1; ▲ – Al-2.

The characters of the temperature variations of thermal conductivity and specific heat of electrons of the superconductor are interrelated. This is shown by a detailed measurement of the exponents $\alpha$ and $\beta$ in the exponential laws for $c_{es}$ and $K_{es}$, although this means of comparing K and c does not appear to be very trustworthy. More accurate evidence on the relation of the specific heat and the thermal conductivity is given by the results of measurement of the thermometric conductivity $a^2 = K/c\rho$; this permits us to establish even a very small difference in the temperature dependence of these quantities. Since the thermal characteristics of Al and Zn are chiefly determined by the electrons in this case,* we have for these metals, with accuracy to within several percent: $a^2 = K_{es}/c_{es}\rho$. For convenience, the value of the temperature conductivity was taken in the normal state at $T_k$, and the dependence of $\xi = a_s^2/a_n^2$ on $T/T_k$ was considered. It turned out that Al and Zn have the same type of dependence of $\xi$ on $T/T_k$, although the possibility is not excluded that, the absolute magnitude of $\xi$ contains the value of $\alpha$ or $\beta$, since $\xi_{Al}/\xi_{Zn}$ is approximately inversely proportional to $\alpha_{Al}/\alpha_{Zn}$.

All these quantities can be considered from the point of view of the new theory of superconductivity. If, within the framework of this theory, we compute the thermal conductivity of the electrons in the temperature range where the path length is determined by scattering from impurities,† then

$$\frac{K_{es}}{K_{es}(T_k)} = \frac{12}{\pi^2}\frac{T}{T_k}\int_{\Delta(T)/2T}^{\infty}\frac{x^2 dx}{\mathrm{ch}^2 x},$$

where $\Delta(T)$ is the width of the energy gap in the superconductor, or

$$K_{es}(T)/K_{es}(T_k) \approx 5.75 \exp(-\beta T_k/T),$$

where $\beta = 1.75$. Although this law agrees qualitatively with the experimentally established dependence of $K_{es}$ on $T_k/T$, the quantity $\beta$, as also $\alpha$ in the specific heat, is not a universal constant, changing from one metal to another. In the same way, starting out from the model developed recently, it is not possible quantitatively to determine the thermal conductivity of the electrons of the superconductor in a sufficiently wide temperature range.

It is natural to expect that the change in $\alpha$ and $\beta$ from one metal to another is determined either by the appearance of anisotropy in the metal or by

*For aluminum, measurements of the temperature conductivity are considered only above 0.3°K where, in accord with the data of Fig. 1, the thermal conductivity of the lattice of specimen Al-2 contributes less than 10% of the total thermal conductivity.

†The author acknowledges his deep gratitude to B. T. Geilikman who kindly reported the results of this computation prior to publication.[22]

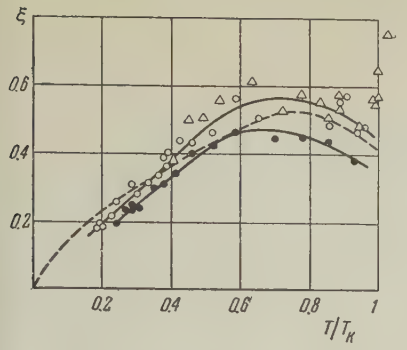


FIG. 11. Dependence of $\xi = a_s^2/a_n^2$ on $T/T_k$: ● – Al-1; ○ – Zn-1; △ – Zn-2. Dashed line – theoretical curve.

a different dependence of $\Delta$ on the temperature. From this point of view, we may assume that the ratio $K_{es}/c_{es}$ can be theoretically determined more accurately than $K_{es}$ or $c_{es}$ alone. Evidently this is so. Thus, for example, while the deviation between the experimental and theoretical values of $K_{es}$ and $c_{es}$ for Zn at 0.2°K amounted to a factor of six, the quantity $\xi$, computed on the basis of the theoretical dependence of $K_{es}$ and $c_{es}$, differs from the experimental value by not more than 10%. However, even in this case, it is still possible that in detail the theory does not accurately determine the dependence of $\xi$ on $T/T_k$ (see Fig. 1).

In conclusion, I take this opportunity to express my deep gratitude to P. L. Kapitza, A. I. Shal'nikov, Iu. B. Sharvin, and P. G. Strekov for valuable remarks in the course of completion of the research, and to V. I. Shishkin for help in the measurements.

[1] N. V. Zavaritskii, J. Exptl. Theoret. Phys. (U.S.S.R.) **33**, 1085 (1957), Soviet Phys. JETP **6**, 837 (1958).

[2] Bardeen, Cooper, and Schrieffer, Phys. Rev. **106**, 162 (1957); **108**, 1175 (1957).

[3] N. N. Bogoliubov, J. Exptl. Theoret. Phys. (U.S.S.R.) **34**, 58 (1958), Soviet Phys. JETP **7**, 41 (1958).

[4] Corak, Goodman, Satterthwaite, and Wexler, Phys. Rev. **102**, 656 (1956).

[5] B. B. Goodman, Conference de physique des basses temperatures, Paris, 1955, p. 506.

[6] W. S. Corak and S. B. Satterthwaite, Phys. Rev. **102**, 662 (1956).

[7] J. L. Snider and J. Nicol, Phys. Rev. **105**, 1242 (1957).

[8] W. H. Keesom and J. A. Kok, Physica **4**, 835 (1937).

[9] Howling, Mengoza and Zimmerman, Proc. Roy. Soc. (London) **229A**, 86 (1955).

[10] W. H. Keesom and J. N. Van den Ende. Leid. Comm. 219 B, 1932.

[11] A. A. Silvidi and J. G. Daunt, Phys. Rev. **77**, 125 (1950).

[12] B. B. Goodman, Compt. rend. **244**, 2899 (1957).

[13] Brown, Zemansky, and Boorse, Phys. Rev. **92**, 52 (1953).

[14] Worley, Zemansky, and Boorse, Phys. Rev. **99**, 447 (1955).

[15] J. R. Clement and E. H. Quinnell, Phys. Rev. **92**, 258 (1953).

[16] E. Maxwell and O. S. Lutes, Phys. Rev. **95**, 333 (1954).

[17] B. N. Samoilov, Dokl. Akad. Nauk SSSR **86**, 281 (1952).

[18] Worley, Zemansky, and Boorse, Conference de physique des basses temperatures, Paris, 1955, p. 499.

[19] P. L. Smith and N. M. Wolcott, Phil. Mag. **1**, 854 (1956).

[20] J. R. Clement and E. H. Quinnell, Phys. Rev. **85**, 502 (1952).

[21] Horowitz, Silvidi, Malaker, and Daunt, Phys. Rev. **88**, 1182 (1952).

[22] B. T. Geilikman, J. Exptl. Theoret. Phys. (U.S.S.R.) **34**, 1042 (1958), Soviet Phys. JETP **7**, 721 (1958).

Translated by R. T. Beyer
232

# COLLECTIVE OSCILLATIONS OF ELECTRONS IN CRYSTALS

E. L. FEINBERG

P. N. Lebedev Institute of Physics, Academy of Sciences, U.S.S.R.

Submitted to JETP editor August 27, 1957; corrected manuscript received February 12, 1958

J. Exptl. Theoret. Phys. (U.S.S.R.) **34**, 1125-1137 (May, 1958)

Collective oscillations of electrons distributed with periodic density in a lattice are considered as quasi-hydrodynamic oscillations of a degenerate non-uniform gas of electrons. Properties of the various levels are analyzed and the probabilities of exciting collective oscillations by light and by charged particles are calculated. Quantitative estimates of the position of the levels are compared with data concerning characteristic losses of electrons in thin films.

## 1. INTRODUCTION

ATTEMPTS have been made to apply the theory of collective oscillations of a plasma to the valence electrons in a crystal by considering them as a degenerate Fermi gas (see, for instance, the review article by Pines[1]). At the present time it is not clear whether such oscillations, "plasmons," are stable enough to be considered as actually existing. There is no doubt that the lifetime of a plasmon is small, and the probability that it will be converted to the excitation of separate electrons and to thermal motion is large. However, the successful interpretation on this basis of certain characteristic energy losses of electrons passing through solid films[1] obliges us to direct ourselves seriously to the problem of the collective oscillations of electrons in crystals and, above all, to attempt to broaden the circle of phenomena under study which are connected with plasmons.

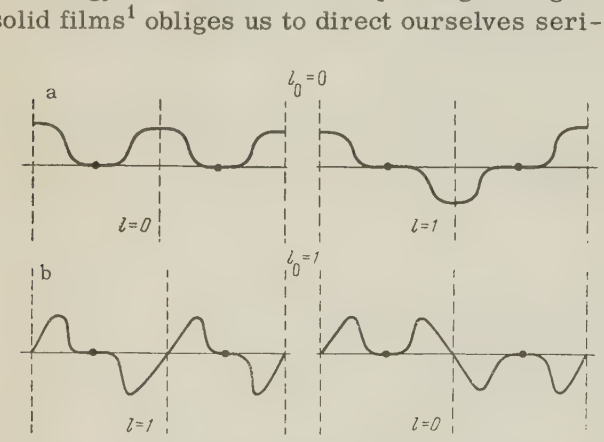


a – Form of the oscillations for even $l_0$, $l_0 = 0$. For $k = 0$ only the term $l = 0$ appears; $\rho$ belongs to the type $\rho_l = \rho_0^{(s)}$ – in neighboring cells the function is the same. For $kd = \pi$ principally the term $l = 1$ is represented; $\rho$ belongs to the type $\rho_1^{(s)}$ – in neighboring cells the functions differs in sign, $\exp(ik \cdot d) = -1$. b – Form of the oscillations for odd $l_0$, $l_0 = 1$. For $k = 0$ only the term $l = 1$ appears; $\rho$ belongs to the type $\rho = \rho_1^{(a)}$ – in neighboring cells the function is the same. For $kd = \pi$ principally the terms $l = 0$ and $l = 2$ are represented; $\rho$ belongs to the type $\rho_0^{(a)}$ and $\rho_2^{(a)}$ – in neighboring cells the functions differ in sign.

The theory of collective oscillations is applied to crystals in a quite elementary way.[1,2] For a uniform degenerate gas of free electrons the following dispersion equations are used:

$$\omega^2 = \omega_p^2 + \langle v^2 \rangle k^2, \qquad \omega_p^2 = 4\pi\rho_0 e^2/m, \tag{1}$$

where $\omega$, $k$ are the frequency and wave number of a plasmon; $\langle v^2 \rangle$ is the average square of the thermal velocity of the electrons,

$$\langle v^2 \rangle = \frac{3}{5} v_{max}^2 = \frac{3}{5} (3\pi)^{2/3} \frac{\hbar^2}{m^2} \rho_0^{2/3};$$

$\rho_0$ is the average number density of the electrons; $e$ is the charge and $m$ the mass of an electron. The relation (1) and the condition of its applicability were obtained from a kinetic equation.[3-5] It was shown that the quantum correction is small.[3] This relation is valid (or, a plasmon exists) so long as the plasmon wavelength is sufficiently large in comparison with interelectronic distances, and therefore the term $\langle v^2 \rangle k^2$ in (1) is small in comparison with $\omega_p^2$, which leads to the conditions $k \lesssim k_c \sim \rho_0^{1/6}$. This is a strong condition, because, in the other direction, the effective wavelength can not be materially larger than the lattice constant (see figure a below). Consequently the success of all ideas can be charged in large part to a favorable relation between the numerical coefficients. If the condition derived above is violated, the motion rapidly breaks up into individual excitations of electrons, so that if indeed plasmon levels exist, they ought to be very broad.

In reality the positive charge in a metal is not spread out as in a plasma. Furthermore it is necessary to take the constitution of the atom into ac-

count by one means or another. Up to the present time this has, in fact, not been included in the theory but has been dealt with on a different basis. One considers the atom only as the source of a periodic field, or else, proceeding from semiqualitative considerations, assumes that in certain cases, that of Cu, for instance, one must understand by $\rho_0$ in (1) not only the valence electrons, but should add to these a certain number of electrons from the shell — for Cu, for instance, three times the number of valence electrons, etc.

The problem obviously consists in studying the collective behavior of all of the electrons of the crystal (including the ionic group) from a single point of view, and the theory itself ought to show what part of these participate effectively in a plasmon. The goal of the present paper is to study this question, although only very roughly because of the roughness of the approximation of collective oscillations.

A study has already been made of a plasma in a periodic field on the basis of a classical kinetic equation, in the approximation of a weak periodicity, for a gas of valence electrons.[6] (For an interesting application of the theory of collective oscillations see also Ref. 7). This investigation does not include the ions and is unsatisfactory for our purposes.

## 2. KINETIC EQUATION METHOD

It is a simple matter to write down the kinetic equation for the electron distribution function $f(\mathbf{r}, \mathbf{p}, t)$ for a non-uniform density if one takes into account the external field created by the atomic nuclei. It is possible to start out from the quantum kinetic equation.[3] However, the quantum corrections are small even for electron interactions, and for a gradually varying nuclear field it is known that one can use the classical approximation, so that the external field $U(\mathbf{r})$ enters only in the form $\nabla_{\mathbf{r}} U \cdot \nabla_{\mathbf{p}} f$ (where $\mathbf{r}$ is the coordinate, $\mathbf{p}$ the momentum). As usual, we put

$$f = f^{(0)}(\mathbf{r}, \mathbf{p}) + f^{(1)}(\mathbf{r}, \mathbf{p}, t), \quad | f^{(1)} | \ll f^{(0)}$$

Now $f^{(0)}$ depends on $\mathbf{r}$, although comparatively weakly. Consequently the difference between this case and the case $f^{(0)} = f^{(0)}(\mathbf{p})$ boils down to the fact that we have to understand $U$ to be the combined potential of the nucleus and the undisturbed distribution of the electrons, satisfying the equation

$$\nabla^2 U = -4\pi\rho_0, \quad \rho_0 = \int f^{(0)}(\mathbf{r}, \mathbf{p})\, d\mathbf{p}.$$

We now carry out the transition from the distribution in multi-dimensional space to the single-particle approximation:

$$f^{(1)}(\mathbf{r}_1, \mathbf{p}_1; \mathbf{r}_2, \mathbf{p}_2; t) = f_1(\mathbf{r}_1, \mathbf{p}_1, t) f_1(\mathbf{r}_2, \mathbf{p}_2, t),$$

which is equivalent to the Hartree approximation, to which, as Wolff has shown,[8] the theory of plasmons corresponds.

From the kinetic equation for $f_1(\mathbf{r}_1, \mathbf{p}_1, t)$ it is possible, following Silin,[3] to go over to the "quasi-hydrodynamic approximation," in which the first moments of the desired distribution are studied:

$$\int f_1 d\mathbf{p} \equiv \rho_1(\mathbf{r}, t), \quad \int f_1 p_i d\mathbf{p}, \quad \int f_1 p_i p_k d\mathbf{p}, \ldots.$$

A system of equations is obtained for these moments, and the succeeding moments are ignored. This system cannot be simplified as readily as for a uniform plasma,[3] but one general property of its solution — that of periodicity — is important for us.

For the case of electrons in a crystal, a system of equations is obtained which is linear and homogeneous, with coefficients which have the periodicity of the lattice. Consequently one can verify that the solution of this system, for instance the excess density, has the form

$$\rho_1(\mathbf{r}, t) = e^{i\mathbf{k}\mathbf{r}} \rho_{1\mathbf{k}}(\mathbf{r}, t), \tag{2}$$

where $\rho_{1\mathbf{k}}(\mathbf{r}, t)$ has the period of the lattice and $\mathbf{k} = (2\pi n_x/L_x, 2\pi n_y/L_y, 2\pi n_z/L_z)$; $L_x$, $L_y$, $L_z$ are the dimensions of the unit cell, and $n_x$, $n_y$, $n_z$ are integers. As a matter of fact, all of the usual arguments which enter, for instance, into the Bloch theory for the wave function of an electron in the periodic field of a crystal, are applicable here. The solutions form a complete orthogonal set of functions of the characteristic oscillations, numbered according to the index $\mathbf{k}$, and the indices of the states $\rho_{1\mathbf{k}}$, determined from the solutions inside the cell. It is obvious that the question of the stability of these new plasmons remains unsolved here also.

## 3. HYDRODYNAMIC APPROXIMATION

Many of the following results require only a knowledge of the above-mentioned property of periodicity of the functions (2). However for the sake of concreteness, it is convenient to have a method, even though a very approximate one, which would permit one to carry out the calculations to the end. The method of hydrodynamics is one of these.[9] In solving the hydrodynamic equations for an electron gas with Coulomb forces guaranteeing a collective interaction, one can take account of collisions and of thermal motion in the term $\int dp/\rho$ ($p$ is the pressure) for the

corresponding equation of state. It is known that this method gave in the classical case an incorrect coefficient of $\frac{1}{3}$ in the correction term $\langle v^2\rangle k^2$ of (1).[3-5] In the case of a uniform degenerate Fermi gas, this method gives a coefficient of $\frac{5}{9}$ in the correction term [see Ref. 10 and Eq. (14) below], which is closer to unity but is still not correct.

The principal equations for a non-uniform degenerate electron gas, neglecting the retardation of the interaction, were written down long ago by Bloch,[9] who made a partial study of their properties for the case of an atom, although he was not engaged in looking for a solution. We will take advantage of this approach for the more general problem.

For plasmons in a crystals, the accounting for the retardation may be essential.

In the linear approximation with respect to the velocity $\mathbf{u}$, for $\rho = \rho_0 + \rho_1$, $|\rho_1| \ll \rho_0$, taking account of the fields $\mathbf{E}$, $\mathbf{H}$ of the electrons themselves and the external fields $\mathbf{E}^{(e)}$, $\mathbf{H}^{(e)}$, we have the following system of equations (the quadratic term $\left(\frac{1}{c}\mathbf{u}\times\mathbf{H}\right)$ is dropped):

$$\frac{\partial\rho_1}{\partial t} = -\operatorname{div}(\rho_0\mathbf{u}),$$
$$m\frac{\partial\mathbf{u}}{\partial t} = -\nabla(D\rho_1) - e\mathbf{E} - e\left\{\mathbf{E}^{(e)} + \left[\frac{1}{c}\,\mathbf{u}\times\mathbf{H}^{(e)}\right]\right\},$$
$$\frac{\partial\mathbf{E}}{\partial t} = 4\pi\rho_0\mathbf{u} + c\operatorname{curl}\mathbf{H},\quad \frac{\partial\mathbf{H}}{\partial t} = -c\operatorname{curl}\mathbf{E}. \tag{3}$$

Here the term $-\nabla(D\rho_1)$ arose from the decomposition

$$\int\frac{dp}{\rho} = \int_0^{\rho_0}\frac{dp}{\rho} + \int_{\rho_0}^{\rho_0+\rho_1}\frac{dp}{\rho} = \left(\int\frac{dp}{\rho}\right)_{\rho=\rho_0} + D\rho_1,$$
$$D = \left(\frac{1}{\rho}\,\frac{dp}{d\rho}\right)_{\rho=\rho_0}$$

(for a uniform Fermi gas $D = 5m\langle v^2\rangle/9\rho_0$).

The quantity $\rho_1$ which, like $\mathbf{u}$, is real, gives the quasi-classical approximation to the density matrix; consequently in a system of n particles with unperturbed wave functions $\psi_j^{(0)}$ and a perturbation $\psi_j^{(1)}$:

$$\rho \to \sum_{j=1}^{n}\psi_j^*(\mathbf{r})\,\psi_j(\mathbf{r}) \approx \sum(\psi_j^{(0)*} + \psi_j^{(1)*})(\psi_j^{(0)} + \psi_j^{(1)}) = \rho_0 + \rho_1,$$
$$\rho_1 \approx \sum_{j=1}^{n}(\psi_j^{(0)*}\psi_j^{(1)} + \psi_j^{(1)*}\psi_j^{(0)}). \tag{4}$$

Let us study the free oscillations in the absence of an external field.

The energy of the oscillations is

$$\mathcal{H} = \frac{1}{2}\int d\mathbf{r}\left\{m\rho_0\mathbf{u}^2 + D\rho^2 + \frac{1}{4\pi}(E^2 + H^2)\right\}. \tag{5}$$

Here and in what follows the index 1 in $\rho_1$ is dropped.

We introduce a four-component quantity whose first component is a scalar and whose remaining three are vectors (thus in fact we have a ten-component quantity):

$$\mathbf{G} = (G^{(1)}, G^{(2)}, G^{(3)}, G^{(4)}) = (\tilde\rho, \tilde{\mathbf{u}}, \tilde{\mathbf{E}}, \tilde{\mathbf{H}}),\quad \tilde\rho = \sqrt{D(\mathbf{r})}\,\rho,$$
$$\tilde{\mathbf{u}} = \sqrt{m\rho_0(\mathbf{r})}\,\mathbf{u},\quad \tilde{\mathbf{E}} = \mathbf{E}/\sqrt{4\pi},\quad \tilde{\mathbf{H}} = \mathbf{H}/\sqrt{4\pi}. \tag{6}$$

If then, with a view to what follows, we multiply the system of equations (3) by i, we can write them in the form

$$i\frac{\partial\mathbf{G}}{\partial t} = \hat L\mathbf{G},\quad \mathcal{H} = \frac{1}{2}\int\mathbf{G}^2 d\mathbf{r}, \tag{7a}$$

$$\mathbf{G}_1\mathbf{G}_2 \equiv \sum_{\alpha=1}^{4} G_1^{(\alpha)}G_2^{(\alpha)},\quad \hat L\mathbf{G} = \sum_{\beta=1}^{4} L^{(\alpha,\beta)}G^{(\beta)},\quad \omega_p^2(\mathbf{r}) = \frac{4\pi e^2\rho_0(\mathbf{r})}{m}.$$

$$L^{(\alpha,\beta)} = \begin{vmatrix} 0 & -\sqrt{D}\nabla\sqrt{\frac{\rho_0}{m}} & 0 & 0\\ -\sqrt{\frac{\rho_0}{m}}\nabla D & 0 & -\omega_p(\mathbf{r}) & 0\\ 0 & \omega_p(\mathbf{r}) & 0 & c\operatorname{curl}\\ 0 & 0 & -c\operatorname{curl} & 0 \end{vmatrix} \tag{7b}$$

Thus $\hat L$ is a self-adjoint operator. We split all real quantities into two parts:

$$\mathbf{G} = \sum_\lambda(\mathbf{G}_\lambda e^{-i\omega_\lambda t} + \mathbf{G}_\lambda^* e^{i\omega_\lambda t}), \tag{8}$$

so that for $\rho$, for instance, we have

$$\rho = \sum_\lambda(\rho_\lambda(\mathbf{r})\,e^{-i\omega_\lambda t} + \rho_\lambda^*(\mathbf{r})\,e^{i\omega_\lambda t}). \tag{9}$$

It is clear that if $\rho_\lambda$ corresponds to a transition with the absorption (emission) of a quantum $\hbar\omega_\lambda$, then $\rho_\lambda^*$ corresponds to a transition with the emission (absorption) of a quantum. In determining by any manner the real oscillation of $\rho(\mathbf{r}, t)$ with the frequency $\omega_\lambda$, we can split it up into two parts, corresponding to (4), and consider $\rho_\lambda$ and $\rho_\lambda^*$ as the quasi-classical approximation for $\sum\psi_j^{(0)*}\psi_j^{(1)}$ and $\sum\psi_j^{(0)}\psi_j^{(1)*}$, in order, for instance, to use them in quantum-mechanical calculations of different processes.

For $\mathbf{G}_\lambda$ there occur the equations

$$\omega_\lambda\mathbf{G}_\lambda = \hat L\mathbf{G}_\lambda. \tag{10}$$

Thus by using the self-adjointness of operator $\hat L$ and the antisymmetry of the real operator $-i\hat L$ one can, by the usual method, obtain the properties of orthogonality and normalization.

The value of the constant of normalization is determined from the requirement that the energy of an oscillation with a certain frequency $\omega_\lambda$ is equal to $\hbar\omega_\lambda$. Substituting one term of the sum (8) into

$\mathcal{H}$ (7) we obtain the normalization conditions:

$$\int G_\lambda^* G_{\lambda'} d\mathbf{r} = \hbar\omega_\lambda \delta_{\lambda\lambda'}, \tag{11a}$$

$$\int G_\lambda^* G_{\lambda'}^* d\mathbf{r} = \int G_\lambda G_{\lambda'} d\mathbf{r} = 0. \tag{11b}$$

If the $G_\lambda$ are understood to be quantities, already normalized, which form a complete set of functions, then an arbitrary state is determined by the set of coefficients $a_\lambda$ in the expansion

$$G(\mathbf{r}, t) = \sum_\lambda (a_\lambda G_\lambda e^{-i\omega_\lambda t} + a_\lambda^* G_\lambda^* e^{i\omega_\lambda t}), \tag{8a}$$

so that the energy turns out to be

$$\mathcal{H} = \sum_\lambda |a_\lambda|^2 \hbar\omega_\lambda. \tag{12}$$

Thus for a uniform plasma, in which $\rho_0 = \text{const}$, $\omega_p = \text{const}$, we have "free plasmons:"

$$\rho = \rho_k e^{i(\mathbf{k}\cdot\mathbf{r}-\omega t)}; \quad \mathbf{u} = \mathbf{u}_k e^{i(\mathbf{k}\cdot\mathbf{r}-\omega t)}, \tag{13}$$

etc. Substituting into (10) and (12) we find two types of solutions: if $\omega^2 = \omega_p^2 + c^2k^2$, then $\mathbf{H} = (c/\omega)(\mathbf{k}\times\mathbf{E})$, $\mathbf{E} = im\omega\mathbf{u}/e$ (transverse waves),

$$u_k = \sqrt{2\pi\hbar e^2/(m\omega V)}, \quad \rho_k = 0. \tag{14a}$$

If however $\omega^2 \neq \omega_p^2 + c^2k^2$, then $\mathbf{H} = 0$, $\mathbf{E} = im\omega\mathbf{u}/e$, $\mathbf{k}\cdot\mathbf{u} = ku$ (longitudinal waves),

$$\omega^2 = \omega_p^2 + {}^5/_9 \langle v^2 \rangle k^2,$$

$$u_k = \sqrt{\frac{2\pi\hbar e^2}{m\omega V}} \frac{\omega}{\omega_p}, \quad \rho_k = \frac{k\rho_0}{\omega} u_k = \sqrt{\frac{\hbar k^2 \rho_0}{2m\omega V}}, \tag{14b}$$

where $V$ is the normalization volume. The dispersion relation obtained by this method has an incorrect factor of ${}^5/_9$ in the correction term.

## CHARACTER OF THE FUNCTIONS FOR A CRYSTAL

In a crystal, $\rho$, $\mathbf{u}$, $\mathbf{E}$, and $\mathbf{H}$ have to be determined from a numerical solution of (10), where $\rho_0$, within the limits of one cell, is taken according to the Thomas-Fermi method. $\rho_0$ has been determined many times for different elements and different degrees of compression (see Refs. 11 and 12, for example).

We will use the cell method,[13,14] which was developed and used to find the wave functions of electrons in crystals. If we make use of the continuity of the functions and their derivatives in going across the boundaries of the cells, in conformance with the condition of periodicity (2) (which is valid for all components of $\mathbf{G}$), we can write the following boundary conditions, for example, for $\rho$: for any point $\mathbf{r}_0$ the surface of the cell has to be[14]

$$\rho(\mathbf{r}_0) = e^{i\mathbf{k}\cdot\mathbf{d}} \rho(\mathbf{r}_0 - \mathbf{d}), \quad \frac{\partial\rho(\mathbf{r}_0)}{\partial n} = -e^{i\mathbf{k}\cdot\mathbf{d}} \frac{\partial\rho(\mathbf{r}_0 - \mathbf{d})}{\partial n}, \tag{15}$$

where $\mathbf{d}$ is a vector connecting the two opposite faces of the cell. We will set $\mathbf{d}$ equal to the lattice constant. $\partial/\partial n$ is the derivative taken normal to the faces.

If we consider waves having the character of longitudinal waves [and going over to longitudinal waves for $\rho_0 \to \text{const}$; see (14b)], we can neglect retardation and set $\mathbf{E} = -\text{grad}\,\Phi$. In this case the coefficients of (10) in each cell will have spherical symmetry and a solution inside the cell can be sought in the form of an expansion in the spherical functions $Y_{lm}(\vartheta, \varphi)$ (normalized to unity),

$$\rho = \sum_{l,m} a_{lm}(\mathbf{k}) \rho_l(r) Y_{lm}(\vartheta\varphi), \tag{16}$$

in which we assume that the polar axis is directed along $\mathbf{k}$. For $m \neq 0$ waves appear which have the character of transverse oscillations and go over to transverse electromagnetic waves for $\rho_0 \to \text{const}$ in a uniform plasma (14a). Generally speaking it is no longer possible here to ignore the magnetic field of the waves and the retardation. However, the waves which most interest us are those having principally a longitudinal character, that is, containing a weak admixture of terms with $m \neq 0$. Consequently we will consider that the average field of distant cells is small in comparison with the field

$$\mathbf{E} = -\text{grad}\,\Phi, \quad \Phi = -e\int \frac{\rho(\mathbf{r}')}{|\mathbf{r}-\mathbf{r}'|} d\mathbf{r}',$$

so long as the $a_{lm}$ for $m \neq 0$ are comparatively small. Since $\rho(\mathbf{r}_0 - \mathbf{d}) = \sum a_{lm}\rho_l(\mathbf{r}_0) \times Y_{lm}(\pi - \vartheta, \pi + \varphi) = \sum a_{lm}\rho_l(\mathbf{r}_0)(-1)^l Y_{lm}(\vartheta, \varphi)$, then (15) has the form

$$\sum_{lm} a_{lm}(\mathbf{k}) \rho_l(r_0) \{1 - (-1)^l e^{i\mathbf{k}\cdot\mathbf{d}}\} Y_{lm}(\vartheta\varphi) = 0, \tag{17a}$$

$$\sum_{lm} a_{lm}(\mathbf{k}) \frac{\partial\rho_l(r_0)}{\partial n} \{1 + (-1)^l e^{i\mathbf{k}\cdot\mathbf{d}}\} Y_{lm}(\vartheta\varphi) = 0 \tag{17b}$$

for all $\vartheta$ and $\varphi$ ($\mathbf{r}_0 = \mathbf{r}_0(\vartheta, \varphi)$). As we see, principally the states with $k = 0$ are important for us. In this case there remains in (17a) only a sum over odd $l$, in (17b) — over even $l$. Consequently for $k = 0$ any solution $\rho_l(r) Y_{lm}(\vartheta, \varphi)$ of (10), taken by itself, will satisfy the conditions (17) if we subject $\rho_l$ to the requirement $\rho_l'(r_0) = 0$ for even $l$ and to the requirement $\rho_l(r_0) = 0$ for odd $l$. We note that for any $l$ the radial equations, for instance for $\rho_l$, have in general many solutions differing in their "radial quantum number" $n_r$; however it is apparently necessary to take only the lowest of these into account, since the remaining ones will correspond to too large a gradient of $\rho$, for which it is already known a plasmon cannot exist and breaks up into individual excitations of

electrons.

Those solutions with $k = 0$ form a basis. For $k \neq 0$ each of these generates its own branch of solutions. Thus if $kd \ll 1$, then expanding $\exp(i\mathbf{k}\cdot\mathbf{d})$ in a series and keeping only the first terms, we can seek a solution in the form of a sum of several first harmonics with coefficients $a^{l_0 m_0}_{lm}(\mathbf{k})$, where the new indices $l_0 m_0$ indicate to which branch the solution belongs, or which harmonic remains when $k \to 0$. It is easily shown that, if for $\mathbf{k} = 0$ a certain $a^{l_0 m_0}_{lm}$ is different from zero (and equal to unity), we find that for $\mathbf{k} \neq 0$ the adjacent harmonic will have $a_{lm}(\mathbf{k}) \sim kd$, the next one $a_{lm}(\mathbf{k}) \sim (kd)^2$, etc.

Let us for simplicity replace the cell by a sphere, $r_0 = \text{const}$, for example. We will study the case $l_0 = 0$, $a^{00}_{lm}(0) = \delta_{l l_0}$, i.e., the branch arising from the state $l = l_0 = 0$. We will look for $\rho$ in the form of a linear combination of the three first harmonics, all with $m = 0$:

$$\rho_k(r) = \sum_{l=0}^{2} a^0_{l_0}(k)\,\rho^{(s)}_l(r)\,Y_{l0}(\vartheta\varphi) \qquad (18)$$

(the index s indicates that $\rho$ has to satisfy a "symmetrical" boundary condition $\rho^{(s)\prime}_l(r_0) = 0$). Condition (17b) drops out here. It is impossible to satisfy (17a) for all $\vartheta, \varphi$, however. We satisfy it, for example, (a) for $\vartheta = 0$, (b) on the average over the sphere. Here, in calculating the normalization, all three coefficients $a^0_{l_0}$ are determined; it turns out that for $kd > 0$, $a^0_{00}$ decreases; $a^0_{10}$ increases, at first linearly with kd, while $a^0_{20}$ increases quadratically. For $kd = \pi$ only $a^0_{10}$ is different from zero [in this approximation see Eq. (18)], then it decreases and for $kd = \pi/2$ the second harmonic is maximum.

Let us now study the branch which for $k = 0$ starts with the state $l = 1$, $m = 0$, that is $a^{10}_{lm}(0) = \delta_{l l_1}\delta_{m m_0}$. Proceeding similarly, we imagine $\rho_l = \rho^{(a)}_l$ to be of an "antisymmetric" type, $\rho^{(a)}_l(r_0) = 0$. It is clear that here the functions have more nodes, and the energy of this state has to be considerably larger than for $l_0 = 0$ (as is substantiated by a calculation; see Sec. 8). For small k, $a^{10}_{10}$ decreases as kd, and $a^{10}_{00}$ and $a^{10}_{20}$ increase linearly. For $kd = \pi$ $a^{10}_{10}$ vanishes, and $a^{10}_{00}$ and $a^{10}_{20}$ have the same order of magnitude. If one does not replace the cell by a sphere, then the generation of longitudinal waves with $m = 0$ becomes generally impossible. For all orders of $(kd)^2 \sim d^2/\lambda^2$, transverse waves are mixed in with waves having a longitudinal character, and conversely.

We obtain the solution in another cell with integral indices $\boldsymbol{\nu} = (\nu_1, \nu_2, \nu_3)$ by multiplying the solution found in one cell by an exponential factor. Introducing for normalization purposes the factor $N^{-1/2}$, where N is the number of cells in the normalization volume V [$\rho_{l n_r}$ is normalized inside the cell in conformance with (11a)], and writing out all the indices, we have

$$\rho_{k n_i} = N^{-1/2} e^{i\mathbf{k}\cdot\boldsymbol{\nu}d} \sum_{lm} a^{(n_i)}_{lm}(k)\,\rho^{(p_{n_i})}_{l n_r}(r)\,Y_{lm}(\vartheta, \varphi), \qquad (19)$$

where $n_i$ denotes the combination of indices of an "internal state" in the cell, $n_i = (n_r, l_0, m_0)$, that is it indicates to which branch the solution belongs, and the index $p_{n_i}$ denotes the type of boundary condition for $\rho$: for even $l$ we have $p_{n_i} = s$, $\rho'(r_0) = 0$; for odd $l_0$, $p_{n_i} \equiv a$, $\rho(r_0) = 0$. All that has been said has to be repeated for the remaining functions $G^{(\alpha)}$, for which all the indices of the different functions $G^{(\alpha)}$ coincide. In practice we do not take the index $n_r$ into account (see below).

The nature of typical solutions is shown schematically in the figure. The solution for $k = 0$, $l_0 = l = 0$ formally is in conflict with the condition $\int \rho d\mathbf{r} = 0$; however this condition would be fulfilled for a k different from zero but arbitrarily small. If one goes over to a uniform plasma $\rho_0 \to \text{const}$, then this solution goes over to the usual longitudinal oscillations. The reduction of $\rho$ to zero in the center of the cell is related to the fact that oscillations of arbitrarily small energy do not penetrate into the depth of the atomic shell.

These collective oscillations have essentially the character of excitons. An excitation inside one cell (also representing a collective oscillations) is propagated in the form of a wave throughout the entire crystal.

## 5. EXCITATION OF THE OSCILLATIONS

If a system of solutions is known for a crystal, then the change of state under the influence of an external field can be found by the usual method.

In the presence of an external electric field $\mathbf{E}^{(e)}$, equation (3) can be written in a form corresponding to Eq. (7a):

$$i\frac{\partial G}{\partial t} = \hat{L}G + \mathbf{K},$$
$$\mathbf{K} = \left(0;\ -\frac{\omega_p(\mathbf{r})}{V 4\pi}\mathbf{E}^{(e)};\ 0;\ 0\right). \qquad (20)$$

Usually the external field is periodic, with a frequency $\omega_0$. We resolve it into components of the type $\exp(-i\omega_0 t)$ and $\exp(i\omega_0 t)$, which give rise to corresponding components in G, and study one of these components, for instance $G \sim \exp(-i\omega_0 t)$. We expand the desired solution in terms of the basic system of functions — the solutions $G^{(0)}_\lambda$ of

Eq. (10):

$$G = \sum_\lambda a_\lambda(t)\, e^{-i\omega_\lambda t} G_\lambda^{(0)}(r). \tag{21a}$$

Substituting in (20), multiplying by $G_\lambda^{(0)*}$, integrating over space and using (11a) we obtain

$$\frac{d}{dt} a_\lambda = -\frac{i}{\hbar\omega_\lambda} \int G_\lambda^{(0)*} K(r, t)\, dr e^{i\omega_\lambda t}. \tag{21b}$$

Let $K = K^{(0)}(r)\, e^{-i\omega_0 t}$. Integrating from the initial condition $a_\lambda = 0$ for $t = 0$ we obtain:

$$a_\lambda(t) = I\,[e^{i(\omega_\lambda - \omega_0)t} - 1]/i(\omega_\lambda - \omega_0),$$

$$I = -\frac{i}{\hbar\omega_\lambda} \int G_\lambda^{(0)*}(r)\, K^{(0)}(r)\, dr = I_1 + I_2,$$

$$I_1 = -\frac{ie}{\hbar c} \int \rho_0 u_\lambda^* A\, dr, \qquad I_2 = \frac{ie}{\hbar} \int \rho_\lambda^* \Phi\, dr, \tag{22}$$

where $E^{(e)}$ is expressed in terms of vector and scalar potentials, $E^{(e)} = -\nabla\Phi - \dot{A}/c$.

According to (12) the weight of the state $\lambda$ at the instant $t$ is $|a_\lambda(t)|^2$. The probability of transition to this state per unit time is

$$W_\lambda = \lim_{t\to\infty} \frac{d}{dt} |a_\lambda(t)|^2 = 2\pi |I_1 + I_2|^2 \delta(\omega_\lambda - \omega_0). \tag{23}$$

## 6. INTERACTION WITH LIGHT

Let us study the absorption of light. For $\mathfrak{N}$ quanta in the volume $V$ let

$$\Phi = 0,\ A = A_0 \exp(i(k_0 \cdot r - \omega_0 t)),\ A_0^2 = 2\pi\hbar\omega_0 \mathfrak{N}/Vk_0^2.$$

We assume that $A_0$ is directed along the z axis, $A_0 = A_0$ grad z. Using the first equation of (3), we have

$$\int \rho_0 u_\lambda^* A_0\, dr = i\omega_\lambda A_0 \int \rho_\lambda^* z\, dr.$$

Hence according to (19):

$$|I_1|^2 = \frac{e^2\omega_\lambda^2}{\hbar^2 c^2} A_0^2 \tag{24}$$

$$\times \left| \sum_\nu N^{-1/2} e^{i(k_0 - k, \nu)d} \sum_{lm} a_{lm}^{l_0 m_0}(k) \int \rho_l^* Y_{lm}^*(\vartheta\varphi)\, e^{ik_0 r} r\cos\vartheta\, dr \right|^2,$$

where the integral is extended throughout the volume of one cell. Since

$$\sum \exp[i(k_0 - k)\cdot\nu d] = N\delta_{kk_0},$$

and, for light, for $\hbar\omega_0 = \hbar\omega_\lambda \sim 5$ to 30 ev, $k_0 d \ll 1$, then the exponential factor in the integral can be dropped. Consequently, just as for ordinary excitons, a plasmon is excited with a $k$ that is practically zero. Only dipole oscillations with $l = 1$ give a contribution For $k = 0$ such oscillations are present only if $l_0 = 1$. Energetically this branch is situated below the branch $l_0 = 0$. Substituting the value of $A_0$, multiplying by the number of initial photon states $(2\pi)^{-3} V dk_0$ and introducing the spectrum of the incident light

$$S_0(\omega_0)\, d\omega_0 d\Omega \text{ erg}\cdot\text{cm}^{-2}\text{sec}^{-1} = \mathfrak{N} c\hbar\omega_0 (2\pi)^{-3}\, dk_0,$$

we obtain, after integration over $\omega_0$, the following expression for the total absorption of energy per unit time, $\hbar\omega_0 W = S$:

$$S_{\text{erg/sec}} = N 3\pi \frac{e^2}{\hbar c} \omega_0 S_0(\omega_0)\, d\Omega \left| \int_0^{r_0} \rho_1^{l_0}(r)\, r^3 dr \right|^2 |a_{10}^{l_0 m_0}(0)|^2. \tag{25}$$

Thus only transverse oscillations with $l = 1$, $m = 0$ can be excited (we recall that here the z axis is directed along the field $A_0$, and not along k, as in Sec. 4). If we designate

$$\left| \frac{4\pi}{3} \int_0^{r_0} \rho_1(r)\, \frac{r}{r_0}\, r^2 dr \right| = n_{\text{eff}}, \tag{26}$$

(the effective number of oscillating electrons), then $S$ takes the usual form[15] for the absorption of light by $N$ atoms, for each of which the effective square of the matrix element of the coordinate is

$$|x_{ab}|^2_{\text{eff}} \sim r_0^2 n_{\text{eff}}^2. \tag{27}$$

However such an absorption indicates that it takes place very rapidly: setting $N = \frac{1}{d^3} T\Sigma$, where $T$ is the width of the crystal and $\Sigma$ is the area of the surface being irradiated, we find for the ratio of the intensities of the incident and absorbed light ($r_0 \sim d$):

$$\frac{S}{S_0\, d\omega_0\, d\Omega\Sigma} \sim \frac{e^2}{\hbar c} \frac{\omega_0}{d\omega_0} \frac{T}{d}.$$

Thus even over a distance much smaller than $137d \sim c/\omega_0 \sim 1/k_0$ the absorption will be total. Consequently even on the surface of a crystal a light wave very rapidly goes over into a transverse plasmon wave, in which the principal component of $\rho$ is a dipole oscillation (in each cell) in the direction of the external electric field. According to the statements made in Sec. 4, there will be present in this oscillation, with a relative weight $(k_0 d)^2 \sim (e^2/\hbar c)^2$, an added wave with $l_0 = 1$, $l = 0$, for which the average value of $\rho$ will not vanish, i.e., a wave of longitudinal type.

## 7. EXCITATION BY FAST CHARGED PARTICLES

Let a particle with charge $e_1$, mass $M$, momentum $p_0$ and energy $E_0 = \hbar^2 p_0^2/2M$ strike the crystal, and as the result of exciting a plasmon make a transition to a state with momentum $p_f$ and energy $E_f$. This will produce a charge density for the transition, expressed in terms of the initial and final wave functions of the particle,

$$\psi = V^{-1/2} e^{i(\mathbf{p}\cdot\mathbf{r} - Et)/\hbar}. \quad (28)$$

There will arise a perturbation potential

$$\Phi = e_1 \int \frac{d\mathbf{r}'}{|\mathbf{r} - \mathbf{r}'|} \psi_f^*(\mathbf{r}', t)\, \psi_0(\mathbf{r}', t)$$

$$= \frac{4\pi e_1 \hbar^2}{V |\mathbf{p}_f - \mathbf{p}_0|^2} e^{\frac{i}{\hbar}(\mathbf{p}_0 - \mathbf{p}_f, \mathbf{r}) - i\omega_{0f} t}. \quad (29)$$

Here

$$\hbar\omega_{0f} = E_f - E_0 = v_0 \hbar\, |\mathbf{p}_0 - \mathbf{p}_f| \cos\theta,$$

$\mathbf{v}_0 = (\mathbf{p}_f + \mathbf{p}_0)/2M$ is the average particle velocity, which for a fast particle is the same as the initial velocity, and $\theta$ is the angle between the outgoing momentum and $\mathbf{v}_0$.

Substituting $\Phi$ into (22) and (23), one can split up the integral over the whole crystal into a sum (over $\nu$) of integrals over the separate cells, since $\rho$ differs from one cell to another only by the factor $\exp(i\,\mathbf{k}\cdot\boldsymbol{\nu}\,d)$. The sum gives $\hbar\mathbf{k}_0 = \mathbf{p}_0 - \mathbf{p}_f$, and after multiplying by the number of final states $(2\pi)^{-3} V\, d\mathbf{k}$ or $(2\pi\hbar)^{-3} V\, d\mathbf{p}_f$ and integrating with respect to $\mathbf{k}$ or $\mathbf{p}_f$ we obtain

$$W = 4N \frac{e_1^2 e^2}{\hbar^2} \int \frac{d\,\mathbf{k}}{k^4} \delta(\omega(k) - k v_0 \cos\theta) \left| \int e^{i\mathbf{k}\cdot\mathbf{r}} \rho^*(\mathbf{r})\, d\,\mathbf{r} \right|^2, \quad (30)$$

where the integral over $\mathbf{r}$ is taken within the limits of one cell.

For the case of a uniform plasma we substitute $\rho$ from (13) and (14b) (here V has to be replaced by the volume V/N of one cell) and obtain

$$W = \frac{e_1^2 \omega_p}{\hbar} \int_0^{k_c} \frac{dk}{k^2} \int_{-1}^{1} d\cos\theta\, \delta(\omega(k) - k v_0 \cos\theta)$$

$$\approx \frac{1}{2} \frac{m v_0 e_1^2}{\hbar^2} \frac{\hbar\omega_p}{E_0} \ln \frac{v_0 k_c}{\omega_p}, \quad (31)$$

where we have ignored the difference between $\omega_p$ and $\omega(k)$. This is the usual formula, which has also been obtained by other methods.[1]

For the case of a crystal the integral over the cell in (30) has the form

$$\int e^{-i\mathbf{k}\cdot\mathbf{r}} \sum_{lm} a_{lm}^{l_0 m_0}(\mathbf{k})\, \rho_l^{l_0}(r)\, Y_{lm}(\vartheta, \varphi)\, d\,\mathbf{r}.$$

We will restrict ourselves to a study of such small k that $kd \ll 1$. Since, as is apparent from (31), the upper limit in the integral with respect to k appears logarithmically, we can ignore it for a small portion of the scattering of the order of $\ln(k_c/k_{max})/\ln(k_c v_0/\omega_p)$. For M = m (excitation by an electron)

$$k_c v_0/\omega_p \sim \sqrt{\hbar^2 E_0/me^4} \gg 1.$$

We will exclude it from a consideration of very large angles of scattering: probably $\cos\theta >$ $(e^2/\hbar c)\sqrt{mc^2/E_0}$. Setting $\exp(i\,\mathbf{k}\cdot\mathbf{r}) \approx 1 + i\,\mathbf{k}\cdot\mathbf{r}$ and directing the z axis along $\mathbf{k}$ we obtain the probability of exciting a plasmon with a given k, $l_0$, and $m_0$ (integrated with respect to the angle $\theta$ between $\mathbf{k}$ and $\mathbf{v}_0$):

$$W_{k_0 l_0 m_0}\, dk = \frac{2e^2 e_1^2}{\hbar^2 v_0} \frac{dk}{k^3} \frac{4\pi}{3} r_0^3$$

$$\times \left\{ |a_{00}^{l_0 m_0}(k)\, \overline{\rho_0^{l_0}}|^2 + \frac{\omega_1^2 r_0^2}{3v_0^2} \left| a_{10}^{l_0 m_0}(k)\, \overline{\rho_l^{l_0} \frac{r}{r_0}} \right|^2 \right\}. \quad (32)$$

Here the term with $\sin^2\theta$ is dropped in comparison with $\cos^2\theta = \omega_1^2/k^2 v_0^2$ and it is considered that in the term $\delta(\omega(k) - k v_0 \cos\theta)$ it is in general necessary to write $\omega_{l_0}(k)$ in place of $\omega(k)$. The bar on top denotes an averaging over the cell. Hence, only longitudinal waves with $m = 0$ are excited. The first term in the brackets corresponds to an ordinary longitudinal plasmon (the average density does not vanish), the second to a longitudinal dipole oscillation in the cell. Since small k play a role, the first, principal term appears if $l_0 = m_0 = 0$, that is if a plasmon is excited in the lower band. But a non-vanishing $\overline{\rho}$ can also be involved in oscillations with $l \neq 0$. Thus for small values $kda_{00}^{1m_0}(k) \sim kda_{1m_0}^{1m_0}(k)$ (see Sec. 4). Hence for $l_0 = 1$ this term is $(kd)^2$ times smaller than the principal term. It is possible to write

$$\left\{ \quad \right\} \approx \left\{ |a_{00}^{00}\overline{\rho_0^0}|^2 \delta_{l_0 0}\delta_{m_0 0} + k^2 d^2 |a_{10}^{1m_0}\overline{\rho_0^1}|^2 \delta_{l_0 1} + \frac{\omega_1^2 r_0^2}{3v_0^2} \left| a_{10}^{10}\rho_1^1 \overline{\frac{r}{r_0}} \right|^2 \delta_{l_0 1}\delta_{m_0 0} \right\}. \quad (32a)$$

The role of the different terms for different k depends essentially on how k enters into the normalization factor. For a uniform plasma the first term in curly brackets is equal to $3\hbar k^2 \rho_0/(2mr_0^3\omega_p)$. Thus one can set

$$|a_{00}^{00}(k)\, \overline{\rho_0^0}|^2 = \frac{3}{r_0^3} \frac{\hbar k^2}{2m} \frac{\rho_{0\,\mathrm{eff}}}{\omega_0} b_0,$$

where $b_0$ is a number of order unity, and $\rho_{0\,\mathrm{eff}}$ can be considered equal to $\rho_0(r_0)$. Then for the lower band the total probability is

$$W_{00} = \frac{m v_0 e_1^2}{2\hbar^2} \frac{\hbar\omega_p(r_0)}{E_0} b_0 \ln \frac{v_0 k_{max}}{\omega_0}. \quad (33)$$

The excitation of higher levels for longitudinally polarized dipole oscillations ($l_0 = 1$, $m_0 = 0$), if they exist, can take place with a probability of order $(kd)^2$ relative to the probability of the principal process, in the form of characteristic losses for scattering through large angles $\theta$, in which the following relation ought to be satisfied:

$\cos\theta \sim \omega_{l_0 m_0}/kv_0 > \omega_{l_0 m_0} r_0/v_0$.

## 8. QUANTITATIVE ESTIMATES

It is possible to estimate the energy of a level by using, for example, a variational method for an almost-longitudinal plasmon, when the retardation of the interaction can be ignored. These calculations have been carried out by D. G. Sannikov for the case of Cu. By selecting test functions in the form of polynomials for $\rho$ and for the velocity potential $\varphi$ in the cell, which satisfied the boundary conditions appropriate to a given $l_0$, and then varying three undetermined parameters, it was possible to obtain eigenvalues of the energy $\hbar\omega_l$ for different $l$. The unperturbed density was substituted from Ref. 12.

The radius of the cell was taken to correspond to the normal density of copper, $\xi_0 = r_0/\mu = 9.4$. The following values were obtained, which represent upper limits, since a variational method was used:

1. $l_0 = 0$; $l = 0$, $\hbar\omega = 30$ ev (which corresponds to the beginning of the band, $k = 0$); $l = 1$, $\hbar\omega = 27$ ev (which corresponds approximately to $kd = \pi$).

2. $l_0 = 1$; $l = 1$, $\hbar\omega = 58$ ev (which corresponds to the beginning of the band, $k = 0$); $l = 0$, $\hbar\omega = 74$ ev (which corresponds approximately to $kd = \pi$).

The relatively small width of the lower band ($\sim 3$ ev) corresponds to the fact the plasma is uniform ($\langle v^2\rangle k_c^2 \ll \omega_p^2$). It indicates that the study of collective oscillations in crystals carried out above is developed within the confines of the usual theory of plasmons. The lower band corresponds to optically inactive oscillations in the sense that it cannot be immediately excited by light. Certainly, however, a more complicated process on the part of an interstitial electron is possible, as a result of which light can excite a plasmon of such a type. This has been the object of a separate study.[16]

The characteristic value of the energy losses in Cu is considered to be about 23 ev (Ref. 1). One can identify the band $l_0 = 0$ with this figure. It follows consequently from (32) and (32a) that just this band can be excited by a charged particle. The existence of longitudinal oscillations with $l = 1$ has to be regarded as extremely improbable; this band is very broad, plasmon oscillations with energies of $\sim 60$ ev will very rapidly go over into excitations of separate electrons. Certainly the application of the Thomas-Fermi method can in general give rise to certain doubts. Here, however, the method is not addressed to such fine effects as the chemical bond or the compressibility, where it is excessively crude, but to energies which exceed the energy of the chemical bond by one or two orders of magnitude; we expect that the results derived above are approximately correct. As a matter of fact it is known that the Thomas-Fermi method gives values for the energies of atomic electrons which are not too far out of line. For a study of other possible optical effects see Ref. 16.

In conclusion I would like to thank V. L. Ginzburg and V. P. Silin for interesting and useful discussions and comments and D. G. Sannikov for submitting the results of his calculations, quoted in Sec. 8.

[1] D. Pines, Rev. Mod. Phys. **28**, 184 (1956); Solid State Physics **1**, 367 (1955).

[2] D. Bohm and E. P. Gross, Phys. Rev. **75**, 1851, 1864 (1949); D. Bohm and D. Pines. Phys. Rev. **82**, 625 (1951); D. Pines and D. Bohm, Phys. Rev. **85**, 338 (1952); D. Bohm and D. Pines, Phys. Rev. **92**, 609 (1953); D. Pines, Phys. Rev. **92**, 626 (1953); D. N. Zubarev, J. Exptl. Theoret. Phys. (U.S.S.R.) **25**, 548 (1953)

[3] V. P. Silin, Тр. Физич. ин-та П. Н. Лебедева АН СССР (Trans. of P. N. Lebedev Physics Inst.) **6**, 201 (1955); J. Exptl. Theoret. Phys. (U.S.S.R.) **23**, 641, 649 (1952).

[4] A. A. Vlasov, Уч. зап. МГУ (Sci. Notes, Moscow State Univ.) No. 75, vol. 2, part 1 (1945).

[5] L. D. Landau, J. Exptl. Theoret. Phys. (U.S.S.R.) **16**, 574 (1946).

[6] P. S. Zirianov, J. Exptl. Theoret. Phys. (U.S.S.R.) **25**, 441 (1953).

[7] V. L. Bonch-Bruevich, Izv. Akad. Nauk. SSSR, Ser. Fiz. 21, **87** (1957); [Columbia Tech. Transl. **21**, 82 (1957)].

[8] P. Wolff. Phys. Rev. **92**, 18 (1953).

[9] F. Bloch, Z. Physik **81**, 363 (1933).

[10] I. I. Gol' dman, J. Exptl. Theoret. Phys. (U.S.S.R.) **17**, 681 (1947).

[11] P. Gombas, Die statistische Theorie des Atoms und ihre Anwendungen, Springer, Wien, 1949 (Russ. Transl. IIL, 1951).

[12] N. Metropolis and J. R. Reitz, J. Chem. Phys. **19**, 555 (1951).

[13] E. Wigner and F. Seitz, Phys. Rev. **43**, 804 (1933).

[14] J. Slater, Revs. Mod. Phys. **6**, 209 (1934).

[15] W. Heitler, Quantum Theory of Radiation, London, 1954, Sec. 17, Eq. (19).

[16] I. I. Sobel' man and E. L. Feinberg, J. Exptl. Theoret. Phys. (U.S.S.R.) **34**, 494 (1958); Soviet Physics JETP **7**, 339 (1958).

Translated by W. M. Whitney
233

# THE EFFECT OF A STRONG ELECTRIC FIELD ON THE OPTICAL PROPERTIES OF INSULATING CRYSTALS

L. V. KELDYSH

P. N. Lebedev Physics Institute, Academy of Sciences, U.S.S.R.

Submitted to JETP editor November 1, 1957; resubmitted February 20, 1958

J. Exptl. Theoret. Phys. (U.S.S.R.) **34**, 1138-1141 (May, 1958)

The absorption coefficient is calculated for a crystal placed in a uniform electric field, for frequencies at which the crystal does not normally absorb in the absence of a field. It is shown that there is a shift in the red absorption limit toward the longer wavelengths, by an amount which may reach hundreds of angstroms for reasonable field strengths.

It is known that a uniform electric field greatly alters the electron states in a crystal. Strictly speaking, there is no stationary state at all under these conditions. Instead of the Bloch functions $\psi_j(\mathbf{p}, \mathbf{r})$ for the electrons, we have functions of the form

$$\psi_j(\mathbf{p}_0, \mathbf{r}, t) = \exp\left\{-\frac{i}{\hbar}\int_0^t \varepsilon_j(\mathbf{p}_0 - e\mathbf{E}x)\,dx\right\}\psi_j(\mathbf{p}_0 - e\mathbf{E}t, \mathbf{r}). \quad (1)$$

even in the zero-order approximation. Here $\epsilon_j(\mathbf{p})$ are functions which define the dependence of electron energy on the quasi-momentum in the j-th band; $\mathbf{E}$ is the electric field strength.

These functions satisfy the time-dependent Schrödinger equation for the model under consideration (an electron in a periodic field plus a uniform electric field), accurately up to the exponentially small terms corresponding to the "leakage" of electrons from one band to another under the influence of the field, and describe a uniform acceleration of the electron which is in the state $\psi_j(\mathbf{p}_0, \mathbf{r})$ at the instant $t = 0$.

In what follows we shall express corrections to the wave function for the system which arise from interaction with light, using an expansion in terms of the functions (1). We could have used for this purpose any other system of functions satisfying the above-mentioned Schrödinger equation, so long as this system is complete and orthogonal at all instants of time (since we shall be considering only those expansion coefficients that change with time). However, the system (1), in addition to its physically descriptive nature, has the further advantage that it is obviously complete and orthogonal. As a matter of fact, although each of the functions varies continuously with time, at every instant the system as a whole is identical with the complete system of Bloch functions for the crystal. The particular choice of functions in which to carry out the expansion is quite immaterial to the final result, since the number of quanta absorbed (or, the number of photoelectrons, which is the same thing) depends on the total sum of the squares of the moduli of the coefficients in the expansion, and therefore does not depend on the choice of the base functions.

The probability that a quantum with frequency $\omega$ and polarization vector $\mathbf{e}$ will be absorbed by an electron in the state $\psi_v(\mathbf{p}_0, \mathbf{r}, t)$ is

$$w(\mathbf{p}_0, \omega, t) = \left(\frac{e}{m}\right)^2 \frac{2\pi\hbar}{\omega}\left|\int_0^t dt \int d\tau \psi_c^*(\mathbf{p}_0, \mathbf{r}, t)\, e^{-i\omega t} e\nabla\psi_v(\mathbf{p}_0, \mathbf{r}, t)\right|^2, \quad (2)$$

where the indices v and c refer to the valence and conduction bands respectively; e and m are the charge and mass of electron.

In the general case, in the absence of an electric field, the integrand varies harmonically with time; this implies that the energy must remain constant. The total probability of absorption of a photon $\hbar\omega$ per unit time per unit volume is then given by the expression

$$W(\omega) = \int \frac{dw(\mathbf{p}, \omega, t)}{dt}\frac{d^3p}{(2\pi\hbar)^3} = \left(\frac{e}{m}\right)^2 \frac{2\pi\hbar}{\omega}\int |e\mathbf{M}_{vc}(\mathbf{p})|^2 \delta\{\varepsilon_c(\mathbf{p}) - \varepsilon_v(\mathbf{p}) - \hbar\omega\}\frac{d^3p}{(2\pi\hbar)^3}, \quad (3)$$

$$\mathbf{M}_{vc}(\mathbf{p}) = \int \psi_c^*(\mathbf{p}, \mathbf{r})\nabla\psi_v(\mathbf{p}, \mathbf{r})\,d\tau, \quad (4)$$

from which it can be seen, in particular, that quanta with frequencies less than $\omega_0 = \epsilon_0/\hbar$, where $\epsilon_0 = \min\{\epsilon_c(\mathbf{p}) - \epsilon_v(\mathbf{p})\}$, are not absorbed at all. To be specific, we shall assume that the transition (4) is not forbidden by symmetry considerations, i.e., $\mathbf{M}_{vc}(\mathbf{p}_m) \neq 0$, where $\mathbf{p}_m$ is the value of the quasi-momentum corresponding to the absolute minimum in the function $\epsilon_c(\mathbf{p}) - \epsilon_v(\mathbf{p})$. This

case corresponds to the steepest absorption edge, and is therefore particularly suitable for observations. In fact, near this edge the expression (3) can be put into an explicit form by noting that in this region the function $\epsilon_c(\mathbf{p}) - \epsilon_v(\mathbf{p})$ can be written as

$$\varepsilon_c(\mathbf{p}) - \varepsilon_v(\mathbf{p}) = \varepsilon_0 + \sum_{i,k}(p_i - p_{im})(p_k - p_{km})/2m_{ik}. \quad (5)$$

Then

$$W(\omega) = \frac{1}{\pi}\frac{e^2}{\hbar c}\frac{c}{\omega}\left[\frac{m_1m_2m_3}{m^3}\frac{2(\hbar\omega - \varepsilon_0)}{m}\right]^{1/2}|\mathbf{eM}_{vc}(\mathbf{p}_m)|^2, \quad (6)$$

where $m_i^{-1}$ is the principal value of the tensor $m_{ik}^{-1}$.

The absorption coefficient is thus seen to vary as $(\omega - \omega_0)^{-1/2}$. In the particular case $\mathbf{M}_{vc}(\mathbf{p}_m) = 0$, the coefficient increases much more slowly,[2] as $(\omega - \omega_0)^{3/2}$.

In the presence of an electric field, expression (2) no longer contains delta functions, and therefore the probability of absorbing a quantum of frequency less than $\omega_0$ is not zero. The probability of photon absorption in this case must be calculated in a different manner. We shall first carry out this derivation under the simplifying assumption that the field is directed along one of the axes of a simple cubic lattice with period d. Then because $\epsilon_j(\mathbf{p})$ and $\psi_j(\mathbf{p}, \mathbf{r})$ are periodic functions of the quasi-momentum, the electron undergoes a periodic motion within the j-th band, with the period $T = 2\pi\hbar/eEd$. In this case it is natural to take the absorption probability for one period of this oscillation, $w(\mathbf{p}_0, \omega, 2\pi\hbar/eEd)$, as the characteristic absorption. In order to calculate this quantity, we transform (2) into the new variables of integration $p_x = p_{0x} - eEt$ (the X axis is assumed to be in the field direction) and note that the factor

$$\exp\left\{\frac{i}{e\hbar E}\int[\varepsilon_c(\mathbf{p}) - \varepsilon_v(\mathbf{p}) - \hbar\omega]\,dp_x\right\}$$

occurring in the integrand has a saddle point $p_x = q(p_y, p_z)$ in the complex $p_x$ plane, determined by the conditions

$$\varepsilon_c(q, p_y, p_z) - \varepsilon_v(q, p_y, p_z) - \hbar\omega = 0.$$

Making use of this circumstance, we obtain

$$w\left(\mathbf{p}_0, \omega, \frac{2\pi\hbar}{eEd}\right) = \left(\frac{e}{m}\right)^2\frac{2\pi\hbar}{\omega}\frac{2\pi\hbar}{eE}|\mathbf{eM}_{vc}(q, p_{0y}, p_{0z})|^2$$

$$\times\left|\frac{\partial[\varepsilon_c(\mathbf{p}) - \varepsilon_v(\mathbf{p})]}{\partial p_x}\right|^{-1}_{p_x=q}$$

$$\times\left|\exp\left\{\frac{i}{e\hbar E}\int_{p_x=q}^{p_x}[\varepsilon_c(\mathbf{p}') - \varepsilon_v(\mathbf{p}') - \hbar\omega]\,dp_x'\right\}\right|^2. \quad (7)$$

Multiplying this expression by the number of oscillations of the electron per unit time, $eEd/2\pi\hbar$, and integrating over all $\mathbf{p}_0$, we obtain the absorption probability for a photon of frequency $\omega$ per unit volume per unit time. Electrons with this same $p_{0y}$ and $p_{0z}$, but different $p_{0x}$, will be found to carry out exactly the same motions, but with a shift in time. Hence integration over $p_x$ is equivalent to a simple multiplication by 1/d, the number of states with a given $p_{0y}$ and $p_{0z}$. Using the expansion (5), and bearing in mind that, for the almost trivial case under consideration, $m_{ik}^{-1} = m^{*-1}\delta_{ik}$, we arrive at the following final result (for frequencies $\omega < \omega_0$):

$$W(\omega) = \frac{e^2}{\hbar c}\frac{c}{\omega}\left(\frac{m^*}{m}\right)^2\sqrt{2\frac{\varepsilon_0 - \hbar\omega}{m^*}}\frac{(e\hbar E)^2}{m^*(\varepsilon_0 - \hbar\omega)^3}|\mathbf{eM}_{vc}(\mathbf{p}_m)|^2$$
$$\times\exp\left\{-\frac{4\sqrt{2m^*}}{3e\hbar E}(\varepsilon_0 - \hbar\omega)^{3/2}\right\}. \quad (8)$$

It is not difficult to repeat all the steps outlined above for more general cases as well — lattices with any symmetry and with arbitrary field directions, in which the electron motion, generally speaking, is aperiodic (see, for instance, Keldysh[3]). The number of photons absorbed per unit volume in unit time is then given by the following expression (under the condition $\omega < \omega_0$)

$$W(\omega) = \frac{e^2}{\hbar c}\frac{c}{\omega}\sqrt{\frac{m_1m_2m_3}{m^3}\frac{2(\varepsilon_0 - \hbar\omega)}{m}}\frac{(e\hbar E)^2}{m_\parallel(\varepsilon_0 - \hbar\omega)^3}|\mathbf{eM}_{vc}(\mathbf{p}_m)|^2$$
$$\times\exp\left\{-\frac{4\sqrt{2m_\parallel}}{3e\hbar E}(\varepsilon_0 - \hbar\omega)^{3/2}\right\},$$
$$m_\parallel^{-1} = \sum_i\cos^2\gamma_i/m_i, \quad (9)$$

where $m_i^{-1}$ are the diagonal terms of the tensor $m_{ik}^{-1}$, and $\gamma_i$ are the angles between the field and the principal axes of the tensor $m_{ik}^{-1}$. This formula applies when $\sqrt{m_\parallel}\,(\epsilon_0 - \hbar\omega)^{3/2}/e\hbar E \gtrsim 1$. For $\omega > \omega_0$ and $\sqrt{m_\parallel}\,(\hbar\omega - \epsilon_0)^{3/2}/e\hbar E \gtrsim 1$, formula (6) is still valid.

Comparison of these two expressions shows that in an electric field $\mathbf{E}$ there is a fundamental change in the frequency dependence of the absorption coefficient near the threshold, which can be integrated between known limits to give a shift of the absorption edge toward the red by a distance of the order of

$$\Delta\omega_E = \frac{1}{\hbar}\left[(eE)^2\frac{\hbar^2}{m_\parallel}\right]^{1/3} = \frac{1}{\hbar}\left[(eEd)^2\frac{\hbar^2}{m_\parallel d^2}\right]^{1/3}. \quad (10)$$

For crystals whose absorption edge is in the visible region of the spectrum, in electric fields E of the order of $10^5$ v/cm, this shift amounts to hundreds of angstroms, if we assume that $m_\parallel \sim m = 10^{-27}$ g. However, it is very seldom that either an electron or a hole will have an effective mass much less than m, which would lead to an

increased $\Delta\omega_E$, since $m_\parallel$ is the resultant effective mass of the electrons and holes, and is therefore determined by the smallest of these masses. Thus the most favorable case for observing this effect is one in which the effective mass is small and the forbidden zone is not too wide (of the order of 1 — 2 ev), so that the relative value of the shift $\Delta\omega_E/\omega_0$ is not too small. The origin of this effect is analogous to the self-ionization which causes widening in the lines of atomic spectra. This case was considered by Lanczos, in whose work[4] it is shown that spectral lines which are separated from the series limit by a frequency $\Delta\omega$ widen and merge into a comlex spectrum when the applied field satisfies the condition $\Delta\omega_E \sim \Delta\omega$. The basic qualitative difference between the two cases is that in crystals this shift has nothing at all to do with the existence of any discrete lines corresponding to bound states of electrons or holes, much less to any broadening of such lines. Furthermore, the cases most suitable for the observation of the effect are those in which such states are completely absent, i.e., when the field E is so strong that $\hbar\Delta\omega_E$ is greater than the binding energy, and consequently bound states are practically non-existent. Under the opposite conditions,[5] the picture is similar to the one put forward by Lanczos.

Obviously there will be an analogous shift of the lower threshold which corresponds to absorption with the formation of phonons.

[1] V. W. Houston, Phys. Rev. **57**, 184 (1940).
[2] G. Dresselhaus, Phys. Rev. **105**, 135 (1957).
[3] L. V. Keldysh, J. Exptl. Theoret. Phys. (U.S.S.R.) **33**, 994 (1957), Soviet Phys. JETP **6**, 763 (1958).
[4] C. Lanczos, Z. Physik **62**, 518 (1930).
[5] E. F. Gross, Progress Phys. Sciences **63**, 575 (1957).

Translated by D. C. West
234

SOVIET PHYSICS JETP VOLUME 34 (7), NUMBER 5 NOVEMBER, 1958

# *DEPENDENCE OF THE HYPERFINE STRUCTURE OF F CENTERS ON THE ORIENTATION OF A CRYSTAL IN AN EXTERNAL MAGNETIC FIELD*

M. F. DEIGEN and V. Ia. ZEVIN

Institute of Physics, Academy of Sciences, Ukrainian S.S.R.

Submitted to JETP editor November 10, 1957

J. Exptl. Theoret. Phys. (U.S.S.R.) **34**, 1142-1147 (May, 1958)

The spin Hamiltonian for the interaction between an F-center electron and the angular momenta of the first and second coordinational spheres surrounding the nuclei have been obtained by using the continual and orbital models of F centers in KCl-type lattices. The dependence of the frequency of spin-nuclear transitions on the orientation of the crystal in an external static magnetic field is considered. Comparison of theory with experiment leads to a satisfactory agreement between the angular dependences and (to order of magnitude) of the spin-Hamiltonian coefficient. The square of the F-center wave function in the potassium and chlorine sites of the lattice have been determined by comparison with experiment.

1. The spin-electron resonance of F center in an ionic crystal was considered in Refs. 1 to 3. The most general form of the spin Hamiltonian was obtained in Ref. 4 for the interaction between the localized electron in the crystal and the momenta of the surrounding nuclei. The same reference gives also the spin Hamiltonian of the F center with allowance for the interaction between the electron of the F center and the nuclei of the first coordinational sphere. It was emphasized in Refs. 2 to 4 that the spin Hamiltonian has an anisotropy which, as indicated, should cause the parameters of the

spin-resonance absorption band to depend on the orientation of the crystal in an external static magnetic field.

In a recently published article, Feher[5] was able to resolve the lines due to a change in orientation of the spins of the individual nuclei surrounding the F center upon absorption of radio waves. It has been indicated in the same reference that it is possible to explain the experimental results by using the following spin Hamiltonian for the interaction between the electron and one of the nuclei surrounding the F center:

$$\mathcal{H}_k = A(\mathbf{I}_k\mathbf{S}) + BI_{zk}S_z + Q'\left[I_{zk}^2 - \frac{1}{3}I_k(I_k+1)\right]. \quad (1)$$

Here S and $I_k$ are the respective spins of the electron of the F center and of the nucleus in the k-th site; A and B are phenomenological coefficients of the hyperfine interaction, and Q′ is the coefficient of quadrupole interaction. The coefficients in (1) were determined by Feher from comparison of the frequencies obtained from (1) with the experimental values.

If the quadrupole interaction is disregarded, the Hamiltonian (1) is contained, as a particular case, in the general spin Hamiltonian obtained in Ref. 4. What is important, however, is the fact that in Refs. 2 to 4 it was possible to calculate the coefficients of the spin Hamiltonian theoretically. Using the results of these works, we shall derive below a general form for the spin Hamiltonian of the hyperfine interaction between the F-center electron and the magnetic momenta of the nuclei of the first and second coordinational spheres. An investigation of the anisotropy of the spin-Hamiltonian coefficients leads to good agreement with the results of Feher's experiments.

**2.** The general form of the spin Hamiltonian of the interaction of a localized electron in a crystal with the magnetic moment of the k-th nucleus of the lattice is of the form[4]:

$$\mathcal{H}_k = 4\pi\frac{\mu\mu_k}{SI_k}|\psi(\rho_k=0)|^2(\mathbf{I}_k\mathbf{S}) + \sum_{p,q}A_{pqk}I_{pk}S_q, \quad (2)$$

where $\psi$ is the electron wave function, while $\mu$ and $\mu_k$ are the Bohr magneton and the magnetic moment of the nucleus in the k-th site respectively; p and q represent the rectangular coordinate axis and assume values from 1 to 3;

$$A_{pqk} = \frac{\mu\mu_k}{SI_k}\int\frac{x_{qk}}{\rho_k^3}\frac{\partial|\psi|^2}{\partial x_{pk}}dV. \quad (3)$$

Here $x_{qk}$ is the q-th component of the radius vector $\boldsymbol{\rho}_k$ drawn to the point from the k-th lattice site.

We shall henceforth take into account the most important interaction, that with the nuclei of the first and second coordinational spheres. We shall choose the rectangular system of coordinates ($x_{1k}$, $x_{2k}$, $x_{3k}$) in such a manner that its center is in the k-th site, and the $x_{3k}$ axis is directed along the radius vector $\mathbf{R}_k$ drawn from the F center to the k-th site.

The form of the $\psi$ function depends on the model of the F center. In the case of the continual model (method of effective mass[6] and strong-coupling approximation) we have

$$\psi = \varphi(r)\sum_k c_k\psi_k(\rho_k),$$

where $\varphi(r)$ is the smoothed wave function, spherically symmetrical about the lattice defect, and $\psi_k(\rho_k)$ are the atomary 4s-functions of K and $Cl^-$. If we make allowance in $\psi$ for the contribution of the ions of the first and second coordinational spheres, and also of the contribution of the central ion $Cl^-$ (the last component), we have

$$\psi = \varphi(r)\left[c_1\sum_{i=1}^{6}\psi_i(\rho_i) + c_2\sum_{i=7}^{18}\psi_i(\rho_i) + c_3\psi_0(r)\right].$$

In the orbital model of the F center[7] we have

$$\psi = c_1\sum_{i=1}^{6}\psi_i(\rho_i) + c_2\sum_{i=7}^{18}\psi_i(\rho_i),$$

where, as in the preceding case, the first sum contains the wave functions of the alkali atoms of the first coordinational sphere, and the second sum contains the corresponding functions of $Cl^{--}$ (Ref. 8). We note that the functions $\psi$ are even with respect to $x_{1k}$ and $x_{2k}$ in both models.

Let us consider first the hyperfine interaction between the F-center electron and one of the nuclei of the first coordinational sphere. In this case the axes of the local system of coordinates are directed along the principal crystallographic axes, and the coordinates $x_{1k}$ and $x_{2k}$ enter in an identical manner in $|\psi|^2$ and $\rho_k$. A consequence of the evenness of $|\psi|^2$ and $\rho_k$ with respect to $x_{1k}$ and $x_{2k}$ is the vanishing of all coefficients $A_{pqk}$ with $p \neq q$. Next, since $x_{1k}$ and $x_{2k}$ enter into $|\psi|^2$ and $\rho_k$ in an identical manner, $A_{11} = A_{22}$. The non-vanishing coefficients are $A_{11} = A_{22}$ and $A_{33}$.

From (2) and (3) we have

$$\mathcal{H}_k = 4\pi\frac{\mu\mu_k}{SI_k}|\psi(\rho_k=0)|^2(\mathbf{I}_k\mathbf{S}) + A_{11}(I_{x_{1k}}S_{x_{1k}} + I_{x_{2k}}S_{x_{2k}}) + A_{33}I_{x_{3k}}S_{x_{3k}} = A(\mathbf{I}_k\mathbf{S}) + B(\mathbf{I}_k\mathbf{R}_k)(\mathbf{S}\mathbf{R}_k), \quad (4)$$

where

$$A = \frac{\mu\mu_k}{SI_k}\left[4\pi|\psi(\rho_k=0)|^2 + \int\frac{x_{1k}}{\rho_k^3}\frac{\partial|\psi|^2}{\partial x_{1k}}dV\right],$$

$$B = \frac{\mu\mu_k}{R_k^2 S I_k}\int\left(x_{3k}\frac{\partial|\psi|^2}{\partial x_{3k}} - x_{1k}\frac{\partial|\psi|^2}{\partial x_{1k}}\right)\frac{1}{\rho_k^3}\,dV. \qquad (5)$$

We note that when A and B are calculated, for example with the aid of the continual model, use is made of integrand components containing two-center functions of the type $\varphi^2(r)\psi_1^2(\rho_1)$ (Refs. 3, 4) and the like.

Let us examine the spin Hamiltonian of the hyperfine interaction between the F-center electron with the chlorine nucleus of the second coordinational sphere. The $x_{3k}$ axis of the local system of coordinates will now be oriented along one of the twelve (110) directions, the $x_{2k}$ axis along another similar direction, and the $x_{1k}$ axis will be directed along one of the (100) crystallographic axes. In this case all the coefficients $A_{ppk}$ are different. The coefficients $A_{pqk}$ with $p \neq q$ vanish as before (the evenness of the $\psi$ functions with respect to $x_{1k}$ and $x_{2k}$). Thus, if k denotes the number of the chlorine nucleus of the second coordination sphere

$$\mathcal{H}_k = 4\pi\frac{\mu\mu_k}{SI_k}|\psi(\rho_k=0)|^2(\mathbf{I}_k\mathbf{S}) + A_{11}I_{x_{1k}}S_{x_{1k}} + A_{22}I_{x_{2k}}S_{x_{2k}}$$
$$+ A_{33}I_{x_{3k}}S_{x_{3k}} = A'(\mathbf{I}_k\mathbf{S}) + B'(\mathbf{I}_k\mathbf{R}_k)(\mathbf{S}\mathbf{R}_k) + CI_{x_{1k}}S_{x_{1k}}. \qquad (6)$$

Here

$$A' = \frac{\mu\mu_k}{SI_k}\left[4\pi|\psi(\rho_k=0)|^2 + \int\frac{x_{2k}}{\rho_k^3}\frac{\partial|\psi|^2}{\partial x_{2k}}dV\right]$$
$$B' = \frac{\mu\mu_k}{R_k^2 SI_k}\int\left(x_{3k}\frac{\partial|\psi|^2}{\partial x_{3k}} - x_{2k}\frac{\partial|\psi|^2}{\partial x_{2k}}\right)\frac{1}{\rho_k^3}\,dV,$$
$$C = \frac{\mu\mu_k}{SI_k}\int\left(x_{1k}\frac{\partial|\psi|^2}{\partial x_{1k}} - x_{2k}\frac{\partial|\psi|^2}{\partial x_{2k}}\right)\frac{1}{\rho_k^3}\,dV. \qquad (6a)$$

It is useful to bear in mind the following relation between the coefficients $A_{11}$, $A_{22}$, and $A_{33}$:

$$A_{11} + A_{22} + A_{33}$$
$$= \frac{\mu\mu_k}{SI_k}\int\left(x_{1k}\frac{\partial|\psi|^2}{\partial x_{1k}} + x_{2k}\frac{\partial|\psi|^2}{\partial x_{2k}} + x_{3k}\frac{\partial|\psi|^2}{\partial x_{3k}}\right)\frac{1}{\rho_k^3}\cdot dV \qquad (7)$$
$$= -\frac{\mu\mu_k}{SI_k}\int \operatorname{grad}\frac{1}{\rho_k}\operatorname{grad}|\psi|^2\,dV = -\frac{\mu\mu_k}{SI_k}4\pi|\psi(\rho_k=0)|^2.$$

If $A_{11} = A_{22}$, a connection is obtained between the coefficients A and BR of Ref. 4. In the general case, however, it follows from (7) that

$$B'R_k^2 = -3\left(A' - \frac{\mu\mu_k}{SI_k}\frac{8\pi}{3}|\psi(\rho_k=0)|^2\right) - C. \qquad (8)$$

In addition, it can be shown that

$$A = \frac{\mu\mu_k}{SI_k}\frac{8\pi}{3}|\psi(\rho_k=0)|^2 - b.$$

Introducing the notation

$$a = \frac{\mu\mu_k}{SI_k}\frac{8\pi}{3}|\psi(\rho_k=0)|^2 \qquad (9)$$

and taking (8) and (9) into account, we get

$$A' = a - b,$$
$$B'R_k^2 = 3b - C. \qquad (10)$$

If $C = 0$, then (5) and (6) lead to formula (1). Thus, in the case of nuclei of alkaline ions, the Hamiltonian (1) is correctly chosen, and in the case of interaction with the chlorine nuclei, the Hamiltonian (1) of Feher's work must be supplemented with a term $CI_{x_{1k}}S_{x_{1k}}$.

3. Feher observed transitions in which $\Delta S_H = 0$ and $\Delta I_H = \pm 1$ ($S_H$ and $I_H$ are the spin projections on the external static magnetic field H). The frequencies of these transitions are $h\nu = g_n\beta_n H + E_{S_H, I_H} - E_{S_H, I_{H_1}}$, where $g_n$, $\beta_n$ are the nuclear g factor and Bohr magneton and $E_{S_H, I_H}$ is the energy of the hyperfine interaction.

Assuming the field H to be in a plane perpendicular to the (001) direction and to make an angle $\theta$ with the (100) direction, we obtain for the transition frequencies the expressions given in Tables I and II.

**TABLE I**

| Directions along which the metal ions are located | Transition frequency | No. of ions |
|---|---|---|
| (001) | $h\nu = g_n\beta_n H + {}^1/_2 A$ | 2 |
| (010) | $h\nu = g_n\beta_n H + {}^1/_2 A +$ $+ {}^1/_2 BR^2_K \sin^2\theta$ | 2 |
| (100) | $h\nu = g_n\beta_n H + {}^1/_2 A +$ $+ {}^1/_2 BR^2_K \cos^2\theta$ | 2 |

The angular variations of the frequencies agree with experiment (diagram). Thus, it is seen that when $\theta = 0$ the frequencies $\nu'_{001}$, $\nu''_{001}$, and $\nu_{010}$ coincide, and when $\theta$ varies from 0 to 45° the frequency $\nu''_{001}$ increases and the other two decrease. Further, the frequency $\nu_{100}$ is less than the frequency $\nu_{010}$ at $\theta = 0$. As $\theta$ increases, $\nu_{100}$ increases and becomes equal to $\nu_{010}$ at $\theta = 45°$.

4. We shall compare quantitatively the angular dependences of Table II with Feher's experimental data. For this purpose it is necessary to determine three parameters. Two of these (A' and $B'R^2_{Cl}$) enter in all four $\nu = \nu(\theta)$ curves, while one parameter, C, is contained in only two curves ($\nu_{010}$ and $\nu_{100}$). It is possible to determine A' and $B'R^2_{Cl}$ from the experimental points of one curve,

TABLE II

| Direction, perpendicular to the plane in which the chlorine ions are located | Transition frequency | No. of ions | Designations of ions in Ref. 5 |
|---|---|---|---|
| (001) | $h\nu'_{001} = g_n\beta_n H + {}^1/_2\ A' + {}^1/_4 B' R^2_{Cl}(1 - \sin 2\theta)$ | 2 | C |
| (010) | $h\nu''_{001} = g_n\beta_n H + {}^1/_2\ A' + {}^1/_4 B' R^2_{Cl}(1 + \sin 2\theta)$ | 2 | A |
| | $h\nu_{010} = g_n\beta_n H + {}^1/_2\ (A' + C) + {}^1/_4\ (B' R^2_{Cl} - 2C)\cos^2\theta$ | 4 | B |
| (100) | $h\nu_{100} = g_n\beta_n H + {}^1/_2\ (A' + C) + {}^1/_4\ (B' R^2_{Cl} - 2C)\sin^2\theta$ | 4 | D |

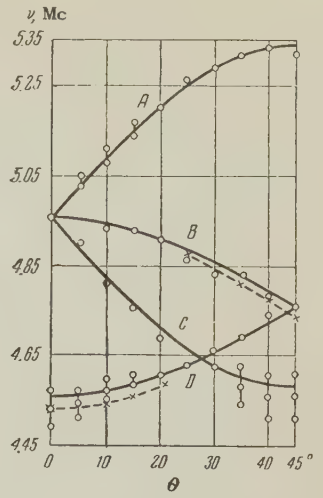


while C can be calculated from the experimental data of another curve (all three parameters cannot be determined from one experimental curve). Inserting the values of the parameters thus obtained into the two other functions $\nu = \nu(\theta)$, we can make an independent quantitative comparison with experiment. We have determined the parameters $g_n\beta_n H + A'/2$ and $B'R^2_{Cl}$ from the experimental points (Ref. 5) of the $\nu''_{001}$ curve, and have evaluated C from the points of $\nu_{100}$.

It must be noted that the spread in the experimental data makes it impossible to obtain a sufficiently accurate value of C (diagram).

The above method was used to find the following values for $Cl^{35}$ (H ≈ 3,000 oersteds)

$$A'/h \approx 6.66\ \text{Mc};\quad B'R^2_{Cl}/h \approx 1.52\ \text{Mc};\qquad C/h \approx -0.04 \div -0.1\ \text{Mc}. \tag{11}$$

Using (10), we get

$$a/h \approx 7.1\ \text{Mc};\qquad b/h \approx 0.5\ \text{Mc}. \tag{11a}$$

a and b of (11a) coincide approximately with the analogous values obtained by Feher (judging from the values of Ref. 5, the field H was somewhat greater than 3,000 oersteds).

Expression (9) makes it possible to find the value of the wave function of the F center in the sites of the first and second coordination spheres. Denoting by $\psi^2_F(K)$ and $\psi^2_F(Cl)$ the squares of the F-center wave functions in the sites indicated, we get

$$\psi^2_F(K) \approx 0.70\cdot 10^{24}\ \text{cm}^{-3};\quad \psi^2_F(Cl) \approx 0.11\cdot 10^{24}\ \text{cm}^{-3};\qquad \psi^2_F(K)/\psi^2_F(Cl) \approx 6.4 \tag{12}$$

We determined $\psi^2_F(K)$ using the experimental value a/h = 21.6 Mc (Ref. 5) for $K^{39}$, while $\psi^2_F(Cl)$ was determined from (11a).

Using the orbital model of the F center, and restricting ourselves to the first coordination sphere, we can determine $\psi^2_K(0)$ (the square of the wave function of the 4s state of potassium in the potassium site) in an approximation that does not take into account the overlapping of the functions:

$$\psi^2_K(0) \approx 6\psi^2_F(K) = 4.2\cdot 10^{24}\text{cm}^{-3}.$$

Reference 3 contains a method for calculating the coefficients of the spin Hamiltonian (5) in the continual F-center model. According to Ref. 3, and also according to Ref. 9, $A'/A \approx 0.2$, whereas experiment yields $A'/A \approx 0.32$ (A' and A are the Hamiltonian coefficients for $Cl^{35}$ and $K^{39}$ respectively). A continual-model computation gives lower values of A'/A. This is readily understood since the smoothed F-center wave function $\varphi(r)$ diminishes very rapidly in KCl (small state radii), making the macroscopic approximation inaccurate. For the same reason, the absolute values of A, A', and $BR^2$ from (5) and (6a), calculated in the continual model (Refs. 3, 9), agree with experiment only in order of magnitude.

It is interesting to calculate the coefficients of the spin Hamiltonian in the orbital model, where better agreement with experiment can be expected.

Experiment[5] leads to the following value of the ratio $A/BR^2 \approx 7$ for the coefficients of the isotropic and anisotropic terms for K. Calculations using a smoothed F-center wave function of the form $\varphi = (2\beta/\pi)^{3/2} e^{-\beta r^2}$ leads to $A/BR^2 \approx 5$. Better agreement can be obtained between theory and experiment by using a more accurate approximation for the smoothed wave function.[10]

$$\varphi = \frac{\alpha^{3/2}}{\sqrt{7\pi}}(1 + \alpha r)\, e^{-\alpha r}.$$

Let us note, finally, that the frequencies of the

spin-nuclear transitions for $Cl^{37}$ are less than the corresponding frequencies for $Cl^{35}$ by approximately a factor of 1.2, which corresponds, within experimental error, to the ratio $\mu_{Cl^{35}}/\mu_{Cl^{37}}$. This should be, according to (5) and (6a).

[1] Kip, Kittel, Levy, and Portis, Phys. Rev. **91**, 1066 (1953).

[2] M. F. Deigen and L. A. Shul' man Оптика и спектроскопия (Optics and Spectroscopy) **3**, 21 (1957).

[3] M. F. Deigen, J. Exptl. Theoret. Phys. (U.S.S.R.) **33**, 773 (1957), Soviet Phys. JETP **6**, 594 (1958).

[4] V. Ia. Zevin, Оптика и спектроскопия (Optics and Spectroscopy) **3**, 660 (1957).

[5] G. Feher, Phys. Rev. **105**, 1122 (1957).

[6] S. I. Pekar, J. Exptl. Theoret. Phys. (U.S.S.R.) **16**, 933 (1946).

[7] T. Muto, Progr. Theoret. Phys. **4**, 243 (1949); T. Inui and J. Uemura, Progr. Theoret. Phys. **5**, 252, 395 (1950).

[8] K. B. Tolpygo and O. F. Tomasevich, Укр. физ. журн. (Ukrainian Physics J.) **3**, No. 1 (1958).

[9] L. A. Shul' man, Оптика и спектроскопия (Optics and Spectroscopy) (in press).

[10] S. I. Pekar, Исследования по электронной теории кристаллов (Investigations on the Electron Theory of Crystals), GTTI, 1951.

Translated by J. G. Adashko
235

SOVIET PHYSICS JETP VOLUME 34(7), NUMBER 5 NOVEMBER, 1958

# *POLARIZATION IN HIGH-ENERGY ELASTIC SCATTERING*

L. I. LAPIDUS

Joint Institute for Nuclear Research

Submitted to JETP editor November 9, 1957

J. Exptl. Theoret. Phys. (U.S.S.R.) **34**, 1148-1153 (May, 1958)

A study is made of polarization phenomena in elastic scattering at high energies. It is shown that nuclear beams with considerable polarization can be obtained by small-angle elastic scattering. The applicability of the "black nucleus" and "gray absorbing nucleus" approximations to high-energy p − p scattering is discussed.

1. The present paper contains a discussion of the problem of polarization phenomena at high energies. We determine what peculiarities appear in the polarization phenomena in the approximation in which "diffraction" expressions appear for the scattering cross-sections averaged over the spins, and what sort of information can be obtained from the results of experiments on the polarization at high energies, at which the elastic scattering is to a large extent determined by the presence of inelastic processes.

We consider first the scattering of particles with spin $\frac{1}{2}$ by spinless particles [the case $(0, \frac{1}{2})$].

In most of the published works,* after introducing the effective potential, one makes various assumptions about the radial variation of the potentials, and discusses the results of comparison with the experimental data from the point of view of determining the parameters of the effective potential

*There are many papers in which polarization phenomena in scattering by nuclei are discussed by the use of the concepts of the optical model. We mention the papers of Riesenfeld and Watson[1] and of Brown,[2] which provide references to other papers. The writer takes occasion to thank Dr. Brown for sending him a number of unpublished notes.

(cf., e.g., Ref. 3).

2. We shall proceed differently. Without introducing the interaction potential explicitly, we determine, in analogy with the procedure used in the spinless case (cf., e.g., Refs. 4, 5), the absorption coefficients $K_1$ and $K_2$ and the indices of refraction $n_1$ and $n_2$. The quantities so introduced are related to the four functions $V_{CI}$, $V_{SI}$, $V_{CR}$, $V_{SR}$ of the paper of Riesenfeld and Watson.[1] For example, the quantity $K_1$ is proportional to the imaginary part, and $(n-1)$ to the real part, of the average amplitude for nucleon-nucleon scattering at $\theta = 0$. In the notation of Ref. 1, $K_1$ and $(n_1 - 1)k$ are proportional to the imaginary and real parts of the quantity

$$\overline{M_0} = {}^1/_8 \{[B+N+G]_{pp} + [B+N+G]_{np}\}_{\theta=0}, \quad (1)$$

and similarly $K_2$ and $(n_2 - 1)k$ are proportional to the imaginary and real parts of

$$\overline{M_1} = -\frac{1}{2i}\left[\frac{1}{\sin\theta}(C_{pp}+C_{np})\right]_{\theta=0} = -\frac{1}{2i}\left[\frac{d}{d\cos\theta}(C_{pp}+C_{np})\right]_{\theta=0}. \quad (2)$$

If we use the usual limiting transition from Legendre polynomials $P_l(\cos\theta)$ to Bessel functions $J_0(l\theta)$, then for the coefficients $A(\theta)$ and $B(\theta)$ of the amplitude

$$M = A(\theta) + B(\theta)(\sigma n), \quad \mathbf{n} = \mathbf{k}_0 \times \mathbf{k}/|\mathbf{k}_0 \times \mathbf{k}| \quad (3)$$

we get

$$2A(\theta) = ik\int_0^R bdbJ_0(kb\theta)\{2 - e^{-[K_1-2i(n_1-1)k]s} \times \left[e^{-[K_2-2i(n_2-1)k]s} + e^{[K_2-2i(n_2-1)k]s}\right]\}$$

$$2B(\theta) = -k\int_0^R bdbJ_1(kb\theta)\, e^{-[K_1-2i(n_1-1)k]s} \times \{e^{-[K_2-2i(n_2-1)k]s} - e^{[K_2-2i(n_2-1)k]s}\}, \quad (4)$$

where $s^2 = R^2 - b^2 = R^2 - l^2\lambda^2$, the remaining notation is obvious, and

$$K_1 > K_2 \geqslant 0. \quad (5)$$

Conditions (5) replace the requirement of definiteness of sign of the imaginary parts of the scattering phase shifts in the spinless case.

3. For infinite absorption ("black nucleus") $K_1 \to \infty$, and

$$A(\theta) = ik\int_0^R J_0(kb\theta)\, bdb = \frac{iR}{\theta}J_1(kR\theta); \quad B = 0;$$

$$\sigma_t = \frac{4\pi}{k}\operatorname{Im}A(0) = 2\pi R^2; \quad \sigma_s = \pi R^2 \quad (6)$$

and the polarization $\mathbf{P}_{uu}$ from the elastic scattering of an unpolarized beam becomes zero. In virtue of time reversibility the cross-section for elastic scattering of a polarized beam does not contain any azimuthal asymmetry and is the same as the cross-section $I_0(\theta)$ for the scattering of an unpolarized beam. For the polarization $\mathbf{P}_{pu}$ (Ref. 6) after scattering of a polarized ($\mathbf{P}^{in}$) beam we get

$$I_0(\theta)\mathbf{P}_{pu} = P^{in}|A(\theta)|^2 \mathbf{n}\times\mathbf{k}_0; \quad \mathbf{P}_{pu} = P^{in}\,\mathbf{n}\times\mathbf{k}_0 = \mathbf{P}^{in}, \quad (7)$$

if we choose $\mathbf{P}^{in}$ perpendicular to $\mathbf{k}_0$ and the normal n. From Eq. (7) it follows that in the approximation of the "black nucleus" there is also no rotation of the polarization. Thus the absence of any polarization effects at all is characteristic of the "black nucleus". Consequently, the observation of a nonvanishing polarization $\mathbf{P}_{uu}$ at high energy can serve as a good "indicator" of the non-applicability of the concept of the "black nucleus." We remark at once that the solution of this problem by the study of unpolarized cross-sections only is a difficult task.

4. In the absence of refraction, i.e., for $n_1 = n_2 = 1$ ("gray absorbing nucleus"),

$$A(\theta) = ik\int_0^R bdbJ_0(kb\theta)(1 - e^{-K_1 s}\cosh K_2 s),$$

$$B(\theta) = k\int_0^R bdbJ_1(kb\theta)\sinh K_2 s; \quad (8)$$

$$\sigma_t = \frac{4\pi}{k}\operatorname{Im}A(0) = 2\pi R^2\{1 - [(K_1-K_2)R]^{-2}[1 - e^{-(K_1-K_2)R} \times (1 + K_1R - K_2R)] - [(K_1+K_2)R]^{-2} \times [1 - e^{-(K_1+K_2)R}(1 + K_1R + K_2R)]\}. \quad (9)$$

The expression for the differential cross-section for elastic scattering

$$I_0(\theta) = |A(\theta)|^2 + |B(\theta)|^2 \quad (10)$$

follows from Eq. (8). Integrating Eq. (10), we get for the total cross-section for elastic scattering

$$\sigma_s = \pi R^2\{1 - {}^1/_2(K_1R)^{-2}[1 - e^{-2K_1R}(1 + 2K_1R)] - 2(K_1-K_2)^{-2}R^{-2}[1 - e^{-(K_1-K_2)R}(1 + K_1R - K_2R)] - 2(K_1+K_2)^{-2}R^{-2}[1 - e^{-(K_1+K_2)R}(1 + K_1R + K_2R)]\}. \quad (11)$$

The expression for the total cross-section $\sigma_c$ for inelastic processes is obtained by taking the difference of the expressions (9) and (11).

Going on to consider the polarization phenomena, we note that $A(\theta)$ is purely imaginary and $B(\theta)$ is purely real, i.e.,

$$A^+(\theta) = -A(\theta), \quad B^+(\theta) = B(\theta). \quad (12)$$

The expression for the polarization $\mathbf{P}_{uu}$

$$I_0(\theta)P_{uu} = (A^+B + AB^+) \quad (13)$$

vanishes for nonvanishing A and B. Since the azimuthal asymmetry in the cross-section for scattering of a polarized beam is proportional to the right member of Eq. (13), such asymmetry is also absent for the region of energies for which the scattering phases are purely imaginary.

For the polarization $\mathbf{P}_{pu}$ after the scattering of a polarized beam we have instead of Eq. (7)

$$I_0(\theta)\mathbf{P}_{pu} = P^{in}\{(a_0^2 - B^2)\mathbf{n}\times\mathbf{k}_0 - 2a_0 B\mathbf{k}_0\}\ . \quad (14)$$

($A = ia_0$). The quantities A and B are given by the formulas (8).

We note that the vanishing of the polarization $\mathbf{P}_{uu}$ for nonvanishing $A(\theta)$ and $B(\theta)$ also occurs, as is well known, in the Born approximation (for real potentials), since, as can be seen from the expressions for $A(\theta)$ and $B(\theta)$ in terms of the scattering phase shifts, for small real phase shifts

$$A_b^+(\theta) = A_b(\theta),\ B_b^+(\theta) = -B_b(\theta).$$

The polarization (even for real potentials) becomes different from zero if one makes the expressions for A and B obtained in the Born approximation exactly unitary.

5. From consideration of limiting cases it can be seen that the presence of a polarization $\mathbf{P}_{uu}$ is connected with deviations of the indices of refraction $n_1$ and $n_2$ from the value 1. The maximum polarization will occur when $n_1 = 1$, $K_2 = 0$. In this case

$$A(\theta) = ik\int_0^R \{1 - e^{-K_1 s}\cos[2(n_2 - 1)ks]\}J_0(kb\vartheta)\,bdb$$
$$= -A^+ = ia_0,$$
$$B(\theta) = -ik\int_0^R bdbJ_1(kb\theta)\,e^{-K_1 s}\sin[2(n_2 - 1)ks]$$
$$= -B^+ = ib_0, \quad (15)$$

and the polarization reaches 100% at a small angle, where $|a_0| = |b_0|$. The fact that such a point can exist in the case under consideration follows from the fact that in the region of small angles $A(\theta)$ is a decreasing function of the angle and $B(\theta)$ is an increasing function. The intersection $a_0 = b_0$ occurs near the first diffraction minimum. As has been shown by the analysis of Brown,[2] precisely this case is found in the interaction of protons of energy $\sim 1$ Bev with carbon. To describe the scattering one needs here two parameters $K_1$ and $n_2$ (if the radius R is known), and the study of the polarization $\mathbf{P}_{pu}$ can serve as a check on the interpretation adopted. For $\mathbf{P}_{pu}$ we have in this case instead of Eq. (14)

$$I_0(\theta)\mathbf{P}_{pu}(\theta) = P^{in}\ (a_0^2 - b_0^2)\mathbf{n}\times\mathbf{k}_0 + P_{uu}\mathbf{n}I_0(\theta). \quad (16)$$

The polarization experiments necessary for the determination of the parameters of the effective potential for nonvanishing $K_1$, $K_2$, $n_1 - 1$, and $n_2 - 1$ ($V_{CI}$, $V_{SI}$, $V_{CR}$, $V_{SR}$) have been discussed by Riesenfeld and Watson.[1]

Electromagnetic effects have not been included in the present discussion. As is shown by an examination of the spinless case,[4] it is essential in some cases to take the electromagnetic interaction into account. Of particular importance for the polarization $\mathbf{P}_{uu}$ is the change of phase of the amplitude, which manifests itself at very small angles.

The expression for the amplitude with inclusion of the effect of the magnetic moment, as obtained in the Born approximation,[7,8] has the disadvantage that the expression for $\mathbf{P}_{uu}$ does not go to zero for $\theta \to 0$. The study of the electromagnetic effects on the polarization may be of great interest in getting information about the electromagnetic properties of nucleons (relaxation of the magnetic moments).

6. We have considered above the elastic scattering of particles with spin $\frac{1}{2}$ by a spinless target [the case $(0, \frac{1}{2})$]. The qualitative results relating to $\mathbf{P}_{uu}$ remain valid also for the cases $(\frac{1}{2}, \frac{1}{2})$ and $(1, 0)$ (nucleon-nucleon scattering and scattering of deuterons by spinless nuclei). We represent the amplitude M for the nucleon-nucleon scattering in the form

$$M = BS + C(\sigma_1 + \sigma_2, \mathbf{n}) + \{{}^1\!/_2 G[(\sigma_1\Delta)(\sigma_2\Delta) + (\sigma_1\pi)(\sigma_2\pi)]$$
$$+ {}^1\!/_2 H[(\sigma_1\Delta)(\sigma_2\Delta) - (\sigma_1\pi)(\sigma_2\pi)] + N(\sigma_1\mathbf{n})(\sigma_2\mathbf{n})\}T. \quad (17)$$

Here

$$S = (1 - \sigma_1\sigma_2)/4,\quad T = (3 + \sigma_1\sigma_2)/4$$

are the singlet and triplet projection operators, and

$$\pi = (\mathbf{k}_0 + \mathbf{k})/|\mathbf{k}_0 + \mathbf{k}|,\ \Delta = (\mathbf{k}_0 - \mathbf{k})/|\mathbf{k}_0 - \mathbf{k}|.$$

From the expressions for the coefficients B, C, . . . obtained by Wright[9] it can be seen that for imaginary phases B, G, H, and N are imaginary quantities and C is real. We note particularly that just this case for $\overline{M}_0$ and $\overline{M}_1$ in Eqs. (1) and (2) leads to the maximum polarization in the scattering of nucleons by nuclei.

For imaginary phase shifts in N-N scattering the polarization $\mathbf{P}_{uu}$ goes to zero, and the cross-section for scattering of a polarized beam by an unpolarized target has no azimuthal symmetry. Thus here too the study of the polarization $\mathbf{P}_{uu}$ can be a good way of checking the correctness of the diffraction approach, with imaginary phases,

to the analysis of the experimental data. A number of other polarization effects (including the correlation of polarizations) are nonvanishing, and the correlation of the polarizations, when the beam is polarized, does not differ from the case of an unpolarized beam with an unpolarized target. The addition to the polarization

$$I_0(\theta) P_{ipq} = \frac{1}{4} \operatorname{Sp} M\sigma_{1i}M^+\sigma_{1p}\sigma_{2q}$$

goes to zero.

For imaginary scattering phase shifts the number of independent experiments is the same as the number of components in the amplitude, since the phases of the coefficients become equal to 0 and $\pi/2$.

To get an idea of what happens in the elastic scattering of particles with higher spins, let us consider briefly the case (1, 0), again confining ourselves to imaginary phase shifts. For this case the amplitude M is essentially identical with the M for the triplet scattering of neutrons by protons, i.e., we can get it by setting B = 0, T = 1 in Eq. (17) and replacing $(\sigma_1 a)(\sigma_2 a)$ by $2(\hat{S}a)^2 - 1$ in the remaining expressions, where $\hat{S}$ is the operator for spin 1. Then, as follows from the work of Wright[9] and Cheishvili,[10] the polarization $P_{uu}$ also goes to zero, while the average values of the tensors

$$\hat{D}_{ik} = {}^1/_2 (\hat{S}_i\hat{S}_k + \hat{S}_k\hat{S}_i) - {}^2/_3\delta_{ik},$$

which, together with $\hat{S}_i$, characterize the state of polarization, are not equal to zero. In general the cross-section for scattering of a polarized beam will contain terms proportional to $\cos\varphi$ and $\cos 2\varphi$, but the term containing $\cos\varphi$ is only proportional to the average value of

$$T_{2,1} = -\frac{\sqrt{3}}{2} \{(\hat{S}_x\hat{S}_z + \hat{S}_z\hat{S}_x) + i(\hat{S}_z\hat{S}_y + \hat{S}_y\hat{S}_z)\}$$

$$= -\sqrt{3}\{\hat{D}_{xy} + i\hat{D}_{yz}\}.$$

7. In the discussion of proposed experiments with nucleons of energies amounting to several Bev it is sometimes assumed that the elastic scattering of nucleons by nucleons and by nuclei will correspond to the simple picture of diffraction by a "black nucleus" or by a "gray nucleus", and that polarization phenomena will be absent. Confirmation for this is found by its proponents in the good agreement of the available experimental data on p-p scattering and the scattering of nucleons by nuclei with the simple formulas for the cross-sections in the approximation of the "black nucleus" or of the "gray absorbing nucleus" with n = 1, although the values of the parameters obtained (with the use of "spinless amplitudes") in the energy region around 1 Bev make these writers express amazement at the good agreement.

Some objections against the applicability of such an argument for the p-p scattering in the region of energies $\sim 1$ Bev have been presented by Rarita.[11]

The results of the discussion in the present paper show that also at high energies, when the elastic scattering is to a large extent determined by the presence of inelastic processes, it may turn out to be possible to obtain beams of nucleons with considerable polarization. The existence of such beams makes possible the performance of additional experiments. Polarization experiments give a sensitive method for studying spin effects in elastic scattering, the existence of which might not be revealed by the study of the differential cross-sections.

The relevance of the predictions of the "black nucleus" or "gray absorbing nucleus" approximations to polarization phenomena appears doubtful, since the quantities $(n_{1,2} - 1)k$ are proportional to the real part of the forward scattering amplitude and to its derivative with respect to the angle at $\theta \to 0$, divided by the momentum k. But even in the high-energy limit these quantities are not zero, as is shown by the dispersion relations, but approach constant nonvanishing values. The decisive quantity is the relation between the limiting values of the real and imaginary parts of the amplitude. In addition to this, the presence of a magnetic moment of the nucleon leads to the presence in the amplitude (3) of a coefficient $B(\theta)$ with a nonvanishing imaginary part.

As for the agreement of the diffraction formulas for the cross-sections with the experimental data in the region $\sim 1$ Bev, this is evidently due to the fact that the main features of the elastic scattering at high energies (the scattering is strongly directed forward and is concentrated in the region of small angles) are expressed by the simple inequality[11-13]

$$I_0(0) \geqslant (k\sigma_t/4\pi)^2, \tag{18}$$

from which one has the result that[12]

$$\pi\theta^2 \leqslant (4\pi/k\sigma_t)^2 \sigma_s. \tag{19}$$

For the n-p scattering one has added to this the quantity

$$I_0(\pi) \geqslant (k/4\pi)^2 (\sigma_{pp}^t - \sigma_{np}^t)^2. \tag{20}$$

The inequalities (18) to (20) are based on the optical theorem, i.e., they follow from the general unitary property of the S matrix, which also is preserved in the optical model. In the framework of the opti-

cal model (for $n = 1$) Eq. (18) becomes an equality, and from (19) it follows that the main range of scattering angles is given by

$$\theta^2 \leqslant (2/kR)^2.$$

These last facts also evidently explain the good agreement of the simple "diffraction" formulas with the experimental data on the elastic scattering at high energies.

Arguments analogous to those given by Okun' and Pomeranchuk[14] lead to the conclusion that in the amplitude (3) the quantity $A(\theta)$ is in general predominant in magnitude as compared with $B(\theta)$, so that the latter can be neglected in the discussion of the unpolarized cross-sections. As is shown by the arguments that have been given, in the range of angles where $A(\theta)$ and $B(\theta)$ turn out to be comparable, a considerable degree of polarization is nevertheless possible. This will also occur for the inelastic processes.

Although the discussion was primarily in terms of the interaction of nucleons with nucleons and nuclei, it of course applies to beams of other nuclei, and also to antinucleons, hyperons, etc.

We remark that beams of antinucleons, hyperons, and antihyperons are in general partially polarized by the processes that produce them. This provides the possibility of using the azimuthal dependence of the cross-sections for interaction of such beams with nucleons or nuclei to obtain information about the spin values for hyperons and antihyperons.[15]

An interesting point for study is the polarization $P_{pu}$. As can be seen from Eq. (16), $P_{pu}(\theta)$ is practically identical with $P^{in}$ in the range of angles in which $a^2 \gg b^2$. The rotation of the polarization is greatest in the region of angles where $a_0 = b_0$. There $P_{uu}$ is at its maximum, and $P_{pu}$, given by the second term in Eq. (16), is turned through an angle $\pi/2$ relative to $P^{in}$.

The writer is grateful to S. M. Bilen'kii, I. I. Levintov, R. M. Ryndin, Ia. A. Smorodinskii, and L. M. Soroko for helpful discussions and valuable comments.

[1] W. B. Riesenfeld and K. M. Watson, Phys. Rev. **102**, 1157 (1956).

[2] G. E. Brown, Proc. Phys. Soc. **A70**, 361 (1957).

[3] I. I. Levintov, Dokl. Akad. Nauk SSSR **107**, 240 (1956), Soviet Phys. "Doklady" **1**, 175 (1956).

[4] A. I. Akhiezer and I. Ia. Pomeranchuk, Некоторые вопросы теории ядра (Certain Problems of Nuclear Theory), GITTL, 1950.

[5] R. M. Sternheimer, Phys. Rev. **101**, 384 (1956).

[6] R. Oehme, Phys. Rev. **98**, 147 (1955).

[7] J. Schwinger, Phys. Rev. **73**, 407 (1948).

[8] J. T. Sample, Canad. J. Phys. **34**, 36 (1956).

[9] S. C. Wright, Phys. Rev. **99**, 996 (1955).

[10] O. D. Cheishvili, J. Exptl. Theoret. Phys. (U.S.S.R.) **30**, 1147 (1956), Soviet Phys. JETP **3**, 974 (1956).

[11] W. Rarita, Phys. Rev. **104**, 221 (1956).

[12] L. I. Lapidus, J. Exptl. Theoret. Phys. (U.S.S.R.) **31**, 1099 (1956), Soviet Phys. JETP **4**, 937 (1957).

[13] G. Wick, Phys. Rev. **75**, 1459(A) (1949).

[14] L. B. Okun' and I. Ia. Pomeranchuk, J. Exptl. Theoret. Phys. (U.S.S.R.) **30**, 424 (1956), Soviet Phys. JETP **3**, 307 (1956).

[15] L. I. Lapidus, J. Exptl. Theoret. Phys. (U.S.S.R.) **31**, 342 (1956), Soviet Phys. JETP **4**, 447 (1957).

Translated by W. H. Furry
236

# CORRELATION RELATIONS FOR RANDOM ELECTRIC CURRENTS AND FIELDS AT LOW TEMPERATURES

F. G. BASS and M. I. KAGANOV

Institute of Radiophysics and Electronics, Academy of Sciences, Ukrainian S.S.R.

Submitted to JETP editor November 26, 1957

J. Exptl. Theoret. Phys. (U.S.S.R.) **34**, 1154-1157 (May, 1958)

Correlation functions have been obtained between the components of a random electric field with account of spatial dispersion. The correlation radius depends on the frequency: for $\delta(\omega) \gg l$ it is identical with the depth of the skin layer, while for $\delta(\omega) \ll l$ it coincides with the length of the mean free path.

As has been shown by Leontovich and Rytov,[1]* the correlation between the random side currents in a metal is determined by the conductivity tensor $\sigma_{ik}$

$$[j_i(\mathbf{r})\, j_k(\mathbf{r}')]_\omega = \frac{\hbar\omega}{2\pi}\sigma_{ik}\coth\frac{\hbar\omega}{2T}\delta(\mathbf{r}-\mathbf{r}'), \tag{1}$$

while for $\hbar\omega \ll T$

$$[j_i(\mathbf{r})\, j_k(\mathbf{r}')]_\omega = \frac{T}{\pi}\sigma_{ik}\delta(\mathbf{r}-\mathbf{r}'). \tag{2}$$

By means of Eqs. (1) or (2) we can find the correlation relations between the components of random fields (for example, see Ref. 4, § 90).

However, at low temperatures, Ohm's law, $j_i = \sigma_{ik}E_k$, which was used in the derivation of Eq. (1), must be replaced by the integral relation between the current density $\mathbf{j}$ and the direction of the electric field $\mathbf{E}$.[5] This connection is obtained from the solution of the kinetic equation. In the general case, the integral connecting the current and the field has the following form:

$$j_i(\mathbf{r}) = \int K_{ik}(\mathbf{r}, \mathbf{r}')\, E_k(\mathbf{r})\, dv'. \tag{3}$$

The space correlation function between the components of the electric current is expressed simply by the components of the kernel $K_{ik}(\mathbf{r}, \mathbf{r}')$. Actually, according to Eq. (90.5) of Ref. 4, we can introduce the generalized coordinates $x_a$ and the generalized forces $f_a$ in the following manner: $x_a \to \mathbf{E}\Delta v/4\pi$ ($\Delta v$ = element of volume), $f_a \to \mathbf{K}$, where $\mathbf{K}$ [ not to be confused with $K_{ik}(\mathbf{r}, \mathbf{r}')$!] is connected with the current density by the relation $\mathbf{j} = -(i\omega/4\pi)\mathbf{K}$. Transforming in Eq. (3) from integration to summation, and replacing $\mathbf{j}$ by $\mathbf{K}$, we find the following connection between the generalized force and the generalized coordinates:

$$K_i(\mathbf{r}) = \frac{16\pi^2 i}{\omega}\sum_{k,\,\mathbf{r}'} K_{ik}(\mathbf{r}, \mathbf{r}')\, E_k(\mathbf{r}')\,\frac{\Delta v}{4\pi}.$$

From a comparison of this expression with (88.10) of Ref. 4, it is seen that the kinetic coefficients $\alpha_{ab}^{-1}$ in the given case are equal to $(16\pi^2 i/\omega)\,K_{ik}(\mathbf{r}, \mathbf{r}')$, whence, in accord with Eq. (88.11) of Ref. 4, we obtain the following relation for the generalized forces $K_i(\mathbf{r})$:

$$[K_i(\mathbf{r})\, K_k(\mathbf{r}')]_\omega = -\frac{8\pi\hbar}{\omega}\,\mathrm{Re}\,K_{ik}(\mathbf{r}, \mathbf{r}')\coth\frac{\hbar\omega}{2T},$$

or, turning again to the currents:

$$[j_i(\mathbf{r})\, j_k(\mathbf{r}')]_\omega = \frac{\hbar\omega}{2\pi}\,\mathrm{Re}\,K_{ik}(\mathbf{r}, \mathbf{r}')\coth\frac{\hbar\omega}{2T}. \tag{4}$$

Thus, to find the correlation relations, it is only necessary to write out the concrete form of the connection between the current density $\mathbf{j}$ and the direction of the electric field $\mathbf{E}$.

For this purpose, we make use of the linearized kinetic equation (for simplicity, the dispersion law is taken to be quadratic and we introduce the relaxation time $\tau$):

$$\frac{\partial f_1}{\partial t} + \frac{\partial f_1}{\partial \mathbf{r}}\mathbf{v} + \frac{f_1}{\tau} = -\frac{\partial f_0}{\partial \varepsilon}\, e\mathbf{E}\cdot\mathbf{v}. \tag{5}$$

Here $\partial f_0/\partial\epsilon = -\delta(\epsilon - \epsilon_0)$, and $\epsilon_0$ is the Fermi energy; the current density is determined by the following:

$$\mathbf{j} = \frac{2e}{(2\pi\hbar)^3}\int f_1 \mathbf{v}\, d\tau_p. \tag{6}$$

In the case of an unbounded metal, replacing $\mathbf{E}$ and $f_1$ in the Fourier integral by (5) and (6), we find

$$K_{ik}(\mathbf{r}, \mathbf{r}') = \frac{\sigma_0}{(2\pi)^3}\,\frac{3}{4\pi}\iint \frac{n_i n_k\, do\, e^{i\mathbf{k}(\mathbf{r}-\mathbf{r}')}}{1 + i(\mathbf{k}nl - \omega\tau)}\, d\tau_{\mathbf{k}}. \tag{7}$$

*See also Refs. 2 and 4. The most satisfactory account of the problem of correlations for our purposes is contained in Electrodynamics of Continuous Media by L. D. Landau and E. M. Lifshitz.[4]

Here $\sigma_0$ is the static conductivity, $\mathbf{n} = \mathbf{v}/v$, do = element of solid angle in momentum space, $l = v/\tau$ = length of the mean free path (v is the constant value of the velocity on the Fermi surface).

It is easy to see that in these cases, when we can neglect spatial dispersion ($l = 0$), we get Eq. (1), wherein in this case,

$$\sigma_{ik} = \sigma_0 \delta_{ik}/(1 + \omega^2\tau^2).$$

Making use of Eq. (7), we compute the dependence of the correlation function on $\rho = \mathbf{r} - \mathbf{r}'$:

$$[j_i(\mathbf{r})\, j_k(\mathbf{r}')]_\omega = \frac{\hbar\omega}{4\pi} \coth\frac{\hbar\omega}{2T} \cdot \frac{3\sigma_0}{4\pi} \left\{ \frac{\delta_{ik}}{\rho l^2} \int_0^1 \left(\frac{1}{u^2} - 1\right) e^{-\rho|u|l} \left(\cos\frac{\rho\omega\tau}{ul} + \omega\tau \sin\frac{\rho\omega\tau}{ul}\right) du + \frac{1}{1+\omega^2\tau^2} \frac{\partial^2}{\partial x_i \partial x_k} \right.$$

$$\left. \times \left[ \frac{1}{\rho} \int_0^1 (3u^2 - 1)\, e^{-\rho|u|l} \left(\cos\frac{\rho\omega\tau}{ul} - \omega\tau \sin\frac{\rho\omega\tau}{ul}\right) du \right] \right\}. \quad (8)$$

Clearly, there is a broad range of frequencies (up to the infrared) in which spatial dispersion is important, while time dispersion can be neglected ($\omega\tau \ll 1$). In this region, Eq. (8) can be materially simplified:

$$[j_i(\mathbf{r})\, j_k(\mathbf{r}')]_\omega = \frac{\hbar\omega}{4\pi} \coth\frac{\hbar\omega}{2T} \cdot \frac{3\sigma_0}{4\pi} \left\{ \frac{\delta_{ik}}{\rho l^2} \int_0^1 \left(\frac{1}{u^2} - 1\right) e^{-\rho|u|l}\, du \right.$$

$$\left. + \frac{\partial^2}{\partial x_i \partial x_k} \left[ \frac{1}{\rho} \int_0^1 (3u^2 - 1)\, e^{-\rho|u|l}\, du \right] \right\} \quad (9)$$

or

$$[j_i(\mathbf{r})\, j_k(\mathbf{r}')]_\omega = \frac{\hbar\omega}{4\pi} \coth\frac{\hbar\omega}{2T} \cdot \frac{3\sigma_0}{4\pi} \left\{ \delta_{ik} \left[ \frac{e^{-\rho/l}}{\rho^2 l} - \frac{1}{\rho l^2} E_2\left(\frac{\rho}{l}\right) \right] \right.$$

$$\left. + \frac{\partial^2}{\partial x_i \partial x_k} \left[ \frac{1}{\rho} \left( 3E_4\left(\frac{\rho}{l}\right) - E_2\left(\frac{\rho}{l}\right) \right) \right] \right\}, \quad (10)$$

where

$$E_n(x) = \int_1^\infty e^{-zx} z^{-n}\, dz.$$

In two limiting cases, it follows from Eq. (10) that

$$[j_i(\mathbf{r})\, j_k(\mathbf{r}')]_\omega \approx \frac{\hbar\omega}{4\pi} \coth\frac{\hbar\omega}{2T} \cdot \frac{3\sigma_0}{4\pi} \frac{\delta_{ik}}{\rho^2 l} \quad (\rho/l \ll 1);$$

$$[j_i(\mathbf{r})\, j_k(\mathbf{r}')]_\omega \approx \frac{\hbar\omega}{4\pi} \coth\frac{\hbar\omega}{2T} \cdot \frac{3\sigma_0}{2\pi} \frac{\nu_i \nu_k}{\rho^2 l} e^{-\rho/l}; \quad \nu_i = \frac{\rho_i}{\rho} \quad \left(\frac{\rho}{l} \gg 1\right). \quad (11)$$

Therefore the random currents, as was to be expected, are correlated at distances of the order of the mean free path length $l$.

Using the correlation relations for the components of the random currents, we can, by means of Maxwell's equations, obtain correlation relations between the components of the electric and magnetic fields.[1]

However, it is better to proceed otherwise; from Maxwell's equations, we have

$$(\operatorname{curl}\mathbf{H})_i = \frac{4\pi}{c} \int K_{ik}(\mathbf{r}, \mathbf{r}')\, E_k(\mathbf{r}')\, dv' + \frac{4\pi}{c} j_i^{\text{for}}, \quad (12)$$

$$\operatorname{curl}\mathbf{E} = -\frac{1}{c}\frac{\partial \mathbf{H}}{\partial t}.$$

Eliminating $\mathbf{H}$ from the system (12), and solving for $\mathbf{E}$, we get the following expression for the electric field:

$$E_i = \frac{4\pi i}{\omega} \int \Lambda_{ik}(\mathbf{r}, \mathbf{r}')\, j_k^{\text{for}}(\mathbf{r}')\, dv'. \quad (13)$$

Introducing the generalized coordinates and generalized forces $x_a \to \mathbf{E}$, $f_a \to \mathbf{K}\Delta v/4\pi$, and also transforming (13) from an integration to a summation, just as was done in deriving Eq. (4), we find

$$[E_i(\mathbf{r})\, E_k(\mathbf{r}')]_\omega = 2\hbar \coth\frac{\hbar\omega}{2T} \cdot \operatorname{Im}\Lambda_{ik}(\mathbf{r}, \mathbf{r}'). \quad (14)$$

It is simplest to find the kernel $\Lambda_{ik}(\mathbf{r}, \mathbf{r}')$ in the case under consideration by going over to Fourier components in (12). Then, solving the resultant system relative to the Fourier components of the electric field intensity, and employing the inverse Fourier transformation, we get the following formulas:

$$\Lambda_{ik}(\rho) = \frac{\omega^2}{4\pi^2 c^2} \left\{ \frac{\delta_{ik}}{i\rho} \int_{-\infty}^{\infty} \frac{e^{ik\rho}}{L_1} k\, dk \right.$$

$$\left. + \frac{\delta^2}{6} \frac{\partial^2}{\partial x_i \partial x_k} \frac{1}{\rho} \int_{-\infty}^{\infty} \frac{L_2}{L_1} \frac{(kl)^2 e^{ik\rho} k\, dk}{1 - \arctan kl/kl} \right\}. \quad (15)$$

Here

$$L_1 = k^2 - \frac{3i}{\delta^2} \left[ \left(1 + \frac{1}{(kl)^2}\right) \frac{\arctan kl}{kl} - \frac{1}{(kl)^2} \right], \quad (16)$$

$$L_2 = -\left\{ 1 + \frac{3i}{(k\delta)^2} \left[ \frac{3}{(kl)^2} - \left(1 + \frac{3}{(kl)^2}\right) \frac{\arctan kl}{kl} \right] \right\},$$

$\delta = c/\sqrt{2\pi\sigma_0\omega}$ is the penetration depth of the low frequency field in metals. As the mean free path approaches zero, Eq. (14) takes the form

$$[E_i(\mathbf{r})\, E_k(\mathbf{r}')]_\omega = \frac{\hbar}{2\pi} \coth\frac{\hbar\omega}{2T} \left\{ \frac{\omega^2}{c^2\rho} e^{-\rho/\delta} \sin\frac{\rho}{\delta} \delta_{ik} \right.$$

$$\left. - \frac{\omega}{4\pi\sigma_0} \frac{\partial^2}{\partial x_i \partial x_k} \frac{e^{-\rho/\delta}}{\rho} \cos\frac{\rho}{\delta} \right\}. \quad (17)$$

This equation can be obtained directly from Eqs. (90.23) of Ref. 4, if we assume the dielectric constant of the metal to be equal to $\epsilon = 4\pi\sigma_0 i/\omega$.

We consider the opposite limiting case (large mean free path, $l \gg \delta$). The general formulas (for any ratio between $\rho$ and $l$) are very rough We limit ourselves to asymptotic expressions in the two cases:

1. $\rho \ll \delta \ll l$:

$$[E_i(\mathbf{r})\,E_k(\mathbf{r}')]_\omega = 2\hbar\coth\frac{\hbar\omega}{2T}\left\{A\,\frac{\omega^2}{c^2(\delta^2 l)^{1/3}}\,\delta_{ik} - \frac{\omega^2}{c^2}\,\frac{\delta^2 l^2}{6}\,\frac{\partial^2}{\partial x_i \partial x_k}\,\delta(\rho)\right\}, \qquad (18)$$

where

$$A = 1729/2^{1/3}\pi^{2/3}3^{1/3} \approx 570.$$

Here the spectral density of the energy per unit volume of the electric field in the metal, $W_\omega$, is equal to

$$W_\omega = \frac{1}{8\pi}\{E^2\}_\omega = \frac{3A\hbar}{4\pi}\coth\frac{\hbar\omega}{2T}\cdot\frac{\omega^2}{c^2(\delta^2 l)^{1/3}}. \qquad (19)$$

In averaging over an infinitely small volume, the second component in Eq. (18) drops out.

2. $\delta \ll l \ll \rho$. For calculation of the integrals entering into Eq. (15), it is appropriate in this case to extend the path of integration to infinity[5] (we consider k a complex variable, Im k → ∞), taking into account all the singularities of the integral. The singularities of the integrand are the zeros of the denominator and k = i (branch point). After transformation, the integrals reduce to a sum of residues and an integral from i to i∞.

It is easy to see that for $\delta \ll l$ the sum of the residues is appreciably less than the integral, the asymptotic value of which leads to a correlation function of the following sort:

$$[E_i(\mathbf{r})\,E_k(\mathbf{r}')]_\omega = \frac{\hbar\omega}{6\pi\sigma_0}\coth\frac{\hbar\omega}{2T}\left[\frac{\delta_{ik}}{\rho} - \frac{\nu_i\nu_k}{l\ln^2(\rho/l)}\right]\frac{e^{-\rho/l}}{\rho^2}. \qquad (20)$$

The authors take this opportunity to express their gratitude to L. D. Landau and E. M. Lifshitz for acquainting us with the book, Electrodynamics of Continuous Media, before publication.

[1] S. M. Rytov, Теория электрических флуктуаций и теплового излучения (Theory of Electrical Fluctuations and Thermal Radiation) Acad. of Sci. Press, 1953.

[2] M. L. Levin, Dokl. Akad. Nauk SSSR **102**, 53 (1955).

[3] F. V. Bunkin, Dissertation, Phys. Inst. Acad. Sci. U.S.S.R., 1955.

[4] L. D. Landau and E. M. Lifshitz, Электродинамика сплошных сред (Electrodynamics of Continuous Media), Gostekhizdat, 1957

[5] G. E. H. Reuter and E. H. Sondheimer, Proc. Roy. Soc. (London) **195**, 336 (1948).

Translated by R. T. Beyer
237

SOVIET PHYSICS JETP VOLUME 34(7), NUMBER 5 NOVEMBER, 1958

# *QUANTUM OSCILLATIONS OF THE HIGH-FREQUENCY SURFACE IMPEDANCE*

M. Ia. AZBEL'

Physico-Technical Institute, Academy of Sciences, Ukrainian S.S.R.

Submitted to JETP editor November 26, 1957

J. Exptl. Theoret. Phys. (U.S.S.R.) **34**, 1158-1168 (May, 1958)

On the basis of general formulas obtained earlier by the author, a quantum-mechanical formula is found for the total surface impedance of metals at high frequencies, where the skin depth is small in comparison with the Larmor radius and with the electronic mean free path. The analysis is carried out for an arbitrary law of dispersion for the conduction electrons. Cases involving constant magnetic fields both parallel to the surface of the metal and inclined with respect to it are studied. The influence of the thickness of the metallic film on the quantum oscillations is ascertained. It is shown that an experimental study of the surface impedance in a strong magnetic field makes it possible in principle to reconstruct the shape of the Fermi surface and to determine the velocities of the electrons on it.

## INTRODUCTION

IN Ref. 1 we found the first non-vanishing quantum correction to the current density $\Delta_j^{qu}$ at high frequencies in a film whose width D satisfies the inequality

$$D > d = \left|\frac{c}{eH}\int_{t_0'}^{t_0''} v_\zeta\,dt_2\right|_{p_z = p_z^{ext}}$$

$$v_\zeta(t_0') = v_\zeta(t_0'') = 0, \quad dv_\zeta/dt_0' > 0, \quad dv_\zeta/dt_0'' < 0, \qquad (1.1)$$

where $t$ is the period of orbital revolution of an electron in a magnetic field; $\mathbf{p}$, $\mathbf{v} = \nabla\epsilon$, and $\epsilon$ are the quasi-momentum, velocity, and energy of an electron; $\zeta$ is the direction of the normal to the surface of the metal; and $z$ is the direction of the constant magnetic field $\mathbf{H}$ (which makes an angle $\Phi$ with $\zeta$).

It was shown that under the conditions of the anomalous skin effect, when the effective skin depth $\delta_{\text{eff}}$ is small in comparison with the mean free path $l = vt_0$, with $v/\omega$, and with the radius of the Larmor orbit $r$.

$$\Delta j_i^{\text{qu}} = \sum \frac{h^3}{2\pi} H^2 \chi_i \left(\frac{d\ln S}{d\varepsilon}\right)^2 \frac{\partial \Delta M^z}{\partial H}\Big|_{\varepsilon=\varepsilon_0,\ p_z = p_z^{\text{ext}};\ 0}, \quad (1.2)$$

$$\chi_i = \frac{4\pi e^2}{h^3 \overline{t_0^{*-1}}} \left\{ v_i(t_1)\, s\left(\zeta - \int_{t_0'}^{t_1} v_\zeta dt_2\right) \times s\left(D - \zeta - \int_{t_1}^{t_0''} v_\zeta dt_2\right) \overline{v_j(t_1')\, E_j\left(\zeta - \int_{t_1'}^{t_1} v_\zeta\, dt_2\right)} \right\}_{\text{av}},$$

$$s(w) = \begin{cases} 1 & (w>0) \\ 0 & (w<0) \end{cases}; \quad \frac{1}{t_0^*} = \frac{1}{t_0} + i\omega. \quad (1.3)$$

Here the averages (denoted by the bar and by "av") are taken with respect to $t_1$ and $t_1'$; the summation is taken over all extreme cross sections of the limiting Fermi surface $\epsilon(\mathbf{p}) = \epsilon_0$, if $\pi/2 - \Phi \ll \delta_{\text{eff}}/l$, and only over central cross sections $\epsilon(\mathbf{p}) = \epsilon_0$, $p_z = 0$ if $\pi/2 - \Phi \gg \delta_{\text{eff}}/r$. In the latter case equation (1.3) is valid only for a sufficiently strong magnetic field:

$$\Omega = \frac{2\pi |e| H}{c\ \partial S/\partial \varepsilon_z} \gg \omega, \frac{1}{t_0};\ \frac{r}{\delta_{\text{eff}}}\left(\frac{\mu H}{\varepsilon_0}\right)^{1/2} \ll 1. \quad (1.4)$$

We note that Eqs. (1.2) and (1.3) give correctly the zero approximation $(\mu H/\epsilon_0)^{1/2}$ also for $D < d$, but this approximation reduces to zero, and it is the next one which is of interest. The functions $s$ in Eq. (1.3) appeared because, as it turns out, the approximation under consideration depends entirely on electrons whose average velocity is very small in the bulk metal and which do not collide with the surfaces of the film.

Equations (1.2) and (1.3) permit us to obtain the quantum correction to the total surface impedance under the conditions indicated.

## 2. CALCULATION OF THE TOTAL SURFACE IMPEDANCE

In order to determine the total surface impedance it is necessary to solve Maxwell's equations, which in our case reduce to

$$E_\alpha''(\zeta) = 4\pi i\omega c^{-2} j_\alpha(\zeta) \quad (\alpha = x,\ \xi), \quad (2.1)$$

$$j_\zeta(\zeta) = 0 \quad (2.2)$$

with the following relation between the current density and the electric field intensity:

$$j_i(\zeta) = j_i^{\text{cl}}(\zeta) + \Delta j_i^{\text{qu}}(\zeta) \quad (2.3)$$

($\xi$ is the direction in the plane of the metal perpendicular to $x$). We will consider first the case of a half space. We write $j_i(\xi)$ in the form $j_i(|\xi|)$ and extend $E_j(\xi)$ as an even function into the region $\xi < 0$, just as was done in Refs. 2 and 3.

Taking a Fourier transform of both sides of (2.1) and (2.2), we obtain

$$-k^2 \mathcal{E}_\alpha(k) - 2E_\alpha'(0) = 4\pi i\omega c^{-2}\{j_\alpha^{\text{cl}} + \Delta j_\alpha^{\text{qu}}(k)\}; \quad (2.4)$$

$$j_\zeta^{\text{cl}}(k) + \Delta j_\zeta^{\text{qu}}(k) = 0. \quad (2.5)$$

The expression for $j_i^{cl}(k)$ was obtained in Ref. 3 (the results of which we shall use repeatedly in what follows), and $\Delta j_i^{\text{qu}}(k)$ has the following form for the case of a half space:

$$\Delta j_i^{\text{qu}}(k) = \sum \frac{h^3}{2\pi} H^2 \chi_i \left(\frac{d\ln S}{d\varepsilon_0}\right)^2 \frac{\partial \Delta M^z}{\partial H}\Big|_{\varepsilon=\varepsilon_0,\ p_z = p_z^{\text{ext}};\ 0} \quad (2.6)$$

$$\chi_i(k) = (4\pi e^2/h^3 \overline{t^{*-1}}) \left[ v_i(t) \left[ v_j(t') \left\{ \cos\left(\frac{kc}{eH}\int_t^{t'} v_\zeta dt_2\right) \mathcal{E}_j(k) - \frac{1}{\pi}\int_{-\infty}^{\infty} \sin\frac{c}{|eH|}\left(k\int_{t_0}^{t} v_\zeta dt_2 + k'\int_{t_0'}^{t'} v_\zeta dt_2\right) \frac{\mathcal{E}_j(k')\,dk'}{k+k'} \right\} \right]_{\text{av}} \right]_{\text{av}},$$

$$\mathcal{E}_j(-k) = \mathcal{E}_j(k) = 2\int_0^\infty E_j(\zeta)\cos k\zeta d\zeta;$$

$$j_i(k) = 2\int_0^\infty j_i(\zeta)\cos k\zeta\, d\zeta. \quad (2.7)$$

For the anomalous skin effect only large $k$ and $k'$ play a substantial role;[3] by the method of steepest descents with respect to $k$ and $k'$ we find

$$\chi_i \approx \frac{8\pi^2 e^2}{h^3 \overline{t_0^{*-1}}} \frac{v_i v_j}{|v_\zeta'(t)|\, T^2} \frac{1}{k} \times \left\{ \mathcal{E}_j(k) - \frac{1}{\pi}\int_0^\infty \frac{\sqrt{k}\,\mathcal{E}_j(k')\,dk'}{\sqrt{k'}\,(k+k')} \right\}\Big|_{\varepsilon=\varepsilon_0;\ p_z = p_z^{\text{ext}};\ 0;\ v_\zeta = 0} \quad (2.8)$$

It is clear that $\chi_\xi(\xi)$ reduces to zero in this approximation (since $v_\xi = 0$). The same thing happens also for $j_\xi^{cl}(k) \sim v_\xi$ because of the fact that, for the anomalous skin effect, only electrons travelling almost parallel to the surface are important at all times. According to the same principle, the term with $\mathcal{E}_\xi(k)$ drops out in the equa-

tions for $j_\alpha$, and it is sufficient to carry out the summation only over two indices j, x and $\xi$.

Thus Eq. (2.5) is satisfied automatically, and there remains only the solution of Eq. (2.4).

In the case of a magnetic field parallel to the surface of the metal, the asymptote of $j_\alpha^{cl}(k)$ with respect to k has the form[3]

$$j_\alpha^{cl}(k) = \frac{3\pi}{4k}\left\{A_{\alpha\beta}^{cl}\mathcal{E}_\beta(k) - \frac{2}{\pi^2}C_{\alpha\beta}^{cl}\int_0^\infty \frac{k\ln(k/k')\,\mathcal{E}_\beta(k')\,dk'}{k^2-k'^2} - \frac{1}{\pi}(A_{\alpha\beta}^{cl}-C_{\alpha\beta}^{cl})\int_0^\infty \sqrt{\frac{k}{k'}}\frac{\mathcal{E}_\beta(k')\,dk'}{(k+k')}\right\}, \quad (2.9)$$

where

$$A_{\alpha\beta}^{cl} = \frac{8e^2}{3h^3}\int_0^{2\pi}\frac{n_\alpha n_\beta}{K}\cdot\frac{d\varphi}{1-\exp\left\{-2\pi i\frac{\omega}{\Omega}-\frac{2\pi}{\Omega t_0}\right\}};$$

$$B_{\alpha\beta}^{cl} = \frac{8e^2}{3h^3}\int_0^{2\pi}\frac{n_\alpha n_\beta}{K}d\varphi; \quad (2.10)$$

$$C_{\alpha\beta}^{cl} = B_{\alpha\beta}^{cl} - \frac{2e^2}{3h^3}\int_0^{2\pi}\frac{n_\alpha n_\beta}{K}\left(1-\exp\left\{-2\pi i\frac{\omega}{\Omega}-\frac{2\pi}{\Omega t_0}\right\}\right)d\varphi;$$

$$\mathbf{n} = \mathbf{v}/v = (n_x,\ n_y,\ n_z) = (\sin\theta\sin\varphi,\ \cos\theta,\ \sin\vartheta\cos\varphi);$$

all quantities are evaluated at $\epsilon = \epsilon_0$, $\theta = \pi/2$ ($v_y = 0$); K is the Gaussian curvature at the corresponding point; $1/t_0$ is averaged over the time of revolution of an electron in its orbit.

In the case most important to us, that of a strong magnetic field ($\Omega \gg \omega$, $1/t_0$) and resonance ($\omega \approx \pm\Omega$, $\pm 2\Omega, \ldots$) it is sufficient to retain in (2.9) only terms with $A_{\alpha\beta}$. Then from (2.9), (2.6), and (2.8) it is clear that the quantum correction changes only $A_{\alpha\beta}$:

$$j_\alpha(k) = \frac{3\pi}{4}A_{\alpha\beta}\frac{1}{k}\left\{\mathcal{E}_\beta(k) - \frac{1}{\pi}\int_0^\infty\frac{\sqrt{k}\mathcal{E}_\beta(k')\,dk'}{\sqrt{k'}(k+k')}\right\}; \quad (2.11)$$

$$A_{\alpha\beta} = A_{\alpha\beta}^{cl} + \Delta A_{\alpha\beta}^{qu}; \quad \Delta A_{\alpha\beta}^{qu} = \sum\frac{16}{3}\frac{e^2}{t_0^*-1}H^2\frac{v_\alpha v_\beta}{|v_y'(t)|T^2} \times\left(\frac{d\ln S}{d\varepsilon}\right)^2\frac{\partial\Delta M^z}{\partial H}\Big|_{\varepsilon=\varepsilon_0,\ p_z=p_z^{ext},\ v_\zeta=0}. \quad (2.12)$$

In Ref. 3 it was shown how one can find, in terms of $A_{\alpha\beta}$, the total surface impedance $Z_{\alpha\beta}$, which is determined by the equation

$$E_\alpha(0) = Z_{\alpha\beta}I_\beta, \quad I_\beta = -(c^2/4\pi i\omega)E_\beta'(0), \quad (2.13)$$

$I_\beta$ is the total current in the direction $\beta$. In the special case when the complex tensor $A_{\alpha\beta}$ is reduced to principal axes, the principal values of $Z_\alpha$ are expressed in terms of the principal values of $A_\alpha$:

$$Z_\alpha \approx \frac{16}{9}\left(\frac{\sqrt{3}\pi\omega^2}{c^4}\right)^{1/3}e^{i\pi/3}A_\alpha^{-1/3}. \quad (2.14)$$

In the general case of a constant magnetic field of arbitrary magnitude and direction, the exact expression for $j_\alpha(k)$ has a very complex form. However, assuming only a small error (of the order of several percent) in the numerical factor in the expression for the impedance, one can write $j_\alpha(k)$ approximately as

$$j_\alpha(k) = \frac{3\pi}{4k}a_{\alpha\beta}; \quad a_{\alpha\beta} = a_{\alpha\beta}^{cl} + \Delta a_{\alpha\beta}^{qu}, \quad (2.15)$$

$\Delta a_{\alpha\beta}^{qu}$ is determined from equation (2.12), where $v_\zeta'$ replaces $v_y'$ and $a_{\alpha\beta}^{cl}$ coincides with $A_{\alpha\beta}^{cl}$ [see (2.10)] for $\pi/2 - \Phi \ll \delta_{eff}/l$ and with $B_{\alpha\beta}^{cl}$ for $\pi/2 - \Phi \gg \delta_{eff}/r$. The impedance $Z_{\alpha\beta}$ is easily found in terms of $a_{\alpha\beta}$:

$$Z_{xx,\ \xi\xi} = \frac{16}{9}\left(\frac{\sqrt{3}\pi\omega^2}{c^4}\right)^{1/3}e^{i\pi/3}\frac{(x_1+x_2)x_1x_2 + a_{\xi\xi,\ xx}}{x_1x_2(x_1^2+x_1x_2+x_2^2)};$$

$$Z_{x\xi} = Z_{\xi x} = -\frac{16}{9}\left(\frac{\sqrt{3}\pi\omega^2}{c^4}\right)^{1/3}e^{i\pi/3}\frac{a_{x\xi}}{x_1x_2(x_1^2+x_1x_2+x_2^2)};$$

$$x_{1,2} = \{{}^1\!/_2(a_{xx}+a_{\xi\xi}) \pm [{}^1\!/_4(a_{xx}-a_{\xi\xi})^2 + a_{x\xi}^2]^{1/2}\}^{1/3}. \quad (2.16)$$

We choose the cubic root whose argument lies in the interval $(-\pi/6,\ +\pi/6)$.

It is clear from the equations derived that the case of equal numbers of "holes" and electrons ($N_1 = N_2$) is not a special one; this result differs from the static case, but is the same as for the classical part of the high-frequency $Z_{\alpha\beta}$.

As already pointed out, the equations derived give the zero- and first-order approximations for the impedance with respect to $(\mu H/\epsilon_0)^{1/2}$ and the zero-order approximation with respect to $\delta_{eff}/r$. This approximation can reduce to zero only in the exceptional cases when $v_x$ or $v_\xi$ equals zero at the point $\epsilon = \epsilon_0$, $p_z = p_z^{ext}$, $v_\zeta = 0$. Such a case occurs, for example, for an isotropic quadratic law of dispersion in a constant magnetic field parallel to the surface and having the same direction as the electric field.

Furthermore, Eqs. (2.15) are inapplicable if the equations $p_z = p_z^{ext}$, $v_\zeta = 0$ coincide, or $\epsilon = \epsilon_0$, $p_z = p_z^{ext}$, $v_\zeta = 0$ determines a line instead of an isolated point. This happens, for instance, when the magnetic field is perpendicular to the surface and the dispersion law is isotropic. Since electrons with $p_z = 0$ are at all times in the skin layer, the skin effect is normal for them, consequently $\bar{v}_x$ or $\bar{v}_y$ becomes zero; the zeroth approximation of the impedance with respect to $(\mu H/\epsilon_0)^{1/2}$ reduces to zero; and in the sums in Eq. (4.4) of Ref. 1 it is necessary to take terms with $l \neq 0$ into account. Since electrons with a vanishing $v_z$ do not generally collide with the

surface, the calculation can be carried out also in this exceptional case (see Sec. 3).

Naturally, because of the "normality" of the skin effect for the electrons which are responsible for the quantum oscillations, and the "anomaly" of the skin effect for the remaining electrons, the relative magnitude of the quantum oscillations turns out to be considerably greater in this case than in the static one.

We note in conclusion that all the equations derived above are valid also for films which are not too thin (according to the criterion $D > d$ given above) struck on one side by an electromagnetic wave. In this case, because of the anomaly of the skin effect, the electrons with $\overline{v}_\zeta = 0$ (which are only important for $\Delta j_i^{qu}$), which do not get into the "skin-layer," in general make no contribution to $\Delta j_i^{qu}$, and the second surface of the film has absolutely no effect on $\Delta j_i^{qu}$.

If the film thickness is $D < d$, then the amplitude of the quantum oscillations with the corresponding period is zero to the approximation under consideration, since $\chi_i = 0$ [see Eq. (1.3)]. This circumstance permits one, by studying $Z_{\alpha\beta}(H)$ in films of width $D < l$, to determine the d and $S_{ext}$ corresponding to exactly this period in terms of the value of the magnetic field for which an abrupt increase occurs in the amplitude of the quantum oscillation with a given period and for a given direction of the constant magnetic field.

## 3. QUANTUM OSCILLATIONS OF THE SURFACE IMPEDANCE IN A MAGNETIC FIELD PERPENDICULAR TO THE SURFACE FOR A QUADRATIC DISPERSION LAW

We assume that $(\mu H/\epsilon_0)^{1/2} l/\delta_{eff} \ll 1$ and $l > r$. Then it is possible to regard the electrons making the essential contribution to the quantum oscillations and having $v_z \sim v(\mu H/\epsilon_0)^{1/2}$ as generally not through the spatial distribution of the electric field $\mathbf{E}$, setting $\mathbf{E} = 0$ outside the metal. Since such an extrapolation of the electric field into the region outside the metal gives simultaneously the correct classical result,[4,5] we shall obtain the exact quantum-mechanical formula for $\mathbf{j}$.

In the case under study the quasi-classical matrix elements are*

$$[\Phi(y, p_y, z, p_z)]_{nn', p_z p_z'} = \frac{1}{Th}\int_{-\infty}^{\infty} \exp\left\{-\frac{i}{\hbar}(p_z - p_z')z\right\} dz \int_0^T e^{-i\Omega(n-n')t}\,\Phi(y(t), p_y(t) z, p_z)\,dt; \quad (3.1)$$

$$\Omega = 2\pi/T = |e|H/m^* c.$$

Once the quasi-classical matrix elements are known, one can calculate $j_{x,y}$ from the equations derived in the preceding sections. It is convenient to introduce

$$j_\pm = j_x \pm i j_y;\ E_\pm = E_x \pm i E_y. \quad (3.2)$$

Then

$$E_\pm''(z) = 4\pi i\omega c^{-2} j_\pm(z); \quad (3.3)$$

$$j_\pm(z) = \int_0^\infty K_\pm(|z - z'|)\,E_\pm(z')\,dz'; \quad (3.4)$$

$$K_\pm(w) = -\frac{|e|^3 H}{ch^3}\int_{-\infty}^{\infty} dp_z \sum_{n=0}^{\infty} v_n^2 \times \frac{f^0(\varepsilon_{np_z} \mp \hbar\Omega + v_z p_z') - f^0(\varepsilon_{np_z})}{\mp\hbar\Omega + v_z p_z'} \frac{\exp\{-ip_z' w/\hbar\}}{1/t_\pm - ip_z' v_z/\hbar}, \quad (3.5)$$

where

$$v_n^2 = 2(n + 1/2)\hbar\Omega/m;\ \varepsilon_{np_z} = (n + 1/2)\hbar\Omega + p_z^2/2m;$$
$$1/t_\pm = 1/t_0 + i(\omega \pm \Omega). \quad (3.6)$$

From (3.5)

$$\Delta K_\pm^{qu}(\omega) = \sum_{s=1}^{\infty} I_s;\ I_s = -\frac{2|e|^3 H}{ch^3}\int_0^\infty e^{2\pi i n s} dn \int_{-\infty}^{\infty} dp_z' v_n^2 \times \frac{f^0(\varepsilon_{np_z} \mp \hbar\Omega + v_z p_z') - f^0(\varepsilon_{np_z})}{\mp\hbar\Omega + v_z p_z'} \frac{e^{-ip_z w/\hbar}}{1/t_\pm - ip_z' v_z/\hbar}. \quad (3.7)$$

Setting $n = n' \pm 1 - v_z p_z'/\hbar\Omega$ and noting that, by hypothesis,

$$|v_z p_z'| \sim (\mu H/\varepsilon_0)^{1/2} r/\delta_{eff} \ll 1,$$

we obtain the following result (the lower limit for

*It is a simple matter to obtain this equation by writing $\Phi$ in the form

$$\Phi = \sum_s \varphi_s(y, p_y)\,\psi_s(z, p_z)$$

and observing that in the quasi-classical approximation

$$(np_z|\varphi_s|n'p_z') = \delta(p_z - p_z')\frac{1}{T}\int_0^T e^{-i\Omega(n-n')t}\varphi_s(t)\,dt;$$

$$(np_z|\psi_s|n'p_z') = \frac{1}{h}\delta_{nn'}\int_{-\infty}^{+\infty} \exp\left\{-\frac{i}{\hbar}(p_z - p_z')z\right\}\psi_s(z, p_z)\,dz.$$

n has no effect on the oscillating part):

$$I_s = \frac{4|e|^3 t_\pm^3 H}{m\,ch^2}\,\delta(w)\int e^{2\pi i s n}dn \int_{-\infty}^{\infty} dp_z \cdot f^0(\varepsilon_{np_z}).$$

We now easily find

$$\Delta K_\pm^{qu}(w) = -\frac{2e^2 t_\pm^3 H}{m\varepsilon_0}\,\delta(w)\,\Delta M^z = -\frac{2H}{\varepsilon_0 N}\sigma_\pm \delta(w)\,\Delta M^z$$

$$\sigma_\pm = Ne^2 t_\pm/m, \qquad (3.8)$$

where N is the electron density. Here

$$\Delta j_\pm^{qu}(z) = -\frac{2H}{\varepsilon_0 N}\,\sigma_\pm \Delta M^z E_\pm(z) = \Delta s_\pm^{qu} E_\pm(z),$$

i.e., as was assumed, the skin effect is normal for the electrons responsible for $\Delta j_\pm^{qu}$, and $\Delta j_\pm^{qu}$ does not depend on the form of the boundary condition. In particular, such a result would also have been obtained for specular reflection, for which Eq. (3.4) has the form

$$j_\pm(z) = \int_{-\infty}^{\infty} K_\pm(|z-z'|)\,E_\pm(z')\,dz'. \qquad (3.9)$$

Since the character of the reflection has only a weak effect on the classical equation for the surface impedance,[3,4] we shall not solve the exact Wiener-Hopf equation, but shall consider the case of specular reflection.

Writing down the Fourier transform of (3.9) and taking into consideration the fact that, according to Ref. 4,

$$K_\pm^{cl}(k) \sim 3\pi\sigma/4kl, \qquad (3.10)$$

we obtain

$$Z_\pm = -\frac{4\pi i\omega}{c^2}\frac{E_\pm(0)}{E'_\pm(0)} = \frac{8i\omega}{c^2}\int_0^\infty \frac{dk}{k^2 + 3\pi i/2\delta^2 l k + \Delta s_\pm^{qu} 4\pi i\omega/c^2}$$

$$= Z_\pm^{cl}(0)\left\{1 - e^{-\pi/3}\,\frac{28\sqrt{3}\sigma_\pm}{c^2\varepsilon_0 N}\,\omega H\left(\frac{2\delta^2 l}{3\pi}\right)^{1/3}\Delta M^z\right\};$$

$$Z_\pm^{cl}(0) \approx \frac{16}{9}\left(\frac{\sqrt{3}\,\pi\omega^2 l}{c^4\sigma}\right)^{1/3} e^{i\pi/3}. \qquad (3.11)$$

Thus the quantum correction to the surface impedance in the zero approximation with respect to $l/\delta$ is purely real; its relative amplitude for $kT < \hbar\Omega$ is of the order of $(k\Omega/\epsilon_0)^{3/2}(l/\delta)^{2/3}$.

The fact that the calculations were carried out in terms of the variables $\zeta_{chem}$, H ($\zeta_{chem}$ is the chemical potential) and not N, H, as already mentioned,[1] is also unimportant here because $(l/\delta)^{2/3} \gg 1$.

## 4. POSSIBILITY OF CONSTRUCTING THE FERMI SURFACE

It has been shown by I. Lifshitz and Pogorelov[6] that the study of quantum oscillations is a very convenient method for ascertaining the form of the Fermi surface in metals. The periods of the quantum oscillations

$$\Delta(1/H) = |e|h/cS_{ext}\ (\varepsilon_0)$$

permit one to determine directly the extreme areas $S_{ext}$ of cross sections of the Fermi surface. Knowledge of these areas for different directions makes it possible to construct $\epsilon(\mathbf{p}) = \epsilon_0$.

From this point of view the study of quantum oscillations of the high-frequency conductivity is particularly convenient for two reasons. First, the quantum oscillations are, generally speaking, $\epsilon_0/\mu H$ times larger at high frequencies than in the static case. In particular, in strong magnetic fields the amplitude of the oscillations of dR/dH and dX/dH ($Z = R + iX$), which can be directly measured experimentally, exceeds the classical values of dR/dH and dX/dH by a factor of $(\epsilon_0/\mu H)^{1/2} \gg 1$ [this conclusion follows at once from (2.15)], which facilitates the observation of the quantum oscillations.

Second, in an inclined magnetic field the oscillations do not yield all the extreme cross sections, as in the static case or in the case of a parallel magnetic field, but only the central sections. Consequently, a study of the oscillations for different angles of inclination of the magnetic field with respect to the surface of the metal can materially simplify the analysis of the experimental curves, which in the static case is quite difficult because of the superposition of a large number of harmonics with different periods.

Up to the present time quantum oscillations of the high-frequency conductivity have not been observed experimentally. However, a study of the classical and quantum-mechanical variation of the surface impedance in a constant magnetic field is of special interest, since in principle it permits a completely determination of the form of the Fermi surface and of the velocities of the electrons over it. (The quantum-mechanical variation can be easily distinguished from the classical one by the sizes of the periods.)

A study of quantum oscillations in films of width $D < l$ is particularly convenient, since by determining $Z_{\alpha\beta}(\mathbf{H})$ one can find all the extreme cross sections without harmonic analysis. For this it would be sufficient to increase the magnetic field and find values of H for which there was an abrupt increase in the amplitude of an oscillation with a given period (different periods would appear one after the other with increasing field). Furthermore, one can obtain d directly: knowledge of this quantity for all directions makes it possible to determine its form, at least for a

convex surface. In particular in a parallel field on a central section, which is easily distinguished from others by the inclination of the field, $d = |(2c/eH)p_x^{max}|$ (the maximum is taken with respect to $t$), so that by rotating $\mathbf{H}$ in the plane of the metal we establish the shape of the cross-section $\epsilon(\mathbf{p}) = \epsilon_0$, $p_y = 0$. If we use films whose surfaces are oriented in various ways with respect to the crystallographic axes, we can plot $\epsilon(\mathbf{p}) = \epsilon_0$ directly.

Finding the magnitudes of the velocities of the electrons on the Fermi surface requires a knowledge of the extreme effective masses $(\partial S/\partial\epsilon)_{ext}/2\pi$ for different directions,[6] which can be determined from the amplitudes of the quantum oscillations of the magnetic susceptibility. However, the magnitude of the amplitude is extremely sensitive to various incidental effects, such as, for example, a mosaic crystal structure. Consequently the determination of $(\partial S/\partial\epsilon)_{ext}$ from quantum oscillations appears to be very unreliable.

$(\partial S/\partial\epsilon)_{ext}$ can be determined with considerable accuracy from the classical variation of the impedance in a magnetic field aligned parallel to the surface. The extremal masses are determined directly from the resonant frequencies of the cyclotron resonance.[3]

$$(\partial S/\partial\varepsilon)_{ext} = 2\pi|e|H_{res}/\omega c,$$

in which the interpretation of the superposition of the resonance curves is naturally simpler than the interpretation of the superposition of the quantum harmonics.

It is not difficult to distinguish the classical variation of $Z_{\alpha\beta}$ from the quantum-mechanical one. There are differences between the classical and quantum oscillations both with respect to their relative magnitudes,

$$(|\Delta Z^{qu}| \ll |Z^{cl}|, \quad |d\Delta Z^{qu}/dH| \gg |dZ^{cl}/dH|),$$

and their periods (the periods of the quantum oscillations are, as a rule, considerably smaller); in a strong magnetic field $(\Omega \gg \omega)$ the classical oscillations (cyclotron resonance) usually vanish, while the quantum-mechanical ones of course remain; for an inclined magnetic field only the quantum oscillations corresponding to central sections are conserved (in this case it is obviously expedient to study $dZ/dH$, since, in the next approximation with respect to the anomaly, the cyclotron resonance is preserved in an inclined field as well[3]). Beyond this, a change of the frequency $\omega$ of the high-frequency field can give a well-defined result: the periods of the quantum oscillations will not change at all, but the periods of the cyclotron resonance will vary directly as $\omega$.

The most convenient way to observe the quantum oscillations of $dZ/dH$ is in strong magnetic fields $\Omega \gg \omega$.

## 5. QUANTUM OSCILLATIONS OF THE STATIC CONDUCTIVITY IN FILMS

We shall make several remarks relating to quantum oscillations in films in the static case.

We note first of all that in films which are not too thin (according to the criterion given above, $D > d$), but also not too thick ($D \sim d$), only those electrons with $\bar{v}_\xi = 0$ which do not collide with the surface are important for determining $\Delta j_i^{qu}$, even in the static case. The point is that the energy spectrum of all the remaining electrons which, clearly, do collide with the surface, is not quasi-classically degenerate with respect to $P_x$, and therefore such electrons give a contribution in the next approximation with respect to $(\mu H/\epsilon_0)^{1/2}$, their contribution being $(\mu H/\epsilon_0)^{1/2} \gg 1$ times smaller than the contribution of the "sub-surface" electrons with $\bar{v}_\xi = 0$ (see Ref. 1). In those cases when the quantum correction, necessitated by those electrons which do not collide with the surface, does not reduce to zero, the problem can be solved in light of the above remark.

This pertains first of all to the de Haas-van Alphen effect in films.[7]

For a film in static fields, the quantum correction to the current density is determined by Eqs. (1.2) and (1.3). It is to be understood that these formulas are not exact in the static case, since it is impossible to introduce a free-path time even in the classical case at low temperatures. One can convince himself, however, that all of the results obtained below are qualitatively correct for any form of the collision integral.

Averaging the current density over the thickness we have

$$\overline{\Delta j_i^{qu}} = \frac{1}{D}\int_0^D \Delta j_i^{qu}(\zeta)\,d\zeta$$

$$= \sum \frac{h^3}{2\pi} H^2 h_i \left(\frac{d\ln S}{d\varepsilon}\right)^2 \frac{\partial \Delta M^z}{\partial H}\bigg|_{\varepsilon=\varepsilon_0, p_z=p_z^{ext}}; \qquad (5.1)$$

$$h_i = \frac{4\pi e^2}{h^3 t_0^{-1}}\,\bar{v}_i\left\{v_i\frac{1}{D}\int_{Q_1}^{D-Q_2} E_i(\mu)\,d\mu\right\}_{av};$$

$$Q_1 = \int_{t_0}^{t_1'} v_\zeta dt_2; \quad Q_2 = \int_{t_1'}^{t_0''} v_\zeta dt_2. \qquad (5.2)$$

In an inclined field in this approximation the summation in (5.1) is carried out only over central

cross-sections, on which (naturally, if they are closed) $\bar{\mathbf{v}} = 0$ and $\overline{\Delta j_i^{qu}} = 0$.

The effect is possible in the first approximation with respect to $(\mu H/\epsilon_0)^{1/2}$ only in a magnetic field parallel to the surface of the film, if the Fermi surface has non-central sections. Then, since $E_x$ and $E_z$ do not depend on y,

$$E_y(\mu) = E_y(D-\mu);\ \bar{v}_x = \bar{v}_y = 0,\ v_y = -|c/eH|\,dp_x/dt;$$

$$\overline{\Delta j_x^{qu}} = \overline{\Delta j_y^{qu}} = 0;\ \overline{\Delta j_z^{qu}}$$

$$= \sum \frac{h^3}{2\pi} H^2 h_z \left(\frac{d\ln S}{d\varepsilon}\right)^2 \frac{\partial \Delta M^z}{\partial H}\bigg|_{\varepsilon=\varepsilon_0,\ p_z = p_z^{ext}};$$

$$h_z = \frac{4\pi e^2}{h^3 \overline{t_0^{-1}}}\bar{v}\left\{\left(1-\frac{d}{D}\right)\bar{v}_z E_z - \left[\frac{v_y}{D}\left(\int_0^{Q_1} E_y(\mu)\,d\mu + \int_0^{Q_2} E_y(\mu)\,d\mu\right)\right]_{av}\right\},$$

where $E_y(y)$ is determined from the condition $j_y(y) = 0$. It is easy to see that in the case of the bulk metal, only $\overline{\Delta\sigma_{zz}^{qu}}$ is different from zero in the approximation under consideration. Thus practically the only case for which there are, generally speaking, "large" quantum oscillations is that of high frequencies. The oscillations of the static conductivity in films apparently do not exceed the oscillations in the bulk metal, in spite of the presence of a substantial anisotropy of the current density.

In order to determine a non-vanishing $\overline{\Delta\sigma_{ik}^{qu}}$ in films it is necessary to solve the very difficult problem of finding the energy spectrum of the electrons in the film for diffuse reflection of electrons from the boundary.

## CONCLUSIONS

1. Quantum oscillations of the high frequency conductivity are predicted, whose relative amplitudes (the amplitudes as compared with the classical quantities) are, generally speaking, $\epsilon_0/\mu H \gg 1$ times larger than the relative amplitudes of the quantum oscillations of the static conductivity.

2. The amplitudes of the quantum oscillations of dR/dH, dX/dH exceed the classical values of dR/dH, dX/dH by a factor of $(\epsilon_0/\mu H)^{1/2} \gg 1$.

3. In a magnetic field aligned parallel to the surface $(\pi/2 - \Phi \ll \delta_{eff}/l)$, the periods of the quantum oscillations are determined by all the extreme cross-sections $p_z = p_z^{ext}$ of the Fermi surface $\epsilon(\mathbf{p}) = \epsilon_0$;

$$\Delta(1/H) = |e|h/cS(\varepsilon_0, p_z^{ext});$$

in an inclined magnetic field $(\pi/2 - \Phi \gg \delta_{eff}/r)$, they are determined only by the central sections $p_z = 0$, $\epsilon(\mathbf{p}) = \epsilon_0$.

4. The tensor of the surface impedance is expressed in Eqs. (2.16) in terms of the tensor $a_{\alpha\beta} = a_{\alpha\beta}^{cl} + \Delta a_{\alpha\beta}^{qu}$, where

$$a_{\alpha\beta}^{cl} =$$

$$\begin{cases} \dfrac{8e^2}{3h^3}\displaystyle\int_0^{2\pi} \frac{n_\alpha n_\beta}{K}\,\frac{d\varphi}{1-\exp(-2\pi i\omega/\Omega - (2\pi/\Omega)\overline{t_0^{-1}})}; & \left(\dfrac{\pi}{2} - \Phi \ll \delta_{eff}/l\right) \\ \dfrac{8e^2}{3h^3}\displaystyle\int_0^{2\pi} \frac{n_\alpha n_\beta}{K}\,d\varphi; & \left(\dfrac{\pi}{2} - \Phi \gg \delta_{eff}/r\right) \end{cases}$$

$$\Omega = 2\pi/T = 2\pi|e|H/c(\partial S/\partial\varepsilon),$$

where all quantities are taken at $v_\zeta = 0$; $\mathbf{n} = \mathbf{v}/v$; $\varphi$ is the angle read along the curve $\epsilon(\mathbf{p}) = \epsilon_0$, $v_\zeta = 0$; K is the Gaussian curvature of the Fermi surface; S is the area of the cross-section $\epsilon(\mathbf{p}) = \epsilon_0$, $p_z = \text{const}$; and $t_0(\mathbf{p})$ is the free-path time, which can always be introduced for the anomalous skin effect, and

$$\Delta a_{\alpha\beta}^{qu} = \sum \frac{16}{3}\frac{e^2}{\overline{t_0^{-1}}} H^2 \frac{v_\alpha v_\beta}{|v_\zeta'|T^2}\left(\frac{d\ln S}{d\varepsilon}\right)^2 \frac{\partial \Delta M^z}{\partial H}\bigg|_{\varepsilon=\varepsilon_0,\ p_z = p_z^s,\ v_\zeta = 0},$$

$$p_z^s = \begin{cases} p_z^{ext} & (\pi/2 - \Phi \ll \delta_{eff}/l), \\ 0 & (\pi/2 - \Phi \gg \delta_{eff}/r). \end{cases}$$

5. A determination of the periods of the oscillations (both classical and quantum-mechanical) of the surface impedance with a magnetic field makes it possible to find $S_{ext}$ (from the quantum periods) and $(\partial S/\partial\epsilon)_{ext}$ (from the resonant frequencies of the cyclotron resonance). Knowledge of these quantities for different directions of the magnetic field makes it theoretically possible to construct completely the form of the Fermi surface and to find the velocities of the electrons on it. A study of $Z_{\alpha\beta}(H)$ in a monocrystalline film permits one, first, to determine $S_{ext}$ and $(\partial S/\partial\epsilon)_{ext}$ without a complicated harmonic analysis, and second, to plot the Fermi surface and the velocities of the electrons on it directly.

I am grateful to I. M. Lifshitz and L. D. Landau for valuable discussions.

Note added in proof (April 5, 1958). We add two more comments.

1. A substantial increase in the amplitude of the quantum oscillations occurs at very low frequencies, corresponding to the normal skin effect $(r \gg \delta)$

$$\Delta j_i^{qu}(t) = \Delta\sigma_{ik}^{qu} E_k(t) - a_{ik}\partial E_k/\partial t;$$

$$a_{ik} = -\sum_s \frac{8\pi e^2}{c^2 \overline{t_0^{-1}}} H^2 \left(\frac{d \ln S}{d\varepsilon}\right)^2 \times \frac{\partial \Delta M^z}{\partial H} v_i(t_1) \int_0^{t_1} v_\eta \, dt_2 \, v_j(t_1') \int_0^{t_1'} v_\eta dt_2 \Big|_{\substack{\varepsilon=\varepsilon_0 \\ p_z=p_z^s}},$$

where $\Delta\sigma_{ik}^{qu}$ is the quantum correction to the static conductivity, found in Ref. 9, and a is the positive solution of Det $|\sigma_{ik} - a\delta_{ik}| = 0$. For $r \gg \delta$ the ratio of the second term to the first is of the order of $(\epsilon_0/\mu H)(r/\delta)^2$.

2. In an inclined field, for $(r/\delta)(\mu H/\epsilon_0)^{1/2} < 1 < (l/\delta)(\mu H/\epsilon_0)^{1/2}$, cyclotron resonance occurs in the amplitude of the quantum oscillations. This make is possible to measure, on one sample of a metal, the cyclotron frequencies [and consequently also $(\partial S/\partial\epsilon)_{ext}$] for all directions of H. An investigation of a monocrystalline film makes it possible to determine all the $(\partial S/\partial\epsilon)_{ext}$ one after the other without additional harmonic analysis. Thus by determining $Z_{ik}(H)$ one can, in principle, construct from experiments with one sample the form of the Fermi surface (from the periods of the quantum oscillations) and determine the velocities of the electrons on it (from the cyclotron frequencies).

[1] M. Ia. Azbel', J. Exptl. Theoret. Phys. (U.S.S.R.) **34**, 969 (1958), Soviet Phys. JETP **7**, 669 (1958).

[2] M. Ia. Azbel', Dokl. Akad. Nauk SSSR **100**, 437 (1955).

[3] M. Ia. Azbel' and E. A. Kaner, J. Exptl. Theoret. Phys. (U.S.S.R.) **30**, 811 (1956) and **32**, 896 (1957); Soviet Phys. JETP **3**, 772 (1956) and **5**, 730 (1957); Journ. Phys. Chem. Solids **4**, 1958.

[4] M. Ia. Azbel' and M. I. Kaganov, Dokl. Akad. Nauk SSSR **95**, 41 (1954).

[5] M. Ia. Azbel' and M. I. Kaganov, Тр. физич. фак-та ХГУ (Trans. Phys. Faculty Khar'kov State University) **6**, 59 (1955).

[6] I. M. Lifshitz and A. V. Pogorelov, Dokl. Akad. Nauk SSSR **96**, 1143 (1954).

[7] M. Ia. Azbel', J. Exptl. Theoret. Phys. (U.S.S.R.) **34**, 754 (1958), Soviet Phys. JETP **7**, 518 (1958).

[8] I. M. Lifshitz, J. Exptl. Theoret. Phys. (U.S.S.R.) **30**, 814 (1956) and **32**, 1509 (1957); Soviet Phys. JETP **3**, 774 (1956) and **5**, 1227 (1957); I. M. Lifshitz and A. M. Kosevich, J. Exptl. Theoret. Phys. (U.S.S.R.) **33**, 88 (1957); Soviet Phys. JETP **6**, 67 (1958).

Translated by W. M. Whitney
238

# ANGULAR DISTRIBUTION OF INELASTICALLY SCATTERED DEUTERONS

V. I. MAMASAKHLISOV and T. I. KOPALEISHVILI

Institute of Physics, Academy of Sciences, Georgian S.S.R.

Submitted to JETP editor November 28, 1957

J. Exptl. Theoret. Phys. (U.S.S.R.) **34**, 1169-1175 (May, 1958)

Inelastic scattering of deuterons on $Mg^{24}$ and $C^{12}$ nuclei is considered on the basis of the generalized nuclear model. The $Mg^{24}$ nucleus is considered to be deformed, and the $C^{12}$ nucleus to be spherical. Assuming that the rotational level is excited in the $Mg^{24}$ nucleus upon collision with deuterons, and that a single phonon is excited in the $C^{12}$ nucleus, the angular distributions of the scattered deuterons have been computed with account of the Coulomb interaction. The results are compared with experimental data.

1. Haffner[1] has carried out an experimental investigation of the angular distribution of inelastically scattered deuterons on some light nuclei. He compared the resultant distributions with the theoretical values.[2,3]

Huby and Newns[2] considered only the nuclear interaction between deuterons and the target nucleus; calculation of the angular distribution was carried out in a fashion similar to the calculation of the distribution of (dp) reactions in Ref. 4.

In the work of Mullin and Guth[3] on obtaining the angular distribution, only the electric interaction of the deuteron with the nucleus was taken into account. Comparison with experimental data, made by Haffner, shows that the theoretical computation of the angular distribution, taking into account only the nuclear interaction, gives a satisfactory agreement at large scattering angles, while the computation taking into account only the electric interaction, leads to satisfactory agreement for small scattering angles.

It is therefore of interest to consider the simultaneous effect of both interactions, with a view to obtaining better agreement of theory with experiment in all regions of angles. In the researches mentioned above, the wave function of the nucleus is considered unknown. As a consequence, within the framework of these researches, it is not possible to clarify the relative role of each of these two interactions.

Clearly, consideration of both interactions is possible only of the basis of a definite nuclear model, which allows us to establish excitation mechanism. As Rakavy has shown,[5] we can consider the lighter nuclei, with mass number 18 to 28, on the basis of a generalized nuclear model, in which the coupling of the subshell particles with the surface shell of $O^{16}$ is strong. This means that one must consider these nuclei to be strongly deformed. Therefore, they must possess rotational levels, among which the levels of the even-even nuclei are known to possess the simplest property.

In the present research, we consider the inelastic scattering of deuterons on certain even-even nuclei on the basis of the generalized model of the nucleus.

We assume that in the collision of the deuteron with the nucleus, only collective degrees of freedom are excited as a consequence. In this situation, two cases are possible: (1) rotational and vibrational levels are excited, and (2) the excitation of the nucleus bears a phonon character. Existence of the first or second case depends on whether the original nucleus is deformed or not.

2. If we assume that the nucleon in the free state interacts with the surface of the nucleus in the same way as in the bound state, we can write for the interaction energy of the deuteron with the nucleus (in the case in which the initial state of the nucleus is deformed*)

$$H = \pm V_0 R_0 \delta (r'_p - R_0) \sum a_\nu Y_{2\nu} (\vartheta'_p, \varphi'_p)$$

$$\pm V_0 R_0 \delta (r'_n - R_0) \sum a_\nu Y_{2\nu} (\vartheta'_n, \varphi'_n) + V' + V(r), \qquad (1)$$

in the case in which the nucleus is initially undeformed,

*The presence of two signs in Eqs. (1) and (2) takes into account the possibility that the interaction of the free nucleon with the surface vibrations of the nucleus can have both an attractive and a repulsive character.

$$H = \pm V_0 R_0 \delta(r_p - R_0) \sum_\mu \alpha_\mu Y_{2\mu}(\vartheta_p, \varphi_p)$$

$$\pm V_0 R_0 \delta(r_n - R_0) \sum_\mu \alpha_\mu Y_{2\mu}(\vartheta_n, \varphi_n) + V' + V(r), \qquad (2)$$

where $V_0$ is the depth of the potential well, $R_0$ is the equilibrium nuclear radius, $(r_p, \vartheta_p, \varphi_p)$ and $(r_n, \vartheta_n, \varphi_n)$ are the coordinates of the components of the deuteron (the proton and the neutron), while the same coordinates, marked with primes in Eq. (1), denote the fact that they refer to a system of coordinates connected to the principal axes of the deformed nucleus. The quantities

$$a_2 = a_{-2} = \frac{\beta}{\sqrt{2}} \sin\gamma, \quad a_0 = \beta\cos\gamma \, (a_1 = a_{-1} = 0)$$

denote the parameters which determine the shape of the deformed nucleus possessing rotational and vibrational levels. The parameters $\alpha_\mu$ must be regarded as the creation operators of the phonons. $V'$ is the operator of electric interaction of the proton with the nucleus, which is equal to[3]

$$V' = 0 \qquad \text{for } r_p \leqslant r_0,$$

$$V' = \sum_{k=1}^{Z} e^2/|\mathbf{r}_p - \mathbf{R}_k| \qquad \text{for } r_p \geqslant r_0, \qquad (3)$$

where $R_k$ are the radius vectors of the protons of the target nucleus, $V(r)$ is the radially symmetric part of the nuclear potential.

We expand the potential $V'$ in multipoles:

$$V' = \sum V'_l, \qquad (4)$$

where

$$V'_l = \sum_{k=1}^{Z} \frac{e^2}{r_p}\left(\frac{R_k}{r_p}\right)^l P_l[\cos(\mathbf{r}_p, \mathbf{R}_k)]$$

$$= \frac{e^2}{r_p^{l+1}} \frac{4\pi}{2l+1} \sum_m Y_{lm}(\vartheta_p, \varphi_p) \sum_{k=1}^{Z} R_k^l Y^*_{lm}(\vartheta''_k, \varphi''_k).$$

We make use of the well-known relations between the parameters of collective motion in the nucleus nnd the variables of the individual particles[6]

$$\alpha_{lm} = \frac{4\pi}{3A} \sum_{k=1}^{A} \left(\frac{R_k}{R_0}\right)^l Y_{lm}(\vartheta''_k, \varphi''_k).$$

If we assume that the neutrons and protons produce identical deformation of the nucleus, then we can write:

$$V'_l = \frac{3Ze^2}{r_p^{l+1}} \frac{R_0^l}{2l+1} \sum \alpha_{lm} Y_{lm}(\vartheta_p, \varphi_p). \qquad (5)$$

In the nuclear interaction of nucleon (1) with (2), consideration is generally limited to surface deformations of second order. Therefore, in the electric interaction (5) also, one should limit oneself to the parameter $\alpha_{2m} \equiv \alpha_m$. Taking this into account and transforming to the coordinates connected with the deformed nucleus, we shall obtain

$$V'_2 = \frac{3Ze^2R_0^2}{5r_p^3} \sum_\mu \alpha_\mu Y_{2\mu}(\vartheta_p, \varphi_p)$$

$$= \frac{3Ze^2R_0^2}{5r_p^3} \sum_\nu a_\nu Y_{2\nu}(\vartheta'_p, \varphi'_p), \qquad (6)$$

where

$$\alpha_\mu = \sum_\nu a_\nu D^2_{\mu\nu}(\vartheta_i),$$

while $D^2_{\mu\nu}$ is the transformation matrix of the spherical harmonics $Y_{2\mu}$ and $\vartheta_i = (\vartheta_1, \vartheta_2, \vartheta_3)$ are the Eulerian angles.

Since the ground state of even-even nuclei is the state $0^+$, while the interaction operators (1), (2), and (6) give transitions only with a change in moment by two units, then, after the process, the nucleus is in the state $2^+$ which is the first excited level of even-even nuclei.

3. The matrix element of the process under consideration, corresponding to the interaction operators (1) and (6), has the form

$$H_{if} = \frac{1}{(2\pi\hbar)^{3/2}\sqrt{v}} \sum_\nu \Big\{ \pm V_0 R_0 \Big[ \int \exp\Big\{ -i\frac{\mathbf{k}'}{2}(\mathbf{r}_p + \mathbf{r}_n)\Big\}$$

$$\times \Phi^*(|\mathbf{r}_p - \mathbf{r}_n|)\, \psi_f^*(x)\, \delta(r'_p - R_0)\, a\, Y_{2\nu}(\vartheta'_p, \varphi'_p)$$

$$\times \exp\Big\{ i\frac{\mathbf{k}}{2}(\mathbf{r}_p + \mathbf{r}_n)\Big\} \Phi(|\mathbf{r}_p - \mathbf{r}_n|)\, \psi_i(x)\, d\mathbf{r}_p d\mathbf{r}_n dx$$

$$+ \int \exp\Big\{ -\frac{i\mathbf{k}'}{2}(\mathbf{r}_p + \mathbf{r}_n)\Big\}$$

$$\times \Phi^*(|\mathbf{r}_p - \mathbf{r}_n|)\, \psi_f^*(x)\, \delta(r'_n - R_0)\, a_\nu Y_{2\nu}(\vartheta'_n, \varphi'_n)$$

$$\times \exp\Big\{ i\frac{\mathbf{k}}{2}(\mathbf{r}_p + \mathbf{r}_n)\Big\} \Phi(|\mathbf{r}_p - \mathbf{r}_n|)\, \psi_i(x)\, d\mathbf{r}_p d\mathbf{r}_n dx \Big]$$

$$+ \frac{3Ze^2R_0^2}{5} \int \exp\Big\{ -i\frac{\mathbf{k}'}{2}(\mathbf{r}_p + \mathbf{r}_n)\Big\}$$

$$\times \Phi^*(|\mathbf{r}_p - \mathbf{r}_n|)\, \psi_f^*(x)\, a_\nu Y_{2\nu}(\vartheta'_p, \varphi'_p)$$

$$\times \exp\Big\{ i\frac{\mathbf{k}}{2}(\mathbf{r}_p + \mathbf{r}_n)\Big\} \Phi(|\mathbf{r}_p - \mathbf{r}_n|)\, \psi_i(x)\, \frac{d\mathbf{r}_p}{r_p^3}\, d\mathbf{r}_n dx \Big\}. \qquad (7)$$

In the case of interaction operators (2) and (6), we have for the matrix element of the transition

$$H_{if}=\frac{1}{(2\pi\hbar)^{3/2}\sqrt{v}}\sum_{\mu}(0\,|\,\alpha_{\mu}\,|\,1)$$

$$\times\left\{\pm V_0R_0\left[\int\exp\left\{-i\frac{\mathbf{k}'}{2}(\mathbf{r}_p+\mathbf{r}_n)\right\}\Phi^*(|\mathbf{r}_p-\mathbf{r}_n|)\right.\right.$$

$$\times\delta(r_p-R_0)\,Y_{2\mu}(\vartheta_p,\varphi_p)$$

$$\times\exp\left\{i\frac{\mathbf{k}}{2}(\mathbf{r}_p+\mathbf{r}_n)\right\}\Phi(|\mathbf{r}_p-\mathbf{r}_n|)\,d\mathbf{r}_p d\mathbf{r}_n$$

$$+\int\exp\left\{-\frac{i\mathbf{k}'}{2}(\mathbf{r}_p+\mathbf{r}_n)\right\}\Phi^*(|\mathbf{r}_p-\mathbf{r}_n|)$$

$$\times\delta(r_n-R_0)\,Y_{2\mu}(\vartheta_n,\varphi_n)$$

$$\left.\times\exp\left\{i\frac{\mathbf{k}}{2}(\mathbf{r}_p+\mathbf{r}_n)\right\}\Phi(|\mathbf{r}_p-\mathbf{r}_n|)\,d\mathbf{r}_p d\mathbf{r}_n\right]$$

$$\left.+\frac{3Ze^2R_0^2}{5}\int\exp\left\{-i\frac{\mathbf{k}'}{2}(\mathbf{r}_p+\mathbf{r}_n)\right\}\right.$$

$$\left.\times\Phi^*(|\mathbf{r}_p-\mathbf{r}_n|)\,Y_{2\mu}(\vartheta_p,\varphi_p)\exp\left\{i\frac{\mathbf{k}}{2}(\mathbf{r}_p+\mathbf{r}_n)\right\}\frac{d\mathbf{r}_p}{r_p^3}d\mathbf{r}_n\right\},\quad(8)$$

where $\Phi(\mathbf{r})=\sqrt{\alpha/2\pi}\;e^{-\alpha r}/r$ is the wave function of the interior state of the deuteron, $\mathbf{k}$ and $\mathbf{k}'$ are the wave vectors of the center of mass of the deuteron before and after scattering, $\psi_f(x)$ and $\psi_i(x)$ are the wave functions of the deformed nucleus in the excited and ground states, respectively. These functions have the form

$$\psi_f=\frac{1}{\sqrt{2\pi}}\,Y_{IM}(\vartheta,\varphi)\cdot\varphi_{n_\beta n_\gamma}'(\beta,\gamma),$$

$$\psi_i=\frac{1}{\sqrt{2\pi}}\,Y_{00}(\vartheta,\varphi)\,\varphi_{n\;n_\gamma}(\beta,\gamma),\quad(9)$$

where I is the spin of the nucleus in the excited state, M is its projection on a fixed axis, and $\varphi$ is the wave function of the vibrational state of the surface of the nucleus.

The quantity $(0|\alpha_\mu|1)$ in Eq. (8) represents the matrix element of the creation of a single phonon. It is equal to[6]

$$(0\,|\,\alpha_\mu\,|\,1)=\sqrt{\hbar\omega/2C},\quad(10)$$

where C is a coefficient characterizing the deformability of the nucleus, $\hbar\omega$ is the energy of the phonon.

Expanding the plane waves in (8) in the form of spherical waves in the fixed system, and in (7) in a system connected with the principal axes of deformation of the nucleus, we get for the matrix elements (after integration):

$$H_{if}=-\frac{4V_0R_0^3\sqrt{5\pi}}{\sqrt{v}\,(2\pi\hbar)^{3/2}}\sqrt{\frac{\hbar\omega}{2C}}\left[\frac{4\alpha}{q}\tan^{-1}\frac{q}{4\alpha}\right]$$

$$\times\left[\pm J_2(qR_0)+\frac{0.3Ze^2}{V_0R_0}\frac{J_1(qr_0)}{qr_0}\right]\quad(11)$$

and

$$H_{if}=-\frac{4V_0R_0^3\sqrt{5\pi}}{\sqrt{v}\,(2\pi\hbar)^{3/2}}\left[\frac{4\alpha}{q}\tan^{-1}\frac{q}{4\alpha}\right]\left[\pm J_2(qR_0)\right.$$

$$\left.+\frac{0.3Ze^2}{R_0V_0}\frac{J_1(qr_0)}{qr_0}\right]\sum\int\psi_f^*a_\nu D_{\nu0}^2(\vartheta\varphi\psi)\,\psi_i d\tau,\quad(12)$$

where $J_1$ and $J_2$ are the spherical Bessel functions, $q=|\mathbf{k}-\mathbf{k}'|$. Making use of the known expression for $D_{\nu0}^2$, we have

$$A=\sum_{\nu}\int\psi_f^*a_\nu D_{\nu0}^2\psi_i d\tau=(n_\beta n_\gamma\,|\,a_M\,|\,n_\beta' n_\gamma')\,\delta_{I2}/\sqrt{5}.\quad(13)$$

If we consider the case in which only rotational levels are excited in the deformed nucleus, then we must set $n_\beta'=n_\beta$ and $n_\gamma'=n_\gamma$ in Eq. (13). Furthermore, we must expect that the mean values of the parameters $a_M$ will differ slightly from their equilibrium values. Therefore, for the sake of simplicity in our case, we can in Eq. (13) take $\beta=\beta_1$ and $\gamma=0,\pi$, where $\beta_1$ is the equilibrium value of $\beta$. As a result, we obtain

$$A=\pm\beta_1\delta_{I2}\delta_{M0}/\sqrt{5},\quad(14)$$

since $a_2=a_{-2}=0$ and $a_0=\pm\beta$ here.

4. For the differential cross section of the process under study, we get (for the case in which the initial nucleus is assumed to be deformed):

$$\left(\frac{d\sigma}{d\Omega}\right)_1=\frac{20\mu^2(V_0R_0^2)^2}{\pi\hbar^4}R_0^2\sqrt{1+\frac{Q}{E_0'}}\,\frac{\beta_1^2}{5}\left[\frac{4\alpha}{q}\tan^{-1}\frac{q}{4\alpha}\right]^2$$

$$\times\left[\pm J_2(qR_0)+\frac{0.3Ze^2}{R_0V_0}\frac{J_1(qr_0)}{qr_0}\right]^2;\quad(15)$$

in the case in which the deformation of the initial nucleus is neglected,

$$\left(\frac{d\sigma}{d\Omega}\right)_2=\frac{5\hbar\omega}{2C\beta_1^2}\left(\frac{d\sigma}{d\Omega}\right)_1,\quad(16)$$

where $\mu$ is the reduced mass of the system, and $E_0$ is the energy of the incident deuteron. The sign $\pm$ in front of $J_2$ is determined by the sign in the expression for the interaction (1) and (2).

5. We compare these theoretical distributions with the experimental data for the $Mg^{24}$ and $C^{12}$ nuclei. We first consider the $Mg^{24}$ nucleus. In accord with Ref. 5, this nucleus must be regarded as deformed. Since its energy of creation is com-

paratively small (1.37 Mev), it is natural to assume that in collisions with deuterons, only rotational states are excited in them. This allows us to apply Eq. (15) to the $Mg^{24}$ nucleus. Before carcying out a comparison of the angular distribution with experimental data, we shall show in what fashion it is possible to find the values of the parameters $\beta_1$, $R_0$, $r_0$, and $V_0$ which enter into Eq. (15).

In the expression for the energy of rotation of even-even nuclei,[6]

$$E_I = (\hbar^2/2J)\, I\,(I+1), \tag{17}$$

where $J = 3B\beta_1^2$ is the effective moment of inertia, $I = 2$, while $B = (3/8\pi)\,MAR_0^2$ (M is the mass of the nucleon and A the mass number), we replace $E_I = E_2$ by the experimentally observed value of the excitation energy 1.37 Mev. At the same time we find the connection between the parameters $\beta_1$ and $R_0$. For a determination of each of these parameters separately, we must also have a second relation between them. As a second relation we can take the express which defines the quadrupole moment of the nucleus[6]

$$Q_0 = \pm (3/\sqrt{5\pi})\, ZR_0^2\beta_1. \tag{18}$$

Making use of the experimental value of the quadrupole moment of the $Mg^{24}$ nucleus ($Q_0 = 0.66 \times 10^{-24}\,cm^2$), and taking it into account that Eq. (18) usually gives values approximately twice as great as the experimental, we can in a rough way determine $R_0$ and $\beta_1$ from the two relations given above. As a result, we get $R_0 = 4 \times 10^{-13}\,cm$ and $\beta_1 = 0.77$. The value of the parameter $r_0$ can be estimated in the following way. Inasmuch as the choice of the electrical interaction in the form (3) denotes that it is essentially small in the region occupied by the nucleus, then it is natural to set $r_0 \approx R_0 + \delta R$, where $\delta R$ is the maximum change in the linear dimensions of the nucleus, produced by the deformations. According to Bohr and Mottelson,[6] it is equal to

$$\delta R = \sqrt{5/4\pi}\,\beta_1 R_0 \tag{19}$$

in our case ($\gamma = 0, \pi$). As a result, we get $r_0 = 5.9 \times 10^{-13}\,cm$ for the parameter $r_0$ for the $Mg^{24}$ nucleus. In so far as the depth $V_0$ of the potential well is concerned, we can determine it from the condition that the value of the principal maximum in the angular distribution is determined only by the nuclear interaction. If we employ this assumption and make use of the experimental value of the principal maximum, we obtain $V_0 = 1.84$ Mev. It is easy to see that in our choice of the parameters, the electric interaction plays a role comparable with the nucleus interaction.

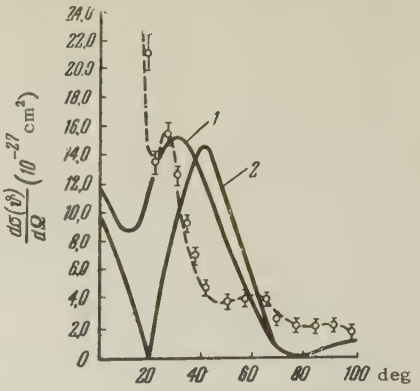


FIG. 1

The angular distribution obtained on the basis of Eq. (15) is shown in Fig. 1, where Curve 2 corresponds to the minus sign in (15) and Curve 1 to the plus sign. The rapid fall-off of Curve 2 at small angles is caused by the electrical term in the interaction, while the principal maximum and the further development of the curve is due to the nuclear term. The principal maximum on Curve 2 is displaced by about 10° relative to the position of the experimental maximum.

Curve 2 possesses a minimum at small angles, while at this same value of the angle, the experimental curve also has a minimum; however, in contrast to the experimental case, the theoretical value of the minimum is zero.

Better agreement with experiment is obtained when we take the plus sign in (15). In this case, the position of the principal maximum coincides with the one observed experimentally. Moreover, in agreement with experiment, the minimum of the theoretical curve does not lie on the axis, although it is displaced somewhat in the direction of smaller angles in comparison with the position of the experimental minimum.

We can apply Eq. (16) to the $C^{12}$ nucleus which, before the reaction, is not deformed. Inasmuch as the excitation energy is comparatively small (4.43 Mev), we consider that a single phonon excitation takes place in the collision with the deuteron. For an estimate of the parameter C entering into Eq. (16), we make use of the well-known formula[6]

$$C = 4R_0^2 S - 3Z^2e^2/10\pi R_0, \tag{20}$$

where the surface tension of the nucleus S is determined from the relation[7]

$$4\pi S R_0^2 = 15.4 A^{2/3}\,\text{Mev}. \tag{21}$$

It should be noted that this way of determining the parameter C is very crude in its application to the $C^{12}$ nucleus, since the formulas employed hold

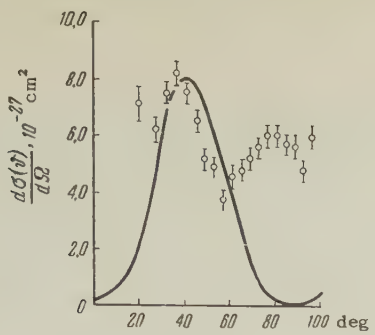


FIG. 2

for heavy nuclei. Inasmuch as the $C^{12}$ nucleus is not considered to be deformed, we have no relation between $r_0$ and $R_0$, in contrast to the $Mg^{24}$ case. Therefore we use the rough values $R_0 = 4 \times 10^{-13}$ cm and $r_0 = 6 \times 10^{-13}$ cm. In such a case, C = 24.4 Mev.

If we assume here too that the principal maximum is connected with the nuclear interaction, we obtain $V_0 = 5.41$ Mev. For the values of the parameters that we have chosen, it is seen that the electrical interaction plays almost no role in the angular distribution. The angular distribution obtained on the basis of Eq. (16) is shown by the solid curve in Fig. 2. As we see, the theoretical curve does not have a minimum and disagrees, in many respects, with the experimental data. It agrees with experiment only in relation to the presence of the principal maximum.

It is possible that this nonconformity is produced by our incorrect assumption that, in the process considered by us, a single phonon excitation arises in the $C^{12}$ nucleus. Nor is it excluded that, in such light nuclei as $C^{12}$, the generalized model is generally non-applicable.

[1] J. W. Haffner, Phys. Rev. **103**, 1398 (1956).
[2] R. Huby and H. C. Newns, Phil. Mag. **42**, 1442 (1951).
[3] C. J. Mullin and E. Guth, Phys. Rev. **82**, 141 (1951).
[4] Bhatia, Huang, Huby, and Newns, Phil. Mag. **43**, 485 (1952).
[5] G. Rakavy, Nucl. Phys. **4**, 375 (1957).
[6] A. Bohr and B. Mottelson, K. Danske Vidensk. Mat. fys. Medd. **27**, No. 16 (1953).
[7] L. Rosenfeld, Nuclear Forces (Amsterdam, 1948).

Translated by R. T. Beyer
239

SOVIET PHYSICS JETP VOLUME 34 (7), NUMBER 5 NOVEMBER, 1958

# *DISPERSION OF LIGHT IN THE EXCITON ABSORPTION REGION OF CRYSTALS*

S. I. PEKAR

Institute of Physics, Academy of Sciences, Ukrainian S.S.R.

Submitted to JETP editor November 22, 1957

J. Exptl. Theoret. Phys. (U.S.S.R.) **34**, 1176-1188 (May, 1958)

The theory of light waves in exciton-absorbing crystals, developed in Ref. 1 on the basis of a new relation between specific polarization and the electric field, is applied to cubic crystals. For each direction of propagation, the existence of three types of light waves is predicted in these crystals. One of these types is similar to ordinary waves, whereas the other two are essentially anomalous. The frequency dependence of the refractive indices of the three types is considered. Fresnel's formulas are generalized for light passing through the boundary between the crystal and a vacuum. New formulas are obtained for the coefficient of reflection from the crystal surface and for the transparency of a plane parallel plate. Methods are suggested for experimental testing of the theory and for obtaining a direct proof of the existence of second and third light in cubic crystals.

THE present article is an immediate continuation of Ref. 1, in which it was shown that in the region of exciton absorption of light the specific dipole moment of dielectric polarization and the electric field are related through a differential equation rather than by a simple linear algebraic expres-

sion. Therefore Maxwell's equations are of a higher order and possess more than the customary number of solutions. Specifically it was shown in Ref. 1 that in a crystal there can exist several plane monochromatic waves of the same frequency, direction of propagation, and polarization but with different refractive indices (different velocities of propagation). This phenomenon differs from ordinary birefringence, where the waves of different refractive indices must be polarized at right angles to each other.

The next step to be taken is the extension of all equations of theoretical crystal optics to the exciton absorption region and the prediction of new effects which could be observed experimentally and thus provide a test of the theory. It is desirable to begin with cubic crystals in order to avoid the complication of these new effects by ordinary birefringence. We shall therefore apply here the theory of Ref. 1 to cubic crystals and predict several effects which are capable of experimental verification.

## 1. REFRACTIVE INDICES OF LIGHT

In Ref. 1 it was shown that when the solution of Maxwell's equations is sought with the electric and magnetic fields proportional to $\exp\{i\omega[n(\mathbf{s}\cdot\mathbf{r})/c - t]\}$ for any given $\omega$ and $\mathbf{s}$, three types of solution are possible in a cubic crystal:

$$\mathbf{E} = \mathbf{E}_+ \exp\left\{i\omega\left[\frac{n_+}{c}(\mathbf{s}\cdot\mathbf{r}) - t\right]\right\}, \quad \mathbf{E}_+ \perp \mathbf{s}; \tag{1}$$

$$\mathbf{E} = \mathbf{E}_- \exp\left\{i\omega\left[\frac{n_-}{c}(\mathbf{s}\cdot\mathbf{r}) - t\right]\right\}, \quad \mathbf{E}_- \perp \mathbf{s}; \tag{2}$$

$$\mathbf{E} = \mathbf{E}_\parallel \exp\left\{i\omega\left[\frac{n_\parallel}{c}(\mathbf{s}\cdot\mathbf{r}) - t\right]\right\}, \quad \mathbf{E}_\parallel \parallel \mathbf{s}. \tag{3}$$

The following expressions are obtained for the refractive indices:

$$n_\pm^2 = {}^1/_2(\mu + \vartheta) \pm \sqrt{{}^1/_4(\mu - \vartheta)^2 + b}, \tag{4}$$

$$n_\parallel^2 = \mu', \tag{5}$$

with

$$\mu \equiv (2Mc^2/\hbar\omega)(1 - \mathcal{E}_0/\hbar\omega), \quad \mu' \equiv \frac{2M'c^2}{\hbar\omega}\left(1 - \frac{\mathcal{E}_0'}{\hbar\omega}\right), \tag{6}$$

where $c$ is the velocity of light in a vacuum, and $M$ and $M'$ are the effective mass of an exciton for transverse and longitudinal polarization, respectively, which can be determined if the expansion of the energy of the exciton state in powers of the wave vector $\mathbf{k}$ has the form

$$\mathcal{E}(\mathbf{k}) = \mathcal{E}_0 + \hbar^2\mathbf{k}^2/2M + \cdots \quad \mathcal{E}'(\mathbf{k}) = \mathcal{E}'_0 + \frac{\hbar^2\mathbf{k}^2}{2M'} + ; \tag{7}$$

The energy of an unexcited crystal is taken as the zero level. Using the notation $\omega_0 = \mathcal{E}_0/\hbar$ and keeping in mind that only frequencies $\omega$ near $\omega_0$ will be of importance, we can rewrite (6) as

$$\mu = \frac{2Mc^2}{\hbar\omega}\left(1 - \frac{\omega_0}{\omega}\right) \approx \frac{2Mc^2}{\hbar\omega_0}\frac{\omega - \omega_0}{\omega_0}, \quad \mu' \approx \frac{2M'c^2}{\hbar\omega'_0}\frac{\omega - \omega'_0}{\omega_0'} \tag{8}$$

Furthermore

$$b \equiv 8\pi Mc^2 a/\hbar^2\omega^3 \approx 8\pi Mc^2 a/\hbar^2\omega_0^3, \tag{9}$$

where $a$ is a constant whose significance for the general case is given in Ref. 1. When we are concerned with the Frenkel type of exciton,[2] and when it is possible in zero approximation to write the wave function of the crystal as the product of the wave functions for the individual unit cells, $a$ can be related to the oscillator strength $f$ for the optical transition of a single cell by the equation

$$a = (e^2\hbar/2m)Nf, \tag{10}$$

where $N$ is the number of cells in unit volume of the crystal and $m$ is the mass of a free electron. From (9) and (10) by introducing the familiar constants $a_0 = \hbar/mc^2 = 0.529$ A and $I = e^2/a_0 = 27.1$ ev, we finally obtain

$$b \approx \frac{4\pi Mc^2}{\mathcal{E}_0}\frac{(I/\mathcal{E}_0)^2}{(d/a_0)^3}f, \tag{11}$$

where $d$ is the lattice constant.

In (4) "$\vartheta$" is the contribution to the dielectric constant from virtual transitions to all excited states except the exciton state under consideration. If the other absorption bands are sufficiently distant from the band that is of interest here, "$\vartheta$" can be regarded as independent of the frequency.

In solutions such as Eqs. (1) and (2), the magnetic field $\mathbf{H}$ can be expressed in terms of the electric field $\mathbf{E}$ by the equation $\mathbf{H}_\pm = n[\mathbf{s}\times\mathbf{E}_\pm]$ of ordinary crystal optics. The electric induction is given by $\mathbf{D}_\pm = n_\pm^2\mathbf{E}_\pm$. In solutions such as (3) we have $\mathbf{H}_\parallel = \mathbf{D}_\parallel = 0$.

The dispersion curves that correspond to (4) are represented by solid lines in Figs. 1 and 2, which depict the following numerical example: $\mathcal{E}_0 = 2$ ev, $d/a_0 = 10$, $\vartheta = 2$, $f = 0.1$. Fig. 1 corresponds to the case of $M = m$, for which we obtain $b = 58400$. Fig. 2 corresponds to the same $M$ and $b$ as in Fig. 1, but negative.

All previous attempts to construct a theory of light dispersion in crystals have tacitly assumed the inviolacy of Maxwell's phenomenological "ma-

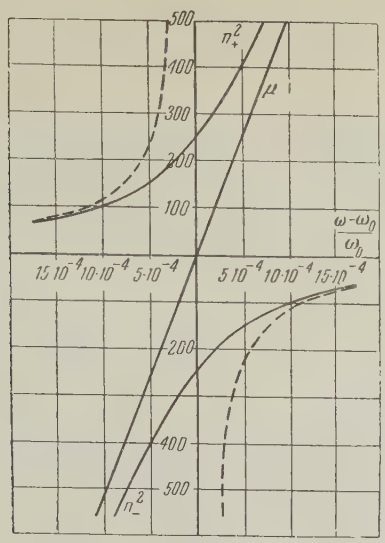


FIG. 1

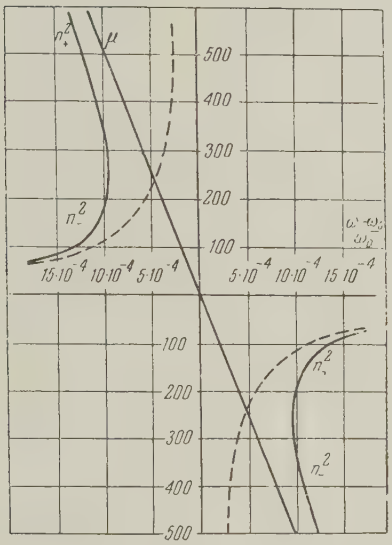


FIG. 2

terial" equations. We believe that this has led to incorrect results. Most of these attempts have resulted in a dispersion formula of the form (for electronic dispersion near an isolated narrow absorption band)

$$n^2 = \vartheta - \frac{4\pi e^2 N f}{m(\omega^2-\omega_0^2)} \approx \vartheta - \frac{2\pi e^2 N f}{m\omega_0(\omega-\omega_0)} = \vartheta - \frac{b}{\mu}. \quad (12)$$

For brevity we shall call this the ordinary dispersion formula, which is represented by a dashed line in Figs. 1 and 2. It will be shown subsequently that this formula is applicable only when light excitation is strongly associated with a lattice site (for large effective exciton mass), in which case the crystal can be regarded as a compressed gas.

As $\omega$ moves away from $\omega_0$ in either direction, we have the inequality $4b/\mu^2 \ll 1$, which in Eq. (4) enables us to expand the radical in powers of $b/\mu^2$. The following asymptotic expressions result:

$$\text{for } \mu>0 \quad n_+^2 \approx \mu + b/\mu, \quad n_-^2 \approx \vartheta - b/\mu,$$
$$\text{for } \mu<0 \quad n_-^2 \approx \mu + b/\mu, \quad n_+^2 \approx \vartheta - b/\mu. \quad (13)$$

It is thus seen that when the subscript of $n_\pm^2$ agrees with the sign of $\mu$, $n_\pm^2$ approaches $\mu$ asymptotically. When the subscript of $n_\pm^2$ is the opposite of the sign of $\mu$, $n_\pm^2$ can be expressed asymptotically by Eq. (12). This can be seen in Figs. 1 and 2, where the solid curve approaches the dashed curve asymptotically. The difference between the new and the ordinary dispersion formula is more pronounced on steep portions of the dispersion curve than on shallow portions. Unlike ordinary dispersion curves the new curves have an inclined rather than a vertical straight asymptote. Therefore for all $\omega$, $n_+^2$, $n_-^2$, and $n_\parallel^2$ remain finite, whereas by Eq. (12) $n^2$ becomes infinite for $\omega = \omega_0$. In the ordinary formula a single value of $n^2$ corresponds to each frequency; in the new formula there are three such values of $n^2$. If the atomic separation is continuously enlarged, thus increasing the lattice constant, we make the transition to a gas; this signifies an unlimited increase of the effective exciton mass M. Then, as is seen from Eq. (8), the inclined asymptote (the straight line $\mu$) in the figures becomes vertical and the new dispersion curve goes over into the ordinary curve, as expected.

In Figs. 1 and 2 only real values of $n^2$ are represented. When $n^2 > 0$ the solution is an ordinary unattenuated monochromatic light wave. When $n^2 < 0$, n is purely imaginary. This denotes that the electric and magnetic fields are gradually attenuated from the crystal surface inwards and cannot appreciably penetrate the crystal; in this case there is zero energy flow into the crystal because of the phase difference $\pi/2$ between the electric and magnetic fields. Only for $M < 0$, since $b < 0$ for $\omega$ near $\omega_0$, the quantity under the radical in (4) becomes negative and $n_\pm^2$ becomes complex (this is not shown in Fig. 2). In this region $-b > (\mu - \vartheta)^2/4$ and

$$n_\pm = \left[\frac{1}{4}(\mu+\vartheta) + \frac{1}{2}\sqrt{-b+\mu\vartheta}\right]^{1/2}$$
$$\pm i\left[\frac{-b-(\mu-\vartheta)^2/4}{\mu+\vartheta+2\sqrt{-b+\mu\vartheta}}\right]^{1/2}. \quad (14)$$

We shall now show that when the ordinary dispersion formula (12) is applied to crystals there is sometimes considerable disagreement with experiment. According to (12) there is a region of

negative values of $n^2$ beginning with $\omega_0$ in the violet direction. This region extends to the frequency $\omega_1$ which is determined from

$$\frac{\omega_1 - \omega_0}{\omega_0} = \frac{2\pi e^2 N f}{\vartheta m \omega_0^2} = \frac{2\pi f}{\vartheta}\left(\frac{I}{\mathscr{E}_0}\right)^2 \left(\frac{a_0}{d}\right)^3 . \qquad (15)$$

Assuming $f = 0.1$ and assuming the same values of the other parameters that were used in plotting the curves of Figs. 1 and 2, we obtain $(\omega_1 - \omega_0)/\omega_0 = 0.058$. When, for example, $\omega_0 = 16200\ \text{cm}^{-1}$, the width of the negative $n^2$ region is given by $\omega_1 - \omega_0 = 940\ \text{cm}^{-1}$ (assuming that there are no other strong bands on the violet side of the given absorption band). In this entire region the crystal would have to exhibit total reflection. This conflicts with experiment, since the widely used transillumination method of photographing crystal absorption spectra at low temperatures indicates that for the given oscillator strength the opaque region of a crystal plate is sometimes only 10 to 20 $\text{cm}^{-1}$.

This difficulty does not arise in the proposed new theory of dispersion. Figure 1 shows that $n_-^2$ is negative as far as the same frequency $\omega_1$, but that there is a second wave whose refractive index $n_+$ is everywhere real. This wave passes freely through the crystal plate and generates an ordinary wave in the vacuum with exactly the same frequency as the original light. For a strictly quantitative determination of transparency under the new theory, Fresnel's equations must be extended to the case of the three waves appearing in a crystal.

## 2. FRESNEL EQUATIONS FOR THE VACUUM-TO-CRYSTAL BOUNDARY

Let the plane $z = 0$ be the crystal surface; the crystal is located in the half-space $z > 0$ while the half-space $z < 0$ is a vacuum. Let the amplitudes of the electric fields of the waves, — the incident wave in the vacuum, the reflected wave in the vacuum and the three transmitted waves in the crystal, be denoted by $\mathbf{A}$, $\mathbf{R}$, $\mathbf{E}_+$, $\mathbf{E}_-$, and $\mathbf{E}_\parallel$, respectively. The electric fields of the incident and reflected waves are given by

$$\mathbf{E} = \mathbf{A}\exp\left\{i\omega\left[\frac{1}{c}(\mathbf{s}\cdot\mathbf{r}) - t\right]\right\},$$

$$\mathbf{E} = \mathbf{R}\exp\left\{i\omega\left[\frac{1}{c}(\tilde{\mathbf{s}}\cdot\mathbf{r}) - t\right]\right\}, \qquad (16)$$

and for the three transmitted waves they are given by Eqs. (1), (2), and (3). We denote the unit vectors of the normals to the wave fronts by $\mathbf{s}$, $\tilde{\mathbf{s}}$, $\mathbf{s}_+$, $\mathbf{s}_-$, and $\mathbf{s}_\parallel$, respectively. We assume that $y = 0$ is the plane of incidence. The incident wave forms the angle $\varphi$ with the $z$ axis, while the transmitted waves form the angles $\psi_+$, $\psi_-$, and $\psi_\parallel$, as shown

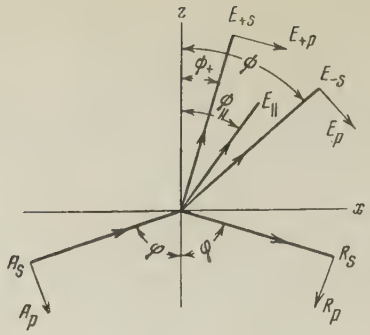


FIG. 3

in Fig. 3. Projections of the field amplitudes on the y axis will be denoted by the subscript s. The y axis in Fig. 3 is into the plane of the paper. Projections of the amplitudes on the plane of incidence will be denoted by the subscript p, with their positive direction indicated by the arrows in Fig. 3. The amplitude of the longitudinal wave will be considered positive in the direction of propagation of this wave.

As usual, the unit vectors of the normals and the amplitudes of all waves except the incident wave are determined from the continuity of the tangential projections of the electric and magnetic fields on the plane $z = 0$. For this purpose it is required, first of all, that in the plane $z = 0$ there be agreement of the phases (the exponential indices) of all five waves for all values of x, y and t. This leads to the relations

$$\begin{aligned} s_x = \tilde{s}_x = n_+ s_{+x} = n_- s_{-x} = n_{||} s_{||x}, \\ s_y = \tilde{s}_y = n_+ s_{+y} = n_- s_{-y} = n_{||} s_{||y} = 0, \end{aligned} \qquad (17)$$

which express Snell's law and the requirement that all five waves possess the same frequency. The continuity of $E_x$, $H_y$, $E_y$ and $H_x$ is expressed by the following equations for the amplitudes:

$$(A_p - R_p)\cos\varphi = E_{+p}\cos\psi_+ + E_{-p}\cos\psi_- + E_{||}\sin\psi_\parallel, \qquad (18)$$

$$A_p + R_p = n_+ E_{+p} + n_- E_{-p}, \qquad (19)$$

$$A_s + R_s = E_{+s} + E_{-s}, \qquad (20)$$

$$(A_s - R_s)\cos\varphi = n_+ E_{+s}\cos\psi_+ + n_- E_{-s}\cos\psi_- \qquad (21)$$

The continuity of the normal projection of the electric induction does not lead to new equations.

It is also necessary to satisfy the boundary condition derived in Ref. 1 for the specific dipole mo-

ment: in the plane $z = 0$ we must have $\mathbf{P}_1 = 0$. In our notation this condition becomes

$$\frac{\mathbf{E}_+}{n_+^2-\mu} + \frac{\mathbf{E}_-}{n_-^2-\mu} - \frac{\vartheta}{b}\mathbf{E}_\parallel = 0. \tag{22}$$

From the set of equations (18) to (21) and (22), the seven quantities $R_S$, $R_p$, $E_{+S}$, $E_{+p}$, $E_{-S}$, $E_{-p}$, and $E_\parallel$ are expressed in terms of $A_S$ and $A_p$ as follows:

s-components:

$$E_{\pm s} = u_\pm A_s, \quad R_s = (u_+ + u_- - 1)\,A_s, \tag{23}$$

$$u_\pm = 2\left[1 + n_\pm \frac{\cos\psi_\pm}{\cos\varphi} - q^{\pm 1}\left(1 + n_\mp \frac{\cos\psi_\mp}{\cos\varphi}\right)\right]^{-1}, \tag{24}$$

$$u_- = -qu_+, \quad q \equiv \frac{n_-^2-\mu}{n_+^2-\mu} = \frac{\vartheta - n_+^2}{\vartheta - n_-^2},$$

$$n_\pm = \frac{\sin\varphi}{\sin\psi_\pm}, \quad n_\parallel = \sqrt{\mu} = \frac{\sin\varphi}{\sin\psi_\parallel}; \tag{25}$$

p-components:

$$E_{\pm p} = v_\pm A_p, \quad R_p = (v_+ n_+ + v_- n_- - 1)\,A_p, \tag{26}$$

$$E_\parallel = \frac{\sin(\psi_- - \psi_+)}{\cos(\psi_- - \psi_\parallel)} \frac{bv_+}{\vartheta(n_+^2-\mu)} A_p, \tag{27}$$

$$v_\pm = 2\left[\frac{\cos\psi_\pm}{\cos\varphi} + n_\pm + \frac{b\sin\psi_\parallel \sin(\psi_\mp - \psi_\pm)}{\vartheta(n_\pm^2-\mu)\cos\varphi\cos(\psi_\mp - \psi_\parallel)}\right.$$
$$\left. - q^{\pm 1}\frac{\cos(\psi_\pm - \psi_\parallel)}{\cos(\psi_\mp - \psi_\parallel)}\left(\frac{\cos\psi_\mp}{\cos\varphi} + n_\mp\right)\right]^{-1}, \tag{28}$$

where

$$v_- = -q\frac{\cos(\psi_+ - \psi_\parallel)}{\cos(\psi_- - \psi_\parallel)} v_+. \tag{29}$$

It can be shown that when $M > 0$, for example, as $\omega$ changes toward the red from $\omega_0$, the (+) wave acquires all the properties of the ordinary wave, while the amplitude of the anomalous (−) wave approaches zero ($|q|$ becomes $\ll 1$). The formulas given above then become the ordinary Fresnel equations with $n_+$ as the refractive index. Similarly, as $\omega$ changes toward the violet from $\omega_0$, the (−) wave becomes the ordinary wave while the amplitude of the anomalous (+) wave approaches zero ($|q|$ becomes $\gg 1$). The above formulas then become the ordinary Fresnel equations with $n_-$ as the refractive index, and the (−) wave becomes the transmitted wave.

The coefficient of reflection from the crystal surface into the vacuum is

for the s-component $r_s = |R_s|^2/|A_s|^2 = |u_+ + u_- - 1|^2$, (30)

for the p-component $r_p = |R_p|^2/|A_p|^2$

$$= |v_+ n_+ + v_- n_- - 1|^2.$$

In the special case of normal incidence

$$r_s = r_p = r = \left|\frac{n_+ - 1 - q(n_- - 1)}{n_+ + 1 - q(n_- + 1)}\right|^2. \tag{31}$$

We shall now consider the passage of light through the boundary between the vacuum and the crystal with the incident wave striking the crystal surface from within. The longitudinal, (+), and (−) waves will be considered separately. As previously, Snell's law applies to all cases; the product of the refractive index and the sine of the angle formed with the z axis is identical for all waves.

**a. For an Incident Longitudinal Wave.**

We retain all of the notation of Fig. 3 with the following necessary changes. In the half-space $z < 0$ there now exists only one wave propagated away from the surface with amplitude $\mathbf{R}(\mathbf{A} = 0)$. In the half-space $z > 0$ the negative-x quadrant contains an additional longitudinal wave whose direction forms the angle $\psi_\parallel$ with the z axis. The amplitude of the latter wave will be denoted by $A_\parallel$. The boundary conditions for the s components of the amplitudes are derived directly from Eqs. (20) and (21) by inserting $A_S = 0$. We require in addition the s projection of the vector equation (22). The solution of these equations is obtained from (23) by inserting $A_S = 0$. Thus $E_{+S} = E_{-S} = R_S = 0$.

For the p-components of the amplitudes we obtain the following equations which express the continuity of $E_x$ and $H_y$:

$$(A_\parallel + E_\parallel)\sin\psi_\parallel + E_{+p}\cos\psi_+ + E_{-p}\cos\psi_- = -R_p\cos\varphi, \tag{32}$$

$$n_+ E_{+p} + n_- E_{-p} = R_p. \tag{33}$$

In addition, the condition $\mathbf{P}_1 = 0$ on the crystal surface[1] leads to

$$\frac{E_{+p}\cos\psi_+}{n_+^2-\mu} + \frac{E_{-p}\cos\psi_-}{n_-^2-\mu} - \frac{\vartheta}{b}(E_\parallel + A_\parallel)\sin\psi_\parallel = 0, \tag{34}$$

$$\frac{E_{+p}\sin\psi_+}{n_+^2-\mu} + \frac{E_{-p}\sin\psi_-}{n_-^2-\mu} + \frac{\vartheta}{b}(E_\parallel - A_\parallel)\cos\psi_\parallel = 0. \tag{35}$$

The solution of Eqs. (32) to (35) is

$$E_{\pm p} = w_{\pm} A_{\parallel}, E_{\parallel} = w_{\parallel} A_{\parallel}, R_p = (n_+ w_+ + n_- w_-) A_{\parallel}, \tag{36}$$

where

$$w_{\pm} = -\frac{\sin 2\psi_{\parallel}\left[\frac{\vartheta}{b}\left(\frac{\cos\psi_{\mp}}{\cos\varphi}+n_{\mp}\right)(n_{\mp}^2-\mu)+\frac{\cos\psi_{\mp}}{\cos\varphi}\right]}{\left(\frac{\cos\psi_{\pm}}{\cos\varphi}+n_{\pm}\right)\cos(\psi_{\parallel}-\psi_{\mp})-q^{\pm 1}\left(\frac{\cos\psi_{\mp}}{\cos\varphi}+n_{\mp}\right)\cos(\psi_{\parallel}-\psi_{\pm})+\frac{b}{\vartheta}\frac{\sin\psi_{\parallel}\sin(\psi_{\mp}-\psi_{\pm})}{\cos\varphi\,(n_{\pm}^2-\mu)}}, \tag{37}$$

$$w_{\parallel} = \frac{\left(\frac{\cos\psi_+}{\cos\varphi}+n_+\right)(n_+^2-\mu)\cos(\psi_{\parallel}+\psi_-)-\left(\frac{\cos\psi_-}{\cos\varphi}+n_-\right)(n_-^2-\mu)\cos(\psi_{\parallel}+\psi_+)-\frac{b}{\vartheta}\frac{\sin\psi_{\parallel}\sin(\psi_--\psi_+)}{\cos\varphi}}{\left(\frac{\cos\psi_+}{\cos\varphi}+n_+\right)(n_+^2-\mu)\cos(\psi_{\parallel}-\psi_-)-\left(\frac{\cos\psi_-}{\cos\varphi}+n_-\right)(n_-^2-\mu)\cos(\psi_{\parallel}-\psi_+)+\frac{b}{\vartheta}\frac{\sin\psi_{\parallel}\sin(\psi_--\psi_+)}{\cos\varphi}} \tag{38}$$

As explained in Ref. 1, the longitudinal wave is the electric field of an exciton wave excited in the crystal. Equations (36) to (38) show that the longitudinal (exciton) wave is only partly reflected from the crystal surface ($|w_{\parallel}|^2 \leq 1$); the rest of its energy is expended for the generation of two electromagnetic waves directed into the crystal [the (+) and (−) waves] and of an additional wave directed into the vacuum. In other words, excitons which reach the crystal surface emit light.

For normal incidence $w_{\parallel} = 1$ and $w_{\pm} = 0$.

**b. For an Incident (+) Wave.**

This case differs from the preceding one only in that the longitudinal wave is replaced by an incident (+) wave of amplitude $\mathbf{A}_+$. The directions of all waves are shown in Fig. 4. The continuity

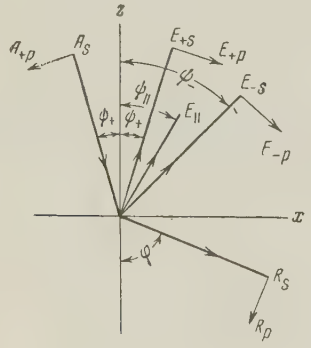


FIG. 4

conditions for $E_x$, $H_y$, $E_y$, and $H_x$ become

$$-R_p\cos\varphi = (E_{+p}-A_{+p})\cos\psi_+ + E_{-p}\cos\psi_- + E_{\parallel}\sin\psi_{\parallel}, \tag{39}$$

$$R_p = n_+(E_{+p}+A_{+p}) + n_-E_{-p}, \tag{40}$$

$$R_s = A_{+s}+E_{+s}+E_{-s}, \tag{41}$$

$$R_s\cos\varphi = n_+(A_{+s}-E_{+s})\cos\psi_+ - n_-E_{-s}\cos\psi_-. \tag{42}$$

The condition $\mathbf{P}_1 = 0$ in the $z = 0$ plane[1] leads to

$$\frac{\mathbf{E}_+ + \mathbf{A}_+}{n_+^2-\mu}+\frac{\mathbf{E}_-}{n_-^2-\mu}-\frac{\vartheta}{b}\mathbf{E}_{\parallel}=0. \tag{43}$$

The solution of Eqs. (39) to (43) is

for s-components:

$$E_{+s} = \frac{n_+\cos\psi_+ + qn_-\cos\psi_- - (1-q)\cos\varphi}{n_+\cos\psi_+ - qn_-\cos\psi_- + (1-q)\cos\varphi}A_{+s}, \tag{44}$$

$$E_{-s} = -\frac{2qn_+\cos\psi_+}{n_+\cos\psi_+ - qn_-\cos\psi_- + (1-q)\cos\varphi}A_{+s}, \tag{45}$$

$$R_s = \frac{2(1-q)n_+\cos\psi_+}{n_+\cos\psi_+ - qn_-\cos\psi_- + (1-q)\cos\varphi}A_{+s}; \tag{46}$$

for p-components:

$$E_{\parallel} = -\frac{bU}{\vartheta(n_+^2-\mu)}A_{+p},$$

$$U = \frac{\sin 2\psi_+\left[(1-q)\frac{\cos\psi_-}{\cos\varphi}-qn_-\right]}{\left(\frac{\cos\psi_+}{\cos\varphi}+n_+\right)\cos(\psi_{\parallel}-\psi_-)-q\left(\frac{\cos\psi_-}{\cos\varphi}+n_-\right)\cos(\psi_{\parallel}-\psi_+)} \rightarrow \frac{+2n_+\sin\psi_-\cos\psi_+}{+\frac{b\sin\psi_{\parallel}\sin(\psi_--\psi_+)}{\vartheta(n_+^2-\mu)\cos\varphi}}, \tag{47}$$

$$E_{+p} = \frac{\sin(\psi_-+\psi_+)-U\cos(\psi_{\parallel}-\psi_-)}{\sin(\psi_--\psi_+)}A_{+p}, \tag{48}$$

$$E_{-p} = q\frac{U\cos(\psi_{\parallel}-\psi_+)-\sin 2\psi_+}{\sin(\psi_--\psi_+)}A_{+p}, \tag{49}$$

$$R_p = \{2n_+\sin\psi_-\cos\psi_+ - qn_-\sin 2\psi_+ - U[n_+\cos(\psi_{\parallel}-\psi_-) - qn_-\cos(\psi_{\parallel}-\psi_+)]\}A_{+p}/\sin(\psi_--\psi_+). \tag{50}$$

**c. For an Incident (−) Wave.**

This is entirely analogous to case b with the single difference that the (+) and (−) waves have exchanged roles. Therefore all equations and solutions for this case are obtainable from Eqs. 39 to 50 simply by interchanging the subscripts + and − and replacing q with 1/q.

## 3. TRANSMISSION OF LIGHT THROUGH A PLANE-PARALLEL PLATE

We take the planes $z = 0$ and $z = l$ as the surfaces of the plate. We limit ourselves to a consideration of normal incidence, where the incident and all secondary waves propagate parallel to the z axis. Then Eqs. 27 and 47 show that longitudinal waves do not arise in the crystal, but that there are four transverse waves, whose electric fields will be denoted as follows:

$$\mathbf{E}_+ e^{i(k_+ z-\omega t)}, \quad \mathbf{E}_- e^{i(k_- z-\omega t)},$$

$$\mathbf{E}'_+ e^{i(-k_+ z-\omega t)}, \quad \mathbf{E}'_- e^{i(-k_- z-\omega t)}, \qquad (51)$$

where

$$k_\pm = n_\pm \omega / c.$$

The electric fields of the incident wave, the wave reflected into the region $z < 0$, and the wave transmitted into the region $z > l$ will be denoted respectively by

$$\mathbf{A}e^{i(k_0 z-\omega t)}, \quad \mathbf{R}e^{i(-k_0 z-\omega t)}, \quad \mathbf{D}e^{i(k_0 z-\omega t)} \quad (k_0 = \omega / c). \qquad (52)$$

Continuity of the tangential electric and magnetic components on the surface $z = 0$ furnishes the equations

$$\mathbf{A} + \mathbf{R} = \mathbf{E}_+ + \mathbf{E}_- + \mathbf{E}'_+ + \mathbf{E}'_-, \qquad (53)$$

$$\mathbf{A} - \mathbf{R} = n_+ (\mathbf{E}_+ - \mathbf{E}'_+) + n_- (\mathbf{E}_- - \mathbf{E}'_-). \qquad (54)$$

The analogous condition on the surface $z = l$ gives

$$\mathbf{E}_+ e^{ik_+ l} + \mathbf{E}_- e^{ik_- l} + \mathbf{E}'_+ e^{-ik_+ l} + \mathbf{E}'_- e^{-ik_- l} = \mathbf{D}e^{ik_0 l}, \qquad (55)$$

$$n_+ (\mathbf{E}_+ e^{ik_+ l} - \mathbf{E}'_+ e^{-ik_+ l}) + n_- (\mathbf{E}_- e^{ik_- l} - \mathbf{E}'_- e^{-ik_- l}) = \mathbf{D}e^{ik_0 l} \qquad (56)$$

The condition $\mathbf{P}_1 = 0$ on the surfaces $z = 0$ and $z = l$ gives, respectively,

$$\mathbf{E}_- + \mathbf{E}'_- = -q (\mathbf{E}_+ + \mathbf{E}'_+), \qquad (57)$$

$$\mathbf{E}_- e^{ik_- l} + \mathbf{E}'_- e^{-ik_- l} = -q (\mathbf{E}_+ e^{ik_+ l} + \mathbf{E}'_+ e^{-ik_+ l}). \qquad (58)$$

Equations 53 to 58 can be used to express the secondary wave amplitudes $\mathbf{E}_+$, $\mathbf{E}_-$, $\mathbf{E}'_+$, $\mathbf{E}'_-$, R, and D in terms of the incident wave amplitude A. From (53), (55), (57), and (58) we obtain

$$\mathbf{E}_+ = \frac{i}{2} \frac{(\mathbf{A} + \mathbf{R}) e^{-ik_+ l} - \mathbf{D}e^{ik_0 l}}{(1 - q) \sin k_+ l},$$

$$\mathbf{E}_- = \frac{i}{2} \frac{(\mathbf{A} + \mathbf{R}) e^{-ik_- l} - \mathbf{D}e^{ik_0 l}}{(1 - 1/q) \sin k_- l},$$

$$\mathbf{E}'_+ = -\frac{i}{2} \frac{(\mathbf{A} + \mathbf{R}) e^{ik_+ l} - \mathbf{D}e^{ik_0 l}}{(1 - q) \sin k_+ l},$$

$$\mathbf{E}'_- = -\frac{i}{2} \frac{(\mathbf{A} + \mathbf{R}) e^{ik_- l} - \mathbf{D}e^{ik_0 l}}{(1 - 1/q) \sin k_- l}. \qquad (59)$$

Substitution of (59) into (54) and (56) gives

$$\mathbf{D} = \frac{2iGe^{-ik_0 l}}{(1 + iF)^2 + G^2} \mathbf{A}; \qquad \mathbf{R} = \frac{1 + F^2 - G^2}{(1 + iF)^2 + G^2} \mathbf{A}, \qquad (60)$$

where

$$F = \frac{n_+}{1 - q} \cot k_+ l + \frac{n_-}{1 - 1/q} \cot k_- l;$$

$$G = n_+ / (1 - q) \sin k_+ l + n_- / (1 - 1/q) \sin k_- l. \qquad (61)$$

Thus far it has been assumed that $\mu$ and $\varepsilon$ are real. Then $n_+$, $n_-$, and $n_\P$ for $M < 0$ are either purely real or purely imaginary. This denotes complete absence of light absorption in the plate. For $M < 0$, in the frequency region to which Eq. 14 is applicable, $n_+$ and $n_-$ are complex conjugates. It can be shown that in this case no light will be absorbed in the plate. It must be emphasized that in virtue of the assumption that the lifetime of the exciton state is determined only by interaction with the electromagnetic field (emission), there can be no exciton absorption of light for any magnitude of the unit-cell oscillator strength f. This becomes obvious from consideration of the stationary state in which an electromagnetic wave entering the crystal for an infinitely long period does not raise the average quantum-mechanical energy level of the crystal. Therefore all of the admitted light energy must be re-emitted by the crystal plate. Unlike a gas, however, the crystal will emit radiation only parallel to the z axis. Radiation in the positive z direction is called a transmitted wave, while radiation in the negative z direction is called a reflected wave. The sum of the transmitted and reflected intensities equals the incident intensity.

Exciton absorption of light in a crystal occurs when the system makes transitions from exciton states produced by light to any state other than the original state. When these transitions are

accompanied by emission, Roman scattering of the primary light occurs. When these transitions are performed thermally, with the excitation of thermal vibrations, ordinary light absorption occurs. It is thus clear that a theoretical study of light absorption must take into account the finite exciton lifetime which results from all possible transitions except a transition to the original state of the system. The finite exciton lifetime can be taken into account formally by a small imaginary correction to the exciton energy $\mathcal{E}(k)$ in Ref. 1. A corresponding imaginary correction appears in $\mu$. All of the equations derived above remain in effect and will describe the case of an absorbing crystal since $n_+$, $n_-$, and $n_\parallel$ now have new complex values.

A special article will be devoted to exciton absorption of light. We shall here confine ourselves to negligibly small absorption, which occurs when $n_+$ and $n_-$ are real or pure imaginary quantities (not necessarily both simultaneously) and also when $n_- = n_+^*$. In such cases Eq. 61 shows that F and G are real. The transmission coefficient $\delta$ and the reflection coefficient $\rho$ are

$$\delta = \frac{|D|^2}{|A|^2} = \frac{4G^2}{(1+F^2-G^2)^2+4G^2},$$

$$\rho = \frac{|R|^2}{|A|^2} = \frac{(1+F^2-G^2)^2}{(1+F^2-G^2)^2+4G^2}. \qquad (62)$$

Hence we obtain $\delta + \rho = 1$, which proves the absence of light absorption.

Interference transmission maxima, when $\delta = 1$ and $\rho = 0$, occur at frequencies determined by the condition $1 + F^2 - G^2 = 0$. Transmission minima, when $\delta = 0$ and $\rho = 1$, occur at frequencies determined by $G = 0$.

Equations 57 and 58 show that for $q \to 0$ both (−) waves disappear in the crystal, and that for $|q| \to \infty$ both (+) waves disappear. In both instances Eqs. 53 to 58 are the same as in ordinary crystal optics. Therefore when in Eqs. 59 to 62 we make the formal transition to the limit $q \to 0$ or $|q| \to \infty$, we obtain the equations of ordinary crystal optics. Equations 60 and 62 then remain unchanged but Eq. 61 is replaced by

$$F_0 = n\cot kl, \quad G_0 = n/\sin kl, \quad k = \omega n/c. \qquad (63)$$

We now turn to the question of crystal transparency in the frequency region $\omega_0 - \omega_1$, where according to the ordinary dispersion equation (12) n is pure imaginary. From (63) we now obtain $G_0 = |n|/\sinh |k| l$. Consequently, $G_0$ decreases exponentially with $l$, and when the thickness of the plate is considerably greater than the wavelength we have practically $G_0 \approx 0$ and $\delta \approx 0$. This represents total reflection in the entire interval from $\omega_0$ to $\omega_1$, which, as noted in Sec. 1, conflicts with experiment. The aforementioned difficulty of ordinary crystal optics does not arise in the proposed theory, where G is expressed by (61). Here we obtain $G \approx 0$ only when $M < 0$ in the frequency region where both $n_+$ and $n_-$ are pure imaginary (Fig. 2). When $M > 0$, owing to the presence of second light with a real refractive index $n_+$, the first term in the expression for G is large. Therefore $G \neq 0$ and $\delta \neq 0$. Thus the plate can be transparent in the frequency interval $\omega_0 - \omega_1$.

## 4. POSSIBLE EXPERIMENTAL TESTS OF THE PROPOSED THEORY

In selecting crystals and absorption bands for testing of the theory it must be borne in mind that these must be exciton absorption bands with the term "exciton" understood according to the definition at the beginning of Ref. 1. Extremely low temperatures are preferable because the theory has been developed, strictly speaking, for absolute zero. Although the theory can be applied to very low temperatures above zero, suitable criteria have not been established. The absorption bands must not be adjacent to other strong bands. It is desirable to begin with cubic crystals, in which the effects under investigation are not complicated by birefringence.

It is desirable to investigate the case of small effective exciton mass, where the straight asymptotes in Figs. 1 and 2 show greater inclination away from the vertical. In such cases second and third light possess appreciable amplitudes in a broader frequency range. Narrow absorption bands must be selected, which are usually associated with photo-transitions that do not induce multiple phonon production. Narrow bands are also more suitable because they permit more complete determination of the dispersion curves.

In using previously published experimental results we can trust the estimate of the elementary cell oscillator strength f based on the low-frequency tail of the dispersion curve, since the ordinary dispersion equation (12) used for this purpose approaches Eq. 4 asymptotically. But the oscillator strength f cannot be evaluated from the "absorption curve area" by the ordinary theory, since the proposed theory includes an entirely different equation.

We shall now give a far from complete list of the experiments that could be performed to test the proposed theory.

1. Determination of the cases of crystal transparency in a considerable portion of the frequency interval from $\omega_0$ to $\omega_1$ [see Eq. (15)].

2. Plotting of dispersion curves such as those in Figs. 1 and 2, by means of experimental determination of the refractive indices of all three waves. Some possible methods are:

a. An interferometer is used to divide the original light beam into two beams; one of the beams passes through a plate of the investigated crystal, after which it interferes with the other beam. Study of this interference enables us to determine the change of amplitude and phase of the light wave as a result of passage through the plate, i.e., the complex quantity D/A (in the notation of Sec. 3). In the ordinary theory this determines the single refractive index but in the proposed theory the fraction in the first equation of (60) is determined, thus giving an equation with the three unknowns $n_+$, $n_-$ $\mu$. By performing the measurement for three thicknesses of the plate, we obtain three equations to determine the three unknown quantities.

It is also possible to make an interference study of the light reflected from the crystal plate, thus determining the fraction in the second equation of (60) and giving an equation for the determination of $n_+$, $n_-$, and $\mu$. Thus two relations can be obtained with a plate of any given thickness.

b. The refractive indices can be determined by sending light through a prism made of the given crystal. In Sec. 2 it was shown that a beam entering the prism is split into three beams (see Fig. 3). The three beams emerge from the crystal prism at different angles with the primary beam which can be measured in the usual way to give all three refractive indices by means of Snell's law. Detection of the three beams emerging from a prism would be a direct proof of the existence of second and third light in a cubic crystal.

Since the frequency of the light is in or near the absorption region, the prism must be a very thin and sharp wedge to insure sufficient transparency. It must be remembered that the refractive indices of second and third light can be very large, amounting to some tens or even hundreds. Therefore if these beams are to emerge from the prism instead of undergoing total internal reflection, their direction within the prism must form a very small angle with the normal to the plane of emergence. After emergence, the beams should be sought at a large angle to the normal.

When the primary beam is normal to the entrance plane, no longitudinal wave arises in the prism. When the direction of a longitudinal wave propagating in the prism is normal to the exit plane of the prism, it undergoes total internal reflection and thus excites no electromagnetic wave in the vacuum. If the refractive index of any one of the three waves is imaginary, that wave will pass through the prism only if the thickness of the latter does not exceed the wavelength in order of magnitude. It is especially interesting to observe the frequency region in which $|q|$ is of the order of unity, in which case the amplitude of second light is of the same order as that of ordinary light.

As a control over any method of determining the refractive indices, the following relation, which is derived from (4), should be verified:

$$n_+^2 + n_-^2 - \mu = \vartheta, \tag{64}$$

where $\vartheta$ should not depend on the frequency if there are no close-lying absorption bands.

3. Interference investigation of a beam reflected from a semi-infinite crystal makes it possible to determine the changes of phase and amplitude upon reflection, i.e., the complex quantities $R_s/A_s$ and $R_p/R_p$. By equating these quantities and their theoretical values as given by Eqs. (23) and (26), we obtain in each instance an equation relating $n_+$, $n_-$, and $\mu$. When the measurement is performed three times at different angles of incidence, or with different polarizations, we obtain three equations for $n_+$, $n_-$, and $\mu$, from which the refractive indices can be determined. When the coefficient b is unknown, it is best to confine the investigation to s-polarization, since Eqs. (23) and (24) do not contain b.

4. When any one of the aforementioned methods is used to determine $n_+$, $n_-$, and $\mu$, the value of $\mu$ can be used in (8) to calculate the effective exciton mass M. Then b can be calculated from (4), using, for example, the value of $n_+^2$. Substitution of the result into (4) for $n_-^2$ serves as a check.

5. By analogy with Brewster's law in the ordinary theory, the proposed theory leads to an angle of incidence at which the p-component is completely unreflected, so that the reflected beam is strictly polarized in the s-direction. Equation (26) shows that this occurs when $v_+n_+ + v_-n_- - 1 = 0$. This equation can also be used to verify the theory after experimental determination of the refractive indices and angle of incidence at which total polarization of the reflected wave is observed.

Exciton absorption of light will be considered in another article.

The author wishes to thank Iu. L. Mentkovskii for checking some of the calculations.

[1] S. I. Pekar, J. Exptl. Theoret. Phys. (U.S.S.R.) **33**, 1022 (1957), Soviet Phys. JETP **6**, 785 (1958); J. Phys. Chem. Solids **5**, 11 (1958).

[2] Ia. I. Frenkel', Phys. Rev. **37**, 17, 1276 (1931).

Translated by I. Emin
240

SOVIET PHYSICS JETP VOLUME 34(7), NUMBER 5 NOVEMBER, 1958

# *THE MOTIONS OF ROTATING MASSES IN THE GENERAL THEORY OF RELATIVITY*

A. P. RIABUSHKO and I. Z. FISHER

Belorussian State University

Submitted to JETP editor November 29, 1957

J. Exptl. Theoret. Phys. (U.S.S.R.) **34**, 1189-1194 (May, 1958)

The relativistic equations of translational and rotational motion for spherically symmetrical rotating bodies, developed in a previous paper,[1] have been integrated. Some novel relativistic effects, due to the proper rotations of the bodies, appear and are discussed.

## 1. INTRODUCTION

In an article by one of the authors[1] the equations of translational and rotational motion for spherically symmetrical rotating bodies were derived from Einstein's gravitational equations. In the present paper we shall study the solutions of these equations. In view of the well-known difficulties in the general problem of celestial mechanics, we shall limit ourselves here to a study of the two-body problem. In their well-known paper,[2] Thirring and Lense studied the relativistic effects of rotation as applied to the very simple (though important) case of a very light, non-rotating body moving in the field of a massive rotating body, by making use of the properties of geodesics. In our problem, however, both bodies are treated on an equal footing — they may be of comparable mass, and each may rotate about its own axis.

Let $a^i$ and $b^i$, $m_a$ and $m_b$, $M_a^{ik}$ and $M_b^{ik}$ be the coordinates, masses, and proper rotational moments of the two bodies, and let $r$ be the distance between them and $\gamma$ the Newtonian gravitational constant. In Ref. 1 the equations

$$\ddot{a}^l - \left(\frac{\gamma m_b}{r}\right)_{,a^l} = F_a^l + D_a^l \tag{1.1}$$

were derived for the translational motion, and

$$\dot{M}_a^{ik} = L_a^{ik} \tag{1.2}$$

for the proper rotation. (Analogous equations hold for body b). Here $F_a^i$ is the relativistic correction to the Newtonian force when the rotation of the body is neglected; it has been discussed by numerous authors.[3,4,5] $D_a^i$ is the relativistic correction due to the rotation derived in Ref. 1 (cf. Eq. (5.6) of that paper). $L_a^{ik}$ is an abbreviation for the right-hand side of equation (6.2) of Ref. 1. We shall not repeat here the complicated expressions for $F_a^i$, $D_a^i$, and $L_a^{ik}$.

In the Newtonian approximation, $F_a^i = D_a^i = L_a^{ik} = 0$, and we obtain the familiar solution, with $r \equiv |\mathbf{a} - \mathbf{b}|$,

$$\frac{1}{r} = \frac{1}{p}(1 + e\cos\varphi), \tag{1.3}$$

$$M_a^{ik} = \text{const}, \quad M_b^{ik} = \text{const}, \tag{1.4}$$

subject to the conservation laws

$$M_1 = M_2 = 0, \quad M_3 \equiv r^2\dot{\varphi} = (\gamma m p)^{1/2} = \text{const}, \tag{1.5}$$

$$E \equiv \frac{1}{2}v^2 - \frac{\gamma m}{r} = -\frac{\gamma m}{2a} = \text{const}. \tag{1.6}$$

Here $e$ is the eccentricity of the orbit, if we take $e < 1$; $p$ is a parameter, $a$ is the major semi-axis of the relative orbit, $v$ is the relative velocity, and $m \equiv m_a + m_b$.

## 2. THE ROTATION OF A BODY ABOUT ITS OWN AXIS

Let us consider the rotation of a body about its axis in the first non-Newtonian approximation. As in Ref. 1, we shall use the specific proper moments $\sigma_a$ and $\sigma_b$ instead of $M_a^{ik}$ and $M_b^{ik}$ in this approximation: $M_a^{ik} = m_a \delta_{ike} \sigma_a^e$. Substituting the first-approximation values given in (1.3) to (1.5) into the right hand side of (1.2) (cf. Eq. (6.2) in Ref. 1), we obtain equations which are easily integrable. Considering only the secular terms for body a, we have:

$$\tilde{\sigma}_a^1 = \sigma_a^1 - \frac{\gamma m_b}{c^2 mp}(2m_a + m_b)\,\sigma_a^2 \varphi.$$

$$+ \frac{\gamma m_b}{c^2 p\,|\mathbf{M}|}\left(\frac{1}{4}\sigma_a^2\sigma_a^3 - \sigma_a^2\sigma_b^3 + \frac{1}{2}\sigma_a^3\sigma_b^2\right)\varphi,$$

$$\tilde{\sigma}_a^2 = \sigma_a^2 + \frac{\gamma m_b}{c^2 mp}(2m_a + m_b)\,\sigma_a^1 \varphi$$

$$+ \frac{\gamma m_b}{c^2 p\,|\mathbf{M}|}\left(-\frac{1}{4}\sigma_a^1\sigma_a^3 + \sigma_a^1\sigma_b^3 - \frac{1}{2}\sigma_a^3\sigma_b^1\right)\varphi,$$

$$\tilde{\sigma}_a^3 = \sigma_a^3 + \frac{\gamma m_b}{c^2 p\,|\mathbf{M}|}\left(\frac{3}{4}\sigma_a^1\sigma_a^2 + \frac{1}{4}\sigma_a^1\sigma_b^2 + \frac{1}{2}\sigma_a^2\sigma_b^1\right)\varphi, \quad (2.1)$$

where $\varphi$ is the angle of rotation from (1.3); analogous equations are also obtained for body b. Here and throughout the rest of this paper we use the following notation: corresponding quantities in the Newtonian and non-Newtonian approximations are denoted by the same letters, the higher approximation being distinguished by a tilde over the letter. Thus, in Eq. (2.1) each $\sigma$ on the right-hand side (and also each m) is Newtonian (i.e., constant), while the $\tilde{\sigma}$ on the left hand side includes the relativistic corrections.

It is easy to see that the ratio of the terms which are bilinear in $\sigma$ to the linear correction terms is of the same order of magnitude as the ratio of the proper moment to the orbital moment, $\sigma/M$; for all astronomical applications this is an extremely small fraction. Therefore we may neglect the bilinear terms and write (2.1) in the form

$$\tilde{\boldsymbol{\sigma}}_a = \boldsymbol{\sigma}_a + \frac{\gamma}{c^2}\frac{m_b(2m_a + m_b)}{mp}[\mathbf{n} \times \boldsymbol{\sigma}_a]\varphi, \quad (2.2)$$

where $\mathbf{n} \equiv \mathbf{M}/|\mathbf{M}|$ is a unit pseudovector normal to the plane of the Newtonian orbit; there is an analogous equation for $\tilde{\boldsymbol{\sigma}}_b$. From this it is evident that $\boldsymbol{\sigma}_a$ changes only when $\boldsymbol{\sigma}_a$ is inclined with respect to $\mathbf{n}$.

Forming the scalar product of (2.2) with $\tilde{\boldsymbol{\sigma}}_a$, and the product of the analogous equation for $\tilde{\boldsymbol{\sigma}}_b$ with $\tilde{\boldsymbol{\sigma}}_b$, we obtain, to the corresponding degree of approximation,

$$\tilde{\sigma}_a^2 = \sigma_a^2 = \text{const}, \quad \tilde{\sigma}_b^2 = \sigma_b^2 = \text{const}, \quad (2.3)$$

i.e., the proper-moment vectors of the bodies remain constant in magnitude. Note that if we take into account the linear terms of (2.1), this condition is violated:

$$\tilde{\sigma}_a^2 = \sigma_a^2 + \frac{3\gamma m_b}{4c^2 p\,|\mathbf{M}|}\sigma_a^1\sigma_a^3(\sigma_a^2 + \sigma_b^2)\varphi, \quad (2.4)$$

so that in the general case there will be a certain, though slight secular variation in the absolute magnitude of the proper rotation of the body.

Returning now to the approximation (2.2), it is evident from (2.2) and (2.3) that the moment $\tilde{\boldsymbol{\sigma}}_a$ (together with $\tilde{\boldsymbol{\sigma}}_b$) executes a pure precession about the axis $\mathbf{n}$. If we denote by $\tau$ the period of motion of the two bodies in their relative orbit (i.e., the time during which $\varphi$ changes by $2\pi$), we can obtain from (2.2) the value of the precessional period

$$T_a^{\text{prec}} = \left[\frac{\gamma}{c^2}\frac{m_b(2m_a + m_b)}{mp}\right]^{-1}\tau. \quad (2.5)$$

The quadratic terms in (2.1) would introduce a weak perturbation of this simple precession.

## 3. ORBITAL ANGULAR MOMENTUM

We now turn to a consideration of the effect of proper rotations of the bodies upon the orbital angular momentum as a constant of motion. Writing $\mathbf{r} \equiv \mathbf{a} - \mathbf{b}$, we can obtain the orbital velocity moment $\mathbf{M} \equiv \mathbf{r} \times \dot{\mathbf{r}}$ from (1.1):

$$\dot{\mathbf{M}} = [\mathbf{r} \times (\mathbf{F}_a - \mathbf{F}_b)] + [\mathbf{r} \times (\mathbf{D}_a - \mathbf{D}_b)]. \quad (3.1)$$

To integrate these equations we substitute into the right hand side (which is similar in form to Eq. (5.6) of Ref. 1) the values of the quantities in the first approximation, (1.3) to (1.5), whereupon the integration can be carried out directly. If we retain only the cyclic terms in the equations thus obtained, we have

$$\tilde{\mathbf{M}} = \mathbf{M} - \frac{\gamma}{c^2 mp}\{(2m_a^2 - m_b^2)[\mathbf{n} \times \boldsymbol{\sigma}_a]$$

$$+ (2m_b^2 - m_a^2)[\mathbf{n} \times \boldsymbol{\sigma}_b]\}\varphi$$

$$+ \frac{3\gamma m}{4c^2 p\,|\mathbf{M}|}\{(\mathbf{n} \cdot \boldsymbol{\sigma}_a)[\mathbf{n} \times \boldsymbol{\sigma}_a] + (\mathbf{n} \cdot \boldsymbol{\sigma}_b)[\mathbf{n} \times \boldsymbol{\sigma}_b]$$

$$- 2(\mathbf{n} \cdot \boldsymbol{\sigma}_a)[\mathbf{n} \times \boldsymbol{\sigma}_b] - 2(\mathbf{n} \cdot \boldsymbol{\sigma}_b)[\mathbf{n} \times \boldsymbol{\sigma}_a]\}\varphi, \quad (3.2)$$

where all the symbols are the same as in (2.1) and (2.2). Here we have omitted the terms arising from

the non-rotational relativistic corrections to the forces $\mathbf{F}_a$ and $\mathbf{F}_b$ in (1.1) or (3.1), since they do not lead to secular terms in $\tilde{\mathbf{M}}$, in agreement with Robertson.[6] It is not difficult to verify that the total moment $(\tilde{m}_a\tilde{m}_b/\tilde{m})\tilde{\mathbf{M}}$ would differ from the right hand side of (3.2) only by a constant factor, since the relativistic correction to the masses of the bodies contains no secular terms.

Hence if the bodies have proper rotations, the orbital moment undergoes a secular deviation from its Newtonian value.

From (3.2) it is evident that the secular perturbations of the orbital moment lie in the plane of the Newtonian orbit: $\mathbf{n}\cdot(\tilde{\mathbf{M}} - \mathbf{M}) = 0$; and to the present degree of approximation, the absolute value of the moment does not change:

$$\tilde{\mathbf{M}}^2 = \mathbf{M}^2 = \gamma mp = \text{const.} \tag{3.3}$$

Hence the perturbation consists of a secular wobble of the orbital moment vector, and consequently a secular deviation of the plane of the relativistic orbit from the Newtonian position. As can be seen from (3.2), the angle of inclination is of the order of

$$\Delta\theta \sim \frac{\gamma m}{c^2 p}\frac{|\boldsymbol{\sigma}|}{|\mathbf{M}|}\varphi, \tag{3.4}$$

where $|\boldsymbol{\sigma}|$ is understood to represent the larger of the quantities $|\boldsymbol{\sigma}_a|$ and $|\boldsymbol{\sigma}_b|$. The exact value of $\Delta\theta$, and also the direction of the wobble, depend on the orientations of $\boldsymbol{\sigma}_a$ and $\boldsymbol{\sigma}_b$ and on the mass ratio of $m_a$ to $m_b$, as can be see from (3.2). The more accurate values of these quantities are easy to obtain but extremely complicated. Note that, just as in the case of the proper moments, the orbital moment undergoes no secular perturbations if both the proper moments $\boldsymbol{\sigma}_a$ and $\boldsymbol{\sigma}_b$ are normal to the orbital plane.

In conclusion, we shall consider the special case where $m_b \ll m_a$, which has been studied previously.[2] From (3.2) and (2.2) without the bilinear terms, we obtain

$$(\tilde{\boldsymbol{\sigma}}_a\cdot\tilde{\mathbf{M}}) = (\boldsymbol{\sigma}_a\cdot\mathbf{M}) - \frac{\gamma m_a}{c^2 p}(\mathbf{n}\cdot[\boldsymbol{\sigma}_a\times\boldsymbol{\sigma}_b])\varphi. \tag{3.5}$$

If we assume, following Lense and Thirring,[2] that $\boldsymbol{\sigma}_b = 0$, we obtain $\tilde{\boldsymbol{\sigma}}_a\cdot\tilde{\mathbf{M}} = \boldsymbol{\sigma}_a\cdot\mathbf{M}$, which together with (2.3) and (3.3) implies that the angle between $\tilde{\boldsymbol{\sigma}}_a$ and $\tilde{\mathbf{M}}$ is constant. Lense and Thirring quote this result, in their system of coordinates, as proof that the angle of inclination is constant. Now, however, we can see that the rotation of the second body (the lighter one) leads to secular variations in the angle of inclination. This effect persists, of course, even in the case of bodies with comparable masses.

## 4. ROTATION OF THE PERIHELION

Let us now consider the effect of the proper rotations of the bodies on their orbital motion. The complete solution of the problem turns out to be very complicated and clumsy. In this paper we shall limit ourselves to the simple case in which the proper moments of both bodies, $\boldsymbol{\sigma}_a$ and $\boldsymbol{\sigma}_b$, are normal to the plane of the Newtonian orbit and where, in consequence, neither $\boldsymbol{\sigma}_a$ nor $\boldsymbol{\sigma}_b$ causes any secular perturbation of the orbital plane.

In this case, a direct integration of Eqs. (3.1), using the Newtonian approximations (1.3) to (1.5) on the right-hand side, leads to $\tilde{M}_1 = \tilde{M}_2 = 0$ and

$$\begin{aligned}\tilde{M}_3 = M_3\Big[1 - \frac{2\gamma}{mc^2 r}\left(2m_a^2 + 2m_b^2 + 3m_a m_b\right)\Big] \\ + \frac{\gamma}{mc^2 r}\left[\left(2m_a^2 - m_b^2 + 3m_a m_b\right)\sigma_a^3\right. \\ \left. + \left(2m_b^2 - m_a^2 + 3m_a m_b\right)\sigma_b^3\right].\end{aligned} \tag{4.1}$$

In the same way, for the energy (in the Newtonian sense of $\tilde{E} = \frac{1}{2}\tilde{v}^2 - \gamma m/\tilde{r}$) we obtain

$$\begin{aligned}\tilde{E} = E\Big\{1 + \frac{\gamma}{mc^2 r}\Big[\left(6m_a^2 + 6m_b^2 + 5m_a m_b\right) \\ - \frac{5a}{r}\left(2m_a^2 + 2m_b^2 + 3m_a m_b\right) + \frac{ap}{r^2}m_a m_b\Big]\Big\} \\ + \frac{\gamma}{c^2}\frac{3M_3}{me^2}\left[\left(2m_a^2 - m_b^2 - m_a m_b\right)\sigma_a^3 + \left(2m_b^2 - m_a^2 - m_a m_b\right)\sigma_b^3\right] \\ \times\left(\frac{7a - 10p}{60ap^3} + \frac{1}{2ar^2} - \frac{2}{3r^3} + \frac{p}{4r^4}\right) + \frac{\gamma}{c^2}\frac{2M_3}{mr^3}m_a m_b\left(\sigma_a^3 + \sigma_b^3\right) \\ + \frac{\gamma}{c^2}\frac{4m}{r^3}\left(-\sigma_a^3\sigma_b^3 + \frac{1}{4}\sigma_a^3\sigma_a^3 + \frac{1}{4}\sigma_b^3\sigma_b^3\right).\end{aligned} \tag{4.2}$$

By eliminating the time variable from the left-hand sides of these equations, expressed in polar coordinates (i.e., from $\frac{1}{2}(\dot{\tilde{r}}^2 + \tilde{r}^2\dot{\tilde{\varphi}}^2) - \gamma m/\tilde{r}$ and $\tilde{r}^2\dot{\tilde{\varphi}}$), we obtain an equation for the trajectories. After carrying out the calculations according to the well-known methods,[6] and considering only the secular correction terms, we arrive at the final result

$$\frac{1}{\tilde{r}} = \frac{1}{p}\{1 + e\cos[(1 - \alpha - \alpha^*)\tilde{\varphi}]\}. \tag{4.3}$$

Here $\alpha \equiv 3\gamma m/c^2 p$, as usual, describes the rotation of the perihelion of a relativistic orbit when the proper rotations of the bodies are neglected. The quantity

$$\begin{aligned}\alpha^* \equiv \frac{\gamma}{c^2}\frac{1}{2p}\Big\{\frac{1}{mM_3}\Big[\Big(-\frac{19}{2}m_a^2 + \frac{19}{4}m_b^2 + \frac{3}{4}m_a m_b\Big)\sigma_a^3 \\ + \Big(-\frac{19}{2}m_b^2 + \frac{19}{4}m_a^2 + \frac{3}{4}m_a m_b\Big)\sigma_b^3\Big] \\ + \frac{24}{\gamma p}\Big(-\sigma_a^3\sigma_b^3 + \frac{1}{4}\sigma_a^3\sigma_a^3 + \frac{1}{4}\sigma_b^3\sigma_b^3\Big)\Big\}\end{aligned} \tag{4.4}$$

leads to an additional rotation of the perihelion caused by the proper rotations. It is easy to show that the order of magnitude of the ratio $\alpha^*/\alpha$ is the same as that of $\sigma/M$, the ratio of proper rotational moments, $\sigma_a$ and $\sigma_b$, to the orbital moment. Hence the effect $\alpha^*$ will be observable only in exceptional cases. Nonetheless, it is still of great physical interest (see, for instance, Ginzburg[7]). The magnitude and sign of $\alpha^*$ depend on the magnitudes and signs of $\sigma_a$ and $\sigma_b$, and on the ratio of the masses $m_a$ and $m_b$. Equation (4.4) is the generalization of the corresponding result of Lense and Thirring[2] to the case of comparable masses and $\sigma_a \neq 0$, $\sigma_b \neq 0$ (but $\sigma_a^1 = \sigma_a^2 = \sigma_b^1 = \sigma_b^2 = 0$).

It can be seen that the right hand side of Eq. (4.2) contains no secular terms, and it can be shown that this remains true in the general case where $\sigma_a$ and $\sigma_b$ havy any arbitrary orientation. We therefore find that the energy, defined in the Newtonian sense, is not subject to secular perturbations.

## 5. MOTION OF THE NEWTONIAN CENTER OF INERTIA

It is also of interest to study the motion of the center of inertia, defined in the Newtonian sense:

$$\tilde{c}^i \equiv \frac{1}{m}(m_a\tilde{a}^i + m_b\tilde{b}^i). \tag{5.1}$$

With the aid of equation (1.1) we have

$$\ddot{\tilde{c}}^i = \frac{1}{m}(m_aF_a^i + m_bF_b^i) + \frac{1}{m}(m_aD_a^i + m_bD_b^i). \tag{5.2}$$

Into the right hand side of this equation we substitute the Newtonian approximations (1.3) to (1.5) and transform to the mean values for one Newtonian period $\tau$:

$$\ddot{\tilde{c}}_\tau^i \equiv \frac{1}{\tau}\int_0^\tau \ddot{\tilde{c}}^i\,dt = \frac{1}{2\pi a\sqrt{ap}}\int_0^{2\pi} \ddot{\tilde{c}}^i r^2 d\varphi. \tag{5.3}$$

Averaging the groups of terms arising from $F_a^i$ and $F_b^i$, which do not involve the proper rotations of the bodies, leads to a null result, in agreement with the work of Robinson.[6] Consideration of the second term in (5.2) leads to

$$\ddot{\tilde{c}}_\tau^1 = \frac{\gamma}{c^2}\frac{3m_am_be}{m^2ap^2}\sqrt{\frac{\gamma m}{a}}\left[(2m_b+m_a)\sigma_b^3 - (2m_a+m_b)\sigma_a^3\right],$$

$$\ddot{\tilde{c}}_\tau^2 = 0, \tag{5.4}$$

$$\ddot{\tilde{c}}_\tau^3 = \frac{\gamma}{c^2}\frac{3m_am_be}{m^2ap^2}\sqrt{\frac{\gamma m}{a}}\left[(2m_b+m_a)\sigma_b^1 - (2m_a+m_b)\sigma_a^1\right].$$

This shows that in the general case the proper rotations of the bodies result in a finite residual mean acceleration of the Newtonian center of inertia. It is not difficult to prove that the substitution of $\tilde{m}_a$, $\tilde{m}_b$, and $\tilde{m}$ for $m_a$, $m_b$, and $m$ in (5.1) does not alter this conclusion from (5.4). This acceleration is absent only when the relativistic orbit is circular (so that $e = 0$), or when both moments $\sigma_a$ and $\sigma_b$ are parallel to the minor axis of the Newtonian ellipse.

The acceleration (5.4) is extremely small, and its ratio to the Newtonian acceleration is of the order

$$|\ddot{\tilde{c}}|/|\ddot{\mathbf{r}}| \sim e\frac{\gamma m}{c^2 p}\frac{|\sigma|}{|M|} \sim e\alpha\frac{|\sigma|}{|M|} \sim e\alpha^* \tag{5.5}$$

[cf. Eq. (4.3)]. The existence of a constant acceleration in (5.4), no matter how small, is rather unexpected. However, it must be borne in mind that the point determined by the condition (5.1) is not really the inertial center of the system.[8,9] In addition, it is quite possible that the constant acceleration (5.4) is actually an artefact of the method of successive approximations which has been used in this paper and in Ref. 1. The question as to what is the true motion of the Newtonian center of inertia over long periods of time remains open.

[1] A. P. Riabushko, J. Exptl. Theoret. Phys. (U.S.S.R.) **33**, 1387 (1957), Soviet Phys. JETP **6**, 1067 (1958).

[2] J. Lense and H. Thirring, Phys. Z. **19**, 156 (1918).

[3] A. Einstein, L. Infeld, and B. Hoffmann, Ann. Math. **39**, 65 (1938).

[4] N. M. Petrova, J. Exptl. Theoret. Phys. (U.S.S.R.) **19**, 989 (1949).

[5] A. Papapetrou, Proc. Phys. Soc. **A64**, 57 (1951).

[6] H. P. Robertson, Ann. Math. **39**, 101 (1938).

[7] V. L. Ginzburg, Usp. Fiz. Nauk **59**, 11 (1956).

[8] V. A. Fock, Dokl. Akad. Nauk SSSR **32**, 28 (1941).

[9] M. F. Shirokov, J. Exptl. Theoret. Phys. (U.S.S.R.) **27**, 251 (1954).

Translated by D. C. West
241

# TWO-PHOTON ANNIHILATION OF POSITRONIUM IN THE P-STATE

A. I. ALEKSEEV

Moscow Engineering Physics Institute

Submitted to JETP editor December 4, 1957

J. Exptl. Theoret. Phys. (U.S.S.R.) **34**, 1195-1201 (May, 1958)

A relativistically invariant expression for the probability amplitude of two-photon annihilation of positronium has been obtained by summing an infinite number of diagrams of a certain particular class. We have calculated the nonrelativistic limit of two-photon positronium annihilation in the S- and P-states, as well as the selection rules for these processes.

In a previous work[1] the author extended the methods of quantum field theory to the problem of annihilation (or creation) of particles in bound states. In the present work, as a specific example of the results there obtained, we shall consider the annihilation of positronium in the P-state, a problem which has not been treated by the usual quantum field theory.* In the present communication we shall not take account of radiative corrections, and shall calculate the probability amplitude for two-photon annihilation simply by summing diagrams. The same results can be obtained, on the other hand, by making use of the Green's function which describes two-photon positronium annihilation.[1] In fact it is advantageous to use this Green's function for calculating the radiative corrections, since the summation of an infinite number of diagrams becomes extremely complicated when virtual particle annihilation is taken into account (see, for instance, the author's above-cited work).

## 1. PROBABILITY AMPLITUDE FOR TWO-PHOTON POSITRONIUM ANNIHILATION

In the lowest approximation the probability amplitude $A_f$ for two-photon annihilation of the free particles is written†

$$A_f = e^2\Phi^*_{kk'}(\xi\xi')\,C(23')\,\gamma(\xi, 3'3)\,G(31')\,\gamma(\xi', 1'1)\,\Psi_f\ (12). \tag{1}$$

Here $\Psi_f(12)$ is the wave function of the electron and positron in the free state, $G(31')$ is the Green's function of the electron,[3] and

$$\Phi_{kk'}(\xi\xi') = (2\pi/\sqrt{k_0k_0'})\,[l_\nu l'_{\nu'}\exp i(-k\xi - k'\xi') + l_{\nu'}l'_\nu\exp i(-k\xi' - k'\xi)]$$

is the symmetrized function of two photons with momenta k and k′ and polarization $\boldsymbol{l}$ and $\boldsymbol{l}'$. The numbers (see Ref. 4) denote the sets of all coordinates and spin indices of the particles, whereas the symbol $\xi$ (or $\xi'$, $\xi''$, . . .) denotes the set of all coordinates and components of the polarization vector of the photon. A repeated symbol denotes summation (for spin indices and polarization vector components) and integration (for the coordinates). Further,

$$\gamma(\xi, 12) = (\gamma_\nu)_{\alpha_1\alpha_2}\delta(\xi - x_1)\,\delta(x_1 - x_2),$$
$$C(12) = C_{\alpha_1\alpha_2}\delta(x_1 - x_2), \tag{2}$$

where $\gamma_{1,2,3} = \beta\alpha_{1,2,3}$ and $\gamma_0 = \beta$, while C is a matrix which transforms an electron-positron field operator to its charge conjugate. We shall set $C = \alpha_2$.

Figure 1 shows the diagram* corresponding to Eq. (1). Since we wish to obtain the probability amplitude for two-photon annihilation of bound particles, we add to the reducible diagram of Fig. 1 all "ladder-type" diagrams (Fig. 2). When this is done, the probability amplitude A for two-photon annihilation is written

$$A = e^2\Phi^*_{kk'}(\xi\xi')\,C(67')\,\gamma(\xi, 7'7)\,G(75')\,\gamma(\xi', 5'5)\,[\Psi_f\ (56)$$
$$+ e^2\,G(51')\,G(62')\,\gamma(\bar\xi, 2'2)\,D(\bar\xi\bar\xi')\,\gamma(\bar\xi', 1'1)\,\Psi_f\ (12)$$
$$+ e^4\,G(53')\,G(64')\,\gamma(\bar\xi, 4'4)\,D(\bar\xi\bar\xi')\,\gamma(\bar\xi', 3'3)\,G(31')\,G(42')$$
$$\times\gamma(\bar{\bar\xi}, 2'2)\,D(\bar{\bar\xi}\bar{\bar\xi}')\,\gamma(\bar{\bar\xi}', 1'1)\,\Psi_f\ (12) + \ldots], \tag{3}$$

where $D(\xi\xi')$ is the photon Green's function.† This kind of an approximation for A means that

*K. Tumanov[2] has calculated the probability of positronium annihilation in the P-state using quantum electrodynamics in configuration space, as suggested by Iu. Shirokov.

†We shall use a system of units in which $\hbar = c = 1$, and the summation convention:

$$ab = a_\nu b_\nu = a_0b_0 - a_1b_1 - a_2b_2 - a_3b_3.$$

*For simplicity, in Figs. 1, 2, and 3 we have omitted similar graphs in which the k and k′ photons are interchanged.

†This function is defined as $D(\xi\xi') \equiv \delta_{\nu\nu'}D(x - x')$, where $\Box D(x - x') = -4\pi i\,\delta(x - x')$.

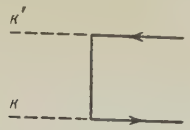

FIG. 1


FIG. 2

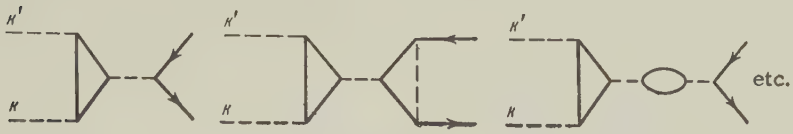


FIG. 3

some graphs of higher powers in $e^2$ are included, while others are not. As is known, the physical meaning of this method may be explained as follows.[5] In the bound state, particles interact for a very long (infinite) time. If $e^2 \ll 1$, the probability of finding one virtual quantum in the field is small and the probability of finding two quanta simultaneously is even smaller. Although the probability for the exchange of one quantum during a small time interval is fairly small, during the infinite time of existence of the bound state an indefinite number of quanta may be exchanged successively. It is just such processes that the "ladder-type" graphs deal with. Omitted diagrams of higher powers of $e^2$ refer to processes in which two or more quanta are in the field simultaneously. If $e^2 \ll 1$, such graphs are not important in the bound state if we restrict ourselves to the first nonzero approximation.

We note that Fig. 2 omits diagrams (Fig. 3) which refer to the electron-positron exchange interaction involving one-photon virtual annihilation. This interaction is also of the type in which at every instant of time there is only a single virtual photon in the field. According to Furry's theorem,[6] the total contribution of such diagrams to the probability amplitude of Eq. (3) must vanish. In general, summation of the "ladder-type" diagrams of Fig. 2 together with those of Fig. 3 will lead to a particle bound state whose wave function is a solution of the Bethe-Salpeter type, which includes, in addition to the usual interaction, the electron-positron exchange interaction which results from their single-photon virtual annihilation.[1,4]

The infinite sum in square brackets in (3) is a solution to the Bethe-Salpeter equation obtained by successive approximation. To show this, let us write the Bethe-Salpeter equation in the integral form

$$\Psi(12) = \Psi_f(12) + e^2 G(13') G(24') \gamma(\xi, 3'1') D(\xi\xi') \gamma(\xi', 4'2') \Psi(1'2'), \quad (4)$$

where $\Psi_f(12)$ satisfies the free-particle equation

$$G^{-1}(11') G^{-1}(22') \Psi_f(1'2') = 0$$

and is the zeroth approximation to the exact wave function $\Psi(12)$. We obtain the first correction to the zeroth approximation by replacing $\Psi(1'2')$ in the right side of (4) by its zeroth approximation $\Psi_f(1'2')$. The second approximation is obtained by replacing $\Psi(1'2')$ on the right side of (4) by its first approximation, etc. Continuing this iteration process ad infinitum, we obtain a representation of the solution of (4) in the form of the infinite sum of Eq. (3), so that we can now write

$$A = e^2 \Phi^*_{kk'}(\xi\xi') C(25) \gamma(\xi, 53') G(3'3) \gamma(\xi', 31) \Psi(12), \quad (5)$$

where $\Psi(12)$ is the positronium wave function satisfying the Bethe-Salpeter equation.[5]

Equation (5) can also be written in terms of $\overline{G}_{ep}(\xi\xi', 21)$, the Green's function describing two-photon positronium annihilation.[1] Indeed, according to the author's previously-cited work we have

$$\overline{G}_{ep}(\xi\xi', 21) = e^2 (D(\xi\bar{\xi}) D(\xi'\bar{\xi}') + D(\xi'\bar{\xi}) D(\xi\bar{\xi}')) C(2'5) \times \gamma(\bar{\xi}, 53') G(3'3) \gamma(\bar{\xi}', 31') K(1'2', 12), \quad (6)$$

in the first nonvanishing approximation. Here $K(1'2', 12)$, which is the Green's function of the interacting electron and positron,[4] and the photon and electron Green's functions D and G, are taken in the lowest approximation in $e^2$. Equation (5) follows directly from (6).

## 2. NONRELATIVISTIC APPROXIMATION FOR THE PROBABILITY AMPLITUDE

Let us rewrite (5) in terms of the relative momentum p. Then in the positronium center-of-mass coordinate system we have

$$A = i\frac{2\pi e^2}{m}\int\left(\frac{C\hat{1}'(\hat{p}+\hat{k}+m)\hat{1}}{p_0^2-[(p-k)^2+m^2]}+\frac{C\hat{1}(\hat{p}-\hat{k}+m)\hat{1}'}{p_0^2-[(p+k)^2+m^2]}\right)_{\alpha_2\alpha_1}$$
$$\times\,\psi_{\alpha_1\alpha_2}(p)\,d^4p\,\delta(K-k-k'), \qquad (7)$$

Here $\psi(p)$ is the positronium wave function in relative momentum space, m is the electron mass, and K is the total positronium momentum. For any vector a we write $\hat{a} = a_\nu\gamma_\nu$, and $\hat{\mathbf{a}} = a_1\gamma_1 + a_2\gamma_2 + a_3\gamma_3$.

In calculating the amplitude as given by (7), we make use of the fact that the relative velocity v of the particles in the positronium atom is small ($v \sim e^2$), so that we shall henceforth neglect all terms of order $v^2$ and higher. For convenience, we shall rewrite (7) in terms of the two-by-two Pauli matrices $\sigma$ rather than the Dirac matrices $\gamma$, and shall consider only those of the small components of $\psi(p)$ to be nonzero which are of order v. We then obtain

$$A = -i\frac{2\pi e^2}{m}\left[\int\left(\frac{\sigma_2(1'\sigma)[(p-k)\sigma](1\sigma)}{p_0-[(p-k)^2+m^2]}\right.\right.$$
$$\left.+\frac{\sigma_2(1\sigma)[(p+k)\sigma](1'\sigma)}{p_0^2-[(p+k)^2+m^2]}\right)_{\alpha_2\alpha_1}\psi^{L}_{\alpha_1\alpha_2}(p)\,d^4p$$
$$+2m\int\left(\frac{\sigma_2(1'\sigma)(1\sigma)}{p_0^2-[(p-k)^2+m^2]}+\frac{\sigma_2(1\sigma)(1'\sigma)}{p_0^2-[(p+k)^2+m^2]}\right)_{\alpha_2\alpha_1}$$
$$\left.\times\,\psi^{S}_{\alpha_1\alpha_2}(p)\,d^4p\right]\delta(K-k-k'), \qquad (8)$$

where $\psi^L(p)$ is the large (two-row) component of $\psi(p)$, and $\psi^S(p)$ is one of the two small (two-row) components of $\psi(p)$, which are of order v. The small components (of order v) give equal contributions to (8), which explains the factor 2 in the second integral of that equation.

When integrating over the fourth component $p_0$ of the momentum in Eq. (8), it is convenient to expand the coefficient of $\psi^L$ or $\psi^S$ in powers of $p_0^2$. This corresponds to expanding the integral in powers of $v^4$. For our purposes the zeroth order term of this series is sufficient, namely

$$\int\frac{\psi^L(p;\,p_0)\,dp_0}{p_0^2-[(p-k)^2+m^2]} = \frac{-1}{(p-k)^2+m^2}\int\psi^L(\mathbf{p},\,p_0)\,dp_0$$
$$= \frac{-1}{(p-k)^2+m^2}\,2\pi\psi^L(\mathbf{p},\,t=0). \qquad (9)$$

A similar expression can be obtained for $\psi^S(p)$. Thus after integrating over $p_0$, the probability amplitude of Eq. (8) contains the functions $\psi^L$ and $\psi^S$ evaluated at the same time $t_1 = t_2$ for both particles. In our approximation $\psi^L(\mathbf{p})$ evaluated at $t = 0$ is just the nonrelativistic two-component positronium wave function in momentum space. We shall evaluate $\psi^S(\mathbf{p})$ at $t = 0$ in the following way.

Up to terms of order v inclusive, the wave function of a single electron (or positron) in an external potential field is of the form

$$\begin{pmatrix}\chi\\(p\sigma)\chi/2m\end{pmatrix}f(x), \qquad (10)$$

where $\chi$ is a two-component spinor depending only on the spin indices, and $\mathbf{p} = -i\nabla$ is a differential operator acting on the nonrelativistic wave function $f(\mathbf{x})$ which depends on the coordinates and describes the motion of the particle in the external potential field (the expression in (10) can be replaced by a superposition of similar four-component functions). Bearing in mind Eq. (10), it is easy to find as accurate a positronium wave function with $t_1 = t_2$. This wave function is

$$\begin{pmatrix}\Phi & -\Phi\frac{(p\sigma^T)}{2m}\\ \frac{(p\sigma)}{2m}\Phi & 0\end{pmatrix}\psi_{nr}(x). \qquad (11)$$

Here $\Phi$ is a two-row spin wave function of two particles, and $\mathbf{p} = -i\nabla$ is a differential operator which acts on the nonrelativistic positronium wave function $\psi_{nr}(\mathbf{x})$. The numbers 1 and 2 in the spin indices $\Phi_{\alpha_1\alpha_2}$ as well as in the relative coordinates $\mathbf{x} = \mathbf{x}_1 - \mathbf{x}_2$ denote the electron and positron, respectively. The superscript T denotes the transposed matrix.

If the positronium is in an eigenstate of the total angular momentum and perhaps of other physical quantities, it is described by a superposition of functions of the form $\Phi\psi_{nr}$. Then the four-row positronium wave function is a superposition of the four-row functions of Eq. (11), and can be written in general as

$$\begin{pmatrix}\varphi(x) & -\varphi(x)\frac{(p\sigma^T)}{2m}\\ \frac{(p\sigma)}{2m}\varphi(x) & 0\end{pmatrix}, \qquad (12)$$

where the nonrelativistic two-row positronium wave function $\varphi(\mathbf{x})$ is an eigenfunction of the total angular momentum of the system (as well as of other physical observables making up a complete set). In Eq. (12) the differential operator $\mathbf{p}$ multiplying $\sigma^T$ acts on the function $\varphi(\mathbf{x})$ on its left.

It follows from (9) and (12) that the remaining integrals in Eq. (8) are of the form

$$\int F(p)\,\varphi(p)\,d^3p, \qquad (13)$$

where $\varphi(\mathbf{p})$ is defined in (12), and $F(\mathbf{p})$ denotes all the other functions of $\mathbf{p}$ which enter into the integral. If we now make use of the fact that the positronium wave function $\varphi(\mathbf{p})$ differs significantly from zero only in the small-momentum region where $p/m = v \ll 1$, we may calculate (13) up to terms of order $v$ inclusive. We then obtain

$$\int F(\mathbf{p})\varphi(\mathbf{p})\,d^3p = \int\left(F(0) + p_n \frac{\partial F(0)}{\partial p_n}\right)\varphi(\mathbf{p})\,d^3p$$

$$= (2\pi)^3 F(\mathbf{p}=0)\varphi(\mathbf{x}=0) + \frac{(2\pi)^3}{i}\frac{\partial F(\mathbf{p}=0)}{\partial p_n}\frac{\partial\varphi(\mathbf{x}=0)}{\partial x_n}. \quad (14)$$

## 3. ANNIHILATION OF POSITRONIUM IN THE S-STATE

Using (8), (9), and (14) the probability amplitude for two-photon annihilation of positronium in the S-state is given by

$$A = i\frac{(2\pi)^5 e^2}{2m^3}(\sigma_2[(\mathbf{l}\sigma)(\mathbf{k}\sigma)(\mathbf{l}'\sigma)$$

$$-(\mathbf{l}'\sigma)(\mathbf{k}\sigma)(\mathbf{l}\sigma)])_{\alpha_2\alpha_1}\varphi_{\alpha_1\alpha_2}(\mathbf{x}=0)\,\delta(K-k-k').$$

$$= \frac{(2\pi)^5 e^2}{m^3}\mathbf{k}[\mathbf{l}\times\mathbf{l}']\,\mathrm{Sp}(\sigma_2\varphi(0))\,\delta(K-k-k'). \quad (15)$$

Since $\sigma_2$ is an antisymmetric matrix, this probability amplitude differs from zero only for states whose wave function is antisymmetric in the spin indices. This means that the probability for two-photon positronium annihilation differs from zero only for states with total spin $s = 0$ (parapositronium), and vanishes if $s = 1$ (orthopositronium).[7] Finally, it follows from (15) that when positronium annihilates in the S-state giving off two photons, the polarizations of these photons are mutually perpendicular.

According to (15), the probability W for two photon annihilation of positronium in the S-state is

$$W = \frac{e^4}{4m^4}\int\sum_{\mathbf{l},\mathbf{l}'}(\mathbf{k}[\mathbf{l}\times\mathbf{l}'])^2\;d\Omega_k\;|\mathrm{Sp}(\sigma_2\varphi(0))|^2$$

$$= \frac{4\pi e^4}{m^2}|\varphi(0)|^2 = \frac{1}{2\pi^3}(e^2)^5 m. \quad (16)$$

If the principal quantum number n takes on its minimum value $n = 1$, we have $W = (e^2)^5 m/2 = 0.8\times10^{10}\,\mathrm{sec}^{-1}$, which agrees with the well known results of Pomeranchuk.[7] We have introduced the factor $\frac{1}{2}$ into the formula for the probability of two-photon annihilation in order to take account of the two identical states of the system in which the photon momenta are interchanged.

## 4. ANNIHILATION OF POSITRONIUM IN THE P-STATE

Equation (5) can be used to calculate the probability of two-photon annihilation of positronium in any excited state. If, in particular, the positronium is in the P-state and its wave function is such that $\varphi(\mathbf{p}) = -\varphi(-\mathbf{p})$, the first term in (14) vanishes and the probability amplitude for two-photon annihilation of positronium in the P-state is given by the second term of the sum, namely

$$A = \frac{(2\pi)^5 e^2}{m}\left(\frac{\partial}{\partial k_n}\frac{\sigma_2[(\mathbf{l}'\sigma)(\mathbf{k}\sigma)(\mathbf{l}\sigma)+(\mathbf{l}\sigma)(\mathbf{k}\sigma)(\mathbf{l}'\sigma)]}{\mathbf{k}^2+m^2} + \frac{(\mathbf{l}\mathbf{l}')\sigma_2\sigma_n}{m^2}\right)_{\alpha_2\alpha_1}$$

$$\times\frac{\partial\varphi_{\alpha_1\alpha_2}(0)}{\partial x_n}\,\delta(K-k-k')$$

$$= \frac{(2\pi)^5 e^2}{m^5}[m^2(l_n l'_m + l_m l'_n)$$

$$+(\mathbf{l}\mathbf{l}')k_n k_m]\frac{\partial}{\partial x_n}\mathrm{Sp}(\sigma_2\sigma_m\varphi(0))\,\delta(K-k-k'). \quad (17)$$

The matrix $\sigma_2\sigma_m$ is symmetric, so that (17) fails to vanish only for states whose total spin $s = 1$ (orthopositronium). If, on the other hand, the total spin $s = 0$ (parapositronium), the probability for two-photon annihilation of positronium in the P-state vanishes by Landau's theorem,[8] which asserts that a two-photon system has no states whose total angular momentum is one. From the symmetry of (17) with respect to interchange of $\mathbf{l}$ and $\mathbf{l}'$ we may conclude that the polarizations of the photons are parallel in the two-photon annihilation of positronium in the P-state.

Equation (17) can be used to find the probability of two-photon annihilation of orthopositronium in the P-states, namely

$$W = \frac{e^4}{4m^8}\int\sum_{\mathbf{l},\mathbf{l}'}\left|[m^2(l_n l'_m + l_m l'_n) + (\mathbf{l}\mathbf{l}')k_n k_m]\,B_{nm}\right|^2 d\Omega_k$$

$$= \frac{2\pi e^4}{15m^4}[11\,|\mathrm{Sp}\,B|^2 + 6\,\mathrm{Sp}\,B^*(B+B^T)], \quad (18)$$

where we have written

$$\partial\,\mathrm{Sp}(\sigma_2\sigma_m\varphi(0))/\partial x_n = B_{nm}.$$

In order to calculate B we must know the total angular momentum eigenfunctions $\varphi_{J,M}(\mathbf{x})$ of orthopositronium with $J = 0$, 1, and 2 and with the z-component of the total angular momentum $M = 0, \pm1, \ldots, \pm J$. Solving the eigenvalue problem in the usual way, we obtain

$$\varphi_{0,0}=\frac{1}{\sqrt{3}}\begin{pmatrix}\psi_{-1} & -1/\sqrt{2}\,\psi_0\\ -1/\sqrt{2}\,\psi_0 & \psi_1\end{pmatrix},\quad \varphi_{1,M}=\frac{1}{2}\begin{pmatrix}-\sqrt{(1+M)(2-M)} & \psi_{M-1}\,M\psi_M\\ M\psi_M & \sqrt{(1-M)(2+M)}\,\psi_{M+1}\end{pmatrix},$$

$$\varphi_{2,M}=\frac{1}{2}\begin{pmatrix}\sqrt{(1+M)(2+M)/3}\,\psi_{M-1} & \sqrt{(2-M)(2+M)/3}\,\psi_M\\ \sqrt{(2-M)(2+M)/3}\,\psi_M & \sqrt{(1-M)(2-M)/3}\,\psi_{M+1}\end{pmatrix}, \tag{19}$$

where $\psi_m \equiv R_{n1}(r)Y_{1m}(\theta,\varphi)$ is the Schroedinger wave function of positronium with principal quantum number n, orbital quantum number $l = 1$, and magnetic quantum number m. The gradient of $\psi_n(\mathbf{x})$ at $\mathbf{x} = 0$ is equal to the gradient of

$$\left(\frac{R_{n1}}{r}\right)_{r=0} rY_{1m}(\theta,\varphi)\equiv\frac{2}{3}\left(\frac{n^2-1}{a^5n^5}\right)^{1/2}\cdot rY_{1m}(\theta,\varphi). \tag{20}$$

Here r, $\theta$, and $\varphi$ are spherical coordinates, $a = 2/me^2$ is the Bohr radius, and the $Y_{1m}(\theta,\varphi)$ are defined in terms of the associated Legendre polynomials $P_1^m(\cos\theta)$ by[9]

$$Y_{1m}(\theta,\varphi)=\frac{1}{\sqrt{2\pi}}\Theta_{1m}(\theta)\,e^{im\varphi}, \tag{21}$$

where

$$\Theta_{1m}(\theta)=(-1)^m\sqrt{\frac{3(1-m)!}{2(1+m)!}}\,P_1^m(\cos\theta)\quad\text{for } m\geqslant 0, \tag{22}$$

$$\Theta_{1,-|m|}(\theta)=(-1)^m\Theta_{1,|m|}(\theta)\quad\text{for } m<0. \tag{23}$$

Finally, in agreement with Tumanov[2] we obtain the following result for the probability W of two-photon annihilation of orthopositronium in the P-state.

(a) For $J = 0$ and $M = 0$ we have

$$W=\frac{n^2-1}{8n^5}\,(e^2)^7\,m,$$

and in particular for $n = 2$, we obtain $W = 1.0 \times 10^4\,\text{sec}^{-1}$.

(b) For $J = 1$ and $M = 0$ or $\pm 1$, we have

$$W=0,$$

which follows also from the work of Landau.[8]

(c) For $J = 2$ and $M = 0$, or $\pm 1$, or $\pm 2$ we have

$$W=\frac{n^2-1}{30n^5}\,(e^2)^7\,m,$$

and in particular for $n = 2$, we obtain $W = 0.26 \times 10^4\,\text{sec}^{-1}$.

As is seen from the above results, the lifetime of positronium with respect to annihilation in the P-state is long enough for its visual spectrum to be observed.

The author is very grateful to V. M. Galitskii and A. D. Galanin for discussion of the results.

[1] A. I. Alekseev, J. Exptl. Theoret. Phys. (U.S.S.R.) **32**, 852 (1957), Soviet Phys. JETP **5**, 696 (1957).

[2] K. A. Tumanov, J. Exptl. Theoret. Phys. (U.S.S.R.) **25**, 385 (1953).

[3] R. P. Feynman, Phys. Rev. **76**, 749 (1949).

[4] R. Karplus and A. Klein, Phys. Rev. **87**, 848 (1952).

[5] H. A. Bethe and E. E. Salpeter, Phys. Rev. **84**, 1232 (1951).

[6] W. H. Furry, Phys. Rev. **51**, 125 (1937).

[7] I. Ia. Pomeranchuk, Dokl. Akad. Nauk SSSR **60**, 213 (1948).

[8] L. D. Landau, Dokl. Akad. Nauk SSSR **60**, 207 (1948).

[9] L. D. Landau and E. M. Lifshitz, Квантовая механика (Quantum Mechanics), GITTL, 1948, pp. 109, 149.

Translated by E. J. Saletan
242

# THE $K_{e3}$ DECAY

I. G. IVANTER

Institute of Scientific Information, Academy of Sciences, U.S.S.R.

Submitted to JETP editor December 4, 1957

J. Exptl. Theoret. Phys. (U.S.S.R.) **34**, 1202-1206 (May, 1958)

The possibility is considered of determining the interaction constants and the properties of the neutrino from studies of the polarizations and spectra of the particles emitted in $K_{e3}$ decays.

AT the present time it is not clear whether or not the neutrino is a two-component particle. The study of $K_{e3}$ decays can provide information about the neutrino and the interaction constants.

All of the experiments on measurements of the spectra and polarizations in $\mu^{\pm}$ decays must be divided into two broad groups: those requiring a knowledge of the energies of neutral $\pi$ mesons, and those not requiring such knowledge. As regards $K^0$ decays, in this case a study of the spectra of the particles can be carried out only if the direction of the $K^0$ particle's momentum is known, since otherwise one cannot transform to the center-of-mass system. If, however, a powerful directed beam of $K^0$ mesons has been produced, the detection of the charged particles does not present the same difficulties as that of $\pi^0$ mesons; therefore we may assume that in this case all the momenta will be known.

The calculation of the polarization on the hypothesis that the neutrino is a longitudinal particle has been carried out by Okun'[1] and Werle.[2] Werle[3] has carried through the calculation of the polarization of the $\mu$ mesons for the pure S, V, and T interactions. Charap[4] has calculated the probabilities of the different polarizations and the spectra of the $\mu$ mesons from $K_{\mu 3}$ decays for the cases of the two-component neutrino and the twin-component neutrino. But Charap did not consider the case of arbitrary constants, and did not discuss the possibility of determining the constants from experiments.

In the present paper the form of the interaction given in Refs. 5 to 7 is used, but on the assumption that the neutrino is not necessarily a two-component particle. The matrix element has the form:

$$\langle \bar{\psi}_e \{ (g_S + i\gamma_5 g'_S) + (g_V + i\gamma_5 g'_V)\gamma_4 + \frac{1}{2M}(g_T + i\gamma_5 g'_T)(\gamma_4 \hat{p}_\pi - i\hat{p}_\pi \gamma_4) \} \psi_\nu \rangle (2M^{3/2} E_\pi^{1/2})^{-1}. \quad (1)$$

The most convenient way of writing the expression for the probability of emission of electrons and $\pi$ mesons has been given in a paper by Okun'.[7] If one includes all 12 constants corresponding to the general form of the interaction with parity nonconservation, and eliminates the momentum of the $\pi$ meson, Eq. (2) of Ref. 7 takes the following form

$$\begin{aligned} W_1(E_\pi, E_e)\, dE_\pi\, dE_e = {} & \{ (|g_S|^2 + |g'_S|^2)[\Delta - 2E_\pi M] \\ & + (|g_V|^2 + |g'_V|^2)[-(M - 2E_e)^2 - m_\pi^2 + 2E_\pi (M - 2E_e)] \\ & + (|g_T|^2 + |g'_T|^2)[\Delta - 2E_\pi M][M - E_\pi - 2E_e]^2 M^{-2} \\ & + 2\mathrm{Re}(g_T g_S^* + g'_T g'^*_S)[\Delta - 2E_\pi M][M - E_\pi - 2E_e] M^{-1} \} \\ & \times (32\pi^3 M^3)^{-1}\, dE_\pi\, dE_e. \end{aligned} \quad (2)$$

Here $\Delta = M^2 + m_\pi^2$, M and $m_\pi$ are the masses of the K particle and $\pi$ meson, $E_\pi$ and $E_e$ are the energies of the $\pi$ meson and electron in the center-of-mass system, and $p_\pi$ and $p_e$ are their momenta.

If in Eq. (2) one introduces the variable $\epsilon = 2E_e/(M - E_\pi)$, the result is the analogue of Eq. (3) of the paper of Okun':

$$W_1(\varepsilon) = \Phi^{SS}_{S'S'} + \Phi^{VV}_{V'V'}[\varepsilon_0^2 - (1 - \varepsilon)^2] + \Phi^{TT}_{T'T'}(1 - \varepsilon)^2 + \Phi^{TS}_{T'S'}(1 - \varepsilon). \quad (3)$$

As in Ref. 7

$$\varepsilon_0 = p_\pi/(M - E_\pi), \quad 1 - \varepsilon_0 \leqslant \varepsilon \leqslant 1 + \varepsilon_0, \quad m_e = 0.$$

This formula differs from Eq. (3) of reference 7 only by the additional indices on the unknown functions $\Phi$ of the $\pi$-meson energy.

If we assume nothing about the nature of the dependence of $\Phi$ on the $\pi$-meson energy, then we can get from experiments measuring the differential spectrum only three equations for the determination of four combinations of constants. The

analysis of the expression (3) has been carried out in Ref. 7, but in one respect this was not done with sufficient completeness: it is stated there that the presence of a maximum (or a minimum) at $\epsilon = 1$ would be evidence of the existence of a V (or T) type of interaction. Actually the condition $\epsilon = 1$ is superfluous, so that the presence of a maximum (or minimum) at any value of $\epsilon$ would indicate the existence of a V (or T) interaction.

If we assume that the constants do not depend on the $\pi$-meson energy, then we can determine all four combinations of constants. Otherwise we can only express three of the combinations in terms of the fourth. There is an exception, however — if the vector interaction is absent. This fact could be ascertained, as noted in Ref. 7, from the shape of the $\pi$-meson spectrum near the maximum $\pi$-meson energy $E_{\pi\,\max} = \Delta/2M$.

If the neutrino is not assumed to be a two-component particle, the corresponding expression given by Okun'[7] for the probability of emission of a $\pi$ meson will have the following appearance:

$$W(E_\pi)\,dE_\pi = \{(|g_S|^2 + |g'_S|^2)(\Delta - 2E_\pi M)\,p_\pi + (|g_V|^2 + |g'_V|^2)\,2p_\pi^3/3 + (|g_T|^2 + |g'_T|^2)(\Delta - 2ME_\pi)\,p_\pi^3/3M^2\}\,dE_\pi/32\pi^3M^3. \quad (4)$$

The study of the polarization of the electrons for fixed momenta of the electron and $\pi$ meson can give additional information about the interaction constants, and thus also about the properties of the neutrino.

It is more convenient to examine the probability distribution of the longitudinal polarizations by using the variables $E_e$ and $E_\pi$, as was done for the spectrum in Ref. 7. The calculations lead to the following expression for the difference of the probabilities of the polarizations parallel and antiparallel to the momentum of the electron:

$$\delta W_2(E_e, E_\pi)\,dE_\pi\,dE_e = (ME_\pi - \Delta/2)\left\{a_2 + a_8[(M - E_\pi) - 2E_e]\,M^{-1} + a_{15}[(M - E_\pi)^2 - 4E_e(M - E_\pi) + 4E_e^2]\,M^{-2} + a_{10}\left[-1 + \frac{2E_e(E_\pi - M)}{ME_\pi - \Delta/2} + \frac{2E_e^2}{ME_\pi - \Delta/2}\right]\right\}\frac{dE_\pi\,dE_e}{32\pi^3M^3}. \quad (5)$$

Here

$$a_2 = -2\mathrm{Re}\,(g'_S g_S^*); \quad a_8 = -2\mathrm{Re}\,(g'_S g_T^* + g_S g'^*_T);$$
$$a_{10} = -2\mathrm{Re}\,(g'_V g_V^*); \quad a_{15} = -2\mathrm{Re}\,(g'_T g_T^*).$$

If we write (5) in the more compact form, we have:

$$\delta W_2(\varepsilon) = F_{SS'} + F_{ST'}^{S'T}(1 - \varepsilon) + F_{T'T}(\varepsilon - 1)^2 + F_{VV'}[(\varepsilon - 1)^2 - \varepsilon_0^2]. \quad (6)$$

Thus the expression for the longitudinal polarization, Eq. (6), is very similar to the expression (3) for the spectrum.

If $F_{ST'}^{S'T} = 0$, the distribution is symmetrical with respect to the point $\epsilon = 1$. The converse statement is also true: if the distribution is symmetrical around the point $\epsilon = 1$, then $F_{ST'}^{S'T} = 0$.

If the distribution has an extremum, then either $F_{VV'}$ or $F_{TT'}$ is different from zero. We call attention to the fact that if we had started with the two-component model of the neutrino, the presence of a minimum would have meant the emission of a neutrino, and a maximum that of an antineutrino. Therefore if it should turn out, for example, that in the $K_{e3}$ decay there is a maximum in the distribution instead of a minimum, this would mean either that the lepton charge is not conserved, or else that the neutrino is not a two-component particle. The same statement could be made if a minimum were observed in the $K_{e3}$ decay or the decay $K^0 \to e^- + \tilde{\nu} + \pi^+$, or if a maximum were observed in the decay $K^0 \to e^+ + \nu + \pi^-$.

We note that if one of the constants of the vector interaction, $g_V$ or $g_{V'}$, is equal to zero, or if these constants are displaced in phase relative to each other by 90°, the distribution passes through zero when the $\pi$-meson energy takes the value $E_{\pi\,\max}$. As was pointed out in Ref. 7, it is improbable that these constants should vanish right at just this point; therefore the absence of one of the vector interaction constants is a condition that can be ascertained experimentally, independently of the determination of the functional dependence of the constants on the $\pi$-meson energy.

Equation (6) contains three powers of $\epsilon$ (0, 1, 2); therefore if $F_{VV'} \neq 0$, one can only express three combinations of constants in terms of the fourth, but if $F_{VV'} = 0$, one can find all four combinations.

If the assumption is made that the constants do not depend on the energy of the $\pi$ meson, then of course all four combinations can be determined.

Let us consider the problem of the transverse polarization in the plane of the decay. By standard calculations one gets the following expression for the difference of the probabilities of the polarizations parallel and antiparallel to the direction $\mathbf{J}_2$ ($\mathbf{J}_2$ lies in the plane of the decay and makes a right angle with the electron momentum and an acute angle with the momentum of the $\pi$ meson):

$$\delta W_3 = -|p_\pi||\sin\theta|\{2\,\mathrm{Re}\,(g'_V g_T^* - g_V g_T'^*) \times [2E_e^2 - (M - E_\pi)E_e]M^{-1} + 2\,\mathrm{Re}\,(g'_S g_V^* - g_S g_V'^*)E_e\}\,dE_\pi\,dE_e/32\pi^3M^3. \quad (7)$$

Writing this in the more compact form, we get

$$\delta W_3 = |\sin\theta|[F_{VT'}^{V'T}(\varepsilon^2 - \varepsilon) + F_{SV'}^{S'V}\varepsilon]. \quad (8)$$

Here $\theta$ is the angle between the momenta of the $\pi$ meson and the electron

$$\sin\theta = [1 - (E_\pi E_e + \Delta/2 - ME_e - ME_\pi)^2/E_e^2(E_\pi^2 - m_\pi^2)]^{1/2}.$$

It is convenient to investigate not the expression (8), but the expression for $\delta W_3/|\sin\theta| \equiv q$. If q does not have an extremum, then $F_{VT'}^{V'T} = 0$. If q passes through zero at $\epsilon = 1$, then $F_{SV'}^{S'V} = 0$. If $F_{VT'}^{V'T} = F_{SV'}^{S'V}$, then q can be drawn as a parabola with its vertex at $\epsilon = 0$.

Let us pause to consider one more kind of polarization — the polarization in the direction perpendicular to the plane of the decay. A polarization in this direction is forbidden by the law of conservation of the combined parity, if such a law exists. Standard calculations give the following expression for the difference of the probabilities of polarizations parallel and antiparallel to the direction $J_3 = [\mathbf{p}_\pi \times \mathbf{p}_e]/|[\mathbf{p}_\pi \times \mathbf{p}_e]|$:

$$\delta W_4\,dE_e\,dE_\pi = E_e p_\pi |\sin\theta|[-2\,\mathrm{Im}\,(g_V g_T^* - g'_V g_T'^*) \times (-2E_e + M - E_\pi)M^{-1} - 2\,\mathrm{Im}\,(g_S g_V^* - g'_S g_V'^*)]\,dE_e dE_\pi/32M^3\pi^3, \quad (9)$$

or in the more compact form:

$$\delta W_4(\varepsilon) = E_e|\sin\theta|[\mathscr{F}_{VT'}^{VT}(1-\varepsilon) + \mathscr{F}_{S'V'}^{SV}]. \quad (10)$$

If $\delta W_4(\epsilon) \neq 0$, the law of conservation of the combined parity is not valid. If $\mathscr{F}_{V'T'}^{VT} = 0$, then $\delta W_4/E_e|\sin\theta| = d$ does not depend on $\epsilon$, and conversely. If $\mathscr{F}_{S'V'}^{SV} = -\mathscr{F}_{V'T'}^{VT}$, then $d(\epsilon)$ corresponds to a straight line passing through the point $\epsilon = 0$. If $\mathscr{F}_{S'V'}^{SV} = 0$, then the plot of $d(\epsilon)$ passes through zero at $\epsilon = 1$.

In order to settle the question as to whether one can determine all the interaction constants from experiments on $K_{e3}$ decays, we write out together all the equations that can be obtained from experiments:

$$\mathscr{F}_{V'T'}^{VT}(1-\varepsilon) + \mathscr{F}_{S'V'}^{SV} = A_1,\quad F_{VT'}^{V'T}(\varepsilon^2 - \varepsilon) + F_{SV'}^{S'V}\varepsilon = A_2,$$

$$F_{SS'} + F_{ST'}^{S'T}(1-\varepsilon) + F_{V'V}[(\varepsilon-1)^2 - \varepsilon_0^2] + F_{T'T}(\varepsilon-1)^2 = A_3,$$

$$\Phi_{S'S'}^{SS} + \Phi_{V'V'}^{VV}[\varepsilon_0^2 - (1-\varepsilon)^2] + \Phi_{T'T'}^{TT}(1-\varepsilon)^2 + \Phi_{T'S'}^{TS}(1-\varepsilon) = A_4.$$

Here $A_1$, $A_2$, $A_3$, and $A_4$ are functions of the energies of the $\pi$ meson and the electron which can be obtained from experiments. The total number of equations is 10, and the number of unknown functions is 11.

If $|g_V|^2 + |g'_V|^2 = 0$, the number of equations is 6, and the number of unknowns is 7. And only if $\mathrm{Re}\,(g_V g_V'^*) = 0$ does one have 11 equations for 11 unknowns, if at the same time these constants are not both zero, i.e., if $|g_V|^2 + |g'_V|^2 \neq 0$. In all other cases we are short one equation.

Thus the constants can be completely determined (apart from an unimportant phase factor) only if one of the constants of the vector interaction vanishes while the other does not, or if $g_V$ and $g'_V$ are displaced in phase relative to each other by 90°. With regard to the neutrino it must be noted that if one of the transverse polarizations exists, the neutrino cannot be a two-component particle. One cannot, however, draw the converse conclusion: if there are no transverse polarizations, this still does not mean that the neutrino is a two-component particle.

Let us go on to the second group of experiments: measurements of the spectrum and the longitudinal polarization of the electrons.

Expressions for the electron spectrum have been obtained by Furuichi and others[5,8,9] and partially by Matinian,[10] and have been discussed in detail. Expressions for the longitudinal polarization have been obtained by Okun'[1] and Werle,[2] who have also discussed them in detail. Therefore we shall give below a very brief discussion of the problem of what changes are made in these expressions by the use of a neutrino of arbitrary type.

First we note that from the spectrum and the longitudinal polarization one can obtain six equations for the determination of the interaction constants, which are assumed independent of the energy of the $\pi$ meson. In this way one can determine the following combinations

$$\overline{\Phi}_{T'T'}^{TT};\quad \overline{\Phi}_{S'T'}^{ST};\quad \overline{\Phi}_{S'S'}^{SS} - \overline{\Phi}_{V'V'}^{VV};$$
$$\overline{F}_{SS'} + \overline{F}_{VV'};\quad \overline{F}_{TT'};\quad \overline{F}_{ST'}^{S'T}$$

(the bar denotes values averaged over the $\pi$-meson energy).

If the neutrino is a two-component particle, then

$$\overline{\Phi}_{T'T'}^{TT} = \overline{F}_{TT'},\quad \overline{\Phi}_{S'T'}^{ST} = \overline{F}_{ST'}^{S'T}. \quad (11)$$

If we assume the constants to be independent of the $\pi$-meson energy, the equations (11) are equivalent to the following:

$$|g_T|^2 + |g'_T|^2 = 2\mathrm{Re}(g_T g'^*_T); \quad (12)$$

$$\mathrm{Re}(g_S g^*_T + g'_S g'^*_T) = \mathrm{Re}(g'_S g^*_T + g_S g'^*_T). \quad (13)$$

We note that it follows unambiguously from Eq. (12) that $g_T = g'_T$. Equation (13), however, is a mere consequence of Eq. (12), i.e., a second independent check on the equality of the two tensor constants. For the case in which the equations (11) hold except that the signs of the left members are changed, we also have as the unambiguous result that the tensor constants are equal in magnitude and opposite in phase, which corresponds to the case of the "two-component antineutrino for the tensor-type interaction". Here we have used an expression for the degree of polarization which is the analogue of the equation obtained by Okun',[1] namely:

$$\bar{P} = \frac{-\bar{\Phi}^{SS}_{S'S'} J_3 + \bar{\Phi}^{VV}_{V'V'} J_3 - \bar{\Phi}^{TT}_{T'T'}(\bar{A}-\bar{B}) - \bar{\Phi}^{ST}_{S'T'}(\bar{C}-\bar{D})}{\bar{F}_{SS'} J_3 + \bar{F}_{VV'} J_3 + \bar{F}_{TT'}(\bar{A}-\bar{B}) + \bar{F}^{S'T}_{ST'}(\bar{C}-\bar{D})}.$$

The values of $J_3$, $\bar{C}$, $\bar{A}$, $\bar{B}$, $\bar{D}$ as functions of the electron energy are given in Ref. 1.

In conclusion we write down the probability for the emission of an electron with given energy and polarization in a given direction and the emission of a $\pi$ meson with a given energy:

$$W(\mathbf{J}, E_\pi, E_e)\, dE_\pi\, dE_e = \frac{1}{2}\{\cos(\mathbf{JJ}_3)\,\delta W_4 + \cos(\widehat{\mathbf{JJ}_2})\,\delta W_3 + \cos(\widehat{\mathbf{JJ}_1})\,\delta W_2 + 2W_1\}.$$

The values of $\delta W_4$, $\delta W_3$, $\delta W_2$, add $W_1$ and the definitions of the three directions $\mathbf{J}_{1,2,3}$ have been given in the text of the present paper.

I thank L. B. Okun' for suggesting this problem and for a discussion.

[1] L. B. Okun', Nuclear Phys. **5**, 355 (1958).
[2] J. Werle, Nuclear Phys. **4**, 171 (1957).
[3] J. Werle, Nuclear Phys. (in press).
[4] J. M. Charap. Preprint, 1957.
[5] S. Furuichi et al., Prog. Theor. Phys. **16**, 64 (1957).
[6] A. Pais and S. B. Treiman, Phys. Rev. **105**, 1616 (1957).
[7] L. B. Okun', J. Exptl. Theoret. Phys. (U.S.S.R.) **33**, 525 (1957), Soviet Phys. JETP **6**, 409 (1958).
[8] S. Furuichi et al., Prog. Theor. Phys. **17**, 89 (1957).
[9] S. Furuichi et al., Nuovo Cim. **5**, 285 (1957).
[10] S. G. Matinian, J. Exptl. Theoret. Phys. (U.S.S.R.) **31**, 529 (1956), Soviet Phys. JETP **4**, 434 (1957).

Translated by W. H. Furry
243

SOVIET PHYSICS JETP VOLUME 34(7), NUMBER 5 NOVEMBER, 1958

## *INELASTIC SCATTERING OF DEUTERONS*

MOHAMMED EL NADI

Cairo University, Egypt

Submitted to JETP editor December 6, 1957

J. Exptl. Theoret. Phys. (U.S.S.R.) **34**, 1207-1210 (May, 1958)

The inelastic scattering of deuterons by nuclei is assumed to occur in some cases through direct interaction. The incident deuteron is merely scattered and forms the outgoing particle. An expression is derived for the angular distribution of the scattered deuterons. This expression agrees with the experimental data on the scattering of 14.4 Mev deuterons from the 4.61 Mev level of $Li^7$.

THE experiments of Holt and Young[1] on inelastic scattering of deuterons show that the angular distribution of the scattered deuterons usually has a maximum in the forward direction. This is a characteristic feature of the stripping and direct-interaction theories. Huby and Newns[2] have explained

such a behavior by assuming that only one of the component parts of the deuteron interacts with the nucleus in the scattering. The other part remains outside the effective radius of the nuclear forces. The interacting nucleon excites the nucleus, and the deuteron then continues its motion as a whole. The resulting formula is similar to those derived in the stripping theory, and agreement with experiment has been obtained in many cases.

Certain discrepancies were observed recently[3] between this formula and the experimental data.

Fairbairn[4] has derived very recently another formula, in which it is also assumed that scattering proceeds through an intermediate state, composed of the bombarding nucleus and one of the deuteron nucleons, i.e., the reaction proceeds through the single-particle mechanism.

In this communication we shall represent the inelastic scattering of the deuteron as a direct process, analogous in certain respects to that examined by Austern, Butler and McManus and more recently by Butler[5] for (p, p) reactions. We assume that the incident deuteron, colliding at a certain instant of time with the proton and neutron on the surface of the nucleus, merely experiences scattering and is itself the outgoing particle.

Let $\mathbf{k}$ and $\mathbf{k}'$ be the wave vectors of the incident and scattered deuterons $\Phi_{l_1 m_1, l_2 m_2}(\mathbf{r}_1, \mathbf{r}_2)$ and $\Phi_{l_1' m_1', l_2' m_2'}(\mathbf{r}_1, \mathbf{r}_2)$ the wave functions representing the states of the proton on the surface of the nucleus prior to and after the collision ($|\mathbf{r}_1| \approx |\mathbf{r}_2| \equiv |\mathbf{r}|$). To simplify the calculations we shall not introduce the spin functions explicitly and will take spins into account only inasmuch as they determine the selection rules. We shall also assume that the target nucleus has an infinite mass. Then, the differential cross section for the direct (d, d′) reaction will be given by the expression

$$\sigma(\mathbf{k}_d, \mathbf{k}_{d'}) = \frac{M_d^2}{(2\pi\hbar^2)^2} \frac{k'}{k} \sum |I|^2,$$

where

$$I = \langle l_1' m_1', \; l_2' m_2', \; \mathbf{k}' | V | l_1 m_1, \; l_2 m_2, \; \mathbf{k} \rangle$$

$$= \int d\mathbf{r}_1 d\mathbf{r}_2 d\mathbf{r}_1' \, d\mathbf{r}_2' \, \Phi^*_{l_1' m_1', \, l_2' m_2'}(\mathbf{r}_1, \mathbf{r}_2)$$

$$\times \exp\{-\alpha r_{12}'^2 - i\mathbf{k}'(\mathbf{r}_1' + \mathbf{r}_2')/2\}$$

$$\times V \Phi_{l_1 m_1, l_2 m_2}(\mathbf{r}_1, \mathbf{r}_2) \exp\{-\alpha r_{12}'^2 + i\mathbf{k}(\mathbf{r}_1' + \mathbf{r}_2')/2\}, \qquad (1)$$

where the Born approximation is used, and a Gaussian expression with $\alpha = 0.23 \times 10^{13}\,\mathrm{cm}^{-1}$ is used for the internal wave function of the deuteron. V is the potential of the interaction between the incident deuteron and the proton-neutron system on the surface of the nucleus. For V we take the expression

$$V = V_0 \delta(\mathbf{r}_1 - \mathbf{r}_1') \delta(\mathbf{r}_2 - \mathbf{r}_2'). \qquad (2)$$

Inserting (2) into (1) we get

$$I = V_0 \int \Phi^*_{l_1' m_1', \, l_2' m_2'}(\mathbf{r}_1, \mathbf{r}_2) \, e^{-2\alpha r_{12}^2} \, e^{i\mathbf{Q}(\mathbf{r}_1 + \mathbf{r}_2)}$$

$$\times \Phi_{l_1 m_1, \, l_2 m_2}(\mathbf{r}_1, \mathbf{r}_2) \, d\mathbf{r}_1 \, d\mathbf{r}_2, \qquad (3)$$

$$\mathbf{Q} = (\mathbf{k} - \mathbf{k}')/2.$$

We also use the expression

$$\Phi_{l_1 m_1, \, l_2 m_2}(\mathbf{r}_1, \mathbf{r}_2) = f_{l_1}(\mathbf{r}_1) f_{l_2}(\mathbf{r}_2) Y_{l_1}^{m_1}(\theta_1, \varphi_1) Y_{l_2}^{m_2}(\theta_2, \varphi_2) \qquad (4)$$

and put $|\mathbf{r}_1| = |\mathbf{r}_2| = |\mathbf{r}|$, so that we can write

$$\exp\{-2\alpha r_{12}^2\} = \exp\{-4\alpha r^2 + 4\alpha r^2 \cos\theta_{12}\}$$

$$= e^{-4\alpha r^2} \sqrt{\frac{\pi}{8\alpha r^2}} \sum_{n=0}^{\infty} (2n+1) I_{n+1/2}(4\alpha r^2) P_n(\cos\theta_{12}), \qquad (5)$$

where $I_{n+\frac{1}{2}}(4\alpha r^2)$ is the modified Bessel function of half-integral order.[6] Inserting the formula

$$P_n(\cos\theta_{12}) = \frac{4\pi}{2n+1} \sum_{m=-n}^{n} Y_n^{m*}(\theta_1, \varphi_1) Y_n^m(\theta_2, \varphi_2) \qquad (6)$$

together with (4) and (5) into (3), inverting the spherical harmonics with respect to $(\theta_1, \varphi_1)$ and $(\theta_2, \varphi_2)$ with the aid of the vector-addition coefficients,[7] and finally integrating over the solid angles $d\Omega_1$ and $d\Omega_2$, we obtain (summation over $L_1$, $L_2$, n, $K_1$, $K_2$, $M_1$, $M_2$, m)

$$I \approx \int 4\pi dr e^{-4\alpha r^2} \sqrt{\frac{\pi}{8\alpha r^2}} f_{l_1}(r) f_{l_2}(r) f_{l_1'}(r) f_{l_2'}(r)$$

$$\times \sqrt{(2l_1+1)(2l_1'+1)(2l_2+1)(2l_2'+1)}$$

$$\times \sum (-1)^{m+m_1'+m_2'} i^{K_1+K_2}$$

$$\times (2n+1) I_{n+1/2}(4\alpha r^2) C_{l_1 l_1'}(L_1 000)$$

$$\times C_{l_1 l_1'}(L_1 M_1 m_1 m_1') C_{l_2 l_2'}(L_2 000)$$

$$\times C_{l_2 l_2'}(L_2 M_2 m_2 m_2') C_{L_1 n}(K_1 000)$$

$$\times C_{l_1 n}(K_1 0 M_1 - m) C_{L_2 n}(K_2 000) C_{L_2 n}(K_2 0 M_2 m)$$

$$\times J_{K_1}(Qr) I_{K_2}(Qr). \qquad (7)$$

$J_{K_1}$ and $J_{K_2}$ are spherical Bessel functions, and C are the vector-addition coefficients. As an approximation, we take the spherical Bessel functions outside the integral sign, using their values on the nuclear boundary r = R. We then find that the transition amplitude is expressed in the form of a sum of terms, in which the angular dependence is contained in $J_{K_1}(QR)\,J_{K_2}(QR)$, with

$$Q^2 = (k^2 + k'^2 - 2kk'\cos\theta)/4, \tag{8}$$

where $\theta$ is the angle between $\mathbf{k}$ and $\mathbf{k}'$.

Squaring (7), summing over the final states, averaging over the initial states, and using the Racah formalism,[8] we obtain an expression for the inelastic scattering differential cross section of the deuterons.

$$\sigma \infty |F(R)|^2 e^{-8\alpha R^2}[(2l_1+1)(2l_1'+1)(2l_2+1)(2l_2'+1)]$$
$$\times \sum_{L_1L_2}[(2L_1+1)(2L_2+1)]^{-1/2} |C_{l_1l_1'}(L_1\,000)\,C_{l_2l_2'}(L_2\,000)|^2$$
$$\times \sum_f (-1)^f \Big|\sum_{nK_1K_2}(2n+1)\,I_{n+1/2}(4\alpha R^2)$$
$$\times C_{L_1n}(K_1\,000)\,C_{L_2n}(K_2\,000)$$
$$\times Z(K_1L_1K_2L_2,\ nf)\,j_{K_1}(QR)\,j_{K_2}(QR)\Big|^2 \tag{9}$$

Here $L_1$ takes on values from $|l_1 - l_1'|$ to $|l_1 + l_1'|$, and $K_1$ ranges from $|L_1 - n|$ to $|L_1 + n|$, with $L_2$ and $K_2$ behaving analogously. Summation over f extends from $L_1 - L_2$ to $L_1 + L_2$. The coefficients Z (Ref. 8) are connected with a Racah coefficient by the relation

$$Z(K_1L_1K_2L_2,\ nf) = i^{f-K_1+K_2}[(2K_1+1)$$
$$\times (2K_2+1)(2L_1+1)(2L_2+1)]^{1/2}$$
$$\times W(K_1L_1K_2L_2,\ nf)\,C_{K_1K_2}(f\,000).$$

The angular distribution of the scattered deuterons, given in (9), depends on the spherical Bessel functions $j_{K_1}$ and $j_{K_2}$. In addition, as can be seen from (9), there is no interference between the different values of $L_1$, $L_2$, and f. Given $L_1$ and $L_2$, which can be obtained from the values of the angular momenta of the levels under examination, it is possible to choose for f an allowed value that gives the best agreement with experiment.

For comparison with experiment, we made use of the measurements of Levine, Bender, and McGruer,[3] who obtained an angular distribution for 14.4-Mev deuterons, inelastically scattered by the 4.61-Mev level of the $Li^7$ nucleus.

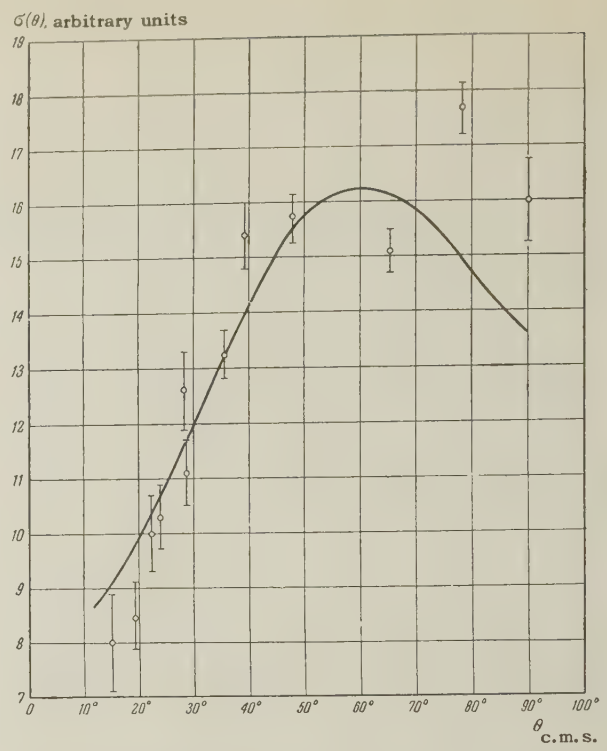


The observed distribution (c.m.s.) increases in the interval from 17° to ~70°. This distribution is not in agreement with the Huby and Newns theory.

In the ground state of $Li^7$, $J = (3/2)^-$, while for the 4.6 Mev level $J = (5/2)^-$. According to the selection rules

$$J_f - J_i = (L_1 + L_2) + I + I,$$

and since the parity does not change in this transition, we can take $L_1 = L_2 = 0$, and then f = 0. In this case, that portion of (9) which determines the angular distribution will be of the form

$$\sigma \infty |j_0^2 + 4.614\,j_1^2 + 7.848\,j_2^2 + 9.17\,j_3^2$$
$$+ 8.37\,j_4^2 + 6.604\,j_5^2 + 5.016\,j_6^2|^2. \tag{10}$$

The angular distribution that follows from (10) is shown in the diagram together with the experimental values obtained from Ref. 3. A satisfactory agreement is seen. The nuclear radius of $Li^7$ was taken to be $6.5 \times 10^{-13}$ cm, the value used in Ref. 3 when discussing the $Li^7(d, d')Li^7$ reactions at the 0.478 Mev level; $\alpha = 0.23 \times 10^{-13}\,cm^{-1}$ (Ref. 9).

The mechanism considered can play a substantial role in the case of inelastic scattering of deuterons, for example, by $N^{14}$ and $C^{12}$ nuclei. Experiments carried out with these two nuclei (and possibly also with others) can be reconciled with the formulas of the stripping and direct-interaction theories. The contribution of each of these processes

will depend on the structures of the nuclei studied. One can hope information on the structures of various nuclei can be obtained in this manner.

[1] J. R. Holt and C. T. Young, Nature **164**, 1000 (1949).

[2] R. Huby and H. C. Newns, Phil. Mag. **42**, 1442 (1951).

[3] Levine, Bender, and McGruer, Phys. Rev. **97**, 1249 (1955). T. S. Green and R. Middleton, Proc. Phys. Soc. **A69**, 28 (1956). S. Hinds and R. Middleton, Proc. Phys. Soc. **A69**, 347 (1956).

[4] W. M. Fairbairn, Proc. Roy. Soc. **A238**, 448 (1957).

[5] Austern, Butler, and McManus, Phys. Rev. **92**, 350 (1953). S. T. Butler, Phys. Rev. **106**, 272 (1957).

[6] G. Petiau, La theorie des functions de Bessel, C.N.R.S., Paris, pp. 87, 170, 1955.

[7] J. M. Blatt and V. F. Weiskopf, Theoretical Nuclear Physics, Wiley, 1952, p. 789.

[8] Biedenharn, Blatt, and Rose, Revs. Mod. Phys. **24**, 258 (1952).

[9] H. C. Newns, Proc. Phys. Soc. **A65**, 916 (1952).

Translated by J. G. Adashko
244

SOVIET PHYSICS JETP VOLUME 34(7), NUMBER 5 NOVEMBER, 1958

# *SEMI-PHENOMENOLOGICAL THEORY OF NUCLEON-NUCLEON INTERACTION*

G. F. ZHARKOV

P. N. Lebedev Physics Institute, Academy of Sciences, U.S.S.R.

Submitted to JETP editor December 6, 1957

J. Exptl. Theoret. Phys. (U.S.S.R.) **34**, 1211-1220 (May, 1958)

Results of the calculation of nucleon-nucleon interaction potentials are presented. The calculations were made within the framework of the semi-phenomenological isobaric theory. The computed deuteron parameters and scattering of low-energy nucleons agree satisfactorily with experiment. An unsuccessful attempt is made to employ the computed potentials for a description of the scattering of high energy nucleons (~100 Mev).

## 1. INTRODUCTION

TAMM, Gol'fand, and Fainberg[1] have proposed a semi-phenomenological theory of nucleon-meson interaction where, in addition to the ordinary nucleon state with mechanical and isotopic spins $\frac{1}{2}$, there is consideration of their excited isobaric state with mechanical and isotopic spins $\frac{3}{2}$. This isobaric state, which is introduced purely phenomenologically, permits us to describe the behavior of the cross sections for the scattering[1] and photoproduction[2] of $\pi$ mesons on nucleons in a fairly large meson energy range up to 400 Mev.

The semi-phenomenological theory of Ref. 1 involves four free parameters: the nucleon excitation energy $\Delta$, the pseudovector meson-nucleon coupling constant $g/\mu$ (where $\mu$ is the mass of the $\pi$ meson), the pseudoscalar coupling constant $g' = sg$ (where $s$ is a number) and the constant $g_1$ which determines the probability of a nucleonic transition from its unexcited state to the isobaric state or vice versa. The values of these parameters were chosen to provide the best possible fit of experimental data on meson-nucleon scattering and meson photoproduction. The success of this procedure induced us to apply the semi-phenomenological isobaric theory to the problem of nuclear forces and specifically to the deuteron and nucleon-nucleon scattering.

Our calculation showed that inclusion of isobaric states greatly changes the results of the ordinary theory of nuclear forces, in which isobars are neglected. For example, when isobars are included the potential energy of nucleons in $^1S$ and $^3S$ states increases proportionally to $1/r^3$ for $r \to 0$, whereas when isobars are not taken into account the potential energy in the $^1S$ state (unlike $^3S$) has, as we know, only the simple pole $1/r$.

It follows that the isobaric theory leads to a nuclear force potential with a high-order singularity, so that, just as in the ordinary theory, the potential must be cut off at small distances. We shall assume that at small distances $r \leq r_0$ the potential represents an infinitely great repulsion; we thus are using the potential model with an impenetrable solid nucleus. In addition to the four parameters already mentioned, the theory will thus include, as a fifth parameter, the cutoff radius $r_0$. The parameters $\Delta$, g, s, and $g_1$ are determined from data on meson-nucleon scattering[1] and photoproduction,[2] and are assumed to be fixed. The single variable parameter $r_0$ can be determined provided that we obtain, on the one hand, the correct deuteron binding energy (triplet state) and, on the other hand, the correct value for the deuteron singlet level. Generally speaking, these two conditions can result, and in the ordinary theory do result (see Ref. 3, for example) in a different cutoff radius $r_0$ for the triplet and singlet states. A fundamental feature of the isobaric theory is that the triplet and singlet cutoff radii are very precisely identical, so that the theory actually includes only one additional parameter $r_0$. The present article presents the results of the application of this semi-phenomenological theory to the deuteron and to nucleon-nucleon scattering.

The general wave equation of a system of two nucleons is given in Sec. 2. Our initial equations could be written in relativistic form but would make the problem too complicated. In the present work we have used the so-called adiabatic approximation, which is essentially as follows. In first approximation the nucleons are regarded as infinitely heavy and fixed at the points $\mathbf{r}_1$ and $\mathbf{r}_2$; their static interaction potential $V(\mathbf{r})$ is then determined, where $\mathbf{r} = \mathbf{r}_1 - \mathbf{r}_2$, and this potential is inserted in the Schrödinger equation. This is the simplest approximation and is fully suitable for the nonrelativistic deuteron problem of interest.

In Secs. 3 and 4 the nucleon interaction potentials are found in adiabatic approximation for states of two-nucleon systems with different isotopic and mechanical spins. Finally, Sec. 5 gives the results of a computation of deuteron parameters and nucleon scattering at low energies. Whereas these results can be regarded as in satisfactory agreement with experiment, the theory was unsuccessfully applied to a description of nucleon scattering at high energies. This is shown by the 100-Mev nucleon scattering phases which are given in Sec. 5.

## 2. WAVE EQUATION OF A TWO-NUCLEON SYSTEM

We take the interaction Lagrangian in the form[1] ($\hbar = c = 1$)

$$L = L_1 + L_2,$$

$$L_1 = \frac{g}{\mu}\bar{\psi}\gamma_5\gamma_\mu\tau\frac{\partial\varphi}{\partial x_\mu}\psi + igs\bar{\psi}\gamma_5\tau\varphi\psi,$$

$$L_2 = \frac{g_1}{\mu}\left(\bar{\psi}\mathbf{S}\frac{\partial\varphi}{\partial x_\mu}B_\mu + \bar{B}_\mu\mathbf{S}^+\frac{\partial\varphi}{\partial x_\mu}\psi\right). \qquad (1)$$

Here $\varphi$ is the wave function of the meson field, $\psi$ is the nucleon field and $B_\mu$ is a spin vector which describes the excited nucleon field (the isobaric field).*

The six-row matrix $\mathbf{S}$ in isotopic space is determined by the requirement of isotopic invariance of the Lagrangian and is analogous to the ordinary isotopic matrices $\tau$. (The explicit form of $\mathbf{S}$ is given in Ref. 1, Appendix A.4).

We shall now write the equation of motion for the wave function $v(\gamma_1\gamma_2)$ of two nucleons with positive energy. Here $\gamma_i$ denotes the set of quantum numbers which characterize the state of the i-th nucleon (its momentum, total mechanical and isotopic spins and their projections on the z axis). In addition to the two-nucleon state we shall consider only states in which an additional single meson is present. The Schrödinger equation is then[4] (summing over repeated subscripts)

$$(W - E_{\gamma_1\gamma_2})\,v(\gamma_2,\gamma_2) = \frac{\langle\gamma_1\gamma_2 0\,|\,\gamma_1'\gamma_2 1\rangle\langle\gamma_1'\gamma_2 1\,|\,\gamma_1'\gamma_2'' 0\rangle}{W - E_{\gamma_1'\gamma_2}^{1}}\,v(\gamma_1',\gamma_2'')$$

$$+\frac{\langle\gamma_1\gamma_2 0\,|\,\gamma_1\gamma_2' 1\rangle\langle\gamma_1\gamma_2' 1\,|\,\gamma_1''\gamma_2' 0\rangle}{W - E_{\gamma_1\gamma_2'}^{1}}\,v(\gamma_1'',\gamma_2'). \qquad (2)$$

Here W is the energy of the system, $E_{\gamma_1\gamma_2}$ is the energy of two free nucleons, $E_{\gamma_1\gamma_2 1}$ is the energy of the state consisting of two free nucleons and a single meson, the quantities $\langle\gamma_1\gamma_2 0\,|\,\gamma_1'\gamma_2' 1\rangle$ are the matrix elements of transitions from a mesonless state to a state with a meson; $\langle\gamma_1\gamma_2 1\,|\,\gamma_1'\gamma_2' 0\rangle$ represents a transition with absorption of the meson. The matrix elements are easily obtained explicitly by means of the Lagrangian (1).

We now pass in Eq. 2 to the approximation whereby the nucleon mass M and the isobar mass $M + \Delta$ are regarded as very large ($M \gg \mu$), and we also assume $W - 2M = 0$ in the denominators of the right member of the equation. The latter approximation provides considerable simplification

*Strictly speaking, the wave function of the isobar is a combination of the spin vector $B_\mu^\sigma$ and the bispinor $D_\sigma$. However, the interaction Lagrangian does not contain $D_\sigma$ and in the limiting case of infinitely heavy nucleons and isobars which is considered below $D_\sigma = 0$.

and is fully justified for the nonrelativistic deuteron and nucleon-nucleon scattering at sufficiently low energies.

We shall use the letter $\alpha$ to denote the state in which both nucleons are unexcited, $\beta$ to denote the state in which the first nucleon* is unexcited while the second is in the isobaric state, $\gamma$ for the state in which the second nucleon is excited but not the first and $\delta$ for the state in which both nucleons are excited. We also introduce the notation

$$\Phi_n(\rho) = \frac{1}{(2\pi)^2}\int d\mathbf{k}\,\frac{e^{i\mathbf{k}\rho|\mu}}{(n\Delta+\varepsilon_k)\varepsilon_k}\ (n=0,\ 1,\ 2);$$
$$W-2M=V\mu;\ r=\rho/\mu;\ \varepsilon_k=\sqrt{k^2+\mu^2};$$
$$G_n=2\rho\ {}^1\Phi_n',\ H_n=2(\Phi_n''-\rho^{-1}\Phi_n');$$
$$N_n(\mathbf{k},\ \mathbf{l})=(\mathbf{kl})\,G_n+(\mathbf{k\rho})(\mathbf{l\rho})\,\rho^{-2}H_n;$$
$$N_{nm}=N_n+N_m. \qquad (3)$$

Using the explicit form of the matrix elements, we rewrite Eq. (2) in the coordinate representation:

$$V\alpha = g^2(\tau_1\tau_2)\,N_0(\sigma_1,\ \sigma_2)\,\alpha + {}^1/_2\,gg_1(\tau_1\mathbf{S}_2)\,N_{01}(\sigma_1,\ \mathbf{c}_2)\,\beta$$
$$+\,{}^1/_2\,gg(\mathbf{S}_1\tau_2)\,N_{01}(\mathbf{c}_s,\ \sigma_2)\,\gamma + g_1^2(\mathbf{S}_1\mathbf{S}_2)\,N_1(\mathbf{c}_1,\ \mathbf{c}_2)\,\delta,$$
$$(V-\Delta)\,\beta = {}^1/_2\,gg_1(\tau_1\mathbf{S}_2)\,N_{01}(\sigma_1,\ \mathbf{c}_2^*)\,\alpha$$
$$+\,{}^1/_2\,g_1^2(\mathbf{S}_1\mathbf{S}_2)\,N_{02}(\mathbf{c}_1\mathbf{c}_2^*)\,\gamma,$$
$$(V-\Delta)\,\gamma = {}^1/_2\,gg_1(\mathbf{S}_1\tau_2)\,N_{01}(\mathbf{c}_1^*,\ \sigma_2)\,\alpha$$
$$+\,{}^1/_2\,g_1^2(\mathbf{S}_1\mathbf{S}_2)\,N_{02}(\mathbf{c}_1^*,\mathbf{c}_2)\,\beta,$$
$$(V-2\Delta)\,\delta = g_1^2(\mathbf{S}_1\mathbf{S}_2)\,N_1(\mathbf{c}_1^*,\ \mathbf{c}_2^*)\,\alpha. \qquad (4)$$

The spin matrices $\mathbf{c}$ are

$$c_x=\frac{1}{\sqrt{2}}\begin{pmatrix}0 & 0 & 1/\sqrt{3} & 0\\ 1 & 1/\sqrt{3} & 0 & 1\end{pmatrix};$$

$$c_y=\frac{1}{\sqrt{2}}\begin{pmatrix}i & 0 & -i/\sqrt{3} & 0\\ 0 & i/\sqrt{3} & 0 & -i\end{pmatrix};$$

$$c_z=\frac{1}{\sqrt{2}}\begin{pmatrix}0 & -2/\sqrt{3} & 0 & 0\\ 0 & 0 & 2/\sqrt{3} & 0\end{pmatrix}. \qquad (5)\dagger$$

In Eq. (4) the following equalities were used:*

$$\bar{u}(\mathbf{k},\ s)\,i\gamma_5(\hat{k}-\hat{p})\,u(\mathbf{p},\ s')$$
$$=2M\bar{u}(\mathbf{k},\ s)\,\gamma_5\,u(\mathbf{p},\ s')=(\sigma,\ \mathbf{p}-\mathbf{k})_{ss'},$$
$$\bar{u}(\mathbf{k},\ s)\,(\mathbf{k}-\mathbf{p})\,\mathbf{B}(\mathbf{p},\ s')=(\mathbf{c},\ \mathbf{k}-\mathbf{p})_{ss'},$$

where u represents the usual Dirac amplitudes of a particle with spin $1/2$, $\mathbf{B}$ is the spin-vector amplitude of a particle with spin $3/2$ (in our approximation ($M\to\infty$), u are two-component spinors and $B_4=0$), and $\sigma$ are the Pauli matrices. The subscripts 1 and 2 of the operators $\tau$, $\mathbf{s}$, $\sigma$ and $\mathbf{c}$ denote the nucleon on whose variables the operations are performed. In order to go over from Eq. (4) to the ordinary non-isobaric theory of nuclear forces, it is sufficient to set $g_1=0$. For the potential energy of the two-nucleon interaction we then obtain the familiar expression

$$V=g^2(\tau_1\tau_2)\,N_0(\sigma_1,\ \sigma_2)$$
$$=g^2(\tau_1\tau_2)\,\frac{e^{-\rho}}{3\rho}\left\{(\sigma_1\sigma_2)+\left(1+\frac{3}{\rho}+\frac{3}{\rho^2}\right)S_{12}\right\}, \qquad (6)$$

where $S_{12}$ is the spin operator

$$S_{12}=3(\sigma_1\rho)(\sigma_2\rho)\rho^{-2}-(\sigma_1\sigma_2). \qquad (7)$$

## 3. THE CASE I = 0

The total isotopic spin I of a two-nucleon system can be either 0 or 1. We shall consider the first of these cases. When $I=0$ it is impossible to have one unexcited and one excited nucleon since two vectors with $I=1/2$ and $3/2$ cannot be added to give zero. Therefore in this case the wave functions $\beta$ and $\gamma$ are zero.

It is easily seen that in isotopic space $\alpha$ and $\delta$ are given by

$$\alpha=a\hat{\alpha}_0,\ \delta=d\hat{\delta}_0, \qquad (8)$$

with the isotopic space matrices

$$\hat{\alpha}_0=\begin{pmatrix}0 & 1\\ -1 & 0\end{pmatrix},\ \hat{\delta}_0=\begin{pmatrix}0 & 0 & 0 & 1\\ 0 & 0 & -1 & 0\\ 0 & 1 & 0 & 0\\ -1 & 0 & 0 & 0\end{pmatrix}, \qquad (8')$$

*Our approximation corresponds to the case of fixed particles so that we can speak of a "first" and a "second" nucleon.

†The following relations are easily verified:

$$\sum_{\lambda=1}^{2}c_{\lambda r}^*\,c_{\lambda s}=\delta_{rs};\ \sum_{r=1}^{4}c_{\lambda r}\,c_{\mu r}=2\delta_{\mu\nu};\ \sum_{r=1}^{4}[c_{\mu r}\,c_{\nu r}^*]=-\frac{2}{3}\,i\sigma_{\mu\nu};$$
$$\sum_{r=1}^{4}(c_{\lambda r}\,\mathbf{k})\,(c_{\mu r}^*\,\mathbf{l})=\frac{2}{3}(\mathbf{kl})\,\delta_{\lambda\mu}-\frac{i}{3}[\mathbf{kl}]\,\sigma_{\lambda\mu}.$$

*The first of these equalities, which demonstrates the so-called equivalence of the pseudovector and pseudoscalar interactions, will cause g in Eq. (4) and subsequent equations to be replaced by $g(1+s/2M)$ when M is regarded as finite (see footnote† on p. 842). The last equality can easily be obtained by means of Ref. 5, where $B_\mu$ is given explicitly.

where a and d are in general matrices with the ordinary spin variable.

In the present case, (4) becomes

$$Va = -3g^2 N_0(\sigma_1, \sigma_2)\, a - 12g_1^2 N_1(\mathbf{c}_1, \mathbf{c}_2)\, d,$$
$$(V - 2\Delta)\, d = -6g_1^2 N_1(\mathbf{c}_1^*, \mathbf{c}_2^*)\, a. \qquad (9)$$

Eliminating d, we obtain

$$Va = -3g^2 N_0(\sigma_1, \sigma_2)\, a + \frac{72g_1^4}{V - 2\Delta} N_1(\mathbf{c}_1, \mathbf{c}_2) N_1(\mathbf{c}_1^*, \mathbf{c}_2^*)\, a. \qquad (10)$$

Using (3) and (7), with the notation

$$F_i = 3G_i + H_i, \qquad (11)$$

we obtain the following expression for the operator $V^{I=0}$ of the potential energy of nucleons in the state I = 0:

$$V = -g^2\{(\sigma_1\sigma_2) F_0 + S_{12}H_0\} + \frac{16g_1^4}{9(V - 2\Delta)}\{6F_1^2 + 12H_1^2 + (\sigma_1\sigma_2)(H_1^2 - F_1^2) + S_{12}H_1(F_1 - H_1)\}. \qquad (12)$$

The first term on the right-hand side agrees (for $\tau_1\tau_2 = -3$) with the usual expression (6) for the potential energy of two nucleons, while the second term takes into account the influence of isobaric states on V. Multiplying (12) by $(V - 2\Delta)$, we obtain a quadratic equation in the interaction operator V. The solution of this equation for triplet states, with respect to the mechanical spin (S = 1), of the two-nucleon system (including the stable $^3$S deuteron state) is given by

$$V^{I=0, S=1} = U^{0,1} + U_T^{0,1} S_{12}, \qquad (13)$$

with the following notation:

$$U^{0,1} = \Delta - \frac{p}{2} - \frac{R_1}{3} - \frac{R_2}{6}, \quad U_T^{0,1} = -\frac{R_1 - R_2}{12} - \frac{q}{2},$$
$$R_1 = \sqrt{(2\Delta + p + 2q)^2 + r + s},$$
$$R_2 = \sqrt{(2\Delta + p - 4q)^2 + r - 2s},$$
$$p = g^2 F_0^*,\ q = g^2 H_0,\ r = \frac{64}{9} g_1^4 (5F_1^2 + 13H_1^2),$$
$$s = \frac{128}{9} g_1^4 H_1 (F_1 - H_1).$$

When S = 0 the eigenvalue of $S_{12}$ is zero and the eigenvalue of $(\sigma_1\sigma_2)$ is $-3$. Substituting these values into (12), we obtain the following equation for the two-nucleon interaction potential:

$$V = 3g^2 F_0 + \frac{16g_1^4}{V - 2\Delta}(F_1^2 + H_4^2),$$

one of whose solutions is

$$V^{I=0, S=0} = \Delta + \frac{3}{2} g^2 F_0 - [(\Delta + {}^3/_2 g^2 F_0)^2 + 16g_1^4 (F_1^2 + H_1^2) - 6g^2 F\Delta]^{1/2}. \qquad (14)$$

As $r \to \infty$ the solution for V with the positive radical approaches $2\Delta$, while the solution with the negative radical approaches zero. The last solution evidently represents the potential energy of two nucleons in the state I = 0, S = 0.

## 4. THE CASE I = 1

We now consider a system of two nucleons with total isotopic spin I = 1. By charge invariance the value of $I_Z$, which is the projection of I on the z axis, is not significant, but for definiteness we shall assume $I_Z = 1$. For $I_Z = 1$ only the following components of the wave functions are nonvanishing:

$$\alpha_{1/2,\,1/2},\ \beta_{1/2,\,1/2},\ \beta_{-1/2,\,3/2},\ \gamma_{3/2,\,-1/2},\ \gamma_{1/2,\,1/2},\ \delta_{3/2,\,-1/2},\ \delta_{1/2,\,1/2},\ \delta_{-1/2,\,3/2},$$

where the subscripts denote the projections of the isotopic spin of the i-th nucleon on the z axis.

Using the fact that the wave function of the system $v(\gamma_1, \gamma_2)$ must satisfy the equation

$$\hat{I}^2 v = I(I+1)\, v,$$

where $\hat{I}$ is the operator of the total isotopic moment, we can represent $\alpha$, $\beta$, $\gamma$, $\delta$ by

$$\alpha = \hat{a}\hat{\alpha}_1,\ \beta = \hat{b}\hat{\beta}_1,\ \gamma = \hat{c}\hat{\gamma}_1,\ \delta = \hat{d}\hat{\delta}_1. \qquad (15)$$

Here we have introduced the following matrices in isotopic space:

$$\hat{\alpha}_1 = \begin{pmatrix} 1 & 0 \\ 0 & 0 \end{pmatrix};\ \hat{\beta}_1 = \begin{pmatrix} 0 & 1 & 0 & 0 \\ -\sqrt{3} & 0 & 0 & 0 \end{pmatrix};$$
$$\hat{\gamma}_1 = \begin{pmatrix} 0 & -\sqrt{3} \\ 1 & 0 \\ 0 & 0 \\ 0 & 0 \end{pmatrix};$$
$$\hat{\delta}_1 = \begin{pmatrix} 0 & 0 & -\sqrt{3}/2 & 0 \\ 0 & 1 & 0 & 0 \\ -\sqrt{3}/2 & 0 & 0 & 0 \\ 0 & 0 & 0 & 0 \end{pmatrix}. \qquad (16)$$

$\hat{a}$, $\hat{b}$, $\hat{c}$, $\hat{d}$ are independent of the isotopic coordinates but are matrices in ordinary spin space. Substituting (15) into the general system (4), we obtain

$$V\hat{a} = g^2 N_0(\sigma_1, \sigma_2)\,\hat{a} + 4gg_1\{N_{01}(\sigma_1, c_2)\,\hat{b} + N_{01}(c_1, \sigma_2)\,\hat{c}\} + 10\,g_1^2 N_1(c_1, c_2)\,\hat{d},$$

$$(V-\Delta)\,\hat{b} = gg_1 N_{01}(\sigma_1, c_2^*)\,\hat{a} - g_1^2 N_{02}(c_1, c_2^*)\,\hat{c},$$

$$(V-\Delta)\,\hat{c} = gg_1 N_{01}(c_1^*, \sigma_2)\,\hat{a} - g_1^2 N_{02}(c_1^*, c_2)\,\hat{b},$$

$$(V-2\Delta)\,\hat{d} = 4\,g_1^2 N_1(c_1^*, c_2^*)\,\hat{a}. \qquad (17)$$

The last of these equations is used to eliminate $\hat{d}$ from the first equation of (17). We proceed as follows to eliminate $\hat{b}$ and $\hat{c}$.

We consider singlet states with respect to the mechanical spin ($S = 0$). Then the four components of $\hat{a}$ ($\hat{a} = a_{\lambda\mu}$, where $\lambda$ and $\mu$ are spin indices) can be represented by

$$\hat{a} = \begin{vmatrix} 0 & a \\ -a & 0 \end{vmatrix}, \qquad (18)$$

where $a$ depends on spatial coordinates alone. We shall obtain the solutions of the second and third equations of (17) in the form

$$\hat{b} = \xi N_{01}(\sigma_1 c_2^*)\,\hat{a}, \quad \hat{c} = \xi N_{01}(c_1^*, \sigma_2)\,\hat{a}, \qquad (19)$$

where $\xi$ is the sought factor. Substituting (19) into (17) for $S = 0$, we obtain a relation for $\xi$:

$$\xi = gg_1[(V-\Delta) - g_1^2(G_{02} + {}^2/_3 H_{02})]^{-1} \qquad (20)$$

Substituting (19) and (20) into (17) and eliminating $\hat{d}$ from the first equation of (17) by means of the fourth equation, we obtain an equation for $\hat{a}$, from which there is derived the following cubic equation for determination of the potential energy $V^{I=1,\,S=0}$ in the system with $I = 1$, $S = 0$:

$$V = -g^2 F_0 + \frac{16g^2 g_1^2 (H_0 + H_1)^2}{3(V-\Delta) - g_1^2(F_0 + F_2 + H_0 + H_2)} + \frac{80 g_1^4 (F_1^2 + H_1^2)}{9(V-2\Delta)}. \qquad (21)$$

It can be shown that for all distances between the nucleons this equation has one negative and two positive roots for $V$, which for $\rho \to \infty$ approach 0, $\Delta$ and $2\Delta$, respectively. The negative root of (21) must obviously be interpreted as the potential energy of nucleons in the state $I = 1$, $S = 0$.

We shall finally consider a system of two nucleons in the state with both total isotopic and ordinary spins equal to unity. Above, in (17), equations were given describing the behavior of a two-nucleon system in state $I = 1$ with arbitrary mechanical spin. (17) is a set of four equations with respect to the functions $\hat{a}$, $\hat{b}$, $\hat{c}$, $\hat{d}$, with $\hat{d}$ easily eliminated by means of the last equation, whereas the elimination of $\hat{b}$ and $\hat{c}$ is more complicated.

We shall obtain the solution of (17) for the triplet state $S = 1$ in the form

$$\hat{b} = \xi_1(\sigma\hat{a}c^*) + \xi_2(\sigma\rho)\,\hat{a}(c^*\rho)\,\rho^{-2} + \xi_3\hat{a}\,\widetilde{(\sigma\rho)}\,(c^*\rho)\,\rho^{-2},$$
$$\hat{c} = \hat{b}, \qquad (22)$$

where $\xi_i$ are coefficients, with the sign $\sim$ denoting transposition. Substituting (22) into the second equation of (17), we obtain a relation for a linear combination of the matrices in (22). By equating coefficients of the different matrices we obtain the following set of equations for the determination of $\xi_i$:

$$(V-\Delta)\,\xi_1 = gg_1 G_{01} + {}^1/_3\,\xi_1 g_1^2 G_{02} + {}^1/_3\,\xi_2 g_1^2 G_{02} + {}^1/_3\,\xi_3 g_1^2 G_{02},$$

$$(V-\Delta)\,\xi_2 = gg_1 H_{01} - {}^2/_3\,\xi_2 g_1^2 G_{02} - \xi_3 g_1^2 G_{02} + {}^1/_3\,\xi_1 g_1^2 H_{02} - {}^2/_3\,\xi_3 g_1^2 H_{02},$$

$$(V-\Delta)\,\xi_3 = -{}^1/_3\,\xi_2 g_1^2 G_{02} - \xi_1 g_1^2 H_{02} - {}^2/_3\,\xi_2 g_1^2 H_{02}. \qquad (23)$$

Obtaining $\xi_i$ from (23) and substituting (22) into the first equation of (17), we obtain an equation for $\hat{a}$, which describes a system of two unexcited nucleons.

The equations for $\hat{a}$ can be written as

$$[V - E_1(V)]\,\hat{a} = E_2(V)\,(\sigma\rho)\,\hat{a}\,\widetilde{(\sigma\rho)}\,\rho^{-2}; \qquad (24)$$

where

$$E_1(V) + E_2(V) = g^2(G_0 + H_0) + \frac{16}{3} gg_1 G_{01}(4\xi_1 + \xi_2 + \xi_3) + \frac{16}{3} gg_1 H_{01}(\xi_1 + \xi_2 + \xi_3) + \frac{80}{9}\frac{g_1^4}{V-2\Delta}(5G_1^2 + 4G_1H_1 + 2H_1^2),$$

$$E_1(V) - E_2(V) = g^2(G_0 - H_0) + \left(\frac{32}{3} gg_1 G_{01} + \frac{16}{3} gg_1 H_{01}\right)(2\xi_1 + \xi_2 - \xi_3) + \frac{80}{9}\frac{g_1^4}{V-2\Delta}(5G_1^2 + 2G_1H_1 + 2H_1^2),$$

with $\xi_1$, $\xi_2$, $\xi_3$ obtained from (23). The operator $(\sigma_1\rho)(\sigma_2\rho)\,\rho^{-2}$ in (24) has in the triplet state ($S = 1$) the three eigenvalues 1, 1, $-1$. We denote by $V_1$ the root of the equation

$$V - [E_1(V) + E_2(V)] = 0, \qquad (25)$$

which corresponds to the eigenvalue 1 of the operator, and by $V_{-1}$ the root of the equation

$$V - [E_1(V) - E_2(V)] = 0, \qquad (26)$$

TABLE I. Values of the nuclear potentials

| r, $\hbar/\mu c$ | $U^{0,1}$, Mev | $U_T^{0,1}$, Mev | $V^{00}$, Mev | $V^{1,0}$, Mev | $U^{1,1}$, Mev | $U_T^{1,1}$, Mev |
|---|---|---|---|---|---|---|
| 0.46 | —846.14 | —219.35 | —456.00 | —1254.8 | —1044.9 | 11.12 |
| 0.5 | —600.57 | —184.07 | —294.77 | — 935.00 | — 768.14 | 11.62 |
| 0.6 | —250.78 | —131.16 | — 89.87 | — 462.36 | — 365.29 | 12.74 |
| 0.7 | —102.87 | — 99.34 | — 18.87 | — 242.68 | — 181.88 | 13.15 |
| 0.8 | — 41.72 | — 73.53 | 5.357 | — 128.5 | — 89.24 | 12.64 |
| 1.0 | — 11.39 | — 38.40 | 12.77 | — 39.18 | — 21.83 | 9.494 |
| 1.2 | — 5.217 | — 21.20 | 10.46 | — 14.02 | — 5.556 | 6.154 |
| 1.5 | — 2.491 | — 9.799 | 6.624 | — 4.352 | — 0.4264 | 3.134 |
| 2.0 | — 1.050 | — 3.346 | 3.077 | — 1.250 | 0.2214 | 1.078 |
| 2.5 | — 0.5022 | — 1.339 | 1.499 | — 0.5330 | 0.1517 | 0.4448 |
| 3.0 | — 0.2522 | — 0.5884 | 0.7564 | — 0.2583 | 0.0800 | 0.1968 |

TABLE II

| $r_s$, $\hbar/\mu c$ | $r_t$, $\hbar/\mu c$ | Q, $(\hbar/\mu c)^2$ | p, % |
|---|---|---|---|
| 2.25 (1.92) | 1.37 (1.22) | 0.17 (0.14) | 8 See Ref. 6 |

which corresponds to the eigenvalue $-1$ of the same operator. (25) and (26) are fifth-degree equations in V, and the roots of these equations which approach 0 in the limit $r \to \infty$ obviously represent to the potential energy of two unexcited nucleons.

When the potential energy of two nucleons in the state $I = 1$, $S = 1$ is represented as

$$V^{I=1,\,S=1} = U^{1,1} + U_T^{1,1} S_{12}, \qquad (27)$$

where $S_{12}$ is the spin operator (7), then for the functions $U^{1,1}$ and $U_T^{1,1}$ depending on the separation we have

$$U^{1,1} = {}^1/_3 (2V_1 + V_{-1}), \quad U_T^{1,1} = {}^1/_6 (V_1 - V_{-1}). \qquad (28)$$

## 5. NUMERICAL RESULTS

Numerical values for the potentials of interest were obtained from Eqs. (12), (14), (21), and (27) of the present article. The constants in the expressions for the potentials were obtained by making the theoretical formulas of Refs. 1 and 2 agree as well as possible with experiments on meson photoproduction and scattering by nucleons. The optimum values of the constants were*

$$\Delta = 2.1\mu; \quad g^2 = 0.085; \quad g_1^2 = 0.063; \quad s = 1.8, \qquad (29)$$

with the nucleonic mass taken as $M = 6.75\,\mu$.

Table I contains the values of the potentials, calculated from the set of constants in (29)†

As already stated in the introduction, these potentials possess a singularity of high order at the origin, thus leading to the difficulty associated with the absence of a stable deuteron state and zero separation of the nucleons. We have therefore replaced our potentials at distances $r \leq r_0$ by an infinitely high repulsive barrier. The cutoff radius $r_0$ was determined separately for the singlet and triplet states of the deuterons; the identical value $r_0 = 0.46\ \hbar/\mu c$ was obtained in both instances. In this respect the isobaric theory differs from the ordinary theory of nuclear forces,[3] since, as we know, the singlet and triplet radii do not coincide in the latter.

The potentials were used to calculate the parameters which describe the deuteron and nucleon scattering at low energies; these are the effective ranges of nuclear forces in the singlet ($r_s$) and triplet ($r_t$) spin states, the quadrupole moment (Q) and the admixture of the D wave in the triplet state (p, %). These quantities and the corresponding experimental values (in parentheses) are seen in Table II. Although the theoretical values generally somewhat exceed the experimental values, on the whole the agreement of theory and experiment at low energies can be regarded as satisfactory.

As has already been indicated, our treatment is essentially nonrelativistic and applicable only to sufficiently low energies. To determine more completely the limits of applicability of the theory developed here it was of interest to use the derived nuclear potentials in a description of nucleon-nucleon scattering at energies as much higher as possible. For this purpose we calculated the phase shifts of nucleon-nucleon scattering at 100 Mev in the laboratory system. The results, which are given in Table III, show that our adiabatic approximation cannot be used to describe nucleon scattering at this energy. This would also be evident simply from the fact that the total cross sections $\sigma_{pp}$ and $\sigma_{pn}$ were 75 and 124 mb, respectively, compared with the experimental values $\sim 34$ and

*In comparing these numerical values of the constants with those given in Ref. 1, it must be remembered that in the present article we have used an isotopically invariant formalism, whereas the formalism employed in Ref. 1 is based on a classification by charge states. It is easily seen that as a result our values of $g^2$ and $g_i^2$ must be one half as large as the corresponding values in Ref. 1.

†Actually, in calculating the potentials from Eqs. (13), (14), (21) and (27) we did not use the constant $g^2$ equal to 0.085 but instead $g^2(1 + s/2\,M)^2 = 0.11$ (see footnote* on p. 839), but the results were very little affected.

**TABLE III.** Phase shifts of nucleon-nucleon scattering at 100 Mev

| State | $^1S_0$ | $^1P_1$ | $^1D_2$ | $^1F_3$ | $^3P_0$ | $^3P_1$ | $^3D_2$ | $^3F_3$ |
|---|---|---|---|---|---|---|---|---|
| Phase shifts | $\delta_0^0$ 0.395 | $\delta_1^0$ −0.2938 | $\delta_0^2$ 0.1034 | $\delta_3^0$ −0.0518 | $\delta_{I=0}$ 0.969 | $\delta_{I=1}^{\beta}$ −0.1238 | $\delta_{I=2}^{\beta}$ 0.609 | $\delta_{I=3}^{\beta}$ −0.0368 |

| State | $^3S_1 + {}^3D_1$ | | | $^3P_2 + {}^3F_2$ | | | $^3D_3 + {}^3G_3$ | | |
|---|---|---|---|---|---|---|---|---|---|
| Phase shifts and parameters of the mixture* | $\delta_{J=1}^{\alpha}$ 0.622 | $\delta_{J=1}^{\gamma}$ −0.344 | $\eta_{J=1}^{\alpha}$ 0.053 | $\delta_{J=2}^{\alpha}$ 0.3328 | $\delta_{J=2}^{\gamma}$ −0.001 | $\eta_{J=2}^{\alpha}$ −0.2544 | $\delta_{J=3}^{\alpha}$ 0.112 | $\delta_{J=3}^{\gamma}$ −0.0879 | $\eta_{J=3}^{\alpha}$ 0.7499 |

*We have followed the notation used in Ref. 7.

~ 70 mb. The angular distributions were also entirely unsatisfactory. A more exact non-adiabatic approximation might to some extent correct this discrepancy, but we are inclined to believe that the semi-phenomenological isobaric theory of nuclear forces which has been developed here is limited to low energies not above a few Mev.

Academician I. E. Tamm suggested this problem and participated in the early part of the work. I am extremely grateful to Academician Tamm for his suggestion and guidance. I also wish to thank L. V. Pariiskaia, A. T. Matachun and L. Ia. Trendeleva for many calculations.

[1] Tamm, Gol' fand, and Fainberg, J. Exptl. Theoret. Phys. (U.S.S.R.) **26**, 649 (1954).

[2] V. I. Ritus, J. Exptl. Theoret. Phys. (U.S.S.R.) **27**, 660 (1954).

[3] H. A. Bethe, Phys. Rev. **57**, 390 (1940).

[4] I. E. Tamm, J. Phys. (U.S.S.R.) **9**, 449 (1945).

[5] V. L. Ginzburg, J. Exptl. Theoret. Phys. (U.S.S.R.) **12**, 425 (1942).

[6] Taketani, Machida and O-Numa, Progr. Theoret. Phys. (Japan) **7**, 45 (1952).

[7] F. Rohrlich and J. Eisenstein, Phys. Rev. **75**, 705 (1946).

Translated by I. Emin
245

# USE OF THE OPTICAL MODEL FOR THE ANALYSIS OF $\pi - p$ AND $p - p$ SCATTERING AT HIGH ENERGIES

V. G. GRISHIN, I. S. SAITOV, and I. V. CHUVILO

Joint Institute for Nuclear Research

Submitted to JETP editor December 6, 1957

J. Exptl. Theoret. Phys. (U.S.S.R.) **34**, 1221-1229 (May, 1958)

$\pi$-p and p-p scattering at energies above 1 Bev in the laboratory system has been analyzed on the basis of a model in which the nucleon is regarded as an optically homogeneous sphere with sharp boundaries and a complex refractive index. It is shown that the available experimental data can be fitted by choosing a sphere of radius $R = (1.08 \pm 0.07) \times 10^{-13}$ cm, which is independent of the type of the interacting particles and of their energy. The optical parameters of the sphere are computed. The contributions to the elastic scattering cross section from the real and imaginary parts of the scattering amplitude are estimated. One can assume that the contribution from the real part of the scattering amplitude is small for $\pi$-meson energies of 1.37 Bev and for proton energies above $\sim 5$ Bev, and thus at higher energies the scattering can be analyzed using the general scattering theory without spin, or else on the basis of the model of a purely absorbing sphere. The possible behavior of the cross sections for $\pi$-p and p-p interaction with increasing energy of the colliding particles is discussed.

## 1. INTRODUCTION

IN 1949, Fernbach, Serber, and Taylor[1] made use of an optical analogy for the analysis of neutron scattering from nuclei at high energies. Nuclear matter was regarded as a refractive and absorptive medium. During the passage of the neutron through the medium its wave vector, which is equal to $k_0$ outside the nucleus, takes on the complex value

$$k = k_0 + k_1 + iK/2, \quad (1)$$

where K denotes the absorption coefficient of the medium, and $k_1$ is the change in the real part of the wave vector of the neutron. Then, in analogy with optics, one can characterize the nuclear matter by a complex refraction index $n = k/k_0$. This optical model received wide attention in the analysis of the experimental data on the scattering of fast particles from nuclei, and led to many valuable results.

The formalism of the optical model of the nucleus was subsequently used in the analysis of the scattering of $\pi$ mesons and protons from protons at energies of order 1 Bev and higher.[2-4] This approach may be called the optical model of the nucleon. It was shown that the experimental data on $\pi$-p scattering at 1.37 Mev (Ref. 3) could be fitted by a model in which the nucleon is represented as a homogeneous sphere of radius $R = (1.18 \pm 0.1) \times 10^{-13}$ cm, characterized by a coefficient of absorption $K = 0.67 \times 10^{-13}$ cm$^{-1}$ and $k_1 = 0$.

Thus the sphere can be considered purely absorbing.

In an analogous manner the data on p-p scattering for the energies 0.8, 1.5, and 2.75 Bev (Ref. 2) were analyzed. The proton was regarded as a homogeneous, purely absorbing sphere ($k_1 = 0$) of radius R, which is independent of the energy. The incoherent scattering was considered insignificant. With these assumptions the experimental data could be fitted by taking for the proton model a sphere of radius $R = 0.93 \times 10^{-13}$ cm with absorption coefficients $K = 4.3$, 3.7, and $2.7 \times 10^{13}$ cm$^{-1}$ for proton energies 0.8, 1.5, and 2.75 Bev, respectively. A comparison of the results of the analysis shows that the proton is more "transparent" for the $\pi$ meson than for a proton, and that the range of the $\pi$-p interaction is greater than that of the p-p interaction. Recently published data on the elastic scattering of protons by protons at 2.24, 4.40, and 6.15 Bev (Ref. 4) were analyzed from the point of view of the extremely simple optical model. In all variants of this model, the nucleon is represented by a disc with different optical parameters. With a certain choice of the parameters of this disc, it was possible to achieve

TABLE I

| $E_p$, Bev | $10^{14}\lambda$, cm | $\sigma_t$, mb | $\sigma_e$, mb | $\sigma_i$, mb |
|---|---|---|---|---|
| 1.5 | 2.35 | 47.2±0.9[10] | 20±2[2] | 27±2[2] |
| 2.24 | 1.92 | 44.1±4[8] | 17±3[4] | 26±2[8] |
| 2.75 | 1.73 | 41 ±1[10] | 15±2[2] | 26±2[2] |
| 4.40 | 1.37 | 34 ±2[8] | 9.7±1.5[4] | 24.2±2[8] |
| 6.15 | 1.16 | 31.3±1.5[8] | 7.5±1.5[4] | 23.8±2[8] |
| $E_\pi$, Bev | | | | |
| 1.37 | 2.7 | 30.6±2.8[9] | 6.6±1[3] | 24.0±1.5[3] |

agreement with experiment.

We made an attempt to analyze all available experimental data on p-p and π-p scattering, in the energy region of several Bev, on the basis of the optical model of the nucleon. The analysis was carried through under the assumption that the range of interaction is determined by an optically homogeneous sphere with sharp boundary, and that the incoherent elastic scattering can be neglected. In light of this analysis, we examined several aspects concerning the use of the general scattering formalism in the problem under consideration, in analogy to the work done earlier.[5-8]

## 2. EXPERIMENTAL DATA AND FORMULAE USED IN THE ANALYSIS

Table I summarizes the experimental data on the scattering cross sections at high energies, including the values of the total cross section ($\sigma_t$), the elastic cross section ($\sigma_e$), and the inelastic cross section ($\sigma_i$) for p-p and π-p interactions. The second column of the table gives the value of the wavelength $\lambda$ of the impinging particle in the center-of-mass system for the corresponding energy E of the impinging particle in the laboratory system. The $\sigma_i$ for $E_p = 2.24$, 4.40, and 6.15 Bev have not been experimentally measured. They have been obtained using the ideas reported in Ref. 8, and appear to be perfectly reasonable, since there are grounds to assume that $\sigma_i$ changes slowly in this energy region. One can judge this from the results of the estimate for the average value of the cross section for the inelastic interactions in the nucleon-nucleon collisions at energies of the order of 50 Bev, (Ref. 11) giving for $\sigma_i$ the value (21 ± 4) mb. Moreover, as will be seen from the following, the results of the analysis change very little for variations of $\sigma_i$ over a wide interval of values. The choice of the value of the cross section for the inelastic interaction thus does not appear to be critical.

Apart from the data in Table I, we have available experimental differential cross sections for the elastic scattering of π mesons and protons from protons at the indicated energies. These data have also been used in the analysis.

We make a few remarks about the formulae with which the experimental results quoted above can be analyzed.

It is known that, neglecting the incoherent scattering and regarding the nucleon as an optically homogeneous sphere, the scattering cross sections can be expressed in terms of the parameters of this sphere.[1] In this case the inelastic scattering cross section is

$$\sigma_i = \pi R^2 \{1 - [1-(1+2KR)\exp(-2KR)]/2K^2R^2\} \quad (2)$$

and the differential cross section for the elastic scattering ( here $\sigma_e = \sigma_d$),

$$d\sigma_d/d\omega = |f(\vartheta)|^2, \quad (3)$$

where the scattering amplitude is

$$f(\vartheta) = ik_0 \int_0^R [1 - \exp\{(-K + 2ik_1)s\}] J_0(k_0\rho \sin\vartheta)\rho d\rho. \quad (4)$$

In these formulae $\vartheta$ is the scattering angle; $s = \sqrt{R^2 - \rho^2}$.

The integration of (3) leads to a rather complicated expression for the total cross section of the elastic diffractional scattering (see, e.g., formula (6) in Ref. 1). It is known, however, that for an opacity $\sigma_i/\pi R^2 \leq 0.9$, which corresponds to $KR \leq 2.3$ and $k_1/K \leq 1$, the expression for the total cross section of the diffractional scattering can be brought into the simpler form[12]

$$\sigma_d = \sigma_d(K, k_1 = 0)\left\{1 + 4\left(\frac{k_1}{K}\right)^2\left[1 - \frac{1}{18}(KR)^2 + \cdots\right]\right\}, \quad (5)$$

where

$$\sigma_d(K, k_1 = 0) = \frac{\pi R^2}{B^2}\{B^2 - 14 - 2(1+B)e^{-B} + 8(2+B)e^{-B/2}\}, \quad B = 2KR, \quad (6)$$

which gives a result differing by not more than 1% from that obtained with the exact expression for

$\sigma_d$. We use expression (5), since the experimental data satisfy the corresponding requirements. The quoted expressions are justified for energies for which the condition $\lambda\!\!\!^{-} \ll R$ is true in the c.m.s.

## 3. PARAMETERS OF THE OPTICAL MODEL OF THE NUCLEON FOR THE DESCRIPTION OF THE SCATTERING AT HIGH ENERGIES

The parameters of the optical model of the nucleon to be determined from the experimental data are the radius of the homogeneous sphere R and its optical parameters K and $k_1$. The radius R of the interaction sphere was taken as the starting quantity in the determination of the parameters. For every given radius R, the values of K and $k_1$ were calculated at different energies of the interacting particles, using formulae (2) and (5) and the data in Table I. These values were determined for the average values of the cross section as well as for their limiting values corresponding to the quoted experimental errors.

It is seen from the curves of Bethe and Wilson[12] that for the available values of $\sigma_e$ and $\sigma_i$ the case $k_1 = 0$ gives maximum values for $\sigma_e/\pi R^2$ $\sigma_i/\pi R^2$, i.e., minimum values for R. Therefore, for each energy, the interval for the values of the radius considered was bounded from below by the radius of the purely absorbing "gray" sphere. The minimum values for the radii for the energies $E_p$ are listed in Table II. For $E = 1.37$ Bev, $R_{min} = 1.01 \times 10^{-13}$ cm.

TABLE II

| $E_p$, Bev | 1.5 | 2.24 | 2.75 | 4.4 | 6.15 |
|---|---|---|---|---|---|
| $10^{13} \cdot R_{min}$, cm | 0.90 | 0.89 | 0.90 | 0.92 | 0.95 |

For each set of values R, K, and $k_1$ the differential cross sections for elastic scattering were calculated using formulae (3) and (4). Expression (3) was integrated numerically using Simpson's rule, with an accuracy not worse than 1% for small scattering angles and several percent for large ones. In the course of the calculation, it appeared that upon a 20% change in $\sigma_i$, with constant R and $\sigma_d$, the change in the value of $d\sigma_d/d\omega$ is still within the limits of error of the numerical integration. Thus the choice of the value of $\sigma_i$ does not appear to be critical for this analysis.

The angular distributions for the elastic scattering were calculated for the limiting values of $\sigma_d$ with fixed values of R. In the same way, the range of possible angular distributions was determined in accordance with the experimental accuracy of the total cross sections. Comparison of

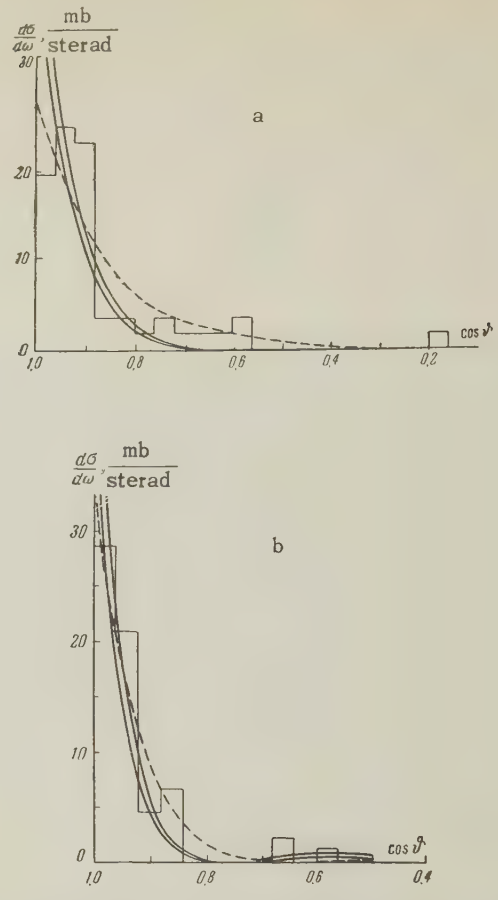


FIG. 1. The solid curves describe the region of possible angular distributions for the elastic p – p scattering in the center of mass system for the radii: (a) $E_p = 1.5$ Bev, $R = 1.3 \times 10^{-13}$ cm, and (b) $E_p = 2.75$ Bev, $R = 1.2 \times 10^{-13}$ cm. The dotted curves describe the angular distributions calculated with the model of a purely absorbing sphere with radius $R = 0.93 \times 10^{-13}$ cm for both energies. The histograms represent the experimental angular distributions of Ref. 2.

these ranges with the experimental data on the differential cross sections allowed us to choose the values of R (together with the corresponding values of $k_1$ and K) satisfying the experimental data with respect to the total as well as with respect to the differential scattering cross sections. We list below the results of the calculations and their comparison with the experimental data.

(a) p-p scattering at 1.5, 2.24, and 2.75 Bev.

The experimental data at 1.5 and 2.75 Bev have been obtained with a diffusion chamber[3] and have poor statistical accuracy. Therefore the experimental distributions are reconciled to an equal degree with an optical model of the nucleon having parameters that fluctuate over a very wide range. (see Fig. 1). The available counter data of Cork et al.[4] at $E_p = 2.24$ Bev, however, allow one to narrow down the range of the fluctuations of the radius of the sphere for this energy region. It

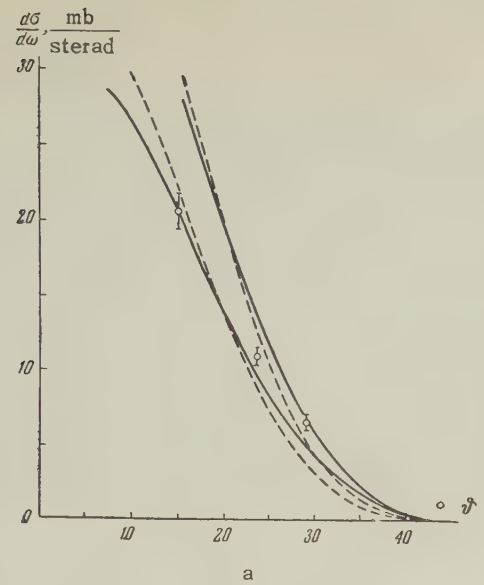


FIG. 2. The solid curves describe the region of possible angular distributions for the elastic p−p scattering in the center of mass system for $R = 1.10 \times 10^{-13}$ cm. The dotted curves describe the region of angular distributions for $R = 1.20 \times 10^{-13}$ cm. The experimental points are taken from Ref 4. a − $E_p$ = 2.24 Bev, b − $E_p$ = 4.40 Bev, c − $E_p$ = 6.15 Bev.

turns out that the homogeneous sphere may have a maximum radius $R = 1.15 \times 10^{-13}$ cm, since definite disagreement with the experimental data occurs even for $R = 1.20 \times 10^{-13}$ cm (see Fig. 2a). For these values of the radius of the sphere, the contribution to the cross section of the elastic interaction from the real part of the scattering amplitude, due to values of $k_1$ different from zero, can reach 35%. It should be noted that for $R \leq 1.15 \times 10^{-13}$ cm agreement with experiment exists only at angles $\vartheta$ not above 30°. The minimum radius for $E_p = 2.24$ Bev is in accordance with the value $0.93 \times 10^{-13}$ cm, which was given in Ref. 2 for the energies 1.5 and 2.75 Bev. Furthermore, the purely absorbing sphere ($k_1 = 0$) may only have a radius below $1.0 \times 10^{-13}$ cm.

It should be noted that the considerations of Rarita[13] in connection with the applicability of the optical model of the nucleon to the p-p scattering at $E_p \approx 1.0$ Bev are equally justified for the energies considered above.

(b) p-p scattering at 4.40 and 6.15 Bev.

The experimental data at $E_p = 4.40$ Bev[4] for $\vartheta < 30°$ are satisfactorily fitted with a homogeneous sphere with a radius from $0.95 \times 10^{-13}$ cm to $1.15 \times 10^{-13}$ cm. The values $R = 0.92$ and $1.20 \times 10^{-13}$ cm lead to definite disagreement with the experimental results (see Figs. 2b and 3a). The purely absorbing sphere may have a radius of not more than $1.10 \times 10^{-13}$ cm. The measured angular distribution of the elastic scattering at $E_p = 6.15$ Bev is satisfactorily fitted with a homogeneous

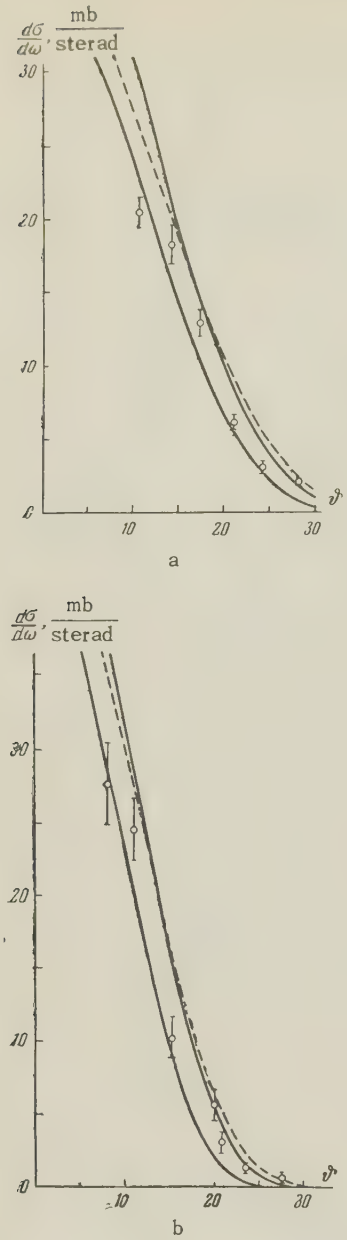


FIG. 3. The solid curves describe the region of possible angular distributions for the elastic p – p scattering in the center-of-mass system, calculated using the model of a purely absorbing sphere, based on the following data: (a) $E_p = 4.40$ Bev, $\sigma_i = 24.2$ mb, $\sigma_d = (9.7 \pm 1.5)$ mb, $R = (0.97 - 1.05) \times 10^{-13}$ cm; (b) $E_p = 6.15$ Bev, $\sigma_i = 23.8$ mb, $\sigma_d = (7.5 \pm 1.5)$ mb, $R = (1.0 - 1.15) \times 10^{-13}$ cm. The dotted curves give the angular distributions for the case of a purely absorbing sphere with minimum radius: (a) $R = 0.92 \times 10^{-13}$ cm, (b) $R = 0.95 \times 10^{-13}$ cm. The experimental points are taken from Ref. 4.

sphere with a radius from $1.0 \times 10^{-13}$ cm to $1.15 \times 10^{-13}$ cm. The disagreement with experiment for $R = 0.95 \times 10^{-13}$ cm and $R = 1.20 \times 10^{-13}$ cm is seen in Figs. 3b and 2c.

In addition, for $E_p = 6.15$ Bev and all values of the radius inside the indicated interval, the sphere may be purely absorbing.

(c) $\pi$-p scattering at $E_\pi = 1.37$ Bev.

The available experimental data on the scattering of $\pi$ mesons by protons[3] were obtained with a diffusion chamber and have therefore bad statistical accuracy. It was found that these data could be fitted with a model of a homogeneous sphere whose radius takes on arbitrary values within a wide interval. Therefore the restriction of the range of values R was achieved with the use of the dispersion relations, which show that the contribution from the real part of the scattering amplitude to the elastic scattering cross section at the angle 0° and at $E_\pi = 1.37$ Bev amounts to about 7%.[9] For the application of the optical model, this means that the radius of the homogeneous sphere may range from $1.01 \times 10^{-13}$ cm to $1.25 \times 10^{-13}$ cm.

## 4. ON THE APPLICABILITY OF THE OPTICAL MODEL OF THE NUCLEON WITH $K_1 = 0$

Let us consider the optical model of the nucleon with $k_1 = 0$, in which the form of interaction range is not specified, in other words, we assume: (1) the elastic interaction has diffraction character and there is no potential scattering; (2) the scattering cross sections are independent of the spins of the interacting particles. These assumptions are equivalent to those made in Refs. 5 to 8. In connection with a discussion of p-p and $\pi$-p interactions from the point of view of the general scattering theory, which permits a more consistent description of the scattering at high energies. It is therefore of interest to investigate the limits of applicability of these notions.

We start from the known formula for the scattering amplitude of spinless particles (see, e.g., Ref. 14):

$$f(\vartheta) = \frac{i\lambda}{2} \sum_{l=0}^{\infty} (2l+1)(1-\beta_l) P_l(\cos\vartheta),$$

$$\beta_l = \exp\{2i\eta_l\}. \qquad (7)$$

Here $\hbar l$ denotes the orbital angular momentum, $P_l(\cos\vartheta)$ are the Legendre polynomials, and $\eta_l$ is the scattering phase. The optical model parameters are combined with the scattering phase in the following way:[1]

$$\eta_l = (k_1 + {}^1/_2 iK)\, s_l. \qquad (8)$$

Here $2s_l$ is the path length of the incident particle with orbital angular momentum $\hbar l$ in nuclear matter.

For the case $k_1 = 0$ the quantity $\beta_l = \exp(-Ks_l)$

must be real and positive, and the scattering amplitude pure imaginary.

We have calculated $\beta_0$ for all the interaction energies mentioned with the help of the analytic expression for $d\sigma/d\omega$ from Ref. 8. It was assumed that the angular distribution is known with an accuracy of $\pm 15\%$ for all angles.

The calculation makes use of the formula (see, e.g., Refs. 7 and 8)

$$(1-\beta_l)\lambda = \int_{-1}^{+1} |f(x)| P_l(x)\, dx, \quad |f(x)|^2 = \frac{d\sigma}{d\omega}. \qquad (9)$$

The results of the calculation are listed in Table III.

Thus the analysis of the p-p scattering under the assumptions enumerated above leads to negative values of $\beta_0$ for energies of 1.5 to 4.4 Bev. This implies that the original conditions of this investigation are not valid for this range of proton energies. Consequently, an investigation of the type of Refs. 5 to 8 and the optical model with $k_1 = 0$ are applicable to the description of the p-p scattering only for energies above $\sim 5$ Bev.

An analogous consideration of the $\pi$-p scattering at $E_\pi = 1.37$ Bev gives $\beta_0 = 0.15 \pm 0.08$. This implies that the assumptions made above do not contradict the experimental data for these $\pi$-meson energies.

TABLE III

| $E_p$, Bev | 1.5 | 2.24 | 2.75 | 4.4 | 6.15 |
|---|---|---|---|---|---|
| $\beta_0$(S wave) | −0.46±0.13 | −0.52±0.13 | −0.39±0.12 | −0.11±0.10 | +0.06±0.08 |

## 5. CONCLUSIONS

All available experimental data on $\pi$-p and p-p scattering in the energy region of several Bev can be fitted satisfactorily with the optical model of the nucleon, where the range of interaction is represented in the form of a homogeneous sphere with sharp boundary and complex refractive index. In the framework of this investigation, there are reasons to assume that the radius for the interaction is independent of the types of the colliding particles and of their energies. This radius ranges from $1.01 \times 10^{-13}$ cm to $1.15 \times 10^{-13}$ cm. Table IV gives the values of the absorption coefficient K as well as the contributions of the real parts of the scattering amplitude for three values of the radius of interaction. It is seen from the data in Table IV that the contribution to the elastic cross section from the real part of the scattering amplitude decreases with increasing energy. This means that $k_1$ decreases, going to zero in the limit, i.e., the homogeneous sphere becomes purely absorbing. In this limiting case the optical model drops the concept of a range of interaction, and is equivalent to an investigation of the scattering at high energies on the basis of the general scattering theory under the assumptions made in the papers of Refs. 5 to 8. On the basis of these considerations we have investigated, in Sec. 4, the limits of applicability of these concepts for the analysis of the scattering at high energies. It was found that the analysis of the experimental data under the assumptions mentioned is valid for the p-p interactions only for energies above $\sim 5$ Bev. The results of the $\pi$-p scattering at 1.37 Bev can be similarly fitted. The question of the applicability of this method for the analysis of the $\pi$-p scattering is still open, since we do not have as yet the necessary experimental data for smaller energies.

If, as seems entirely possible, the "form factor" of the nucleon is independent of the energy, we can draw the following conclusions about the behavior of the cross sections for the $\pi$-p and p-p interactions with increasing energy of the colliding particles. It is known that, for high energies, the cross sections for the interactions of $\pi$ mesons and protons with nucleons tend towards a constant limiting value. This appears to be a consequence of the finite dimensions of the nucleon. (We neglect the Coulomb interaction.) If this limiting value for $\pi$ mesons is $\approx 30$ mb, then the total cross section at the $\pi$-meson energy 1.37 Bev, as considered above, is already equal to its limit calculated with the help of the dispersion relations.[15] There are grounds to expect that the values of the elastic and inelastic cross sections for the $\pi$-p interaction will not change with increasing energy, since the elastic cross section can at these energies be regarded as a consequence of the inelastic cross section. An increase or a decrease of the inelastic interaction entails a corresponding increase or decrease of the elastic interaction, leading to a change in $\sigma_t$. If these considerations are right then, for $E_\pi \to \infty$, $\sigma_t \approx 30$ mb, $\sigma_i \approx 24$ mb, and $\sigma_e \approx 6$ mb.

Similarly, it is known for the nucleon-nucleon interaction that $\sigma_i = 21 \pm 4$ mb at $E_N = 50$ Bev. This implies that the inelastic cross section

TABLE IV

| $E_p$, Bev | $K \cdot 10^{13}$ cm$^{-1}$ | $\lvert \mathrm{Re}\, f(\vartheta)\rvert^2 / \lvert f(\vartheta)\rvert^2$, % | | |
|---|---|---|---|---|
| | | $R = 1.05 \cdot 10^{-13}$, cm | $R = 1.1 \cdot 10^{-13}$, cm | $R = 1.15 \cdot 10^{-13}$, cm |
| 1.5 | 0.64÷2.6 | 6÷21 | 12÷27 | 20÷35 |
| 2.24 | 0.60÷2.1 | 8÷23 | 15÷30 | 22÷35 |
| 2.75 | 0.60÷2.0 | 5÷22 | 9÷28 | 15÷35 |
| 4.4 | 0.53÷1.3 | 0÷21 | 0÷29 | 5÷35 |
| 6.15 | 0.51÷1.0 | 0÷16 | 0÷23 | 0÷30 |
| $E_\pi = 1.37$ Bev | 0.53÷1.0 | ~7 | ~7 | ~7 |

changes slowly with energy. As our considerations above showed, one can interpret the elastic p-p interaction at $E_p = 6.15$ Bev as a consequence of the inelastic interaction. Then one may expect that, for $E_p \to \infty$, $\sigma_i \approx 24$ mb and $\sigma_e \approx 7$ mg, with $\sigma_t = 30$ to 31 mb. We thus arrive at the conclusion that for high energies of the colliding particles the total cross sections of the elastic and inelastic interactions of $\pi$ mesons and nucleons with nucleons have the same values.

We thank L. Z. Isaeva and L. A. Shustrova for numerical calculations done for this work.

[1] Fernbach, Serber, and Taylor, Phys. Rev. **75**, 1352 (1949).

[2] Fowler, Shutt, Thorndike et al., Phys. Rev. **103**, 1489 (1956).

[3] L. M. Eisberg, W. B. Fowler et al., Phys. Rev. **97**, 797 (1955).

[4] Cork, Wenzel, and Causey, Phys. Rev. **107**, 859 (1957).

[5] D. Ito and S. Minami, Progr. Theor. Phys. **14**, 198 (1955).

[6] S. Z. Belen'kii, J. Exptl. Theoret. Phys. (U.S.S.R.) **30**, 983 (1956); Soviet Phys. JETP **3**, 813 (1956).

[7] Ito, Yamazaki, Kobayashi, and Minami, Progr. Theor. Phys. **18**, 264 (1957).

[8] V. G. Grishin and I. S. Saitov, J. Exptl. Theoret. Phys. (U.S.S.R.) **33**, 1051 (1957); Soviet Phys. JETP **6**, 809 (1958).

[9] Cool, Piccioni, and Clark, Phys. Rev. **103**, 1082 (1956).

[10] Chen, Leavitt, and Shapiro, Phys. Rev. **103**, 211 (1956).

[11] A. E. Brenner and R. W. Williams, Phys. Rev. **106**, 1020 (1957).

[12] H. A. Bethe and R. R. Wilson, Phys. Rev. **83**, 690 (1951).

[13] W. Rarita, Phys. Rev. **104**, 221 (1956).

[14] A. Akhiezer and I. Pomeranchuk, Некоторые вопросы теории ядра (Certain Problems in Nuclear Theory), GTTI, 1950.

[15] P. V. Vavilov, J. Exptl. Theoret. Phys. (U.S.S.R.) **32**, 940 (1957); Soviet Phys. JETP **5**, 768 (1957).

Translated by R. Lipperheide
246

# THE RELATIVISTIC THEORY OF REACTIONS INVOLVING POLARIZED PARTICLES

CHOU KUANG-CHAO and M. I. SHIROKOV

Joint Institute for Nuclear Research

Submitted to JETP editor December 6, 1957

J. Exptl. Theoret. Phys. (U.S.S.R.) **34**, 1230-1239 (May, 1958)

It is shown that, in the rest system, the relativistic formulas for the angular distribution and the polarization vectors and tensors for a reaction of the type $a + b \rightarrow c + d$ are essentially the same as the nonrelativistic formulas, if the spin of a particle is defined as its internal angular momentum around its center of mass. The square of this internal angular momentum is Lorentz invariant. The spins of the particles are arbitrary, and their rest masses are nonvanishing.

The main difference from the nonrelativistic case is that the description of the spin state is not the same in different Lorentz reference systems. Therefore for cascades of reactions (for example, for experiments on double scattering) corrections must be applied to the nonrelativistic formal theory. The relativistic changes in the angular correlations are indicated for successive reactions of the type $\pi + p \rightarrow Y + K$, $Y \rightarrow N + \pi$.

## INTRODUCTION

FOR reactions of the type $a + b \rightarrow c + d$, formal theories are known which express the angular distribution and the state of polarization of the products of a reaction in terms of the states of polarization of the incident beam and the target and unknown parameters which are the elements of the S matrix for the process $a + b \rightarrow c + d$. The simplest example is the well-known formula for the function $f(\theta)$ which appears in the expression

$$\psi(r) = e^{ikr} + f(\theta)\, e^{ikr}/r$$

for the wave function of a stationary scattering process of particles of spin zero. In this case the unknown parameters are called the scattering phase shifts.

These theories are based on the use of the conservation laws (in particular the law of the conservation of the total angular momentum). Coester and Jauch[1] were the first to obtain formulas for the angular distribution and polarization in the case of particles a, b, c, d of arbitrary spins; their starting point was the explicit formulation of the conservation laws in terms of the diagonal property of the S matrix with respect to the conserved quantities. These same formulas have been obtained by Simon and Welton, but by a different method (cf., e.g., Ref. 2).

These formulas are nonrelativistic, but only because the spin state of the particles is described in the Pauli approximation (so that it has the same appearance in all Lorentz reference systems). The theory of the scattering of spinless particles is essentially relativistic. In order to obtain the angular distribution in any Lorentz system, one has only to transform $\sigma(\theta) = |f(\theta)|^2$ from the center-of-mass system into the desired system by using known formulas. What is therefore required for the relativistic generalization is the definition of the relativistic spin operator. The spin operator which we introduce satisfies all the requirements which can be demanded in terms of the concept of the spin as the intrinsic angular momentum of a particle.*

To obtain the relativistic formulas we use the method of Coester and Jauch in a form presented in a paper by one of us.[3] We emphasize that in this method one needs only the ability to describe the state of a free particle possessing spin; we do not need relativistic equations (for free particles) like the Dirac equation (which plays an essential part in Stapp's relativistic theory[4] of the scattering of particles with spin $\frac{1}{2}$).

## 1. THE CONSERVED PHYSICAL QUANTITIES IN A RELATIVISTIC THEORY

The conservation laws are simply an expression of the fact that the physical processes in an isolated system must not depend on the means used to de-

*Iu. M. Shirokov has informed us that he has employed this same description of the spin state (which was obtained by him from the theory of the irreducible representations of the inhomogeneous Lorentz group) to the formulation of a similar relativistic theory of polarization and correlation effects.

scribe it, in particular on the choice of the reference system. Here it is of course assumed that space-time is homogeneous and isotropic (we can suppose, however, that this assumption is contained in the concept of an isolated system). In quantum mechanics this fact is expressed by the requirement that the S matrix of a physical process must commute with ten operators, the infinitesimal displacements of the origin of the space and time coordinates providing operators $P_\mu$, and infinitesimal space-time rotations giving operators $M_{\mu\nu}$. The fact that an operator commutes with the S matrix means that the S matrix is diagonal with respect to the eigenvalues of this operator,* and consequently that the corresponding physical quantity is conserved, i.e., remains unchanged in all internal processes.

Four conservation laws have the clear physical meaning of the conservation of the total momentum and energy $P_\mu \{P_x, P_y, P_z, iP_0\}$. Of the six other operators $M_{\mu\nu}$, three operators $M_{k4}$ ($k = 1, 2, 3$) do not have an immediate physical meaning, and instead of $M_{\mu\nu}$ we shall introduce six other operators, which have the physical meaning of the coordinates of the center of mass of the physical system and its total angular momentum around its center of mass.

The properties of the center of mass follow directly from its conceptual meaning: the motion of the system as a whole can be characterized primarily (in the very first approximation) as the motion of a material point with mass equal to the rest mass (or energy) of the system and with momentum equal to the total momentum **P** of the system. The center of mass of an isolated system must therefore move uniformly in a straight line. Furthermore, in quantum mechanics we must require that the center of mass **R** actually be the coordinate operator of a certain particle, i.e., in particular, that the well known commutation relations hold between $R_x$, $R_y$, $R_z$, $P_x$, $P_y$, $P_z$.

We can obtain such an operator **R** in the following way. It is well known that the following are the commutation relations which must be satisfied by the operators $P_i$ and $M_{\mu\nu}$ (cf. Ref. 6 and Sec. 3 of Ref. 5):

$$[P_i, P_j] = 0;\ [P_i, E] = 0;\ [M_i, P_j] = i\varepsilon_{ijk}P_k; \quad (1.1)$$

$$[M_i, E] = 0;\ [M_i, M_j] = i\varepsilon_{ijk}M_k; \quad (1.2)$$

$$[N_i, P_j] = i\delta_{ij}E;\ [N_i, E] = iP_i;\ [M_i, N_j] = i\varepsilon_{ijk}N_k; \quad (1.3)$$

$$[N_i, N_j] = -i\varepsilon_{ijk}M_k. \quad (1.4)$$

Notations: $[A, B] = AB - BA$; i, j, k take the values 1, 2, 3; and

$$\{M_1, M_2, M_3\} = \{M_{23}, M_{31}, M_{12}\};\ iN_j = M_{j4};$$

$$E = (\mathbf{P}^2 + m_0^2)^{1/2};\ \hbar = c = 1;$$

$\epsilon_{ijk}$ is a tensor antisymmetric in all its indices, with $\epsilon_{123} = 1$. It is understood that we confine ourselves to those state vectors $\psi_0$ which describe states with a definite rest mass $m_0$, i.e., for which $P_\mu P_\mu \psi_0 = -m_0^2\psi_0$, or $(P_0 - E)\psi_0 = 0$ (the time displacement operator $P_0$ is equivalent to the factor E). We note that since $[N_i, E] = iP_i$ the average value of $N_i$ is a linear function of the time. Therefore $N_i$ is "conserved" in the sense that internal processes have no effect on this time dependence.

We introduce three new operators $R_x$, $R_y$, $R_z$, for which

$$[R_i, R_j] = 0, \quad [R_i, P_j] = i\delta_{ij}$$

(from which if follows that $[R_i, E] = iP_i/E$). We represent **M** in the form

$$M_k = \sum_{i,j} \varepsilon_{kij} R_i P_j + J_k,$$

and find from Eq. (1.1) that $[J_i, P_j] = 0$. If we require that $R_x$, $R_y$, $R_z$ be the components of a spatial vector (as must indeed be the case), i.e., that $[M_i, R_j] = i\epsilon_{ijk}R_k$, then $[J_i, R_j] = 0$, and $J_x$, $J_y$, $J_z$ also form a three-dimensional vector. It then follows from Eq. (1.2) that $[J_i, J_j] = i\epsilon_{ijk}J_k$. In like fashion, representing **N** in the form

$$N_i = {}^1/_2(R_iE + ER_i) + K_i \equiv R_iE - iP_i/2E + K_i,$$

we find that $[K_i, P_j] = 0$. Therefore also $[K_i, E] = 0$, and the average value of $K_i$ is constant in time.

We now pose the problem of expressing **M** and **N** in terms of the operators **R** and **J** which we have introduced. For **M** this has already been done. It remains only to express the spatial polar vector **K** in terms of **P** and **J**. It can be shown that if $R_x$, $R_y$, $R_z$ are the first three components of any four-vector (i.e., for example, $[N, R] = 0$ if $i \neq j$), then **K** cannot be expressed in terms of **J** and **P** only so as to satisfy all the commutation relations for **N**. This means that if **K** is constructed from **P** and **J** alone, then $[\mathbf{R}, \mathbf{P}]_k$ and $J_k$ are not the spatial components of a four-dimensional tensor of the second rank.

*Let us write out $AS - SA = 0$ as a matrix product. In doing so, we choose a representation in which the operator A is diagonal (i.e., we label matrix elements with its eigenvalues). Then

$$A_{ik}S_{kl} - S_{im}A_{ml} = (A_i - A_l)S_{il} = 0,$$

i.e., $S_{il}$ must be equal to zero if $i \neq l$.

The simplest $\mathbf{K}$ (namely one linear in $J_x$, $J_y$, $J_z$) satisfying Eqs. (1.3) and (1.4) has the form

$$\mathbf{K} = [\mathbf{PJ}](E \pm m)^{-1}$$

(cf. Refs. 7 and 6).*

Since the problem has a solution, it follows that: (1) $\mathbf{R}$ is "conserved" (in the same sence as $\mathbf{N}$), since it can be expressed in terms of the conserved operators $M_{\mu\nu}$ (see Appendix). $\mathbf{R}$ can be called the center-of-mass operator. It is the same as definition (e) of the center-of-mass in the papers of Pryce.[8] (2) $\mathbf{J}$ is also conserved and, what is particularly important for our purpose, $J^2 = J_x^2 + J_y^2 + J_z^2$ is Lorentz invariant, since $[\mathbf{N}, J^2] = 0$. We emphasize that this is true for arbitrary $\mathbf{K} = \mathbf{K}(\mathbf{P}, \mathbf{J})$.

## 2. USE OF THE CONSERVATION LAWS. RELATIVISTIC DEFINITION OF THE SPIN OF A PARTICLE

The four conservation laws for the total momentum and energy and the three conservation laws for the center of mass can be expressed very simply. The argument is usually carried through in the Lorentz system of reference $K_S$ in which the (conserved) total momentum is zero (the so-called center-of-mass system). The origin of the coordinate system can be taken at the center of mass (more precisely, at the point given by the average value of the operator $\mathbf{R}$† for the particles a and b (or c and d). Then $\mathbf{J}$ is the total angular momentum. Since the commutation relations between $J_x$, $J_y$, $J_z$ are the same as for the total angular momentum or for the Pauli spin matrices, the eigenvalues of $\hat{J}^2$ and $\hat{J}_z$ are respectively equal to $h^2J(J+1)$ and $M = J, J-1, \ldots, -J$.

The conservation law for $\mathbf{J}$ is expressed by the fact that the S matrix is diagonal with respect to the eigenvalues of $\hat{J}^2$ and $\hat{J}_z$:

$$(\ldots J'M'|S|\ldots JM) = (\ldots|S^{JM}|\ldots)\delta_{J'J}\delta_{M'M} \qquad (2)$$

and also the fact that $(\ldots|S^{JM}|\ldots)$ is independent of the value of M, which follows from $[J_x, S] = 0$.

To find, for example, the angular distribution of particles c and d, we need to know the explicit expression of the elements of the S matrix in the representation of the particle momenta. In order to express these elements in terms of the elements (2), we must first of all enumerate the remaining variables of a complete set (denoted in Eq. (2) by dots), which commute with each other and with $J^2$ and $J_z$.

The initial and final states of the process a + b → c + d are states of systems consisting of two free noninteracting particles. From the meaning of the S matrix, its elements are the transition amplitudes between such states. Therefore to label the elements of the S matrix we must take as our variables a complete set of quantum mechanical quantities describing the free particles a and b or c and d. The total angular momentum $\mathbf{J}$ (in the system $K_S$) is represented in the form $\mathbf{J} = \mathbf{j}_1 + \mathbf{j}_2$, where $\mathbf{j}$ is the total angular momentum of a single particle in $K_S$.

The procedure stated in Sec. 1 for obtaining the conserved angular momentum relative to the center of mass can be applied to a system of arbitrary physical nature (for example, to a system of fields). One needs only to know a concrete representation of the operators P and M. Therefore it is natural to apply this procedure to an "elementary" particle, whose physical nature is in general unknown (by the definition of "elementary"). Besides the coordinates $\mathbf{r}$ of the center of mass and the momentum $\mathbf{p}$ we then get just one conserved external characteristic of the particle, its angular momentum $\mathbf{s}$ relative to its center of mass $\mathbf{r}$. In defining the spin s of a particle, we are only fixing precisely the concept of the spin as the intrinsic angular momentum of the particle.

Accordingly, $\mathbf{j} = [\mathbf{r} \times \mathbf{p}] + \mathbf{s}$, and in the system $K_S$, in which $\mathbf{p}_1 = -\mathbf{p}_2 = \mathbf{p}$, we get

$$\begin{aligned}\mathbf{J} &= [\mathbf{r}_1 \times \mathbf{p}_1] + \mathbf{s}_1 + [\mathbf{r}_2 \times \mathbf{p}_2] + \mathbf{s}_2 \\ &= [(\mathbf{r}_1 - \mathbf{r}_2) \times \mathbf{p}] + \mathbf{s}_1 + \mathbf{s}_2 \equiv \mathbf{l} + \mathbf{s}_1 + \mathbf{s}_2.\end{aligned} \qquad (3)$$

In the system $K_S$ we can now proceed in complete formal analogy with the nonrelativistic treatment to introduce the total spin operator $\mathbf{s} = \mathbf{s}_1 + \mathbf{s}_2$ (the square of which, however, is not a Lorentz-invariant quantity). The eigenfunctions of the square of this quantity, $s^2$, and its component $s_z$ can be expressed in terms of the products $\psi_{i_1 m_1} \times \psi_{i_2 m_2}$ of the eigenfunctions of the squares and components of the operators $\mathbf{s}_1$ and $\mathbf{s}_2$ (the eigenvalues of $s_1^2$ are denoted by $h^2 i_1(i_1+1)$). Since

*We have not been able to show that no other $\mathbf{K}$'s exist. Beginning with different considerations, L. G. Zastavenko has evidently proved the uniqueness of $\mathbf{K}$. We are grateful to him for a discussion of this question.

†The conservation law for $\mathbf{R}$ means something more than the conservation of the average value. The requirement $[\mathbf{R}, S] = 0$ means that if the system is in a state with a definite value of $\mathbf{R}$ (we note that in the interaction representation the wave function for the external behavior of the system does not change with the time), internal processes in the system will not take it out of this state. This property does not get used explicitly, but an operator $\mathbf{R}$ of this kind is required for the definition of the conserved angular momentum $\mathbf{J}$ of the system (and of the spin of a particle, see below).

the commutation relations for $\mathbf{s}$, $\mathbf{s}_1$, $\mathbf{s}_2$ have the usual form, $[s_x, s_y] = is_z$ and so on, the coefficients in these expressions will be the well known Clebsch-Gordan coefficients $(i_1 i_2 m_1 m_2 | i_1 i_2 s m)$, which are also the transformation functions for the transformation from the representation in the variables $i_1$, $i_2$, $m_1$, $m_2$ into the $i_1$, $i_2$, s, m-representation (and inversely). A similar meaning attaches to the coefficient $(ls\mu m | lsJM)$.

We can now take as the variables denoted by dots in Eq. (2) s, $l$, and the absolute values of the momenta in $K_S$ (or the total energy of the system, which in $K_S$ is equal to an invariant, the rest mass of the system).

## 3. FORMULAS FOR THE CROSS-SECTION AND THE POLARIZATION VECTOR AND TENSORS. RELATIVISTIC ROTATION OF THE SPIN

We can now express the elements of the S matrix in the representation of the momenta of the particles and their spin components in terms of the elements $(p_c, s', l', J', M' | S | p_a, s, l, J, M)$. The transformation function from the representation in the variables p, s, $l$, J, M into the representation of the momenta and the spin components is the product of three transformation functions. We can write out the transformation as follows (cf. Ref. 9):

$$(p_c;\ m_c,\ m_d \mid S \mid p_a,\ m_a,\ m_b) = (\vartheta_c \varphi_c p_c \mid l'\mu' p_c) \times (i_c i_d m_c m_d \mid i_c i_d s' m')\,(l's'\mu' m' \mid l's'JM)\,(s'l' \mid S^{J, E(p_a)} \mid sl) \times (lsJM \mid ls\mu m)\,(i_a i_b sm \mid i_a i_b m_a m_b)\,(l\mu p_a \mid \vartheta_a \varphi_a p_a). \tag{4}$$

We have used Eq. (2) and the law of the conservation of the total energy. $\mathbf{p}_c$ and $\mathbf{p}_a$ are the momenta of particles c and d and a and b respectively in K; $\vartheta_c$, $\varphi_c$, $p_c$, $\vartheta_a$, $\varphi_a$, $p_a$ are their spherical angles and absolute values. It is recalled that $p_c$ is a function of $p_a$:

$$\sqrt{p_a^2 + \varkappa_a^2} + \sqrt{p_a^2 + \varkappa_b^2} = \sqrt{p_c^2 + \varkappa_c^2} + \sqrt{p_c^2 + \varkappa_d^2}.$$

Summation over the labels $l'$, $\mu'$, s', m', J, M, $l$, $\mu$, s, m is understood.

$$(\vartheta\varphi p \mid l\mu p_0) = 2\pi\hbar \sqrt{\frac{2R}{V}}\, \frac{i^{-l}}{p}\, Y_{l\mu}(\vartheta, \varphi)\,(p \mid p_0),$$

where $Y_{l\mu}(\vartheta, \varphi)$ is a spherical harmonic. For the other notations see Ref. 3 (in particular, Appendix II).

From the formula $\rho' = S\rho S^+$ we can now get the density matrix $\rho'$ of the products of the reaction in the representation of their momenta and spin components ($\rho$ is the density matrix for beam and target in the same representation). The problems of normalization and of deducing the cross-section in the system $K_S$ are solved in just the same way as in the nonrelativistic case (cf. Ref. 3). One can also introduce in just the same way the statistical polarization tensors instead of the density matrices. All the formulas will have the same form as those of the nonrelativistic case.[3] The difference lies in the fact that the quantities $m_a$, $m_b$, $m_c$, $m_d$ (or $\tau$, $\nu$), and also the total spin and other variables are relative to the system $K_S$. The same spin state has a different form in a different Lorentz system K (for example, in the laboratory system).

In order to learn how a spin state specified in $K_S$ is described in K, we must find the transformation function from the representation in the eigenvalues of $s^2$ and $s_z$ in the system $K_S$ to the representation in the eigenvalues of $\tilde{s}^2$ and $\tilde{s}_z$, which are the square and component of the same operator, but in the system K. In view of the fact that $s^2$ is Lorentz invariant, the spin operator $\tilde{\mathbf{s}}$ is a vector rotated as compared with $\mathbf{s}$. Consequently, the transformation function is the same as is obtained in the solution of the problem of describing a given spin state in a rotated system of spatial axes:

$$(\tilde{m} \mid m) = D^i_{\tilde{m}m}(\Phi_2, \theta, \Phi_1) = e^{-i\tilde{m}\Phi_2} i^{m-\tilde{m}} P^i_{\tilde{m}m}(\cos\theta)\, e^{-im\Phi_1}; \tag{5}$$

The matrices $P^i_{mm}(\cos\theta)$ are defined in Ref. 10 [Eq. (22) on page 77; we note that the matrix $P^1_{mn}$ written out explicitly on page 78 does not agree with Eq. (22) and is incorrect]. If the rotation is interpreted as a turning of a vector in a stationary coordinate system, then it consists of (a) a rotation of the vector around the z axis by the angle $\Phi_1$, (b) a rotation around the y axis by the angle $\theta$, and (c) a rotation around the z axis by the angle $\Phi_2$. All these rotations are counterclockwise. In the Appendix we show how to find the axis of rotation and the rotation angle $\Omega$ of the spin vector for the transformation from $K_S$ to K. For the transformation of the spin state of the reaction products from $K_S$ to the laboratory system we get as the Eulerian angles of the rotation

$$\{\Phi_1,\ \theta,\ \Phi_2\} = \{+\varphi,\ \Omega,\ -\varphi\},$$
$$\sin\Omega = \frac{\beta v \sin\vartheta\,(1 + \gamma + \gamma_\beta + \gamma')}{(1+\gamma)(1+\gamma_\beta)(1+\gamma')}\,\gamma\gamma_\beta, \tag{6}$$

where

$$v = |\mathbf{p}|/\omega = \sqrt{\omega^2 - \varkappa^2}/\omega;\ \gamma = \omega/\varkappa;$$
$$\gamma_\beta = (1 - \beta^2)^{-1/2};\ \gamma' = \omega'/\varkappa;$$

$\omega'$ is the energy of a reaction product in the laboratory system, and $\vartheta$ and $\varphi$ are the spherical

angles of its momentum $\mathbf{p}$ in $K_S$, measured in an axis system with the z axis parallel to $\boldsymbol{\beta}$ (the x and y axes are chosen arbitrarily).

In Stapp's[4] Eq. (48) for $\sin\Omega$ there is a mistake (or a missprint): it does not have the factors $\gamma\gamma_\beta$ [$\gamma^{(a)}\gamma^{(b)}$ in his notation]. If one repeats Stapp's calculations (in accordance with his arguments), the result is just the present Eq. (6). The rotation by the angle $\Omega$ must be applied counterclockwise around the vector $\boldsymbol{\beta}[\mathbf{p}]$, $\boldsymbol{\beta}$ being the velocity of the laboratory system relative to the center-of-mass system of the reaction (see Appendix).

This relativistic effect of rotation of the spin state of course does not show up at all in the transformation of the angular distribution into the laboratory system (since the angular distribution is a polarization tensor of rank zero). One needs only to carry out the ordinary (kinematic) relativistic transformation of the angles from $K_S$ to the laboratory system. The nonrelativistic theory of the angular distribution in reactions with unpolarized beams and targets remains valid also in the relativistic domain (except for changes or increased precision in the meanings of the quantities involved in the formulas).

As for the polarization vector and the polarization tensors, they are not directly measured in the experiments. In order to measure the polarization vector for the product c of the reaction $a + b \to c + d$, we must scatter c from a target e and measure the asymmetry in the angular distribution of the scattered particles c. Then we obtain information about the polarization vector $\mathbf{P}'$ in the center-of-mass system $K'_S$ of the reaction $c + e \to c + e$. The desired polarization vector is obtained from $\mathbf{P}'$ by a rotation. The angle of this rotation is found from Eq. (6). In fact, in the successive Lorentz transformations from $K_S$ to the laboratory system (by means of the known velocity $\boldsymbol{\beta}$) and then to the system K′ (velocity $\boldsymbol{\beta}'$) a rotation occurs only in the first transformation, since the momentum $\mathbf{p}'_c$ of particle c in the laboratory system is parallel to $\boldsymbol{\beta}'$, so that $\sin\Omega_2 \sim \sin(\hat{\boldsymbol{\beta}}'\mathbf{p}'_c) = 0$. This question is analyzed in more detail in Ref. 4, and the treatment carried through there is valid for arbitrary spin.

Quite generally, the relativistic rotation of the spin is seen to be of importance only for the treatment of cascades of reactions. In the following section we shall deal with the problem of the relativistic changes of the angular correlations in successions of reactions of type $a + b \to c + d$, $c \to e + f$.

In conclusion we point out that in the change from $K_S$ to the system $K_0$ in which a particle is at rest the description of the spin state does not undergo any changes, since here $\boldsymbol{\beta} \parallel \mathbf{p}$ and $\Omega = 0$. Therefore we can regard the quantities $m_a$, $m_b$, and so on as describing the spin states of the particles in their rest systems $K_0$. This interpretation is preferable to the preceding one: the spin states of particles are described by quantities whose definition does not depend on the system $K_S$, i.e., on what target the particle is interacting with, on what its energy is, or on the energy balance of a particular reaction.*

## 4. THE RELATIVISTIC ANGULAR CORRELATIONS IN CASCADES OF THE TYPE $a + b \to c + d$, $c \to e + f$

We shall consider first the cascade $\pi^- + p \to Y + K$, $Y \to N + \pi$, which is well known in the literature. If the first reaction occurs near threshold, the correlation in the angle $\gamma$ between the directions of the incident $\pi^-$ mesons and the decay nucleons provides a way of determining the spin j of the hyperon Y. This correlation can be found if one substitutes into the expression

$$F(\vartheta,\varphi) = \frac{w}{\sqrt{4\pi}} \sum_{q=0,2\ldots}^{2j-1} (2q+1)^{-1/2} Q(j,q) \sum_{\nu=-q}^{q} Y_{q\nu}(\vartheta,\varphi)\,\rho(q,\nu) \tag{7}$$

for the angular distribution of the decay products of the hyperon in its rest system $K_Y$ the concrete expression for the statistical polarization tensors $\rho(q,\nu)$ of the hyperon (cf. Refs. 12 and 13). In the center-of-mass system $K_S$ of the reaction $\pi^- + p \to Y + K$ we have near threshold (the z axis is directed along the $\pi^-$ meson beam)

$$\rho_s(q,\nu) \sim Q(j,q)\,\delta_{\nu,0}. \tag{8}$$

The nonrelativistic correlation in the angle $\gamma$ is

*In connection with this interpretation, however, the following misunderstanding can arise. Since there is only one system $K_0$ in which a particle is at rest, in any reaction the m values mean always the same thing: the spin components in the rest systems. Consequently it might seem that no transformations of the spin state are actually necessary. The point is that if we are given the velocity $\mathbf{v}_{21}$ of a system $K_2$ relative to $K_1$ and the velocity $\mathbf{v}_{32}$ of $K_3$ relative to $K_2$, then the velocity $\mathbf{v}_{31}$ (which is of course a function of $\mathbf{v}_{21}$ and $\mathbf{v}_{32}$) turns out not to be parallel to $\mathbf{v}_{13}$ if $[\mathbf{v}_{21}\mathbf{v}_{32}] \neq 0$ (cf. Ref. 11, Sec. 22). The transformation from $K_1$ to $K_3$ must have the form of a Lorentz transformation with a spatial rotation [see Eq. (58) of Ref. 11]. If the particle was at rest in $K_1$, then in $K_3$ it has the velocity $\mathbf{v}_{13}$, and by using this velocity we can go over to a system $K_4$ in which the particle is again at rest. Calculations show that the product of the transformations from $K_1$ to $K_3$ and then on to $K_4$ has the form of a pure spatial rotation: $\mathbf{s}_{(4)} = D^{-1}\mathbf{s}_{(1)}$, if $D\mathbf{v}_{13} = -\mathbf{v}_{31}$ (the space axes of the Lorentz systems $K_1$, $K_2$, $K_3$, $K_4$ are of course assumed parallel).

obtained by simply substituting Eq. (8) into Eq. (7):

$$F_{nr}(\vartheta, \varphi) \sim \sum_{q=0}^{2j-1} (2q+1)^{-1/2} Q^2(j,q) Y_{q,0}(\vartheta, 0) \quad (9)$$

$$\sim \sum_{q=0}^{2j-1} Q^2(j,q) P_q(\cos\gamma).$$

In actual fact one must substitute into Eq. (7) not the $\rho_S(q, \nu)$, but the statistical tensors of the hyperon referred to the system $K_Y$:

$$\rho(q,\nu) = \sum_{\nu'} D^q_{\nu,\nu'}(\varphi_c, \Omega(\vartheta_c), -\varphi_c)\rho_s(q,\nu')$$

$$= \sqrt{4\pi/(2q+1)}\, Y^*_{q,\nu}(\Omega, \varphi_c) Q(j,q). \quad (10)$$

Here $\varphi_C$ and $\vartheta_C$ are the spherical angles of the emission of the hyperon in the system $K_S$. The angle $\Omega$ is determined by Eq. (6), since in the transformation from $K_S$ to the laboratory system and then on into $K_Y$ a rotation occurs only in the passage from $K_S$ to the laboratory system. (We note that in the experiment $F(\vartheta, \varphi)$ is obtained by translating the measured distribution from the laboratory system into $K_Y$, and not by going from $K_S$ to the rest system of the hyperon).

Substituting Eq. (10) into Eq. (7), we get

$$F_r(\vartheta, \varphi) \sim \sum_{q=0}^{2j-1} (2q+1)^{-1} Q^2(j,q) \sum_{\nu=-q}^{+q} Y_{q\nu}(\vartheta, \varphi) Y^*_{q\nu}(\Omega, \varphi_c)$$

$$= (1/4\pi) \sum_{q=0}^{2j-1} Q^2(j,q) P_q(\cos\gamma_r), \quad (11)$$

where $\gamma_r$ is now the angle between the direction of emergence of the decay products and the direction $\{\Omega(\vartheta_C), \varphi_C\}$. Thus the expression for the correlation has its old form, if we change the definition of the angle $\gamma$.

In the experiment we are discussing $\Omega$ does not exceed 1.5°. If we construct the distribution in $\gamma$, choosing only cases with fixed $\vartheta_C \approx 90°$ and fixed $\varphi_C$, then the difference between the nonrelativistic and the relativistic correlations can amount to 3% for $j = 3/2$ and 5% for $j = 5/2$. In the actual experimental procedure, of course, all cases of the cascade are used in the construction of the correlation $F(\gamma)$. If Eq. (11) is just integrated over $\varphi_C$, the difference between the resulting correlation $F_r(\gamma, \Omega(\vartheta_C))$ and the nonrelativistic result (9) does not exceed 0.1% over the entire range of angles $\gamma$ and $\vartheta_C$ (for $j \le 5/2$).

In the case of the cascade $K^- + p \to Y + \pi$, $Y \to N + \pi$, the angular correlation again does not contain any unknown parameters and depends only on the spin j of the hyperon, if the energies of the $K^-$ particles do not exceed 20 or 30 Mev but are large enough (> 0.1 Mev) so that mesic atoms are not formed (for more details see Ref. 9). In the center-of-mass system of the reaction $K^- + p \to Y + \pi$, with the z axis parallel to the direction of $[\mathbf{n}_K \times \mathbf{n}_Y]$, where $\mathbf{n}_K$ is the direction of the incident beam of K particles,

$$\rho_s(q,\tau) \sim Q(j,q)\delta_{\tau,0}.$$

Relative to this same set of axes, but in the rest system $K_Y$ of the hyperon

$$\rho(q,\tau) = \sum_{\tau'} D^q_{\tau\tau'}(0, \Omega, 0)\rho_s(q,\tau')$$

$$= \sqrt{4\pi/(2q+1)}\, Y^*_{q,\tau}(\Omega, 0) Q(j,q). \quad (12)$$

The difference between the relativistic correlation $F_r(\vartheta, \varphi)$ and the nonrelativistic function is basically the same: substituting Eq. (12) into Eq. (7), we get the correlation $F_r(\theta)$ of the angle $\theta$ between the direction $\mathbf{n}$ of the emission of the decay products and the vector obtained by rotating $\mathbf{n}_Y$ by the angle $\Omega$ around the vector $[\mathbf{n}_K \times \mathbf{n}_Y]$ (i.e., in the plane of the reaction). The nonrelativistic correlation had the same form, but $\theta$ was the angle between $\mathbf{n}$ and $\mathbf{n}_Y$.

The correlation proposed by Adair[13] (cf. also Ref. 9) admits of energies larger than those near threshold, but does not change when treated relativistically: for this correlation one uses cases in which the hyperons are emitted at small angles with the direction of the incident beam, and then $\Omega \approx 0$.

Since the most general case of the cascade $a + b \to c + d$, $c \to e + f$, in which all the spins are arbitrary and the correlation depends on unknown parameters, is of no practical interest, we simply note without proof that the nonrelativistic form of the angular correlation can be retained. To do this one finds for each case of the cascade, using the measured angles of emission of the particle c, a particular system of coordinates belonging to this case. The angles of emission of the products from the decay of c are calculated relative to this system. The distribution in these recalculated angles has the old, nonrelativistic, form (but one has, of course, changed the rule for constructing the angular correlation from the experimental data).

## APPENDIX

1. Let us express $\mathbf{s}$ in terms of $M_{\mu\nu}$ and $p_\mu$. Let $\kappa$ be the rest mass of the particle and $\omega = (p^2 + \kappa^2)^{1/2}$, and

$$\mathbf{M} = [\mathbf{r} \times \mathbf{p}] + \mathbf{s},$$
$$\mathbf{N} = \mathbf{r}\omega - i\mathbf{p}/2\omega + [\mathbf{p} \times \mathbf{s}]/(\omega + \varkappa). \quad (A.1)$$

The four-dimensional vector

$$\Gamma_\sigma = (1/2i)\,\varepsilon_{\mu\nu\sigma\lambda} M_{\mu\nu} p_\lambda$$

($\epsilon_{\mu\nu\sigma\lambda}$ is the completely antisymmetric tensor of the fourth rank with $\epsilon_{1234} = 1$) then has the form:

$$\Gamma = s\varkappa + (ps)\,p/(\omega + \varkappa), \quad \Gamma_4 = i\,(sp). \tag{A.2}$$

Noting that $(\Gamma p) = \omega\,(sp)$, we find from Eq. (A.2):

$$s = \Gamma/\varkappa - (\Gamma p)\,p/\varkappa\omega\,(\omega + \varkappa). \tag{A.3}$$

All these operator equations are to be understood as being in the momentum representation.

From the second of the relations (A.1) we now get

$$r\omega = N + ip/2\omega - [p\times\Gamma]/\varkappa\,(\omega + \varkappa). \tag{A.4}$$

2. The vector $\tilde{s}$ in the new system K, which moves relative to $K_S$ with the velocity $\beta$ (in units of the speed of light) can now be found in the following way. Substituting into the right and left members of the equations [cf. Ref. 11, Sec. 18, Eq. (25)]

$$\tilde{\Gamma} = \Gamma + \beta\,\{(\Gamma\beta)\,(\gamma_\beta - 1)\,\beta^{-2} - \gamma_\beta \Gamma_{4l}\},$$

$$\tilde{\Gamma}_{4l} = \gamma_\beta\,\{\Gamma_{4l} - (\beta\Gamma)\} \tag{A.5}$$

the expressions (A.2) for $\Gamma$ and $\tilde{\Gamma}$ in terms of $s$, $p_\mu$ and $\tilde{s}$, $\tilde{p}_\mu$, respectively, and replacing the $\tilde{p}_\mu$ by their expressions in terms of $p_\mu$ (which have the same form (A.5)), we get the expressions for $\tilde{s}$ in terms of $s$. First of all we establish the fact that $\tilde{s}$ is a linear combination of the vectors $s$, $\beta$, and $p$. This means that the vector $\tilde{s}$ is obtained from $s$ by a rotation around an axis perpendicular to $\beta$ and $p$. There remains only the determination of the magnitude and sign of the angle of rotation around this axis. For this purpose we choose a convenient set of three space axes (it is obvious that the angle of rotation cannot depend on the choice of the axes): $z \parallel \beta$, $y \parallel [\beta\times p]$. A rotation of the vector around the y axis in the counterclockwise direction through the angle $\Omega$ must have the form

$$\tilde{s}_x = \cos\Omega s_x + \sin\Omega s_z \qquad \tilde{s}_z = -\sin\Omega s_x + \cos\Omega s_z. \tag{A.6}$$

Representing the expression for $\tilde{s}$ in terms of $s$ (in the chosen set of axes) in the form (A.6), and finding the coefficient of $s_z$ in the expression for $\tilde{s}_x$ (as that having the simplest form), after cumbersome calculations we get the formula (6) of Sec. 3 for $\sin\Omega$.


[1] F. Coester and J. M. Jauch, Helv. Phys. Acta **26**, 3 (1953).

[2] A. Simon, Prob. Sovr. Fiz. 1955, No. 6, p. 21 (Russian translation); Phys. Rev. **92**, 1050 (1953).

[3] M. I. Shirokov, J. Exptl. Theoret. Phys. (U.S.S.R.) **32**, 1022 (1957), Soviet Phys. JETP **5**, 835 (1958).

[4] H. P. Stapp, Phys. Rev. **103**, 425 (1956).

[5] C. Møller, Dansk. Mat-Fys. Medd. **23**, No. 1 (1945).

[6] L. L. Foldy, Phys. Rev. **102**, 568 (1956).

[7] Iu. M. Shirokov, Dokl. Akad. Nauk SSSR **94**, 857 (1954).

[8] M. H. L. Pryce, Proc. Roy. Soc. **A150**, 166 (1935); **A195**, 62 (1948).

[9] Chou Kuang-Chao and M. I. Shirokov, Nuclear Phys. **6**, 10 (1958).

[10] I. M. Gel' fand and Z. Ia. Shapiro, Usp. Mat. Nauk **7**, 3 (1952).

[11] C. Møller, The Theory of Relativity. Oxford 1952.

[12] M. I. Shirokov, J. Exptl. Theoret. Phys. (U.S.S.R.) **31**, 734 (1956), Soviet Phys. JETP **4**, 620 (1957).

[13] R. K. Adair, Phys. Rev. **100**, 1540 (1956).


Translated by W. H. Furry
247

# ON THE THEORY OF SUPERFLUIDITY

V. L. GINZBURG and L. P. PITAEVSKII

P. N. Lebedev Physics Institute of the Academy of Sciences, U.S.S.R., and Institute of Physical Problems, Academy of Sciences, U.S.S.R.

Submitted to JETP editor December 10, 1957

J. Exptl. Theoret. Phys. (U.S.S.R.) **34**, 1240-1245 (May, 1958)

Taking quantum effects into account, we have obtained equations describing the behavior of superfluid helium near the $\lambda$-point in the stationary case. We have considered the properties of thin films of helium and the vortex line in helium near the $\lambda$-point.

## 1. THE FUNDAMENTAL EQUATION

THE present paper is devoted to the properties of helium near the $\lambda$-point. It is well known that the usual quasi-microscopic approach to a superfluid liquid, where the normal part is considered as an assembly of weakly interacting elementary excitations,[1] cannot be used in the immediate neighborhood of the transition point. In that temperature region there is a natural, different approach which is applied in the phenomenological theory of phase transitions of the second order.[2] In this theory one expands the thermodynamic potential of the system in a series of powers of some "order parameter" (and its derivatives) which in equilibrium is equal to zero on one side of the transition point. The equilibrium value of this parameter on the other side of the phase transition point is determined by requiring the thermodynamic potential to be a minimum with respect to this parameter. It is clear that in our case the expansion parameter must be connected with the density $\rho_S$ of the superfluid part of the liquid which is different from zero in He II and equal to zero in He I.

Bearing in mind the quantum nature of the phenomena in liquid helium, it is natural to take for this parameter a complex function $\psi(x, y, z) = \eta e^{i\varphi}$, which plays the role of "the effective wave function" of the superfluid part of the liquid, so that the density $\rho_S$ and the velocity $v_S$ of the superfluid part can be expressed as follows in terms of $\psi$,

$$\rho_s = m|\psi|^2, \quad v_s = \frac{\hbar}{\sqrt{mm^*}}\nabla\varphi \tag{1}$$

where $m$ is the mass of a helium atom and $m^*$ some effective mass. There are grounds for assuming that the $\psi$-function introduced by us is closely connected with the true wave function of liquid helium; it can, for instance, be expressed in terms of the single particle density matrix.

In the present paper we restrict ourselves to those stationary problems where we can assume the normal part to be at rest, that is, where we can put $v_n = 0$. In that case we can write the thermodynamic potential $F$ per unit volume of the liquid in the following form (if we take only the first term of the expansion in the gradient of $\psi$),

$$F = \frac{\hbar^2}{2m^*}|\nabla\psi|^2 + F_0(p, T, |\psi|^2). \tag{2}$$

The total thermodynamic potential can be written as $\int F\,dV$. If we take the variation with respect to $\psi^*$ and $\psi$ (with the boundary condition $\psi = 0$, vide infra) we get the equation

$$-\frac{\hbar^2}{2}\nabla\left(\frac{\nabla\psi}{m^*}\right) + \frac{\partial F_0}{\partial|\psi|^2}\psi = 0, \tag{3}$$

and also its complex conjugate for $\psi^*$.

We note that Eq. (3) is completely analogous to the one used in the phenomenological theory of superconductivity.[3] In the stationary case with $v_n = 0$ one can also use the equation of continuity in the form

$$\operatorname{div}(\rho_s v_s) = 0. \tag{4}$$

One can, however, easily satisfy oneself that (4) follows from (3) and its complex conjugate only if $m^*$ does not depend on the coordinates and hence neither on the temperature or pressure, since the latter may depend on the coordinates. This shows that $m^*$ must coincide with the true mass $m$ of the helium atom [any "effective mass" would depend on temperature and pressure; see also the footnote to equation (18)]. We replace therefore $m^*$ by $m$ in (3). We finally have

$$-\frac{\hbar^2}{2m}\Delta\psi + \frac{\partial F_0}{\partial|\psi|^2}\psi = 0. \tag{5}$$

We could, of course, also use the free energy $F'(\rho, T)$ instead of the potential $F(p, T)$.

For applications, the boundary conditions for Eq. (5) are also important. Bearing in mind the assumed connection between the function $\psi$ and the true wave function of helium which tends to zero at the boundary, we must assume that $\psi = 0$ on the boundary. The following argument leads to this condition. We consider the flow of a superfluid liquid along a solid wall. If $\rho_S \neq 0$ at the wall, the current of the superfluid part must experience a jump at the wall: liquid helium wets a solid body, that is, sticks to it, and $v_S$ can not gradually decrease coming to the wall since curl $v_S = 0$. The occurrence of a break in the current when a body moves relative to the liquid must lead to an effect of the "dry friction" kind, since the jump will be connected with a surface energy.[4] However, specially arranged experiments showed that no such effect is present,[5] leading to the conclusion that at the wall $\rho_S = 0$.

The boundary conditions at a free surface of helium are not so obvious. We shall, however, also in that case assume that $\psi = 0$ at the surface.

We expand the thermodynamic potential $F_0$, as in the usual theory of phase transitions, in powers of $|\psi|^2$,

$$F_0 = F_I(p, T) - \alpha|\psi|^2 + \frac{\beta}{2}|\psi|^4 \qquad (6)$$

(expansion (6) was already applied to helium in Ref. 6; $F_I$ is the potential of helium I). At the $\lambda$-point $\alpha(p, t_\lambda) = 0$ and expanding in powers of $T - T_\lambda$ we get

$$\alpha = \left(\frac{d\alpha}{dT}\right)_{T_\lambda}(T - T_\lambda) = \alpha'_\lambda(T_\lambda - T).$$

As far as expansion (6) is concerned, we must note that it is not completely well founded, since the true character of the singularity at the transition point of a second-order transition is not known at the present time. Apart from that, the large value of the anomalous heat capacity in helium near the $\lambda$-point and the strong dependence of the jump on the pressure possibly indicate the proximity of a critical Curie point where $\beta = 0$. In that case we must also take into account in the expansion the term of the form $\gamma|\psi|^6$. However, bearing in mind the insufficiency of the experimental data, we shall for the sake of simplicity restrict ourselves to the expansion (6). The transition to another form of the function $F_0(|\psi|^2)$ does not introduce any fundamental difficulties.

If the state is uniform in space, and in equilibrium, we have

$$\frac{\partial F_0}{\partial|\psi|^2} = 0, \quad |\psi|_e^2 = \frac{\rho_s}{m} = \frac{\alpha}{\beta} = \frac{\alpha'_\lambda(T_\lambda - T)}{\beta},$$

$$\Delta c_p = c_{p\,II} - c_{p\,I} = T_\lambda(\alpha'_\lambda)^2/\beta_\lambda.$$

Hence

$$\alpha'_\lambda = \Delta c_p m/T_\lambda\left|\frac{\partial\rho_s}{\partial T}\right|_\lambda, \qquad \beta_\lambda = \alpha'_\lambda m\Big/\left|\frac{\partial\rho_s}{\partial T}\right|_\lambda.$$

If we put

$$\Delta c_p = 1.0\cdot10^7 \text{ erg-degree}^{-1}\text{cm}^{-3},$$

$$\left|\frac{\partial\rho_s}{\partial T}\right|_\lambda = 0.7 \text{ g-degree}^{-1}\text{cm}^{-3},$$

we get

$$\alpha'_\lambda \approx 4.5\cdot10^{-17} \text{ erg/degree and } \beta_\lambda \approx 4\cdot10^{-40} \text{ erg-cm}^3.$$

We note the tentative nature of these estimates.

We turn now to Eq. (5) and introduce new variables (the $x_i$ are Cartesian coordinates)

$$\psi_0 = \psi/|\psi|_e = \psi/\sqrt{\alpha/\beta}; \quad \xi_k = x_k/l, \quad l = \hbar/\sqrt{2m\alpha}.$$

The expression for the thermodynamic potential then becomes

$$F = F_I + \frac{\alpha^2}{2\beta}\{-2|\psi_0|^2 + |\psi_0|^4 + 2|\nabla_\xi\psi_0|^2\}, \qquad (7)$$

and instead of (5) we have

$$\Delta_\xi\psi_0 = (|\psi_0|^2 - 1)\psi_0. \qquad (8)$$

Using the calculated value of $\alpha$ we get

$$l \approx 4\cdot10^{-8}/\sqrt{T_\lambda - T}.$$

In order that this macroscopic theory be applicable, it is necessary that $l$ be much larger than the interatomic distances, i.e., that the condition $l \gg a \sim 3\times10^{-8}$ cm be satisfied. If $l \sim a$, there are no special reasons to restrict ourselves in (2) to only the squares of the first derivatives. In that sense (2) gives us the first terms in an expansion in $(a/l)^2$. It is thus clear that the theory under consideration can only be applied in the immediate neighborhood of the $\lambda$-point.

## 2. SOLUTIONS OF SOME PROBLEMS

We consider first of all helium near a solid wall which we shall take as the xy plane. We shall assume that the helium is not moving; the presence of some velocity $v_S$ leads only to a change in the coefficient of $\psi_0$ in Eq. (8), completely insignificant for all real velocities. If $v_S = 0$, the function $\psi$ can be considered to be real and to depend on the z coordinate only. Equation (8) is then of the form

$$d^2\psi_0/d\xi^2 = (\psi_0^2 - 1)\psi_0 \qquad (9)$$

with the boundary conditions

$$\xi = 0, \ \psi_0 = 0; \ \xi \to \infty, \ \psi_0 \to 1. \qquad (10)$$

Equation (9) has a first integral

$$\left(\frac{d\psi_0}{d\xi}\right)^2 + \psi_0^2 - \frac{\psi_0^4}{2} = C = \text{const.}$$

The solution of equation (9) with the boundary conditions (10) is of the form

$$\psi_0(\xi) = \tanh(\xi/\sqrt{2}).$$

Here

$$\rho_s = \rho_{s_e} \tanh^2(z/\sqrt{2}l).$$

The presence of a boundary leads to the appearance of an additional surface energy

$$\sigma = \int (F - F_{0e})\, dz = \frac{\alpha^2}{2\beta} l \int_0^\infty \left(\psi_0^4 - 2\psi_0^2 + 2\left(\frac{d\psi_0}{d\xi}\right)^2 + 1\right) d\xi$$

$$= \frac{4\sqrt{2}}{3}\left(\frac{\alpha^2}{2\beta}\right) l. \qquad (11)$$

We note that $\sigma \sim (T_\lambda - T)^{3/2}$ while

$$F_I - F_{0e} = \alpha^2/2\beta \sim (T_\lambda - T)^2.$$

We consider now a helium film, that is, a layer of helium of thickness $\alpha$. The boundary conditions of Eq. (9) are now of the form*

$$\xi = 0,\ \psi_0 = 0;\ \xi = d/2,\ d\psi_0/d\xi = 0.$$

The corresponding solution of Eq. (9) is as follows

$$\xi = \int_0^{\psi_0} \frac{d\psi_0}{\sqrt{\psi_0^4/2 - \psi_0^2 + C}} = \frac{\sqrt{2}}{b} \int_0^{\psi_0/a} \frac{du}{\sqrt{(1-u^2)(1-k^2u^2)}}$$

$$\equiv \frac{\sqrt{2}}{b} F(\varphi, k), \quad \varphi = \arcsin(\psi_0/a),\ k = a/b,$$

$$a^2 = (1 - \sqrt{1-2C}),\ b^2 = (1 + \sqrt{1-2C}), \qquad (12)$$

where C follows from the equation

$$\frac{d}{2l} = \frac{\sqrt{2}}{b} F\left(\frac{\pi}{2}, \frac{a}{b}\right) \equiv \frac{\sqrt{2}}{b} K\left(\frac{a}{b}\right). \qquad (13)$$

A plot of the function $\psi_0(\xi)$ has the form of a dome, which is symmetric with respect to the middle of the film and the height of which decreases with decreasing film thickness d. Also, starting from some thickness $d_k$ there is no solution with $\psi_0 \neq 0$, that is, the film ceases to be superfluid.

To find $d_k$ it is sufficient to note that the complete elliptic integral $K(a/b)$ reaches its minimum value $\frac{1}{2}\pi$ for $a/b = 0$, that is, when $b = \sqrt{2 - a^2} = \sqrt{2}$. We get thus

$$d_k = \pi l = \pi\hbar/\sqrt{2m\alpha}. \qquad (14)$$

This result means that the temperature of the $\lambda$-point in the film is lower than in the case of large volumes of helium. The corresponding change $\Delta T_\lambda$ can be found from Eq. (14) which we can consider to be the equation determining $T_\lambda$ for a given thickness d. We get finally

$$\Delta T_\lambda = \pi^2\hbar^2/2m\alpha'_\lambda d^2 \approx 2 \cdot 10^{-14}/d^2. \qquad (15)$$

The fact that $T_\lambda$ was lower in films was observed experimentally.[7,8] Unfortunately, the film thickness in those experiments was only known as to order of magnitude. At the same time the theory can only be applied to films of thickness $d \gg a \sim 3 \times 10^{-8}$ cm since in the opposite case it is impossible, in particular, to take for $\alpha'_\lambda$ data referring to He II in bulk, and one must consider in detail the nature of the interaction with the solid wall. We shall thus give only one estimate. In Ref. 7, $\Delta T_\lambda = 0.146°$ for a film of thickness of about 18 atomic layers. At the same time we get from Eq. (15), for $d = 18 \times 3.6 \times 10^{-8} = 6.5 \times 10^{-7}$ cm, a change $\Delta T_\lambda \approx 5 \times 10^{-2}$. The discrepancy by a factor of 3, which we have found, can completely be caused by the inaccuracy of the values of $\Delta T_\lambda$, d, and $l$ we have used, even apart from the possible inapplicability of the expansion (6).

The thermodynamic potential of the film per unit volume is equal to

$$\overline{F} = F_I + \frac{\alpha^2}{2\beta}\frac{2l}{d}\int_0^{d/l} (C - 2\psi_0^2 + \psi_0^4)\, d\xi$$

$$= F_I + \frac{4\alpha^2 l}{3\beta d}\left\{\left(\frac{C}{2} - b^2\right)\frac{d}{2l} + \sqrt{2}\, bE\left(\frac{a}{b}\right)\right\}, \qquad (16)$$

where

$$E(a/b) = \int_0^{\pi/2} \sqrt{1 - (a/b)^2 \sin^2\varphi}\, d\varphi$$

is the complete elliptical integral of the second kind, and where the quantities a, b, and C are determined in terms of the film thickness [see Eqs. (12) and (13)].

The quantity $F_I - \overline{F}$ decreases with decreasing film thickness and for $d = d_k$ we have, of course, $\overline{F} = F_I$, that is, the transition to He I takes place. The heat capacity of the film decreases also when it gets thinner, which is in agreement with Frederikse's results.[9] Unfortunately the available data are insufficient for a quantitative comparison of the theory with experiment.

We shall now consider, on the basis of Eq. (8), a vortex filament in He II. The function $\psi$ in that case can be written in the form

$$\psi(r, \varphi) = \Phi(r)\, e^{in\varphi}, \qquad n = 1, 2 \ldots . \qquad (17)$$

*The boundary conditions which we have written down are, under the assumptions we have made, strictly valid for the case of a film enclosed between solid walls. In the case of a free surface the problem of the boundary conditions is insufficiently clear.

where r, $\varphi$, and z are cylindrical coordinates; the z axis is taken along the axis of the filament. We shall see below that vortices with $n > 1$ are energetically unfavorable.

The velocity $v_s$ has only a component $v_{s\varphi}$, and (see also Ref. 10)*

$$\oint v_s ds = v_{s\varphi} \cdot 2\pi r = \frac{2\pi n\hbar}{m}. \qquad (18)$$

Furthermore, Eq. (8) will be of the form ($\xi = r/l$, $\psi_0 = \Phi\sqrt{\alpha/\beta}$)

$$\xi^2 \frac{d^2\psi_0}{d\xi^2} + \xi \frac{d\psi_0}{d\xi} + (\xi^2 - n^2)\psi_0 - \xi^2\psi_0^3 = 0. \qquad (19)$$

As $\xi \to 0$, the function $\psi_0$ is of the form $c_1 r^{\pm|n|}$. The solution with $\psi_0 \sim c_1 r^{-|n|}$ ($\psi_0 \to \infty$ as $\xi \to 0$) has no physical meaning and must be discarded. As $\xi \to \infty$ the density $\rho_s = m\psi_0^2$ must equal the unperturbed density $\rho_{se}$, i.e., $\psi_0^2 = 1$. One sees easily that in the region of large $\xi$ Eq. (19) has the approximate solution

$$\psi_0^2 = 1 - n^2/\xi^2, \qquad \xi \gg 1. \qquad (20)$$

Equation (19) cannot be solved by quadrature over the whole range, and has been solved numerically. The result for $n = 1$ is given in the figure.

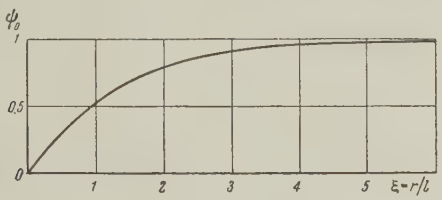


The thermodynamic potential per unit length of filament is equal to (the problem is here to find the difference of the potential when a solenoidal velocity is present or not)

$$f = (\alpha^2/2\beta)\,4\pi l^2 N = (\pi\hbar^2/m^2)\rho_{se}N, \qquad N = N_1 + N_2, \qquad (21)$$

$$N_1 = \frac{1}{2}\int_0^\infty \left[\psi_0^4 - 2\psi_0^2 + 2\left(\frac{d\psi_0}{d\xi}\right)^2 + 1\right]\xi\, d\xi, \quad N_2 = n^2 \int_0^{R/l} \psi_0^2 \frac{d\xi}{\xi}.$$

In this equation R is some maximum radius of integration (for instance, the diameter of the container, or the distance between vortex filaments) which must be introduced in connection with our consideration of an infinitely long filament. If we put $\rho = \rho_{se} = \text{const.}$, as should be the case, and if we do not take the gradient term into consideration, we find $N = N_e = n^2 \ln(R/a)$, where a is some distance of atomic dimensions. From a numerical calculation it follows that for $n = 1$, $N = \ln(1.46\, R/l)$, for $n = 2$, $N = 4\ln(0.59\, R/l)$, and for $n = 3$, $N = \ln(0.38\, R/l)$. If R is sufficiently large, the difference between N and $N_e$ is of small importance; this is also natural since the main contribution to f comes from the distant, classical region. For the same reason we find that for large values of R the energy is roughly proportional to $n^2$ and states with $n > 1$ need not be taken into account (it is more favorable to form two vortex lines with $n = 1$ than one with $n > 1$). We note that solutions related to the one considered for the vortex line were earlier investigated by Abrikosov[11] on the basis of a theory of superconductivity.[3]

In conclusion the authors use this opportunity to thank Academician L. D. Landau for discussing the problems considered in the present paper.

*If we had in Eq. (5) instead of the helium atom mass m some effective mass m*, the right hand side of Eq. (18) would be $2\pi n\hbar/\sqrt{mm^*}$. This circulation can, however, not change with temperature. If $T = 0$, Eq. (18) is valid as follows from the arguments given in Ref. 10. It follows thus that $m^* = m$, as followed also from the considerations at the beginning of the present paper.

[1] L. D. Landau, J. Exptl. Theoret. Phys. (U.S.S.R.) **11**, 592 (1941).

[2] L. D. Landau and E. M. Lifshitz, Статистическая физика (Statistical Physics), Ch. XIV, Gostekhizdat, 1951.

[3] V. L. Ginzburg and L. D. Landau, J. Exptl. Theoret. Phys. (U.S.S.R.) **20**, 1064 (1950).

[4] V. L. Ginzburg, J. Exptl. Theoret. Phys. (U.S.S.R.) **29**, 244 (1955), Soviet Phys. JETP **2**, 170 (1956).

[5] G. A. Gamtsemlidze, Paper at the Fourth All-Soviet Meeting on Low Temperature Physics, Moscow, 1957.

[6] V. L. Ginzburg, Dokl. Akad. Nauk SSSR **69**, 161 (1949).

[7] D. F. Brewer and K. Mendelssohn, Phil. Mag. **44**, 340 (1953).

[8] E. Long and L. Meyer, Phys. Rev. **85**, 1030 (1952).

[9] H. P. R. Frederikse, Physica **15**, 860 (1949).

[10] R. P. Feynman, Progr. Low Temp. Phys. **1**, 17 (1955).

[11] A. A. Abrikosov, J. Exptl. Theoret. Phys. (U.S.S.R.) **32**, 1442 (1957), Soviet Phys. JETP, **5**, 1174 (1957).

Translated by D. ter Haar
248

# ON THE INTERACTION OF $\Xi^-$-HYPERONS WITH NUCLEONS AND LIGHT NUCLEI

L. B. OKUN', I. Ia. POMERANCHUK and I. M. SHMUSHKEVICH

Submitted to JETP editor December 10, 1957

J. Exptl. Theoret. Phys. (U.S.S.R.) **34**, 1246-1249 (May, 1958)

Spin correlations are determined for $\Lambda$ particles produced in $\Xi^- + p \to \Lambda + \Lambda$ reactions (slow $\Xi^-$). An experimental study of such correlations would make it possible to establish the parity of $\Lambda$ particles.

In the interaction of a slow $\Xi^-$ hyperon with protons, the following reactions are possible:

$$\Xi^- + p \to \Xi^- + p, \quad \text{elastic scattering,} \quad (1)$$

$$\Xi^- + p \to \Xi^0 + n, \quad \text{charge exchange,} \quad (2)$$

$$\Xi^- + p \to \Lambda^0 + \Lambda^0, \quad \text{absorption.} \quad (3)$$

Other processes (of the type $\Xi^- + p \to \Sigma^0 + \Lambda^0$ and others) have a threshold and can be neglected at low energies. (We proceed on the assumption that the $\Xi^-$ strangeness is equal to 2). If it turns out that the lifetime of the $\Xi^-$ hyperon is sufficiently long (see the Report of the Seventh Rochester Conference), and that it is possible to experiment with slow $\Xi^-$ hyperons, then it would be of particular interest to study the reaction (3), observing the subsequent decays of the $\Xi^-$ hyperons. In particular, study of this reaction would make it possible to establish the parity of the $\Xi^-$ hyperon relative to the nucleon.

The following analysis is based on the assumption that the decay of the $\Lambda$ hyperon proceeds with nonconservation of parity. If parity is not conserved in the decay $\Lambda^0 \to p + \pi^-$, then the amplitude of this decay can be written in the form

$$a_\Lambda = a + b\sigma\mathbf{n}. \quad (4)$$

Here a and b are, in general, complex numbers and $\mathbf{n}$ is a unit vector in the direction of emission of the $\pi$ meson.

The angular distribution of $\pi$ mesons in the decay of polarized $\Lambda$ hyperons has the form

$$1 + \varkappa\mathbf{sn}, \quad (5)$$

where $\mathbf{s}$ is a unit vector in the direction of spin of the $\Lambda$ hyperon and the asymmetry parameter $\kappa$ is equal to

$$\varkappa = (a^*b + b^*a)/(|a|^2 + |b|^2). \quad (6)$$

Thus, the $\pi$ meson should be emitted mainly parallel (or antiparallel) to the direction of polarization of the $\Lambda$ hyperon.

On the other hand, the spins of two $\Lambda$ hyperons produced in the reaction (3) are correlated because of the Pauli principle. In the table are given the

| States of the system $\Xi^- + p$ | States of the system $\Lambda + \Lambda$ | |
|---|---|---|
| | $\Xi$ parity + 1 | $\Xi$ parity − 1 |
| $^1S_0$ | $^1S_0$ | $^3P_0$ |
| $^3S_1$ | Reaction (3) forbidden | $^3P_1$ |

spin and orbital states of two $\Lambda$ hyperons for the case in which the $\Xi^-$ hyperon is captured from an S-state by the proton. (We assume that the spin of the $\Xi^-$ hyperon, as well as the spin of the $\Lambda$ hyperon, is equal to $\frac{1}{2}$.)

Consequently, for a positive parity of the $\Xi^-$ particle, only the amplitude for the one transition ($^1S_0 \to {}^1S_0$) has to be taken into account. Calculating the angular distribution of $\pi$ mesons arising in the decay of two $\Lambda$ hyperons with the aid of Eq. (4), we obtain

$$W(\mathbf{n}_1, \mathbf{n}_2) = 1 - \varkappa^2(\mathbf{n}_1\mathbf{n}_2). \quad (7)$$

Here $\mathbf{n}_i$ ($i = 1, 2$) is a unit vector in the direction of motion of the $\pi$ meson in the rest system of that hyperon in the decay of which the $\pi$ meson arises.

It is essential that Eq. (7) is valid for both polarized and unpolarized $\Xi$ particles, and the resulting distribution does not depend on the direction of flight of the $\Lambda$ particle.

For a negative parity of the $\Xi$ hyperon, one must consider two amplitudes $\lambda$ and $\mu$ for the two possible transitions $^3S_1 \to {}^3P_1$ and $^1S_0 \to {}^3P_0$, respectively, possible in the process (3). In this case, calculation gives for the angular distribution of $\pi$ mesons produced in the decay of the $\Lambda$ particle

$$W(\mathbf{n}_1, \mathbf{n}_2) = 1 + \frac{|\alpha|^2}{3 + |\alpha|^2}\varkappa^2(\mathbf{n}_1\mathbf{n}_2) + \frac{3 - 2|\alpha|^2}{3 + |\alpha|^2}\varkappa^2(\mathbf{kn}_1)(\mathbf{kn}_2)$$

$$+\frac{3}{3+|\alpha|^2}(\zeta\mathbf{k})(\mathbf{k}\cdot(\mathbf{n}_1+\mathbf{n}_2))$$
$$+\sqrt{\frac{3}{2}}\frac{\alpha^*+\alpha}{3+|\alpha|^2}([\mathbf{k}\times[\mathbf{k}\times\zeta]]\cdot(\mathbf{n}_1+\mathbf{n}_2))$$
$$+i\sqrt{\frac{3}{2}}\frac{\alpha-\alpha^*}{3+|\alpha|^2}\{([\mathbf{k}\times\zeta]\cdot\mathbf{n}_1)(\mathbf{k}\mathbf{n}_2)$$
$$+([\mathbf{k}\times\zeta]\cdot\mathbf{n}_2)(\mathbf{k}\mathbf{n}_1)\}. \quad (8)$$

Here $\alpha=\mu/\lambda$, $\mathbf{k}$ is a unit vector in the direction of flight of the $\Lambda^0$ hyperons, and $\zeta$ is the polarization vector of the $\Xi^-$ hyperons, i.e., the mean value of the spin of the $\Xi$ particles.

Averaging Eq. (8) over direction $\mathbf{k}$ gives

$$W(\mathbf{n}_1,\mathbf{n}_2)=1+\frac{1}{3}\varkappa^2(\mathbf{n}_1\mathbf{n}_2)$$
$$+\frac{1-\sqrt{2/3}(\alpha+\alpha^*)}{3+|\alpha|^2}\varkappa\zeta(\mathbf{n}_1+\mathbf{n}_2). \quad (9)$$

Comparison of experimental data with (7) or (8) and (9) could facilitate the determination of the parity of the $\Xi$ hyperon. We note in this connection that if the $\Xi^-$ is not polarized ($\zeta=0$), then, if the parity of the $\Xi^-$ is negative, $\pi$ mesons produced in the decay should be emitted mainly in the same direction. If the parity of the $\Xi^-$ is positive, then the $\pi$ mesons should be mainly emitted in opposite directions. Further, if Eq. (9) is averaged over $\mathbf{n}_2$, one obtains

$$W(\mathbf{n}_1)=1+\frac{1-\sqrt{2/3}(\alpha+\alpha^*)}{3+|\alpha|^2}\varkappa(\zeta\mathbf{n}_1). \quad (10)$$

Averaging Eq. (7) over $\mathbf{n}$ leads to an isotropic distribution for $\mathbf{n}_1$:

$$W(\mathbf{n}_1)=1. \quad (11)$$

Equations (7) to (11) for process (3) are valid for the capture of slow $\Xi^-$ particles out of the continuous spectrum, as well as the capture from bound states of the $\Xi^-+p$ system. It is not clear, however, what contribution will come from capture out of bound P-states. If this contribution is sufficiently large, then the angular distributions of the $\pi$ mesons produced will differ essentially from those obtained here. Thus, the experimental data can be analyzed using Eqs. (8) to (10) or (7) and (11) and choosing the cases which correspond to capture out of the continuous spectrum, i.e., for capture out of a beam of slow $\Xi$ particles. The criterion for this choice, in principle, can be that the sum of momenta of the four particles produced ($2p+2\pi^-$), although small, is not equal to zero.

If the parity of the $\Xi^-$ is equal to +1, and if the interaction between $\Xi$ and p is such that there is a level* in the $^3S_1$ state, then, as can be seen from the table, the $\Xi^-+p$ system will be metastable, since the decay into two $\Lambda^0$ hyperons is forbidden.

Such a system would have a greater probability of decay by emission of a hard $\gamma$-quantum

$$\Xi^-+p\to\Lambda^0+\Lambda^0+\gamma, \quad (12)$$

which could be detected either directly, or by the lack of energy-momentum balance.

If the $\Xi$ + nucleon system has a bound state and if the splitting of the $(\Xi^-+p)$ and $(\Xi^0+n)$ levels, which comes basically from the difference in masses of the $\Xi^-$ and $\Xi^0$ hyperons, is small compared with the splitting of the levels with T = 1, $(\Xi^-p+\Xi^0n)/\sqrt{2}$, and T = 0, $(\Xi^-p-\Xi^0n)/\sqrt{2}$, then the $\Xi$ + nucleon system will be in a state of well-defined isotopic spin T. Here the $^3S_1$-state with T = 0 will be analogous to the deuteron ($J=1$, $T=0$, $P=+1$).

It should be noted that if isotopic spin is a good quantum number for the $\Xi$ + nucleon system, then all bound states of this system with T = 1 will be metastable, since the reaction (3) is forbidden for them.

The reaction (12) can be observed if there is no nuclear bound state of the $\Xi$ + nucleon system, but

$$m_{\Xi^-}+m_p-V_{\text{Coul}}<m_n+m_{\Xi^0}.$$

In this case the Coulomb level $^3S_1$ will be metastable because the charge exchange reaction (2) will be energetically forbidden.

It is of interest to represent also the interaction of a slow $\Xi^-$ hyperon with the deuteron

$$\Xi^-+d\to\Lambda^0+\Lambda^0+n. \quad (13)$$

Study of the angular distribution of hyperons in this case can give information about the mutual interaction of two $\Lambda$ hyperons. For example, presence of a level near zero in the system of two $\Lambda$ hyperons would lead to the fact that small angles between them are preferred. For this, the still unknown amplitude for interaction between the $\Lambda$ and neutron, knowledge of which is necessary for the interpretation of reaction (13), can be obtained directly from the reaction of the type

$$K^-+d\to\Lambda+p+\pi^-,$$

considered in Ref. (2).

*These requirements do not contradict the models of strange particles proposed recently be Gell-Mann;[11] according to which the parity of all hyperons is equal to + 1, and their interaction with $\pi$ mesons is just as strong as the interaction of $\pi$ mesons with nucleons.

Capture of the $\Xi^-$ in $He^4$ can lead to a series of inelastic processes; included in the possible reactions is the production of hypernuclei containing two $\Lambda$ hyperons

$$\Xi^- + He^4 \rightarrow \begin{matrix} p + (\Lambda\Lambda nn), \\ n + (\Lambda\Lambda np), \ldots \end{matrix}$$

The existence of such hypernuclei should lead to a characteristic cascade decay.

We note that the ratio of cross sections for inelastic and elastic interactions on $He^4$ will depend on the relative parity of the $\Xi$ and nucleon (in the case of negative parity of the $\Xi$, inelastic scattering will be suppressed since one of the particles produced in the inelastic scattering must be emitted in a P-state, and the energy given up in this case is small (30 Mev minus the binding energy of $He^4$ plus the binding energy of the fragments produced)).

The authors are grateful to V. V. Sudakov for useful discussion.

[1] M. Gell-Mann, Phys. Rev. **106**, 1296 (1957).

[2] L. B. Okun' and I. M. Shmushkevich, J. Exptl. Theoret. Phys. (U.S.S.R.) **30**, 979 (1956), Soviet Phys. JETP **3**, 792 (1956).

Translated by G. E. Brown
249

SOVIET PHYSICS JETP VOLUME 34 (7), NUMBER 5 NOVEMBER, 1958

# *ON THE POLARIZATION OF THE ELECTRONS EMITTED IN THE DECAY OF MU MESONS*

L. B. OKUN' and V M. SHEKHTER

Submitted to JETP editor December 11, 1957

J. Exptl. Theoret. Phys. (U.S.S.R.) **34**, 1250-1253 (May, 1958)

Expressions have been obtained for the energy spectrum, the angular distribution, and the polarization of the electrons emitted in the decay of polarized $\mu$ mesons. The calculations have been carried out for a decay interaction Hamiltonian of the most general form, characterized by ten complex constants, It is shown that the experiments carried out up to the present time are insufficient to test the validity of the predictions made in Refs. 4 and 5; in addition to these experiments, it is necessary to measure the sign of the polarization of the decaying $\mu$ mesons.

THE experimental data from studies of the spectrum, angular asymmetry, and polarization of the electrons from the decay of polarized $\mu$ mesons are in evident agreement with the predictions of the theory of the two-component neutrino, proposed by Salam,[1] Landau,[2] and Lee and Yang.[3] Within the framework of this theory, if we take into account the experimentally observed spectrum of the electrons, out of the ten complex constants C and C′ which describe the decay of the $\mu$ meson in the general case [cf. Eq. (I) of the Appendix] only four are different from zero:

$$C_V = C_A' \neq 0, \quad C_A = C_V' \neq 0; \tag{1}$$

$$C_S = C_S' = C_P = C_P' = C_T = C_T' = 0. \tag{2}$$

It can be hoped that more precise experimental data will be found to be in agreement with the more restrictive hypothesis of Feynman and Gell-Mann[4] and Marshak and Sudarshan[5] about the two-component nature of the electronic interaction, according to which

$$C_V = \pm C_V', \quad C_A = \pm C_A'. \tag{3}$$

In this latter case the distribution of the electrons from the decay of stationary $\mu$ mesons must be proportional to

$$(1 \mp \zeta\mathbf{n})(3 - 2\varepsilon \pm \eta\mathbf{n}(1 - 2\varepsilon))\varepsilon^2 d\varepsilon. \tag{4}$$

Here $\epsilon$ is the energy of the electron divided by its maximum possible energy, $\mathbf{n}$ is the unit vector in the direction of motion of the electron, $\boldsymbol{\zeta}$ is the unit vector in the direction of the spin of the electron in the rest system of the electron, and $\boldsymbol{\eta}$ is the unit vector in the direction of the spin of the

$\mu$ meson in the rest system of the $\mu$ meson.

The formula (4) is obtained from Eq. (II) of the Appendix if the conditions (1), (2), and (3) are fulfilled and if we neglect the mass $m_e$ of the electron in comparison with its energy.

The first factor in Eq. (4) indicates that the electrons must be completely longitudinally polarized. It has been established experimentally[6,7] that the positrons from the decay of $\mu^+$ mesons are polarized in the direction of motion. Therefore the lower signs in Eq. (4) must be assigned to the decay of the $\mu^+$ meson, and the upper signs to the decay of the $\mu^-$ meson. Furthermore, since the positrons with large energies emerge predominantly backward relative to the momentum of the $\mu^+$ meson,[8] and according to Eq. (4) they emerge along the spin of the $\mu^+$ meson, if Eq. (4) is valid we can conclude that the spin of a $\mu^+$ meson produced in the decay of a $\pi^+$ meson is directed oppositely to its momentum. An experimental test of this prediction is very important.

It is of interest to ascertain to what extent the experimental verification of Eq. (4) would carry with it the two-component nature of the neutrino. In other words, suppose the electron enters the interaction through only two components ($C_i = \pm C_i'$. In this case, are the conditions (1) and (2) not only sufficient for the formula (4) to be valid, but also necessary?

As for the condition (1), it is obvious that if we dispense with it, postulating, for example, that $C_A = C_A' = 0$, $C_V = \pm C_V' \neq 0$, then Eq. (4) will hold as before. Thus the condition (1) is not a necessary one for the validity of Eq. (4), and the experimental confirmation of this formula does not mean that the neutrino is a two-component particle.

As for the condition (2), from the results of a number of researches[9-12] it follows that one can get just the same spectrum and angular asymmetry of the electrons as in the formula (4) if one assumes that $C_V = C_V' = C_A = C_A' = 0$ and chooses the constants $C_S$, $C_S'$, $C_P$, $C_P'$, $C_T$, $C_T'$ in a suitable way. It is obvious that if one is not interested in the angular asymmetry of the electrons it is not hard to get also the required (experimentally observed) sign for their polarization. The question arises: cannot a happily chosen combination of the S, P, and T interaction types give a formula in complete agreement with Eq. (4)?

An analysis of Eq. (II) gives a negative answer to this question. Actually, by combining the S, P, and T types, one can get the formula

$$(1 \mp \zeta\mathbf{n})\,(3 - 2\varepsilon \mp \eta\mathbf{n}\,(1 - 2\varepsilon))\,\varepsilon^2 d\varepsilon, \qquad (5)$$

which differs from Eq. (4) by the sign of the angular asymmetry of the electrons if the sign of their polarization is prescribed. Consequently, if it is shown that the polarization of the $\mu^+$ mesons from the decay of $\pi^+$ mesons agrees with the consequence of the two-component theory of the neutrino as stated above, this will mean that the formula (5) is incorrect. Thus the condition (2) is a necessary one for the validity of the formula (4).

We have carried through the investigation of the necessity of the conditions (1) and (2) on the assumption that the condition of the two-component nature of the electronic interaction is valid. If it turns out that this latter condition is not borne out by experiment, then a consideration like that set forth above can be easily carried through by means of Eq. (II) for this more general case.

## APPENDIX

We present here the result of the calculation of the angular asymmetry and polarization of the electrons emitted in the decay of polarized $\mu$ mesons. The calculation is carried out for the case in which the Hamiltonian has the following form:

$$H = \sum_{i=S,\,V,\,T,\,A,\,P} (\bar{\psi}_e\,(C_i + C_i'\gamma_5)\,O_i\psi_\mu)\,(\bar{\psi}_\nu O_i\psi_\nu),$$

$$O_S = 1,\ O_V = -i\gamma_\alpha,\ O_T = \frac{i}{2\sqrt{2}}(\gamma_\alpha\gamma_\beta - \gamma_\beta\gamma_\alpha),$$

$$O_A = \gamma_\alpha\gamma_5,\ O_P = \gamma_5,\qquad \gamma_5 = i\gamma_0\gamma_1\gamma_2\gamma_3. \qquad (I)$$

It is convenient to carry through the calculation by using the method of Lenard[13] and the spin projection operators of Michel and Wightman.[14] The probability that in the decay of a $\mu$ meson with its spin directed along $\eta$ an electron is emitted in the direction $\mathbf{n}$ with energy $\epsilon$ and with spin directed along $\zeta$ is given by the following formula:

$$d^2W / d\varepsilon d\Omega = (\mu w^4 / 96\pi^4)\sqrt{\varepsilon^2 - u^2}\,\{3S + 2V + 2T\},$$

$$S = (C_S C_S^* + C_P' C_P'^*)\,(1 - \varepsilon)\,(\varepsilon + u)\,\{1 + [\eta\zeta - (\eta\mathbf{n})(\zeta\mathbf{n})] + (\eta\mathbf{n})(\zeta\mathbf{n})\}$$
$$+ (C_S' C_S'^* + C_P C_P^*)\,(1 - \varepsilon)\,(\varepsilon - u)\,\{1 - [\eta\zeta - (\eta\mathbf{n})(\zeta\mathbf{n})] + (\eta\mathbf{n})(\zeta\mathbf{n})\}$$
$$+ (C_S C_S'^* + C_S' C_S^* + C_P C_P'^* + C_P' C_P^*)\,(1 - \varepsilon)\sqrt{\varepsilon^2 - u^2}\,\{\eta\mathbf{n} + \zeta\mathbf{n}\}$$
$$+ i\,(C_S' C_S^* - C_S C_S'^* + C_P C_P'^* - C_P' C_P^*)\,(1 - \varepsilon)\sqrt{\varepsilon^2 - u^2}\,\zeta\,[\eta\times\mathbf{n}],$$

$$V = (C_V C_V^* + C_A' C_A'^*)\,(\varepsilon - u)\,\{(3 - 2\varepsilon + u) + (1 + u)\,[\eta\zeta - (\eta\mathbf{n})\,(\zeta\mathbf{n})]$$
$$- (1 - 2\varepsilon - u)(\eta\mathbf{n})(\zeta\mathbf{n})\} + (C_V' C_V'^* + C_A C_A^*)\,(\varepsilon + u)\,\{(3 - 2\varepsilon - u)$$

$$
\begin{aligned}
&-(1-u)\,[\eta\zeta-(\eta\mathbf{n})(\zeta\mathbf{n})]-(1-2\varepsilon+u)(\eta\mathbf{n})(\zeta\mathbf{n})\}\\
&+(C_VC_V'^{*}+C_V'C_V^{*}+C_AC_A'^{*}+C_A'C_A^{*})\sqrt{\varepsilon^2-u^2}\,\{(1-2\varepsilon+v)\,\eta\mathbf{n}\\
&-(3-2\varepsilon-v)\,\zeta\mathbf{n}\}+i\,(C_V'C_V^{*}-C_VC_V'^{*}+C_AC_A'^{*}-C_A'C_A^{*})\sqrt{\varepsilon^2-u^2}\,(1-v)\,\zeta\,[\eta\times\mathbf{n}],\\
T=&(C_TC_T^{*}+C_T'C_T'^{*})\{\varepsilon(3-\varepsilon)-2u^2-u(1-\varepsilon)\,[\eta\zeta-(\eta\mathbf{n})(\zeta\mathbf{n})]\\
&-[\varepsilon(1+\varepsilon)-2u^2](\eta\mathbf{n})(\zeta\mathbf{n})\}+(C_TC_T'^{*}+C_T'C_T^{*})\sqrt{\varepsilon^2-u^2}\\
&\times\{(3-\varepsilon-2v)\,\mathbf{n}\zeta-(1+\varepsilon-2v)\,\mathbf{n}\eta\};\\
&\varepsilon=E_e/w,\quad u=m_e/w,\quad v=m_e^2/m_\mu w,\quad w=(m_\mu^2+m_e^2)/2m_\mu.
\end{aligned}
\tag{II}
$$

The expression proportional to $\zeta[\mathbf{n}\times\eta]$ determines the transverse polarization of the electrons, perpendicular to the plane $\eta\mathbf{n}$. For conservation of the parity with respect to time reversal, when all the constants C and C′ are real, it can be seen from Eq. (II) that this type of polarization is absent. The expression proportional to $[\eta\zeta-(\eta\mathbf{n})(\zeta\mathbf{n})]$ determines the transverse polarization of the electrons in the plane $\eta\mathbf{n}$.

If we stipulate that the formula (II) describes the decay of the $\mu^+$ meson, then in order to get the formula for the $\mu^-$ meson we must make the replacements

$$C_S,\ C_A,\ C_P,\ C_V',\ C_T'\to C_S^{*},\ C_A^{*},\ C_P^{*},\ C_V'^{*},\ C_T'^{*}$$
$$C_S',\ C_A',\ C_P',\ C_V,\ C_T\to -C_S'^{*},\ -C_A'^{*},\ -C_P'^{*},\ -C_V^{*},\ -C_T^{*}.$$

Various special cases of the formula (II) have been obtained previously in a number of papers. Thus, if we average Eq. (II) with respect to the spin states of the $\mu$ meson and the electron ($\eta=0$, $\zeta=0$), then we have the expression for the electron spectrum first obtained by Tiomno, Wheeler, and Rau[15] and by Michel.[16] If we average Eq. (II) only over the polarizations of the electron ($\zeta=0$), we get the expression obtained by Rudik and one of the present writers[9] (on the assumption $m_e=0$), by Bouchiat and Michel[10] ($m_e\neq 0$), by Kinoshita and Sirlin[11] ($m_e=0$), and by Larsen, Lubkin, and Tausner[12] ($m_e=0$). If we assume that the conditions (1) and (2) hold, then from Eq. (II) we get a formula analogous to those contained in the papers of Kinoshita and Sirlin[17] ($m_e=0$), Überall,[18] and Candlin ($m_e\neq 0$). A formula analogous to Eq. (II) for the case when only the tensor interaction is absent has been obtained by Sharp and Bach[20] ($m_e\neq 0$).

If we set all the primed constants C′ equal to zero and take $m_e=0$, Eq. (II) goes over into the formula obtained by one of the present writers[21] for the Hamiltonian conserving parity.

The writers express their gratitude to V. N. Gumen for aid in carrying out the calculations.

[1] A. Salam, Nuovo cimento **5**, 299 (1957).
[2] L. Landau, J. Exptl. Theoret. Phys. (U.S.S.R.) **32**, 405 (1957); Soviet Phys. JETP **5**, 336 (1957).
[3] T. D. Lee and C. N. Yang, Phys. Rev. **105**, 1671 (1957).
[4] R. Feynman and M. Gell-Mann, Phys. Rev. **109**, 193 (1958).
[5] R. Marshak and E. Sudarshan, Phys. Rev. (in press).
[6] M. Lederman, Notes of the Seventh Rochester Conference, 1957.
[7] Culligan, Frank, and Klyver, Notes of the Conference in Venice, 1957.
[8] Garwin, Lederman, and Weinrich, Phys. Rev. **105**, 1415 (1957).
[9] L. Okun' and A. Rudik, J. Exptl. Theoret. Phys. (U.S.S.R.) **32**, 627 (1957), Soviet Phys. JETP **5**, 520 (1957).
[10] C. Bouchiat and L. Michel, Phys. Rev. **106**, 170 (1957).
[11] T. Kinoshita and A. Sirlin, Phys. Rev. **107**, 593 (1957).
[12] Larsen, Lubkin, and Tausner, Phys. Rev. **107**, 856 (1957).
[13] A. Lenard, Phys. Rev. **90**, 968 (1953).
[14] L. Michel and A. S. Wightman; Phys. Rev. **98**, 1190 (1955).
[15] Tiomno, Wheeler, and Rau, Revs. Mod. Phys. **21**, 144 (1949).
[16] L. Michel, Proc. Phys. Soc. **A63**, 514 (1950).
[17] T. Kinoshita and A. Sirlin, Phys. Rev. **106**, 1110 (1957).
[18] H. Überall, Nuovo cimento **6**, 376 (1957).
[19] D. J. Canclin, Nuovo cimento **6**, 390 (1957).
[20] R. T. Sharp and G. Bach, Canad. J. Phys. **35**, 1199 (1957).
[21] L. B. Okun', Dokl. Akad Nauk SSSR **104**, 840 (1955).

Translated by W. H. Furry
250

# THE INTERACTION OF ELECTRONS WITH LATTICE VIBRATIONS

S. V. TIABLIKOV and V. V. TOLMACHEV

Mathematics Institute, Academy of Science, U.S.S.R.

Submitted to JETP editor December 10, 1957

J. Exptl. Theoret. Phys. (U.S.S.R.) **34**, 1254-1257 (May, 1958)

This work investigates the stability of the lattice is investigated with account of the interaction of the electrons with the phonon field. A criterion for stability is established without the aid of perturbation theory.

In his well known work, Wentzel[1] investigated the limits of applicability of perturbation theory to the interaction of electrons with the phonon field. By calculating the second-order correction to the phonon self-energy in perturbation theory, he found that the velocity of sound of the phonons is renormalized by writing

$$s = s_0(1-\rho), \quad \rho = (g^2/2\pi^2)\,k_F^2/\varepsilon'(k_F), \tag{1}$$

where $s_0$ is the velocity of sound before renormalization, $s$ is its renormalized value, $k_F$ is the wave vector at the Fermi boundary, $\epsilon'(k_F)$ is the derivative of the electron self-energy with respect to the wave vector, and $g$ is the coupling constant. Wentzel concludes that a necessary condition for the applicability of perturbation theory is that

$$\rho \ll 1. \tag{2}$$

As to what will occur if (2) is not satisfied, Wentzel asserts, on the basis of an analysis of the one-dimensional problem, that if in this case the coupling constant is sufficiently great, the phonon self-energy will become imaginary rather than negative. This, in turn, leads to breakdown of the lattice. We shall show below how an exact criterion for the stability of a crystal lattice can be established without the aid of perturbation theory.

We start with the Hamiltonian describing the interaction of electrons with lattice vibrations in the form proposed by Fröhlich. This is

$$H = H_0 + H_{\text{int}},$$

where

$$H_0 = \sum_{k,\sigma} \varepsilon(k)\, a_{k\sigma}^+ a_{k\sigma} + \sum_q \hbar\omega(q)\, b_q^+ b_q, \tag{3}$$

$$H_{\text{int}} = \frac{g}{\sqrt{2V}} \sum_{k,k',\sigma} \sqrt{\hbar\omega(k'-k)}\,(a_{k'\sigma}^+ a_{k\sigma} b_{k'-k} + a_{k\sigma}^+ a_{k'\sigma} b_{k'-k}^+),$$

in which $a_{k\sigma}^+$ and $a_{k\sigma}$ are electron creation and annihilation operators, $b_k^+$ and $b_k$ are phonon creation and annihilation operators, and $V$ is the volume of the region of periodicity.

In what follows we shall be interested in phonons whose energies are so low that

$$\hbar\omega \ll \Delta\varepsilon,$$

where $\Delta\epsilon$ is the mean energy difference in electron transitions. A rather good idea of the situation which arises can be obtained with the aid of the so-called adiabatic approximation in the form given by Bogoliubov and Tiablikov.[2,3] In agreement with the basic concept of this approximation, we shall formally introduce in (3) a small parameter into the phonon frequency $\hbar\omega$ and project our Hamiltonian with the necessary accuracy onto the subspace of states each of which is an electron Fermi vacuum.* We obtain

$$(E-E_0)\Phi = \sum_q (\hbar\omega(q)\, b_q^+ b_q - g^2\hbar\omega(q)\, A(q) \times (b_q b_{-q} + b_q^+ b_q + b_q b_q^+ + b_q^+ b_{-q}^+))\,\Phi, \tag{4}$$

where $\Phi$ is the wave function in the above-mentioned subspace,

$$E_0 = 2 \sum_{|k|<k_F} \varepsilon(k)$$

is the energy of the Fermi vacuum, and

$$A(q) = \frac{1}{V} \sum_{\substack{|k|<k_F \\ |k+q|>k_F}} \frac{1}{\varepsilon(k+q)-\varepsilon(k)}. \tag{5}$$

Equation (4) is easily solved, since the Hamiltonian entering into it is a quadratic form in the Bose operators. We set up the secular equations (for more details see Bogoliubov and Tiablikov[3] and the monograph mentioned in the last footnote)

*A detailed description of the technique of projection can be found in N. N. Bogoliubov's monograph Лекції з квантової статистики (Lectures on Quantum Statistics) (in Ukranian).

$$(\hbar\omega(q) - 2g^2\hbar\omega(q)A(q) - E)C_q - 2g^2\hbar\omega(q)A(q)C^+_{-q} = 0,$$
$$(\hbar\omega(q) - 2g^2\hbar\omega(q)A(q) + E)C^+_{-q} - 2g^2\hbar\omega(q)A(q)C_q = 0, \quad (6)$$

where $C_q$ and $C^+_q$ are treated as c-numbers, and E is the energy of an elementary excitation (the energy difference between an excited state and the ground state). The condition that (6) be a soluble set of equations is that its determinant vanish.

Solving (6), we obtain

$$E(q) = \hbar\omega(q)\sqrt{1 - 4g^2A(q)} \quad (7)$$

(it follows from the general theory that the negative root of (6) may be ignored). Equation (7) shows immediately that if $g^2$ is sufficiently large, E(q) becomes imaginary so that the state under consideration becomes unstable due to the breakdown of the crystal lattice. Thus the criterion for stability is

$$4g^2A(q) < 1, \quad (8)$$

for all q. Noting that $\epsilon(q) = \hbar^2q^2/2m$, we can calculate the integral in (5). Calculation gives

$$4g^2A(q) = \rho f(x), \quad (9)$$

where

$$f(x) = 1 + \frac{4-x^2}{4x}\ln\left|\frac{x+2}{x-2}\right|; \quad x = \frac{q}{k_F}. \quad (10)$$

The function f(x) takes on its maximum value f = 2 at x = 0. If this maximum value is used in the stability condition (8), we obtain finally

$$\rho \leqslant 1/2. \quad (11)$$

Since it is the phonons with low momenta, and therefore also with low energies, which are responsible for the breakdown of the crystal lattice, we have an a posteriori verification of the consistency of the approximation being used.

It is interesting to note that if, in the spirit of perturbation theory, we had expanded the root of (7) in powers of $\rho$, we would have obtained just Wentzel's Eq. (1). We note also that the stability criterion of (1) remains valid if we project the original Hamiltonian on a subspace of states close to the Fermi vacuum such as, in particular, the superconducting state.

We have treated the case in which the Hamiltonian does not involve the Coulomb interaction of electrons. When the Coulomb interaction is included, the stability criterion (8) will differ because of the different variation of A(q) for small q. One may suppose, however, that the lattice will remain unstable for sufficiently high coupling constants.

We have established the stability criterion in the adiabatic approximation. We will now show that the same expression is easily obtained by using the principle of compensation of "dangerous" diagrams.[4]

Let us perform the canonical transformation

$$b_q + b^+_{-q} = \sqrt{\frac{\omega(q)}{\Omega(q)}}(B_q + B^+_{-q});$$
$$b_q - b^+_{-q} = \sqrt{\frac{\Omega(q)}{\omega(q)}}(B_q - B^+_{-q}), \quad (12)$$

on the Bose operators $b_k$, where $\Omega(q)$ is the renormalized phonon energy, which will be found below. Equation (3) then becomes

$$H = E_0 + H_0 + H_1$$
$$E_0 = \frac{1}{2}\sum_q(\hbar\Omega(q) - \hbar\omega(q));$$
$$H_0 = \sum_{k,\sigma}\varepsilon(k)a^+_{k\sigma}a_{k\sigma} + \sum_q\hbar\Omega(q)B^+_qB_q;$$
$$H_1 = \frac{g}{\sqrt{2V}}\sum_{k,\sigma,q}\sqrt{\hbar\Omega(q)}\,\frac{\omega(q)}{\Omega(q)}(a^+_{k+q,\sigma}a_{k\sigma}B_q + a^+_{k-q,\sigma}a_{k\sigma}B^+_q)$$
$$+ \sum_q\hbar\Omega(q)\,\frac{\omega^2(q) - \Omega^2(q)}{4\Omega^2(q)}$$
$$\times (B_{-q}B_q + B^+_qB^+_{-q} + B^+_qB_q + B_{-q}B^+_{-q}). \quad (13)$$

We shall treat the term $H_1$ as a perturbation. It should be noted that the second term in $H_1$ is in fact of order $g^2$.

Let us now determine $\Omega$ from the requirement that in the second approximation in g all diagrams with two phonon lines at the output must compensate.[4] This leads to an equation for the heretofore unknown function $\Omega(q)$. As a result we obtain

$$\Omega^2(q) = \omega^2(q)\left\{1 - \frac{4g^2}{V}\sum_{\substack{|k|<k_F\\ |k-q|>k_F}}\frac{1}{\varepsilon(k-q) - \varepsilon(k) + \hbar\Omega(q)}\right\}, \quad (14)$$

and we may make the approximation

$$\Omega(q) = \omega(q)\left\{1 - \frac{4g^2}{V}\sum_{|k|<k_F,\ |k-q|>k_F}\frac{1}{\varepsilon(k-q) - \varepsilon(q) + \hbar\omega(q)}\right\}^{1/2}. \quad (15)$$

It is clear that the lattice will be stable if the expression in curly brackets in (14) or (15) is positive. It is easily seen that this condition

$$\frac{4g^2}{V}\sum_{|k|<k_F,\ |k-q|>k_F}\frac{1}{\varepsilon(k-q) - \varepsilon(q) + \hbar\omega(q)} > 1$$

becomes identical with (8) if the term $\hbar\omega(q)$ is neglected in the denominator.

It should be noted that obtaining $\Omega$ from the requirement that the "dangerous" diagrams compen-

sate in the second order in g is equivalent to obtaining it by minimizing the ground state energy to the same approximation in g. One may suppose that this equivalence will be true also in higher orders in g.

The authors take this opportunity to express their gratitude to N. N. Bogoliubov for discussing the work.

[1] G. Wentzel, Phys. Rev. **83**, 168 (1952).
[2] N. N. Bogoliubov and S. V. Tiablikov, Вестник МГУ (Bulletin, Moscow State Univ.) **3**, 35, (1949); J. Exptl. Theoret. Phys. (U.S.S.R.) **19**, 151 (1949).
[3] N. N. Bogoliubov and S. V. Tiablikov, J. Exptl. Theoret. Phys. (U.S.S.R.) **19**, 257 (1949).
[4] N. N. Bogoliubov, J. Exptl. Theoret. Phys. (U.S.S.R.) **34**, 58 (1958), Soviet Phys. JETP **7**, 41 (1958).

Translated by E. J. Saletan
251

SOVIET PHYSICS JETP VOLUME 34 (7), NUMBER 5 NOVEMBER, 1958

# *RADIATIVE CORRECTIONS TO COMPTON SCATTERING TAKING INTO ACCOUNT POLARIZATION OF THE SURROUNDING MEDIUM*

M. I. RIAZANOV

Moscow Engineering-Physical Institute

Submitted to JETP editor December 16, 1957

J. Exptl. Theoret. Phys. (U.S.S.R.) **34**, 1258-1266 (May, 1958)

A general method for taking into account polarization of the medium in the calculation of radiative corrections in phenomenological quantum mechanics is developed. The effect of a nonconducting medium on radiative corrections to Compton scattering is taken into account for an arbitrary dependence of the dielectric constant of the medium on frequency. It is shown that in some cases, account of the medium substantially changes the cross section in the region of small scattering angles.

## 1. INTRODUCTION

THE influence of the medium in the calculation of higher approximations in perturbation theory must, in general, be taken into account, because the integrations over the 4-momenta of virtual photons include a region of long-wave photons for which it is impossible to ignore the presence of neighboring atoms of the medium. This situation was first indicated by Landau and Pomeranchuk,[1] who noted that multiple scattering by the atoms of the medium should lead to a change in radiative corrections in those cases in which infrared catastrophes occur, i.e., where the region of soft quanta is essential. Ter-Mikaelian[2] noted that the difference of the dielectric constant of the medium from unity for soft quanta should strongly influence the radiative corrections.

A method of taking into account the multiple scattering by atoms of the medium was developed by Migdal.[3] In the following, we consider the influence of the medium on radiative corrections, connected with the difference of the dielectric constant and magnetic permeability of the medium, $\epsilon$ and $\mu$, from unity in the region of soft quanta; we shall not take account of multiple scattering.

In order to develop a general method for taking into account the polarization of the medium in higher orders of perturbation theory, it is convenient to use a generalization by the author[4] of the Feynman-Dyson covariant perturbation theory to the case of phenomenological quantum electrodynamics in media. The general method obtained in this way will be applied to the Compton scattering, in order to obtain the cross section of sixth power in e, with account of the polarization of the

surrounding medium. The notation of Feynman[5] will be used.

## 2. COVARIANT PERTURBATION THEORY

In the formulation of the Heisenberg representation[4] of phenomenological quantum electrodynamics in media, it is easy to see that the only difference of the theory from electrodynamics in vacuo is the equation for the potential of the electromagnetic field and the commutation relations for the operators of the noninteracting electromagnetic field. The supplementary relation can be put in the same form as in electrodynamics in vacuo by using a covariant method of separation of the longitudinal and scalar components of the potential, analogous to that employed in Ref. 6. Therefore, in the formulation of the perturbation theory, the usual Green's function for the photon will be replaced everywhere by the Green's function

$$G_{\lambda\nu}(x, x') = (2\pi)^{-2}\int d^4k g_{i\lambda}\{k_\rho^2 + \varkappa (u_\rho k_\rho)^2\}^{-1} g_{i\nu} \exp ik(x - x'), \tag{1}$$

where $\varkappa = \epsilon\mu - 1$, $u_\nu$ is the 4-velocity of the medium, and $e_{i\nu}$ are the unit 4-vector directions of polarization of the photon, such that

$$e_{i\lambda}e_{i\nu} = \delta_{\lambda\nu}; \quad e_{i\lambda}e_{j\lambda} = \delta_{ij}; \tag{2}$$

$$g_{i\nu} = \mu^{1/2}e_{i\sigma}(\delta_{\nu\sigma} - u_\nu u_\sigma [1 - (1 + \varkappa)^{-1/2}]). \tag{3}$$

In the following we shall take the imaginary parts of $\epsilon$ and $\mu$ to be small, limiting the consideration to dispersion in the region of transparency. It should be noted that the usual choice of sign of the imaginary parts of $\epsilon$ and $\mu$ does not lead to a causal Green's function, but to a retarded one, as can be seen from the fact that in going over to the vacuum, the way of going around the pole is not the same as that of Feynman. (This is connected with the fact that only retarded potentials were employed in the derivation of the expressions for $\epsilon$ and $\mu$.) Therefore, the prescription for going around the pole in Eq. (1) should be obtained from the requirement that (1) be the causal Green's function.[7] The prescription obtained from this can be, for example, given for positive frequencies in the form of the condition that there be an infinitesimal absorption, and for negative frequencies in the form of the requirement of symmetry of the theory with respect to past and future.

As is well known, in a dispersive medium, $\epsilon$ and $\mu$ are functions of that invariant variable, which, in the system of the medium, becomes the frequency. The only variable of this type is the scalar uk, and $\epsilon$, $\mu$, and $\varkappa$ are functions of it.

Thus, $\varkappa$ and $\mu$ are, in general, some complicated operators, and this leads to additional difficulties in formulating the theory. In order to get rid of these difficulties, it is possible from the very beginning to consider the theory in the momentum representation; however, one can obtain the same results by employing the usual simple method, introducing the dependence of $\varkappa$ and $\mu$ on uk only after going to the momentum representation.

Just as in the case of the vacuum, all divergences in the region of large momenta can be eliminated by renormalization of mass and charge. Consideration of possible types of diagrams shows that all conclusions about number and behavior of primitive divergences obtained for electrodynamics in vacuo[8] remain valid for electrodynamics in media. This follows from the fact that in the region of large momenta, $\epsilon$ and $\mu$ tend to unity and the matrix element for an arbitrary process in media in the region of large momenta coincides with the expression for the matrix element of the same process in vacuo.

The general rule for eliminating divergences from the scattering matrix element, analogous to that obtained by Dyson[8] for electrodynamics in vacuo, consists in subtracting several terms in an expansion of the divergent matrix element in $\hat{k}$ or $(\hat{p} - m)$, where one must set $\epsilon = \mu = 1$ in the subtracted matrix elements, i.e., these terms must be defined from the corresponding matrix element for the process in vacuo. The latter condition comes from the fact that the subtracted terms correspond to unobservable effects. The number of subtracted terms should be the minimum number for convergence of the remainder, which is that value matrix-element having physical significance.

Thus, the finite part of the self energy of an electron in media will differ from that in vacuo, leading to a difference in the mass of a free electron in media from that of a free electron in vacuo. From this it follows that after renormalization of the Green's function for an electron in media is carried out, it coincides with the Green's function for an electron in vacuo only in the zero order approximation of perturbation theory.

Taking account of the subsequent terms in perturbation theory leads to the appearance of additions to the mass if the electron moves in media, but not if it is in vacuo.

This leads to an essential difference in the Green's functions for a free electron in media and in vacuo, in spite of the fact that the equation for the operators of the electron-positron field in media has the same form as that in vacuo. The

finite additions to the electron mass in the Green's function are essential in the infrared region and lead to the fact that the so called infrared catastrophe never arises in media. This effect, in essence, is a result of the fact that, strictly speaking, the electron moving in the potential field of the atoms of the medium cannot be considered as free, and therefore $p^2 \neq m^2$.

From this it follows that in order to eliminate the infrared catastrophe for electrodynamics in media, it is sufficient to take into account the corrections to the electron Green's function from the emission and absorption of a single virtual quantum, i.e., the change in mass connected with calculation of the self-energy diagram of second order. From the result in the same order, it is possible to obtain the expression for the Green's function of the electron in media in the form

$$i\,(2\pi)^{-2}\int d^4p\,(\hat{p} - m - \Delta)^{-1}\exp ik\,(x - x'), \qquad (4)$$

where $\Delta$ is the difference in the change in mass for a free electron in media and in vacuo. We note that $\Delta$ depends on the invariants m and up, i.e., on the energy of the electron relative to the medium.

In the future, we consider only the experimentally observed cross section of Compton scattering, in which the possibility of production of additional soft quanta, not registered by the apparatus, is taken into account. Then the cross section in the region of soft quanta drops out of consideration, the infrared catastrophe does not arise, and it is not necessary to take account of $\Delta$ in Eq. (4).

## 3. COMPTON SCATTERING

In considering the influence of the medium on Compton scattering, it is of greatest interest to represent the scattering of photons sufficiently hard in the system of the medium so that $\epsilon$ and $\mu$ can be considered equal to unity for the frequencies of both the incident and scattered photons. The influence of the medium in this case will show up only in the virtual quanta and, consequently, the matrix element of second order in e for Compton scattering will not depend on polarization of the medium. (The corresponding diagrams do not include virtual photons.)

The matrix element of fourth order in e includes virtual photons and, consequently, will depend on the presence of the medium. We shall calculate the radiative corrections by the method of Feynman.[5]

Since the radiative corrections for Compton scattering were calculated in the work of Feynman and Brown,[9] it is then necessary for us to find the difference between radiative corrections in media and in vacuo. In view of the fact that we restrict the calculation to only terms of sixth order in e in the cross section, the matrix element of fourth order enters into the cross section linearly, so that we only need to calculate the difference of the matrix elements of fourth order for Compton scattering in media and in vacuo. This significantly simplifies the necessary calculations, since in the region of large momenta the difference of matrix elements which interests us goes to zero.

Denoting the 4-momenta of the incident and scattered photons by $k_1$ and $k_2$, respectively, and describing the initial and final states of the electron by the 4-momenta $p_1$ and $p_2$ and the spinors $v_1$ and $v_2$, it is easy to obtain the well known expression for the matrix element of second order

$$W^0_{st} = \hat{e}_s\,(\hat{p}_1 + \hat{k}_1 - m)^{-1}\hat{e}_t + \hat{e}_t\,(\hat{p}_1 - \hat{k}_2 - m)^{-1}\hat{e}_s, \qquad (5)$$

in which the 4-vector polarizations of the incident and emitted photons are denoted by $e_s$ and $e_t$.

The diagrams of fourth order for Compton scattering are given in Refs. 10, 5, and 9. The difference of fourth-order matrix elements which interests us does not contain divergences in the ultra violet region; therefore, for simplicity, we shall not explicitly introduce the Feynman cut off factor.

We write the matrix element of fourth order for Compton scattering in vacuo in the form

$$W^{(1)}_{st}(0, \lambda) = \int d^4q\,(q^2 - \lambda^2)^{-1}F_1(q), \qquad (6)$$

where $F_1(q)$ is a matrix function of momenta and polarization of the electron and the photons, $\lambda$ is a fictitious mass of the photon, which is introduced in electrodynamics in vacuo in order to eliminate the infrared catastrophe.

The explicit form of $F_1(q)$ was obtained by Brown and Feynman.[9] As noted above, in media the infrared catastrophe does not arise; however, in the following it is also convenient to introduce $\lambda$ into the matrix element of fourth order for Compton scattering in media, denoting it by $W^1_{st}(\kappa, \lambda)$:

$$W^{(1)}_{st}(\varkappa, \lambda) = \int \frac{\mu d^4q}{q^2 + \varkappa (uq)^2 - \lambda^2}\left\{F_1(q) - \frac{\varkappa}{1+\varkappa}F_2(q)\right\}, \qquad (7)$$

where $F_2(q)$ differs from $F_1(q)$ only by the replacement of the 4-vector polarizations of the virtual photon by the 4-velocity of the medium, $u_\nu$.

Calculating the integral in Eq. (7)

$$\int d^4q\,(q^2 - a^2 - \lambda^2)^{-1}F_1(q),$$

in which $a^2$ is determined from the asymptotic form of $\kappa$ for large uq:

$$\varkappa(uq) \approx -(a/uq)^2; \quad a^2 = 4\pi ZNe^2/m, \tag{8}$$

it is easy to transform Eq. (7) to the form

$$W_{st}^{(1)}(\varkappa, \lambda) = W_{st}^{(1)}(0, \sqrt{a^2+\lambda^2}) + \int \frac{d^4q}{q^2-a^2-\lambda^2} \left\{ \frac{(\mu-1)q^2 - \mu a^2 - \varkappa(uq)^2}{q^2+(uq)^2\varkappa-\lambda^2} \right\} F_1(q) - \int \frac{d^4q}{q^2+(uq)^2\varkappa-\lambda^2} \frac{\mu\varkappa}{1+\varkappa} F_2(q). \tag{9}$$

The second term in Eq. (9) differs from the integral in Eq. (6) only by the presence in the integrand of the additional factor

$$\left(\frac{q^2-\lambda^2}{q^2-a^2-\lambda^2}\right)\left(\frac{(\mu-1)q^2-\mu a^2-\varkappa(uq)^2}{q^2+(uq)^2\varkappa-\lambda^2}\right),$$

which is small for $q^2 \gg a^2$, $\omega_1^2$ or $(uq)^2 \gg a^2, \omega_1^2$. This means that the region of q essential for the integration is bounded, in the system of coordinates connected with the medium, so that the values of all components of the 4-momentum of the virtual photon $q_\nu$ are small compared with the momentum transfer $\xi > a$.

If terms of order $a/\xi$ and $\omega_i/\xi$ (where $\omega_i$ is the proper frequency) are neglected henceforth, then the calculation of the integral considered is limited to the first nonvanishing term in the expansion of $F_1(q)$ in powers of q.

Analogous considerations can be made also for the third term in Eq. (9), since $F_2(q)$ has the same structure as $F_1(q)$.

Employing an expansion in powers of q/m, it is easy to find that the principal contribution in the expression of interest comes from the diagrams denoted in Ref. 9 as J, M′, and M″. In the approximation indicated, it is possible to obtain the expression

$$W_{st}^{(1)}(\varkappa, \lambda) = W_{st}^{(1)}(0, \sqrt{a^2+\lambda^2}) + \frac{4e^2}{\pi i}\int \frac{d^4q\,[(\mu-1)q^2-\mu a^2-\varkappa(uq)^2]}{(q^2-a^2-\lambda^2)(q^2+(uq)^2\varkappa-\lambda^2)} W_{st}^0 \left\{ \frac{e_1p_1}{(p_1+q)^2-(m+\Delta)^2} - \frac{e_1p_2}{(p_2+q)^2-(m+\Delta)^2} \right\}^2 - \frac{4e^2}{\pi i}\int \frac{d^4q}{q^2+(uq)^2\varkappa-\lambda^2} \frac{\mu\varkappa}{1+\varkappa} W_{st}^0 \times \left\{ \frac{up_1}{(p_1+q)^2-(m+\Delta)^2} - \frac{up_2}{(p_2+q)^2-(m+\Delta)^2} \right\}^2, \tag{10}$$

in which $W_{st}^0$ and $\Delta$ are defined in Eqs. (5) and (4). The first term in Eq. (10) can be obtained from the result of Brown and Feynman by replacing $\lambda^2$ by $a^2+\lambda^2$. It is easy to see that Eq. (10) remains finite for $\lambda = 0$, if the $\Delta$ in the denominator is not neglected, and the infrared catastrophe does not arise. Therefore, there is no necessity of adding the cross section for double Compton scattering, integrated over the momentum of an additional small quantum, to that obtained from Eq. (10), as is done in the case of electrodynamics in vacuo to eliminate the infrared divergence. However, such an addition is desirable to carry out in order to take into account experimental conditions in which it is impossible to discriminate between single Compton scattering and double Compton scattering with emission of an additional quantum sufficiently small so that it is not registered by the experimental apparatus. It is natural for the experimentally-observed cross section to depend on the threshold of the apparatus, i.e., on the maximum energy of the photon $\omega_m$ for which the photon will not be measured.

Since in the following we will be interested only in the experimentally-observed cross section for Compton scattering, it is possible to neglect the quantity $\Delta$ in Eq. (10), disregarding $\lambda$ for convenience of calculation.

## 4. EXPERIMENTALLY-OBSERVED CROSS SECTION

Denoting the cross section for Compton scattering with account of terms of sixth order in e in vacuo and in media by $d\sigma_K(0, \lambda)$ and $d\sigma_K(\kappa, \lambda)$, respectively, we easily obtain from Eq. (10)

$$d\sigma_K(\varkappa, \lambda) = d\sigma_K(0, \sqrt{a^2+\lambda^2}) - \frac{4e^2}{\pi i} d\sigma_0 \times \int \frac{d^4q\,[(\mu-1)q^2-\mu a^2-\varkappa(uq)^2]}{(q^2-a^2-\lambda^2)(q^2+(uq)^2\varkappa-\lambda^2)} \left\{ \frac{e_1p_1}{q^2+2p_1q} - \frac{e_1p_2}{q^2+2p_2q} \right\}^2 + \frac{4e^2}{\pi i} d\sigma_0 \int \frac{d^4q}{(q^2+(uq)^2\varkappa-\lambda^2)} \frac{\mu\varkappa}{1+\varkappa} \left\{ \frac{up_1}{q^2+2p_1q} - \frac{up_2}{q^2+2p_2q} \right\}^2, \tag{11}$$

in which the usual cross section for the Compton effect without radiative corrections is denoted by $d\sigma_0$, where

$$d\sigma_0 = \left(\frac{e^2}{mc^2}\right)^2 \left(\frac{\omega_2^2}{2\omega_1^2}\right)\left(\frac{\omega_1}{\omega_2} + \frac{\omega_2}{\omega_1} - \sin^2\vartheta\right) d\Omega_2. \tag{12}$$

It is important to note that the integral over q in Eq. (11) was obtained for arbitrary $\epsilon$ and $\mu$; it was derived only by assuming absence of absorption and by assuming the asymptotic behavior of $\kappa$ for large uq, Eq. (8). Therefore, it is desirable to calculate the integrals without introducing additional assumptions about the specific form of $\epsilon$ and $\mu$. This is easy to do if, instead of integrating over components $q_\mu$, one integrates over components $Q_\mu$ and over s, connected with $q_\mu$ by the relations

$$s = uq; \quad Q_\mu = q_\mu - u_\mu u_\rho q_\rho; \quad q_\mu = Q_\mu + u_\mu s. \tag{13}$$

The indicated change of variables makes it possible to resolve the difficulty which arises in consideration of those forms of the dependence of $\epsilon$ on (uq), which do not lead to a single-valued in-

verse function $uq(\epsilon)$, i.e., to the situation where, in the system of the media, several frequencies of the particle correspond to one and the same momentum of the real photon. This difficulty arises in case one tries to carry out the integration in Eq. (11) just as in electrodynamics in vacuo, i.e., first over the fourth component of the 4-momentum of the virtual photon. The change of variables, Eq. (13), makes it possible to first carry out the integration over $Q_\nu$ and then over $s = uq$, so that the fact that $uq(\epsilon)$ is not single valued does not show up in the integration. In this way, the transformation, Eq. (13), makes it possible to generalize the usual methods of quantum electrodynamics to such types of dependency of $\epsilon$ on uq which occur in practice.

The integration over $Q_\nu$ can be conveniently carried out as in Ref. 7. For example, for an integral analogous to those in Eq. (11), one easily obtains

$$\int \frac{d^4k\,(1; k_\sigma)\,F(uk)}{(k^2-2pk-A(uk)+i\eta)^3} \qquad (14)$$

$$= \int_{-\infty}^{\infty} dsF(s) \int \frac{d^4Q\,\delta(uQ)\,(1; Q_\sigma + u_\sigma s)}{[Q^2-2pQ+s^2-2ups+A(s)+i\eta]^3}$$

$$= \frac{1}{16i}\int_{-\infty}^{\infty} \frac{dsF(s)\,(1; p_\sigma + u_\sigma(s-up))}{[s^2-2sup-A(s)+(up)^2-p^2+i\eta]^{3/2}}.$$

To obtain the experimentally observed cross section, it is necessary to put (11) together with the cross section for double Compton scattering, integrated over small values of the additional quantum.

It is convenient to write this cross section as a 4-dimensional integral over the 4-momentum of the additional small quantum, employing a method analogous to that proposed by Abrikosov[11] for quantum electrodynamics in vacuo

$$d\sigma_D(\varkappa, \lambda) = d\sigma_0 \frac{e^2}{\pi i}\int_{(uq)^2\leqslant\omega_m^2} \frac{4d^4q}{q^2+\varkappa(uq)^2-\lambda^2}$$

$$\times\left(\frac{g_l p_1}{(p_1+q)^2-(m+\Delta)^2} - \frac{g_l p_2}{(p_2+q)^2-(m+\Delta)^2}\right)^2, \qquad (15)$$

where the integration is carried out over a region bounded by the condition that the frequency of the additional quantum in the system of the medium, uq, does not exceed the threshold of the experimental apparatus.

Denoting by $d\sigma_D(0, \lambda)$ the cross section for the double Compton effect in vacuo [integrated over the momentum of the small quantum, as in Eq. (15)], it is easy to bring Eq. (15) to a form analogous to Eq. (11).

$$d\sigma_D(\varkappa, \lambda) = d\sigma_D(0, \sqrt{a^2+\lambda^2})$$

$$+\frac{4e^2}{\pi i}d\sigma_0 \int_{(uq)^2\leqslant\omega_m^2} \frac{d^4q\,[(\mu-1)q^2-\mu a^2-(uq)^2\varkappa]}{(q^2+(uq)^2\varkappa-\lambda^2)(q^2-a^2-\lambda^2)}$$

$$\times\left\{\frac{e_l p_1}{q^2+2p_1q} - \frac{e_l p_2}{q^2+2p_2q}\right\}^2 - \frac{4e^2}{\pi i}d\sigma_0 \qquad (16)$$

$$\times\int_{(uq)^2\leqslant\omega_m^2} \frac{d^4q}{(q^2+(uq)^2\varkappa-\lambda^2)}\frac{\mu\varkappa}{(1+\varkappa)}\left\{\frac{up_1}{q^2+2p_1q} - \frac{up_2}{q^2+2p_2q}\right\}^2$$

[where, just as in Eq. (11), $\Delta$ is neglected].

Putting together Eqs. (11) and (16), one easily finds for the experimentally observable cross section for Compton scattering

$$d\sigma = d\sigma_{\text{vac}} - \frac{4e^2}{\pi i}d\sigma_0 \int_{(uq)^2\geqslant\omega_m^2} \frac{d^4q\,[(\mu-1)q^2-\mu a^2-(uq)^2\varkappa]}{(q^2+(uq)^2\varkappa-\lambda^2)(q^2-a^2-\lambda^2)}$$

$$\times\left\{\frac{e_l p_1}{q^2+2p_1q} - \frac{e_l p_2}{q^2+2p_2q}\right\}^2 + \frac{4e^2}{\pi i}d\sigma_0 \qquad (17)$$

$$\times\int_{(uq)^2\geqslant\omega_m^2} \frac{d^4q}{q^2+(uq)^2\varkappa-\lambda^2}\frac{\mu\varkappa}{1+\varkappa}\left\{\frac{up_1}{q^2+2p_1q} - \frac{up_2}{q^2+2p_2q}\right\}^2,$$

in which the first term $d\sigma_{\text{vac}}$ does not depend on the properties of the medium, since in putting together $d\sigma_K(0, \lambda)$ and $d\sigma_D(0, \lambda)$, the terms depending on $\lambda$ cancel[9] and, consequently, $d\sigma_{\text{vac}}$ is the experimentally observable cross section for the Compton effect in vacuo. The second and third terms are corrections, connected with the polarization of the medium. The region of integration in them is bounded by the condition $(uq)^2 \geq \omega_m^2$, so that the integrals remain finite in the infrared region. This makes it possible to set $\lambda = 0$ in the future.

It should be noted that in the expression obtained there are terms with different powers of q in the denominators of the integrands. This is explained by the fact that in the form given, it was more convenient to employ a technique of covariant integration after the substitution (13). After the integration over Q, terms of higher order in s/m naturally had to be thrown away, since terms of these orders were dropped earlier.

We cannot consider values of $\omega_m$ very close to the proper frequencies of the atoms of the medium, since absorption in the medium has not been taken into account. Therefore, in our case the threshold of sensitivity of the apparatus cannot be less than the atomic frequencies. In this case $\mu$ can be considered equal to unity, which makes it possible to obtain from Eq. (17) the expression

$$\frac{d\sigma - d\sigma_{\text{vac}}}{d\sigma_0} = \frac{8e^2}{\pi i}\int_{\omega_m}^{\infty} ds\,(a^2+\varkappa s^2)$$

$$\times\int \frac{d^4Q\,\delta(uQ)}{(Q^2+s^2(1+\varkappa))(Q^2+s^2-a^2)}$$

$$\times\left[\frac{e_1p_1}{Q^2+2p_1Q+2sup_1+s^2}-\frac{e_1p_2}{Q^2+2p_2Q+2sup_2+s^2}\right]^2$$

$$+\frac{8e^2}{\pi i}\int\limits_{\omega_m}^{\infty}\frac{\varkappa ds}{1+\varkappa}\int\frac{d^4Q\,\delta(uQ)}{Q^2+s^2(1+\varkappa)} \qquad (18)$$

$$\times\left[\frac{up_1}{Q^2+2p_1Q+2sup_1+s^2}-\frac{up_2}{Q^2+2p_2Q+2sup_2+s^2}\right]^2$$

In the following, we consider the special case in which the electron is at rest in the medium before the collision. In this case it is possible to obtain the final formulas in an especially simple form. The momentum transfer will be equal to the momentum of the electron after the collision. Since a macroscopic description of properties of media is not possible for collisions with a large momentum transfer, we limit the calculation to only the first terms in an expansion in powers of the ratio of the momentum transfer to the mass. In this approximation, the second integral in Eqs. (17) and (18) is most important, containing the factor $\kappa/(1+\kappa)$ in the integrand. The final result can be conveniently written in the form of the ratio of the difference between the experimentally observable cross section of sixth power in e for Compton scattering in media and in vacuo to the cross section of fourth order in e for Compton scattering. In the first nonvanishing approximation in powers of the ratio $\xi/m$ and $q/\xi$, where $\xi$ is the momentum transfer and q is the 4-momentum of the virtual photon, one easily finds that

$$\frac{d\sigma-d\sigma_{\text{vac}}}{d\sigma_0}=\frac{e^2m}{2\pi\sqrt{2m}}\int\limits_{\omega_m}^{\infty}\frac{ds}{s^{3/2}}\frac{\varkappa(s)}{1+\varkappa(s)}\left\{1+y\left(1-2\ln\frac{2}{y}\right)\right\}, \qquad (19)$$

where it is assumed that $y^2=\frac{2ms}{\xi^2}<1$.

## 5. DISCUSSION OF RESULTS

The applicability of the formulas obtained is determined by the following considerations. It is well known (see, for example, Ref. 12) that a phenomenological description of the surrounding medium is possible for those collisions in which the longitudinal momentum transfer is sufficiently small so that its inverse is larger than the interatomic distances in the medium. Thus, Eq. (19) remains valid in the region of sufficiently small photon-scattering angles satisfying the condition

$$2\sin\frac{\vartheta}{2}<N^{1/6}\sqrt{\frac{m}{\omega_1(\omega_1+m)}}=\left(\frac{\pi}{2}Ze^2\frac{(m+\omega_1)\omega_1^3}{m^2a^2}\right)^{-1/6}, \qquad (20)$$

which relates to the case in which the electron is at rest before scattering. The notation $a^2=4\pi NZe^2/m$, where N is the number of atoms per unit volume and Z is the atomic charge, has been used.

This condition is of a general type, connected with a phenomenological description of media; besides this, the region of angles in which Eq. (19) is valid, is limited by the supplementary conditions under which (19) was derived. Since, for small scattering angles and for an initial photon energy comparable with rest mass energy of the electron, it is possible to consider $\xi^2\approx\omega_1^2\vartheta^2$, then instead of Eq. (20), the region of angles in which Eq. (19) is applicable, is limited by the condition

$$\vartheta>\frac{m}{\omega_1}\sqrt{\frac{\omega_m}{m}}, \qquad (20')$$

which, for example, for liquid hydrogen at a density $\sim 0.07$ g-cm$^{-3}$, $\omega_m\sim 30$ ev, $\omega_1\sim 0.5$ m, gives angles of the order of 1°.

To estimate the magnitude of the corrections connected with the presence of the medium, we consider a simple form of dependence $\kappa(s)$, obtained under the assumption that in the medium there is only one proper frequency.

$$\varkappa(s)=a^2(b^2-s^2)^{-1}. \qquad (21)$$

Using the explicit form $\kappa(s)$ of Eq. (21), it is easy to obtain from Eq. (19)

$$\frac{d\sigma-d\sigma_{\text{vac}}}{d\sigma_0}=\frac{e^2}{2\pi\sqrt{2}}\frac{a^2}{a^2+b^2}\left(\frac{m}{\omega_m}\right)^{1/2}\Phi\left(\sqrt{\frac{\omega_m}{\sqrt{a^2+b^2}}}\right), \qquad (22)$$

where $\Phi(z)$ is defined by

$$\Phi(z)=2-z\left[\tan^{-1}\frac{1}{z}+\frac{1}{2}\ln\left|\frac{1+z}{1-z}\right|\right].$$

In the case that $\omega_m$ is substantially larger than the atomic frequencies, the formula simplifies considerably:

$$\frac{d\sigma-d\sigma_{\text{vac}}}{d\sigma_0}=\frac{-e^2}{5\pi\sqrt{2}}\left(\frac{a^2}{\omega_m^2}\right)\sqrt{\frac{m}{\omega_m}}. \qquad (23)$$

The result shows that in this case, for liquid hydrogen of density $\sim 0.07$ g-cm$^{-3}$, a $\sim 7$ ev, b $\sim 10$ ev, for $\omega_m\sim 30$ ev and $\xi>5$ kev, we have from Eq. (23) $(d\sigma-d\sigma_{\text{vac}})/d\sigma_0=-0.3\times10^{-2}$, i.e., the medium corrections are comparable with the radiative corrections. Particularly large corrections are obtained, as can be seen from Eq. (19), when $\omega_m$ is near to a zero of the function $\epsilon(\omega)$. When $\omega_m$ exactly coincides with a zero of $\epsilon(\omega)$ [in the particular case (21), when $\omega_m=(a^2+b^2)^{1/2}$] the expression $(d\sigma-d\sigma_{\text{vac}})/d\sigma_0$ becomes infinite. This divergence has no physical significance and is connected with the fact that in our approximation of infinitesimal absorption it is not possible to consider frequencies close to zeros and to poles of $\epsilon(\omega)$. However, this circumstance can be an indication that for $\omega_m$ close to zero the real part of

$\epsilon(\omega)$ and, for small absorption, the corrections connected with the medium, will be anomalously large.

In the experimental study of radiative corrections, it must be kept in mind that the accidental coincidence of $\omega_m$ with a zero of the real part of $\epsilon(\omega)$ can substantially distort the results for small scattering angles.

With diminishing momentum transfer $\xi$, i.e., with decreasing angle of scattering, the ratio $(d\sigma - d\sigma_{vac})/d\sigma_0$ decreases to zero, from which it follows that corrections of large magnitude coming from the medium can be expected only at certain scattering angles.

Thus, in the experimental measurement of the cross section for Compton scattering at small angles, it is necessary to take into account the possibility of a significant change in the differential cross section as a result of the influence of the medium.

In conclusion, I would like to use this opportunity to express deep gratitude to E. L. Feinberg for suggesting this problem and constant interest in this work, and M. L. Ter-Mikaelian for valuable discussion.

[1] L. D. Landau and I. Ia. Pomeranchuk, Dokl. Akad. Nauk SSSR **92**, 735 (1953).

[2] M. L. Ter-Mikaelian, Izv. Akad. Nauk SSSR, Ser. Fiz. **19**, 657 (1955) [Columbia Tech. Transl. p. 595].

[3] A. B. Migdal, Dokl. Akad. Nauk SSSR **96**, 49 (1954); **105**, 77 (1955).

[4] M. I. Riazanov, J. Exptl. Theoret. Phys. (U.S.S.R.) **32**, 1244 (1957); Soviet Phys. JETP **5**, 1013 (1957).

[5] R. P. Feynman, Phys. Rev. **76**, 749, 769 (1949).

[6] J. Schwinger, Phys. Rev. **74**, 1439 (1948).

[7] N. N. Bogoliubov and D. V. Shirkov, Введение в теорию квантованных полей (Introduction to the Theory of Quantized Fields), M. 1957.

[8] F. J. Dyson, Phys. Rev. **75**, 1736 (1949).

[9] L. M. Brown and R. P. Feynman, Phys. Rev. **85**, 231 (1952).

[10] A. I. Akhiezer and V. B. Berestetskii, Квантовая электродинамика (Quantum Electrodynamics), M. 1953. [Transl., publ. by U. S. Dept. of Commerce]

[11] A. A. Abrikosov, J. Exptl. Theoret. Phys. (U.S.S.R.) **30**, 96 (1956), Soviet Phys. JETP **3**, 71 (1956).

[12] E. L. Feinberg, Usp. Fiz. Nauk **58**, 198 (1956).

Translated by G. E. Brown
252

SOVIET PHYSICS JETP VOLUME 34(7), NUMBER 5 NOVEMBER, 1958

# *ON THE THEORY OF THE THERMAL CONDUCTIVITY AND ABSORPTION OF SOUND IN FERROMAGNETIC DIELECTRICS*

A. I. AKHIEZER and L. A. SHISHKIN

Khar'kov State University

Submitted to JETP editor December 12, 1957

J. Exptl. Theoret. Phys. (U.S.S.R.) **34**, 1267-1271 (May, 1958)

The temperature dependence of the thermal conductivity and the coefficient of absorption of sound in ferromagnetic dielectrics is determined. It is shown that spin waves play the principal role in these processes at low temperatures.

1. As is well known, the kinetic properties of ordinary dielectrics are determined by the phonon spectrum. In ferromagnetic dielectrics the elementary excitations consist of spin waves in addition to phonons. It is therefore of interest to ascertain the role of the spin waves in thermal conduction and sound absorption in these substances.

We will show that at low temperatures the thermal conductivity in an unbounded ferromagnetic dielectric which contains no impurities is deter-

mined principally by the interactions of spin waves with each other and with phonons. If the Curie temperature $\Theta_c$ is lower than the Debye temperature $\Theta$, the temperature dependence of the thermal conductivity is determined not by the exponential factor $\exp(\Theta/2T)$, as in ordinary dielectrics,[1] but by the factor $\exp(\Theta_c/4T)$.

The dissipation function of a ferromagnetic dielectric at low temperatures in the presence of a sound field is also determined by the interaction of spin waves with each other, and turns out not to depend on the temperature, while in ordinary dielectrics it is inversely proportional to the temperature.

**2.** The principal elementary interaction processes in a system of spin waves and phonons, which we shall take into account here, are the conversion of two phonons into one phonon, the conversion of two spin waves into one spin wave, the scattering of a spin wave by a phonon, and the conversion of two spin waves into one phonon. The respective probabilities of these processes are as follows:[2]

$$W_{f,\,-f',\,-f''} = (\Theta a\hbar/\rho)\, ff'f'', \tag{1}$$

$$W_{k,\,-k',\,-k''} = \frac{64\pi^3 w^2 a^3}{\hbar} \left|\sin 2\vartheta' e^{i\varphi'} + \sin 2\vartheta'' e^{i\varphi''}\right|^2, \tag{2}$$

$$W_{f,\,-k',\,-k} = \frac{2\pi\Theta_c^2 a^3}{\Theta\rho}\frac{\hbar}{f}\left|2(\mathbf{kf})(\mathbf{e}_f, \mathbf{k}+\mathbf{f}) + \mathbf{e}_f(\mathbf{k}f^2 + \mathbf{f}k^2)\right|^2, \tag{3}$$

$$W_{f,\,-k',\,-k} = \frac{4\pi^3 w^2}{\Theta a}\frac{\hbar}{\rho}\frac{1}{f}\left|f^- e_f^- + 2\mathbf{k}\mathbf{e}_f \sin^2\vartheta e^{-2\varphi i}\right.$$

$$\left. + 2\mathbf{k}'\mathbf{e}_f \sin^2\vartheta' e^{-2i\varphi'}\right|^2, \tag{4}$$

where $\mathbf{f}$ and $\mathbf{k}$ are the wave vectors of phonons and spin waves in different states: a is the lattice constant; $\rho$ is the density of the substance; $w = \beta^2/a^3$ is the magnetic interaction energy of the two spins of neighboring atoms ($\beta$ is the Bohr magneton); $\mathbf{e}_f$ is the polarization vector of phonon $\mathbf{f}$; $f^- \equiv f_x - if_y$; $e_f^- = e_{fx} - ie_{fy}$; and $\theta$, $\varphi$, $\theta'$, $\varphi'$, and $\theta''$, $\varphi''$ are the polar angles of the vectors $\mathbf{k}$, $\mathbf{k}'$, and $\mathbf{k}''$.

We now write the kinetic equations for the spin-wave and phonon distribution functions, taking these interaction processes into account. Setting

$$n_k = n_k^0 + (\varphi_k/T)/(e^{\varepsilon_k/T} - 1)(e^{-\varepsilon_k/T} - 1),$$
$$N_f = N_f^0 + (\Phi_f/T)/(e^{E_f/T} - 1)(e^{-E_f/T} - 1), \tag{5}$$

where $n_k^0$ and $N_f^0$ are equilibrium Planck functions, it is a simple matter to obtain the following linearized equations for determining the unknown functions $\varphi_k$ and $\Phi_f$:

$$\int W_{f,\,-f',\,-f''}\,\delta(E_f - E_{f'} - E_{f''})\frac{\Phi_{f''} + \Phi_{f'} - \Phi_f}{(e^{E_{f''}/T}-1)(e^{E_{f'}/T}-1)(e^{-E_f/T}-1)}\,d\tau_{f'}$$
$$+\int W_{f,\,+k,\,-k'}\,\delta(E_f + \varepsilon_k - \varepsilon_{k'})\frac{\Phi_f + \varphi_k - \varphi_{k'}}{(e^{\varepsilon_k/T}-1)(e^{-\varepsilon_k/T}-1)(e^{-E_f/T}-1)}\,d\tau_k$$
$$+\int W_{f,\,-k',\,-k}\,\delta(E_f - \varepsilon_k - \varepsilon_{k'})\frac{\varphi_k + \varphi_{k'} - \Phi_f}{(e^{\varepsilon_k/T}-1)(e^{\varepsilon_{k'}/T}-1)(e^{-E_f/T}-1)}\,d\tau_k$$
$$= \frac{(\partial T/\partial z)\, v_z^{(f)} E_f/T}{(e^{E_f/T}-1)(e^{-E_f/T}-1)}. \tag{6}$$

$$\int W_{k,\,-k',\,-k''}\,\delta(\varepsilon_k - \varepsilon_{k'} - \varepsilon_{k''})\frac{\varphi_{k''} + \varphi_{k'} - \varphi_k}{(e^{\varepsilon_{k''}/T}-1)(e^{\varepsilon_{k'}/T}-1)(e^{-\varepsilon_k/T}-1)}\,d\tau_{k'}$$
$$+\int W_{f,\,+k,\,-k'}\,\delta(E_f + \varepsilon_k - \varepsilon_{k'})\frac{\Phi_f + \varphi_k - \varphi_{k'}}{(e^{\varepsilon_{k'}/T}-1)(e^{-\varepsilon_k/T}-1)(e^{-E_f/T}-1)}\,d\tau_{k'}$$
$$+\int W_{f,\,-k,\,-k'}\,\delta(E_f - \varepsilon_k - \varepsilon_{k'})\frac{\varphi_k + \varphi_{k'} - \Phi_f}{(e^{\varepsilon_k/T}-1)(e^{\varepsilon_{k'}/T}-1)(e^{-E_f/T}-1)}\,d\tau_{k'}$$
$$= \frac{(\partial T/\partial z)\, v_z^{(k)} \varepsilon_k/T}{(e^{\varepsilon_k/T}-1)(e^{-\varepsilon_k/T}-1)}, \tag{6'}$$

where $v_z^{(f)}$ and $v_z^{(k)}$ are the projections of the group velocities of the phonons and of the spin waves onto the z axis, along which the temperature gradient is directed; E and $\epsilon$ are the energies of the phonons and spin waves in their respective states;

$$d\tau_f = (2\pi)^{-3} f^2 df\, do_f, \qquad d\tau_k = (2\pi)^{-3} k^2\, dk\, do_k,$$

($do_f$, $do_k$ are elements of solid angle of the vectors $\mathbf{f}$ and $\mathbf{k}$).

In the first terms of (6) and (6′) the following conservation laws of the wave vectors are satisfied:

$$\mathbf{f} - \mathbf{f}' - \mathbf{f}'' = 0, \pm 2\pi\mathbf{b},$$
$$\mathbf{k} - \mathbf{k}' - \mathbf{k}'' = 0, \pm 2\pi\mathbf{b},$$

in the second terms,

$$\mathbf{f} + \mathbf{k} - \mathbf{k}' = 0, \pm 2\pi\mathbf{b},$$

and in the third terms

$$\mathbf{f} - \mathbf{k} - \mathbf{k}' = 0, \pm 2\pi\mathbf{b},$$

where $\mathbf{b}$ is a vector of the reciprocal lattice.

We will consider further the case of low temperatures, when $\alpha = \Theta^2/\Theta_C T \gg 1$. Retaining the most essential terms in the equations, we can write (6) and (6′) symbolically in the form

$$L_2\{\Phi, \varphi\} + e^{-\Theta/2T} L_1^u\{\Phi\} + e^{-\Theta_c/4T}\alpha^{1/2} L_2^u\{\Phi, \varphi\} = \frac{\frac{\partial T}{\partial z}\frac{a}{\hbar}\frac{\Theta_c}{\Theta}\alpha\cos\vartheta_f\gamma_1}{(e^{\eta}-1)(e^{-\eta}-1)},$$

$$\alpha^{1/2} M_1\{\varphi\} + e^{-\Theta_c/4T} M_1^u\{\varphi\} + e^{-\Theta/2T}\alpha^{1/2} M_2^u\{\Phi, \varphi\} = \frac{\frac{\partial T}{\partial z}\frac{a}{\hbar}\frac{\Theta_c}{\Theta}x^{3/2}\cos\vartheta_k}{(e^{x}-1)(e^{-x}-1)}, \qquad (7)$$

where $\eta = E_f/T$, $\kappa = \epsilon_k/T$; $L_2\{\Phi, \varphi\}$ is an operator, corresponding to the second term of (6) when the conservation law of the wave vector is strictly satisfied, describing the scattering of spin waves by phonons; $M_1\{\varphi\}$ is an operator, corresponding to the first term of (6′), describing the interaction of spin waves with each other also when the wave-vector conservation law is strictly fulfilled; and the operators with the index u correspond to terms taking account of transfer processes. These operators do not contain the temperature explicitly.

Multiplying (6) by $f_z$ and (6′) by $k_z$ and adding both equations we obtain, after integrating over the phonon states f and the spin-wave states k:

$$\frac{2\pi}{aT}\int W_{f,-f',-f''}\,\delta(E_f - E_{f'} - E_{f''})\,\frac{\Phi_{f''}+\Phi_{f'}-\Phi_f}{(e^{E_{f''}/T}-1)(e^{E_{f'}/T}-1)(e^{-E_f/T}-1)}\,d\tau_{f'}\,d\tau_f$$
$$+\frac{2\pi}{aT}\int W_{k,-k',-k''}\,\delta(\varepsilon_k - \varepsilon_{k'} - \varepsilon_{k''})\,\frac{\varphi_{k''}+\varphi_{k'}-\varphi_k}{(e^{\varepsilon_{k''}/T}-1)(e^{\varepsilon_{k'}/T}-1)(e^{-\varepsilon_k/T}-1)}\,d\tau_{k'}d\tau_k$$
$$+\frac{2\pi}{aT}\int W_{f,+k,-k'}\,\delta(E_f + \varepsilon_k - \varepsilon_{k'})\,\frac{\Phi_f+\varphi_k-\varphi_{k'}}{(e^{\varepsilon_{k'}/T}-1)(e^{-\varepsilon_k/T}-1)(e^{-E_f/T}-1)}\,d\tau_f d\tau_k \qquad (8)$$
$$+\frac{2\pi}{aT}\int W_{f,-k,-k'}\,\delta(E_f - \varepsilon_k - \varepsilon_{k'})$$
$$\times\frac{\varphi_k+\varphi_{k'}-\Phi_f}{(e^{\varepsilon_k/T}-1)(e^{\varepsilon_{k'}/T}-1)(e^{-E_f/T}-1)}\,d\tau_f\,d\tau_k = R_f + R_k,$$

where

$$R_f = -\sum_f \frac{\partial T}{\partial z}\frac{v_z^{(f)} f_z}{T}\frac{E_f/T}{(e^{E_f/T}-1)(e^{-E_f/T}-1)} \approx \frac{1}{(2\pi)^3}\frac{1}{\hbar}\frac{\partial T}{\partial z}\frac{1}{a^3}\left(\frac{T}{\Theta}\right)^3,$$
$$R_k = -\sum_k \frac{\partial T}{\partial z}\frac{v_z^{(k)} k_z}{T}\frac{\varepsilon_k/T}{(e^{\varepsilon_k/T}-1)(e^{-\varepsilon_k/T}-1)} \approx \frac{1}{(2\pi)^3}\frac{1}{\hbar}\frac{\partial T}{\partial z}\frac{1}{a^3}\left(\frac{T}{\Theta_c}\right)^{3/2}.$$

Equation (8) is satisfied if we set

$$\varphi_k = \Psi k_z, \quad \Phi_f = \Psi f_z, \qquad (9)$$

where the quantity $\Psi$ does not depend on f and k and has the following form:

$$\Psi \approx \frac{a^2\Theta^2}{w^2}\frac{1}{\alpha}\frac{\partial T}{\partial z}e^{\Theta_c/4T} \quad \text{for} \quad \Theta \gg \Theta_c,\ \Theta^2/\Theta_c \gg T,$$
$$\Psi \approx \frac{\rho}{\hbar^2}\Theta a^7\frac{\partial T}{\partial z}\alpha^{1/2}e^{\Theta/2T} \quad \text{for} \quad \Theta \ll \Theta_c,\ T \ll \Theta^2/\Theta_c.$$

The functions (9) transform $L_2$ and $M_1$ to zero. Hence, following Ref. 3, we readily conclude that these functions are the principal parts of the solutions of the kinetic equations.

Using these functions we calculate the heat currents $\Pi_f$ and $\Pi_k$ carried by the phonons and by the spin waves:

$$\Pi_f = \int v_z^{(f)}\Phi_f\frac{(E_f/T)d\tau_f}{(e^{E_f/T}-1)(e^{-E_f/T}-1)},$$

$$\Pi_k = \int v_z^{(k)}\varphi_k\frac{(\varepsilon_k/T)d\tau_k}{(e^{\varepsilon_k/T}-1)(e^{-\varepsilon_k/T}-1)}.$$

Corresponding to these equations, the coefficients of thermal conductivity of the phonon and spin-wave gases are, for $\Theta \gg \Theta_C$, $\Theta^2/\Theta_C \gg T$:

$$\varkappa_f \sim \frac{\Theta_c\Theta^2}{\hbar a w^2}\left(\frac{T}{\Theta}\right)^5 e^{\Theta_c/4T}, \quad \varkappa_k \sim \frac{\Theta_c^3}{\hbar a w^2}\left(\frac{T}{\Theta_c}\right)^{7/2} e^{\Theta_c/4T}.$$

In this case $\kappa_k \gg \kappa_f$.

If $\Theta_C \gg \Theta$, $\Theta^2/\Theta_C \gg T$, then

$$\varkappa_f \sim \frac{\rho a^4}{\hbar^3}\frac{\Theta_c^3}{\Theta}\left(\frac{T}{\Theta_c}\right)^{7/2} e^{\Theta/2T}, \quad \varkappa_k \sim \frac{\rho a^4}{\hbar^3}\Theta^{1/2}\Theta_c^{3/2}\left(\frac{T}{\Theta}\right) e^{\Theta/2T}.$$

In this case also $\kappa_k \gg \kappa_f$, that is, the thermal conductivity, as in the preceding case, is determined principally by the spin waves. In contrast to the previous case, however, it is the Debye temperature and not the Curie temperature which

enters into the exponent.

3. We now study sound absorption in a ferromagnetic dielectric. To this end it is necessary, as in the case of ordinary dielectrics,[4] to find the deviations of the phonon and spin-wave distribution functions from their equilibrium values and to determine the entropy increase of the crystal due to these deviations.

Assuming that the sound wavelength is sufficiently large, we can consider that in a system of phonons and spin waves it is possible for an equilibrium to be established which corresponds to the instantaneous value of the sound field.[4] The influence of the sound field on the phonons and spin waves amounts to a change in their energies. These quantities can be represented in the presence of sound in the form

$$E_f = E_f^0(1 + \Lambda_{ij}u_{ij}), \quad \varepsilon_k = \varepsilon_k^0 + \lambda_{ij}u_{ij},$$

where $E_f^0 = \Theta af$, $\epsilon_k^0 = \Theta_c a^2 k^2$ are the equilibrium values of the phonon and spin-wave energies in the absence of sound, and $u_{ij}$ is the deformation tensor due to the sound.

In contrast to the phonon energies, which become zero for $f = 0$ both in deformed and non-deformed crystals, the spin-wave energies acquire an addition which, generally speaking, does not reduce to zero for $k = 0$.

The changes of the phonon and spin-wave distribution functions due to the sound field are

$$\dot{N}_f^s = \frac{1}{T}\frac{E_f - E_f\dot{T}/T}{(e^{E_f/T}-1)(e^{-E_f/T}-1)},$$

$$\dot{n}_k^s = \frac{1}{T}\frac{\dot{\varepsilon}_k - \varepsilon_k\dot{T}/T}{(e^{\varepsilon_k/T}-1)(e^{-\varepsilon_k/T}-1)}.$$

In contrast to the problem of thermal conductivity, it is possible in this case to ignore transfer processes.[4]

The linearized kinetic equations for the phonon and spin-wave distribution functions in an external sound field for $\alpha \gg 1$ have the form

$$L_2\{\Phi, \varphi\} \sim \eta_l \Lambda_{ij}\dot{u}_{ij}N_f^0(N_f^0+1),$$

$$\alpha^{1/2}M_1\{\varphi\} \sim \Theta_c\Theta^{-2}\alpha\lambda_{ij}\dot{u}_{ij}n_k^0(n_k^0+1), \tag{10}$$

where $L_2$ and $M_1$ are the operators appearing in Eq. (7). The largest terms have been retained in the left side of (10).

The solutions of these equations have the form

$$\varphi_k = \alpha^{1/2}\lambda_{ij}\dot{u}_{ij}F_1, \quad \Phi_f = \Lambda_{ij}\dot{u}_{ij}F_2, \tag{11}$$

where $F_1$ and $F_2$ are certain functions of $\mathbf{x}$, $\eta$, and of the angles determining the directions of $\mathbf{k}$ and $\mathbf{f}$.

The dissipation function of the system of phonons and spin waves is

$$T\dot{S} = T\dot{S}_f + T\dot{S}_k,$$

where $S_f$ and $S_k$ are the phonon and spin-wave entropies:

$$S_f = \sum_f \{(N_f+1)\ln(N_f+1) - N_f\ln N_f\},$$

$$S_k = \sum_k \{(n_k+1)\ln(n_k+1) - n_k\ln n_k\}.$$

Substituting $n_k$ and $N_f$ in the form of (5) here, we obtain

$$T\dot{S} = \frac{1}{(2\pi a)^3}\left\{\left(\frac{T}{\Theta}\right)^3\int \Phi_f\Lambda_{ij}\dot{u}_{ij}N_f^0(N_f^0+1)\eta_l^3\,d\eta_l\,do_f + \left(\frac{T}{\Theta_c}\right)^{3/2}\int \varphi_k\frac{\Theta_c}{\Theta^2}\alpha\lambda_{ij}\dot{u}_{ij}n_k^0(n_k^0+1)x^{1/2}\,dx\,do_k\right\}.$$

Making further use of (11), we readily conclude that when $T \ll \Theta^2/\Theta_c$ the dissipation function does not depend on the temperature and has the form

$$T\dot{S} = C(\bar{\lambda}_{ji}\dot{u}_{ji})^2, \tag{12}$$

where $C$ is a certain constant and $\bar{\lambda}_{ij}$ is the value of $\lambda_{ij}$ averaged with respect to the angles.

It is thus clear that for $T \ll \Theta^2/\Theta_c$ the absorption of sound is determined principally by the spin waves and is independent of the temperature.

The authors are grateful to M. I. Kaganov for valuable discussions.

[1] R. Peierls, Ann. Physik (Fifth Series) **3**, 1055 (1929).

[2] A. I. Akhiezer, Journ. of Phys. **10**, 217 (1946).

[3] A. I. Akhiezer, J. Exptl. Theoret. Phys. (U.S.S.R.) **10**, 1934 (1940).

[4] A. I. Akhiezer, J. Exptl. Theoret. Phys. (U.S.S.R.) **8**, 1330 (1938).

Translated by W. M. Whitney
253

# REFLECTION FROM A BARRIER IN THE QUASI-CLASSICAL APPROXIMATION

V. L. POKROVSKII, S. K. SAVVINYKH, and F. R. ULINICH

Institute of Radiophysics and Electronics, Siberian Branch, Academy of Sciences, U.S.S.R.

Submitted to JETP editor December 14, 1957; resubmitted January 26, 1958

J. Exptl. Theoret. Phys. (U.S.S.R.) **34**, 1272-1277 (May, 1958)

The asymptotic expression for the coefficient of reflection from a one-dimensional potential barrier has been found for the case when the wavelength is much smaller than the characteristic dimensions of the barrier.

## 1. STATEMENT OF THE PROBLEM

THE determination of the reflection coefficient for the case when the de Broglie wavelength $\lambda$ is commensurable with the characteristic dimensions of the potential barrier is a very complicated mathematical problem, which has been solved only in rare cases. For short wavelengths the Schrödinger equation is usually solved using the well-known Wentzel-Kramers-Brillouin (WKB) method, which in general gives no reflection.

The task of this paper is to find an asymptotic expression for the reflection coefficient for small wavelengths. We consider only the one-dimensional case.

The problem consists in solving the Schrödinger equation:

$$\alpha^2 \frac{d^2\psi}{d\xi^2} + k^2(\xi)\psi = 0, \tag{1.1}$$

where

$$\alpha = \lambda\!\!\!^{-}/a; \quad \xi = x/a; \quad k^2(\xi) = 1 - U(\xi)/E; \tag{1.1a}$$

$\lambda\!\!\!^{-}$ is the de Broglie wavelength of the free particle; a denotes the extent of the region where $U(\xi)$ changes significantly; E is the energy of the particle. Our fundamental assumption is

$$\alpha \ll 1. \tag{1.2}$$

In the following we shall always restrict ourselves to the case $E > U(\xi)$ on the entire $\xi$ axis.

According to the familiar WKB method, the solution of Eq. (1.1) is sought in the form

$$\psi = e^{S/\alpha} \tag{1.3}$$

and S is expanded into a power series in $\alpha$. The zeroth and first approximations give

$$\psi = \frac{1}{\sqrt{k}} \exp\left\{\frac{i}{\alpha}\int^{\xi} k d\xi\right\}. \tag{1.4}$$

The next corrections are small quantities of higher order in $\alpha$ and change the phase and the amplitude of solution (1.4) only insignificantly. For $\xi \to \pm\infty$ solution (1.4) goes over into $A_{\pm}\exp\{ik_{\pm}\xi/\alpha\}$ asymptotically, i.e., into a plane wave going in only one direction at both ends of the straight line ($k_{\pm} = \lim k(\xi)$, $\xi \to \pm\infty$).

In the WKB approximation the quantum effect of the reflection from a potential barrier is thus completely absent.

The reason for this lies in the fact that in the WKB method the function S is expanded into an asymptotic series in powers of $\alpha$, and the method by its very nature, cannot take into account the reflection effect, which, for small $\alpha$, has an amplitude of order $\exp(-A/\alpha)$ ($A > 0$). In order to find the reflection of the wave we must therefore change the method.

We introduce the variable t:

$$\alpha t = \int^{\xi} k d\xi \tag{1.5}$$

and make the transformation

$$\psi = y/\sqrt{k}. \tag{1.6}$$

Equation (1.1) takes the form

$$\frac{d^2y}{dt^2} + (1 + \alpha^2 q(\alpha t))\, y = 0, \tag{1.7}$$

where q is determined by k through the relation

$$q = \frac{3(k')^2 - 2kk''}{4k^4}. \tag{1.8}$$

(The prime denotes differentiation with respect to $\xi$.)

We formally apply to Eq. (1.7) the perturbation theory for the continuous spectrum. It turns out that all the terms in the perturbation expansion have the same order of smallness in $\alpha$.

## 2. CALCULATION OF THE REFLECTION COEFFICIENT

Our task is to find the amplitude for transition from the eigenstate of the Hamiltonian $H_0 = d^2/dt^2$ with momentum 1 to the state with momentum $-1$. This amplitude is expressed with the help of the well-known perturbation expansion

$$R = \frac{1}{2i}\left[V_{-1,1} + \frac{1}{2\pi}\int \frac{V_{-1,k}V_{k,1}}{1-k^2}\,dk + \frac{1}{(2\pi)^2}\iint \frac{V_{-1,k_1}V_{k_1,k_2}V_{k_2,1}}{(1-k_1^2)(1-k_2^2)}\,dk_1\,dk_2 + \ldots\right], \quad (2.1)$$

where $V_{k,k'}$ is the matrix element of the "perturbation" $V = \alpha^2 q$. The path of integration over $k_i$ in formula (2.1) is taken along the real axis, circumventing the singular points $k_i = -1$ and $k_i = 1$ above and below the axis respectively. It will be shown in the Appendix that only a slight error is introduced if the path of integration is taken along the real axis without the by-passes.

We calculate the matrix element $V_{k,k'}$. We have

$$V_{k,k'} = -\alpha\int_{-\infty}^{\infty} \exp\left\{\frac{i}{\alpha}(k'-k)\tau\right\} q(\tau)\,d\tau. \quad (2.2)$$

We investigate the singularities of the function $q(\tau)$ in the complex plane $\tau$. It follows from (1.8) that the singularities of $q(\tau)$ coincide with the roots and singularities of the function $k^2(\xi)$. We restrict ourselves to the case where the singular point $\tau_0$ whose imaginary part has the smallest absolute value corresponds to a simple root. Clearly, this situation holds precisely for not too large energies E. The case where the term making the main contribution to the reflection coefficient involves a simple pole of $k^2(\xi)$ is treated analogously and leads to the same result.

Let $\xi_0$ be the simple root of $k^2(\xi)$. Near $\xi_0$ the function $k(\xi)$ has the form

$$k(\xi) = A\sqrt{\xi - \xi_0}. \quad (2.3)$$

The function $q(\xi)$, in the neighborhood of $\xi_0$, is of the form

$$q(\xi) = \frac{5}{16A^2(\xi-\xi_0)^3}[1 + O(\xi-\xi_0)]. \quad (2.4)$$

The leading term in $q(\xi)$, as is seen from (2.2), contains the constant A, which is determined by the form of the function $k(\xi)$. However, after transformation to the variable $\tau = \int^{\xi} k\,d\xi$ the point $\xi_0$ goes over into the point $\tau_0 = \int^{\xi_0} k\,d\xi$, in the vicinity of which $q(\tau)$ has the form

$$q(\tau) = \frac{5}{36(\tau-\tau_0)^2}[1 + O(\tau-\tau_0)^{2/3}]. \quad (2.5)$$

We see that the leading term in $q(\tau)$ does not depend on the form of the function $k(\xi)$ in the neighborhood of $\tau_0$.

We now apply the theory of residues to the integral (2.2). Here we consider only the pole $\tau_0$, as the contributions from the remaining singularities are exponentially small compared with the contribution of the point $\tau_0$. We assume here that the different singular points of $q(\tau)$ are not too close to each other. With these assumptions, the calculation gives

$$V_{k,k'} = 2\pi\frac{5}{36}|k-k'|\exp\left\{\frac{i}{\alpha}(k'-k)\rho - \frac{1}{\alpha}|k-k'|\sigma\right\} \times (1 + O(\alpha^{2/3})), \quad (2.6)$$

where $\tau_0 = \rho + i\sigma\,(\sigma > 0)$. We note that the leading term in the coefficient of the exponential in $V_{k,k'}$ does not depend on the form of function $k(\xi)$.

In particular, we have

$$V_{-1,1} = \frac{5}{36}\pi e^{2i\tau_0/\alpha}(1 + O(\alpha^{2/3})). \quad (2.7)$$

We show that in all the other corrections of the perturbation theory the leading terms are also proportional to the same exponential $\exp(2i\tau_0/\alpha)$, whose coefficients are universal constants independent of the form of the function $k(\xi)$. We examine the general term in the series (2.1):

$$J_n = \frac{1}{(2\pi)^n}\int\ldots\int dk_1\ldots dk_n\,\frac{V_{-1,k_1}V_{k_1,k_2}\ldots V_{k_n,1}}{(1-k_1^2)^2(1-k_2^2)\ldots(1-k_n^2)} = 2\pi\left(\frac{5}{36}\right)^{n+1}e^{2i\rho/\alpha}\int\ldots\int dk_1 dk_2\ldots dk_n \times \frac{|1+k_1|\,|k_2-k_1|\ldots|1-k_n|}{(1-k_1^2)\ldots(1-k_n^2)} \times \exp\left\{-\frac{\sigma}{\alpha}(|1+k_1| + \ldots + |1-k_n|)\right\}. \quad (2.8)$$

We separate the region of integration into the n-dimensional "tetrahedron" $-1 \le k_1 \le k_2 \ldots \le k_n \le 1$ and the whole remaining space. Inside the "tetrahedron" the exponent of the exponential in the integral (2.8) is equal to $-2\sigma/\alpha$; in the remaining region of integration it is everywhere smaller than this quantity, and therefore the latter region gives to the integral a contribution which is small in comparison with the contribution of the "tetrahedron" (of order $2^n\alpha/n!$). We can thus restrict the integration to the "tetrahedron," with the result

$$J_n = (5/36)^{n+1}\,2\pi A_n e^{2i\tau_0/\alpha}(1 + O(\alpha^{2/3})), \quad (2.9)$$

where

$$A_n = \int_{-1}^{1} dk_1 \int_{k_1}^{1} dk_2 \ldots \int_{k_{n-1}}^{1} dk_n \frac{(1+k_1)(k_2-k_1)\ldots(1-k_n)}{(1-k_1^2)(1-k_2^2)\ldots(1-k_n^2)}. \quad (2.10)$$

We thus convince ourselves that the coefficients $A_n$ indeed do not depend on the form of the function $k(\xi)$. Hence the amplitude of the reflection coefficient has the form

$$R = -i\pi e^{2i\tau_0/\alpha} \sum_{n=0}^{\infty} A_n \left(\frac{5}{36}\right)^{n+1}, \quad (2.11)$$

where $A_0 = 2$. It is not necessary to compute the sum in formula (2.11), since its value does not depend on the form of the function $k(\xi)$, and can thus be determined using any known exact solution of the Schrödinger equation.

A number of cases is known where the Schrödinger equation (1.1) admits of an exact solution.[1,2] The asymptotic expression for the reflection coefficient leads in all these cases to the formula

$$R = -ie^{2i\tau_0/\alpha} = -i\exp\left\{\frac{2i}{\alpha}\int_{\xi}^{\xi_0} k\,d\xi\right\}. \quad (2.12)$$

Consequently, formula (2.12) gives the leading term in the reflection coefficient for arbitrary form of the potential.*

## 3. RANGE OF APPLICABILITY

The formula for the coefficient for barrier reflection (2.12) obtained in the preceding section is valid only in the case where the singular points of the plane $\tau$ are separated from each other by distances much greater than $\alpha$. Otherwise the expression (2.5) for the function $q(\tau)$ becomes incorrect.

We investigate, what limitations on the range of parameters of the problem follow from this requirement.

1. Region of high energies: $U_0/E \ll 1$. ($U_0$ denotes the maximal value of the potential $U$). In this case the root of $k^2 = 1 - U/E$ is clearly located in the vicinity of the singularity of $U$.

The criterion for the applicability of formula (2.12) depends essentially on the kind of singularity of $U$. We examine the case where the singularity of $U$ is a simple pole. Near the pole $\xi_1$ the function $U$ has the form

$$U = U_0 A/(\xi - \xi_1), \quad (3.1)$$

where $A$ is a quantity of order unity. The function $k^2(\xi)$ near $\xi_1$ is of the form

$$k^2(\xi) = (\xi - \xi_0)/(\xi - \xi_1), \quad (3.2)$$

where $\xi_0 = \xi_1 + AU_0/E$. For the corresponding values of $\tau_0$, $\tau_1$ we find

$$\tau_0 - \tau_1 = \int_{\xi_1}^{\xi_0} \sqrt{\frac{\xi - \xi_0}{\xi - \xi_1}}\, d\xi = \frac{i\pi}{2}(\xi_0 - \xi_1) = \frac{i\pi}{2} A \frac{U_0}{E}. \quad (3.3)$$

Hence the required criterion is

$$U_0/E\alpha \gg 1. \quad (3.4)$$

We note that in the case $U_0/E \ll 1$ the usual perturbation theory is applicable.

For the "Gaussian" potential $U = U_0 \exp(-\xi^2)$ the criterion for the applicability of the quasi-classical approximation (2.12) is much less stringent, namely

$$\frac{U_0}{E} e^{\alpha^{-2}} \gg 1. \quad (3.5)$$

It is interesting to note that in this case the region of applicability of perturbation theory lies outside the region (3.5):

$$U_0 e^{\alpha^{-2}}/E \ll 1.$$

2. Region of energies close to $U_0$. In this case the two roots $\xi_0$, $\xi_0^*$ of the function $k^2(\xi)$ lie close to one another (they are also close to the point $\xi_m$ where $U(\xi)'$ takes its maximum). From the condition that the distance between corresponding points $\tau_0$, $\tau_0^*$ must be larger than $\alpha$ we obtain the criterion

$$(E - U_0)/U_0\alpha \gg 1. \quad (3.6)$$

In the region $(E - U_0)/U_0\alpha \lesssim 1$ the amplitude of reflection may be obtained by other means (see, e.g., Refs. 4 and 5). We note that the expression for the reflection amplitude (66) of the paper of Fock,[5] obtained under the assumption $(E - U_0)/U_0\alpha \lesssim 1$, may be extrapolated into the region $(E - U_0)/U_0\alpha \gg 1$, as this work shows.

In closing the authors express their sincere gratitude to L. D. Landau for valuable advice leading to significant simplifications of the mathematical calculations.

## APPENDIX

The asymptotic expression (2.6) for the matrix element $V_{k,k'}$, obtained in Sec. 2, becomes incorrect for $|k - k'| \lesssim \alpha$. However, for the absolute value of the matrix element $V_{k,k'}$ there exists a simple estimate, which is valid for arbitrary $|k - k'|$:

$$|V_{k,k'}| \leqslant \alpha \int_{-\infty}^{\infty} |q(\tau)|\, d\tau = M\alpha, \quad (A.1)$$

where $M$ is a quantity of order unity.

Consider, for example, the integral

*The formula for the reflection coefficient obtained in Ref. 3 proves to be wrong; it takes into account only the first term in the series (2.11).

$$J_1 = \int \frac{V_{-1,k} V_{k1}}{1-k^2}\, dk. \qquad \text{(A.2)}$$

The integral along the real axis of k, by-passing the singularities $k = \pm 1$, is broken up in the following way:

$$J_1 = \int_{-\infty}^{-1-\alpha} + \int_{-1+\alpha}^{1-\alpha} + \int_{1+\alpha}^{\infty} + \int_{\Gamma_1} + \int_{\Gamma_2}, \qquad \text{(A.3)}$$

where $\Gamma_1$ and $\Gamma_2$ are semicircles of radius $\alpha$ about the singular points. Making an error of order $\alpha$ in comparison with the leading term, we replace the exact values $V_{k,k'}$ by their asymptotic expressions (2.6) in the integrals along the straight lines, and extend the second integral to an interval from $-1$ to 1. The integrals over the semicircles are estimated with the help of (A.1). They give a contribution of order $\alpha$ as compared to the leading term.

In an analogous manner one can justify the application of formulae (2.9), (2.10) for the general term in the iteration series.

[1] L. D. Landau and E. M. Lifshitz, Квантовая механика (Quantum Mechanics), GITTL, 1948, vol. 1, pp 96-98.

[2] L. M. Brekhovskikh, Волны в слоистых средах (Waves in Layered Media), Acad. Sci. Press, 1957, pp. 154-159.

[3] I. I. Gol' dman and A. B. Migdal, J. Exptl. Theoret. Phys. (U.S.S.R.) **28**, 394 (1955), Soviet Physics JETP **1**, 304 (1955).

[4] P. M. Morse and H. Feshbach, Methods of Theoretical Physics, McGraw-Hill Book Co., 1953, p. 1103.

[5] V. A. Fok, Радиотехника и электроника (Radio Engg. and Electronics) **1**, 560 (1956).

Translated by R. Lipperheide
254

SOVIET PHYSICS JETP VOLUME 34(7), NUMBER 5 NOVEMBER, 1958

# *RADIATION COOLING OF AIR. I. GENERAL DESCRIPTION OF THE PHENOMENON AND THE WEAK COOLING WAVE*

Ia. B. ZEL' DOVICH, A. S. KOMPANEETS, and Iu. P. RAIZER

Institute of Chemical Physics

Submitted to JETP editor December 20, 1957

J. Exptl. Theoret. Phys. (U.S.S.R.) **34**, 1278-1287 (May, 1958)

We consider non-stationary radiation cooling of a large volume of air heated to a high temperature (on the order of tens and hundreds of thoudands degrees) by a strong explosion. It is shown that, owing to the strong temperature dependence of light absorption in the air, the cooling involves the propagation of a sharp temperature jump, i.e., of a cooling wave. Cooling from the initial high temperature to that at which the air becomes almost transparent and ceases to radiate occurs in a narrow wave front. A system of equations is derived, which permits an investigation of the internal structure of the cooling wave and leads to a connection between its parameters and the propagation velocity. A weak wave with a small temperature difference is considered.

## 1. QUALITATIVE DESCRIPTION OF THE PROCESS OF COOLING HEATED AIR

THE problem of a strong explosion in air was considered by Sedov[1] (see also Ref. 2). A strong shock wave heats the air irreversibly to a very high temperature, so that a large mass of very hot air is produced after the explosion, when the pressure returns to atmospheric.

Imagine a large mass of air with linear dimensions on the order of several hundreds of meters, heated to a high temperature — above 100,000° at the center; the temperature towards the periphery drops to below 1,000°. How is such a mass cooled? Obviously, the molecular heat conduction does not play any role at all: with a heat-diffusion coefficient

(temperature conductivity) on the order of 1 $cm^2$/sec and with dimensions on the order of $10^4$ cm, it would take a year for the air to cool. The convective rise due to the difference between the densities of the hot and cold air and the mixing of the hot air with the surrounding masses of cold air, caused by the rise, are more substantial. However, the rise is small during the first 2 to 3 seconds. Obviously, the convective rise cannot exceed $gt^2/2$, which amounts to 5 m after one second, 20 m after two seconds, and 45 m after three seconds. Therefore, if we consider the first few seconds, convection can also be disregarded. The fundamental factor is the radiation of light from the air, to which this article is devoted.

A characteristic feature of this problem is that the transparency of the air depends strongly on the temperature. Cold air, as is known, is transparent to visible light, which indeed makes possible radiant cooling of a heated volume.

The continuous spectrum of light absorption in heated air is principally due to photoionization of the excited atoms. The ionization energy of a nitrogen or oxygen atom in the ground state ($I \approx 14$ ev) at temperatures on the order of 10,000° is considerably higher than the energies of the quanta, which play the principal role in a flux of energy $h\nu$ on the order of several kT. These quanta can be absorbed only by atoms excited to energies $I - h\nu$, the equilibrium number of which is proportional to the Boltzmann factor $\exp\{-(I + H\nu/kT)\}$. Therefore the free path of the light, which equals the reciprocal of the coefficient of absorption, depends very strongly on the temperature. The free path varies from kilometers at $T \approx 6{,}000°$ to meters at $T \approx 10{,}000°$ and centimeters at $T \approx 13{,}000°$.

Obviously, the radiation that cools the air is determined essentially by the layer in which the radiation free path is on the order of the dimensions of the system, i.e., by a layer of temperature on the order of 10,000°, which can be called the transparency temperature $T_2$. The colder air is transparent and does not radiate, the hotter air is opaque and radiates intensely, but its radiation is absorbed on the spot. These concepts, defining the effective radiating layer, are by no means new, and are universally used in the study of stars. However, unlike in the stars, the energy radiated by the air is not compensated for by an energy influx from an inner hotter region, since the temperature distribution is determined in our case principally by the past history of the phenomenon and is not stationary. It is therefore to be expected that if, as shown in Fig. 1, a certain smooth temperature distribution exists at the initial instant of time, the

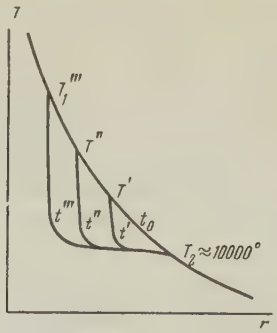


FIG. 1

first to begin cooling by radiation would be the layer with a temperature on the order of $T_2 \sim 10{,}000°$; in the subsequent instants the temperature distribution will change under the influence of radiation as shown in Fig. 1. One layer of air after another will be cooled to the transparency temperature. Propagating over the gas hotter then $T_2$ will be a temperature jump, a cooling wave (CW), in which the temperature drops sharply from an initial value $T_1$ to the transparency temperature $T_2$.

By representing the successive changes in temperature distribution as shown in Fig. 1, we disregard the changes in distribution due to purely hydrodynamic motion. Actually, the jump is formed even before the air pressure drops to atmospheric, and the hydrodynamic scattering stops at approximately that instant, when the radiant cooling of the layer of temperature $\sim 10{,}000°$ becomes comparable with the adiabatic cooling of the expanding air. Later on, when the adiabatic cooling diminishes rapidly with falling pressure, radiant cooling begins to play the principal role. To the contrary, prior to the formation of the jump, the principal role is played by the adiabatic cooling and the radiation losses are small.

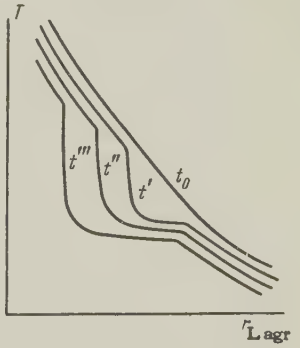


FIG. 2

Thus, taking the adiabatic cooling into account, the successive changes in the temperature distribution are shown in Fig. 2, where the abscissa represents the Lagrangian rather than the Eulerian

coordinate.

It can be said that the CW propagates through air that is undisturbed by the radiation. The air temperature prior to the arrival of the wave, $T_1$, is determined only by the past history of the process and by purely hydrodynamic motion, if present. The point is that at temperatures on the order of tens and hundreds of thousands of degrees, and at temperature gradients on the order of thousands of degrees per meter, which frequently occur in the initial distribution, the radiant heat conduction is too small, owing to the strong absorption, to produce any noticeable energy flux in the region with initial temperature $T_1$. The radiant heat conduction, the coefficient of which (coefficient of proportionality between the thermal flux and the temperature gradient) is proportional to the free path of the light $l(T)$ and to the cube of the temperature, increases sharply with increasing temperature and plays a substantial role only at hundreds of thousands of degrees, limiting the temperature rise to the same order and equalizing the temperature near the center.*

Thanks to the low heat conduction on the upper edge of the CW at the temperature $T_1$, the energy flux into the wave from within is nearly zero and cannot have a significant value. All the properties of the CW, particularly its rate of propagation through the hot gas, are determined essentially by one quantity, the temperature $T_1$, of the initial gas. (The properties of the gas and its pressure are assumed specified.) The fundamental problem of the theory of the cooling wave is to find the energy flux $S_2$ radiated away from the surface of the wave. This flux lies obviously between the limits $\sigma T_1^4 > S_2 > \sigma T_2^4$ ($\sigma$ is the Stefan-Boltzmann constant). This problem is non-trivial, for the temperature changes very abruptly within the front of the CW. Once we find the flux $S_2$, the velocity of the wave is readily derived from energy-balance considerations

$$S_2 = u\rho_1 c_p (T_1 - T_2), \tag{1}$$

where $c_p$ is the specific of air at constant pressure, which we shall assume for simplicity to be constant, and $\rho_1$ is the density of the air through which the wave travels. The basis for writing such a balance is the fact that the velocity of the wave, according to estimates made, is subsonic, so that the pressure p is practically constant over the narrow front of the CW (as the air becomes cooler, it becomes compressed, so that $p \sim \rho T \approx$ const).

The lower temperature of the CW or the transparency temperature is not a strictly defined quantity. This is that temperature, below which the absorption and radiation of light become very small. More accurately, it is the temperature at which the free path of the light becomes comparable with the characteristic dimension R, over which the temperature drops from $T_2$ to a sufficiently low value, say 1,000°,

$$l(T_2) \approx R. \tag{2}$$

When the wave propagates through expanding air, this dimension is determined by the hydrodynamics of the entire motion as a whole. The faster the adiabatic cooling, the smaller this dimension. Thanks to the exceedingly sharp exponential dependence of the free path on the temperature, the transparency temperature has a rather narrow range, in spite of the arbitrariness in its definition, and depends logarithmically on the dimension R and on the air density $\rho_1$.

If the free path, suitably averaged over the spectrum, is

$$l = a(T)(\rho_0/\rho)\, e^{I/kT}, \tag{3}$$

where a is a slowly-varying function of T (we assume for air $a = 2.8 \times 10^{-12} \times T^2$ cm), $\rho_0$ is the normal air density (see below), than the transparency temperature, according to (2) is

$$T_2 = \frac{I}{k}\left(\ln \frac{R\rho}{a\rho_0}\right)^{-1}. \tag{4}$$

It will be shown below that the radiation from the surface of the CW is always generated at the lower edge of the step, regardless how high the step, i.e., at initial gas temperatures $T_1$ as high as convenient. The flux $S_2$ radiated by the CW is determined principally by the transparency temperature and equals approximately $2\sigma T_2^4$.

The speed of propagation of the CW, which is proportional to

$$u \sim 2\sigma T_2^4 / p(1 - T_2/T_1), \tag{5}$$

in the case of a sufficiently strong wave, when $T_2 \ll T_1$, thus depends principally only on the pressure.* The table gives several calculated

*The coefficient of radiant heat conduction again becomes large at low temperatures (below ~ 10,000°), owing to the sharp increase in the free path $l$, which passes through a minimum at $T \sim 50{,}000°$ [$l(T)T^3$ has a minimum at $T \sim 10{,}000°$]. However, at larger free paths, comparable with the dimensions of the system, the radiation transfer no longer has the nature of heat conduction.

*If it is taken into account that at high temperatures ionization causes the specific heat to increase with temperature, then the relations (1) and (5) become somewhat more complicated. In this case it becomes necessary to write the specific enthalpies $W(T_1p)$ and $W(T_2p)$ in lieu of $c_pT_1$ and $C_pT_2$.

u, km/sec at p = 1 atmos

| R, m / $T_2°$ | 10 / 10 700 | 50 / 9 700 | 100 / 9 300 |
|---|---|---|---|
| $T_1°$ | | | |
| 20 000 | 2.7 | 2.1 | 1.7 |
| 50 000 | 1.8 | 1.4 | 1.1 |
| 100 000 | 1.6 | 1.2 | 1.0 |

values of the velocity u in kilometers per second in air at atmospheric pressure, at various values of $T_1$ and $T_2$. The same table indicates also the values of R, from which the temperature $T_2$ was obtained with formula (4).

It is shown in the theory of heat conduction that the time t required to cool a hot body is proportional to $R_0^2 c_p \rho / \kappa$, where $\kappa$ is the coefficient of heat conduction, and $R_0$ is the dimension of the body. The relation $t \sim R_0^2$ is based on the assumption of a gradual similar reduction in temperature of the entire mass of the body. If a hot body is cooled by radiation, with a cooling wave traveling from the periphery toward the center, the cooling time is quite different, namely $t \sim R_0/u$. Thus, a mass of air approximately 100 m in radius, heated at atmospheric pressure to temperatures on the order of tens and hundreds of thousands of degrees, cools down by radiation to about 10,000° within approximately 0.1 seconds. The radiation cooling that follows is considerably slower and is of an entirely different, three-dimensional character (since the free path of the light becomes comparable with the dimensions of the body). The mechanism of absorption and radiation of light now becomes different.

Owing to the great extent of the lower edge of the CW, and also owing to absorption and radiation of light by the air cooled by the CW, the front of the CW almost always remains invisible. All these questions, including that of the possibility of experimental observation of the CW, are beyond the scope of this investigation.

We develop below an approximate theory of the CW, i.e., we examine in detail that narrow layer, in which the temperature drops sharply from $T_1$ to $T_2$.

## 2. STATEMENT OF THE COOLING-WAVE PROBLEM

Disregarding the specific dimensions and shape of the cooled air mass, we seek a solution for the non-stationary equations of radiant heat exchange in the form $T(x - ut)$, corresponding to a plane wave propagating at constant speed u in a gas of specified temperature $T_1$ and density $\rho_1$. The speed u itself should be found from equations similar to those used to determine the speed of a flame in an explosive mixture.

Actually, the equations do not have an exact solution of the form $T(x - ut)$. The point is that as the wave propagation leads to an increase in the thickness of the layer of cooled air in which the absorption of light, although small, is nevertheless different from zero, and the transparency temperature changes with time. In an unbounded medium, the layer of gas cooled to as low a temperature as desired owing to its infinite extent, turns out to be quite opaque. The flux then vanishes at infinity and no CW mode exists in the strict sense of the word.* This factor, of prime significance in the case of an unbounded medium, raises only an apparent difficulty under real conditions. In fact, the hot region is always bounded and the transparency temperature changes but little with increasing distance covered by the wave, being contained within a rather narrow interval if the system is of practical dimensions. An additional, very slow time variation of the solution, occurs only at the very lowest edge of the wave, which is quite elongated, in the almost-transparent region of the already cooled air.

If the CW propagates in expanding air, adiabatic cooling soon lowers the temperature of the radiation-cooled layers enough to make them practically transparent. An additional slow time variation of T will exist only in the region of adiabatic cooling and will hardly affect the temperature profile in the CW itself.

We shall not consider here the additional absorption of light in the region of low temperatures, on the order of several thousands of degrees, due to the nitrogen oxide and the dioxide formed in the hot air. This absorption hardly affects the wave, although it may play a substantial role in the absorption of the radiation flux from the surface of the wave in the peripheral layers of the air.†

We shall neglect, in addition, the intense molecular absorption in the low-temperature region, a substantial factor for ultraviolet radiation with $\lambda < 2{,}000$ A, since at temperatures on the order of 10,000° and below this part of the spectrum contains only a small fraction of the energy (less than

*To a certain extent, an analogous situation exists in the theory of the stationary propagation of a flame. If the speed of the chemical reaction in the uncombusted mixture is not assumed to be exactly zero, although actually it is a finite but vanishingly small quantity, the mixture will burn out before the flame front reaches it.

†The unique optical effects connected with the formation of oxides of nitrogen in a strong explosion have been considered in detail by one of the authors in Ref. 3.

4%), hardly affecting the energy balance of the CW. To formulate a cooling-wave theory it is necessary to examine, as is usually done in the theory of modes, a plane stationary process in the coordinate system in which the CW is at rest. In order to eliminate the difficulty indicated above and to make the problem stationary, i.e., to change from the true solution $T(x - ut, t)$ (with an additional slow time variation) to the idealized solution $T(x - ut)$, it is possible to employ one of two formally artificial measures. These, however are quite justified physically and, by virtue of what has been said, correspond to the real state of affairs.

It is possible, first, to introduce into the energy equation an additional constant term A, which plays the role of adiabatic cooling. This term specifies the constant dimension R which determines the transparency temperature $T_2$ and makes the absorption in the radiation-cooled region finite. The energy-balance equation becomes in the stationary case

$$u\rho_1 c_p \frac{dT}{dx} + \frac{dS}{dx} = -A, \tag{6}$$

where S is the radiation-energy flux at the point x.

It is possible to disregard completely the weakly-absorbing region of the gas, cooled below the transparency temperature, by determining the transparency temperature $T_2$ at the very outset from formula (4), and by assuming that the medium is absolutely transparent at $T < T_2$ ($l = \infty$).

To determine the radiation flux we employ the diffusion approximation of the rigorous kinetic equation. This approximation takes the angular distribution of the radiation into account in an approximate manner. In the diffusion approximation we add to the rigorous equation for the radiation balance

$$dS/dx = c(U_{eq} - U)/l \tag{7}$$

the approximate connection between the flux S and the radiation energy density* U

$$S = -{}^1/_3 lcdU/dx. \tag{8}$$

Here

$$U_{eq} = 4\sigma T^4/c \tag{9}$$

is the equilibrium radiation density, and c is the velocity of light. We disregard the spectral composition of the radiation, characterizing the radiation transfer in a suitable manner by means of a free path $l$ averaged over the spectrum.

It will be shown below that in a considerable portion of the CW the true radiation density U is quite close to the equilibrium density $U_{eq}$. In this case, as is known,[4] the free path is averaged as done by Rosseland. In the region of the cooled air, U differs greatly from $U_{eq}$ and the free path should be averaged, quite differently. For simplicity we shall use everywhere the Rosseland average, taking advantage of the fact that the Boltzmann exponential factor remains equal to $l$ for any averaging method, and that all the important effects in the CW depend only logarithmically on the multiplier in front of the exponential, which naturally depends on the method of averaging. The Rosseland averaging of the Kramers formula for the photoelectric absorption of quanta by excited atoms[4] yields, after substitution of known constants, the multiplier $a(T)$ in front of the exponential of formula (3) for the free path.

In Eqs. (7) and (8) it is convenient to change from the geometrical coordinate x to the optical thickness $\tau$, using the formula

$$d\tau = -dx/l, \quad \tau = -\int dx/l, \tag{10}$$

and reckoning $\tau$ from the place where $l = \infty$, in the direction of increasing absorption, i.e., of higher temperature:

$$dS/d\tau = -c(U_{eq} - U); \tag{11}$$

$$S = {}^1/_3 cdU/d\tau \tag{12}$$

Dispensing with exact calculation of the angular distribution of the radiation, it is also possible to write approximate integral expressions for the flux and for the density by assuming that all the quanta move "forward" and "backward" parallel to the x axis

$$S = \frac{c}{4}\left[\int_\tau^\infty U_{eq} e^{\tau - \tau'} d\tau' - \int_0^\tau U_{eq} e^{\tau' - \tau} d\tau'\right]; \tag{13}$$

$$U = \frac{1}{2}\left[\int_\tau^\infty U_{eq} e^{\tau - \tau'} d\tau' + \int_0^\tau U_{eq} e^{\tau' - \tau} d\tau'\right]. \tag{14}$$

The coefficients in front of the square brackets are chosen such as to make formulas (13) and (14) give the correct values of the flux from the surface of an absolutely black body and the correct density inside the black body, away from the boundary. To take effective account of the angular distribution it is necessary to employ in these formulas not the true free path, but half its value. It is easy to check that in this case (13) and (14) satisfy Eqs. (11) and (12), which are of the diffusion type, with a coefficient of diffusion proportional to $1/4$ instead

*One must not confuse the diffusion approximation with the approximation of radiant heat conduction, which is one particular case in which the true density U in Eq. (8) is replaced by the equilibrium value $U_{eq}$.

of to $\frac{1}{3}$.* On the upper edge of the CW, as already mentioned above, the flux is nearly zero, and therefore one of the boundary conditions for Eqs. (11) and (12) is

$$\tau = \infty, \quad S = 0. \tag{15}$$

The second boundary condition should be specified on the boundary between the absorbing and absolutely transparent media, i.e., at $\tau = 0$. This is the well known diffusion condition, by which the diffusion flux on the boundary with the "vacuum" equals half the kinetic flux

$$\tau = 0, \quad S = cU/2. \tag{16}$$

Integral expressions (13) and (14) satisfy this condition automatically.

## 3. WEAK COOLING WAVE

Let us consider the limiting case of a weak CW, in which the upper temperature $T_1$ barely exceeds the lower one $T_2$. The free path, however will be assumed here quite strongly dependent on the temperature, so that the following conditions become compatible: the condition $l(T_1) \ll l(T_2)$, which is necessary for the very existence of the CW, and the condition $T_1 \approx T_2$, $T_1^4 \approx T_2^4$, which is necessary if the wave is to be considered a weak one.

The examination of the weak wave is of interest essentially as far as method goes. With this example, by simplification of the initial equations, we can obtain an exact analytical solution of the equations. Let us use the first of the artifices indicated in the preceding section and assume that constant adiabatic cooling A exists along with radiant heat exchange, so that the energy equation is written in form (6). The integral of the energy equation (6) contains an integration constant C, determined by the choice of the origin for the coordinate x, i.e., arbitrary (the equation has a translation group):

$$u\rho_1 c_p T + S = -Ax + C. \tag{17}$$

On the lower and upper edges of the CW, where the flux S tends to $S_2$ (the flux that goes to infinity) and to zero, the quantity $u\rho_1 c_p T$ tends asymptotically to two straight lines

$$u\rho_1 c_p T = -Ax - S_2 + C_2, \quad x \to \infty; \tag{18}$$

$$u\rho_1 c_p T = -Ax + C, \quad x \to -\infty, \tag{19}$$

whose ordinates are apart by the amount of flux $S_2$ that goes to infinity.

The step in the CW is contained between these two lines: our problem consists of finding the position of this step. Let us now use the condition that the wave is weak. Since the phenomenon plays itself out in a narrow temperature range, it is possible to assume approximately in the equations for the radiation transfer that the factor $U_{eq}$, to which the radiating ability is proportional, is a constant. Obviously this factor, whose limits in the wave are

$$4\sigma T_2^4/c < U_{eq} < 4\sigma T_1^4/c,$$

can be set equal to any of these limits, since the two limits are nearly equal. We shall assume specifically that $U_{eq} = 4\sigma T_2^4/c$. Here obviously the flux going to infinity is

$$S_2 = \sigma T_2^4, \tag{20}$$

If $U_{eq}$ is constant, the equations for the radiation transfer become much simpler. We start with the integral expression (13) and obtain

$$S = S_2 e^{-\tau}. \tag{21}$$

Inserting (21) into (17) we get

$$u\rho_1 c_p T = -Ax - S_2 e^{-\tau} + C. \tag{22}$$

When the temperature obtained from this formula is inserted into (10) we get a first-order differential equation for the function $x(\tau)$ and, returning to (22), we get $T(\tau, S_2)$ and $T(x, S_2)$. To solve this equation we note that, in the narrow temperature range of interest to us, the actual Boltzmann dependence of the free path on the temperature, which is given by formula (3) (we neglect the weak temperature dependence of the multiplier ahead of the exponent), can be approximated by an exponential one

$$l = (a\rho_0/\rho)\exp\left\{\frac{I}{kT_0} - (T - T_0)\frac{I}{kT_0^2}\right\}$$

$$= l(T_0)\exp\left\{-\frac{(T - T_0)I}{kT_0^2}\right\}, \tag{23}$$

where $T_0$ is a certain temperature about which the exponent is expanded.

Such an approximation was made by Frank-Kamenetskii in the theory of thermal explosions.[5] This formula automatically insures that the flux tends to zero at $x \to -\infty$, where the temperature tends to infinity [and its gradient, according to (22), is finite], which is essential for the existence of the mode. The temperature $T_0$, about which the expansion is made and which can be specified arbitrarily, will be defined by the equation

*Using half the value of the free path means that the average cosine of the "forward" and "backward" quanta is assumed to be one-half. The differential equations equivalent to the integral expressions in (13) and (14) are known in astrophysics as the Schwarzschild approximation.[4]

$$Al(T_0)\, I/u\rho_1 c_p T_0 kT_0 = 1. \tag{24}$$

Let us change to dimensionless quantities, using the formulas

$$\Theta = (T - T_0)\, I/T_0 kT_0, \tag{25}$$

$$d\xi = dx/l(T_0); \tag{26}$$

$$s = \frac{S_2}{u\rho_1 c_p T_0}\frac{I}{kT_0} = \frac{S_2}{Al(T_0)}\frac{I}{kT_0}\frac{(T_1 - T_2)}{T_0}. \tag{27}$$

Equations (22) and (10) assume the following form in dimensionless quantities

$$\Theta = -\xi - se^{-\tau} + C, \tag{28}$$

$$d\xi = -e^{-\Theta}\, d\tau. \tag{29}$$

Their solutions, with the boundary conditions $\tau = 0$, $\xi = \infty$ $(x = \infty)$

$$\xi = -\ln\left[\int_0^\tau e^{se^{-\tau}} d\tau\right] + C, \tag{30}$$

$$\Theta = \ln\left[\int_0^\tau e^{se^{-\tau}}\, d\tau\right] - se^{-\tau} \tag{31}$$

yields the parametric relation for $\Theta(\xi)$ i.e., the temperature profile in a weak CW. Using the substitution $z = e^{-\tau}$, the integral in (30) or (31) is expressed in terms of the tabulated $\overline{\mathrm{Ei}}(x)$ functions (Ref. 6)

$$\overline{\mathrm{Ei}}(x) = \int_{-\infty}^{x} e^y \frac{dy}{y}, \tag{32}$$

namely:

$$J = \int_0^t e^{se^{-\tau}}\, d\tau = \overline{\mathrm{Ei}}(s) - \overline{\mathrm{Ei}}(se^{-\tau}). \tag{33}$$

On the lower edge of the CW, the temperature approaches the lower straight line asymptotically (at $\tau \ll 1$, $s\tau \ll 1$, $\Theta \to -\infty$), in accordance with

$$\xi = -\Theta - s + s(1 - \exp(-e^{\Theta}) + C. \tag{34}$$

On the higher-temperature side the profile $\Theta(\xi)$ has the character of a step, whose slope increases all the time with increasing $\Theta$. Only when $\Theta$ almost reaches the upper straight line does the curve $\Theta(\xi)$ pass through the point of inflection and begins to approach the upper straight line asymptotically, again in accordance with (34), but for

$$\tau \gg 1,\ se^{-\tau} \ll 1,\ \Theta \to +\infty,$$

These laws are illustrated in Fig. 3, which shows the plot of $\Theta(\xi)$ at $s = 5$. $\xi$ is measured from the point at which $\Theta = 0$. It is natural to assume the front of the CW to be the point of inflection of $\Theta(\xi)$, a point at which the slope of the step has a maximum, and to assume the upper and lower

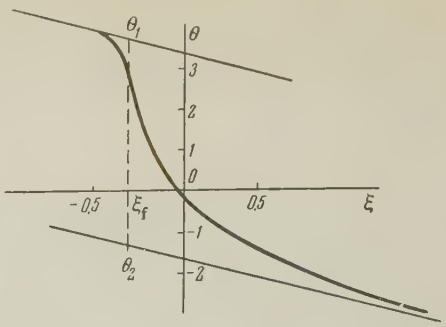


FIG. 3

temperatures of the CW to be the values of $\Theta$ on the asymptotic lines at the coordinate of the point of inflection (see Fig. 3).

The optical thickness $\tau_f$ corresponding to the front of the CW can be found from the equation $d^2\Theta/d\xi^2 = 0$. Differentiation of (30) and (31) gives a transcendental equation for $\tau_f$ as a function of the parameter s.

$$J_f = \overline{\mathrm{Ei}}(s) - \overline{\mathrm{Ei}}(\beta) = e^{\beta}/(1 - \beta),\ \beta = se^{-\tau_f}. \tag{35}$$

The temperature at the point of inflection, $\Theta_f$, and also the upper and lower temperatures $\Theta_1$ and $\Theta_2$ of the CW, are

$$\Theta_f = -\ln(1 - \beta), \tag{36}$$

$$\Theta_1 = \Theta_f + \beta, \tag{37}$$

$$\Theta_2 = \Theta_f + \beta - s. \tag{38}$$

The problem of finding the lower temperature $T_2$ of the CW, and consequently the velocity u of the CW for specified upper temperature $T_1$ and for adiabatic cooling A, is readily solved by successive approximations. We assume some value of the parameter s and use Eqs. (34) to (38) to calculate $\Theta_1$ and $\Theta_2$. Then, changing to real temperatures in accordance with (25), we determine $T_0$ and $T_2$. Inserting these values into (27) we find the parameter s in the next approximation, etc. The successive approximations converge rapidly, since $T_0$ depends logarithmically on s.

It is more convenient to proceed in the reverse manner: specify the values of the parameter s and any one of the two quantities characterizing the CW, either $T_1$ or $T_2$, and then determine the second quantity and the adiabatic cooling A necessary to insure the existence of a stationary mode. Thus, for the case $s = 5$ illustrated in Fig. 3, we obtain from Eqs. (35) to (38): $\beta = 0.93$, $\tau_f = 1.69$, $\Theta_f = 2.7$, $\Theta_1 = 3.7$, and $\Theta_2 = -1.3$. For example, at an upper temperature $T_1 = 12{,}250°$, the lower temperature turns out to be $T_2 = 9200°$, with $T_0 = 10{,}000°$ (I is assumed to be 14 ev for air).

The only really interesting values of the parameter s are those much greater than unity. In fact, it follows from (23) that

$$s = \Theta_1 - \Theta_2 = l(T_1)/l(T_2), \tag{39}$$

and the ratio of the free paths must be greater than unity for the very existence of the CW, as already mentioned at the beginning of this section. (On the other hand, s is bounded from above by the condition that the wave must be weak.) In the case when $s \gg 1$, all the formulas become substantially simplified and an approximate relation can be established in explicit form between the lower temperature of the CW and the value of the adiabatic cooling. In this case the temperature $T_0$ about which the range is expanded drops out entirely from the equation.

Using the asymptotic expression $\overline{\mathrm{Ei}}(s) \approx e^s/s$ for $s \gg 1$, and noting that when $s \gg 1$ the root of (35) is $\beta \approx 1$, ($\tau_f \approx \ln s$), we obtain from (31) and (35)

$$\Theta_f \approx \ln \overline{\mathrm{Ei}}(s) - 1 \approx s - \ln s - 1. \tag{40}$$

From this we obtain from (38)

$$\Theta_2 \approx -\ln s. \tag{41}$$

Returning to the true temperature with the aid of (25) and taking (27) and (23) into account, we obtain the desired relation

$$Al(T_2) = S_2 = \sigma T_2^4, \tag{42}$$

It must be noted that according to (37) $\Theta_1 > \Theta_f > 0$, and according to (41) $\Theta_2 < 0$, i.e., the free path is expanded in accordance with (23) about the intermediate temperature in the CW:

$$T_2 < T_0 < T_f < T_1.$$

[1] L. I. Sedov, Методы подобия и размерности в механике (Similitude and Dimensionality Methods in Mechanics) Moscow 3d Ed., Gostekhizdat, 1954.

[2] G. Taylor, Proc. Roy. Soc. **201**, 175 (1950).

[3] Iu. P. Raizer, J. Exptl. Theoret. Phys. (U.S.S.R.) **34**, 483 (1958), Soviet Phys. JETP **7**, 331 (1958).

[4] A. Unsold, Physics of Stellar Atmospheres, (Russ. Transl.), IIL, 1949.

[5] D. A. Frank-Kamenetskii, J. Phys. Chem. (U.S.S.R.) 13, 738 (1939). Диффузия и теплопередача в химической кинетике (Diffusion and Heat Transfer in Chemical Kinetics), Acad. Sci. Press, 1947.

[6] E. Jahnke and F. Emde, Tables of Functions, N. Y. Dover, 1945.

Translated by J. G. Adashko
255

SOVIET PHYSICS JETP VOLUME 34(7), NUMBER 5 NOVEMBER, 1958

# *EXCITATION OF VIBRATIONAL AND ROTATIONAL STATES OF NUCLEI DUE TO SCATTERING OF NUCLEONS*

S. I. DROZDOV

Submitted to JETP editor December 22, 1957

J. Exptl. Theoret. Phys. (U.S.S.R.) **34**, 1288-1291 (May, 1958)

Scattering of fast nucleons by black nuclei possessing vibrational or rotational levels is considered in the adiabatic approximation. It is shown that, in the diffraction region of scattering angles, the shape of the angular distributions of nucleons of definite energy, scattered with excitation of a given collective level of an even-even nucleus, does not depend on whether the level is a rotational or vibrational one.

WE consider the scattering of fast neutrons or protons from nuclei possessing vibrational or rotational excited states.[1] We shall assume that the wavelength of the incident particle $k^{-1}$ is much smaller than the nuclear dimension R ($kR \ll 1$), that the energy of the proton significantly exceeds the value of the Coulomb barrier ($Ze^2/RE \ll 1$), and that the nucleus absorbs all particles incident upon it (black nucleus). These assumptions correspond to neutron energies $E \gtrsim 10$ Mev and pro-

ton energies $E \gtrsim 20$ Mev. In this case, it is appropriate to make use of the adiabatic approximation, according to which the nucleus can be regarded as fixed during the scattering process. The condition of applicability of this approximation[2] can be written in the form $(\Delta\epsilon/E)kR \ll 1$, where $\Delta\epsilon$ is the energy of the collective excitation.

As is known, the determination of the effective cross sections in the adiabatic approximation reduces to the calculation of the amplitude of elastic scattering of particles by a nucleus of fixed orientation $f(\alpha_{lm}, \Omega)$. This amplitude depends not only on the direction of the scattering $\Omega = (\vartheta, \Phi)$, but also on the parameters $\alpha_{lm}$ which determine the shape of the nucleus (in the fixed system of reference):

$$r(\mathbf{n}) = R\left(1 + \sum_{lm} \alpha_{lm} Y_{lm}(\mathbf{n})\right),$$

where $Y_{lm}(\mathbf{n})$ are the normalized spherical harmonics. In the case of nuclei possessing vibrational levels,[1] the quantities $\alpha_{lm}$ can be connected with the operators of creation and annihilation of excitation quanta (phonons) having a momentum $l$ with a projection $m$ on the fixed axis:

$$\alpha_{lm} = \sqrt{\frac{4\pi}{2l+1}} \frac{p_l}{R} (b_{lm} + (-)^m b^*_{l,-m}), \qquad (1)$$

where $p_l$ is the amplitude of the zero vibrations about the equilibrium sphere of radius R. The operators $b_{lm}$, $b^*_{lm}$ act as usual on the wave functions of the vibrational states $\psi_n(\alpha_{lm})$:

$$b\psi_n(\alpha) = \sqrt{n}\,\psi_{n-1}(\alpha); \quad b^*\psi_n(\alpha) = \sqrt{n+1}\,\psi_{n+1}(\alpha). \qquad (2)$$

If, on the other hand, the nucleus possesses rotational levels, and its surface in the characteristic system of reference of the nucleus is described by the equation

$$R(\mu) = R\left(1 + \sum_l \alpha_l P_l(\mu)\right),$$

then the parameters $\alpha_{lm}$ depend in the following way on the angles $\omega(\theta, \varphi)$ which define the direction of the axis of symmetry of the nucleus in the fixed system of coordinates:

$$\alpha_{lm}(\omega) = \frac{4\pi\alpha_l}{2l+1} Y^*_{lm}(\omega). \qquad (3)$$

In small-angle scattering $\theta < 1$ and for the conditions given above the amplitude of the elastic scattering of nucleons from a fixed nucleus can be given in the form[2]

$$f(\omega, \Omega) = f_e(\omega, \Omega) + f_d(\omega, \Omega). \qquad (4)$$

Here $f_e(\omega, \Omega)$ is the scattering amplitude of particles in the electric field of the fixed nucleus.

Considering scattering at small angles, we can neglect the finite charge distribution in the nucleus. For a sufficiently small departure of the nuclear shape from spherical, when the conditions

$$\alpha_2 Ze^2/\hbar v \ll 1 \quad \text{or} \quad (p_2/R)\,Ze^2/\hbar v \ll 1 \qquad (5)$$

are satisfied for nuclei with rotational or vibrational levels, respectively, the effect of multipole electric interaction on the scattering can be taken into account by perturbation theory. In this case, we can write down the scattering amplitude in the electric field of the nucleus in the form

$$f_e(\omega, \Omega) = f_c(\theta) + \sum_{lm} \alpha_{lm}(\omega) \langle \mathbf{k}' | V_{lm} | \mathbf{k} \rangle;$$

$$f_c(\theta) = -\frac{2\eta}{k} \frac{\Gamma(1+i\eta)}{\Gamma(1-i\eta)} \exp\left\{-2\eta i \ln \frac{\theta}{2}\right\}; \quad \eta = \frac{Ze^2}{\hbar v}, \qquad (6)$$

$$\langle \mathbf{k}' | V_{lm} | \mathbf{k} \rangle = -\frac{\mu}{2\pi\hbar^2} \frac{3Ze^2R^l}{(2l+1)} \int \psi^+_{-\mathbf{k}'}(\mathbf{r})\, r^{-l-1} Y_{lm}\left(\frac{\mathbf{r}}{r}\right) \psi^+_{\mathbf{k}}(\mathbf{r})\, d\mathbf{r},$$

where $\mathbf{k}$ and $\mathbf{k}'$ are the wave vectors of the incident and scattered particle, respectively, and the $\psi^+_{\mathbf{k}}(\mathbf{r})$ are the wave functions that describe the scattering in the Coulomb field $Ze^2/r$ (Ref. 3).

According to Ref. 2, the second term in Eq. (4) has the form

$$f_d(\omega, \Omega) = i \frac{(kR)^{2(1+i\eta)}}{k} \xi(\omega)\, t^{-2(1+i\eta)} \int_0^t x^{1+2i\eta} J_0(x)\, dx;$$

$$t = kR\theta\,[\xi^2(\omega)\cos^2(\varphi - \Phi) + \sin^2(\varphi - \Phi)]^{1/2}; \qquad (7)$$

$$\xi(\omega) = [1 + \varepsilon]^{-1}; \quad \varepsilon = \sum_l \sqrt{\frac{2l+1}{4\pi}}\, \alpha_{l0}(\omega).$$

When $\eta = 0$, the amplitude of $f_d(\omega, \Omega)$ describes the diffraction scattering of neutrons; it is therefore natural to call it the diffraction part of the amplitude of $f(\omega, \Omega)$.

We shall assume that the nucleus is in the ground state prior to scattering, and shall limit ourselves below to a consideration of elastic scattering with a transition of the nucleus from the ground to the first excited state. We shall consider only quadrupole deformations of the nucleus, assuming that the only $\alpha_{lm}$ different from zero are those with $l = 2$. In this case it is appropriate, for calculation of the effective cross section, to expand the amplitude $f(\omega, \Omega)$ in a series of powers of the deformation parameter $\alpha_{lm}$. If condition (5) is satisfied, then Eq. (6) already gives essentially this expansion for the amplitude $f_e(\omega, \Omega)$. In order to obtain a similar expansion of the diffraction part $f_d(\omega, \Omega)$, it is useful to expand in powers of $\epsilon$ in Eq. (7). Denoting $kR\theta = a$, we get

$$f_d(\omega, \Omega) = \frac{i}{k} (kR)^{2(1+i\eta)} \left\{ a^{-2(1+i\eta)} \int_0^a x^{1+2i\eta} J_0(x)\, dx \right.$$

$$+\alpha_{20}(\omega)\sqrt{\frac{5}{4\pi}}\left[i\eta a^{-2(1+i\eta)}\int_0^a x^{1+2i\eta}J_0(x)\,dx-\frac{1}{2}J_0(a)\right]$$

$$-(e^{i2\Phi}\alpha_{22}(\omega)+e^{-i2\Phi}\alpha_{2-2}(\omega))\frac{1}{4}\sqrt{\frac{5}{6\pi}} \qquad (8)$$

$$\times\left[(1+i\eta)\,a^{-2(1+i\eta)}\int_0^a x^{1+2i\eta}J_0(x)\,dx-\frac{1}{2}J_0(a)\right]\Big\}+\ldots$$

When calculating the effective cross sections, we can limit ourselves to the expansion terms written down, if

$$\alpha_2 kR\theta\ll 1 \text{ or } (p_2/R)\,kR\theta\ll 1. \qquad (9)$$

We can obtain these conditions if we compute the terms of order $\alpha_{2m}^2$ and $\alpha_{2m}^3$ and compare their contribution to the scattering cross section with the contribution from terms of zeroth and first order in $\alpha_{2m}$, putting $\eta\sim 1$.

In adiabatic approximation, as is well known, the differential scattering cross section, for which the nucleus undergoes a transition from the state $\varphi_\nu(\omega)$ to the state $\varphi_{\nu'}(\omega)$, is determined by the square of the modulus of the matrix element $\langle\varphi^*_{\nu'}(\omega)\,f(\omega,\Omega)\,\varphi_\nu(\omega)\rangle$. In particular, the excitation cross section of the rotational state (I, M) of the even-even nucleus has the form

$$\sigma_{IM}(\Omega)=|\langle Y^*_{IM}(\omega)\,f(\omega,\Omega)\,Y_{00}(\omega)\rangle|^2. \qquad (10)$$

Similarly, in the case of scattering from a nucleus with vibrational levels, the excitation cross section of n phonons $(l, m)$ is equal to

$$\sigma^{(n)}_{lm}(\Omega)=|\langle\psi^*_n(\alpha_{lm})\,f(\alpha_{lm},\Omega)\,\psi_0(\alpha_{lm})\rangle|^2. \qquad (11)$$

In this case the matrix elements of the amplitude $f(\alpha_{2m},\Omega)$, which determine the elastic and inelastic scattering cross sections, have in accord with Eqs. (1, 2, 4, 6, and 8), the form:

$$\langle\psi^*_0(\alpha_{2m})\,f(\alpha_{2m},\Omega)\,\psi_0(\alpha_{2m})\rangle=\frac{i}{k}(kR)^{2(1+i\eta)}a^{-2(1+i\eta)}\int_0^a x^{1+2i\eta}J_0(x)\,dx+f_c(\theta);$$

$$\langle\psi^*_1(\alpha_{20})\,f(\alpha_{2m},\Omega)\,\psi_0(\alpha_{20})\rangle=\frac{p_2}{R}\left\{i\frac{(kR)^{2(1+i\eta)}}{k}\left[i\eta a^{-2(1+i\eta)}\int_0^a x^{1+2i\eta}J_0(x)\,dx\right.\right.$$

$$\left.\left.-\frac{1}{2}J_0(a)\right]+\sqrt{\frac{4\pi}{5}}\langle\mathbf{k}'|V_{20}|\mathbf{k}\rangle\right\}, \qquad (12)$$

$$\langle\psi^*_1(\alpha_{2\pm1})\,f(\alpha_{2m},\Omega)\,\psi_0(\alpha_{2\pm1})\rangle=-\frac{p_2}{R}\sqrt{\frac{4\pi}{5}}\langle\mathbf{k}'|V_{2\mp1}|\mathbf{k}\rangle;$$

$$\langle\psi^*_1(\alpha_{2\pm2})\,f(\alpha_{2m},\Omega)\,\psi_0(\alpha_{2\pm2})\rangle$$

$$=\frac{p_2}{R}\left\{-\frac{e^{\pm i2\Phi}}{2\sqrt{6}}i\frac{(kR)^{2(1+i\eta)}}{k}\left[(1+i\eta)\,\alpha^{-2(1+i\eta)}\int_0^a x^{1+2i\eta}J_0(x)\,dx\right.\right.$$

$$\left.\left.-\frac{1}{2}J_0(a)\right]+\sqrt{\frac{4\pi}{5}}\langle\mathbf{k}'|V_{2\mp2}|\mathbf{k}\rangle\right\}.$$

Making use of the relation (3), we note that the matrix elements that determine the scattering cross section from a nucleus with rotational levels differ from the matrix elements (12) only by a factor which is independent of the scattering angle, namely,

$$\langle Y^*_{00}(\omega)\,f(\omega,\Omega)\,Y_{00}(\omega)\rangle$$
$$=\langle\psi^*_0(\alpha_{2m})\,f(\alpha_{2m},\Omega)\,\psi_0(\alpha_{2m})\rangle;$$
$$\langle Y^*_{2m}(\omega)\,f(\omega,\Omega)\,Y_{00}(\omega)\rangle$$
$$=\frac{R}{p_2}\frac{\alpha_2}{\sqrt{5}}\langle\psi^*_1(\alpha_{2m})\,f(\alpha_{2m},\Omega)\,\psi_0(\alpha_{2m})\rangle. \qquad (13)$$

It is seen from Eqs. (10) to (13) that in a region of sufficiently small angles (9), the form of the angular distribution of the nucleons of a given energy, which scatter with the excitation of a given collective state of the black nucleus, does not depend on whether this state is rotation or vibrational. The forms of the angular distributions

$$\sigma_2(\Omega)=\sum_M\sigma_{2M}(\Omega) \quad \text{and} \quad \sigma^{(1)}_2(\Omega)=\sum_m\sigma^{(1)}_{2m}(\Omega),$$

of the corresponding excited levels are also independent of the nature of the level.

It is curious to note that the collective states of an even-even nucleus with odd projections of the moment are excited only because of the electrical interaction, i.e., they do not arise in neutron scattering. We also note that the equations in (4), which describe the scattering of neutrons on nuclei with vibrational levels, follow from Eqs. (11) and (12) for $\eta=0$.

The author thanks B. T. Geilikman for discussion of this research.

[1] K. Alder, A. Bohr et al., Revs. Mod. Phys. **28**, 432 (1956); A. Bohr, K. Danske Vidensk. Selsk. Mat. fys. Medd. **26**, No. 14 (1952).

[2] S. I. Drozdov, J. Exptl. Theoret. Phys. (U.S.S.R.)

28, 734 (1955), Soviet Phys. JETP 1, 591 (1955); Атомная энергия (Atomic Energy), 2, 501 (1957).

[3] L. D. Landau and E. M. Lifshitz, Квантовая механика (Quantum Mechanics), Moscow, 1948 [English translation, Addison Wesley, 1957].

[4] E. V. Inopin, J. Exptl. Theoret. Phys. (U.S.S.R.) 31, 901 (1956), Soviet Phys. JETP 4, 764 (1957).

Translated by R. T. Beyer
256

SOVIET PHYSICS JETP VOLUME 34(7), NUMBER 5 NOVEMBER, 1958

# *KINETIC THEORY OF MAGNETOHYDRODYNAMIC WAVES*

K. N. STEPANOV

Physico-Technical Institute, Academy of Sciences, Ukrainian S.S.R.

Submitted to JETP editor December 24, 1957

J. Exptl. Theoret. Phys. (U.S.S.R.) 34, 1292-1301 (May, 1958)

We take account of thermal motion of electrons and ions in considering the propagation of magnetohydrodynamic waves in an ionized gas.

As has been shown by Åström[1,2] and Ginzburg,[3] magnetohydrodynamic waves in an ionized gas are nothing more than low-frequency ordinary and extraordinary electromagnetic waves, familiar from the theory of the propagation of radio waves in the ionosphere. The frequency of these waves is much less than the Larmor frequency of the ions. In the above-cited works the electron and ion motions were described by equations for their mean velocities. The phase velocity $V_\Phi$ of a magnetohydrodynamic wave is usually much less than the velocity of light $c$, and may be comparable with the mean thermal velocity $v_T^e$ and $v_T^i$ of the electrons and ions. One can therefore expect that if $V_\Phi \lesssim v_T^e$, the thermal velocity of the charged particles will strongly influence the propagation of the magnetohydrodynamic waves.

If the frequency $\omega$ of the magnetohydrodynamic waves is much less than the frequency $\nu_c$ of "short-range" collisions, and if the wavelength $\lambda$ is large compared with the mean free path, a local Maxwell distribution is established during a time on the order of $2\pi/\omega$. In this case, as is well known, the equations of hydrodynamics can be used, and it follows that in addition to magnetohydrodynamic waves of the Alfven type, two mixed magnetosound waves may propagate in the plasma. If, on the other hand, $\omega \gg \nu_c$, the thermal motion of the charged particles can be taken into account by finding the magnetohydrodynamic wave propagation using the kinetic equation with self-consistent interaction.[4]

The present work is devoted to the kinetic theory of magnetohydrodynamic waves propagating in a plasma at any angle $\theta$ with respect to an external magnetic field. "Short-range" collisions leading to damping of the waves are not included. The case $\theta = 0$ has been treated by Gershman[5] (see also Dungey[6]). It is found that if $\theta = 0$, the "short-range" collisions give only a small contribution even if it is not true that $\nu_c \ll \omega$.[3,5,6] In any case, the effect of "short-range" collisions will be small for arbitrary $\theta$ if $\nu_c \ll \omega$.

## 1. DISPERSION EQUATION

Consider electromagnetic waves propagating in a plasma of electrons and singly ionized ions. Let $f_{0\alpha}$ be the equilibrium value of the distribution function for particles of type $\alpha$ ($\alpha = e$ denotes electrons, and $\alpha = i$ denotes ions). We shall write a kinetic equation for $f_\alpha(\mathbf{v}, \mathbf{r}, t)$, the small difference between the actual value of the distribution function and $f_{0\alpha}$, assuming that the frequency of the waves is so high that we may neglect the collision integral in this equation. We then have

$$\frac{\partial f_\alpha}{\partial t} + \mathbf{v}\frac{\partial f_\alpha}{\partial \mathbf{r}} + \frac{e_\alpha}{m_\alpha}\mathbf{E}\frac{\partial f_{0\alpha}}{\partial \mathbf{v}} - \omega_H^\alpha \frac{\partial f_\alpha}{\partial \vartheta} = 0, \qquad (1)$$

$$\omega_H^\alpha = e_\alpha H_0 / m_\alpha c, \quad f_{0\alpha} = n_0 (m_\alpha / 2\pi T_\alpha)^{3/2} \exp(-m_\alpha v^2 / 2T_\alpha).$$

Here $e_\alpha$ and $m_\alpha$ are the charge and mass of the particles of type $\alpha$ (with $e_i = e > 0$), $H_0$ is the external magnetic field strength, $\vartheta$ is the polar angle in velocity space ($\mathbf{v}$ is the velocity of par-

ticles of type $\alpha$, and the z axis is parallel to $\mathbf{H}_0$), $T_\alpha$ is the temperature of the gas of particles of type $\alpha$, and $n_0$ is the equilibrium electron density, which is equal to the equilibrium ion density. The electric field strength is given by

$$\Delta\mathbf{E} - \operatorname{grad}\operatorname{div}\mathbf{E} - \frac{1}{c^2}\frac{\partial^2\mathbf{E}}{\partial t^2} = \frac{4\pi e}{c^2}\frac{\partial}{\partial t}\left(\int \mathbf{v} f_i\, d\mathbf{v} - \int \mathbf{v} f_e\, d\mathbf{v}\right). \tag{2}$$

Let the external action perturbing the equilibrium state of the plasma be turned off at time $t = 0$. Then, using a Fourier-Laplace method to solve Eqs. (1) and (2), it can be shown that after a sufficiently long time $t$ the Fourier components of the electric field strength will be proportional to $e^{-i\omega' t}$. The complex frequencies $\omega' = \omega - i\gamma$ are defined as the solutions of the dispersion equation for the lowest $\gamma$. To obtain the dispersion equation we insert expressions for $f_\alpha$ and $\mathbf{E}$ proportional to $e^{i(\mathbf{kr}-\omega' t)}$ into (1) and (2), where $\mathbf{k}$ is a given real vector and $\operatorname{Im}\omega' < 0$, which means that $f_\alpha$ and $\mathbf{E}$ are in the form of plane waves. The condition on $\omega'$ corresponds to solving Eqs. (1) and (2) by a Laplace transform in time. The dispersion equation will then be of the form[7]

$$An'^4 + Bn'^2 + C = 0, \quad n' = kc/\omega', \tag{3}$$

where

$$\begin{aligned} A &= \varepsilon_{11}\sin^2\theta + \varepsilon_{33}\cos^2\theta + 2\varepsilon_{13}\cos\theta\sin\theta, \\ B &= 2(\varepsilon_{12}\varepsilon_{23} - \varepsilon_{22}\varepsilon_{13})\cos\theta\sin\theta + \varepsilon_{13}^2 - \varepsilon_{11}\varepsilon_{33} \\ &\quad - (\varepsilon_{22}\varepsilon_{33} + \varepsilon_{23}^2)\cos^2\theta - (\varepsilon_{11}\varepsilon_{22} + \varepsilon_{12}^2)\sin^2\theta, \\ C &= \operatorname{Det}|\varepsilon_{ik}| = \varepsilon_{33}(\varepsilon_{11}\varepsilon_{22} + \varepsilon_{12}^2) + \varepsilon_{11}\varepsilon_{23}^2 + 2\varepsilon_{12}\varepsilon_{23}\varepsilon_{13} - \varepsilon_{22}\varepsilon_{13}^2. \end{aligned} \tag{4}$$

Here $\theta$ is the angle between the wave vector $\mathbf{k}$ and the magnetic field $\mathbf{H}_0$. If $\operatorname{Im}\omega' < 0$, the dielectric constant $\epsilon_{ik}(\omega', k)$ (with $i, k = 1, 2, 3$) is of the form

$$\begin{aligned} \varepsilon_{ik}(\omega', \mathbf{k}) &= \delta_{ik} - i\sum_\alpha \frac{4\pi e e_\alpha}{\omega'\omega_H^\alpha T_\alpha}\int v_i f_{0\alpha} \exp\,(ia_\alpha\sin\vartheta + ib_\alpha\vartheta) \\ &\quad \times \int^{\vartheta} v_k \exp\,(-ia_\alpha\sin\psi - ib_\alpha\psi)\, d\psi\, d\mathbf{v}, \\ a_\alpha &= k_x v_\perp/\omega_H^\alpha, \quad b_\alpha = (k_z v_z - \omega')/\omega_H^\alpha. \end{aligned} \tag{5}$$

The z axis is parallel to $\mathbf{H}_0$, and the x axis lies in the plane containing $\mathbf{k}$ and $\mathbf{H}_0$.

Let us write Eq. (5) in a different form. Consider, for example, $\epsilon_{11}$. Bearing in mind the relations

$$e^{-ia\sin\psi} = \sum_{n=-\infty}^{\infty} J_n(a)\, e^{-in\psi}; \quad \int_0^{2\pi} e^{ia\sin\psi - in\psi}\, d\psi = 2\pi J_n(a) \tag{6}$$

and the expression for the second exponential integral of Weber,[8] we find that

$$\varepsilon_{11} = 1 - \sum_\alpha \frac{v_\alpha z_0^\alpha}{\sqrt{\pi}\,\mu_\alpha} e^{-\mu_\alpha} \sum_{n=-\infty}^{\infty} n^2 I_n(\mu_\alpha) \int_{-\infty}^{\infty} \frac{e^{-t^2}}{z_n^\alpha - t}\, dt, \tag{7}$$

where $I_n(\mu_\alpha)$ is the modified Bessel function, and

$$\begin{aligned} &v_\alpha = \Omega_\alpha^2/\omega'^2, \ \Omega_\alpha = (4\pi n_0 e^2/m_\alpha)^{1/2}, \quad \mu_\alpha = (k_x v_T^\alpha/\omega_H^\alpha)^2; \\ &z_n^\alpha = (\omega' - n|\omega_H^\alpha|)/\sqrt{2}k_z v_T^\alpha; \ v_T^\alpha = (T_\alpha/m_\alpha)^{1/2}. \end{aligned} \tag{8}$$

The series of Eq. (7) can be summed by noting that

$$\int_0^\infty e^{i\lambda\cos\varphi + i\gamma\varphi}\, d\varphi = i\sum_{n=-\infty}^{\infty} \frac{I_n(\lambda)}{\gamma - n} \quad (\operatorname{Im}\gamma > 0). \tag{9}$$

After integrating over $t$, we obtain an expression for $\epsilon_{11}$ in the form of a single integral. The other components of $\epsilon_{ik}$ can be expressed similarly. As a result we arrive at

$$\begin{aligned} \varepsilon_{11} &= 1 - i\sum_\alpha \frac{\Omega_\alpha^2}{\omega'|\omega_H^\alpha|}\int_0^\infty \exp\left\{\mu_\alpha(\cos\varphi - 1)\right. \\ &\quad \left. + \frac{i\omega'}{|\omega_H^\alpha|}\varphi - \frac{\varkappa_\alpha^2}{4}\varphi^2\right\}\left(i\frac{\omega'}{|\omega_H^\alpha|} - \frac{1}{2}\varkappa_\alpha^2\varphi\right)\sin\varphi\, d\varphi, \\ \varepsilon_{12} &= i\sum_\alpha \frac{\Omega_\alpha^2}{\omega'\omega_H^\alpha}\int_0^\infty \exp\left\{\mu_\alpha(\cos\varphi - 1)\right. \\ &\quad \left. + \frac{i\omega'}{|\omega_H^\alpha|}\varphi - \frac{\varkappa_\alpha^2}{4}\varphi^2\right\}(\cos\varphi - 1)\left(\frac{i\omega'}{|\omega_H^\alpha|} - \frac{1}{2}\varkappa_\alpha^2\varphi\right)d\varphi, \\ \varepsilon_{13} &= -i\cot\theta\sum_\alpha \frac{\Omega_\alpha^2}{\omega'|\omega_H^\alpha|}\int_0^\infty \exp\left\{\mu_\alpha(\cos\varphi - 1)\right. \\ &\quad \left. + \frac{i\omega'}{|\omega_H^\alpha|}\varphi - \frac{\varkappa_\alpha^2}{4}\varphi^2\right\}\left(1 + \frac{i\omega'}{|\omega_H^\alpha|}\varphi - \frac{1}{2}\varkappa_\alpha^2\varphi^2\right)d\varphi, \\ \varepsilon_{22} &= 1 + i\sum_\alpha \frac{\Omega_\alpha^2}{\omega'|\omega_H^\alpha|}\int_0^\infty \exp\left\{\mu_\alpha(\cos\varphi - 1)\right. \\ &\quad \left. + \frac{i\omega'}{|\omega_H^\alpha|}\varphi - \frac{\varkappa_\alpha^2}{4}\varphi\right\}\{\mu_\alpha + (1 - 2\mu_\alpha)\cos\varphi + \mu_\alpha\cos^2\varphi\}\, d\varphi, \\ \varepsilon_{23} &= i\sum_\alpha \frac{\Omega_\alpha^2\varkappa_\alpha\sqrt{\mu_\alpha}}{\sqrt{2}\omega'\omega_H^\alpha} \\ &\quad \times \int_0^\infty \exp\left\{\mu_\alpha(\cos\varphi - 1) + \frac{i\omega'}{|\omega_H^\alpha|}\varphi - \frac{\varkappa_2^\alpha}{4}\varphi\right\}(1 - \cos\varphi)\, d\varphi, \\ \varepsilon_{33} &= 1 + i\sum_\alpha \frac{\Omega_\alpha^2}{\omega'|\omega_H^\alpha|} \\ &\quad \times \int_0^\infty \exp\left\{\mu_\alpha(\cos\varphi - 1) + \frac{i\omega'}{|\omega_H^\alpha|}\varphi - \frac{\varkappa_\alpha^2}{4}\varphi\right\}\left(1 - \frac{1}{2}\varkappa_\alpha^2\varphi^2\right)d\varphi, \\ \varepsilon_{21} &= -\varepsilon_{12}; \ \varepsilon_{31} = \varepsilon_{13}; \ \varepsilon_{32} = -\varepsilon_{23}, \\ \varkappa_\alpha &= \sqrt{2}k_z v_T^\alpha/|\omega_H^\alpha|. \end{aligned} \tag{10}$$

Equations (10) for the $\epsilon_{ik}$ are analytic functions of $\omega'$ over the whole $\omega'$ plane. We shall use them in solving the dispersion equation (3). We note that if $\mathbf{H}_0$ is replaced by $-\mathbf{H}_0$, the components $\epsilon_{11}$, $\epsilon_{22}$, $\epsilon_{33}$, and $\epsilon_{13}$ remain invariant,

whereas $\epsilon_{12}$ and $\epsilon_{23}$ change sign.

Let us rewrite Eq. (10). Expanding $\exp(\mu_\alpha \cos\varphi)$ in Eq. (10) in a series of the $I_n(\mu_\alpha)$ functions and making use of the relation[9]

$$I(z) = \frac{z}{\sqrt{\pi}} \int_C \frac{e^{-t^2}}{z-t}\,dt = -i\sqrt{\pi}\, z w(z),$$

$$w(z) = e^{-z^2}\left(1 + \frac{2i}{\sqrt{\pi}} \int_0^z e^{t^2}\,dt\right), \qquad (11)$$

where the integration over t is taken along a contour C going from $-\infty$ to $+\infty$ and circling the point $t = z$ from below, we obtain

$$\varepsilon_{11} = 1 - \sum_\alpha \frac{v_\alpha z_0^\alpha}{\sqrt{\pi}\mu_\alpha} e^{-\mu_\alpha} \sum_{n=-\infty}^{\infty} n^2 I_n(\mu_\alpha) \int_C \frac{e^{-t^2}}{z_n^\alpha - t}\,dt,$$

$$\varepsilon_{12} = -i \sum_\alpha \frac{e_\alpha v_\alpha z_0^\alpha}{\sqrt{\pi}} e^{-\mu_\alpha} \sum_{n=-\infty}^{\infty} n\,[I_n'(\mu_\alpha) - I_n(\mu_\alpha)] \int_C \frac{e^{-t^2}}{z_n^\alpha - t}\,dt,$$

$$\varepsilon_{13} = -\sum_\alpha \frac{\sqrt{2} v_\alpha z_0^\alpha}{\sqrt{\pi}\mu_\alpha} e^{-\mu_\alpha} \sum_{n=-\infty}^{\infty} n I_n(\mu_\alpha) \int_C \frac{te^{-t^2}}{z_n^\alpha - t}\,dt,$$

$$\varepsilon_{22} = 1 - \sum_\alpha \frac{v_\alpha z_0^\alpha}{\sqrt{\pi}} e^{-\mu_\alpha}$$

$$\times \sum_{n=-\infty}^{\infty} \left[\left(\frac{n^2}{\mu_\alpha} + 2\mu_\alpha\right) I_n(\mu_\alpha) - 2\mu_\alpha I_n'(\mu_\alpha)\right] \int_C \frac{e^{-t^2}}{z_n^\alpha - t}\,dt,$$

$$\varepsilon_{23} = i \sum_\alpha \frac{\sqrt{2} e_\alpha v_\alpha z_0^\alpha \sqrt{\mu_\alpha}}{\sqrt{\pi}} e^{-\mu_\alpha}$$

$$\times \sum_{n=-\infty}^{\infty} [I_n'(\mu_\alpha) - I_n(\mu_\alpha)] \int_C \frac{te^{-t^2}}{z_n^\alpha - t}\,dt, \qquad (12)$$

$$\varepsilon_{33} = 1 - \sum_\alpha \frac{2 v_\alpha z_0^\alpha}{\sqrt{\pi}} e^{-\mu_\alpha} \sum_{n=-\infty}^{\infty} I_n(\mu_\alpha) \int_C \frac{t^2 e^{-t^2}}{z_n^\alpha - t}\,dt,$$

where $e_i = 1$ and $e_e = -1$. If $\cos\theta > 0$, the integral over t in (12) is taken along a contour C that circles $t = z_n^\alpha$ from below, whereas if $\cos\theta < 0$, the contour C passes above $t = z_n^\alpha$. To be specific, we shall assume below that $\cos\theta > 0$. We note that expression (12) for $\epsilon_{ik}$ can be obtained directly from an equation of the form of (7) by replacing the integral over t along the real axis by an integral along C.

In attempting to determine the excitation of electromagnetic vibrations in a plasma by external currents, one must also consider Eq. (3), which defines the wave number $k' = k + i\kappa$ as a function of the frequency $\omega$ [in Eqs. (3), (4), and (10) to (12) one must set $\omega' = \omega - i\delta$, where $\omega$ is a given real number and $\delta \to +0$].

Equation (3) can be solved in several limiting cases. If $V_\Phi \gg v_T^\alpha$ (and $T_\alpha \to 0$), Eq. (12) leads to known expressions for the $\epsilon_{ik}$ (quasi-hydrodynamic approximation), and Eq. (3) gives the index of refraction for the ordinary and extraordinary waves. If the separate terms entering into A are much greater than $|B/n^2|$ and $|C/n^4|$, we obtain by setting $A = 0$ the dispersion equation for longitudinal vibrations of the plasma in the magnetic field. In the present work the dispersion equation (3) is treated for low-frequency waves, when $\omega \ll \omega_H^i$.

## 2. ANALYSIS OF THE DISPERSION EQUATION

We shall now consider the dispersion equation (3) for a strong magnetic field, when $kv_T^\alpha \ll \omega_H^\alpha$. In view of these inequalities, we may consider that $\mu_\alpha \ll 1$ and $|z_n^\alpha| \gg 1$ for $n = \pm 1, \pm 2, \ldots$. The functions $I_n(\mu_\alpha)$ and $e^{-\mu_\alpha}$ in (12) can therefore be expanded in powers of $\mu_\alpha$, and in the resulting sums we need retain only the first few terms. In addition, the integrals taken along C which contain $z_n^\alpha$ (with $n = \pm 1, \pm 2, \ldots$) will be expanded in the asymptotic series

$$I(z) = \frac{z}{\sqrt{\pi}} \int_C \frac{e^{-t^2}}{z-t}\,dt \sim 1 + \frac{1}{2z^2} + \frac{3}{4z^4} + \ldots - i\sqrt{\pi} z e^{-z^2}$$
$$(|\mathrm{Re}\, z| \gg 1, \quad \mathrm{Im}\, z \ll 1). \qquad (13)$$

Considering further that $|\omega'| \ll \omega_H^\alpha$, we obtain the following expressions for the $\epsilon_{ik}$:

$$\varepsilon_{11} = n_A^2\left[1 + \frac{u_i}{v_i} + \frac{1}{u_i} + \frac{3\beta_i^2 n'^2}{u_i}\left(\cos^2\theta - \frac{1}{4}\sin^2\theta\right) + \frac{m_e}{m_i}\right],$$

$$\varepsilon_{12} = \frac{in_A^2}{\sqrt{u_i}}\left[1 + \beta_i^2 n'^2\left(\cos^2\theta - \frac{3}{2}\sin^2\theta\right)\right],$$

$$\varepsilon_{13} = -\frac{2\beta_i^2 n'^2 n_A^2}{u_i}\cos\theta\sin\theta; \qquad (14)$$

$$\varepsilon_{22} = \varepsilon_{11} - 2\beta_i^2 n'^2 n_A^2 \sin^2\theta\left[I(z_0^i) + \frac{T_e}{T_i} I(z_0^e)\right],$$

$$\varepsilon_{23} = -\frac{iv_i \sin\theta}{\sqrt{u_i}\cos\theta}[I(z_0^i) - I(z_0^e)],$$

$$\varepsilon_{33} = \frac{v_i}{\beta_i^2 n'^2 \cos^2\theta}\left[1 + \frac{T_i}{T_e} - I(z_0^i) - \frac{T_i}{T_e} I(z_0^e)\right], \qquad (15)$$

where

$$n_A = (v_i/u_i)^{1/2} = (4\pi n_0 m_i c^2/H_0^2)^{1/2}, \quad \beta_\alpha = v_T^\alpha/c, \quad u_\alpha = \omega^2/(\omega_H^\alpha)^2.$$

If $y_\alpha = -\mathrm{Im}\, z_0^\alpha \ll 1$, expressions (15) for $\epsilon_{22}$, $\epsilon_{23}$, and $\epsilon_{33}$, which contain the integral $I(z_0^\alpha)$, can be simplified. In this case we expand $w(z)$ in Eq. (11) in powers of $y = -\mathrm{Im}\, z$. Dropping terms of order y, we obtain (noting that $z = x - iy$)

$$I(z) = I(x) + O(y); \quad I(x) = 2xF(x) - i\sqrt{\pi}\, x e^{-x^2},$$

$$F(x) = e^{-x^2} \int_0^x e^{t^2} dt. \qquad (16)$$

Taking (16) into account, (15) can be written

$$\varepsilon_{11}-\varepsilon_{22}=2\beta_i^2 n'^2 n_A^2\sin^2\theta\,[2x_iF(x_i)+2x_eF(x_e)\,T_e/T_i$$
$$-i\sqrt{\pi}\,x_i e^{-x_i^2}-i\sqrt{\pi}x_e e^{-x_e^2}\,T_e/T_i],$$
$$\varepsilon_{23}=-\frac{iv_i\sin\theta}{\sqrt{v_i}\cos\theta}[2x_iF(x_i)-2x_eF(x_e)$$
$$-i\sqrt{\pi}\,x_i e^{-x_i^2}+i\sqrt{\pi}\,x_e e^{-x_e^2}],$$
$$\varepsilon_{33}=\frac{v_i}{\beta_i^2 n^2\cos^2\theta}[1+T_i/T_e-2x_iF(x_i)-2x_eF(x_e)\,T_i/T_e$$
$$+i\sqrt{\pi}\,x_i e^{-x_i^2}-i\sqrt{\pi}\,x_e e^{-x_e^2}T_i/T_e], \qquad (17)$$

where

$$x_\alpha=(\sqrt{2}\,\beta_\alpha n\cos\theta)^{-1},\quad n=kc/\omega.$$

In the most interesting cases, in which it is possible to speak of wave propagation at all, the index of refraction $n$ for magnetohydrodynamic waves is on the order of $n_A$. We shall assume that $n_A \gg 1$, or that $V_\Phi \ll c$, since only then will the inclusion of thermal motion give significant corrections to $n'$. Equation (3) then becomes

$$(\cos^2\theta\,n'^2-\varepsilon_{11})(n'^2-\varepsilon_{22}-\varepsilon_{23}^2/\varepsilon_{33})$$
$$=-\varepsilon_{12}^2-2n'^2\cos\theta\sin\theta\varepsilon_{12}\varepsilon_{23}/\varepsilon_{33}+\ldots. \qquad (18)$$

In view of the fundamental inequalities

$$v_e\gg v_i\gg u_i\gg 1\gg\beta_i^2 n^2/u_i\gg\beta_e^2 n^2/u_e. \qquad (19)$$

the terms discarded in (18) are small compared with those which remain.

Let us now go on to a consideration of (18) for various special cases.

(a) Consider first propagation of magnetohydrodynamic waves along the magnetic field. Setting $\theta = 0$, we obtain $\epsilon_{11} = \epsilon_{22}$ and $\epsilon_{13} = \epsilon_{23} = 0$. The left side of (3) then breaks up into the product of three factors. We equate each of these to zero, obtaining

$$\varepsilon_{33}=0;\quad n'^2-\varepsilon_{11}\mp\sqrt{-\varepsilon_{12}^2}=0. \qquad (20)$$

The first relation in (20) gives the dispersion equation for the longitudinal plasma vibrations investigated by Vlasov[4] and Landau.[10] The second is the dispersion equation for ordinary and extraordinary electromagnetic waves which, for $\theta = 0$, are purely transverse (div $\mathbf{E} = 0$). This equation agrees with the dispersion equation obtained by Gershman.[5] If we take account of (19), Eq. (20) gives the indices of refraction for the ordinary and extraordinary waves in the form

$$n_{1,2}^2=n_A^2/(1\mp\sigma);\qquad \sigma=\beta_i^2 n_A^2/\sqrt{u_i}. \qquad (21)$$

According to this equation, the thermal motion of the ions gives corrections to the indices of refraction which are significant only if $V_\Phi \ll v_T^i$, when $\beta_i^2 n_A^2/\sqrt{u_i} \sim 1$. If we include the exponentially small terms in (13), we obtain the damping constant

$$\left(\frac{\gamma}{\omega}\right)_{1,2}=\sqrt{\frac{\pi}{8}}\frac{u_i}{\beta_i n_{1,2}}\frac{1\mp\sigma}{2\mp\sigma}\exp\{-(z_{\pm1}^i)^2\};$$
$$(z_{\pm1}^i)^2=\frac{(1\mp\omega_H^i/\omega)^2}{2\beta_i^2 n_{1,2}^2} \qquad (22)$$

The imaginary part of the wave vector $k'$ will be equal to (the frequency $\omega$ is given)

$$(\varkappa/k)_{1,2}=\sqrt{\frac{\pi}{8}}\frac{u_i}{\beta_i n_{1,2}}\exp\{-(z_{\pm1}^i)^2\}. \qquad (23)$$

Both $(\gamma/\omega)_{1,2}$ and $(\kappa/k)_{1,2}$ are extremely small because $\beta_i n/\sqrt{u_i} \ll 1$ even if $\beta_i^2 n_A^2 \sim \sqrt{u_i}$.

(b) Let us now consider the propagation of magnetohydrodynamic waves at a small angle $\theta \ll 1$ to the magnetic field. We find from (18) that if $\beta_i^2 n_A^2/\sqrt{u_i} \ll 1$, then $n_1 \approx n_2 \approx n_A$. Writing

$$n'_{1,2}=n_A(1+q'_{1,2});\quad q'_{1,2}=q_{1,2}+i\gamma_{1,2}/\omega;$$
$$\gamma_{1,2}=\varkappa_{1,2}c/n_A\quad(|q'_{1,2}|\ll 1), \qquad (24)$$

we find that the quantity

$$q''_{1,2}=q'_{1,2}-\frac{1}{2}\left(\frac{1}{n_A^2}+\frac{1}{u_i}+\frac{3\beta_i^2 n_A^2}{u_i}+\frac{m_e}{m_i}+\cdots\right), \qquad (25)$$

is given by

$$q''^2_{1,2}+\frac{1}{2}\left(\frac{\varepsilon_{11}-\varepsilon_{22}}{n_A^2}-\frac{\varepsilon_{23}^2}{n_A^2\varepsilon_{33}}-\theta^2\right)q''_{1,2}$$
$$+\frac{1}{4}\left(\frac{\varepsilon_{12}^2}{n_A^4}+\theta^2\frac{\varepsilon_{22}-\varepsilon_{11}}{n_A^2}+\theta^2\frac{\varepsilon_{23}^2}{n_A^2\varepsilon_{33}}+2\frac{\varepsilon_{12}\varepsilon_{23}\theta}{n_A^2\varepsilon_{33}}\right)=0. \qquad (26)$$

We now make use of expressions (17) for $\epsilon_{11} - \epsilon_{22}$, $\epsilon_{23}$, and $\epsilon_{33}$, obtaining

$$q''_{1,2}=\frac{\theta^2}{4}(1-\beta_i^2 n_A^2 D)\pm\left\{\frac{\theta^4}{16}(1+\beta_i^2 n_A^2 D)^2\right.$$
$$\left.+\frac{(1+\beta_i^2 n_A^2)}{4u_i}[1+\beta_i^2 n_A^2-2\theta^2\beta_i^2 n_A^2(I_i-I_e)\,G]\right\}^{1/2}, \qquad (27)$$

$$D=2I_i+2I_eT_e/T_i+(I_i-I_e)^2/(1+T_i/T_e-I_i-I_eT_i/T_e),$$
$$G=[1+T_i/T_e-I_i-I_eT_i/T_e]^{-1},$$
$$I_\alpha=I(x_\alpha),\quad x_\alpha=(\sqrt{2}\,\beta_\alpha n_A)^{-1}.$$

Let us now consider (27) in some special cases. Let the phase velocity $V_\Phi = c/n_A$ be much greater than the mean thermal velocity of the ions, or $\beta_i n_A \ll 1$. Equation (27) then leads to

$$\mathrm{Re}\,q''_{1,2}=\frac{\theta^2}{4}\pm\frac{1}{2}\sqrt{\frac{\theta^4}{4}+\frac{1}{u_i}}; \qquad (28)$$

$$\left(\frac{\gamma}{\omega}\right)_{1,2}=\sqrt{\frac{\pi}{32}}\theta^2\frac{m_e}{m_i}\beta_e n_A\left(1\mp\frac{\theta^2}{\sqrt{\theta^4+4/u_i}}\right)\exp\left\{-\frac{1}{2\beta_e^2 n_A^2}\right\}. \qquad (29)$$

It follows from (29) that as the phase velocity decreases, the damping increases. If $\beta_e n_A \ll 1$, the ratio $\gamma/\omega$ is exponentially small. The damp-

ing given by (29), however, will be much greater than that given by (22) for all except the smallest values of $\theta$, since the quantity $u_i/2\beta_i^2 n_A^2$, whose exponential enters into (22), is much greater than $1/2\beta_e^2 n_A^2$. If $V_\Phi \lesssim v_T^e$, then $(\gamma/\omega)_{1,2} \sim \theta^2 \beta_e n_A m_e/m_i$. As is seen from (29), the extraordinary wave is more highly damped than the ordinary one, or $\gamma_2 > \gamma_1$.

Equation (29) is valid if $\beta_i n_A \ll 1$. If, however, $\beta_i n_A \sim 1$, which means that $V_\Phi \sim v_T^i$, then as follows from (27) we have

$$\mathrm{Re}\, q''_{1,2} \sim 1/\sqrt{u_i}, \quad (\gamma/\omega)_{1,2} \sim a_1\theta^2 + a_2\theta^4/\sqrt{u_i},$$

where $a_{1,2} \sim 1$ and $\theta^2 \lesssim 1/\sqrt{u_i}$.

For $V_\Phi \ll v_T^i$, Eq. (27) gives

$$q''_{1,2} = i\sqrt{\frac{\pi}{8}}\beta_i n_A\theta^2 \pm \frac{1}{2}\left[\frac{\beta_i^4 n_A^4}{u_i} - \frac{\pi}{2}\beta_i^2 n_A^2\theta^4\right]^{1/2}, \tag{30}$$

or

$$(\gamma/\omega)_{1,2} = \sqrt{\pi/8}\,\beta_i n_A\theta^2 \quad \text{for } 1/u_i > \pi\theta^4/2\beta_i^2 n_A^2, \tag{31}$$

$$(\gamma/\omega)_{1,2} = \sqrt{\frac{\pi}{8}}\beta_i n_A\theta^2 \mp \frac{1}{2}\left[\frac{\pi}{2}\beta_i^2 n_A^2\theta^4 - \frac{\beta_i^4 n_A^4}{u_i}\right]^{1/2} \quad \text{for } \frac{1}{u_i} < \frac{\pi}{2}\frac{1}{\beta_i^2 n_A^2}\theta^4. \tag{32}$$

Equations (30) to (32) are valid only if $\beta_i n_A \gg 1$, $\beta_i^2 n_A^2/\sqrt{u_i} \ll 1$, and $\beta_i n_A\theta^2 \ll 1$. If however, $\beta_i n_A \gg 1$, but the inequality $\beta_i^2 n_A^2/\sqrt{u_i} \ll 1$ is not fulfilled, the initial approximation $n_1 \approx n_2 \approx n_A$ becomes invalid. Let $\beta_i^2 n_A^2 \sim \sqrt{u_i}$. Then assuming that in the zeroth approximation the indices of refraction of the ordinary and extraordinary waves are given by (21), we obtain

$$\left(\frac{\gamma}{\omega}\right)_{1,2} = \sqrt{\frac{\pi}{2}}\frac{1 \mp \sigma}{2 \mp \sigma}\beta_i n_{1,2}\theta^2, \qquad \left(\frac{\varkappa}{k}\right)_{1,2} = \sqrt{\frac{\pi}{8}}\beta_i n_{1,2}\theta^2,$$

$$(\beta_i n_A\theta^2 \ll 1). \tag{33}$$

If $\sigma = \beta_i^2 n_A^2/\sqrt{u_i} \ll 1$, then (33) leads to Eq. (31) for $\gamma_{1,2}$. Thus Eqs. (27) to (33) for small $\theta$ will give $\gamma_{1,2}$ for all $\sigma$.

(c) Let $\theta \sim 1$. The right side of (18) contains quantities small compared with the individual terms on the left side. Therefore we can obtain an approximate solution of (18) by equating each of the factors on the left side to zero. The index of refraction of the ordinary wave is then given by

$$n_1 = n_A/\cos\theta. \tag{34}$$

We note that Åström calls the wave whose index of refraction is that given by (34) the extraordinary wave.

Let us find the corrections to (34). Writing

$$n'_1 = n_A(1 + q'_1)/\cos\theta, \quad q'_1 = q_1 + i(\gamma/\omega)_1.$$
$$\gamma_1 = \varkappa_1 c\cos\theta/n_A, \quad |q'_1| \ll 1, \tag{35}$$

we find from (18) that

$$q'_1 = q''_1 + \frac{1}{2}\left(\frac{1}{n_A^2} + \frac{1}{u_i} + \frac{3\beta_i^2 n_A^2}{u_i}\left(1 - \frac{1}{4}\tan^2\theta\right) + \frac{m_e}{m_i}\right), \tag{36}$$

$$q''_1 = \frac{[1 + \beta_i^2 n_A^2(1 - {}^3/_2\tan^2\theta)]^2\,[\cot^2\theta + 2\beta_i^2 n_A^2(I_e - I_i)\,a]}{2u_i(1 + \beta_i^2 n_A^2 b)}, \tag{37}$$

$$a^{-1} = [1 + \beta_i^2 n_A^2(1 - {}^3/_2\tan^2\theta)]\,[1 + T_i/T_e - I_i - I_e T_i/T_e],$$
$$b = (I_i - I_e)^2/(1 + T_i/T_e - I_i - I_e T_i/T_e) + 2I_i + 2I_e T_e/T_i,$$
$$I_\alpha = I(x_\alpha), \quad x_\alpha = (\sqrt{2}\,\beta_i n_A)^{-1}.$$

If $\beta_i n_A \ll 1$, we obtain

$$q_1 = \frac{1}{2}\left(\frac{1}{n_A^2} + \frac{1 + \cot^2\theta}{u_i} + \frac{m_e}{m_i}\right), \tag{38}$$

$$\left(\frac{\gamma}{\omega}\right)_1 = \sqrt{\frac{\pi}{8}}\frac{m_e}{m_i}\frac{\beta_e n_A}{u_i}\cot^2\theta\exp\{-x_e^2\}. \tag{39}$$

If $\beta_e n_A \ll 1$, the quantity $(\gamma/\omega)_1$ is exponentially small, while if $\beta_e n_A \sim 1$, we have $(\gamma/\omega)_1 \sim m_e\beta_e n_A/m_i u_i$.

If $\beta_i n_A \sim 1$, it is easily seen from (37) that

$$\mathrm{Re}\, q''_1 \sim \mathrm{Im}\, q''_1 \sim 1\, u_i^{-1}.$$

Finally, if $\beta_i n_A \gg 1$, Eq. (37) leads to

$$\left(\frac{\gamma}{\omega}\right)_1 = \frac{\cot^2\theta\,(1 - {}^3/_2\tan^2\theta)^2}{\sqrt{8\pi}}\frac{\beta_i^3 n_A^3}{u_i}, \tag{40}$$

and $\mathrm{Im}\, q''_1 \gg \mathrm{Re}\, q''_1$. Equation (40) is valid if $(\gamma/\omega)_1 \ll 1$, or if $\beta_i^3 n_A^3/u_i \ll 1$. If $\beta_i^3 n_A^3/u_i \sim 1$, it follows from (18) that $\mathrm{Re}\, n' \sim \mathrm{Im}\, n' \sim n_A$. Thus the ordinary wave is weakly damped ($\gamma_1 \ll \omega_1$) only if $\beta_i^3 n_A^3/u_i \ll 1$.

(d) Let us now consider the propagation of the extraordinary wave for $\theta \sim 1$. We equate the second factor on the left side of (18) to zero, writing

$$n'^2 - \varepsilon_{11} + (\varepsilon_{11} - \varepsilon_{22}) - \varepsilon_{23}^2/\varepsilon_{33} = 0. \tag{41}$$

Assuming that $\epsilon_{11} \approx n_A^2$ is much greater than either $|\epsilon_{11} - \epsilon_{22}|$ or $|\epsilon_{23}^2/\epsilon_{33}|$, we can use (41) to find the index of refraction of the extraordinary wave (which Åström calls the ordinary wave). This is

$$n_2 = n_A. \tag{42}$$

Let us now find the corrections to (42). We set

$$n'_2 = n_A(1 + q'_2); \quad q'_2 = q_2 + i(\gamma/\omega)_2;$$
$$\gamma_2 = \varkappa_2 c/n_A; \quad |q'_2| \ll 1. \tag{43}$$

Then it follows from (18) that

$$q_2 = \frac{1}{2}\left(\frac{1}{n_A^2} + \frac{m_e}{m_i} - \frac{\cot^2\theta}{u_i}\right)$$

$$- \frac{1}{2}\beta_i^2 n_A^2\sin^2\theta\left(2 + \frac{T_e}{T_i} + 2x_e F(x_e)\frac{T_e}{T_i}\right), \tag{44}$$

$$\left(\frac{\gamma}{\omega}\right)_2 = \sqrt{\frac{\pi}{2}}\frac{m_e}{m_i}\frac{\sin^2\theta}{\cos\theta}\beta_e n_A e^{-x_e^2}, \quad x_e = (\sqrt{2}\beta_e n_A \cos\theta)^{-1}. \tag{45}$$

Comparison of (29) and (45) shows that if $\beta_e n_A \lesssim 1$, the extraordinary wave is damped much more strongly than the ordinary one, or $\gamma_2/\gamma_1 \sim u_i \gg 1$.

If $\beta_i n_A \ll 1$, then $|q_2'| \ll 1$. If, on the other hand, $\beta_i n_A \sim 1$, then $n'$ must be found from (41), which then becomes

$$n'^2 - n_A^2 + \beta_i^2 n'^2 n_A^2 \sin^2\theta \left[\frac{I^2(z_0^i)}{1 + T_e/T_i - I(z_0^i)} + 2I(z_0^i)\right] = 0, \tag{46}$$

where $I(z_0^i)$ is the integral defined by (11). Equation (46) is obtained on the assumption that $|\beta_e n' \cos\theta| \gg 1$. It follows from (46) that $\mathrm{Re}\, n_2' \sim \mathrm{Im}\, n_2' \sim n_A$, which means that if $\beta_i n_A \sim 1$, the extraordinary wave is strongly damped. Exact solutions of (46) can be obtained numerically, using the tables of Faddeeva and Terent'ev.[9]

We now make one remark regarding the propagation of electromagnetic waves perpendicular to the magnetic field. As $\theta \to \pi/2$, we find that $|z_n^\alpha| \to \infty$, and the imaginary parts of $\epsilon_{ik}$ in (12) vanish. Therefore the damping of the electromagnetic waves for $\theta = \pi/2$ is determined entirely by "short-range" collisions.

## 3. CONCLUSIONS

The kinetic equation was used to investigate the propagation of magnetohydrodynamic waves whose frequency is much greater than the frequency of "short-range" collisions of charged particles both with each other and with neutral particles. It is shown that magnetohydrodynamic waves propagating at an angle $\theta \neq \pi/2$ are damped (damping is similar to that found by Landau[10] for longitudinal plasma waves). The damping constant increases as the phase velocity $V_\Phi \sim c/n_A$ decreases, and is no longer exponentially small when $V_\Phi \sim v_T^e$. If $\theta \ll 1$ and $V_\Phi \ll v_T^i$, the damping of magnetohydrodynamic waves is small only in a very narrow angle interval $\theta^2 \ll 1/\beta_i n_A \ll 1$. If $\theta \sim 1$ and $V_\Phi \sim v_T^e$, the damping constant $\gamma_2$ for the extraordinary wave is much greater than the damping constant $\gamma_1$ for the ordinary wave, and we may write $\gamma_2/\gamma_1 \sim u_i \gg 1$. The ordinary wave is strongly damped ($\mathrm{Re}\, n_1' \sim \mathrm{Im}\, n_1'$) for $V_\Phi \ll v_T^i$, when $\beta_i^3 n_A^3 \sim u_i$. Strong damping ($\mathrm{Re}\, n_2' \sim \mathrm{Im}\, n_2' \sim n_A$) does not allow the extraordinary wave to propagate when the phase velocity becomes of the order of $v_T^i$.


[1] E. Åström, Ark. f. Fysik **2**, 443 (1951).

[2] E. Åström, Nature **165**, 1019 (1950).

[3] V. L. Ginzburg, J. Exptl. Theoret. Phys. (U.S.S.R.) **21**, 788 (1951).

[4] A. A. Vlasov, J. Exptl. Theoret. Phys. (U.S.S.R.) **8**, 291 (1938).

[5] B. N. Gershman, J. Exptl. Theoret. Phys. (U.S.S.R.) **24**, 453 (1953).

[6] J. W. Dungey, J. Geophys. Research 59, **323** (1954).

[7] A. G. Sitenko and K. N. Stepanov, J. Exptl. Theoret. Phys. (U.S.S.R.) **31**, 642 (1956), Soviet Phys. JETP **4**, 512 (1957).

[8] G. N. Watson, A Treatise on the Theory of Bessel Functions (Russ. Transl.), IIL, M. 1948, part 1, p. 432.

[9] V. N. Faddeeva and M. N. Terent'ev, Таблицы значений интеграла вероятностей от комплексного аргумента (Tables of the Probability Integral of a Complex Argument), edited by Academician V. A. Fock, GITTL, M. 1954.

[10] L. D. Landau, J. Exptl. Theoret. Phys. (U.S.S.R.) **16**, 574 (1946).


Translated by E. J. Saletan
257

# THE INFLUENCE OF SHORT-RANGE ORDER ON THE SPECIFIC HEAT CLOSE TO A SECOND ORDER PHASE TRANSITION POINT

V. M. ZAITSEV

Perm State University

Submitted to JETP editor December 24, 1957

J. Exptl. Theoret. Phys. (U.S.S.R.) **34**, 1302-1305 (May, 1958)

An approximate expression has been obtained for the binary distribution function near a second-order phase transition point. This expression is used to find the specific heat above the Curie point.

LANDAU's[1] thermodynamic theory of second-order phase transitions explains many phenomena close to the transition point. Many properties of matter in more symmetric phases, however, are not explained by this theory. This is due to the fact that only long-range order is considered, because the thermodynamic potential is treated as a functional of the density function or of the unary distribution function $\rho(\mathbf{r})$.

The binary distribution function $\rho(\mathbf{r}_1, \mathbf{r}_2)$ plays an important role in describing the properties of matter. Allowance for the function $\rho(\mathbf{r})$ alone is equivalent to representing the binary function as the product of unary distribution functions. This causes the degree of the short-range order to be replaced by the square of the degree of the long-range order. Although such a description is sufficient in a less symmetric phase, a detailed knowledge of the binary distribution function is necessary in a phase with higher symmetry.

Let us consider the specific heat close to a second-order phase transition, using the binary distribution function. The greater the rate at which disordering proceeds as the temperature is increased, the higher the specific heat, so that inclusion of short-range order should lead to a slower increase of the specific heat below the Curie point and to anomalous behavior of the specific heat above the Curie point.

To find the binary distribution function, let us consider $n_\alpha(\mathbf{r})$, the density of particles of type $\alpha$ at the point $\mathbf{r}$. The mean value $\overline{n_\alpha(\mathbf{r})}$ of this function is the unary distribution function $\rho_\alpha(\mathbf{r})$, whereas $\overline{n_\alpha(\mathbf{r}_1) n_\beta(\mathbf{r}_2)}$ is the binary distribution function $\rho_{\alpha\beta}(\mathbf{r}_1, \mathbf{r}_2)$. Let us first consider the binary distribution $\rho_{\alpha\beta}(\mathbf{r}_1, \mathbf{r}_2)$ for a binary alloy with a superlattice. Ordinarily this function is approximated in the form of a product of unary distribution functions, assuming first that the probability of finding any atom on a lattice site is independent of the position of any other atom. Second, it is assumed that the probability of finding an atom of type $\alpha$ at a given site is independent of the types of atoms occupying the neighboring sites. The first assumption is of almost the same accuracy near and far from a phase transition point, and we may maintain it without introducing any significant error. The second assumption, on the other hand, becomes invalid close to the Curie point and must thus be dropped. Therefore in averaging $n_\alpha(\mathbf{r}_1) n_\beta(\mathbf{r}_2)$ we must take into account the correlation which thus arises.

Similar considerations, obviously, can also be applied to other second-order phase transitions related to symmetry changes in a body. In this connection, the time average of $n_\alpha(\mathbf{r}_1) n_\beta(\mathbf{r}_2)$ is performed in two stages. We first average each factor separately over a time interval large compared with the period of vibration of the atom, but smaller than the resorption time of fluctuations in the order. This leads to the expression

$$[\rho_\alpha(\mathbf{r}_1) + \Delta\eta(\mathbf{r}_1)\rho_{1\alpha}(\mathbf{r}_1)][\rho_\beta(\mathbf{r}_2) + \Delta\eta(\mathbf{r}_2)\rho_{1\beta}(\mathbf{r}_2)], \qquad (1)$$

where $\rho_\alpha(\mathbf{r}) = \rho_{0\alpha}(\mathbf{r}) + \eta_0\rho_{1\alpha}(\mathbf{r})$ is the unary distribution function, $\eta_0$ is the equilibrium value of the degree of long-range order, and $\Delta\eta(\mathbf{r})$ is the fluctuation in the long-range order at the point $\mathbf{r}$. The function $\rho_{0\alpha}(\mathbf{r})$ has the symmetry of the more symmetric phase, whereas $\rho_{1\alpha}(\mathbf{r})$ has that of the less symmetric phase.

Expression (1) is then averaged over a time interval long compared with the resorption time of fluctuations in the order, as a result of which we obtain

$$\rho_{\alpha\beta}(\mathbf{r}_1, \mathbf{r}_2) = \rho_\alpha(\mathbf{r}_1)\rho_\beta(\mathbf{r}_2) + \overline{\Delta\eta(\mathbf{r}_1)\Delta\eta(\mathbf{r}_2)}\rho_{1\alpha}(\mathbf{r}_1)\rho_{1\beta}(\mathbf{r}_2). \qquad (2)$$

The mean value $\overline{\Delta\eta(\mathbf{r}_1)\Delta\eta(\mathbf{r}_2)}$ can be found by means of the thermodynamic theory of fluctuations. We expand $\Delta\eta(\mathbf{r})$ in a Fourier series

$$\Delta\eta(\mathbf{r}) = \sum_{\mathbf{f}} c_{\mathbf{f}} e^{i\mathbf{f}\mathbf{r}}. \tag{3}$$

Then

$$\overline{\Delta\eta(\mathbf{r}_1)\,\Delta\eta(\mathbf{r}_2)} = \sum_{\mathbf{f}}\sum_{\mathbf{f}'} \overline{c_{\mathbf{f}}\,\bar{c}_{\mathbf{f}'}}\, e^{i(\mathbf{f}\mathbf{r}_1+\mathbf{f}'\mathbf{r}_2)}.$$

Averaging this expression over the volume of the crystal, we obtain

$$\overline{\Delta\eta(\mathbf{r}_1)\,\Delta\eta(\mathbf{r}_2)} = \sum_{\mathbf{f}} \overline{c_{\mathbf{f}}^{*} c_{\mathbf{f}}}\, e^{i\mathbf{f}\mathbf{R}}, \tag{4}$$

where

$$\mathbf{R} = \mathbf{r}_1 - \mathbf{r}_2.$$

According to Landau,[2] if there are fluctuations in the order, the thermodynamic potential of the crystal can be written

$$\Phi = \Phi_0 + \int\left[\frac{A}{2}\eta^2 + \frac{C}{4}\eta^4 + \frac{\alpha}{2}(\nabla\eta)^2\right] dV, \tag{5}$$

where $\eta = \eta_0 + \Delta\eta(\mathbf{r})$. Inserting the value of $\Delta\eta(\mathbf{r})$ from (3) into (5) and keeping only those terms which are linear in $c_{\mathbf{f}}^{*}c_{\mathbf{f}}$, we obtain

$$\Phi = \Phi_{\text{equil}} + \Delta\Phi,$$

where $\Phi_{\text{equil}}$ is the equilibrium value of the thermodynamic potential when $\eta = \eta_0$, and

$$\Delta\Phi = \frac{V}{2}\sum_{\mathbf{f}} (A + \alpha f^2)\,\overline{c_{\mathbf{f}}^{*} c_{\mathbf{f}_0}} \quad T > \Theta, \tag{6}$$

$$\Delta\Phi = \frac{V}{2}\sum_{\mathbf{f}} (2|A| + \alpha f^2)\,\overline{c_{\mathbf{f}}^{*} c_{\mathbf{f}}}, \quad T < \Theta, \tag{7}$$

where $\Theta$ is the temperature of the Curie point.

From this we obtain

$$\overline{c_{\mathbf{f}}^{*} c_{\mathbf{f}}} = kT/(A + \alpha f^2)V, \quad T > \Theta, \tag{8}$$

$$\overline{c_{\mathbf{f}}^{*} c_{\mathbf{f}}} = kT/(2|A| + \alpha f^2)V, \quad T < \Theta. \tag{9}$$

It should be noted that in the immediate neighborhood of a second-order phase transition point at which A vanishes, Eqs. (8) and (9) become invalid for small $\mathbf{f}$, for in this case one cannot retain only the linear terms in $\overline{c_{\mathbf{f}}^{*} c_{\mathbf{f}}}$ in the expression for $\Delta\Phi$.

Using the inverse Fourier transform and inserting (8) into (4), we find that for $T > \Theta$

$$\overline{\Delta\eta(\mathbf{r}_1)\,\Delta\eta(\mathbf{r}_2)} = (kT/4\pi\alpha R)\exp\{-(A/\alpha)^{1/2}R\}. \tag{10}$$

Similarly, for $T < \Theta$

$$\overline{\Delta\eta(\mathbf{r}_1)\,\Delta\eta(\mathbf{r}_2)} = (kT/4\pi\alpha R)\exp\{-(2|A|/\alpha)^{1/2}R\}. \tag{11}$$

This gives the expression

$$\rho_{\alpha\beta}(\mathbf{r}_1, \mathbf{r}_2) = \rho_{\alpha}(\mathbf{r}_1)\,\rho_{\beta}(\mathbf{r}_2) + (kT/4\pi\alpha R)\exp\{-(A/\alpha)^{1/2}R\}\,\rho_{1\alpha}(\mathbf{r}_1)\,\rho_{1\beta}(\mathbf{r}_2) \tag{12}$$

for the binary distribution function for $T > \Theta$, and

$$\rho_{\alpha\beta}(\mathbf{r}_1, \mathbf{r}_2) = \rho_{\alpha}(\mathbf{r}_1)\rho_{\beta}(\mathbf{r}_2) + (kT/4\pi\alpha R)\exp\{-(2|A|/\alpha)^{1/2}R\}\,\rho_{1\alpha}(\mathbf{r}_1)\,\rho_{1\beta}(\mathbf{r}_2) \tag{13}$$

for $T < \Theta$.

The binary distribution function can be used to find the energy and specific heat of a crystal. As an example, let us consider the specific heat of a binary alloy of the type of $\beta$-brass close to the second-order phase transition point. The interaction energy of the atoms of the alloy will be

$$E_{\text{int}} = \frac{N_a(N_a-1)}{2V^2}\iint u_{aa}(\mathbf{r}_1-\mathbf{r}_2)\,\rho_{aa}(\mathbf{r}_1,\mathbf{r}_2)\,dV_1\,dV_2 + \frac{N_a N_b}{V^2}\iint u_{ab}(\mathbf{r}_1-\mathbf{r}_2)\,\rho_{ab}(\mathbf{r}_1,\mathbf{r}_2)\,dV_1\,dV_2 + \frac{N_b(N_b-1)}{2V^2}\iint u_{bb}(\mathbf{r}_1-\mathbf{r}_2)\,\rho_{bb}(\mathbf{r}_1,\mathbf{r}_2)\,dV_1\,dV_2,$$

where $N_\alpha$ is the number of atoms of type $\alpha$, and $u_{\alpha\beta}$ is the interaction energy between atoms of type $\alpha$ and type $\beta$. We shall use the binary distribution function as given by Eqs. (12) and (13), where the unary distribution function can be written in the form $\rho_\alpha(\mathbf{r}) = \rho_{0\alpha}(\mathbf{r}) + \eta_0\rho_{1\alpha}(\mathbf{r})$. If we now recall that for an alloy of the type of $\beta$-brass $\rho_{1a}(\mathbf{r}) = -\rho_{1b}(\mathbf{r})$ and neglect unity compared with $N_a$ and $N_b$, we obtain

$$E_{\text{int}} = E_0 + \frac{N^2}{8V^2}\iint u(\mathbf{r}_1-\mathbf{r}_2) \times\left[\eta_0^2 + \frac{kT}{4\pi\alpha|\mathbf{r}_1-\mathbf{r}_2|}\exp\{-(2|A|/\alpha)^{1/2}|\mathbf{r}_1-\mathbf{r}_2|\}\right] \times \rho_1(\mathbf{r}_1)\,\rho_1(\mathbf{r}_2)\,dV_1\,dV_2, \quad T < \Theta,$$

$$E_{\text{int}} = E_0 + \frac{N^2}{8V^2}\iint u(\mathbf{r}_1-\mathbf{r}_2) \times\frac{kT}{4\pi\alpha|\mathbf{r}_1-\mathbf{r}_2|}\exp\{-(A/\alpha)^{1/2}|\mathbf{r}_1-\mathbf{r}_2|\} \times \rho_1(\mathbf{r}_1)\,\rho_1(\mathbf{r}_2)\,dV_1\,dV_2, \quad T > \Theta,$$

where $u = u_{aa} + u_{bb} - 2u_{ab}$, N is the total number of atoms in the alloy, and $E_0$ is the interaction energy of the atom in the completely disordered alloy.

We now make use of the fact that close to the phase transition point $\eta_0^2 = -A/C$ and $A = a(T - \Theta)$ and keep only the largest terms. This leads to the following expressions for the specific heat at constant volume:

$$C_v = C_{v0} + \left(-\frac{a}{C} + \frac{k\Theta a^{1/2}}{4\pi\alpha^{3/2}\sqrt{2(\Theta - T)}}\right) \iint u(\mathbf{r}_1-\mathbf{r}_2)\,\rho_1(\mathbf{r}_1)\,\rho_1(\mathbf{r}_2)\,dV_1\,dV_2, \quad T < \Theta, \tag{14}$$

$$C_v = C_{v0} - \frac{k\Theta a^{3/2}}{8\pi\alpha^{3/2}\sqrt{T-\Theta}} \iint u(\mathbf{r}_1 - \mathbf{r}_2)\,\rho_1(\mathbf{r}_1)\,\rho_1(\mathbf{r}_2)\,dV_1\,dV_2,$$

$$T > \Theta. \qquad (15)$$

As has already been noted, Eqs. (8) and (9) are invalid for small $\mathbf{f}$ in the immediate neighborhood of the phase-transition point. This is true also for Eqs. (14) and (15). A necessary condition for their validity is $A\eta^2/2 \gg C\eta^4/4$, if $\eta^2 = (kT/4\pi\alpha d)\,e^{-nd}$. Here d is the distance between neighboring atoms, and $n = (a|T-\Theta|/\alpha)^{1/2}$

Noting that $a^2/2C$ is equal to the discontinuity in the specific heat per unit volume $\Delta C_p$, and[2] that $\alpha \approx \Theta a d^2$, we obtain the following condition for the validity of Eqs. (14) and (15):

$$|T-\Theta|/\Theta \gg (k/16\pi d^3 \Delta C_p)\exp\{-(|T-\Theta|/\Theta)^{1/2}\}.$$

Using the value of Sykes and Wilkinson[3] for $\Delta C_p$ of $\beta$-brass, we obtain $|T-\Theta|/\Theta \gg 0.007$.

Within the limits of applicability of the expressions obtained, the inclusion of short-range order in the ordered phase leads to an insignificant decrease in the specific heat. In the disordered phase, the inclusion of short-range order adds the following correction term to the specific heat:

$$C_v = C_{v0} + \text{const}/\sqrt{T-\Theta}.$$

For $\beta$-brass, with $(T-\Theta)/\Theta = 3\times10^{-2}$, this additional correction term supplies about 5% of the discontinuity in the specific heat at the Curie point. This conclusion is in satisfactory agreement with the measurements performed by Sykes and Wilkinson.[3]

[1] L. D. Landau and E. M. Lifshits, Статистическая физика (Statistical Physics), Gostekhizdat, 1951.

[2] L. D. Landau, J. Exptl. Theoret. Phys. (U.S.S.R.) **7**, 1232 (1937).

[3] C. Sykes and H. Wilkinson, J. Inst. Metals **61**, 223 (1937).

Translated by E. J. Saletan
258

SOVIET PHYSICS JETP VOLUME 34 (7), NUMBER 5 NOVEMBER, 1958

# *CERTAIN SOURCES OF THE LOW-ENERGY ELECTRON-PHOTON COMPONENT OF COSMIC RAYS IN THE STRATOSPHERE*

I. D. RAPOPORT

Moscow State University

Submitted to JETP editor December 30, 1957

J. Exptl. Theoret. Phys. (U.S.S.R.) **34**, 1306-1309 (May, 1958)

It is shown that part (20 to 30%) of the low-energy flux (range $R < 1.7$ g-cm$^{-2}$ Al) registered in the cosmic radiation of the stratosphere, is genetically related to nuclear-disintegration products.

FROM the number of particles N ($cm^{-2}\,sec^{-1}$) and the produced ionization I (pairs of ions per $cm^3$/sec), measured in the global intensity of cosmic rays,[1,2] it follows that the average ionizing ability of charged particles in the atmosphere, $K = I/N$, increases considerably with altitude, and that at an altitude of 10 to 17 km it exceeds the average ionizing ability of relativistic particles by a factor of 1.5 to 1.7 (Ref 3). This is evidence that there exists at these altitudes a considerable flux of secondary strongly-ionizing particles. The ionization due to these particles can be estimated from the value of the "excess" ionization, defined as the difference $I_{exc} = I - k_r N$ where $k_r$ is the average ionizing ability of relativistic particles. The value of $I_{exc}$ reaches one-third of the total ionization current.[4] Experiment has shown[4,5] that the variation of $I_{exc}$ with altitude and its latitudinal effect are identical with the corresponding relations observed for stars in photoemulsions, and for ionization impacts observed in chambers. This suggests a possible genetic relationship between this variation and nuclear disintegrations.

Quantitative measurements of the ionization impacts, which experiments[5] have shown to be essentially due to strongly-ionizing protons and to heavi-

er charged particles generated in nuclear disintegrations, account for a considerable portion[4] of the excess ionization — up to 57% at the threshold of registration of impacts of 5.5 relativistic particles,[6] corresponding under the experimental conditions to a proton energy range 1 Mev < $E_p$ < 50 Mev. The ionizing contribution (~12% of $I_{exc}$) of the faster strongly-ionizing particles (particularly protons with energies $E_p$ > 50 Mev) that were not recorded in the experiments of Refs. 4 and 6, were determined by measurement of the ionizing abilities of single particles with ranges R > 1.7 g-cm$^{-2}$ in the experiments of Refs. 3 and 7. It was established[3] that, upon approaching the boundary of the atmosphere, most excess ionization is produced by multiply-charged particles from primary cosmic rays (primary $\alpha$ particles).

Comparison of the results of preceding experiments leads to the conclusion that approximately 0.3 $I_{exc}$, observed at an altitude of 10 to 19 km, cannot be attributed to a flux of strongly-ionizing protons and stronger particles generated in nuclear disintegrations. On the other hand, a study of the small ionization impacts observed at very low registration threshholds (~0.5 of the average ionization produced by relativistic particles) makes it possible to separate out the flux of particles that make up this portion of $I_{exc}$ and to identify them as low-energy electrons that produce excess ionization $I'_{exc}$ by multiple scattering.[3] The flux $N_{el}$ of these short-range electrons (R < 1.7 g/cm$^2$), which travel in equilibrium with the photons that generate them (these photons have for the most part, low energies, ~10 Mev), makes up a considerable fraction (~20 percent) of the entire global flux of the charged particles at an altitude of 19 km (Ref. 3). (Further evidence of the considerable flux of low-energy photons in the stratosphere is found in the data of Ref. 8.)

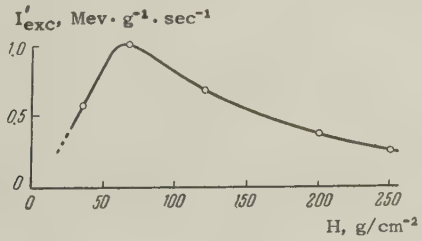


This component, as follows from the excess ionization it produces (see diagram), has an altitude dependence that is characteristic of secondary radiation: the particle flux $N_{el}$ increases from the boundary of the atmosphere, reaches a maximum at an altitude corresponding to 60 to 65 g/cm$^2$, and diminishes monotonically with increasing depth, following approximately an exponential law with an exponent $1/\mu = 130$ g/cm$^2$. The energy $E_{el}$ scattered in the air by this flux can be determined from the equation

$$E_{el} = I'_{exc} + k_t N_{el} \approx 2 I'_{exc},$$

since the average ionization momentum produced by the short-range electrons in a chamber is approximately double the relativistic ionization.[3]

This naturally raises the question of the extent to which the value of $I'_{exc}$, in parallel with the other components of excess ionization, is genetically related to nuclear disintegrations. Since $I'_{exc}$ is due to low-energy electrons, it is possible to take into consideration the $\gamma$ and $\beta$ activities of the residual nuclei, namely the products of disintegrations and of those reactions that can be excited in the air nuclei by the flux of secondary nucleons evaporated at low energies ($\lesssim$ 30 Mev) in the process of nuclear disintegration.

Along with radiation capture,[9] the neutron flux in the atmosphere can cause (nn), (np), or (n$\alpha$) reactions with the air nuclei, causing production of the excited $N^{14*}$, $C^{14*}$ and $B^{11*}$ nuclei.[10-14] To estimate the average excitation energy $\epsilon_{ex}(E_n)$ produced in air ($N^{14}$) by a neutron of initial energy $E_n$ we must know the relative probability $\sigma_{ri}$ of the competing processes and the value of the average excitation energy $\epsilon_{exi}$ of the residual nuclei resulting from each reaction. The lack of literature data was made up, for the energy range 2 Mev < $E_n$ < 30 Mev, by calculating (for reactions on nitrogen) the approximate values of $\sigma_{ri}$ and $\epsilon_{exi}$, in accordance with the "nonresonant" theory of nuclear reactions[15] and known data[16] on the energy levels of the produced nuclei. The resulting values of $\epsilon_{exi}$ are justified by an agreement, satisfactory for our purposes, with the individual experimental data available.[10,11] Also important is the fact that the quantity $\bar{\epsilon}_{ex}$ turns out to be little sensitive to a relative change in the cross sections of the various reactions. As a result, we obtained $\epsilon_{ex} \approx 0.5(E_n - 2.5)$ Mev.

Averaging this quantity over the spectrum of the neutron energies in the act of generation leads to a value $\bar{\epsilon}_{ex} = 3.5$ Mev, assuming a differential spectrum of the form $\sim E \exp\{-E/T\}$ (Ref. 17) and an average energy ~10 Mev at the instant of generation.[18] The excitation energy $\bar{\epsilon}_{ex}$, in view of the low probability of secondary emission of particles for the range of $E_n$ under consideration[10,11,16] is radiated as $\gamma$ quanta. Measured values of the $\gamma$-ray yield[12] confirm this fact. It is necessary to add to the quantity $\epsilon_{ex}$ the energy $\epsilon_\gamma$ of the $\gamma$ radiation that occurs upon radiation

capture of slow neutrons by the $N^{14}$ nuclei. Comparing the various experimental data for absorption cross sections of slow neutrons[19] and for (np) and (nγ) reactions on nitrogen,[9,20] and taking into account the energy yield of the capture reaction (Q = 10.8 Mev),[16] we obtain as an average $\bar{\epsilon}_r$ = 1.6 Mev per neutron absorbed in air.

The dominant reaction in the absorption of slow neutrons in the atmosphere is $N^{14}(np)C^{14}$ (Ref. 17), which leads to the formation of the β-active $C^{14}$ nucleus. But the very long half life (~6,000 years) makes this activity unimportant to the value of $I'_{exc}$.

The energies of the recoil nuclei, formed by elastic collision between the neutrons and the gas of the ionization chamber, are recorded as "excess" ionization, whose average value, for the equilibrium spectrum of neutrons in the atmosphere, turns out to be $\epsilon_0$ = 1.1 Mev/sec-g (referred to one neutron generated per gram of air per second).

The flux of secondary protons, the generation density of which can be assumed in the atmosphere to equal the generation density of the neutrons,[6] can produce various reactions with the $N^{14}$ nucleus, resulting in excited and β-active residual nuclei. However, the ionization ranges of the protons turn out to be on the average considerably less than the average range for nuclear interactions, and consequently, the energy contributions of the latter to the production of electrons and photons does not exceed ~3% of the corresponding contribution of the reactions on neutrons. Even less significant here is the deuteron flux.

It is difficult to give an exact estimate of the excitation energy $\epsilon_d$ for the nuclei resulting from nuclear disintegration. Assuming this value to be bounded from above by the binding energy $\epsilon_b$, we put as a rough approximation $\bar{\epsilon}_d \sim \epsilon_b/2$, which gives $\bar{\epsilon}_d \approx 1.8$ Mev for a single neutron (if the multiplicity of neutron generation in a light substance is assumed to be approximately 2, see Ref. 21). As to the β activity of the disintegration products, the data on observation of stars in photoemulsions exposed at high altitudes[22] apparently give no grounds for assuming this activity (with a short half-life) to be considerable.

A possible source of instrumental error in ionization measurements of cosmic rays[1-3] can be the occurrence of radioactivity in the material, namely the gas (argon) or the walls of the chamber (aluminum). The most significant here may be the radiation capture of slow neutrons, with production of β-active $Al^{28}$ (half-life 2.3 minutes, maximum energy of radiated electrons 3 Mev).[23] The excess ionization due to this activity corresponds to $\bar{\epsilon}_\beta$ = 1.0 Mev/sec-g (referred to one neutron absorbed in an equilibrium flux in one gram of air per second).

It is now possible to determine the total energy $E_\gamma$ contributed by the above processes to the production of electrons and photons of low energy by making use of data on the generation density of neutrons in the atmosphere. For depths H > 200 g/cm², where the neutron flux can be assumed to be in equilibrium,[24] the necessary data are found in the absolute measurements of the absorption of slow neutrons in the atmosphere.[24,25] Extrapolation of these data, using an exponential law with exponent $1/\mu$ = 156 g/cm² yields[25] the approximate values of the generation densities at lower depths (~100 g/cm²). The calculated values of $E_\gamma$ would be somewhat too high for low depths (~100 g/cm²), owing to the shortage of slow neutrons in the observed spectrum compared with the equilibrium spectrum. The table gives the calculated values of $E_\gamma$ for various depths, compared with the experimentally measured energy $E_{el}$ (Ref. 3), after making suitable corrections in the latter for the values of $\bar{\epsilon}_0$ and $\bar{\epsilon}_\beta$.

Value of $E_\gamma$ Compared with the Energy $E_{el}$ at Various Depths in the Atmosphere (Geomagnetic latitude λ = 52°)

| Depth, H, g/cm² | 65 | 120 | 200 | 250 |
|---|---|---|---|---|
| $E_{el}$, Mev/g-sec | 1.9 | 1.3 | 0.7 | 0.44 |
| $E_\gamma$, Mev/g-sec | 0.4 | 0.3 | 0.173 | 0.13 |
| $E_\gamma/E_{el}$ | 0.21 | 0.23 | 0.25 | 0.3 |

It follows from these data that 20 to 30% (referred to the energy) of the short-range electrons (R < 1.7 g/cm²), which produce approximately 10% of the total excess ionization, are genetically related to the products of nuclear disintegrations. The estimated value of $E_\gamma$ can vary by ±80%, owing to the low accuracy of the initial data, principally the inaccuracy of the average neutron energy during the act of generation. The remaining portion of the flux of short-range electrons, which produces approximately 20 percent of the excess ionization, can be assumed due to the cascade process of the development of the electron-photon component in the atmosphere.

The author expresses his gratitude to S. N. Vernov and N. L. Grigorov for advice and discussions.

[1] Vernov, Grigorov, and Savin, Dokl. Akad. Nauk SSSR 57, 137 (1947).

[2] Brikker, Vernov, et al., Dokl. Akad. Nauk SSSR **57**, 141 (1947).
[3] I. D. Rapoport, Izv. Akad. Nauk SSSR, Ser. Fiz. **19**, 419 (1955), Columbia Techn. Transl. **19**, 466 (1955).
[4] Grigorov, Evreinova, and Sokolov, Dokl. Akad. Nauk SSSR **81**, 379 (1951).
[5] N. L. Grigorov, Dissertation, Phys. Inst. Acad. Sci. 1954.
[6] A. D. Solov' ev, Dissertation, Moscow State Univ. 1953.
[7] Grigorov, Rapoport, and Shupilo, Dokl. Akad. Nauk SSSR **91**, 491 (1953).
[8] Rest, Reiffel, and Stone, Phys. Rev. **81**, 894 (1950).
[9] Kinsey, Bartholomew, and Walker, Phys. Rev. **77**, 723 (1950).
[10] A. B. Lillie, Phys. Rev. **87**, 716 (1952).
[11] J. R. Smith, Phys. Rev. **95**, 730 (1954).
[12] Scherrer, Theus, and Faust, Phys. Rev. **91**, 1476 (1953).
[13] H. I. Zagor and F. A. Valente, Phys. Rev. **67**, 133 (1945).
[14] A. Stebler and P. Huber, Helv. Phys. Acta **21**, 59 (1948).
[15] J. Blatt and V. Weiskopf, Theoretical Nuclear Physics, N. Y. Wiley, 1952.
[16] Hornyak, Lauritsen, Morrison, and Fowler, Revs. Mod. Phys. **22**, 291 (1950).
[17] E. Freese and P. Meyer, Kosmische Strahlung (Publ. by Heisenberg), 1953.
[18] Bethe, Korff, and Placzek, Phys. Rev. **57**, 573 (1940).
[19] E. Melkonian, Phys. Rev. **76**, 1750 (1949).
[20] J. H. Coon and R. A. Nobles, Phys. Rev. **75**, 1358 (1949).
[21] V. Tongiorgi, Phys. Rev. **76**, 517 (1949).
[22] E. Pickup and L. Voyvodic, Phys. Rev. **80**, 1100 (1950).
[23] Hughes, Garth, and Levin, Phys. Rev. **91**, 1423 (1953).
[24] J. A. Simpson, Phys. Rev. **83**, 1175 (1951).
[25] L. C. L. Yuan, Phys. Rev. **81**, 175 (1951).

Translated by J. G. Adashko
259

SOVIET PHYSICS JETP VOLUME 34 (7), NUMBER 5 NOVEMBER, 1958

# *THE CAUSALITY CONDITION AND SPECTRAL REPRESENTATIONS OF GREEN'S FUNCTIONS*

V. N. GRIBOV

Leningrad Physico-Technical Institute, Academy of Sciences, U.S.S.R.

Submitted to JETP editor December 12, 1957; resubmitted February 21, 1958

J. Exptl. Theoret. Phys. (U.S.S.R.) **34**, 1310-1318 (May, 1958)

By means of the causality condition in the form of the requirement that field operators commute on a space-like surface, spectral representations are obtained for the vacuum expectation values of T-products of three Heisenberg operators. The analytic properties of these functions in the complex plane are discussed.

THE present paper presents a method for obtaining spectral representations for the vacuum expectation values of T-products of Heisenberg operators (Green's functions).

These representations [Eqs. (8), (9), (18), and (19)], being natural extensions of the Källén-Lehmann formulas[1,2] for the vacuum expectation values of T-products of two operators, provide a convenient means for investigating the analytic properties of these functions in the complex plane.

In the present paper, which is the first installment of this work, spectral representations are

obtained for vacuum expectation values of T-products of three operators, and their analytic properties are studied.

## I. THE CASE OF THE SCALAR FIELD

### 1. Derivation of the Spectral Representation

For simplicity we first consider the Green's function constructed from three scalar operators $\varphi(x_1)$, $\varphi(x_2)$, $\varphi(x_3)$,

$$\langle T\varphi(x_1)\varphi(x_2)\varphi(x_3)\rangle.$$

The vacuum expectation value of the simple (unordered) product of these operators can be written in the form

$$\langle\varphi(x_1)\varphi(x_2)\varphi(x_3)\rangle$$
$$=\frac{1}{(2\pi)^9}\int d^4p_1 d^4p_3 e^{ip_1(x_1-x_2)+ip_3(x_2-x_3)}\vartheta(p_{10})\vartheta(p_{30})\rho(p_1^2, q^2, p_3^2),$$
$$\vartheta(p_{10})\vartheta(p_{30})\rho(p_1^2, q^2, p_3^2)=(2\pi)^3\sum\varphi_{0p_1}\varphi_{p_1p_3}\varphi_{p_30}, \quad (1)$$
$$\varphi_{p_1p_3}=\langle p_1|\varphi(0)|p_3\rangle, \quad q^2=(p_1-p_3)^2, \vartheta(x)=\begin{cases}1 & x>0\\ 0 & x<0\end{cases}$$

The summation is taken over all states with definite values of $p_1$ and $p_3$. If $x_{10}=x_{20}$, then the requirement

$$\langle\varphi(x_1)\varphi(x_2)\varphi(x_3)\rangle=\langle\varphi(x_2)\varphi(x_1)\varphi(x_3)\rangle \quad (2)$$

imposes the following condition on the function $\rho(p_1^2, q^2, p_3^2)$:

$$\int dp_{10}\vartheta(p_{10})\rho(p_1^2, q^2, p_3^2)$$
$$=\int dp_{10}\vartheta(p_{10})\rho((p_3-p_1)^2-p_{10}^2, p_1^2-(p_{30}-p_{10})^2, p_3^2). \quad (3)$$

Equation (3) is easily obtained from Eqs. (1) and (2) if one notes that for $x_{10}=x_{20}$ interchange of $x_1$ and $x_2$ is equivalent to replacement of the space components of the vector $p_1$ by $p_3-p_1$.

A similar condition is obtained by considering the case $x_{20}=x_{30}$. These conditions are satisfied if we write $\rho(p_1^2, q^2, p_3^2)$ in the form

$$\vartheta(p_{10})\vartheta(p_{20})\rho(p_1^2, q^2, p_3^2)$$
$$=\int\vartheta(k_{10})\vartheta(k_{20})\vartheta(k_{30})f(-k_1^2, -k_2^2, -k_3^2)\,d^4l. \quad (4)$$
$$k_1=\tfrac{1}{2}(-p_1+l+p_3), \quad k_2=\tfrac{1}{2}(p_1-l+p_3),$$
$$k_3=\tfrac{1}{2}(p_1+l-p_3)$$

and postulate that $f(-k_1^2, -k_2^2, -k_3^2)$ is a symmetric function of its arguments which vanishes if any of them is less than zero.

In fact, if we substitute Eq. (4) into Eq. (3) and in the resulting integral over $l$ and $p_{10}$ make the change of variables $I=p_3-I'$, $p_{10}=l'_{10}$, $l_{10}=p'_{10}$, then instead of Eq. (3) we get

$$\int dl\,dp_{10}[f(-k_1^2, -k_2^2, -k_3^2)-f(-k_2^2, -k_1^2, -k_3^2)]$$
$$\times\vartheta(k_{10})\vartheta(k_{20})\vartheta(k_{30})=0. \quad (5)$$

The condition that $f(-k_1^2, -k_2^2, -k_3^2)$ vanish for positive $k_1^2, k_2^2, k_3^2$ is necessary in order that the integrals containing $\vartheta(k_{10})$, $\vartheta(k_{20})$, $\vartheta(k_{30})$ be relativistically invariant.

Somewhat later (Sec. 2) we shall see that Eq. (4), regarded as an equation for $f(-k_1^2, -k_2^2, -k_3^2)$ for prescribed $\rho(p_1^2, q^2, p_3^2)$, has a very simple structure and determines f under sufficiently general assumptions regarding $\rho$. At present we shall assume that Eq. (4) is satisfied, and by considering the causality condition in invariant form we shall show that the symmetry of f is not only a sufficient but also a necessary condition for this equation to be true.

Substituting Eq. (4) into Eq. (1) and replacing $f(-k_1^2, -k_2^2, -k_3^2)$ by $\int d\kappa_1^2 d\kappa_2^2 d\kappa_3^2 f(\kappa_1^2, \kappa_2^2, \kappa_3^2)\times\delta(k_1^2+\kappa_1^2)\delta(k_2^2+\kappa_2^2)\delta(k_3^2+\kappa_3^2)$, we get

$$\langle\varphi(x_1)\varphi(x_2)\varphi(x_3)\rangle=\int d\varkappa_1^2 d\varkappa_2^2 d\varkappa_3^2 f(\varkappa_1^2, \varkappa_2^2, \varkappa_3^2)$$
$$\times\Delta^+(x_{12}, \varkappa_3)\Delta^+(x_{13}, \varkappa_2)\Delta^+(x_{23}, \varkappa_1),$$
$$\Delta^+(x, \varkappa)=\frac{1}{(2\pi)^3}\int d^4k\vartheta(k)\delta(k^2+\varkappa^2)e^{ikx}. \quad (6)$$

If the interval $x_{12}^2$ is space-like, then by Eqs. (2) and (6) we have $\Delta^+(x_{12}, \kappa_3)=\Delta^+(x_{21}, \kappa_3)$ and we get

$$\int d\varkappa_1^2 d\varkappa_2^2 d\varkappa_3^2\Delta^+(x_{12}, \varkappa_3)\Delta^+(x_{13}, \varkappa_2)\Delta^+(x_{23}, \varkappa_1)[f(\varkappa_1^2, \varkappa_2^2, \varkappa_3^2)$$
$$-f(\varkappa_2^2, \varkappa_1^2, \varkappa_3^2)]=0. \quad (7)$$

Since the expression (7) must vanish for arbitrary $x_{12}^2$, $x_{23}^2$, $x_{13}^2$, restricted only by weak inequalities (for example $x_{12}^2>0$, $x_{13}^2<0$, $x_{23}^2<0$), $f(\kappa_1^2, \kappa_2^2, \kappa_3^2)$ is a symmetric function.

Possessing the representation (6) and the symmetry property of $f(\kappa_1^2, \kappa_2^2, \kappa_3^2)$, we can easily write out the representation for $\langle T\varphi(x_1)\varphi(x_2)\times\varphi(x_3)\rangle$. Using the definition of the T-product and the relation

$$^1/_2\Delta_F(x, \varkappa)=\vartheta(x)\Delta^+(x, \varkappa)+\vartheta(-x)\Delta^+(-x, \varkappa),$$

we get

$$\langle T\varphi(x_1)\varphi(x_2)\varphi(x_3)\rangle \quad (8)$$
$$=\int d\varkappa_1^2 d\varkappa_2^2 d\varkappa_3^2\Delta_F(x_{12}, \varkappa_3)\Delta_F(x_{13}, \varkappa_2)\Delta_F(x_{23}, \varkappa_1)f(\varkappa_1^2, \varkappa_2^2, \varkappa_3^2).$$

Equation (8) is the desired spectral representation of the Green's function in coordinate space.

To obtain the corresponding representation in momentum space it is necessary to calculate the integral

$$\int e^{il_1x_1+il_2x_2+il_3x_3}\Delta_F(x_{12}, \varkappa_3)\Delta_F(x_{13}, \varkappa_2)\Delta_F(x_{23}, \varkappa_1)\,d^4x_1 d^4x_2 d^4x_3,$$

which is calculated in the usual way and can be written in the following symmetrical form

$$\int_0^1\int_0^1\int_0^1 d\alpha\, d\beta\, d\gamma\, \delta(\alpha+\beta+\gamma-1) \times \frac{\delta(l_1+l_2+l_3)}{l_1^2\beta\gamma + l_2^2\alpha\gamma + l_3^2\alpha\beta + \alpha\varkappa_1^2 + \beta\varkappa_2^2 + \gamma\varkappa_3^2 - i\varepsilon}.$$

Consequently the desired representation has the form

$$\tau(l_1,l_2,l_3) = \delta(l_1+l_2+l_3)\int d\varkappa_1^2\, d\varkappa_2^2\, d\varkappa_3^2 \int d\alpha\, d\beta\, d\gamma \times \frac{\delta(\alpha+\beta+\gamma-1)\, f(\varkappa_1^2,\varkappa_2^2,\varkappa_3^2)}{l_1^2\beta\gamma + l_2^2\alpha\gamma + l_3^2\alpha\beta + \alpha\varkappa_1^2 + \beta\varkappa_2^2 + \gamma\varkappa_3^2 - i\varepsilon} \tag{9}$$

A more detailed study of the properties of $f(\kappa_1^2, \kappa_2^2, \kappa_3^2)$ is necessary for the further analysis of $\tau(l_1, l_2, l_3)$.

## 2. Properties of $f(\kappa_1^2, \kappa_2^2, \kappa_3^2)$

(a) We shall show that f is a real function. Using the Hermitian character of $\varphi(x_i)$, we have

$$\langle \varphi(x_1)\varphi(x_2)\varphi(x_3)\rangle^* = \langle \varphi(x_3)\varphi(x_2)\varphi(x_1)\rangle$$

and consequently

$$\rho^*(p_1^2, q^2, p_3^2) = \rho(p_3^2, q, p_1^2).$$

But according to Eq. (4) it follows from the symmetry of f that

$$\rho(p_1^2, q^2, p_3^2) = \rho(p_3^2, q^2, p_1^2).$$

Consequently $\rho$ is real, and therefore f can also be taken to be a real function.

(b) Let us now determine more precisely the region of values of $\kappa_1^2$ for which $f(\kappa_1^2, \kappa_2^2, \kappa_3^2) \neq 0$. For this purpose we write Eq. (4) in the form

$$\rho(p_1^2, q^2, p_3^2) = \int d\varkappa_1^2\, d\varkappa_2^2 d\varkappa_3^2\, f(\varkappa_1^2, \varkappa_2^2, \varkappa_3^2) \int d^4l\, \vartheta(k_{10})\,\vartheta(k_{20})\,\vartheta(k_{30}) \times \delta(k_1^2+\varkappa_1^2)\,\delta(k_2^2+\varkappa_2^2)\,\delta(k_3^2+\varkappa_3^2) \tag{10}$$

Calculating the integral over $l$, we get (see Appendix):

$$\rho(-m_1^2, q^2, -m_3^2) = \frac{\pi}{2} S^{-1}(q^2, m_1, m_3) \int d\varkappa_1^2\, d\varkappa_2^2\, d\varkappa_3^2 f(\varkappa_1^2, \varkappa_2^2, \varkappa_3^2) \times \vartheta(m_1-\varkappa_2-\varkappa_3)\,\vartheta(m_3-\varkappa_1-\varkappa_3)\,\vartheta(\xi), \tag{10'}$$

$$m_1 = \sqrt{-p_1^2},\quad m_3 = \sqrt{-p_3^2},$$

$$S(q^2, m_1, m_3) = [q^2 + (m_1+m_3)^2]^{1/2}[q^2 + (m_1-m_3)^2]^{1/2},$$

$$\xi = S^2(q^2, m_1, m_3) - [(m_1^2 + m_3^2 + 2\varkappa_2^2 - \varkappa_1^2 - \varkappa_3^2)^2 - 4(q^2 + 2m_1^2 + 2m_3^2)\varkappa_2^2] - [(q^2 + 2m_1^2 + 2m_3^2)(m_1^2 + \varkappa_1^2 - m_3^2 - \varkappa_3^2) + (m_3^2 - m_1^2)(m_1^2 + m_3^2 + 2\varkappa_2^2 - \varkappa_1^2 - \varkappa_3^2)].$$

Equation (10) has the following simple structure:

$$\frac{2}{\pi} S(q^2, m_1, m_3)\,\rho(-m_1^2, q^2, -m_3^2) = \int_V d\varkappa_1^2\, d\varkappa_2^2\, d\varkappa_3^2\, f(\varkappa_1^2, \varkappa_2^2, \varkappa_3^2); \tag{11}$$

V is a volume in the space of $\kappa_1^2, \kappa_2^2, \kappa_3^2$ whose shape depends on $m_1$, $m_3$, and $q^2$. It can easily be shown that for given $m_1$, $m_3$, and $q^2$ the volume V defined by the conditions $\kappa_1 + \kappa_2 < m_3$, $\kappa_3 + \kappa_2 < m_1$, and $\xi > 0$ has the form shown in the diagram.

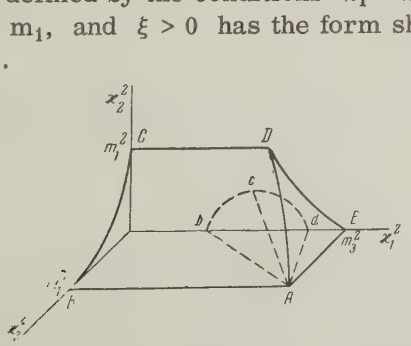


The volume of integration is bounded by the surface Abcd. The surface ABCDE bounds the volume obtained if we do not include the condition $\xi > 0$ ($OB = OC = m_1^2$, $OE = BA = m_3^2$, $m_1 < m_3$). For fixed values of $m_1$ and $m_3$, $q^2$ ranges from $-(m_3-m_1)^2$ to $\infty$. For $q^2 = -(m_3-m_1)^2$ the straight lines Ab and Ad coincide, and the curve Ac coincides with the curve AD. In this limit the volume of integration goes to zero, in accordance with the fact that the factor $S(q^2, m_1, m_3)$ in the left member of Eq. (11) goes to zero. For $q^2 \to \infty$ the straight line Ab coincides with the line AB, the line Ad with AE, and the point c lies on the plane $\kappa_2^2 = 0$. In this limit, the volume of integration also goes to zero. But unlike the case $q^2 = -(m_3-m_1)^2$, the left member is not necessarily equal to zero for $q^2 \to \infty$, since $f(\kappa_1^2, \kappa_2^2, \kappa_3^2)$ can have a $\delta$-function singularity on the plane $\kappa_2^2 = 0$. An equation of such simple structure as Eq. (11) possesses a solution under very general assumptions regarding the function $\rho(-m_1^2, q^2, -m_3^2)$,

if this latter function satisfies the conditions

$$q^2\rho(-m_1^2, q^2, -m_3^2) < \infty \text{ for } q^2 \to \infty,$$
$$\rho(-m_1^2, -(m_3-m_1)^2, -m_3^2) < \infty \qquad (12)$$

which we shall assume are satisfied.

To establish more precisely the properties of the function $f(\kappa_1^2, \kappa_2^2, \kappa_3^2)$ we use the fact that $\rho(-m_1^2, q^2, -m_3^2) = 0$ if either $m_1$ or $m_3$ is less than m, where m is the mass for the state with the smallest energy for which $\varphi_{0p} \neq 0$. Thus we get

$$\int_V d\varkappa_1^2 d\varkappa_2^2 d\varkappa_3^2 f(\varkappa_1^2, \varkappa_2^2, \varkappa_3^2) = 0 \qquad (13)$$

for arbitrary $q^2$ and $m_3$ if $m_1 < m$, and for arbitrary $q^2$ and $m_1$ if $m_3 < m$.

Since the surface Abcd for various values of $q^2$ and $m_3$ contains inside it all parts of the volume bounded by the surface $\kappa_3 + \kappa_2 = m_1$, it follows from Eq. (13) that $f(\kappa_1^2, \kappa_2^2, \kappa_3^2) = 0$ if $\kappa_1 + \kappa_2 < m$ or $\kappa_3 + \kappa_2 < m$. In virtue of its symmetry, the function $f(\kappa_1^2, \kappa_2^2, \kappa_3^2)$ must also equal zero for $\kappa_1 + \kappa_3 < m$.

Thus we have for the T-product of three scalar operators the spectral representations (8) and (9), where $f(\kappa_1^2, \kappa_2^2, \kappa_3^2)$ is a real symmetric function which is nonvanishing if the conditions

$$\varkappa_1 + \varkappa_2 > m, \quad \varkappa_1 + \varkappa_3 > m, \quad \varkappa_2 + \varkappa_3 > m$$

are fulfilled.

### 3. Analytical Properties

Assuming that the integral over $\kappa_1^2, \kappa_2^2, \kappa_3^2$ in Eq. (9) converges for real $l_1^2, l_2^2$, and $l_3^2$ [the function $\tau(l_1^2, l_2^2, l_3^2)$ exists], we find that it defines an analytic function off the real axis for any one of the complex variables $l_1^2, l_2^2, l_3^2$ if the two others are real. This function can have singularities only at values of the variables for which the denominator in Eq. (9) can vanish. In such cases the integration must be carried out by using the stipulation that the denominator with which we are concerned has an infinitely small negative imaginary part. The imaginary part of $\tau(l_1^2, l_2^2, l_3^2)$ will also be different from zero. A simple analysis of the denominator (which we shall denote by $\square$) shows that if even a single one of the arguments, for example $l_1^2$, is greater than zero, then $\square > 0$ for $l_2^2 > -(\kappa_1 + \kappa_3)^2$ and $l_3^2 > -(\kappa_1 + \kappa_2)^2$. That is, if we recall the properties of the function $f(\kappa_1^2, \kappa_2^2, \kappa_3^2)$, we get $\square > 0$ for $l_2^2, l_3^2 > -m^2$. If all the $l_i^2 < 0$, then $\square$ can equal zero also for $l_i^2 > -m^2$; for example, for $\kappa_1 = \kappa_2 = \kappa_3 = m/2$ and $\alpha = \beta = \gamma = 1/3$, $\square = 0$ for $l_1^2 = l_2^2 = l_3^2 = -3m^2/4$. But in this deduction we have not taken into account the condition $l_1 + l_2 + l_3 = 0$. If we include this, then we come to the conclusion that also in the case in which all $l_1^2 < 0$, $\square > 0$ if $l_i^2 > -m^2$.

Consequently, $\operatorname{Im}\tau(l_1, l_2, l_3) = 0$ if all $l_i^2 - m^2$ and these quantities satisfy the inequalities arising from the condition* $l_1 + l_2 + l_3 = 0$.

## II. THE GREEN'S FUNCTION IN THE PSEUDOSCALAR MESON THEORY

In this chapter we shall obtain the spectral representation for

$$\langle T\psi(x_1)\varphi_i(x_2)\bar{\psi}(x_3)\rangle.$$

Just as in the preceding case, we consider first the simple products

$$\langle\psi(x_1)\varphi_i(x_2)\bar{\psi}(x_3)\rangle, \quad \langle\varphi_i(x_2)\psi(x_1)\bar{\psi}(x_3)\rangle,$$
$$\langle\psi(x_1)\bar{\psi}(x_3)\varphi_i(x_2)\rangle \text{ etc.}$$

For example, the first two can be written in the forms

$$\langle\psi(x_1)\varphi_i(x_2)\bar{\psi}(x_3)\rangle$$
$$= \frac{1}{(2\pi)^9}\int d^4p_1 d^4p_3 e^{ip_1(x_1-x_2)+ip_3(x_3-x_2)}\vartheta(p_{10})\vartheta(p_{30})\gamma_5\tau$$
$$\times\Big\{\rho_0^{\psi\varphi\bar{\psi}}(p_1^2, q^2, p_3^2) + \hat{p}_1\rho_1^{\psi\varphi\bar{\psi}}(p_1^2, q^2, p_3^2) + \hat{p}_3\rho_3^{\psi\varphi\bar{\psi}}(p_1^2, q^2, p_3^2)$$
$$+ \frac{1}{2i}(\hat{p}_1\hat{p}_3 - \hat{p}_3\hat{p}_1)\rho_{13}^{\psi\varphi\bar{\psi}}(p_1^2, q^2, p_3^2)\Big\}, \qquad (14)$$

$$\langle\varphi_i(x_2)\psi(x_1)\bar{\psi}(x_3)\rangle$$
$$= \frac{1}{(2\pi)^9}\int d^4p_1 d^4p_3 e^{ip_1(x_2-x_1)+ip_3(x_1-x_3)}\vartheta(p_{10})\vartheta(p_{30})\gamma_5\tau_i$$
$$\times\Big\{\rho_0^{\varphi\psi\bar{\psi}}(p_1^2, q^2, p_3^2) + \hat{p}_1\rho_1^{\varphi\psi\bar{\psi}}(p_1^2, q^2, p_3^2) + \hat{p}_3\rho_3^{\varphi\psi\bar{\psi}}(p_1^2, q^2, p_3^2)$$
$$+ \frac{1}{2i}(\hat{p}_1\hat{p}_3 - \hat{p}_3\hat{p}_1)\rho_{13}^{\varphi\psi\bar{\psi}}(p_1^2, q^2, p_3^2)\Big\}. \qquad (14a)$$

The causality condition establishes a connection between $\rho_i^{\psi\varphi\bar{\psi}}$ and $\rho_i^{\varphi\psi\bar{\psi}}$. In order to bring out this connection we shall, as before, seek to express $\rho_i^{\psi\varphi\bar{\psi}}$, $\rho_i^{\varphi\psi\bar{\psi}}$, etc., in the forms

$$\vartheta(p_{10})\vartheta(p_{30})\rho_0^{\psi\varphi\bar{\psi}}(p_1^2, q^2, p_3^2)$$
$$= \int d^4l\,\vartheta(k_{10})\vartheta(k_{20})\vartheta(k_{30})f_0^{\psi\varphi\bar{\psi}}(-k_1^2, -k_2^2, -k_3^2),$$

$$\vartheta(p_{10})\vartheta(p_{30})[\hat{p}_1\rho_1^{\psi\varphi\bar{\psi}} + \hat{p}_3\rho_3^{\psi\varphi\bar{\psi}}]$$

---

*Nambu[3] took this rule as the basis for his derivation of the spectral representations of the Green's functions, but used it also for $l_i^2$ not satisfying the condition $l_1 + l_2 + l_3 = 0$. This last fact obviously makes his representations incorrect.

After the present paper was completed, the writer learned of a report by Schwinger at the Seventh Rochester Conference, in which similar representations were considered from a different point of view.

$$=\int d^4l\vartheta(k_{10})\vartheta(k_{20})\vartheta(k_{30})[(\hat{k}_1+\hat{k}_3)f_1^{\psi\varphi\bar{\psi}}(-k_1^2,-k_2^2,-k_3^2)+\hat{k}_2 f_2^{\psi\varphi\bar{\psi}}(-k_1^2,-k_2^2,-k_3^2)],$$

$$\vartheta(p_{10})\vartheta(p_{30})\frac{1}{2i}(\hat{p}_1\hat{p}_3-\hat{p}_3\hat{p}_1)\rho_{13}^{\psi\varphi\bar{\psi}}$$

$$=\int d^4l\vartheta(k_{10})\vartheta(k_{20})\vartheta(k_{30})\frac{1}{2i}(\hat{k}_1\hat{k}_3-\hat{k}_3\hat{k}_1)f_3^{\psi\varphi\bar{\psi}}(-k_1^2,-k_2^2,-k_3^2); \tag{15}$$

$$\vartheta(p_{10})\vartheta(p_{30})\rho^{\varphi\psi\bar{\psi}}(p_1^2,q^2,p_3^2)=\int d^4l\vartheta(k_{10})\vartheta(k_{20})\vartheta(k_{30})f_0^{\varphi\psi\bar{\psi}}(-k_1^2,-k_2^2,-k_3^2),$$

$$\vartheta(p_{10})\vartheta(p_{30})[\hat{p}_1\rho_1^{\varphi\psi\bar{\psi}}+\hat{p}_3\rho_3^{\varphi\psi\bar{\psi}}]$$

$$=\int d^4l\vartheta(k_{10})\vartheta(k_{20})\vartheta(k_{30})[(\hat{k}_2+\hat{k}_3)f_1^{\varphi\psi\bar{\psi}}(-k_1^2,-k_2^2,-k_3^2)$$

$$+\hat{k}_1 f_2^{\varphi\psi\bar{\psi}}(-k_1^2,-k_2^2,-k_3^2)], \tag{15a}$$

$$\vartheta(p_{10})\vartheta(p_{30})\frac{1}{2i}(\hat{p}_1\hat{p}_3-\hat{p}_3\hat{p}_1)\rho_{13}^{\varphi\psi\bar{\psi}}$$

$$=\int d^4l\vartheta(k_{10})\vartheta(k_{20})\vartheta(k_{30})\frac{1}{2i}(\hat{k}_2\hat{k}_3-\hat{k}_3\hat{k}_2)f_3^{\varphi\psi\bar{\psi}}(-k_1^2,-k_2^2,-k_3^2).$$

The convenience of just such a choice of the $f_i$ will be evident in what follows.

Substituting Eq. (15) into the causality condition

$$\langle\psi(x_1)\varphi_i(x_2)\bar{\psi}(x_3)\rangle=\langle\varphi_i(x_2)\psi(x_1)\bar{\psi}(x_3)\rangle,\quad x_{12}^2>0,$$

we get (here $\partial=\hat{\gamma}_\mu\partial/\partial x_\mu$)

$$\int dx_1^2\,dx_2^2\,dx_3^2\gamma_5\tau_i\Delta^+(x_{12},x_3)\Delta^+(x_{13},x_2)\Delta^+(x_{23},x_1)$$

$$\times\{f_0^{\psi\varphi\bar{\psi}}(x_1^2,x_2^2,x_3^2)-f_0^{\varphi\psi\bar{\psi}}(x_2^2,x_1^2,x_3^2)\}=0,$$

$$\int dx_1^2\,dx_2^2\,dx_3^2\gamma_5\tau_i\{[\Delta^+(x_{12},x_3)\Delta^+(x_{13},x_2)\hat{\partial}\Delta^+(x_{23},x_1)$$

$$+\hat{\partial}\Delta^+(x_{12},x_3)\Delta^+(x_{13},x_2)\Delta^+(x_{23},x_1)]$$

$$\times[f_1^{\psi\varphi\bar{\psi}}(x_1^2,x_2^2,x_3^2)-f_1^{\varphi\psi\bar{\psi}}(x_2^2,x_1^2,x_3^2)]+\Delta^+(x_{12},x_3)\hat{\partial}\Delta^+(x_{13},x_2)\Delta^+(x_{23},x_1)$$

$$\times[f_2^{\psi\varphi\bar{\psi}}(x_1^2,x_2^2,x_3^2)-f_2^{\varphi\psi\bar{\psi}}(x_2^2,x_1^2,x_3^2)]\}=0,$$

$$\int dx_1^2\,dx_2^2\,dx_3^2\gamma_5\tau_i\frac{1}{2i}[\hat{\partial}\Delta^+(x_{12},x_3)\Delta^+(x_{13},x_2)+\hat{\partial}\Delta^+(x_{13},x_2)\Delta^+(x_{12},x_3)]\Delta^+(x_{23},x_1) \tag{16}$$

$$\times[f_3^{\psi\varphi\bar{\psi}}(x_1^2,x_2^2,x_3^2)-f_3^{\varphi\psi\bar{\psi}}(x_2^2,x_1^2,x_3^2)]=0,$$

from which it follows that

$$f_k^{\psi\varphi\bar{\psi}}(x_1^2,x_2^2,x_3^2)=f_k^{\varphi\psi\bar{\psi}}(x_2^2,x_1^2,x_3^2). \tag{17}$$

Analogous relations can be obtained for $f_k^{\psi\varphi\bar{\psi}}$, $f_k^{\psi\bar{\psi}\varphi}$, etc. Using them and the definition of the functions $\Delta_F(x,\kappa)$, we can proceed as in the previous case to go over to the spectral representation of $\langle T\psi(x_1)\varphi_i(x_2)\bar{\psi}(x_3)\rangle$. We get here:

$$\langle T\psi(x_1)\varphi_i(x_2)\bar{\psi}(x_3)\rangle=\int dx_1^2\,dx_2^2\,dx_3^2\gamma_5\tau_i\Big\{f_0^{\psi\varphi\bar{\psi}}(x_1^2,x_2^2,x_3^2)$$

$$+f_1^{\psi\varphi\bar{\psi}}(x_1^2,x_2^2,x_3^2)\,i(\hat{\partial}_1+\hat{\partial}_3)+f_2^{\psi\varphi\bar{\psi}}(x_1^2,x_2^2,x_3^2)\,i\hat{\partial}_2$$

$$+\frac{1}{2i}(\hat{\partial}_3\hat{\partial}_1-\hat{\partial}_1\hat{\partial}_3)f_3^{\psi\varphi\bar{\psi}}(x_1^2,x_2^2,x_3^2)\Big\}\Delta_F(x_{12},x_3)\,\Delta_F(x_{13},x_2)\Delta_F(x_{23},x_1) \tag{18}$$

and correspondingly in the momentum representation

$$\tau(l_1,l_2,l_3)=\frac{\pi^2}{2}\delta(l_1+l_2+l_3)\gamma_5\tau_i\int dx_1^2\,dx_2^2\,dx_3^2\int_0^1 d\alpha\int_0^1 d\beta\int_0^1 d\gamma\,\delta(\alpha+\beta+\gamma-1)$$

$$\times\Bigg\{\frac{f_0^{\psi\varphi\bar{\psi}}(x_1^2,x_2^2,x_3^2)+(\gamma\hat{l}_1-\alpha\hat{l}_3+\beta\hat{l}_2)f_1^{\psi\varphi\bar{\psi}}(x_1^2,x_2^2,x_3^2)+(\alpha\hat{l}_1-\gamma\hat{l}_3)f_2^{\psi\varphi\bar{\psi}}(x_1^2,x_2^2,x_3^2)}{l_1^2\beta\gamma+l_2^2\alpha\gamma+l_3^2\alpha\beta+\alpha x_1^2+\beta x_2^2+\gamma x_3^2-i\varepsilon}$$

$$+\frac{\frac{\beta}{2i}(\hat{l}_1\hat{l}_3-\hat{l}_3\hat{l}_1)f_3^{\psi\varphi\bar{\psi}}(x_1^2,x_2^2,x_3^2)}{l_1^2\beta\gamma+l_2^2\alpha\gamma+l_3^2\alpha\beta+\alpha x_1^2+\beta x_2^2+\gamma x_3^2-i\varepsilon}\Bigg\}. \tag{19}$$

Using the invariance of the theory with respect to charge conjugation, we get:

$$\langle T\psi(x_1)\varphi_i(x_2)\bar{\psi}(x_3)\rangle = -(C^{-1}\langle T\psi(x_3)\varphi_i(x_2)\bar{\psi}(x_1)\rangle C)^T;$$

$$\bar{\psi}' = C^{-1}\psi; \quad \psi' = C\bar{\psi}; \quad \varphi_i' = -\varphi_i; \quad C^{-1}\gamma_\mu C = -\gamma_\mu^T; \; C^{-1}\tau_j C = -\tau_j^T. \tag{20}$$

From this we find, by considerations analogous to those used in Sec. 2, that the $f_k^{\psi\varphi\bar{\psi}}(\kappa_1^2, \kappa_2^2, \kappa_3^2)$ are real functions. $f_0^{\psi\varphi\bar{\psi}}(\kappa_1^2, \kappa_2^2, \kappa_3^2)$ is an antisymmetric function and $f_1^{\psi\varphi\bar{\psi}}$, $f_2^{\psi\varphi\bar{\psi}}$, and $f_3^{\psi\varphi\bar{\psi}}$ are symmetric functions, with respect to interchange of $\kappa_1^2$ and $\kappa_3^2$.

We obtain further information about the $f_k^{\psi\varphi\bar{\psi}}(\kappa_1^2, \kappa_2^2, \kappa_3^2)$ in just the same way as in the previous case. From the condition that $\rho_k^{\psi\varphi\bar{\psi}}(p_1^2, q^2, p_3^2) = 0$ if $-p_1^2 \leq m^2$ or $-p_3^2 \leq m^2$ and from Eq. (15) it follows, just as in Sec. 2, that $f_k^{\psi\varphi\bar{\psi}}(\kappa_1^2, \kappa_2^2, \kappa_3^2) = 0$ if $\kappa_1 + \kappa_2 \leq m$ or $\kappa_2 + \kappa_3 \leq m$ ($m$ is the mass of the nucleon). From the condition $\rho_k^{\varphi\psi\bar{\psi}}(p_1^2, q^2, p_3^2) = 0$ if $-p_1^2 \leq \mu^2$ or $-p_3^2 \leq m^2$ and from Eq. (15a) it follows that $f_k^{\varphi\psi\bar{\psi}}(\kappa_1^2, \kappa_2^2, \kappa_3^2) = 0$ if $\kappa_1 + \kappa_2 \leq m$ or $\kappa_2 + \kappa_3 \leq \mu$ ($\mu$ is the mass of the meson).

Combining these conditions with the condition (17), we get

$$f_k^{\psi\varphi\bar{\psi}}(\varkappa_1^2, \varkappa_2^2, \varkappa_3^2) \neq 0 \text{ for } \varkappa_1 + \varkappa_2 \geq m,$$
$$\varkappa_2 + \varkappa_3 \geq m, \; \varkappa_1 + \varkappa_3 \geq \mu. \tag{21}$$

The last result means that if we disregard the imaginary quantities occurring in $\hat{l}_i$ and $\gamma_5$, $\tau_i$,

$$\mathrm{Im}''\tau(l_1, l_2, l_3) = 0, \tag{22}$$
$$\text{if } -l_1^2 < m_1^2, \; -l_3^2 < m^2, \; -l_2^2 < \mu^2.$$

We obtain a more complete representation for $\tau(l_1, l_2, l_3)$ if we note that it can be written in the form

$$\tau(l_1, l_2, l_3) = -\frac{1}{l_2^2 + \mu^2}\frac{1}{i\hat{l}_1 + m}\tau'(l_1, l_2, l_3)\frac{1}{i\hat{l}_3 - m}. \tag{23}$$

We get an expression for $\tau'(l_1, l_2, l_3)$ if we go back to the coordinate representation

$$\tau'(x_1, x_2, x_3)$$
$$= (\Box_2 - \mu^2)(\hat{\partial}_1 + m)(\hat{\partial}_3^T - m)\langle T\psi(x_1)\varphi_i(x_2)\psi(x_3)\rangle$$
$$= \langle Tu(x_1) j_i(x_2)\bar{u}(x_3)\rangle$$
$$+ \gamma_4\delta(t_1 - t_2)\langle T[\psi(x_1)\; j_i(x_2)]u(x_3)\rangle$$
$$+ \delta(t_2 - t_3)\langle Tu(x_1)[\bar{\psi}(x_3) j(x_2)]\rangle\gamma_4$$
$$+ \delta(t_1 - t_2)\delta(t_2 - t_3)\gamma_4\langle\{\bar{\psi}(x_3),\; [\psi(x_1) j_i(x_2)]\}\rangle\gamma_4;$$

$$j_i(x) = (\Box - \mu^2)\varphi_i(x); \quad u(x) = (i\hat{\partial} + m)\psi(x);$$
$$\bar{u}(x) = (i\hat{\partial}^T - m)\bar{\psi}(x). \tag{24}$$

Setting $\langle \mathrm{T}u(x_1) j_i(x_2)\bar{u}(x_3)\rangle = \tau_c(x_1, x_2, x_3)$, we see that $\tau_c(x_1, x_2, x_3)$ has precisely the same structure as $\tau(x_1, x_2, x_3)$, i.e., it is a T-product of Heisenberg operators. Therefore we can repeat all the arguments of this chapter with respect to $\tau_c(x_1, x_2, x_3)$. By so doing we arrive at formulas which coincide with Eqs. (18) and (19) in the coordinate and momentum representations, respectively. The corresponding functions $f_k^{uj\bar{u}}$ will satisfy the same conditions of symmetry and reality. The condition (22) is changed, however, since the matrix elements of the operators $u$, $\bar{u}$, and $j_i$ between the vacuum and one-particle states are equal to zero.

Instead of the previous conditions we get

$$\rho_k^{uj\bar{u}}(p_1^2, q^2, p_3^2) = 0,$$
$$\text{if } -p_1^2 < (m+\mu)^2 \text{ or } -p_3^2 < (m+\mu)^2,$$
$$\rho_k^{ju\bar{u}}(p_1^2, q^2, p_3^2) = 0,$$
$$\text{if } -p_1^2 < 9\mu^2 \text{ or } -p_3^2 < (m+\mu)^2,$$

from which it follows that

$$f_k^{uj\bar{u}}(\varkappa_1^2, \varkappa_2^2, \varkappa_3^2) \neq 0, \quad \text{if } \varkappa_1 + \varkappa_2 \geq m + \mu; \tag{25}$$
$$\varkappa_2 + \varkappa_3 \geq m + \mu, \; \varkappa_1 + \varkappa_3 \geq 3\mu.$$

From this it follows in turn that

$$\mathrm{Im}''\tau_c(l_1, l_2, l_3) = 0, \quad \text{if } -l_1^2 < (m+\mu)^2, \tag{26}$$
$$-l_3^2 < (m+\mu)^2, \; -l_2^2 < 9\mu^2.$$

If $j_i(x) = ig\psi\gamma_5\tau_i\psi + \lambda(\varphi_i\varphi_k\varphi_k - \delta\mu^2\varphi)$, then the terms

$$\delta(t_1 - t_2)\gamma_4\langle T[\psi(x_1) j_i(x_2)]\bar{u}(x_3)\rangle$$
$$+ \delta(t_2 - t_3)\langle Tu(x_1)[\psi(x_3) j(x_2)]\rangle\gamma_4$$
$$+ \delta(t_1 - t_2)\delta(t_2 - t_3)\gamma_4\langle\{[\psi(x_1) j_i(x_2)]\psi(x_3)\}\rangle\gamma_4$$
$$= ig\gamma_5\tau_i\langle T\psi(x_2)\bar{u}(x_3)\rangle\delta(x_1 - x_2)$$
$$- ig\delta(x_2 - x_3)\langle Tu(x_1)\bar{\psi}(x_2)\rangle\gamma_5\tau_i$$
$$+ ig\gamma_5\tau_i\delta(x_1 - x_2)\delta(x_2 - x_3) \tag{27}$$

reduce to the vacuum expectation values of T-products of two operators, for which the spectral representations are well known.

In conclusion I wish to express my gratitude to V. V. Anisovich, K. A. Ter-Martirosian, and I. M. Shmushkevich for a helpful discussion.

## APPENDIX

Calculation of the integral (10)

$$I = \int \vartheta(p_1 - k)\,\vartheta(p_3 - k)\,\vartheta(k)\,\delta(k^2 + \varkappa_2^2) \times \delta((p_1 - k)^2 + \varkappa_3^2)\,\delta((p_3 - k)^2 + \varkappa_1^2)\,d^4k.$$

The most important point is to find out the conditions under which $I \neq 0$. In order that the products

$$\begin{aligned} &\vartheta(k)\,\vartheta(p_1 - k)\,\delta(k^2 + \varkappa_2^2)\,\delta((p_1 - k)^2 + \varkappa_3^2), \\ &\vartheta(k)\,\vartheta(p_3 - k)\,\delta(k^2 + \varkappa_2^2)\,\delta((p_3 - k)^2 + \varkappa_1^2) \end{aligned} \tag{A1}$$

be not equal to zero, it is necessary that

$$-p_1^2 \geqslant (\varkappa_2 + \varkappa_3)^2, \qquad -p_3^2 \geqslant (\varkappa_1 + \varkappa_2)^2 \tag{A2}$$

These conditions are not, however, sufficient to secure that $I \neq 0$. What is needed is the existence of common values of k for which these products are nonvanishing. To obtain the sufficient conditions we go over to a definite reference system with

$$\mathbf{p}_1 = -\mathbf{p}_3 = \mathbf{p}.$$

In this system we have

$$\begin{aligned} &p_1^2 + \varkappa_3^2 - \varkappa_2^2 + 2p_{10}k_0 - 2pkx = 0, \\ &p_3^2 + \varkappa_1^2 - \varkappa_2^2 + 2p_{30}k_0 + 2pkx = 0, \quad x = \cos(\mathbf{pk}). \end{aligned} \tag{A3}$$

Solving these equations and substituting the resulting solutions into the condition

$$k_0^2 - \varkappa_2^2 \geqslant k^2x^2,$$

we get

$$\frac{1}{4(p_{10} + p_{30})^2}(2\varkappa_2^2 - \varkappa_1^2 - \varkappa_3^2 - p_1^2 - p_3^2)^2 - \varkappa_2^2 \geqslant \frac{1}{16p^2}\Big[\varkappa_1^2 - \varkappa_3^2 - p_1^2 + p_3^2 + \frac{p_{30} - p_{10}}{p_{30} + p_{10}}(2\varkappa_2^2 - \varkappa_1^2 - \varkappa_3^2 - p_1^2 - p_3^2)\Big]^2. \tag{A4}$$

The conditions (A2) and (A4) are sufficient conditions for $I \neq 0$. When the conditions (A2) and (A4) are satisfied,

$$I = \pi / 4p\,(p_{10} + p_{30}). \tag{A5}$$

It can easily be shown that

$$p_{10} + p_{30} = [q^2 - 2p_1^2 - 2p_3^2]^{1/2},$$

$$p^2 = \frac{[q^2 + (\sqrt{-p_1^2} + \sqrt{-p_3^2})^2]\,[q^2 + (\sqrt{-p_1^2} - \sqrt{-p_3^2})^2]}{4(q^2 - 2p_1^2 - 2p_3^2)}. \tag{A6}$$

By means of these formulas we can write I in invariant form. Substituting (A6) into Eqs. (A5) and (A4), we obtain the result given in the text.

[1] G. Källen, Helv. Phys. Acta **25**, 417 (1952).
[2] H. Lehmann, Nuovo cimento **11**, 342 (1954).
[3] Y. Nambu, Phys. Rev. **100**, 394 (1955).

Translated by W. H. Furry
260

# Letters to the Editor

## *THE ENERGY OF AN EXCITON IN ALKALI-HALIDE CRYSTALS*

I. M. DYKMAN and A. A. TSERTSVADZE

Tbilisi State University

Submitted to JETP editor October 29, 1957

J. Exptl. Theoret. Phys. (U.S.S.R.) **34**, 1319-1321 (May, 1958)

In Ref. 1 a model for excitons in alkali-halides crystals was constructed, according to which the exciton excitation was connected with the transition of one of the six p-electrons of the outer shell of the halide ion to the s-shell of the nearest alkali ions. Such a model made it possible, even without knowing the electronic functions, to calculate the change in polarization energy of the lattice, the half-width of the band of exciton absorption and its temperature dependence, the field mass of the exciton,[2] and a number of other quantities characterizing, on the whole, an excited state, but not the ground state of the crystal. However, to evaluate the energy of an exciton transition and its probability, the interaction cross section of excitons with different impurity centers, and so on, it is necessary to use the eigenfunctions of the system both in an excited, and in the ground state.

In Ref. 3 the wave function $\Psi_0$ of the ground state of the system (corresponding to a non-excited crystal) was chosen in the form of an antisymmetrized product of electron functions at the various ions. To describe the exciton state of the crystal, the wave function $\Psi_{exc}$ was also written as an antisymmetrized product of electron functions, in correspondence with the model considered in Ref. 1, but it was assumed that in one, say the $l$-th, elementary cell one of the external p-electrons was absent from a halide ion, and at the six nearest alkali ions there was, with equal probability, an extra electron.

Substituting $\Psi_0$ and $\Psi_{exc}$ into the Hamiltonian of the system, which describes all possible electrical pair interactions between the electrons and the atomic nuclei of the crystal, we are able to evaluate the energies $E_0$ and $E_{exc}$ of the ground state and excited (exciton) state, respectively. Their difference determines the energy of the exciton excitation and can be transformed to the form

$$E_{exc} - E_0 = \varepsilon_2 - \varepsilon_1 - \frac{e^2}{1+4A+B} \times \sum_{(s',\, l'\neq 1,\, l_1)}{}' \sum_{l_1=1}^{6} \int V_{s'}^{l'}(\rho)\, \varphi_1^{l_1}(\rho)\, \varphi_1^{l'_1}(\rho)\, d\tau - \text{exch. term}$$

$$- \frac{e^2}{3} \sum_{(s',\, l'\neq 2,\, l)}{}' \int V_{s'}^{l'}(\rho)\, |\varphi_{2p}^{l}(\rho)|^2\, d\tau + \text{exch. term}$$

$$- \frac{1}{6(1+4A+B)} \sum_{x\alpha,\, y\beta} \sum_{l_1'=1}^{6} \int [\varphi_1^{*l_1}(\rho)\, \varphi_{2x\alpha}^{*l}(\rho')\, \varphi_1^{l'_1}(\rho)\, \varphi_{2y\beta}^{l}(\rho')$$

$$- \varphi_1^{*l_1}(\rho)\, \varphi_{2x\alpha}^{*l}(\rho')\, \varphi_1^{l_1'}(\rho')\, \varphi_{2y\beta}^{l}(\rho)] \frac{e^2}{|\rho-\rho'|}\, d\tau\, d\tau'. \qquad (1)$$

In this equation A and B are constants occurring in the normalization of $\Psi_{exc}$ and equal to the overlap integrals of the s-functions of different alkali ions at distances $a\sqrt{2}$ and $2a$ apart, where $a$ is the lattice constant. The index 1 refers everywhere to an atom (ion) of the metal, and 2 to those of the halides: $\epsilon_1$ is the ionization energy of an alkali atom, $\epsilon_2$ is the affinity energy of a halide atom, $\varphi_1^{l_1}(\rho)$ is the wave function of a valence electron of an alkali atom in the $l_1$-th elementary cell, $\varphi_{2x\alpha}^{l}(\rho)$ the p-electron function of a halide atom ($x\alpha$ indicates the magnetic and spin quantum numbers), $\varphi_{2p}^{l}(\rho)$ is the radial part of the p-electron wave function, and $V_s^l(\rho)$ is the potential of the ion s, $l$ at a point with radius vector $\rho$.

Equation (1) was numerically evaluated for an NaCl crystal. We took for $V_s^l(\rho)$ and $\varphi_{2x\alpha}^{l}(\rho)$ Hartree functions.[4] In the evaluation of $E_0$ and $E_{exc}$ we can use here these functions as the functions of the zeroth approximation because the overlap integrals of even the nearest ions in the NaCl lattice are very small ($\sim 10^{-2}$). However, we can not use directly the Hartree function for the 3s-electron of atomic Na since the corresponding overlap integrals are not small. For the functions $\varphi_1^{l_1}(\rho)$ we took thus the functions found by Tolpygo and Tomasevich.[5] After evaluating the polarization of the electronic shells of the ions without inertial effects, we got for the energy of the exciton transiton in NaCl $\Delta E = 7.5$ ev. The exchange terms which were not written down explicitly in Eq. (1) turned out to have practically no influence on the final value of $\Delta E$.

Muto and Okuno[6] have evaluated by numerical methods the energy of the exciton transition in KCl and NaCl crystals. They were, however, not able to determine the absolute value of the energy but only the distance of the exciton energy level from the bottom of the conduction band, the position of which was found in addition from experi-

mental data. To get agreement with experiment they could essentially still use two parameters. The method proposed by us is free of these shortcomings and enables us to consider the interaction of excitons with light and various centers. One can consider that the result obtained is in satisfactory agreement with the experimental value of $\Delta E$ determined from the position of the maximum of the exciton absorption band at $\lambda = 1580$ A ($\sim 7.85$ ev).

In conclusion we note that if we take the translational symmetry of our problem into consideration we can write the wave function in the following form

$$\Psi_k = N^{-1/2} \sum_l \exp(i\mathbf{k}\mathbf{r}_2^l)\, \Psi_B^l. \qquad (2)$$

Expression (2) determines the exciton band, whose width is of the order of

$$\frac{1}{36(1+4A+B)} \sum_{l'(\neq l)}' \sum_{l_1, l_1'}^{6} \sum_{x\alpha,\, y\beta}^{6} \int \varphi_1^{*l_1}(\rho)\, \varphi_{2x\alpha}^{*l'}(\rho')$$

$$\times \frac{e^2}{|\rho - \rho'|} \varphi_{2y\beta}^{l}(\rho)\, \varphi_1^{l_1'}(\rho')\, d\tau d\tau' - \text{exch. term.} \qquad (3)$$

The width (3) of the exciton band is, as follows from a numerical calculation, far smaller than $\Delta E$. This is, though, clear from the fact that in (3) functions occur referring to different halide ions and the integrals in (3) are thus much less than the analogous integrals in (1).

Since the width of the exciton band is much smaller than $\Delta E$, the energy of the excitation can be evaluated using the simpler function $\Psi_{exc}$ as was done in the foregoing calculations. In those cases, however, where one is interested in effects which depend essentially on the form and width of the exciton band, it is necessary to use the more exact function (2).

[1] I. M. Dykman, J. Exptl. Theoret. Phys. (U.S.S.R.) **26**, 307 (1954).

[2] Dykman, Kaplunova, and Tolpygo, J. Tech. Phys. (U.S.S.R.) **26**, 2459 (1956), Soviet Phys. JTP **1**, 2376 (1956).

[3] A. A. Tsetsvadze, Труды Тбилисск. ун-та (Trans. Tbilisi Univ.) **62**, 149 (1957).

[4] D. Hartree and W. Hartree, Proc. Roy. Soc. **166**, 450 (1938).

[5] O. F. Tomasevich and K. B. Tolpygo, Укр. физ. журн. (Ukrainian Phys. Journal)(in press).

[6] T. Muto and H. Okuno, J. Phys. Soc. Japan **11**, 633 (1956); **12**, 108 (1957).

Translated by D. ter Haar
261

## *CONSEQUENCES OF THE TWO-COMPONENT BEHAVIOR OF THE ELECTRON IN THE BETA INTERACTION*

B. L. IOFFE and V. A. LIUBIMOV

Submitted to JETP editor December 12, 1957

J. Exptl. Theoret. Phys. (U.S.S.R.) **34**, 1321-1323 (May, 1958)

THE latest measurements[1-3] of the longitudinal polarization of the electrons emitted in $\beta$ decay show that the values of the longitudinal polarization $\langle \sigma_\parallel \rangle$ in cases of allowed transitions and first-forbidden transitions in heavy nuclei are to good accuracy equal to v/c. As can be rigorously proved from the formulas[4] for the longitudinal polarization of the electrons from such transitions, a necessary and sufficient condition for the relation $\langle \sigma_\parallel \rangle = v/c$ is the existence of the following relations between the interaction constants conserving parity and violating its conservation:

$$C_S = -C_S', \quad C_T = -C_T', \quad C_A = C_A', \quad C_V = C_V'. \qquad (1)$$

With these conditions the interaction Hamiltonian takes the form

$$H = \sum_\alpha C_\alpha (\bar{\Psi}_p O_\alpha \Psi_n)(\bar{\psi}_e (1 - \gamma_5) O_\alpha \psi_\nu) + \text{c. c.}, \qquad (2)$$

and the electronic $\psi$ function is involved in all the types of $\beta$ interaction through only two components.

Let us examine the consequences of the relations (1), i.e., of the two-component behavior of the electron in the $\beta$ interaction. When the conditions (1) hold the expressions for the various effects in $\beta$ decay are decidedly simplified, so that in the case of allowed transitions there remain all told just six independent combinations of the constants and matrix elements:

$$N_0 = (|C_S|^2 + |C_V|^2)\,|M_F|^2 + (|C_T|^2 + |C_A|^2)\,|M_{GT}|^2,$$

$$N_1 = -\lambda_{jj'}(|C_T|^2 + |C_A|^2)\,|M_{GT}|^2 - 2\delta_{jj'}\sqrt{j/(j+1)}\,\mathrm{Re}(C_S C_T^* + C_V C_A^*) M_F M_{GT}^*,$$

$$N_3 = (|C_V|^2 - |C_S|^2)\,|M_F|^2 + {}^1/_3 (|C_T|^2 - |C_A|^2)\,|M_{GT}|^2,$$

$$N_4 = 2\delta_{jj'}\sqrt{j/(j+1)}\,\mathrm{Im}(C_V C_A^* - C_S C_T^*) M_F M_{GT}^*,$$

$$N_\nu = -\lambda_{jj'}(|C_T|^2 - |C_A|^2)\,|M_{GT}|^2 + 2\delta_{jj'}\sqrt{j/(j+1)}\,\mathrm{Re}(C_S C_T^* - C_V C_A^*) M_F M_{GT}^*,$$

$$N_5 = 2\delta_{jj'}\sqrt{j/(j+1)}\,\mathrm{Im}(C_V C_A^* + C_S C_T^*) M_F M_{GT}^*. \qquad (3)$$

Here

$$\lambda_{jj'} = [j(j+1) - j'(j'+1) + 2]/2(j+1),$$

and $M_F = \left(\int 1\right)$ and $M_{GT} = \left(\int \sigma\right)$ are the nuclear matrix elements. The quantity $N_0$ determines the total probability of the $\beta$ transition, $N_3$ the electron-neutrino angular correlation,

$$W_{e\nu} = 1 + (v/c)(N_3/N_0)(\mathbf{n}_e\boldsymbol{\nu}),$$

and $N_1$ the angular distribution of the electrons from oriented nuclei:

$$W_{je} = 1 + x(v/c)(N_1/N_0)(\mathbf{n}_e\mathbf{n}_j), \quad x = \langle j_z\rangle/j$$

($\mathbf{n}_e$, $\boldsymbol{\nu}$, and $\mathbf{n}_j$ are unit vectors giving the directions of the momenta of the electron and neutrino and of the spin of the nucleus).

The quantities $N_0$, $N_1$, and $N_3$ have already been determined experimentally. As can be seen from the formulas (3), information new in principle can now be obtained only from experiments in which $N_4$, $N_\nu$, and $N_5$ would be measured. The quantity $N_\nu$ determines the angular distribution of the neutrinos from oriented nuclei (averaged over directions of emission of the electron)

$$W_{j\nu} = 1 + x(N_\nu/N_0)(\mathbf{n}_j\boldsymbol{\nu}).$$

Therefore the simplest experiment in which the quantity $N_\nu$ could be determined is a measurement of the angular distribution of the recoil nuclei from the decay of oriented nuclei.* The coefficient $N_4$ could be found from a study of the asymmetry of the distribution of recoil nuclei relative to the plane of the electron momentum and the nuclear spin. If, for example, we select electrons with momenta perpendicular to the nuclear spin, the ratio of the numbers of recoil nuclei with directions of motion on opposite sides of this plane will be

$$\left(1 - \frac{x}{2}\frac{v}{c}\frac{N_4}{N_0}\right)\Big/\left(1 + \frac{x}{2}\frac{v}{c}\frac{N_4}{N_0}\right).$$

The quantity $N_5$ could be obtained from experiments on the decay of oriented (or aligned) nuclei in which, besides the direction of emission of the electron, one also measured the polarization of the recoil nucleus or the direction of the $\gamma$-quantum from a subsequent $\gamma$-transition.†

Measurements of the polarization of the electrons (both longitudinal and transverse) from oriented nuclei and in correlation with the neutrinos cannot give anything new as compared with the experiments indicated above. For example, the polarization of the electrons from the decay of oriented nuclei is given by:

$$\langle\sigma\rangle_{je} = \frac{1}{W_{je}}\left\{-\mathbf{n}_e\frac{v}{c}\left[1 + x\frac{c}{v}\frac{N_1}{N_0}(\mathbf{n}_e\mathbf{n}_j)\right] + x\frac{Z}{137\varepsilon}\bar{\eta}_0\frac{N_1}{N_0}[\mathbf{n}_e\times\mathbf{n}_j] + x\frac{\gamma_1\bar{\mu}_0}{\varepsilon}\frac{N_1}{N_0}[\mathbf{n}_e\times(\mathbf{n}_e\times\mathbf{n}_j)]\right\},$$

and the correlation of the polarization with the direction of emission of the neutrino (for unpolarized nuclei) by:

$$\langle\sigma\rangle_{e\nu} = \frac{1}{W_{e\nu}}\left\{-\mathbf{n}_e\frac{v}{c}\left[1 + \frac{c}{v}\frac{N_1}{N_0}(\mathbf{n}_e\boldsymbol{\nu})\right] + \frac{Z}{137\varepsilon}\bar{\eta}_0\frac{N_3}{N_0}[\mathbf{n}_e\times\boldsymbol{\nu}] + \frac{\gamma_1\bar{\mu}_0}{\varepsilon}\frac{N_3}{N_0}[\mathbf{n}_e\times(\mathbf{n}_e\times\boldsymbol{\nu})]\right\}.$$

Here $\epsilon$ is the energy of the electron (in units $m_ec^2$), $\gamma_1 = [1-(Z/137)^2]^{1/2}$, and $\bar{\mu}_0$ and $\bar{\eta}_0$ are coefficients nearly equal to unity which allow for the finite size of the nucleus. Thus measurement of $\langle\sigma\rangle_{je}$ and $\langle\sigma\rangle_{e\nu}$ does not give information that is in principle new as compared with the experiments that have already been carried out, in which the quantities $N_0$, $N_1$, and $N_3$ have been measured.

It is not hard to see that if we write the coefficients $C_\alpha$ in the form $|C_\alpha|e^{i\varphi_\alpha}$, the quantities $N_i$ ($i = 0, \ldots 5, \nu$) are expressed in terms of only six unknown coefficients: four absolute values $|C_\alpha|$ and the two phase differences $\varphi_T - \varphi_S$ and $\varphi_V - \varphi_A$, since with the two-component behavior of the electron the types A and V do not interfere with S and T. Therefore to obtain complete information about the $\beta$ interaction in allowed transitions there is in principle no need to measure experimentally all six quantities $N_i$ in Fermi and Gamow-Teller transitions; it is enough if one confines oneself to four of them.

The writers express their sincere gratitude to Academician A. I. Alikhanov, K. A. Ter-Martirosian, and A. P. Rudik for valuable discussions and remarks.

*An equivalent of this would be an experiment on a $\beta-\gamma$ transition which measured the correlation between the directions of emission of $\gamma$-quanta of a given circular polarization and of recoil nuclei.

†The problem of determining the quantity $N_5$ from experiments on the $\beta-\gamma$ correlation in the decay of oriented (or aligned) nuclei has been considered in detail in Refs. 5 to 7.

[1] Alikhanov, Eliseev, and Liubimov, J. Exptl. Theoret. Phys. (U.S.S.R.) **34**, 1045 (1958), Soviet Phys. JETP **7**, 723 (1958).

[2] Cavanagh, Coleman, Turner, and Ridley, Nuclear Phys. **5**, 31 (1958).

[3] Boehm, Novey, Barnes, and Stech, Phys. Rev. **108**, 1497 (1958).

[4] Berestetsky, Ioffe, Rudik, and Ter-Martirosian, Phys. Rev. **111**, 522 (1958).

[5] A. Z. Dolginov, J. Exptl. Theoret. Phys. (U.S.S.R.) **33**, 1363 (1957), Soviet Phys. JETP **6**, 1047 (1958).

[6] M. Morita and R. S. Morita, Phys. Rev. **107**, 1316 (1957).

[7] R. B. Curtis and R. R. Lewis, Phys. Rev. **107**, 1381 (1957).

Translated by W. H. Furry
262

## *PROTON WAVE EQUATIONS*

A. A. BORGARDT

Dnepropetrovsk State University

Submitted to JETP editor December 19, 1957; resubmitted February 12, 1958

J. Exptl. Theoret. Phys. (U.S.S.R.) **34**, 1323-1325 (May, 1958)

THE existing techniques of treatment of the electromagnetic field do not allow to handle the interaction of photons with other fields in terms of quantum field theory in a number of cases. These problems include the whole complex of gravitation-electromagnetic interactions: graviton-photon scattering, graviton bremsstrahlung by photons, etc. In order to treat such problems one has to formulate the wave equation of light quanta in matrix form.

The fundamental difficulty in formulating a matrix theory of the photon field lies in the fact that the rest mass of the photon vanishes and further that the wave function contains both electromagnetic potentials and fields. This makes the application of the Kemmer formalism exceedingly difficult.[1,2] However, by applying the Dirac algebra[3] one can remove this difficulty and it is possible to formulate a photon theory analogously to the Lee-Yang theory[4] of rest-mass-zero fermions.

In Ref. 5 it was shown explicitly how to achieve a representation of the 16-row Kemmer algebra by 8- or 4-row representations of the Dirac algebra. These same representations will have to be applied to the photon theory. (A detailed investigation of these algebrae will be published in Nuovo cimento.)

For the photon wave function we shall take the half-undor $\psi$ which includes, besides the fields E and H, two new quantities, a scalar, $\psi$, and pseudoscalar, $\tilde{\psi}$. Using an 8-row representation of the Dirac algebra one can write the free field wave equation in the form

$$(\boldsymbol{\alpha},\ \nabla + \partial/c\,\partial t)\,\psi(\mathrm{x},\ t) = 0 \qquad (1)$$

or

$$(\boldsymbol{\alpha}^*,\ \nabla + \partial/c\,\partial t)\,\psi(\mathrm{x},\ t) = 0, \qquad (2)$$

where

$$^1/_2\{\alpha_i\alpha_k\} - \delta_{ik}I = {}^1/_2\{\alpha_i^*\alpha_k^*\} - \delta_{ik}I = [\alpha_i\alpha_k^*] = 0. \qquad (3)$$

We define a matrix $\alpha_L \neq I$ with the properties

$$[\alpha_L\alpha_i] = [\alpha_L\alpha_i^*] = [r_i\alpha_L] = 0, \quad \alpha_L^2 = I \qquad (4)$$

where $r_i = \alpha_i\alpha_i^*$ are reflection matrices (here one does not sum over the indices i). It leads to the Larmor transformation for $\psi$: $\psi' = \alpha_L\psi$. The corresponding transformation in the neutrino theory is the Salam transformation[6] $\varphi' = \gamma_5\varphi$.

An explicit expression for $\alpha_L$ is

$$\alpha_L = i\alpha_1\alpha_2\alpha_3 = i\alpha_1^*\alpha_2^*\alpha_3^*, \qquad (5)$$

Besides $\alpha_L$ there exists another pseudoscalar operator, $i\alpha_0 = r\alpha_L$, where r has the properties

$$\{r\alpha_i\} = \{r\alpha_i^*\} = [r_i r] = 0. \qquad (6)$$

Equations (1) and (2) are invariant under Larmor transformations. In order to go over to a 4-row representation one introduces the Larmor-invariant wave function[7] $(I + \alpha_L)\psi$. Then both anticommutative groups $G_\alpha$ and $G_{\alpha^*}$ go over into the group $G_\gamma$ of the Dirac matrix theory of the electron in the representation where charge conjugation is represented by complex conjugation.[5,8]

It is interesting to note that these matrices are identical with the matrices describing the two internal degrees of freedom of Fock's electron.[9,10] However, they enter linearly the operator of van Wyk's generalized gauge transformation.[11]

The Larmor photons can have different parity and can have a spin of $\hbar$ even in the case of longitudinal polarization (longitudinal-magnetic photons). In order to describe Larmor-nonsymmetrical, Maxwell photons one has to go over to a wave function which is a simultaneous solution of (1) and (2), or, of the following system of equations which is equivalent to (1), (2) in this particular case:

$$(\beta^{(+)},\ \nabla + \partial/c\,\partial t)\,\psi(\mathrm{x},\ t) = 0, \quad \beta^{(-)},\ \nabla\psi(\mathrm{x},\ t) = 0,$$
$$\beta^{(\pm)} = (\boldsymbol{\alpha} \pm \boldsymbol{\alpha}^*)/2. \qquad (7)$$

The wave equations (1) and (2) are derived from the Lagrangian

$$L \sim \bar{\psi}(\boldsymbol{\alpha},\ \nabla + \partial/c\,\partial t)\,\psi \qquad (8)$$

(for ordinary photons $\boldsymbol{\alpha}$ here has to be replaced by $\beta^{(+)}$).

The commutation relations are, as usual,

$$[\psi(\mathrm{x},\ t),\ \bar{\psi}(\mathrm{x}',\ t')] = iS(\mathrm{x} - \mathrm{x}',\ t - t'), \qquad (9)$$

where the commuting function S is different for the Larmor and Maxwell photons:

$$= (\alpha, \nabla - \partial/c\,\partial t)\,D(x, t), \quad (10)$$

$$S_M(x, t) = (\alpha, \nabla - \partial/c\,\partial t)(\alpha^*, \nabla - \partial/c\,\partial t)\,D(x, t). \quad (11)$$

In momentum space $S_M$ reduces to the form of the Cayley-Klein transformation of the unit wave vector $k^0 = k/k$

$$S_M = (I + \alpha^*, k^0)/(I - \alpha, k^0). \quad (12)$$

For the Maxwell field it is possible to utilize Eqs. (1) and (2) with the reduced wave function $\psi_M = T\psi$, where

$$T = (3 + M)/4, \quad M = r_1 + r_2 + r_3. \quad (13)$$

The photon theory, like the new neutrino theory, is intrinsically three-dimensional, since both groups $G_\alpha$ and $G_{\alpha^*}$ have a diagonal matrix in common: $\alpha_4 = \alpha_4^* = r$. Taking this into account, one can write the wave equations in a symmetric four dimensional form $(-ir\alpha_k \to \gamma_k,\ r \to \gamma_4)$.

The interaction of photons with the gravitational field is described by the equations

$$\gamma_\lambda\,\partial\varphi/\partial x_\lambda = 0, \quad \text{or} \quad \beta_\lambda\partial\varphi/\partial x_\lambda = 0,$$

where

$$\varphi(x) = (I + g\gamma_\mu\gamma_\nu^* h_{\mu\nu}(x))\,\psi(x) \quad (14)$$

($h_{\mu\nu}(x)$ is the gravitational potential). The application of perturbation theory to this equation is facilitated by the smallness of the coupling constant g. The usual formulae apply for the traces of products of $\alpha_i$ and $\alpha_i^*$. The traces of products $\alpha_i\alpha_k^*$ vanish identically.

[1] D. C. Peaslee, Progr. Theor. Phys. **7**, 639 (1951).

[2] F. I. Fedorov, J. Exptl. Theoret. Phys. (U.S.S.R.) **31**, 140 (1956), Soviet Phys. JETP **4**, 139 (1957).

[3] A. A. Borgardt, Dokl. Akad. Nauk SSSR **78**, 1113 (1951).

[4] T. D. Lee and C. N. Yang, Phys. Rev. **104**, 254 (1956).

[5] A. A. Borgardt, J. Exptl. Theoret. Phys. (U.S.S.R.) **30**, 334 (1956), Soviet Phys. JETP **3**, 238 (1956).

[6] A. Salam, Nuovo cimento **5**, 299 (1957).

[7] A. A. Borgardt, J. Exptl. Theoret. Phys. (U.S.S.R.) **33**, 791 (1957), Soviet Phys. JETP **6**, 608 (1958).

[8] T. Ohmura, Progr. Theor. Phys. **16**, 684 (1956).

[9] V. Fock, Z. Physik **68**, 522 (1931).

[10] S. Tani, Progr. Theoret. Phys. **6**, 267 (1951).

[11] C. B. van Wyk, Nuovo cimento **6**, 522 (1957)

Translated by M. Danos
263

## *CERTAIN NEW MAGIC NUCLEON NUMBERS*

I. A. VAISMAN

Submitted to JETP editor April 23, 1957; resubmitted February 6, 1958

J. Exptl. Theoret. Phys. (U.S.S.R.) **34**, 1325-1327 (May, 1958)

NUCLEI containing 30 neutrons have, in most cases, some rare distinguishing properties. The nuclide $^{26}Fe_{30}$ is the most abundant of all nuclides having $Z > 10$. The relative abundance of this iron isotope is 91.7%, while, for example, the isotope $^{26}Fe_{28}$ (in spite of its containing 28 neutrons) has an abundance of only 5.8%. The relative abundance of the lightest nickel isotope $^{28}Ni_{30}$ is 67.8%, although in the case of analogous isotopes of other elements it usually does not exceed several percent or fractions of a percent. The nuclide $^{24}Cr_{30}$ is different in having a low effective capture cross-section for thermal neutrons. (0.36 barns), like nuclides containing the usual magic numbers of neutrons. Along with this, the iron and nickel isotopes having $N = 30$ have very high effective cross-sections for coherent scattering (without change in spin) of thermal neutrons compared with other isotopes of the same elements, and very high total scattering cross-section ($\sigma_{free}$), multiplied by $[(A + 1)/A]^2$ to reduce it to the case of the nucleus at rest. The corresponding data (in barns) are given in Table I.

TABLE I

| Element | N | A | $\sigma_{free}\,[(A+1)/A]^2$ | $\sigma_{coh}$ |
|---|---|---|---|---|
| Fe | 28 | 54 | 2.5 | 2.20 |
| | 30 | 56 | 12.8 | 12.8 |
| | 31 | 57 | 2.0 | 0.64 |
| Ni | 30 | 58 | 24.4 | 25.9 |
| | 32 | 60 | 1.0 | 1.1 |
| | 34 | 62 | 9.0 | 9.5 |

The effective scattering cross-section of $^{28}Ni_{30}$ is particularly high. It is possible that the properties of a 30-neutron configuration manifest themselves differently in different nuclides, depending

on the properties of the proton system of each individual nuclide. The properties of nuclides with N = 30, particularly the isotopes of iron and nickel, lead to the view that 30 is a magic number for neutrons.*

Very characteristic phenomena are seen to follow the filling of configurations of 42 and 60 protons or neutrons. (See Table II; the dash indicates the absence of a stable nuclide).

TABLE II

| Element | Z | A | I | Element | N | A | I |
|---|---|---|---|---|---|---|---|
| Nb | 41 | 93 | 9/2 | Ge | 41 | 73 | 9/2 |
| Tc | 43 | — | — | Se | 43 | 77 | 1/2 |
| Rh | 45 | 103 | 1/2 | Se | 45 | — | — |
| Ag | 47 | 107,109 | 1/2 | Kr | 47 | 83 | 9/2 |
| Pr | 59 | 141 | 5/2 | Pd | 59 | 105 | 5/2 |
| Pm | 61 | — | — | Pd | 61 | — | — |
| Eu | 63 | 151 | 5/2 | Cd | 63 | 111 | 1/2 |
| Tb | 65 | 159 | 3/2 | Cd | 65 | 113 | 1/2 |

The filling of the shell terms $5g_{9/2}$ and $4d_{5/2}$ begins (in the case of nuclides with 59 and 41 protons or neutrons) in a quite normal manner, but when the number of the same nucleons is one more than 60, the nuclide loses its stability, and it is quite characteristic that this takes place both for 61 protons and for 61 neutrons. Nor does a stable nuclide containing 43 protons exist. Thus, of the four cases considered, three exhibit loss of stability.

As to the nuclide $Se^{77}$, which contains 43 neutrons, its spin is not $9/2$ like that of the $^{32}Ge_{41}$ nuclide, but $1/2$. This must be compared with the fact that the unstable nuclides with 43 protons or 61 neutrons are followed by nuclides having an odd number of protons (Rh, Ag) or neutrons (Cd, Sn, and the following) whose spin also drops to one-half.† Neither the level-crossing hypothesis (Ref. 1 and others) nor any other modern theory is capable of explaining why the spin diminishes not immediately after the closing of the subshells that contain 40 protons or 40 and 50 neutrons, but only at N = 43 and only after Z exceeds 43 or N exceeds 61.

The cause of absence of $\beta$-stable nuclides with Z = 43 and 61 has been the subject of many investigations (Ref. 2 and others). This absence is usually made dependent on the closing of the magic configurations of 50 and 82 neutrons. The influence of the reduced binding energy of the neutrons must naturally be taken into account in both cases. However, such an explanation cannot be considered exhaustive, particularly for the following reasons:

(1) One cannot ignore the fact that the absence of a stable nuclide, or certain other post-magic phenomena, are observed not only past 42 and 60 protons, but also past 60 and 42 neutrons; in many elements with even Z, from $^{42}Mo$ to $^{56}Ba$, there at least two isotopes with odd N, and only in the case of Pd does the nuclide $^{46}Pd_{61}^{107}$ lose stability, unlike its isobar $^{47}Ag_{60}^{107}$. (2) It is known that the only nuclide with N = 51 that remains stable, in spite of the presence of a post-magic neutron configuration, is $^{40}Zr_{51}$, and the stability of this nuclide must be ascribed to the properties of its proton configuration, i.e., to the closing of the $3p_{1/2}$ term. In exactly the same way, the only stable nuclide with N = 83 is $^{60}Nd_{83}$, and in this case the nuclide probably owes its stability to the magic properties of its proton configuration. We see that, in addition to the usual explanation for the absence of stable isotopes of Tc and Pm, it is necessary to take into account also the peculiarities of the numbers 42 and 60.

Thus, it becomes quite probable that a configuration of 30 neutrons and of 42 and 60 protons or neutrons has certain magic properties. These configurations do not coincide with shell configurations, and it must be emphasized that the nature of their stability may be entirely different than that due to closing of the shell terms.

This probably does not exhaust the list of new magic numbers. However, recognition of these three numbers alone is enough to raise the question of the existence of some other uninvestigated properties of the nucleus, along with those already known at the present time.

*Such a conclusion is not disproved by the fact that a configuration consisting of 30 protons does not have clearly pronounced magic properties. It must be taken into account that the $^{30}Zn$ nuclides lie in that portion of the periodic system (between copper and bromine) which is, in general, characterized by a considerably lower binding energy compared with the general course of the packing-fraction curve.

†A similar reduction in spin, as compared with its theoretical value is absent only for odd Z > 61 (it is known that heavy nuclides retain high values of spin for odd Z to a considerably greater extent than for odd N).

[1] M. G. Mayer and J. Jensen, Elementary Theory of Nuclear Shell Structure, 1955.

[2] L. Kowarski, Phys. Rev. **78**, 477 (1950). H. E. Suess, Phys. Rev. **81**, 1071 (1951).

Translated by J. G. Adashko
264

# THEORY OF STRANGE PARTICLES

L. A. MANAKIN

Kamenets-Podol' sk Pedagogical Institute

Submitted to JETP editor August 22, 1957; resubmitted December 24, 1957

J. Exptl. Theoret. Phys. (U.S.S.R.) 34, 1327-1329 (May, 1958)

IN the mathematical interpretation of the scheme of Gell-Mann[1-3] proposed by d'Espagnat and Prentki,[4,5] a new constant of motion appeared — the isofermion charge of a system of elementary particles u, conserved in all strong and electromagnetic interactions. For a single particle, the isofermion charge u characterizes the transformation properties of the particle relative to inversion in a three-dimensional isotopic space.

Under the very general postulates adopted by d'Espagnat and Prentki, only four types of particles are allowable: isoscalar ($u = 0$), isopseudovector ($u = 0$), isospinor of the first type ($u = +1$) and isospinor of the second type ($u = -1$). Therefore, for a single particle only three values $u = \pm 1, 0$ are permissible.*

The connection between the electric charge Q and third component of isotopic spin $I_3$ in the theory of d'Espagnat and Prentki is expressed by the same relation

$$Q = I_3 + u/2, \qquad (1)$$

for all mesons and baryons. The value of u is preserved in strong and electromagnetic interactions and $\Delta u = \pm 1$ are allowable in weak interactions,[5] which is equivalent to the Gell-Mann $\Delta S = \pm 1$. It is of interest to consider all conclusions coming from such a theory.

In comparing (1) with the scheme of Gell-Mann, we note that the Gell-Mann strangeness S is the difference between the isofermion charge of the particle u and its nucleon (baryon) charge n:

$$S = u - n. \qquad (2)$$

The nucleon charge n of a particle can take on only one of three values: +1 (baryon), −1 (antibaryon), 0 (meson).

Only three values of the electric charge $Q = \pm 1, 0$ are allowed and, in connection with Eq. (1), only three values of the total isotopic spin I: $\frac{1}{2}$, 0, 1 (Ref. 2).

The isofermion charge of a particle u also takes on, according to the above, only three values: +1 for isofermions having $I = \frac{1}{2}$; −1 for antiisofermions; 0 for isobosons, having $I = 0$ or $I = 1$.

The limitations on n and u, together with Eq. (2), leave for S only the possibilities: $S = 1, 0, -1$ for mesons; $S = 0, -1, -2$ for baryons; $S = 2, 1, 0$ for antibaryons. Consequently, the hyperons, allowed by Gell-Mann[1-3] and Terletskii,[6] $Z^+(S = +1)$, $\Omega^-(S = -3)$ and mesons $\omega^+(S = +2)$ and $\omega^-(S = -2)$† are completely excluded.

The isofermion charge u can be considered, together with n and I, as a primary characteristic of the particle, and the strangeness S as only one of the possible combinations of them.

In the rational symbolism of elementary particles proposed by Terletskii, in which together with the electric charge Q, there are also the nuclear (n), neutrino ($\nu$) and neutron ($\epsilon$) charges of the particle, in place of the latter it is natural to use the isofermion charge u, connected with it, as is easily established, by the relation: $u = \epsilon + Q$ (Ref. 6).

| Basic characteristics | | | Charge Q | Multiplets |
|---|---|---|---|---|
| n | u | I | | |
| 0 | +1 | 1/2 | +1, 0 | $K^+$, $K^0$ |
| | −1 | | 0, −1 | $\bar{K}^0$, $K^-$ |
| | 0 | 1 | +1, 0, −1 | $\pi^+$, $\pi^0$, $\pi^-$ |
| | 0 | 0 | 0 | $\omega^0$ |
| +1 | +1 | 1/2 | +1, 0 | $N^+$, $N^0$ |
| | −1 | | −1, 0 | $\Xi^-$, $\Xi^0$ |
| | 0 | 1 | +1, 0, −1 | $\Sigma^+$, $\Sigma^0$, $\Sigma^-$ |
| | 0 | 0 | 0 | $\Lambda^0$ |
| −1 | −1 | | −1, 0 | Antinucleons |
| | 1 | 1/2 | +1, 0 | Anti Ξ hyperons |
| | 0 | 1 | −1, 0, +1 | Anti Σ hyperons |
| | 0 | 0 | 0 | Anti Λ hyperons |

Exhausting the possible multiplets of particles with all possible allowable combinations of n, u, and I, it is easy to see that the number of them is limited to those given above in the table. The only new one, aside from those given above, could be the neutral meson noted in the review of Okun'[2] having total isotopic spin $I = 0$, which we denote as a $\omega^0$ meson.‡ This truly neutral particle differs from the $\pi^0$ meson.

Within the framework of the theory of d'Espagnat and Prentki, it is impossible to use the hypothetical $\omega^-$ meson to explain the $K^-$-decays of secondary particles,[7,8] as assumed by Karpman.[5] Only the $\omega^0$ meson can be used for their explanation.

*For example, the values $u = \pm 2$ would correspond to isopseudoscalar and isovector particles, which are not acceptable within the framework of this theory.

†The conclusion of Karpman[5] about the admissibility of a $\omega$ meson of strangeness $S = -2$ within the framework of the theory of d'Espagnat and Prentki is in error.

‡For mesons (n = 0), which are bosons in ordinary space (but not for hyperons with n = 1), the number of possible multiplets can be doubled, corresponding to the two possibilities for ordinary spin of the boson, 1 or 0 (Ref. 9).

[1] M. Gell-Mann, Proc. Pisa Conference, 1955 (see Ref. 3).

[2] L. Okun', Usp. Fiz. Nauk **61**, 535 (1957).

[3] Проблемы современной физики (Probl. of Mod. Phys.) IIL, November, 1956.

[4] B. d'Espagnat and J. Prentki, Phys. Rev. **99**, 328 (1955); **102**, 1684 (1956).

[5] V. I. Karpman, J. Exptl. Theoret. Phys. (U.S.S.R.) **32**, 939 (1957), Soviet Phys. JETP **5**, 767 (1957).

[6] Ia. P. Terletskii, J. Exptl. Theoret. Phys. (U.S.S.R.) **31**, 703 (1956), Soviet Phys. JETP **4**, 575 (1957).

[7] Varfolomeev, Gerasimova and Karpova, Dokl. Akad. Nauk SSSR **110**, 959 (1956). Soviet Phys. "Doklady" **1**, 594 (1956).

[8] Grigor' ev, Toporkova and Fesenko, J. Exptl. Theoret. Phys. (U.S.S.R.) **32**, 1589 (1957), Soviet Phys. **5**, 1299 (1957).

[9] L. A. Manakin, Научные записки Каменец-Подольского Пединститута (Scientific Reports of Kamenets-Podol'ski Ped. Institute) **6**, 113 (1958).

Translated by G. E. Brown
265

## *ON THE THEORY OF THE STABILITY OF LIQUID JETS IN AN ELECTRIC FIELD*

G. A. GLONTI

Taganrog Pedagogical Institute

Submitted to JETP editor September 25, 1957; resubmitted February 17, 1958

J. Exptl. Theoret. Phys. (U.S.S.R.) **34**, 1329-1330 (May, 1958)

We shall consider the behavior of a cylindrical jet (of radius $R_0$) of a liquid dielectric in an electric field. (All that follows is also applicable to a magnetic liquid in a magnetic field). The behavior of an incompressible viscous fluid, in the absence of body forces, is described by the hydrodynamic equations

$$\operatorname{div}\mathbf{v}=0,\quad \frac{\partial \mathbf{v}}{\partial t}+\mathbf{v}\cdot\nabla\mathbf{v}=-\frac{1}{\rho}\operatorname{grad}p+\nu\nabla^2\mathbf{v}. \quad (1)$$

To these must be added the electrostatic equation

$$\operatorname{div}(\varepsilon\mathbf{E})=0. \quad (2)$$

Let the jet be subjected to a perturbation which is symmetrical about the axis. Then, introducing the flow function $\Psi$ and making use of Eq. (1), we obtain

$$(\nu L-\partial/\partial t)L\Psi=(v_x\partial/\partial x+v_r\partial/\partial r-2v_r/r)L\Psi \quad (3)$$

and the following conditions for force equilibrium at the surface $r = R_0$:

$$p_{rx}=p_{xr}=0,\qquad p_{rr}=-(N+T_{rr}), \quad (4)$$

where

$$L=\partial^2/\partial r^2-r^{-1}\partial/\partial r+\partial^2/\partial x^2,$$
$$p_{rx}=\nu\rho(\partial v_r/\partial x+\partial v_x/\partial r),\qquad p_{rr}=-p+2\nu\rho\,\partial v_r/\partial r,$$

$T_{rr}$ is the normal component of the stress tensor in the electric field, and N represents the effect of the surface forces.

Consider a perturbation of the type

$$q=q_0+q(r)\exp[i(kx+\omega t)], \quad (5)$$

where $q_0$ is the equilibrium value and $q(r)$ is to be determined. Solving Eqs. (1) to (3) for such a perturbation, assuming that the amplitudes are small (linearized theory) and using the boundary conditions (4), we obtain the following dispersion equation for the perturbation frequency in the presence of a longitudinal field $E_0$:

$$(\omega-2ik^2\nu)^2\frac{I_0(z)}{kI_1(z)}+2i\frac{\nu}{R_0}(\omega-2ik^2\nu)$$
$$+\frac{4k^2\nu^2}{R_0I_1(nR_0)}[nR_0I_0(nR_0)-I_1(nR_0)]$$
$$-\frac{\sigma}{\rho R_0^2}(z^2-1)-\frac{(\varepsilon-1)^2E_0^2k}{4\pi\rho}\frac{I_0(z)K_0(z)}{\varepsilon I_1(z)K_0(z)+K_1(z)I_0(z)}=0,$$
$$z=kR_0,\quad n^2=k^2+i\omega/\nu, \quad (6)$$

where $I_0$, $I_1$, $K_0$, and $K_1$ are the Bessel functions of the first and second kind for imaginary argument, and $\sigma$ is the surface tension.

The solution of (6) leads to the following conclusions. (1) The viscosity has a stabilizing effect (as Rayleigh has already shown). (2) A jet is always dynamically stable for $kR_0 > 1$. (3) For $kR_0 < 1$ a jet of incompressible non-viscous liquid dielectric is stable under the conditions

$$E_0^2>\frac{4\pi\sigma}{(\varepsilon-1)^2R_0^2k}\frac{\varepsilon I_1(z)K_0(z)+K_1(z)I_0(z)}{I_0(z)K_0(z)}. \quad (7)$$

For a water jet with $\epsilon = 81$, $\sigma = 74$ dynes/cm, and $R_0 = 2$ cm, (7) gives $E_0 > 597$ v/cm for $kR_0 = 0.2$; and $E_0 > 729$ v/cm for $kR_0 = 0.1$.

Investigation shows that a transverse electric field has no effect on the dynamic stability of jets.

I wish to thank Prof. A. A. Vlasov sincerely for his interest in the accomplishment of this work.

Translated by D. C. West
266

## *LIBERATION OF GAS UPON CLEAVAGE OF CRYSTALLINE QUARTZ*

V. V. KARASEV

Institute of Physical Chemistry, Academy of Sciences, U.S.S.R.

Submitted to JETP editor January 20, 1958

J. Exptl. Theoret. Phys. (U.S.S.R.) **34**, 1330-1331 (May, 1958)

PREVIOUSLY reported experiments[1] disclosed electron emission upon cleavage of certain crystals in a vacuum of $10^{-4}$ to $10^{5}$ mm Hg.

To study and to explain further the nature of the emission, it was necessary to use higher vacuum, which in turn called for development of a new procedure. To attain high vacuum in the simplest possible manner, it was decided to make the equipment completely of glass, like the instruments used for the study of the kinetics of chemical reactions

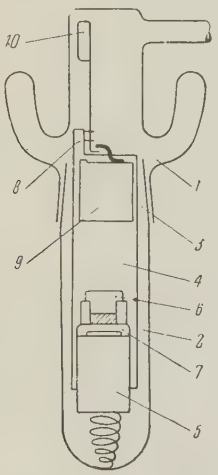


(see diagram). The upper portion of the instrument consisted of a trap 1 for the lubricant vapor with a ground neck. The lower portion of the instrument consists of a sealed tube 2 which was inserted into ground section 3. Placed inside the instrument was a setup for cleaving solid specimens to incandescence, consisting of stainless steel tube 4 with windows, and of a brass cylinder with spring 5. Attached to this cylinder were guides for a knife 6 and a holder for x-ray film 7. Located in the upper portion of the tube was a trigger 8 for falling weight 9.

The instrument was sealed to a vacuum mercury pump and evacuated to a pressure of approximately $10^{-7}$ mm Hg (the vacuum was measured with an ionization manometer). After evacuating the instrument, lever 10 of the trigger was rotated with an electromagnet, and the weight fell and fractured a plate approximately 4 mm. The photographic film was exposed to the electrons emitted from the gap formed upon cleavage of the plate.

It was observed in the preliminary experiments that upon cleavage of glass and diffused quartz there is no noticeable change in the vacuum, and no electron emission was observed (like in the previous experiments).

Cleavage of crystalline quartz (like in the previous experiments) caused electron emission, and the pressure rose to $10^{-4}$ to $10^{-5}$ mm Hg (measured with an ionization manometer). The area of the fresh surface obtained upon cleavage of crystalline quartz was approximately 1 $cm^2$. The capacity of the vacuum system was about 1300 cubic cm. Liberation of gas was observed also upon splitting of mica and stripping of high-polymer films from glass.

The author is grateful to Professor B. V. Deriagin for valuable advice.

[1] N. A. Krotova and V. V. Karasev, Dokl. Akad. Nauk SSSR **92**, 607 (1953).

Translated by J. G. Adashko
267

## *ON ELECTRON CAPTURE IN BETATRONS*

A. N. MATVEEV

Moscow State University

Submitted to JETP editor January 22, 1958

J. Exptl. Theoret. Phys. (U.S.S.R.) **34**, 1331-1333 (May, 1958)

LOGUNOV and Semenov[1] have pointed out the existence of statistical capture of electrons into betatron orbits and have estimated the efficiency of this mechanism. This calls for the following two essential remarks.

1. This mechanism can work only at not too large densities of the injected electrons. In par-

ticular, it will not work at the conditions of the example treated in Ref. 1. This can be seen from the following estimates.

The electrons are injected in a beam with an area $S = 1\ cm^2$ and a density $N_0 = 4.22 \times 10^8$ electrons/$cm^3$. We shall assume a beam of round cross section. The electrostatic force repelling an electron situated on the edge of the beam is given by

$$F_{rep} = 2N_0 e^2 \sqrt{\pi S}. \quad (1)$$

On the other hand, the same electron will be attracted to the center of the beam by a force due to magnetic focusing:

$$F_{att} = -m(v/R)^2(1-n)\sqrt{S/\pi}, \quad (2)$$

where m is the electron mass, v the velocity of the injected electrons, R the radius of the equilibrium orbit, and n the magnetic field decrement index. From (1) and (2) we have

$$|F_{rep}/F_{att}| = 2\pi r_0 R^2 N_0/\beta^2(1-n), \quad (3)$$
$$r_0 = e^2/mc^2, \quad \beta = v/c.$$

For the conditions of the example of Ref. 1 this yields

$$|F_{rep}/F_{att}| \approx 22. \quad (4)$$

Thus the beam will begin to spread right after injection, and the electron dynamics will differ considerably from that assumed in Ref. 1. Electron-electron scattering of the kind on which the proposed capture mechanism was based will thus not occur for the majority of the electrons. Actually a large fraction of the electrons will be lost to the walls already within the first revolution and will thus not be able to experience even a single scattering event of the required kind. If one takes into account this and the loss of electrons in the subsequent revolutions, one finds that the estimate of the number of captured electrons obtained in Ref. 1 has to be decreased by a factor approximately equal to the ratio of the number of injected to captured electrons, i.e., by approximately two orders of magnitude. Mathematically this is expressed by a suitable decrease of N in the numerator of Eq. (4) in Ref. 1. Secondly, the capture efficiency will be decreased by another order of magnitude, owing to the decrease of the factor $N_0$ in the same formula. Thirdly, the following facts have to be considered. Besides radial oscillations the electrons oscillate also in the z direction and longitudinally. Only the transfer of energy from the radial oscillations into other oscillations was considered in Ref. 1. However, if these other oscillations are already excited, then energy will also be transferred into the radial oscillations. This actually will be the case in the example considered, and thus the efficiency of the proposed mechanism will be further decreased. So one finds that for large densities of the injected electrons, where the capture is most effective, this capture mechanism does not work. It therefore can not explain that part of the electron capture for which it was adduced in the first place. It plays only a subordinate role and only at sufficiently low densities, in the range between single electron capture and collective capture. We shall make a few remarks on this subject in the second comment.

2. The decisive capture mechanism is due to the Coulomb interaction and consists, in our example, of the following.

Right after the instant of injection, electrons begin to be lost to the walls close to the injector. The region of contact of the electron beam with the walls of the donut will increase at a rapid rate and after a time of one revolution electrons will hit the donut walls all around. The donut at that time will be filled with an electron cloud of decreasing density. At the time when the beam will stop expanding the electron density will be roughly

$$N_k \approx N_e/\ln(N_0/N_e), \quad N_e = \beta^2/4\pi r_0 R^2 = 0.3 \cdot 10^8. \quad (5)$$

From now on the electrons will start contracting toward the center of the beam, which itself will oscillate about the equilibrium orbit with a very small amplitude. This oscillation is due to the loss of electrons. Thus the survival of some electrons is due to the loss of others to the walls. The electrons which have survived the first revolution [their number is given by Eq. (5)] will now interact with the electrons which are being injected at this time and so a large number of electrons will be lost during the second revolution. Thus the mean life of electrons in the beam is approximately two revolutions or even a little less; for lower densities it would be a little more. During the second revolution the picture remains essentially the same except for the slight modification introduced by the presence of the electrons which have survived from the first revolution, etc. The number of electrons captured with the right momentum and being accelerated is given by

$$N_\gamma = N_k\, 2\pi R S_{eff} \approx 0.45 \cdot 10^{10}, \quad (6)$$

where $S_{eff}$ denotes the area of the effective donut cross section. The obtained numerical value corresponds to the conditions discussed in Ref. 1. Equation (6) is valid for injection currents equal to or larger than the saturation current and has been derived for $N_0/N_e \gg S_{eff} > 1$. For smaller cur-

rents and densities the formula has to be modified.

This way one can give a mathematical description of the treated physical picture of the capture process. The theory then gives good agreement with experiment, both qualitatively and quantitatively.

[1] V. I. Logunov and S. S. Semenov, J. Exptl. Theoret. Phys. (U.S.S.R.) **33**, 1513 (1957), Soviet Phys. JETP **6**, 1168 (1958).

Translated by M. Danos
268

## *ANALYTICITY OF THE NONRELATIVISTIC SCATTERING AMPLITUDE AND THE POTENTIAL*

Ia. A. SMORODINSKII

Joint Institute for Nuclear Research

Submitted to JETP editor January 24, 1958

J. Exptl. Theoret. Phys. (U.S.S.R.) **34**, 1333-1335 (May, 1958)

As is well known, the amplitude for scattering of a particle of given angular momentum $l$ by a central field of force cannot be analytically continued into the upper half plane of the variable k. An interesting proof of this is connected with the inverse problem of scattering theory (Gelfand and Levitan,[1] Marchenko[2]).

For brevity we assume that there are no bound states and that scattering takes place in the s state; the generalization of the problem is obvious.

Following Marchenko,[2] the solution of the equation

$$d^2\psi(x,k)/dx^2 + (k^2 - V(x))\psi(x,k) = 0 \qquad (1)$$

can be given as an expansion in integrals over the system of functions

$$\varphi(y,k) = (2/\pi)^{1/2}\sin[ky + \delta(k)] \qquad (2)$$

[$\delta(k)$ is the scattering phase, known from experiment] in the following way

$$\psi(x,k) = \varphi(x,k) + \int_x^\infty A(x,y)\varphi(y,k)\,dy. \qquad (3)$$

In this equation A(x, y) is determined from the integral equation, the kernel and inhomogeneity of which are expressed through the Fourier component of the scattering amplitude $M(k) = \exp\{2\pi i\delta(k)\} - 1$:

$$m(z) = \frac{1}{2\pi}\int_{-\infty}^{+\infty} M(k)e^{ikz}dk, \quad \text{for } z > 0. \qquad (4)$$

If $m(z) = 0$ for $z > 0$, then it follows from the equation of Marchenko that $A(x, y) = 0$ and, according to Eq. (1), the wave function $\psi(x, k)$ coincides with the solution of the free equation everywhere except at the origin (contact interaction). On the other hand, $m(z)$ going to zero for $z > 0$ means, according to Eq. (3), that the scattering amplitude does not have poles for $\mathrm{Im}\, k > 0$ and grows with $k \to \infty$ ($\mathrm{Im}\, k > 0$) no faster than as a power of k, since in this case the contour of integration can be closed around a half circle of large radius lying in the upper half plane.

From this it follows that, if the scattering is described by a potential, then either the amplitude has a pole (a so-called spurious pole, since we assumed that the system did not have a level), or it grows faster than a polynomial for $k \to \infty$ ($\mathrm{Im}\, k > 0$).

If the potential is bounded in space [$V(x) = 0$ for $x > a$], then $m(z)$ goes to zero for $z > 2a$. This follows from the relation

$$\int \varphi(y,k)\varphi(x,k)\,dk = \delta(y-x) - m(x+y). \qquad (5)$$

In fact, for (x and y) > a, $\varphi(x, k)$ and $\varphi(y, k)$ coincide with the solution of the Schrödinger equation and, therefore, should be orthogonal. But then it follows from Eq. (4) that the function

$$M_a(k) = M(k)e^{2ika} \qquad (6)$$

is analytic in the upper half plane. This result was obtained by Van Kampen[3] from other considerations.

If the scattering amplitude is known for all energies, then, as was shown most rigorously in the work of Khuri,[4] the function

$$g(E) = M(E,\tau) - V_\tau/4\pi \qquad (7)$$

(where $M(E, \tau)$ is the scattering amplitude, viewed as a function of energy E and given momentum $\tau$, and $V_\tau$ is the Fourier component of the potential) can be analytically continued in the complex E plane (or upper half plane of k) and a dispersion relation can be given for it.*

From the dispersion relation for the function (7) obtained by Khuri, it can be seen that if the scattering amplitude is known, then the potential is determined by the amplitude without solution of the integral equation.

We emphasize that this assertion is valid if the scattering amplitude is known for all energies. Since even the Schrödinger equation is valid only in a limited region of energy, then the scattering am-

plitude can be given only for some energy interval. This problem will be treated in another communication.

*The conditions imposed on the potential by this coincide with the condition that for $k \to \infty$ the scattering amplitude be given by the first Born approximation. Then the dispersion relations are valid for $\tau < 2\alpha$, where $\alpha$ is the maximum positive number for which the integral

$$\int_0^\infty e^{2\alpha} |V(y)| dy.$$

exists. We note, in addition, that if this integral exists for arbitrary $\alpha$, then the scattering amplitude does not have "spurious poles."

[1] I. M. Gel'fand and B. M. Levitan, Izv. Akad. Nauk SSSR, Ser. Mat. **15**, 309 (1951).
[2] V. A. Marchenko, Dokl. Akad. Nauk SSSR **104**, 695 (1955).
[3] N. G. van Kampen, Phys. Rev. **91**, 1267 (1953).
[4] N. N. Khuri, Phys. Rev. **107**, 1148 (1957).

Translated by G. E. Brown
269

## *TWO CLASSES OF INTERACTION LAGRANGIANS*

V. G. SOLOV' EV

Joint Institute for Nuclear Studies

Submitted to JETP editor January 24, 1958

J. Exptl. Theoret. Phys. (U.S.S.R.) **34**, 1335-1336 (May, 1958)

LET us consider Lagrangians of the strong interaction of baryons and mesons, retaining their isotopic structure as given by Salam.[1] We note that the wave functions of particles belonging to the same isotopic multiplet behave similarly under all transformations.

We divide strong interaction Lagrangians into two classes. To the first class we assign interactions that contain at least one vertex where the fermion does not change a single one of its fundamental characteristics: mass, electric charge, strangeness. These are the electromagnetic interactions, the interactions of $\pi$ mesons with nucleons, of $\pi$ mesons with $\Sigma$ particles, and of $\pi$ mesons with $\Xi$ particles. To the second class we assign interactions that contain only vertices at which the fermion necessarily changes at least one of its fundamental characteristics: mass, electric charge, strangeness. These are the interactions of $\pi$ mesons with $\Lambda$ and $\Sigma$ particles, and also all interactions of K particles with baryons.

Let $\varphi$, $\chi$, $\phi$, $\xi$ be operators of fields of spin zero which transform in the following ways under the operations of space inversion P, charge conjugation C, and time reversal T:

$$\begin{aligned} P:&\ \varphi' = \varphi \quad \chi' = \chi \quad \phi' = -\phi \quad \xi' = -\xi \\ C:&\ \varphi' = \varphi^* \quad \chi' = -\chi^* \quad \phi' = \phi^* \quad \xi' = -\xi^* \\ T:&\ \varphi' = \varphi^* \quad \chi' = -\chi^* \quad \phi' = -\phi^* \quad \xi' = \xi^*. \end{aligned} \tag{1}$$

The interaction Lagrangians of the first class for the fields $\varphi$, $\chi$, $\phi$, $\xi$ (taken truly neutral for simplicity) have different forms which cannot be reduced to each other, namely:

$$L_\varphi = g_\varphi \bar{\psi}\psi\varphi_0, \tag{2}$$

$$L_\chi = f_\chi \bar{\psi}\gamma_\mu\psi\, \partial\chi_0/\partial x_\mu, \tag{3}$$

$$L_\phi = g_\phi \bar{\psi}\gamma_5\psi \quad \phi_0 + f_\phi \bar{\psi}\gamma_5\gamma_\mu\psi\, \partial\phi_0/\partial x_\mu. \tag{4}$$

A characteristic feature of the Lagrangians assigned to the second class is the presence, in addition to the usual terms, of interactions of the form $i(\bar{\psi}_1 O\psi_2\theta - \bar{\psi}_2 O\psi_1\theta^*)$. The Lagrangians of the second class describing the interaction of the bosons $\varphi$, $\chi$, $\phi$, $\xi$ with the fermions $\psi_1$ and $\psi_2$, which have the same phase factors under the operations P, C, T, are written in the following form:

$$L_\varphi = g_\varphi (\bar{\psi}_1\psi_2\varphi + \bar{\psi}_2\psi_1\varphi^*)$$
$$+ if_\varphi \left(\bar{\psi}_1\gamma_\mu\psi_2 \frac{\partial\varphi}{\partial x_\mu} - \bar{\psi}_2\gamma_\mu\psi_1 \frac{\partial\varphi^*}{\partial x_\mu}\right), \tag{5}$$

$$L_\chi = ig_\chi (\bar{\psi}_1\psi_2\chi - \bar{\psi}_2\psi_1\chi^*)$$
$$+ f_\chi \left(\bar{\psi}_1\gamma_\mu\psi_2 \frac{\partial\chi}{\partial x_\mu} + \bar{\psi}_2\gamma_\mu\psi_1 \frac{\partial\chi^*}{\partial x_\mu}\right), \tag{6}$$

$$L_\phi = g_\phi \ (\bar{\psi}_1\gamma_5\psi_2\phi + \bar{\psi}_2\gamma_5\psi_1\phi^*)$$
$$+ f_\phi \left(\bar{\psi}_1\gamma_5\gamma_\mu\psi_2 \frac{\partial\phi}{\partial x_\mu} + \bar{\psi}_2\gamma_5\gamma_\mu\psi_1 \frac{\partial\phi^*}{\partial x_\mu}\right), \tag{7}$$

$$L_\xi = ig_\xi (\bar{\psi}_1\gamma_5\psi_2\xi - \bar{\psi}_2\gamma_5\psi_1\xi^*)$$
$$+ if_\xi \left(\bar{\psi}_1\gamma_5\gamma_\mu\psi_2 \frac{\partial\chi}{\partial x_\mu} - \bar{\psi}_2\gamma_5\gamma_\mu\psi_1 \frac{\partial\chi^*}{\partial x_\mu}\right). \tag{8}$$

The interchanges*

$$\psi_2 \to -i\psi_2, \quad \chi \to \varphi, \quad g_\chi \to g_\varphi, \quad f_\chi \to -f_\varphi$$

bring the expression (6) to the form (5), and the interchanges

$$\psi_2 \to -i\psi_2, \quad \xi \to \phi, \quad g_\xi \to g_\phi, \quad f_\xi \to f_\phi$$

bring (8) to the form (7). Thus there are two types of Lagrangians of the second kind, namely (5) and (7), and the type of interaction is determined by the behavior of the boson field operator under the operation P.

As has been shown by Pais and Jost,[2] the requirement of invariance under C forbids the combination of the scalar and vector couplings for scalar particles. This is true, however, only for interactions of the first class; as can be seen from Eq. (5), a combination of scalar and vector couplings is possible for interactions of the second class.

Following the hypothesis put forward by the writer,[3] let us consider strong interactions invariant with respect to T, but possibly non-invariant with respect to P. As has been shown in Ref. 4, interactions of the second class contain terms in which the parity is not conserved, but isotopically invariant interactions of the first class without gradient coupling do not contain such terms.

In view of the possibility of the replacements $\psi_2 \to -i\psi_2$ and so on, there is only one form of Lagrangian of the second class that is invariant with respect to T, namely (gradient terms are omitted):

$$L = g(\bar{\psi}_1\gamma_5\psi_2\phi + \bar{\psi}_2\gamma_5\psi_1\phi^*) + ig'(\bar{\psi}_1\psi_2\phi - \bar{\psi}_2\psi_1\phi^*). \quad (9)$$

We note that the Lagrangians of the first class invariant with respect to T will be different for the operators $\varphi$ and $\phi$.

Since the behavior of the $\pi$-meson field under the transformation T is known, the terms of the interaction Lagrangian of baryons and mesons belonging to the first class are completely determined, and there exists only one form for the interaction of the second class. Therefore the isotopically invariant Lagrangian of the strong interaction of baryons and mesons, invariant with respect to T, is uniquely determined. The part of this Lagrangian invariant with respect to P has been given in Ref. 1, and the other part in Ref. 4.

*My attention was called to the possibility of this sort of replacements by Chzhou Guan-Chzhao, to whom I express my gratitude.

[1] A. Salam, Nuclear Phys. **2**, 173 (1956).
[2] A. Pais and R. Jost, Phys. Rev. **87**, 871 (1952).
[3] V. G. Solov' ev, J. Exptl. Theoret. Phys. (U.S.S.R.) **33**, 537 (1957), Soviet Phys. JETP **6**, 419 (1958).
[4] V. G. Solov' ev, J. Exptl. Theoret. Phys. (U.S.S.R.) **33**, 796 (1957), Soviet Phys. JETP **6**, 613 (1958).

Translated by W. H. Furry
270

## *ON THE SYSTEMATICS OF MESONS AND BARYONS*

H. OIGLANE

Institute of Physics and Astronomy, Academy of Sciences, Estonian S.S.R.

Submitted to JETP editor January 31, 1958

J. Exptl. Theoret. Phys. (U.S.S.R.) **34**, 1337-1338 (May, 1958)

In a paper by the writer[1] a classification of baryons has been given on the basis of two quantum numbers — the third component of the isotopic spin, $t_3$, and the third component of the so-called isotopic moment, $v_3$. The results obtained can be represented as shown in Table I.

TABLE I

| Type of baryon | $p$ | $n$ | $\Xi^0$ | $\Xi^-$ | $\Sigma^-$ | $\Sigma^0$ | $\Sigma^+$ | $\Omega^-$ | $\Lambda^0$ | $Z^+$ |
|---|---|---|---|---|---|---|---|---|---|---|
| $t_3$ | $-\frac{1}{2}$ | $+\frac{1}{2}$ | $-\frac{1}{2}$ | $+\frac{1}{2}$ | 1 | 0 | −1 | 0 | | |
| $v_3$ | $-\frac{1}{2}$ | | $+\frac{1}{2}$ | | 0 | | | 1 | 0 | −1 |

In order to obtain the analogous scheme for the mesons, one must set up the irreducible equations for the multiplets of free bosons.

We note that from the equation

$$[\beta_\nu \partial/\partial x_\nu + k_0 \exp(a\eta_5)]\psi = 0 \quad (1)$$

there follows the ordinary second-order wave equation. Here $\beta_\nu$ and $\eta_\nu$ are the Kemmer-Duffin matrices,[2] a is a constant, and

$$\eta_5 = \eta_1\eta_2\eta_3\eta_4. \quad (2)$$

Equation (1) is a generalization of the Proca-

Kemmer-Duffin equation. But for reasons that have been considered by the writer in Ref. 3, Eq. (1) is not useful for the description of multiplets of particles.

Let us generalize Eq. (1) in the following way:

$$[B_\nu \partial/\partial x_\nu + k_0 I \exp(aT_3)]\psi = 0. \quad (3)$$

Here the operators $B_\nu$, I, and $T_3$ satisfy the commutation relations

$$B_\nu B_\rho B_\sigma + B_\sigma B_\rho B_\nu = \delta_{\nu\rho} B_\sigma + \delta_{\sigma\rho} B_\nu,$$

$$B_\nu T_3 + T_3 B_\nu = 0, \qquad IT_3 + T_3 I = 0,$$

$$IB_\nu - B_\nu I = 0. \quad (4)$$

For these operators we can choose the following irreducible representation (notations of Ref. 3):

$$B_\nu = 1^{II} \times \beta_\nu, \qquad T_3 = \sigma_3 \times \eta_5,$$

$$I = \begin{pmatrix} 0 & 1 \\ 1 & 0 \end{pmatrix} \times 1^{V}. \quad (5)$$

With the choice (5), Eq. (3) describes isotopic spin multiplets of free mesons.

In complete analogy with the case of the fermions,[1] we can introduce here also the isotopic moment operator $V_3$. Then the mesons will be characterized by the quantum numbers shown in Table II.

TABLE II

| Type of meson | $K^+$ | $K^*$ | $K^0$ | $K^-$ | $\pi^-$ | $\pi^0$ | $\pi^+$ |
|---|---|---|---|---|---|---|---|
| $t_3$ | $-\frac{1}{2}$ | $+\frac{1}{2}$ | $-\frac{1}{2}$ | $+\frac{1}{2}$ | 1 | 0 | −1 |
| $v_3$ | $-\frac{1}{2}$ | | $+\frac{1}{2}$ | | 0 | | |

It is interesting to note that the system of mesons coincides completely with the system of baryons; the only thing absent is the isotopic-moment triplet corresponding to the baryons $\Omega^-$, $\Lambda^0$, $Z^+$.

The electric charges of baryons and mesons are expressed by a common formula

$$q = -e(t_3 + v_3). \quad (6)$$

A study of the experimental material[4] gives the following rules: (a) In the strong and electromagnetic interactions there is conservation of both the third component of the isotopic spin and also the third component of the isotopic moment of the system (the electric charge is of course also conserved). (b) In the weak interactions only the charge of the system is conserved, since the third component of the isotopic spin and the third component of the isotopic moment change by $\pm\frac{1}{2}$. All processes that do not satisfy these rules are forbidden.

[1] H. Oiglane, J. Exptl. Theoret. Phys. (U.S.S.R.) **33**, 1537 (1957), Soviet Phys. JETP **6**, 1189 (1958).

[2] W. Pauli, Relativistic Theory of Elementary Particles (Russian translation), Moscow, 1947.

[3] H. Oiglane, J. Exptl. Theoret. Phys. (U.S.S.R.) **33**, 1511 (1957), Soviet Phys. JETP **6**, 1167 (1958).

[4] L. Okun', Usp. Fiz. Nauk **61**, 535 (1957).

Translated by W. H. Furry
271

## *CONCERNING AMBIPOLAR DIFFUSION IN A MAGNETIC FIELD*

A. V. NEDOSPASOV

Submitted to JETP editor February 1, 1958

J. Exptl. Theoret. Phys. (U.S.S.R.) **34**, 1338-1339 (May, 1958)

THE basic characteristics of the low-voltage arc region are determined by ambipolar diffusion both in radial and axial directions, from the region of the cathode spot.[1,2] If the low-voltage region is placed in a homogeneous longitudinal magnetic field of intensity H, the distribution of electron concentration of the current on the wall, and also the dimensions of the low-voltage region, change with the ratio $D_\parallel/B_\perp$ of the diffusion coefficients parallel and perpendicular to the magnetic field. This makes it possible to determine the value of the above ratio for various values of H. In particular, the ion current on the wall varies, within a certain range of z, in accordance with

$$j_w = c\exp\left(-\frac{\mu_1 z}{r_0}\sqrt{\frac{D_\perp}{D_\parallel}}\right), \quad (1)$$

where $r_0$ is the radius of the tube, z the coordinate along the tube axis, and $\mu_1$ the eigenvalue of the boundary problem, which can be determined from measurements at H = 0.

The author, helped by G. I. Pankova, measured the distribution of the ion-current density on the walls, in the low-voltage arc region, at various values of H. The measurement procedure was analogous to that described in Ref. 2. The general pattern of the observed redistribution, for

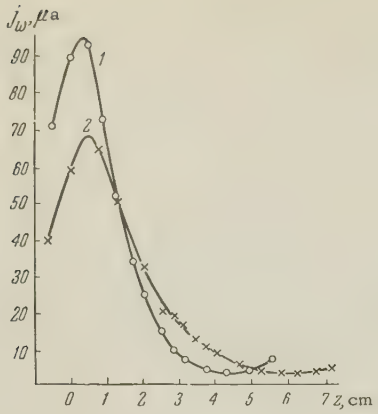


FIG. 1. Distribution of ion current on the walls: 1 – H = 0, 2 – H = 840 oersted.

an argon pressure of 0.7 mm Hg, is shown in Fig. 1. The electrons and ions diffuse farther along the axis, owing to the reduced diffusion towards the walls in the magnetic field. At a certain distance from the cathode, $j_\omega$ increases in the magnetic field, since it decreases near the cathode. The total value of the ion current remains almost constant at H = 840 gausses from z = 0 to the minimum, as shown on the curves of Fig. 1, even though the ratio $D_\parallel/D_\perp$ equals 2.5.

The variation of $D_\parallel/D_\perp$ obtained in the first experiments is shown in Fig. 2, where the abscissa

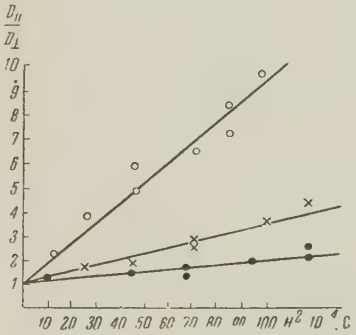


FIG. 2. Dependence of $D_\parallel/D_\perp$ on the square of the magnetic-field intensity. Pressure in argon: o – 0.25 mm Hg, × – 0.7 mm Hg, • – 1.0 mm Hg.

represents the square of the magnetic field intensity. The value of $D_\parallel/D_\perp$ was determined in accordance with (1) from the slope of the lines on the semi-logarithmic graph. Figure 2 agrees fully with the classical formula

$$D_\perp = \frac{D_\parallel}{1 + k\,(b_e H / c_0)^2}\,; \qquad (2)$$

where $b_e$ is the mobility of the electrons, $c_0$ the velocity of light, and k is the ratio of the ion and electron mobilities.

The advantage of the method proposed here over those described in the literature is that there is no need for measuring the electron concentration in the plasma. The results obtained show that when the plasma is no longer longitudinally homogeneous, a decrease in $D_\perp$ is not accompanied by the same decrease in diffusion current on the walls. A frequently-encountered masked case of an inhomogeneous column is a column with moving strata. Here charge diffusion along the tube is characteristic of the strata as well as of the low-voltage arc region.[3-5] Results of measurements in a positive column[6] must therefore be accepted with caution.

[1] B. N. Kliarfel' d and V. D. Sobolev, J. Tech. Phys. (U.S.S.R.) **17**, 319 (1947).

[2] A. V. Nedospasov and K. E. Torgonenko Радиотехника и электроника (Radio Engg. and Electronics) **2**, 494 (1957).

[3] B. N. Kliarfel' d, J. Exptl. Theoret. Phys. (U.S.S.R.) **22**, 66 (1952).

[4] A. B. Stewart, J. Appl. Phys. **27**, 911 (1958).

[5] W. H. Bostick and M. A. Levine, Phys. Rev. **97**, 13 (1955).

Translated by J. G. Adashko
272

## *ANOMALOUS GALVANOMAGNETIC PROPERTIES OF METALS AT LOW TEMPERATURES*

N. E. ALEKSEEVSKII, N. B. BRANDT, and T. I. KOSTINA

Institute of Physical Problems, Academy of Sciences, U.S.S.R; Moscow State University

Submitted to JETP editor February 5, 1958

J. Exptl. Theoret. Phys. (U.S.S.R.) **34**, 1339-1341 (May, 1958)

In many works devoted to the study of galvanomagnetic properties of metals not enough attention is paid to the technique used to bring in the current and potential leads. In strong effective fields [$H_{ef} = H_0\sigma_0(T)/\sigma_0(300°K)$] this can lead to a distortion of the observed phenomena. Thus, for example, in Refs. 1 to 4 the potential difference $V_x$, measured across the potential electrodes, increases as usual in weak magnetic field, passes through a maximum, diminishes to zero, and sometimes reverses its sign.

Since analogous anomalous changes in potential difference were observed by us in an investigation of the galvanomagnetic properties of bismuth in longitudinal and transverse magnetic fields,* supplementary experiments were performed to determine how the shapes of the electrodes and the methods by which they are interconnected influence the variation of $V_x$ in a magnetic field. It becomes possible to attribute the anomalies in the variation of $V_x$ observed in Refs. 1 to 4 to quadratic effects, particularly, the "quadratic" Hall effect, observed up to now only in germanium,[5] HgSe,[6,7] and Ga.[8] This effect is the appearance of a transverse potential difference in specimens located in a magnetic field. This potential difference, $V_y$, is in the plane passing through the current and magnetic field vectors, and is a quadratic function of the magnetic field. For isotropic specimens it attains its maximum at an angle of 45° between the current and field. Investigations of the "quadratic" Hall effect in bismuth of varying purity, in aluminum, and in tin[9] have shown that $V_y$ increases sharply with decreasing temperature and with increasing purity of the specimens. In sufficiently pure specimens, at a temperature of 4.2°K and at $H = 13{,}000$ Oe, $V_y$ of the "quadratic" Hall effect exceeded $V_x$, measured at $H = 0$, by thousands and sometimes tens of thousands times.

It is obvious that in those cases when the change in the resistance in the magnetic field is small (for example, in measurements in a longitudinal field), a slight $V_y$ component along the specimen is sufficient to distort qualitatively the curve of the true variation of resistance in the magnetic field, for this additional component cannot be eliminated by double reversal of the directions of the current in field, as is usually done in the measurement of resistance. The results are particularly badly distorted when the current contact area is small compared with the specimen cross section area and the potential electrodes are located near to the specimen ends. In this case the current-density gradients on the ends of the specimen (which usually are not strictly symmetrical) will give rise to stray currents which may interact with the magnetic field to produce an additional potential difference at the potential electrodes, a difference which cannot be eliminated by reversing the current or the field.

Furthermore, if the line passing through the potential electrodes is not quite parallel with the axis of the specimen, an additional voltage component of the "quadratic" Hall effect may arise between the two. Even in the absence of such a deviation from parallelism, if the current electrodes are not symmetric about the specimen axis, an additional potential difference of either sign can occur, owing to either the first or the second reasons above.

Experiments with specimens of different geometries have shown that increasing the specimen length to diameter ratio, while retaining an identical relative placement of the potential electrodes, does not lead to a substantial reduction in the anomalous effects. However, increasing the distance between the ends of the specimens to the potential-electrodes, and also changing the ratio of the contact area to the specimen cross-section area, affects quite strongly the variation of the potential difference in a longitudinal magnetic field (see diagram).

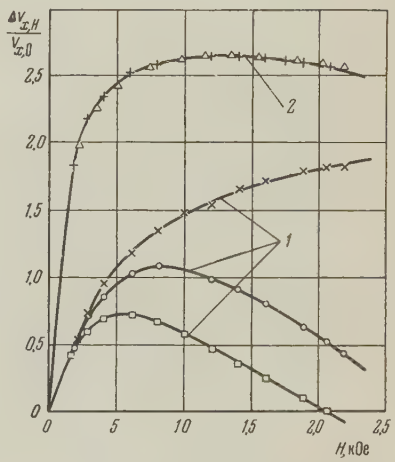


Relative variation of $V_x$ in a longitudinal magnetic field at $T = 77°K$ in Bi specimens of various shapes. Curves 1 – polycrystalline plate measuring $0.7 \times 6.0 \times 3.8$ mm; ○ – current electrodes make point contact, × – flat copper current electrodes, □ – repeated fusing of point electrodes (flat contacts removed and specimen shortened somewhat). Curves 2 – monocrystalline cylindrical specimens of identical crystal orientation, 15 mm long and with diameters of 2 mm (+) and 0.5 mm (Δ); the distance from the end of either specimen to the potential-electrode lead-in is on the order of two diameters.

In connection with this it appears rational to perform measurements on a specimen having a cross section equal to those of the current electrodes. In this case the potential electrodes must be located as far away as possible from the ends of the specimen and as parallel as possible to its axis. Failure to observe these precautions in Refs. 1 to 4 has most probably caused the indicated "anomalies." This likelihood is emphasized by the fact that in Ref. 2 a substantial change in the magnitude of the observed effect was noted when the current and potential electrodes were interchanged.

One cannot exclude the existence of more complicated mechanisms leading to an added longitudinal potential difference in a magnetic field exist. These added effects are, however, apparently substantially less than the effects noted above.

We consider it our pleasant duty to thank Academician P. L. Kapitza for discussing this communication.

*Reported at the All-Union Conference on Low Temperature Physics, Moscow June 1957.

[1] M. C. Steele, Phys. Rev. **97**, 1720 (1955).
[2] D. K. C. MacDonald, Phil. Mag. **2**, 97 (1957).
[3] C. J. Gorter, Progress in Low Temperature Physics **2**, 182 (1957).
[4] J. Babiskin, Phys. Rev. **107**, 981 (1957).
[5] Colman, Soldberg, and Davis, Phys. Rev. **94**, 1121 (1954).
[6] F. G. Bass and I. M. Tsidil'kovskii, J. Tech. Phys. (U.S.S.R.) **24**, 1834 (1954).
[7] I. M. Tsidil'kovskii, J. Tech. Phys. (U.S.S.R.) **27**, 12 (1957), Soviet Phys. JTP **2**, 9 (1957).
[8] J. Jahia and J. A. Marcus, International Conference on Low Temperature Physics and Chemistry, Wisconsin, 1957.
[9] Alekseevskii, Brandt, and Kostina, Вестник МГУ (Bull. Moscow State Univ.) (in press).

Translated by J. G. Adashko
273

## *THE DIFFERENTIAL FORM OF THE KINETIC EQUATION OF A PLASMA FOR THE CASE OF COULOMB COLLISIONS*

B. A. TRUBNIKOV

Moscow Engineering-Physics Institute

Submitted to JETP editor February 20, 1958

J. Exptl. Theoret. Phys. (U.S.S.R.) **34**, 1341-1343 (May, 1958)

As is known,[1] the kinetic equation for the particle distribution function $f_\alpha(t, \mathbf{r}, \mathbf{v})$ of a completely ionized plasma ($\alpha = e$ and $\alpha = i$ denote electrons and ions, respectively) can be written for the case of Coulomb collisions in the form

$$\frac{\partial f_\alpha}{\partial t} + (\mathbf{v}\,\mathrm{grad}_r) f_\alpha + \frac{1}{m_\alpha}(\mathbf{F}_\alpha \nabla_v f_\alpha) = -\sum_\beta (\nabla_v \mathbf{j}_{\alpha\beta}), \qquad (1)$$

$$(\mathbf{j}_{\alpha\beta})_i = \frac{2\pi\lambda e_\alpha^2 e_\beta^2}{m_\alpha}\int d\mathbf{v}' U_{ik}\left(\frac{f_\alpha}{m_\beta}\frac{\partial f_\beta'}{\partial v_k'} - \frac{f_\beta'}{m_\alpha}\frac{\partial f_\alpha}{\partial v_k}\right), \qquad (2)$$

$$U_{ik} = \partial^2 |V| / \partial v_i \partial v_k = (V^2\delta_{ik} - V_i V_k)/V^3;$$

$$V_i = v_i - v_i'.$$

The present note shows that the particular structure of the integrals in Eq. (2) for the current allows one to introduce new variables in the form of new unknown "potential" functions

$$\Phi_\alpha(t, \mathbf{r}, \mathbf{v}) = \int d\mathbf{v}' f_\alpha(\mathbf{v}')\,|\mathbf{v} - \mathbf{v}'|, \qquad (3)$$

which will transform the integro-differential equations (1) into pure differential form.

Let us consider the first integral in the expression for $\mathbf{j}_{\alpha\beta}$. If we make use of the expression for $U_{ik}$, we obtain

$$\int d\mathbf{v}' U_{ik}\frac{\partial f_\beta'}{\partial v_k} = 2\frac{\partial \varphi_\beta}{\partial v_i}, \quad \varphi_\beta(t, \mathbf{r}, \mathbf{v}) = \int \frac{f_\beta(\mathbf{v}')\,d\mathbf{v}'}{|\mathbf{v} - \mathbf{v}'|}. \qquad (4)$$

Further, noting the identity

$$V^{-3}\{V^2\nabla_v f_\alpha - \mathbf{V}(\mathbf{V}\nabla_v f_\alpha)\} = (\nabla_v f_\alpha \nabla_v)\nabla_v |\mathbf{v} - \mathbf{v}'|, \qquad (5)$$

we can transform the second integral in (2) according to

$$\int d\mathbf{v}' f_\beta' U_{ik}\frac{\partial f_\alpha}{\partial v_k} = \frac{\partial f_\alpha}{\partial v_k}\cdot\frac{\partial^2 \Phi_\beta}{\partial v_k \partial v_i}. \qquad (6)$$

The other quantities entering into (1) are also easy to express in terms of the $\Phi_\beta$. In particular,

$$\varphi_\beta = \frac{1}{2}\nabla_v^2 \Phi_\beta, \quad f_\beta = -\frac{1}{4\pi}\Delta_v \varphi_\beta = -\frac{1}{8\pi}\nabla_v^4 \Phi_\beta. \qquad (7)$$

Inserting (4), (6), and (7) into (1), we obtain the differential equation

$$\frac{\partial}{\partial t}(\nabla_v^4 \Phi_\alpha) + (\mathbf{v}\,\mathrm{grad}_r)(\nabla_v^4 \Phi_\alpha) + \frac{1}{m_\alpha}(\mathbf{F}_\alpha \nabla_v^5 \Phi_\alpha)$$
$$= -\sum_\beta \frac{2\pi\lambda e_\alpha^2 e_\beta^2}{m_\alpha}\left(\nabla_v\left[\frac{1}{m_\beta}(\nabla_v^4 \Phi_\alpha)\nabla_v^3 \Phi_\beta - \frac{1}{m_\alpha}(\nabla_v^5 \Phi_\alpha \nabla_v)\nabla_v \Phi_\beta\right]\right) \qquad (8)$$

for the "potential" functions. In the special case of a "moving" Maxwell distribution given by

$$f_\alpha^{(0)}(\mathbf{v}) = n_\alpha (m_\alpha / 2\pi T_\alpha)^{3/2} \exp\{-s_\alpha^2\}, \qquad (9)$$

$$s_\alpha = \sqrt{\frac{m_\alpha}{2T_\alpha}}(\mathbf{v} - \mathbf{v}_\alpha^0)$$

(where $n_\alpha(t, \mathbf{r})$ is the density, $\mathbf{v}_\alpha^0(t, \mathbf{r})$ is the mean velocity, and $T_\alpha(t, \mathbf{r})$ is the temperature) we have

$$\Phi_\alpha^{(0)}(\mathbf{v}) = n_\alpha \left(\frac{2T_\alpha}{\pi m_\alpha}\right)^{3/2} M(s_\alpha),$$

$$M(s) = e^{-s^2} + (1 + 2s^2)\int_0^1 e^{-s^2x^2}dx. \qquad (10)$$

It is easy to verify that $\Phi_\alpha^0(\mathbf{v})$ causes the self-current $\mathbf{j}_{\alpha\alpha}$ to vanish, which is as it should be.

From the definition (3) one easily obtains the asymptotic potential function (for $v \gg \langle v\rangle_\alpha$; we drop terms of order $v^{-3}$), namely

$$\Phi_\alpha(\mathbf{v}) = vn_\alpha\left\{1 - \frac{(\mathbf{v}\mathbf{v}_\alpha^0)}{v^2}\right.$$

$$\left. + \left[\frac{T_\alpha}{m_\alpha v^2} - \frac{v_\alpha^{02}}{2v^2} - \frac{(\mathbf{v}\mathbf{v}_\alpha^0)^2}{2v^4} - \frac{(\mathbf{v}\Pi_\alpha\mathbf{v})}{2v^4}\right]\right\}, \qquad (11)$$

where we make use of the tensor

$$\Pi_{\alpha ik} = \frac{1}{n_\alpha}\int d\mathbf{v}' f_\alpha'\left(u_{\alpha i}'u_{\alpha k}' - \frac{u_\alpha'^2}{3}\delta_{ik}\right), \quad \mathbf{u}_\alpha' = \mathbf{v}' - \mathbf{v}_\alpha^0.$$

If the distribution differs only slightly from a Maxwell distribution, so that we may write

$$\Phi_\alpha(\mathbf{v}) \approx \Phi_\alpha^0 + \Phi_\beta^{(1)}$$

$$= n_\alpha^0 (2T_\alpha/\pi m_\alpha)^{3/2}[M(s_\alpha) + \chi(s_\alpha)], \quad \chi \ll M, \qquad (12)$$

the linear approximation gives the following expression for the current $\mathbf{j}_{\alpha\alpha}$ due to collisions among particles only of type $\alpha$:

$$\mathbf{j}_{\alpha\alpha} = (\lambda e_\alpha^4/4m_\alpha^2)[(\nabla_v^5\Phi_\alpha\nabla_v)\nabla_v\Phi_\alpha - (\nabla_v^4\Phi_\alpha)\nabla_v^3\Phi_\alpha]$$

$$\approx (\lambda e_\alpha^4 n_\alpha^2/4\pi m_\alpha^2)(m_\alpha/2T_\alpha)^{6/2}[16e^{-s^2}(s\nabla_s)\nabla_s\chi + 8e^{-s^2}\nabla_s^3\chi$$

$$+ (\nabla_s^5\chi\nabla_s)\nabla_s M - (\nabla_s^4\chi)\nabla_s^3 M]. \qquad (13)$$

In this case all the equations can be linearized.

Under certain special conditions, it is possible to lower the order of the differential equation. Such a situation may occur, for instance, when the distribution depends only on the absolute value of the velocity. Since the use of Eq. (8) for the "potential" functions may lead to extra solutions, the final result must be verified by inserting it into the initial equation (1).

[1] L. D. Landau, J. Exptl. Theoret. Phys. (U.S.S.R.) 7, 203 (1937).

Translated by E. J. Saletan
274

## *PROOF OF THE ABSENCE OF RENORMALIZATION OF THE VECTOR COUPLING CONSTANT IN BETA-DECAY*

B. L. IOFFE

Submitted to JETP editor February 20, 1958

J. Exptl. Theoret. Phys. (U.S.S.R.) **34**, 1343-1345 (May, 1958)

GELL-MANN and Feynman have proposed[1] that the vector coupling constant of the $\beta$-decay interaction is not subject to renormalizations due to the strong meson-nucleon interaction, if a direct interaction between the $\pi$ meson and electron-neutrino fields is introduced such as to make the vector part of the meson-nucleon $\beta$-interaction Hamiltonian of the form

$$H = G_V[\bar\psi\gamma_\mu\tau^+\psi + 2i(\Phi^+T^+\nabla_\mu\Phi$$

$$- (\nabla_\mu\Phi^+)T^+\Phi)]J_\mu + \text{Herm. conj.}$$

$$\cdot J_\mu = {}^1/_2\bar\psi_e\gamma_\mu(1+\gamma_5)\psi_\nu, \qquad (1)$$

where $\tau^+ = \frac{1}{2}(\tau_x + i\tau_y)$, $T^+ = \frac{1}{2}(T_x + iT_y)$ are the isotopic spin operators and $\Phi = (\varphi, \varphi^0, \varphi^+)$ is the meson wave function.

This assumption of Gell-Mann and Feynman may be rigorously proved if it is noted that in the presence of the $\beta$-interaction (1) the complete nucleon — $\pi$ meson Lagrangian (in which the meson-nucleon interaction is included but interactions with the electromagnetic field are not) admits the group of infinitesimal transformations

$$\psi = [1 - i(\tau^+\chi + \tau\chi^*)]\psi'; \qquad \Phi = [1 - 2i(T^+\chi + T\chi^*)]\Phi';$$

$$J_\mu = J_\mu' + \partial\chi/\partial x_\mu \qquad (2)$$

where $\chi$ is an infinitesimal numerical function. The existence of the group of transformations (2) makes possible the proof of a theorem analogous to the Ward theorem in quantum electrodynamics. To obtain the proof it is only necessary to calculate the nucleon Green's function $G(x, y, J_\mu)$ in the presence of a time and space independent external $\beta$-current $J_\mu$, and to define the vertex part as

$$\Gamma_\mu^+(x, y; \xi) = \partial G^{-1}(x, y; J_\mu)/\partial J_\mu|_{J_\mu=0}\,\delta(\xi).$$

Putting $\chi(x) = J_\mu x_\mu$, one obtains from the definition of the Green's function

$$G(x, y; J_\mu) = \langle 0 \mid T\{\psi(x), \bar\psi(y)\} \mid 0\rangle$$

and from the relations (2):

$$\left.\frac{\partial G(x, y; J_\mu)}{\partial J_\mu}\right|_{J_\mu=0} = i \langle 0 \mid T\{\tau^+ x_\mu \psi(x), \bar{\psi}(y)\} \mid 0\rangle$$

$$- i \langle 0 \mid T\{\psi(x), \bar{\psi}(y)\tau^+ y_\mu\} \mid 0\rangle. \quad (3)$$

However, this quantity, when viewed as a matrix in isotopic spin space, should be of the form $F(x,y)\tau^+$. Taking this into account one may bring (3) into the form

$$\left.\frac{\partial G(x, y; J_\mu)}{\partial J_\mu}\right|_{J_\mu=0} = i(x_\mu - y_\mu)\langle 0 \mid T\{\psi(x), \bar{\psi}(y)\} \mid 0\rangle\tau^+$$

$$= i(x_\mu - y_\mu) G(x, y)\tau^+$$

and, consequently,

$$\Gamma_\mu^+(x, y; \xi) = -i(x_\mu - y_\mu) G^{-1}(x - y)\delta(\xi)\tau^+. \quad (4)$$

Going over to the momentum representation, we obtain a relation analogous to the Ward theorem in quantum electrodynamics:

$$\Gamma_\mu^+(p, p; 0) = \tau^+ \partial G^{-1}(p)/\partial p_\mu. \quad (5)$$

The remainder of the proof of the absence of charge renormalization is the same as in quantum electrodynamics when vacuum polarization is ignored.

If, in addition to the $\pi$ meson — nucleon interactions, it is also desired to take into account the interactions of nucleons with K mesons and hyperons, the group of transformations (2) must be extended to include the strange particles, so as to have no renormalization of the vector coupling constant of the $\beta$-interaction. This can be achieved by assuming that the K meson and $\Xi$ hyperon wave functions transform as the nucleon wave function, the $\Sigma$ hyperon wave function transforms as the $\pi$ meson wave function, and the wave function of the $\Lambda^0$ particle remains unchanged. The existence of such a group of transformations of the strange particles requires that the vector part of the $\beta$-interaction Hamiltonian of K mesons and hyperons be of the form

$$H = G_V[2\bar{\psi}_\Sigma \gamma_\mu T^+ \psi_\Sigma + i(\varphi_K^+ \tau^+ \nabla_\mu \varphi_K - (\nabla_\mu \varphi_K^+)\tau^+ \varphi_K)$$

$$+ \bar{\psi}_\Xi \gamma_\mu \tau^+ \psi_\Xi] J_\mu + \text{Herm. conj.} \quad (6)$$

The Hamiltonian (6) describes $\beta$-decays of strange particles in which strangeness does not change* (e.g., $\Sigma^- \to \Sigma^0 + e^- + \nu$, $K^- \to K^0 + e^- + \nu$). The constant $G_V$ in the Hamiltonian (6) corresponds to the constant in the Hamiltonian (1) and, just like the latter, does not get renormalized by strong interactions.

We note that radiation corrections due to the electromagnetic field have been neglected in the present proof. The interaction of the particles with the electromagnetic field is not invariant under the group of transformations (2) and should, in general, lead to a renormalization of the constant $G_V$.

*Processes involving a strangeness change, cannot, clearly, influence the magnitude of the renormalization in processes in which strangeness does not change.

[1] R. Feynman and M. Gell-Mann, Phys. Rev. **109**, 193 (1958).

Translated by A. Bincer
275

## *LOWER EXCITED (ROTATIONAL) LEVELS OF* $T^{234}$

A. P. KOMAR, G. A. KOROLEV, and G. E. KOCHAROV

Leningrad Physico-Technical Institute, Academy of Sciences, U.S.S.R.

Submitted to JETP editor February 20, 1958

J. Exptl. Theoret. Phys. (U.S.S.R.) **34**, 1345-1346 (May, 1958)

USING an ionization chamber with grid,[1] we investigated the energy spectrum of $\alpha$-particles from $U^{238}$. The spectrum obtained is shown in Fig. 1

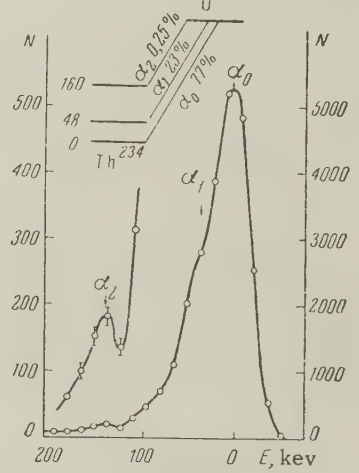


FIG. 1

where $\alpha_0$ is the ground-state group of 4.182-Mev $\alpha$ particles from $U^{238}$. In our opinion, $\alpha_2$ is the group of particles corresponding to the transition

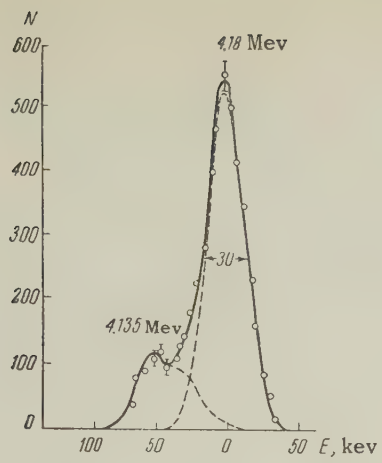


FIG. 2

to the $Th^{234}$ second level. The transition intensity is $(0.25 \pm 0.1)\%$. The level energy is approximately 160 kev. The second to first level energy ratio coincides with the theoretical value obtained using the generalized model of the nucleus. It is most probable that this is the +4 level.

The $\alpha_1$ group corresponds to a transition of the daughter nucleus to the +2 level. This group of particles is readily separated in the $\alpha$-particle spectrum by using electric collimation and a narrower analyzer channel (Fig. 2). The intensity of transition to the +2 level is 23%.

This intensity value is in good agreement with the results of Refs. 2 to 5. The decay scheme of $U^{238}$, plotted in accordance with the results of this work, is shown in Fig. 1.

At the present time further measurements are being made with a view towards a better separation of the $\alpha_2$ group, so as to increase the accuracy of the results obtained.

[1] Bochagov, Kocharov, and Kirshin Приборы и техника эксперимента (Instr. and Meas. Engg.) No. 6, 1957, p. 72.

[2] B. B. Zajac, Phil. Mag. **43**, 264 (1952).

[3] D. C. Dunleavy and G. T. Seaborg, Phys. Rev. **87**, 165 (1952).

[4] G. Albouy and J. Teillac, Compt. rend. **234**, 829 (1952).

[5] Georges Valladac, Dissertation, Paris, 1955.

Translated by J. G. Adashko
276

## *ANISOTROPY OF THE EVEN PHOTOMAGNETIC EFFECT*

Iu. A. KAGAN and Ia. A. SMORODINSKII

Submitted to JETP editor February 21, 1958

J. Exptl. Theoret. Phys. (U.S.S.R.) **34**, 1346-1347 (May, 1958)

KIKOIN and Bykovskii[1] have recently observed the presence of a clearly pronounced anisotropy in an investigation of the even photomagnetic effect in semiconductors with cubic lattice. By "even photomagnetic effect," first discovered by I. K. Kikoin,[2] is meant the appearance of a potential difference in a direction perpendicular to the incident light, independent of the direction of the magnetic field.) In this communication we give a purely phenomenological description of the character of this anisotropy.

The problem under consideration is characterized by three vectors: the magnetic field **H**, the outer normal **n** to the illuminated surface of the semiconductor (along which the liberated carriers diffuse), and the resultant electric field **E**. Let the magnetic field be sufficiently small. Then, with accuracy to terms quadratic in **H**, one can write the following general expression

$$E_i = L_{ik}n_k + L_{ikl}n_kH_l + L_{iklm}n_kH_lH_m. \qquad (1)$$

Let the Cartesian coordinate axes coincide with the axes of the cubic crystal. From the symmetry properties of this crystal it follows that

$$L_{ik} = L_1\delta_{ik}, \quad L_{ikl} = L_2e_{ikl},$$

where $\delta_{ik}$ is the unit tensor of second rank and $e_{ikl}$ is the unit totally-antisymmetrical tensor of third rank.

As is known (see, for example, Ref. 3) the fourth-rank tensor will have only three independent components in a cubic crystal.

$$L_{aabb} = L_{bbaa} \equiv L_3,$$

$$L_{abba} = L_{abab} = L_{baba} \equiv L_4, \quad L_{aaaa} = L_5.$$

As a result the expression for $E_i$ is transformed into

$$E_i = L_1n_i + L_2e_{ikl}n_kH_l + L_3n_iH^2 + 2L_4H_in_kH_k + L'_5n_i\underline{H_i^3},$$

$$L'_5 = L_5 - L_3 - 2L_4 \qquad (2)$$

(there is no summation over the underscored indices).

The first term in (2) corresponds to the Dember effect,[4] the second to the odd photomagnetic effect,[5] and the third determines the variation of the Dember effect with the magnetic field. As to the fourth term, it describes the even photomagnetic effect in that form, in which it takes place in an isotropic semiconductor. If E is measured along a direction $\boldsymbol{l}$ perpendicular to **n**, and if $\boldsymbol{l}$, **n**, and **H** are in the same plane, then this term signifies a simple dependence on the angle $\vartheta_0$ between **n** and **H**, namely $L_4H^2 \sin 2\vartheta_0$, which was observed in polycrystalline specimens.[2]

The last term in (2) determines the presence of anisotropy in the even photomagnetic effect. $L_5'$ vanishes in a completely isotropic specimen.

If **H** is perpendicular to **n** the isotropic portion of the even photomagnetic effect vanishes and the general expression for $E_{\boldsymbol{l}}' = \frac{1}{2}[E_{\boldsymbol{l}}(\mathbf{H}) + E_{\boldsymbol{l}}(-\mathbf{H})]$ ($\boldsymbol{l}$ perpendicular to **H**) is written as

$$E_1' = L_5' \sum_i n_i l_i H_i^2. \qquad (3)$$

It follows from (3) that, at a sufficiently small magnetic field and a known orientation of the monocrystalline specimen axes, the change in the even photomagnetic effect makes it possible to determine the anistropic constant $L_5'$

In the particular case when **n** coincides with the direction of the principal diagonal axis, expression (3) becomes particularly simple

$$E_1'' = \frac{2\sqrt{2}}{9} L_5' H^2 \left\{ \cos^2(\varphi - \varphi_0)\cos\varphi + \cos^2\left(\varphi + \frac{2}{3}\pi - \varphi_0\right)\cos\left(\varphi + \frac{2}{3}\pi\right) + \cos^2\left(\varphi + \frac{4}{3}\pi - \varphi_0\right)\cos\left(\varphi + \frac{4}{3}\pi\right)\right\}. \qquad (4)$$

Here $\varphi_0$ is the angle between **H** and $\boldsymbol{l}$ and $\varphi$ is the angle of rotation of the specimen about **n**. The character of the dependence of $E_{\boldsymbol{l}}''$ on $\varphi$, as obtained in Ref. 1, is very close to that given by (4)

It must be noted in conclusion that the first to indicate that anistropy in a semiconductor with cubic lattice is possible, in connection with the dependence of the resistance on the magnetic field, was Seitz,[6] who introduced a term analogous to the last term in (2).

The authors are indebted to Academician I. K. Kikoin for valuable discussions.

[1] I. K. Kikoin and Iu. A. Bykovskii, Dokl. Akad. Nauk SSSR **116**, 381 (1957), Soviet Phys. "Doklady" **2**, 447 (1957).

[2] I. K. Kikoin, Dokl. Akad. Nauk SSSR **3**, 418 (1934).

[3] L. D. Landau and E. M. Lifshitz, Механика сплошных сред (Mechanics of Continuous Media) Part II, Ch. 1, 2d Ed., 1953.

[4] H. Dember, Phys. Z. **32**, 554 (1931).

[5] I. K. Kikoin and M. M. Noskov, Phys. Z. Sowjetun. **5**, 586 (1934).

[6] F. Seitz, Phys. Rev. **79**, 372 (1950).

Translated by J. G. Adashko
277

## *ON THE DETERMINATION OF THE COVARIANTS IN THE* $K_{e3}$ *DECAY*

I. Iu. KOBZAREV

Submitted to JETP editor February 24, 1958

J. Exptl. Theoret. Phys. (U.S.S.R.) **34**, 1347-1349 (May, 1958)

IF all weak interactions are described by a universal A — V interaction as proposed by Gell-Mann and Feynman[1] and Marshak and Sudarshan[2] then the matrix element for the decay $K \to e + \nu + \pi$ should be of the form:[3]

$$M \sim GMf\,(\bar{\psi}_\nu p_K (1 + \gamma_5)\psi_e)$$

(in perturbation theory $f \sim \ln(\Lambda^2/M^2)$ where $\Lambda$ is the cutoff parameter and M the nucleon mass; however, in general, f may be a function of the $\pi$-meson energy). Additional interest is raised thereby in the determination of the decay interaction.

For purposes of analysis the decay of the long-lived $K_2^0$ meson, $K_2^0 \to e^\pm + \nu + \pi^\mp$, is the most convenient since the presence of two charged particles permits a complete determination of the kinematics.

In the present note we propose to analyze the decay by a method analogous to the Dalitz analysis for the $\tau^+$ decay,[4] on the assumption that the decay interaction is of the general form discussed by Pais and Treiman:[5]

$$M \sim \bar{\psi}_\nu (f_S + f_S'\gamma_5)\psi_e + \frac{ip_\mu^K}{M}\bar{\psi}_\nu\gamma_\mu (f_V + f_V'\gamma_5)\psi_e + \frac{p_\mu^K p_\nu^\pi}{M^2}\bar{\psi}_\nu\sigma_{\mu\nu}(f_T + f_T'\gamma_5)\psi_e.$$

The Gell-Mann and Feynman scheme corresponds

to a pure V covariant, i.e., $f_S = f'_S = f_T = f'_T = 0$ (and $f_V = f'_V$).

The decay probability may be written in the form form

$$W \sim \Phi(E_\pi, E_e)\, dE_\pi dE_e.$$

Theoretically, only the dependence of $\Phi(E_\pi, E_e)$ on $E_e$ can be determined; the necessary calculations are contained in the work of Okun',[6] whose results are used below.

Let us represent the decays by points P(x, y) inside an equilateral triangle ABC, such that the distances from P to AB, AC and BC are proportional to the energies of the electron, neutrino, and $\pi$ meson respectively (see figure). The region allowed by the momentum conservation law is bounded by the straight line

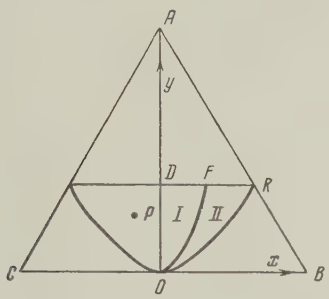


$$y = E_{\pi\,(\max)} = (M_K - m_\pi)^2 / 2M_K$$

and the hyperbola

$$x = \sqrt{(y^2 + 2m_\pi y)/3}.$$

From the observed decays one obtains a certain distribution of points inside of this region. Then, according to the results of Ref. 6, the analysis may be carried out as follows:

1. It is first determined whether the distribution of decays is symmetric or not about the y axis. An asymmetry can occur only if both the S and T covariants are present simultaneously (with, possibly, admixtures of V).

2. If the distribution is symmetric then it may be "folded" relative to the y axis by replacing points P to the left of the y axis with points placed symmetrically relative to this axis; thus one need only consider the segment ROD. This segment is further divided into two parts of equal area, I and II, by the hyperbola $y = \frac{1}{2}\sqrt{(y^2 + 2my)/3}$ Let n(I) and n(II) denote the number of decays in regions I and II and let $\rho(x, y)$ denote the density of decays. Then:

(a) If n(I) > n(II) we have the V covariant with possible admixtures of T or S; a pure V covariant is characterized by the vanishing of $\rho$ on the hyperbola RO.

(b) If n(I) < n(II) then the dominant covariant is T with possible admixtures of V; a pure T covariant is characterized by the vanishing of $\rho$ on the y axis.

(c) If n(I) = n(II) we have either the S covariant or a mixture of V and T; a pure S covariant is characterized by a $\rho$ independent of x.

Let us point out the characteristic feature which indicates the presence of the V covariant: namely, it is the only covariant for which $\rho$ does not vanish on the straight line DR.

[1] M. Gell-Mann and R. P. Feynman, Phys. Rev. **109**, 193 (1958).

[2] R. E. Marshak and E. C. G. Sudarshan, Phys. Rev. **109**, 1860 (1958).

[3] I. Iu. Kobzarev and I. E. Tamm, J. Exptl. Theoret. Phys. **34**, 899 (1958), Soviet Phys. JETP **7**, 622 (1958).

[4] R. H. Dalitz, Phil. Mag. **44**, 1068 (1953), Phys. Rev. **94**, 1046 (1954).

[5] A. Pais and S. B. Treiman, Phys. Rev. **105**, 1616 (1957).

[6] L. B. Okun', J. Exptl. Theoret. Phys. **33**, 525 (1957), Soviet Phys. JETP **6**, 409 (1958).

Translated by A. Bincer
278

## *0 → 0 BETA TRANSITIONS WITH PARITY CHANGE*

B. V. GESHKENBEIN

Submitted to JETP editor February 24, 1958

J. Exptl. Theoret. Phys. (U.S.S.R.) **34**, 1349-1350 (May, 1958)

THE possible variants of $\beta$-decay interaction have recently been undergoing a reexamination. Whereas in the past it has been considered experimentally established that the vector and axial-vector interactions do not contribute to $\beta$-decay, now the validity of these experiments is in doubt. Furthermore, if the universal theory of weak interactions proposed in Refs. 1 and 2 is valid, then only the A and V covariants contribute to $\beta$-decay.

As is well known, the spectrum of 0 → 0 (yes) transitions is given to a high accuracy by the Fermi

spectrum, i.e., the correction factor C is energy independent. Only the tensor interaction fails to give the required spectrum shape; it has been necessary to explain the spectrum shape by introducing the pseudoscalar interaction and assuming $g_P \gg g_T$ (Ref. 3).

The purpose of the present note is to focus attention on the fact that the spectrum shape of $0 \to 0$ (yes) transitions is in good agreement with the A covariant (the V covariant does not contribute due to selection rules), and to derive expressions for the electron polarization and electron-neutrino correlation. The required formulae may be obtained from the corresponding formulae valid for the T — P covariant,[4] provided one replaces q by $-q$ and $\lambda_P = -ig_P \int \gamma_5 / g_T \int \sigma \cdot \mathbf{r}$ by $\lambda = -i \int \gamma_5 / \int \sigma \cdot \mathbf{r}$, which now will be real:

$$C = \{(1/9 L_0 q^2 + M_0 - 2/3 q N_0) + (2N_0 - 2/3 L_0 q)\lambda + L_0 \lambda^2\} \left| g_A \int \sigma \mathbf{r} \right|^2, \quad (1)$$

$$\langle \sigma \mathbf{n} \rangle = -C^{-1} \left| g_A \int \sigma \mathbf{r} \right|^2 \{1/9 q^2 \sqrt{L_0^2 - P_0^2} + \sqrt{M_0^2 - Q_0^2} + 1/3 q (\sqrt{(L_0 + P_0)(M_0 + Q_0)} + \sqrt{(L_0 - P_0)(M_0 - Q_0)}) - (\sqrt{(L_0 + P_0)(M_0 + Q_0)} + \sqrt{(L_0 - P_0)(M_0 - Q_0)} + 2/3 q \sqrt{L_0^2 - P_0^2}) \lambda + \sqrt{L_0^2 - P_0^2} \lambda^2\} \sin(\delta_{-1} - \delta_1), \quad (2)$$

$$W_{ev}(\theta) = 1 + \langle \sigma \mathbf{n} \rangle \cos\theta.$$

The term $L_0 q^2/9 + M_0$ in the correction factor C increases with increasing energy, whereas $-2qN_0/3$ decreases, so that, to an accuracy of 5%, the expression $1/9\ L_0 q^2 + M_0 - 2/3\ qN_0$ is constant. The expression $2N_0 - 2/3\ L_0 q$ is constant to within 2%. In the case of the T — P covariant the analogous quantities varied by a factor of 2 and by 40% respectively (for $Pr^{144}$). If we assume that the deviation from a Fermi shape does not exceed 5% then $\lambda$ must satisfy $\lambda > 24$ or $\lambda < 3$ (the sign of $\lambda$ is unknown). Under these conditions the electron polarization is practically indistinguishable from $-v/c$.

In conclusion I thank Prof. V. B. Berestetskii, B. L. Ioffe, and A. P. Rudik for discussions.

[1] R. P. Feynman and M. Gell-Mann, Phys. Rev. **109**, 193 (1958).

[2] R. E. Marshak and E. C. G. Sudarshan, Phys. Rev. **109**, 1860 (1958).

[3] L. N. Zyrianova, Izv. Akad. Nauk SSSR, Ser. Fiz. **20**, 1399 (1956), (Columbia Tech. Transl. p. 1280).

[4] B. V. Geshkenbein, J. Exptl. Theoret. Phys. **33**, 1535 (1957), Soviet Phys. JETP **6**, 1187 (1958).

Translated by A. Bincer
279

## *CROSS SECTIONS FOR THE INELASTIC SCATTERING OF 4.5-Mev DEUTERONS BY CERTAIN LIGHT NUCLEI*

E. A. ROMANOVSKII and G. F. TIMUSHEV

Moscow State University

Submitted to JETP editor February 24, 1958

J. Exptl. Theoret. Phys. (U.S.S.R.) **34**, 1350-1351 (May, 1958)

INELASTIC scattering of deuterons by atomic nuclei was studied essentially at two energy values: $E_d \sim 15$ Mev (Refs. 1 and 2) and $E_d \sim 9$ Mev (Refs. 3 to 5). There was hardly any investigation of inelastic deuteron scattering at lower energies.

When this investigation was started, it was known that the differential cross section of the (d, d') reaction on $Mg^{24}$ ($\Delta E = 1.37$ Mev, $E_d = 4.5$ Mev) scattering angle ($\vartheta_{lab} = 70°$) was 4 mbn/sterad.[6] One could conclude from the work of Khromchenko[7] that in many nuclei there is little probability for the (d, d') reaction at $E_d \sim 4$ to 5 Mev, with the exception of $Li^7$. In the latter case the group of deuterons from the $Li^7$(d, d')$Li^{7*}$ reaction ($\Delta E = 0.476$ Mev), at $E_d \sim 3.7$ to 4.7 Mev and $\vartheta = 110°$, would be comparable in intensity with the group of deuterons elastically scattered from $Li^7$.

In this investigation we measured the differential cross sections for inelastic scattering of deuterons with $E_d \sim 4$ to 4.5 Mev from nuclei of $Li^7$, $F^{19}$, $Na^{23}$, $Mg^{24}$, and $Al^{27}$. A double-focusing magnetic analyzer[8] was used to sort the groups of inelastically-scattered deuterons. The deuterons were accelerated in the 72 cm cyclotron of the Institute of Nuclear Physics of the Moscow State University. To check the correctness of the identification of the deuteron group, the measurements were made at different energies $E_d$. The values obtained for the differential inelastic-scattering cross sections are given in the table for $E_d = 4.5$ Mev and $\vartheta_{lab} = 91°$.

The fourth and fifth columns of the table give the differential cross sections $d\sigma_{F_2}/d\Omega$ and the total cross sections $\sigma_{E_2}$ for Coulomb excitation

| nucleus | $\Delta E$, Mev | $\frac{d\sigma}{d\Omega}$, mbn/sterad | $\frac{d\sigma_{E_2}}{d\Omega}$, mbn/sterad | $\sigma_{E_2}$, mbn | nucleus | $\Delta L$, Mev | $\frac{d\sigma}{d\Omega}$, mbn/sterad | $\frac{d\sigma_{E_2}}{d\Omega}$, mbn/sterad | $\sigma_{E_2}$, mbn |
|---|---|---|---|---|---|---|---|---|---|
| $Li^7$ | 0.476 | 35 | | | $Na^{23}$ | 0.439 | 9 | 0.15 | 2 |
| $F^{19}$ | 0.197 | 16 | 0.06 | 0.7 | $Mg^{24}$ | 1.370 | 7 | 0.20 | 3.5 |
| $F^{19}$ | 1.355 | 2 | | | $Al^{27}$ | 0.843 | 1.5 | | |
| $F^{19}$ | 1.426 | 2 | | | $Al^{27}$ | 1.013 | 2.5 | | |
| $F^{19}$ | 1.558 | 8 | | | | | | | |

of the levels in $F^{19}$, $Na^{23}$, and $Mg^{24}$. The calculations were made with formulas (B-32) and (B-38) of Ref. 9. The probabilities given in the table for the transitions from the ground state into excited states with energies $\Delta E$ are taken from Refs. 9 and 10.

The tabulated results indicate that when $E_d$ = 4.5 Mev the contribution of $\sigma_{E_2}$ to the experimental value of $\sigma_{tot}$ ($\sigma_{tot}$ = 30 to 50 mbn for (d, d′) reactions on $Mg^{24}$, $Na^{23}$, and $F^{19}$) amounts to several percent. One can therefore conclude that at $E_d$ = 4 to 4.5 Mev and above the process of nuclear excitation by the Coulomb field of the incident deuterons cannot be the dominant process that leads to inealstic scattering of the deuterons. This conclusion contradicts the (d, d′) reaction theory developed by Mullin and Guth.[11]

In conclusion the authors express their gratitude to S. S. Vasil'ev for interest in this work and for discussion of the results, to Z. F. Kalacheva and T. P. Tupikina for aid in this work, and also to the cyclotron crew, particularly to G. V. Koshelyaev, A. A. Danilov and V. P. Khlapov.

[1] J. Haffner, Phys. Rev. **103**, 1398 (1956).
[2] Levine, Bender, and McGuer, Phys. Rev. **97**, 1249 (1956).
[3] R. Middleton, Proc. Phys. Soc. **A69**, 28 (1956).
[4] S. Hinds and R. Middleton, Proc. Phys. Soc. **A69**, 347 (1956).
[5] F. A. Bedewi, Proc. Phys. Soc. **A69**, 221 (1956).
[6] G. W. Greenless, Proc. Phys. Soc. **A68**, 97 (1955).
[7] L. M. Khromchenko, Izv. Akad. Nauk SSSR, Ser. Fiz. **19**, 277 (1956), (Columbia Tech. Transl. p. 252).
[8] G. F. Timushev, Приборы и техника эксперимента (Instr. and Meas. Engg.) (in press).
[9] Alder, Bohr, Huus, and Mottelson, Revs. Mod. Phys. **28**, 432 (1956).
[10] G. Rakavy, Nucl. Phys. **4**, 375 (1957).
[11] C. Mullin and E. Guth, Phys. Rev. **82**, 141 (1951).

Translated by J. G. Adashko
280

## *COMPTON SCATTERING OF CIRCULARLY POLARIZED PHOTONS BY ELECTRONS WITH ORIENTED SPIN*

A. A. SOKOLOV and B. A. LYSOV

Moscow State University

Submitted to JETP editor February 27, 1958

J. Exptl. Theoret. Phys. (U.S.S.R.) **34**, 1351-1354 (May, 1958)

THE further development of the quantum electrodynamics of longitudinally polarized electrons and photons assumes new significance in connection with the discovery of parity nonconservation. As we have already noted,[1,2] to take longitudinal polarization of electrons into account one must, in the calculation of matrix elements, use not the Casimir formula but formula 2.12 of Ref. 3, in which s stands for the eigenvalue of the operator $(\Delta\sigma)/i\sqrt{-\nabla^2}$. This operator gives double the electron spin projection onto its direction of motion.

It is of interest to observe that the above-mentioned formula can also be used if the electron is initially at rest. In that case the formula may be brought into the form

$$\langle \alpha_{n'}, \alpha_n \rangle = \frac{1}{16} \mathrm{Sp}\, \alpha_{n'} \left(1 + \rho_1 \varepsilon' s' \frac{k'}{K'} + \rho_3 \varepsilon' \frac{k_0}{K'}\right) \times \left(1 + s' \frac{\sigma k'}{k'}\right) \alpha_n (1 + \rho_3 \varepsilon)(1 + \sigma s), \quad (1)$$

where $\alpha_{n'}$, $\alpha_n$ are Dirac matrices characterizing the electron velocity, $\epsilon = \pm 1$ stands for the sign of the energy, the primed quantities refer to the final state of the electron, and the initial spin direction is chosen to be $\mathbf{s} = s\mathbf{k}/k$ ($\hbar\mathbf{k}$ is the elec-

tron initial momentum, which tends to zero; $\hbar cK = \hbar c\sqrt{\mathbf{k}^2 + k_0^2}$ is its proper energy).

Summing Eq. (1) over the spins of the final state we obtain:

$$\sum_{s'=\pm 1} \langle \alpha_{n'}, \alpha_n \rangle$$

$$= \frac{1}{8} \mathrm{Sp}\, \alpha_{n'} \left(1 + \varepsilon' \frac{\boldsymbol{\alpha}\mathbf{k}'}{K'} + \rho_3 \varepsilon' \frac{k_0}{K'}\right) \alpha_n (1 + \rho_3 \varepsilon)(1 + \boldsymbol{\sigma}\mathbf{s}). \quad (2)$$

Similarly, the circular polarization of the photons will be taken into account provided we do not average over the photon polarization states.

The appropriate matrix element is then of the form:[4]

$$S_l = {}^1/_2 \{(\bar{\alpha}^+ \bar{\alpha}) - (\bar{\alpha}^+ \varkappa^0)(\bar{\alpha}\varkappa^0) + il(\varkappa^0 [\bar{\alpha}^+ \bar{\alpha}])\}, \quad (3)$$

where $l = 1$ and $l = -1$ correspond to a right-circular (right handed screw) and left-circular photon polarization, respectively (see also Ref. 2). The quantity $\boldsymbol{\kappa}'$ describes the photon wave vector and $\bar{\alpha}$ stands for the matrix element

$$\bar{\alpha} = \int \psi^+ \alpha \psi d^3x.$$

The corresponding quantities referring to the scattered photon are denoted by a prime.

From (2) and (3) one obtains a generalization of the Klein-Nishina formula which includes the dependence on the polarization of the incident ($l$) and scattered ($l'$) photons and on the spin orientation s of the initial electron (the final electron spin has been summed over):

$$d\sigma_{ll'} = \frac{r_0^2 \varkappa'^2 d\Omega}{4\varkappa^2} \left\{ \frac{\varkappa}{\varkappa'} + \frac{\varkappa'}{\varkappa} - \sin^2\vartheta \right.$$

$$+ ll' \left(\frac{\varkappa}{\varkappa'} + \frac{\varkappa'}{\varkappa}\right) \cos\theta - l \left[ \left(\frac{\varkappa}{\varkappa'} - \frac{\varkappa'}{\varkappa}\right) \right.$$

$$\times \cos\vartheta \cos\psi + \left(1 - \frac{\varkappa'}{\varkappa}\right) \sin\theta \sin\psi \cos\varphi \Big]$$

$$- l' \left[ \left( \frac{\varkappa}{\varkappa'} - \frac{\varkappa'}{\varkappa} \cos^2\theta - \sin^2\theta \right) \cos\psi \right.$$

$$\left. \left. + \frac{1}{2} \left(1 - \frac{\varkappa'}{\varkappa}\right) \sin 2\theta \sin\psi \cos\varphi \right] \right\}, \quad (4)$$

where $\cos\psi = \boldsymbol{\kappa}^0 \cdot \mathbf{s}$, $\cos\theta = \boldsymbol{\kappa}^0 \cdot \boldsymbol{\kappa}'^0$ and $\varphi$ is the angle between the $(\boldsymbol{\kappa}^0, \mathbf{s})$ and $(\boldsymbol{\kappa}^0, \boldsymbol{\kappa}'^0)$ planes. Summing in (4) over the final photon polarization ($l'$) we obtain

$$d\sigma_l = \frac{r_0^2 \varkappa'^2 d\Omega}{2\varkappa^2} \left\{ \frac{\varkappa}{\varkappa'} + \frac{\varkappa'}{\varkappa} - \sin^2\vartheta - l \left[ \left( \frac{\varkappa}{\varkappa'} - \frac{\varkappa'}{\varkappa} \right) \cos\theta \cos\psi \right. \right.$$

$$\left. \left. + \left(1 - \frac{\varkappa'}{\varkappa}\right) \sin\vartheta \sin\psi \cos\varphi \right] \right\}, \quad (5)$$

which agrees with the formula of Gunst and Page,[5] found by a different method. Finally, if one averages over $l$, the usual Klein-Nishina formula is obtained. It follows that in the scattering of unpolarized radiation the spin orientation of the electron does not enter into the integral scattering law.

The degree of circular polarization of the scattered radiation may be calculated from the formula

$$P = \{d\sigma_{ll'}(l' = 1) - d\sigma_{ll'}(l' = -1)\} \Big/ \sum_{l'=\pm 1} d\sigma_{ll'}. \quad (6)$$

In the non-relativistic case we obtain

$$P_{\text{n.r.}} = 2l \cos\vartheta / (1 + \cos^2\vartheta). \quad (7)$$

Thus if the incident radiation is unpolarized then $P_{\text{n.r.}} = 0$. In the extreme relativistic case, for small scattering angles ($\cos\theta \gg 1 - k_0/\kappa$) we again obtain formula (7). On the other hand, for large scattering angles ($\cos\theta \ll 1 - k_0/\kappa$), we obtain

$$P_{\text{rel.}} = (l \cos\vartheta - \cos\psi) / (1 - l \cos\vartheta \cos\psi). \quad (8)$$

Hence, in the extreme relativistic approximation and for large scattering angles the scattered radiation will be partially circularly polarized even if the incident radiation is unpolarized.

As the inverse of the above problem we may consider two-photon annihilation of longitudinally polarized positrons by electrons at rest with definite spin directions. Considering the two-photon pair annihilation as a transition of an electron into a free negative energy level we may use, in the calculation of the corresponding matrix element, the expression (1) provided we put in it $\mathbf{k}' = -\mathbf{k}_+$, $\epsilon' = -1$, $s' = s_+$. We then find, after summing over the polarizations of the produced photons,

$$d\sigma = \frac{r_0^2 k_0 (K_+ + k_0)\, d\Omega}{4k_+ (K_+ + k_0 - k_+ \cos\theta)^2} \{J_0 + s_+ (J_1 \cos\psi - J_2 \sin\psi \cos\varphi)\}. \quad (9)$$

Here

$$J_0 = K_+ (1 - \cos\alpha) - k_0 (1 + \cos\alpha) \cos\alpha;$$

$$J_1 = K_+ (1 - \cos\alpha) \cos\alpha + k_0 (1 + \cos\alpha)$$

$$- \frac{k_0}{k_+} (K_+ + k_0)(1 + \cos\alpha)(\cos\vartheta + \cos(\alpha - \vartheta));$$

$$J_2 = \frac{k_0}{k_+} (K_+ + k_0)(1 + \cos\alpha)(\sin\vartheta - \sin(\alpha - \vartheta));$$

$$\cos\alpha = \frac{(\boldsymbol{\varkappa} \cdot \boldsymbol{\varkappa}')}{\varkappa\varkappa'} = \frac{K_+ \cos^2\theta + k_0 \sin^2\theta - k_+ \cos\theta}{k_+ \cos\theta - K_+};$$

$$\cos\vartheta = (\boldsymbol{\varkappa} \cdot \mathbf{k}_+) / \varkappa k_+; \qquad \cos\psi = (\mathbf{s} \cdot \mathbf{k}_+) / k_+;$$

$\varphi$ is the angle between the $(\mathbf{k}_+, \mathbf{s})$ and $(\mathbf{k}_+, \boldsymbol{\kappa})$ planes, $\hbar\mathbf{k}_+$, $c\hbar K_+$ is the momentum and energy of the positron, $s_+$ is double the positron spin projection onto its direction of motion, and $\boldsymbol{\kappa}$, $\boldsymbol{\kappa}'$

are the wave vectors of the produced photons. Let us note that in the non-relativistic case $\alpha \to \pi$ and therefore (9) yields, after integration over $d\Omega$, the well known formula

$$\sigma_{n.r.} = \pi r_0^2 \frac{c}{v_+} (1 - s_+ \cos \psi), \qquad (10)$$

with the consequence that two-photon annihilation is forbidden in this approximation if the electron and positron spins are parallel, i.e., $s_+ \cos \psi = 1$.

One sees from (9) that there is polar ($\psi$ is replaced by $\pi - \psi$) and azimuthal ($\varphi$ is replaced by $\pi - \varphi$) asymmetry. This fact allows the use of two-photon annihilation of positrons by oriented electrons for experimental determination of the degree of longitudinal polarization of the positrons.

It is known[6] that the asymmetry in the scattering of positrons by oriented electrons is small at low energies and becomes appreciable only at relatively high energies.

On the other hand, two photon annihilation of oriented positrons and electrons gives a noticeable asymmetry in the produced photons only at comparatively low energies. In the high-energy region observation of the asymmetry will apparently be difficult, owing to the decrease in the absolute value of the cross section.

[1] A. A. Sokolov, J. Exptl. Theoret. Phys. (U.S.S.R.) **33**, 794 (1957), Soviet Phys. JETP **6**, 611 (1958).

[2] A. A. Sokolov and Iu. M. Loskutov, J. Exptl. Theoret. Phys. (U.S.S.R.) **34**, 1022 (1958), Soviet Phys. JETP **7**, 706 (1958).

[3] A. A. Sokolov and D. D. Ivanenko, Квантовая теория поля (Quantum Field Theory), M.— L., 1952.

[4] A. A. Sokolov and I. M. Ternov, J. Exptl. Theoret. Phys. (U.S.S.R.) **31**, 473 (1956), Soviet Phys. JETP **4**, 396 (1957).

[5] S. B. Gunst and L. A. Page, Phys. Rev. **92**, 970 (1953).

[6] H. Frauenfelder et al., Phys. Rev. **107**, 643, 909 (1957).

Translated by A. Bincer
281

## *QUANTUM YIELD OF PHOTOIONIZATION IN SILICON*

V. S. VAVILOV and K. I. BRITSYN

Moscow State University

Submitted to JETP editor February 27, 1958

J. Exptl. Theoret. Phys. (U.S.S.R.) **34**, 1354-1355 (May, 1958)

It was shown in earlier works[1,2] that, if the photon energies are high enough, the quantum yield of the internal photoeffect in germanium crystals increases to values much above unity. As was already indicated,[2] the increased quantum yield must be ascribed to impact ionization by primary electrons or holes liberated upon absorption of a photon and having the necessary excess energy.

One would expect a similar phenomenon to take place in silicon. To study the photoeffect in silicon we have used crystals with p-n junctions obtained by thermal diffusion of phosphorus into type-p silicon.[3,4]

Since the diffusion length of the nonequilibrium carriers in the silicon employed was relatively low, we prepared crystals in which the depth of the p-n junction under the illuminated surface did not exceed 2 microns, in order to obtain the necessary sensitivity in the short-wave region. To measure the short-circuit current between the p and n regions of the crystal, and to determine the light flux and the reflection coefficients, we employed a setup similar to that used in the germanium experiments.[2] The interpretation of the results obtained was more difficult in our case than in the determination of the quantum yield in germanium, owing to the following circumstance: The expression for the carrier-collection coefficient $\alpha$ contains the carrier mobility and the diffusion length of the nonequilibrium carriers. However, in the case of a p-n junction obtained by diffusion of impurities from the surface, the mobility changes greatly with depth, increasing inward from the surface where the concentration of the impurity (phosphorus) is high. The carrier diffusion length also undoubtedly varies with depth. In view of this, the formula for the quantum yield Q

$$Q = I_{sc} / N_{h\nu} q \alpha (1 - R),$$

derived for germanium, cannot be used here ($I_{sc}$ is the short circuit current between the p and n regions, q the electron charge, R the reflection coefficient, and $N_{h\nu}$ the number of photons incident per second. It is therefore necessary to as-

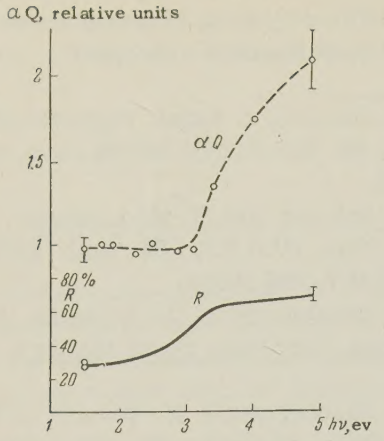


sume that in the photon energy region $E_g < h\nu < 2E_g$, where $E_g \approx 1.1$ ev is the width of the forbidden band for silicon, the quantum yield is unity.

The figure shows the experimental variations of the reflection coefficient R and of the product of the quantum yield Q by the collection coefficient $\alpha$ with the photon energy $h\nu$. A considerable rise in the $\alpha Q$ vs. $h\nu$ curve is seen, starting with approximately $h\nu = 3.25$ ev. In view of the fact that $\alpha$ cannot increase with diminishing wavelength (and consequently with increasing absorption coefficient[5]) the course of the curve indicates an increase in quantum yield and consequently the presence of impact ionization by the carriers liberated upon absorption of the photons.

It would be interesting to compare the photon energies at which this increase is observed (3.2 to 3.3 ev) with the limiting energy of impact ionization in silicon, recently determined by McKay,[6] who studied the multiplication of carriers in strong electric fields. According to his data $E_{i\ min} \approx 2.25$ ev. The value we obtained is quite close to it (3.25 − 1.1 = 2.15 ev).

The authors thank V. M. Malovetskaia, V. M. Patskevich, and L. V. Belova for aid in preparation of crystals with p-n junctions.

[1] S. Koc. Ceskoslov. Casopis pro fisiku, List, Rochik, **6**, 668 (1956).

[2] V. S. Vavilov and K. I. Britsyn, J. Exptl. Theoret. Phys. (U.S.S.R.) **34**, 521 (1958), Soviet Phys. JETP **7**, 359 (1958).

[3] Vavilov, Malovetskaia, Galikin, and Landsman, Usp. Fiz. Nauk **63**, 123 (1957).

[4] Vavilov, Galkin, and Malovetskaia, Атомная энергия (Atomic Energy) June, 1958.

[5] E. Burstein and P. Egli, Coll., Физикаxx полупроводников (Semiconductor Physics), IIL, 1957, p. 15 [Probably: Adv. in Electronics and Electron Physics, **7**, pp. 1 — 86 (1955)].

[6] McKay, Phys. Rev. **108**, 29 (1957).

Translated by J. G. Adashko
282

## *LAMBDA-NUCLEON POTENTIAL FROM MESON THEORY AND THE ENERGIES OF LAMBDA-PARTICLES IN LIGHT HYPERNUCLEI*

V. A. FILIMONOV

Moscow State University

Submitted to JETP editor January 15, 1958

J. Exptl. Theoret. Phys. (U.S.S.R.) **34**, 1355-1356 (May, 1958)

AN attempt was made in Refs. 1 and 2 to obtain the $\Lambda$-nucleon force and to consider the energy of the $\Lambda$ particles in hypernuclei from the point of view of quantum field theory. In order to eliminate the divergences at small distances, a repulsive wall was introduced, in analogy to the nucleon-nucleon interaction. The existence of such a wall in the nucleon-nucleon interaction follows from the scattering of high-energy nucleons; however, the existence of such a repulsion for the $\Lambda$-nucleon interaction cannot be considered established at the present time. The introduction of a repulsive wall in the $\Lambda$-nucleon force causes considerable difficulty in the calculations. However, the nucleon-nucleon forces obtained[3] from meson theory by introducing a cutoff in the momenta of virtual mesons agree well with the experimental data having to do with the low-energy interaction of nucleons. Since the interaction of $\Lambda$-particles with the nucleons in the nucleus has to do with the low-energy region, one might expect that the $\Lambda$-nucleon potential obtained from the theory by cutting off the momenta of virtual mesons will give sensible results.

On the basis of these considerations, we calculated the $\Lambda$-nucleon potential, starting from a Hamiltonian of the form

$$H = \frac{g\hbar}{2V^{1/2}} \sum_{l=1}^{N} \sum_{k} v(k)\,(\sigma_l k)\,\hat{a}^l \Big\{ \sqrt{\frac{\hbar}{2\omega^{(\pi)}}} \sum_{j=1}^{3} iT_j^{(\pi)(l)} (a_{jk} + a^*_{l,-k}) \times \exp\{ikx_l\} + \sqrt{\frac{\hbar}{2\omega^{(K)}}} \Big[ \sum_{j=1}^{2} iT_j^{(K)(l)} (c_{jk} + b^*_{jk}) \times \exp\{ikx_l\} + \text{Hermitian conj.} \Big] \Big\}. \quad (1)$$

The Hamiltonian H was obtained from the interactions of baryons with $\pi$- and K-meson fields,[4] after carrying out the transformation of Dyson assuming the baryons to be at rest at the points $x_l$. Only terms linear in the coupling constant were retained in H. It was also assumed that all coupling constants are the same. $T_j^{(\pi)}$ and $T_j^{(K)}$ are eight-row matrices that account for the transformation of baryons into each other upon meson exchange; $v(k)$ is a function which cuts off the momenta of the virtual mesons; $\hat{a}$ is an eight-row diagonal matrix, the elements of which are the inverses of the baryon masses.

Starting from the Hamiltonian (1), we calculated the forces between $\Lambda$ and nucleon, connected with the exchange of a single K, two $\pi$'s, a K and a $\pi$, and two K mesons. The forces were obtained as in Ref. 3, the only difference being that the matrices $\tau$ were replaced by $T_i\hat{a}$. The forces obtained were used to calculate the binding energies of the light hypernuclei ${}_\Lambda H^3$, ${}_\Lambda He^4$, and ${}_\Lambda He^5$. The results of calculation showed that the potential energy of the $\Lambda$-particle in hypernuclei, connected with the $2\pi$- and 2K-meson forces, was almost independent of the spin of the hypernucleus. The potential energy from the 1K-meson force comprised $\sim 1/10$ of the total potential energy, was positive, and was approximately the same for all hypernuclei. The smallness of the energy from the 1K-meson force is connected with the fact that the corresponding potential is nonmonotonic. The energies from the $\pi$K-meson force depend strongly on the spin of the hypernucleus. The lowest potential energy is obtained for the lowest spin of the hypernucleus.

If the cut-off parameter is taken to be $k_m = 6m_\pi c/\hbar$ (Ref. 3) and a coupling constant is chosen so that for ${}_\Lambda He^5$ the experimental value[5] for the energy of the $\Lambda$-particle, $B_\Lambda \sim 2.6$ Mev, is obtained, then it turns out that $g/\sqrt{\hbar c} = 11.8$ and the energy $B_\Lambda$ of the $He^3$ and $He^4$ hypernuclei is $\sim 2.1$ and $\sim 2.2$ Mev respectively. Here ${}_\Lambda H^2$ is not bound. Probable experimental values for the energy of the hypernuclei ${}_\Lambda He^3$ and ${}_\Lambda He^4$ are $B_\Lambda = 0.3$ Mev and 1.7 Mev, respectively.[5]

Thus, the theory considered gives binding energies too close to each other. Although there is not quantitative agreement, the theory considered correctly reproduces the fact that the force between the $\Lambda$ and nucleons is not of a purely Wigner type. Purely Wigner forces would give a substantially stronger increase in the binding energies of $\Lambda$-particles in light hypernuclei than is actually observed. This tendency for the binding energies of light hypernuclei to be the same is correctly reproduced by the theory considered. Various types of corrections to the forces considered may improve the agreement between experiment and theory.

The author would like to express his gratitude to Prof. D. D. Ivanenko for encouragement in carrying out the present work.

Note added in proof (April 21, 1958). In the calculations described, the effect of the motion of the remaining nucleus in the calculation of the kinetic energy of the $\Lambda$ particle was neglected. If this is taken into account, then for $g^2/4\pi\hbar c = 12.3$, the values 0.48 Mev, 1.53 Mev and 2.30 Mev are obtained for the energies of ${}_\Lambda H^3$, ${}_\Lambda He^4$, and ${}_\Lambda He^5$, respectively, in satisfactory agreement with experiment.

[1] M. Dallaporta and F. Ferrari, Nuovo cimento **5**, 111 (1957).

[2] D. Lichtenberg and M. Ross, Phys. Rev. **103**, 1131 (1956).

[3] S. Gartenhaus, Phys. Rev. **100**, 900 (1955).

[4] B. d'Espagnat and J. Prentki, Nuclear Phys. **1**, 33 (1956).

[5] Levisetti, Slater, and Telegdi, preprint.

Translated by G. E. Brown
283